frontiers | Research Topics

Biodegradable polymers for biomedical applications
volume II

Edited by
Liqun Yang, Jianshe Hu, Shuai Jiang, Hongli Mao and Himansu Sekhar Nanda

Published in
Frontiers in Bioengineering and Biotechnology
Frontiers in Materials

ISSN 1664-8714
ISBN 978-2-8325-2882-2
DOI 10.3389/978-2-8325-2882-2

About Frontiers

Frontiers is more than just an open access publisher of scholarly articles: it is a pioneering approach to the world of academia, radically improving the way scholarly research is managed. The grand vision of Frontiers is a world where all people have an equal opportunity to seek, share and generate knowledge. Frontiers provides immediate and permanent online open access to all its publications, but this alone is not enough to realize our grand goals.

Frontiers journal series

The Frontiers journal series is a multi-tier and interdisciplinary set of open-access, online journals, promising a paradigm shift from the current review, selection and dissemination processes in academic publishing. All Frontiers journals are driven by researchers for researchers; therefore, they constitute a service to the scholarly community. At the same time, the *Frontiers journal series* operates on a revolutionary invention, the tiered publishing system, initially addressing specific communities of scholars, and gradually climbing up to broader public understanding, thus serving the interests of the lay society, too.

Dedication to quality

Each Frontiers article is a landmark of the highest quality, thanks to genuinely collaborative interactions between authors and review editors, who include some of the world's best academicians. Research must be certified by peers before entering a stream of knowledge that may eventually reach the public - and shape society; therefore, Frontiers only applies the most rigorous and unbiased reviews. Frontiers revolutionizes research publishing by freely delivering the most outstanding research, evaluated with no bias from both the academic and social point of view. By applying the most advanced information technologies, Frontiers is catapulting scholarly publishing into a new generation.

What are Frontiers Research Topics?

Frontiers Research Topics are very popular trademarks of the *Frontiers journals series*: they are collections of at least ten articles, all centered on a particular subject. With their unique mix of varied contributions from Original Research to Review Articles, Frontiers Research Topics unify the most influential researchers, the latest key findings and historical advances in a hot research area.

Find out more on how to host your own Frontiers Research Topic or contribute to one as an author by contacting the Frontiers editorial office: frontiersin.org/about/contact

Biodegradable polymers for biomedical applications - volume II

Topic editors

Liqun Yang — Liaoning Research Institute of Family Planning (The Affiliated Reproductive Hospital of China Medical University), China

Jianshe Hu — Northeastern University, China

Shuai Jiang — Ocean University of China, China

Hongli Mao — Nanjing Tech University, China

Himansu Sekhar Nanda — PDPM Indian Institute of Information Technology, Design and Manufacturing, India

Citation

Yang, L., Hu, J., Jiang, S., Mao, H., Nanda, H. S., eds. (2023). *Biodegradable polymers for biomedical applications - volume II*. Lausanne: Frontiers Media SA. doi: 10.3389/978-2-8325-2882-2

Table of contents

frontiers | Frontiers in Materials

TYPE Editorial
PUBLISHED 16 June 2023
DOI 10.3389/fmats.2023.1231445

OPEN ACCESS

EDITED AND REVIEWED BY
Hafiz M. N. Iqbal,
Monterrey Institute of Technology and Higher Education (ITESM), Mexico

*CORRESPONDENCE
Himansu Sekhar Nanda,
himansu@iiitdmj.ac.in
Liqun Yang,
yanglq@lnszjk.com.cn

RECEIVED 30 May 2023
ACCEPTED 09 June 2023
PUBLISHED 16 June 2023

CITATION
Nanda HS, Yang L, Hu J, Jiang S and Mao H (2023), Editorial: Biodegradable polymers for biomedical applications-Volume II.
Front. Mater. 10:1231445.
doi: 10.3389/fmats.2023.1231445

Editorial: Biodegradable polymers for biomedical applications-Volume II

Himansu Sekhar Nanda[1,2]*, Liqun Yang[3,4]*, Jianshe Hu[5], Shuai Jiang[6] and Hongli Mao[7]

[1]Mechanical Engineering Discipline, PDPM Indian Institute of Information Technology, Design and Manufacturing Jabalpur, Jabalpur, Madhya Pradesh, India, [2]Terasaki Institute for Biomedical Innovation (TIBI), Los Angeles, CA, United States, [3]Department of Biomaterials, Shengjing Hospital of China Medical University, Shenyang, China, [4]Liaoning Research Institute of Family Planning (The Reproductive Hospital of China Medical University), Shenyang, China, [5]Center for Molecular Science and Engineering, College of Science, Northeastern University, Shenyang, China, [6]School of Medicine and Pharmacy, Ocean University of China, Qingdao, China, [7]School of Materials Science and Engineering, Nanjing Tech University, Nanjing, China

KEYWORDS

biodegradable polymers, chemical synthesis, degradation behavior, drug delivery system, tissue engineering

Editorial on the Research Topic
Biodegradable polymers for biomedical applications-Volume II

Degradable polymers are desirable due to their capacity to undergo breakdown, excretion, or resorption without requiring removal or surgical alteration (Kirillova et al, 2021). Designing biodegradable polymers for biomedical applications involves vital considerations such as mechanical properties, chemical properties, and degradation mechanisms (Mukherjee et al., 2023). Biodegradable polymers have been extensively employed in biomedical applications due to their unique properties, such as variable copolymer block composition, surface charge, and film-forming capabilities (Pires et al., 2023). The articles featured in this Research Topic focus on the latest and most promising advancements in biomaterials for controlled drug delivery, tissue engineering, and various biomedical applications.

The considerable interest in poly-lactic acid (PLA) and other biodegradable polymers stems from their natural degradation capability, which eliminates the necessity of a second surgical procedure for removal, unlike non-biodegradable materials such as Polymethyl methacrylate (PMMA) (da Silva et al., 2018). The heat generated during the preparation of PMMA beads could compromise the stability of combined antibiotics for treating chronic osteomyelitis. Liu et al. examined the advancements in research on drug delivery systems based on biodegradable polymers for treating chronic osteomyelitis. The article highlights the utilization of natural biodegradable polymers like collagen, chitosan, and silk protein, as well as synthetic polymers such as PLA, poly(trimethylene carbonate) (PTMC), poly(ε-caprolactone) (PCL), and poly(lactic-co-glycolic) acid (PLGA) for developing delivery systems capable of locally administering antimicrobial agents to infected sites. PLGA-based micro/nanoparticle drug delivery systems offer promising prospects due to their higher efficiency and reduced adverse effects, resulting in extensive utilization in drug-resistant tuberculosis that occurred due to low plasma concentration of orally administered drugs (Pires et al., 2023). To combat this issue of drug-resistant tuberculosis, Shao et al.

reviewed recent advancements in PLGA micro/nanoparticle delivery systems for enhancing the delivery efficiency of tuberculosis drugs to lesion sites, thereby improving their overall efficacy. The article covers the current research achievements and shortcomings of the PLGA micro/nanoparticles to facilitate the translation of microtechnology/nanotechnology from successful experimental outcomes to clinical practice. Like PLGA, Poly(l-lactide) (PLLA) has attracted attention in tissue engineering and orthopedics due to its favorable mechanical properties, ability to degrade naturally, and ease of processing (DeStefano et al., 2020). However, PLLA has certain drawbacks, including low toughness and a relatively slow degradation rate, which limit its extensive utilization on a larger scale. To alter the structure and properties of PLLA, Fan et al. fabricated membranes using a combination of poly(l-lactide acid-p-dioxanone-glycolide) (PLPG) and stereo complex poly(lactic acid) (sc-PLA). The study aimed to assess the impact of different quantities of sc-PLA on PLLA crystallization within the PLPG matrix and to evaluate the biocompatibility of PLPG copolymers. Additionally, the mechanisms that can enhance the control over the mechanical properties and biocompatibility of the PLGP polymers are also explored to address skin trauma and bone tissue engineering.

Advancements in osteogenesis research, biomaterial development, and material science and technology offer promising prospects for creating ideal materials that fulfill the requirements of human bone repair (Zhang et al., 2019). Yu et al. primarily discussed the emerging developments in the field of synthetic biodegradable polymer materials for bone repair, with a particular emphasis on exploring their antitumor properties. The article emphasizes the potential benefits of integrating composite materials, including polymer substances such as PLA, PGA, PLGA, and PVA. This integration addresses the difficulties associated with postoperative bone defects and patients' risk of tumor recurrence. Apart from PVA, there is a requirement to progress the development of additional allogeneic materials to restore Achilles tendon injuries effectively. Biomedical polymers offer a versatile solution for treating and repairing soft tissues, ligaments, muscles, and organs that have suffered damage from living organisms (Liu et al., 2023a). Zhang et al. developed PTMC films loaded with degradable Doxycycline hydrochloride to enable a sustained and prolonged release of the drug to treat Achilles tendon rupture.

Despite standardized treatment, achieving optimal wound healing remains challenging, and patients still face the risk of amputation (Malone and Schultz, 2022). The direct use of biomaterials continues to pose difficulties in attaining definitive benefits for wound healing. It may even result in minor adverse effects due to the characteristics of their degradation products. Ren et al. provided an overview of the intricate integration of biomaterials with drugs, stem cells, and active agents. The article includes utilizing and evaluating composite biomaterials in clinical trials and exploring research concepts and future investigations focused on addressing wound repair issues in diabetes.

Intrauterine surgery-induced damage to the endometrium frequently triggers alterations in the intrauterine environment's physiological processes, consequently leading to infertility among women in their reproductive years (Lee et al., 2020). Stem cell therapy stands out as the most appealing therapeutic strategy for addressing endometrial damage (Wani et al., 2022). However, stem cell transplantation for endometrial repair continues to face significant long-term challenges in terms of safety and efficacy. These challenges include difficulties in preserving the cells, the potential risk of tumor formation, and transplanted cells often needing higher rates of successful migration to the desired location. To address these issues, Cai et al. provided a comprehensive review of biopolymer-based hydrogels as delivery systems for effectively regulating the microenvironment at the site of endometrial injury. In addition, the article also emphasizes the importance of designing hydrogels that incorporate estrogen, stem cells, and therapeutic factors with multifunctional capabilities. These hydrogel systems should not only facilitate uterine cavity formation but also effectively respond to various external or internal triggers. In response to the limitations of chemotherapeutic drugs in breast cancer treatment, extensive research has focused on nanotechnology-based nano-drug delivery systems (NDDSs) to enable stable and sustained release of therapeutic agents, similar to hydrogels for sustained release (Liu et al., 2023b). Jia et al. summarize the research progress on utilizing hyaluronic acid (HA) as a hydrophilic carrier for encapsulating chemotherapeutic drugs. This approach enables targeted delivery to breast tumors through CD44 targeting, improving drug utilization and reducing systemic toxicity. The article includes a detailed compilation of HA-based NDDSs, modified HA-based NDDSs, and HA nanohybrid NDDS containing organic or inorganic substances as practical approaches for treating, preventing, and diagnosing breast cancer.

In dental implantology, a crucial aim is to achieve a long-term integration of the implant in the alveolar ridge (Liang, 2023). However, bone resorption resulting from traumas and tumors can compromise the successful integration of prosthetic teeth replacements. GBR (Guided Bone Regeneration) is a commonly used technique for correcting horizontal and vertical defects or preserving alveolar sockets following tooth extraction. The barrier membranes used in GBR prevent cells from the surrounding epithelium and connective tissue from entering the site, which allows osteoprogenitor cells to multiply and create new bone tissue at the implant site. Yang et al. provided a thorough overview of the applications of biomaterials in GBR to repair alveolar ridge and discussed the future advancement in barrier membranes. The study envelops the clinical operability, biocompatibility, tissue selectivity, and antibacterial properties required for barrier membranes. The work provided insights into polymeric membranes, non-polymeric membranes, and techniques for preparing barrier membranes. The polymeric and non-polymeric meshes utilized for Pelvic Floor Dysfunction (PFD) exhibit inadequate mechanical properties and a rapid degradation rate (Wu et al., 2020). Consequently, they result in suboptimal anatomical reduction and impose limitations on their clinical application in PFD treatment. Lin et al. featured an article on tissue-engineered repair materials that use cells and other additional cues for treating PFD. The work provides insight into cells, scaffolds, cell-combined scaffolds, and the cross-talk between cells and scaffolds. The use of tissue-engineered repair material to restore the damaged sphincter function in case of stress urinary incontinence and strengthening of the pelvic floor and supporting structures in pelvic organ prolapse has been highlighted.

In conclusion, this Research Topic has presented insightful and innovative reports focusing on the biodegradable polymers for biomedical applications, aiming to provide valuable insights and thought-provoking ideas to professionals interested in biomaterials. With the current trend of organ regeneration and reconstruction, personalized therapy and precision medicine, the design and development of bioactive biodegradable polymers will be the future research focus and development direction. Of course, with the rapid development of materials science and medicine, especially the increasing attention to medical-industrial integration, the challenges of biodegradable polymers require more attention.

We sincerely thank all the authors and reviewers for their contributions to this Research Topic.

Author contributions

All authors listed have made a substantial, direct, and intellectual contribution to the work and approved it for publication.

Acknowledgments

All authors' contributions, and those of the editorial staff of Frontiers, are appreciated to make this Research Topic possible.

Conflict of interest

The authors declare that the research was conducted in the absence of any commercial or financial relationships that could be construed as a potential conflict of interest.

Publisher's note

References

da Silva, D., Kaduri, M., Poley, M., Adir, O., Krinsky, N., Shainsky-Roitman, J., et al. (2018). Biocompatibility, biodegradation and excretion of polylactic acid (PLA) in medical implants and theranostic systems. *Chem. Eng. J.* 340, 9–14. doi:10.1016/j.cej.2018.01.010

DeStefano, V., Khan, S., and Tabada, A. (2020). Applications of PLA in modern medicine. *Eng. Regen.* 1, 76–87. doi:10.1016/j.engreg.2020.08.002

Kirillova, A., Yeazel, T. R., Asheghali, D., Petersen, S. R., Dort, S., Gall, K., et al. (2021). Fabrication of biomedical scaffolds using biodegradable polymers. *Chem. Rev.* 121 (18), 11238–11304. doi:10.1021/acs.chemrev.0c01200

Lee, D., Kim, S. K., Lee, J. R., and Jee, B. C. (2020). Management of endometriosis-related infertility: Considerations and treatment options. *Clin. Exp. Reproductive Med.* 47 (1), 1–11. doi:10.5653/cerm.2019.02971

Liang, W. (2023). Natural implant restoration in stable alveolar bone (NIRISAB)—concepts in clinical practice: Long-term follow-up on three cases of ridge reconstruction using the tunnel approach with remote incision. *J. Oral Implant.* 49 (2), 130–146. doi:10.1563/aaid-joi-D-22-00032

Liu, J., Li, S., Wang, J., Li, N., Zhou, J., and Chen, H. (2023a). Application of nano drug delivery system (NDDS) in cancer therapy: A perspective. *Recent Pat. Anti-Cancer Drug Discov.* 18 (2), 125–132. doi:10.2174/1574892817666220713150521

Liu, S., Yu, J.-M., Gan, Y.-C., Qiu, X.-Z., Gao, Z.-C., Wang, H., et al. (2023b). Biomimetic natural biomaterials for tissue engineering and regenerative medicine: New biosynthesis methods, recent advances, and emerging applications. *Mil. Med. Res.* 10 (1), 16. doi:10.1186/s40779-023-00448-w

Malone, M., and Schultz, G. (2022). Challenges in the diagnosis and management of wound infection. *Br. J. Dermatology* 187 (2), 159–166. doi:10.1111/bjd.21612

Mukherjee, C., Varghese, D., Krishna, J. S., Boominathan, T., Rakeshkumar, R., Dineshkumar, S., et al. (2023). Recent advances in biodegradable polymers – properties, applications and future prospects. *Eur. Polym. J.* 192, 112068. doi:10.1016/j.eurpolymj.2023.112068

Pires, P. C., Mascarenhas-Melo, F., Pedrosa, K., Lopes, D., Lopes, J., Macário-Soares, A., et al. (2023). Polymer-based biomaterials for pharmaceutical and biomedical applications: A focus on topical drug administration. *Eur. Polym. J.* 187, 111868. doi:10.1016/j.eurpolymj.2023.111868

Wani, S., Dar, T., Koli, S., Wani, W. Y., Anwar, M., and Farooq, Z. (2022). "Stem cell technology in medical biotechnology," in *Fundamentals and advances in medical biotechnology* (Berlin, Germany: Springer International Publishing), 233–267.

Wu, X., Jia, Y., Sun, X., and Wang, J. (2020). Tissue engineering in female pelvic floor reconstruction. *Eng. Life Sci.* 20 (7), 275–286. doi:10.1002/elsc.202000003

Zhang, L., Yang, G., Johnson, B. N., and Jia, X. (2019). Three-dimensional (3D) printed scaffold and material selection for bone repair. *Acta Biomater.* 84, 16–33. doi:10.1016/j.actbio.2018.11.039

frontiers | Frontiers in Bioengineering and Biotechnology

REVIEW
published: 20 June 2022
doi: 10.3389/fbioe.2022.894252

Recent Developments in Biomaterial-Based Hydrogel as the Delivery System for Repairing Endometrial Injury

Guiyang Cai[1†], Zhipeng Hou[2,3†], Wei Sun[4], Peng Li[3], Jinzhe Zhang[3], Liqun Yang[3] and Jing Chen[1]**

[1]Department of Obstetrics and Gynecology, Shengjing Hospital of China Medical University, Shenyang, China, [2]Center for Molecular Science and Engineering, College of Science, Northeastern University, Shenyang, China, [3]NHC Key Laboratory of Reproductive Health and Medical Genetics (China Medical University), Liaoning Research Institute of Family Planning (The Reproductive Hospital of China Medical University), Shenyang, China, [4]Department of Cell Biology, Key Laboratory of Cell Biology, Ministry of Public Health, and Key Laboratory of Medical Cell Biology, Ministry of Education, China Medical University, Shenyang, China

OPEN ACCESS

Edited by:
Yilong Cheng,
Xi'an Jiaotong University, China

Reviewed by:
Philippa Saunders,
University of Edinburgh, United Kingdom
Stacey Schutte,
University of Cincinnati, United States

***Correspondence:**
Liqun Yang
yanglq@lnszjk.com.cn
Jing Chen
chenj@sj-hospital.org

[†]These authors have contributed equally to this work

Specialty section:
This article was submitted to Biomaterials, a section of the journal Frontiers in Bioengineering and Biotechnology

Received: *11 March 2022*
Accepted: *23 May 2022*
Published: *20 June 2022*

Citation:
Cai G, Hou Z, Sun W, Li P, Zhang J, Yang L and Chen J (2022) Recent Developments in Biomaterial-Based Hydrogel as the Delivery System for Repairing Endometrial Injury. Front. Bioeng. Biotechnol. 10:894252. doi: 10.3389/fbioe.2022.894252

Endometrial injury caused by intrauterine surgery often leads to pathophysiological changes in the intrauterine environment, resulting in infertility in women of childbearing age. However, clinical treatment strategies, especially for moderate to severe injuries, often fail to provide satisfactory therapeutic effects and pregnancy outcomes. With the development of reproductive medicine and materials engineering, researchers have developed bioactive hydrogel materials, which can be used as a physical anti-adhesion barrier alone or as functional delivery systems for intrauterine injury treatment by loading stem cells or various active substances. Studies have demonstrated that the biomaterial-based hydrogel delivery system can provide sufficient mechanical support and improve the intrauterine microenvironment, enhance the delivery efficiency of therapeutic agents, prolong intrauterine retention time, and perform efficiently targeted repair compared with ordinary drug therapy or stem cell therapy. It shows the promising application prospects of the hydrogel delivery system in reproductive medicine. Herein, we review the recent advances in endometrial repair methods, focusing on the current application status of biomaterial-based hydrogel delivery systems in intrauterine injury repair, including preparation principles, therapeutic efficacy, repair mechanisms, and current limitations and development perspectives.

Keywords: biomaterial-based hydrogel, endometrial injury repair, intrauterine adhesion, delivery system, IUA

INTRODUCTION

The human endometrium is a dynamically remodeling tissue that lines the inner surface of the uterine cavity and is structurally divided into functional and basal layers (Salazar et al., 2017). As part of the menstrual cycle, the endometrium undergoes a monthly proliferative cycle (follicular phase regeneration), a differentiation cycle (luteal phase), and a shedding cycle (menstrual phase) induced by cyclic changes in estrogen and progesterone levels. (Salamonsen, 2003; Jabbour et al., 2006; Gargett et al., 2008; Mihm et al., 2011; Gargett and Ye, 2012). The proliferative changes in the follicular phase are affected by estradiol, and progesterone inhibits endometrial growth and plays a

role in differentiation during the subsequent secretory phase. The onset of menstruation is due to the lack of trophoblast and human chorionic gonadotrophin (hCG) secretion in the late secretory phase, followed by an endometrial response of progesterone and estradiol withdrawal during luteal regression (Jabbour et al., 2006). The upper functional layer is where the physiological activities of proliferation, secretion, and degeneration occur and where the blastocyst implantation after conception (Strassmann, 1996). In contrast, regeneration usually occurs in the lower basal layer (Jabbour et al., 2006). In the normal non-pregnancy cycle, the endometrium area that does not fall off, fall off, and heals coexists, and the repair process is both rapid and scar-free. This periodic shedding ensures that the amount of exposed endometrium and damaged blood vessels at any given moment is minimized (Garry et al., 2009).

As the most common endometrial injury disease, intrauterine adhesions (IUA) refer to the various degrees of adhesion of the uterine cavity and cervical canal wall induced by various injury factors, and the endometrium is replaced by fibrotic tissue (Robinson et al., 2008). This condition was first described in detail by Asherman in 1948 and is therefore clinically known as "Asherman's syndrome" (AS). Injury factors include repeated induced abortion, mid-term labor induction, uterine submucosal myomectomy and cesarean section, which can cause damage to the endometrial basal layer, endometrial repair obstacles, and fibrous tissue hyperplasia, resulting in the disappearance of the standard shape of the uterine cavity (Hooker et al., 2014). The clinical manifestations of IUA include abnormal menstrual bleeding or even amenorrhea, infertility due to uterine factors, recurrent miscarriage, placenta accreta, and other obstetric complications (Sun et al., 2018; Zhu et al., 2019). As one of the major causes of secondary infertility in women of childbearing age, IUA will hinder the implantation of blastocysts, damage the blood supply of the uterus and the early fetus, and eventually lead to miscarriage or complete infertility in patients, which has become an urgent public health problem for women of childbearing age.

According to different types of IUA, seeking active and effective treatment measures to separate adhesions, restore the normal shape of the uterine cavity, promote endometrial repair, and restore reproductive function is an urgent clinical problem to be solved, and it is also a hot spot and difficulty in clinical research in recent years. Traditional methods such as hysteroscopy adhesiolysis, artificial hormone therapy, and the placement of intrauterine devices are currently used clinically. Still, the therapeutic results obtained are minimal and remain poor effect in severe cases. There is insufficient evidence that these treatment modalities effectively promote regeneration or improve pregnancy outcomes after severe endometrial injury (Johary et al., 2014; Lin et al., 2015). In addition, the recurrence rate of severe IUA is as high as more than 62%, showing a poor prognosis despite an excellent initial treatment effect (Abudukeyoumu et al., 2020).

The introduction of various biological substances that stimulate tissue regeneration can promote endometrial injury repair (Cervelló et al., 2015; Almeida et al., 2021; Ma et al., 2021). Stem cell therapy is currently the most attractive therapeutic approach to repairing endometrial damage (Keyhanvar et al., 2021; Gharibeh et al., 2022). Among them, endometrial mesenchymal stem/progenitor cells (eMSC), a highly proliferative class of cells derived from the dynamic, cyclically regenerating human endometrium, show promise in regenerative medicine through paracrine immunomodulatory effects and enhancing endogenous stem cell function (Hennes et al., 2021). The pericyte and perivascular properties of eMSC indicate their specific roles in regulating angiogenesis, inflammation, and fibrosis (Thomas et al., 2017). Several reports have further demonstrated the feasibility of eMSC as a source of stem cells for regenerative medicine in uterine biology (Campo et al., 2017; Olalekan et al., 2017). The ease of sampling, culture potency and reduced rate of spontaneous differentiation into fibroblasts under specific culture conditions also serve as advantageous features in the application of eMSC (Gurung et al., 2015). Similar to eMSC, menstrual fluid-derived endometrial stem/progenitor cells (MenSC) have shown considerable potential in endometrial injury repair (Bozorgmehr et al., 2020; Wyatt et al., 2021). The results in the animal model showed a good repair effect (Zhang et al., 2016; Zhang et al., 2019). Then it was applied clinically to patients with severe AS, who showed varying degrees of increase in endometrial thickness and improved embryo implantation success, indicating that MenSC reduced fibrosis and promoted the repair of damaged endometrium (Tan et al., 2016). In addition, the endometrial stem/progenitor cell population includes the elusive endometrial epithelial stem/progenitor cells and a systematic review of the identification and use of epithelial stem cells in endometrial diseases (especially endometriosis) has been conducted (Cousins et al., 2021; Kong et al., 2021). However, stem cell transplantation for endometrial repair still has long-term safety and efficacy limitations, such as preservation difficulty, tumorigenicity, and low homing rates of transplanted cells. In addition, there is no uniform guidance or consensus available for a clinical reference regarding stem cell-related therapies (Bai et al., 2019; Song et al., 2021).

With the development of studies in recent years, some researchers have combined tissue engineering with regenerative medicine, using biomaterials for loading stem cells, therapeutic factors, or constructing *in situ* delivery systems as a therapeutic strategy for endometrial damage repair with remarkable results, thus opening up new avenues for the treatment of endometrium-related defects by integrating biomaterials with conventional therapies (Zhao et al., 2017). Biomaterials have the advantage of providing structural support that mimics natural endometrial tissue while allowing for the controlled release of drugs, growth factors, or other biologically active substances, with the expectation of more efficient drug delivery and improved therapeutic outcomes (Zhang et al., 2020a; Yoshimasa and Maruyama, 2021). Hydrogels have excellent water retention properties, swell in volume without dissolving and retain a certain elasticity, which is very similar to the properties of soft tissues in the body. The low interfacial tension and adhesion properties can reduce the irritation of the hydrogel to the tissue and provide good diffusion and longer retention time of the contents (Drury

and Mooney, 2003; Peppas et al., 2006; Brandon et al., 2009; Milcovich et al., 2017). Therefore, hydrogels have become the most attractive carrier material for treating IUA or promoting endometrial regeneration. Herein, we focus on reviewing the different types of biopolymer-based hydrogels used to construct delivery systems such as estrogen, stem cells, or therapeutic factors for endometrial injury repair in recent years. The design principles and future trends of hydrogel materials are also discussed in anticipation of providing useful references for subsequent research.

Design Principles of Hydrogel in Endometrial Repair

When hydrogels are used in the biomedical field, the design principles are often based on the specific microenvironment and application requirements of the target disease. In the treatment of IUA, the main objectives of hydrogel material applications are to prevent the occurrence of adhesions, repair endometrial damage and promote its regeneration. More specifically, the biocompatibility, biodegradability, mechanical properties, immunogenicity, ability to restore endometrial repair and reproductive function, controlled drug release properties, and even ethical issues of the candidate hydrogel matrix materials are all taken into account (López-Martínez et al., 2021a).

First of all, good biocompatibility is a necessary condition in biomedical applications. Most biomaterial-based hydrogels have excellent biocompatibility. Low immune rejection and biomimetics are the two most noteworthy indicators, as low immunogenicity ensures that the hydrogel and its loaded biomolecules are not removed as foreign bodies and can reach the injury to be effective. At the same time, biomimetics enhances the adhesion and growth of cells in the material and molecular responses, resulting in better repair. Secondly, the mechanical strength of the hydrogel needs to be sufficient to support the uterine cavity to reduce the formation of fibrosis, the degradation rate can match the repair process of the endometrium, and then it can be completely non-toxic metabolically excreted. Third, the hydrogel matrix can provide a gently controlled release of drugs, stem cells, or growth factors. Stem cell therapy is usually the first choice for treating severe IUA, but the delivery of hydrogels to stem cells is often insufficient. Ideally, a delivery system that promotes stem cell survival, proliferation, and directed differentiation can be constructed through hydrogels (Cervelló et al., 2015). In addition, the hydrogel formed *in situ* should have a suitable gelation time; too long time may cause the ungelatinized material to be diluted and washed by uterine fluid, unable to form a gel at the injury site, and too short a time may result in poor adhesion of the gel, which is not conducive to injury treatment (Lin et al., 2020). Finally, the sterilization steps of hydrogels. Generally speaking, the sterilization of the prepared hydrogel mainly goes through four stages: cleaning, disinfection, sterilization, and dehydrogenation. The most suitable sterilization method should be selected by comprehensively evaluating the hydrogel material itself, the preparation process, and the physicochemical properties of the loaded therapeutic agent.

Application of Hydrogel in Endometrial Repair

Current research in the treatment of IUA is focused on the repair of the endometrium by using hydrogels as a matrix loaded with various bioactive substances. In the later sections, we will summarize the recent studies according to different sources of biomaterial-based hydrogel delivery systems (Thubert et al., 2015; Hooker et al., 2018) (**Table 1**).

Natural Biomaterial-Based Hydrogels

Due to its unique biocompatibility and enzymatic biodegradability, Hyaluronic acid (HA) has been widely used in the field of biomedicine. Linear HA molecules were typically prepared using cross-linking techniques into hydrogels with a stable three-dimensional network architecture that provides the necessary structural and mechanical support for surrounding cells. In addition, the widely expressed hyaluronidase *in vivo* can completely degrade HA into non-toxic and harmless small molecular products (Weissmann, 1955; Koliakos et al., 2008). The cross-linked hyaluronic acid gel has been adopted and studied by many researchers as an excellent carrier for intrauterine administration.

Liu et al. reported a new strategy for constructing an intrauterine sustained-release system by combining the mesenchymal stem cell secretome (MSC-Sec) with cross-linked hyaluronic acid gel. MSC-Sec has a good effect on endometrial cells and endothelial cells. Then the labeled MSC-Sec were used to monitor the concentration and distribution of stem cells *in utero* by stereo fluorescence imaging technology to study HA hydrogel release kinetics. In the study, MSC-Sec-HA hydrogel was used to repair uterine damage in a rat model, and the research results showed that the endometrial morphology and fertility of the experimental rats were restored (**Figure 1**) (Liu et al., 2019).

The human placenta-derived mesenchymal stem cells (HP-MSCs) were loaded into cross-linked hyaluronic acid hydrogels to prepare HP-MSCs-HA hydrogels for the treatment of endometrial injury successfully. The collection process of HP-MSCs is safe and non-invasive (Zhu et al., 2013) and presents vigorous expansion ability and greater proliferation capacity (Feng et al., 2020). The low immunogenicity also ensures that no immune response will be caused during the treatment (Rinaldi et al., 1996; El-Toukhy et al., 2008; Cenksoy et al., 2013). Therefore, HP-MSCs are fully capable of becoming a new alternative source of stem cell therapy. Compared with the control group, the HP-MSCs-HA hydrogel system can significantly reduce the fiber area, increase the endometrial thickness and the number of glands in the damaged endometrium, and improve embryo implantation rate, demonstrating the good recovery of uterine function. The research group analyzed the potential treatment mechanisms. It concluded that the paracrine action of HP-MSCs could promote the proliferation of human endometrial stromal cells by activating the JNK/Erk1/2-Stat3-VEGF pathway and the

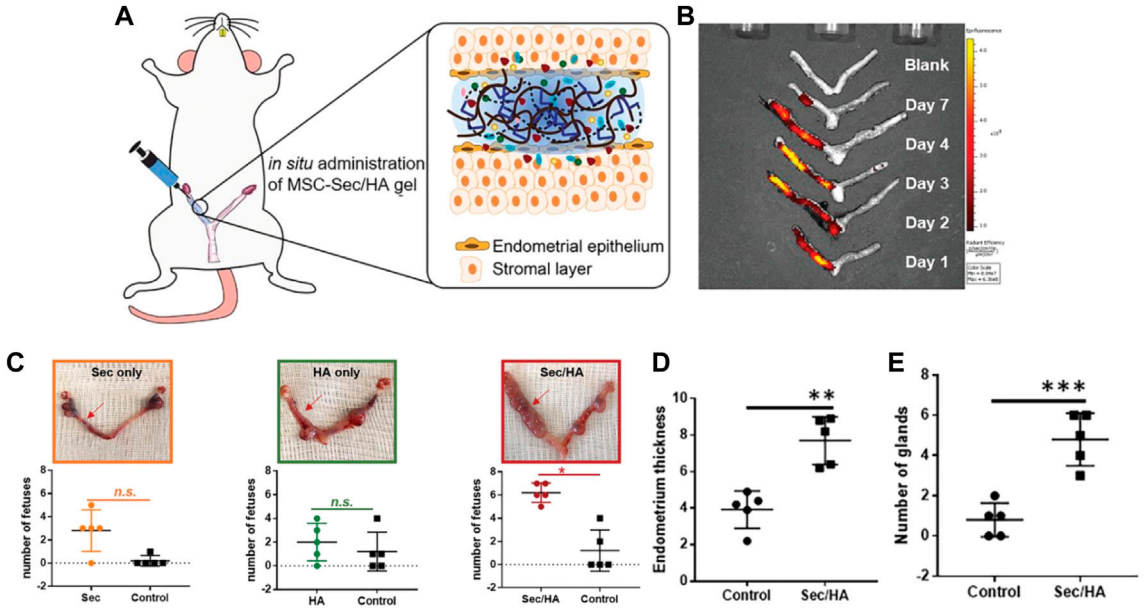

FIGURE 1 | MSC-Sec/HA gel injection and a rodent model of endometrium injury **(A)** Schematic showing intrauterine injection of MSC-Sec/HA gel. **(B)** *Ex vivo* fluorescent imaging of rat uteri at days 1, 2, 3, 4, and 7 after injection. **(C)** Representative uterus images and quantitative data comparing the numbers of fetuses on both sides (red arrow indicates treated side). * indicates $p < 0.05$ when compared to the other side. **(D)** Comparison of endometrium thickness between the control side and the treated side of MSC-Sec/HA group. **(E)** Comparison of number of glands between the control side and the treated side of MSC-Sec/HA group. n = 5, ** indicates $p < 0.01$, *** indicates $p < 0.001$ when compared to the other group. Reproduced with permission from ref (Liu et al., 2019). Copyright 2019 WILEY-VCH Verlag GmbH & Co. KGaA, Weinheim.

proliferation and migration of glandular cells through the Jak2-Stat5 and c-Fos-VEGF pathways. This study provides a theoretical and experimental basis for the clinical application of HP-MSCs-HA in the treatment of endometrial injury (**Figure 2**) (Lin et al., 2022).

Xin et al. recently developed a cell-free therapeutic strategy for IUA treatment by combining mesenchymal stem cell-derived apoptotic bodies (Abs) with hyaluronic acid (HA) hydrogels to construct an Abs delivery system. Studies have shown that ABs contain a variety of functional biomolecules that play a crucial role in compensatory tissue regeneration and maintaining tissue homeostasis. They can induce macrophage immunomodulation, cell proliferation, and angiogenesis *in vitro* (Ryoo et al., 2004; Brock et al., 2019; Xu et al., 2019; Medina et al., 2020). The use of HA hydrogel delivery promoted the retention and sustained-release of Abs. In the mouse acute endometrial injury models and rat IUAs models, *in situ* injections of Abs-HA hydrogel significantly increased the thickness of the endometrium and the number of endometrial glands, effectively reducing fibrosis and promoting endometrial regeneration, thus restoring fertility. This study has validated the therapeutic potential of the Abs-loaded HA hydrogel, providing a clinically feasible cell-free therapy for endometrial regeneration and IUA therapy (**Figure 3**) (Xin et al., 2022).

A meta-analysis of recent clinical studies in which patients were administered the hyaluronic acid gel to prevent adhesions after intrauterine surgery was performed, with strict univariate and randomization principles followed in selecting clinical reports. The analysis results showed that the incidence of severe IUA in the HA gel group was significantly lower than that in the control group, while there was no significant effect on the incidence of mild adhesions. In addition, a broader clinical sample needs to be studied to determine the effectiveness and safety of HA gel in the fertility protection (Can et al., 2018; Liu et al., 2018; Fei et al., 2019; Fei et al., 2020; Mao et al., 2020; Zheng et al., 2020; Liu et al., 2022).

Qi et al. prepared a chitosan-heparin hydrogel through a mild process and verified the good stability of the material through *in vitro* release experiments. Subsequently, SDF-1α-loaded chitosan-heparin hydrogel was used to repair the intrauterine injury rat model. It was found by immunohistochemical staining and immunofluorescence staining that the treatment process was caused by hematopoietic stem cells recruited to the injury site, which promoted the recovery of the wound. And the recovery level of the experimental group was not statistically different from that of the control group. The experimental results demonstrate that the *in-situ* delivery of SDF-1α using chitosan-heparin hydrogel as a carrier can accurately repair the injured uterus in rats and be used as a candidate material for uterine injury healing and other wound dressing drug delivery systems (Wenbo et al., 2020).

Growth factors (GFs) therapy stimulates the body's natural healing process by modulating the inflammatory response, promoting tissue formation, and inducing vascular regeneration (Farnebo et al., 2017). In recent years, researchers have often used biomaterials such as hydrogels loaded with GFs

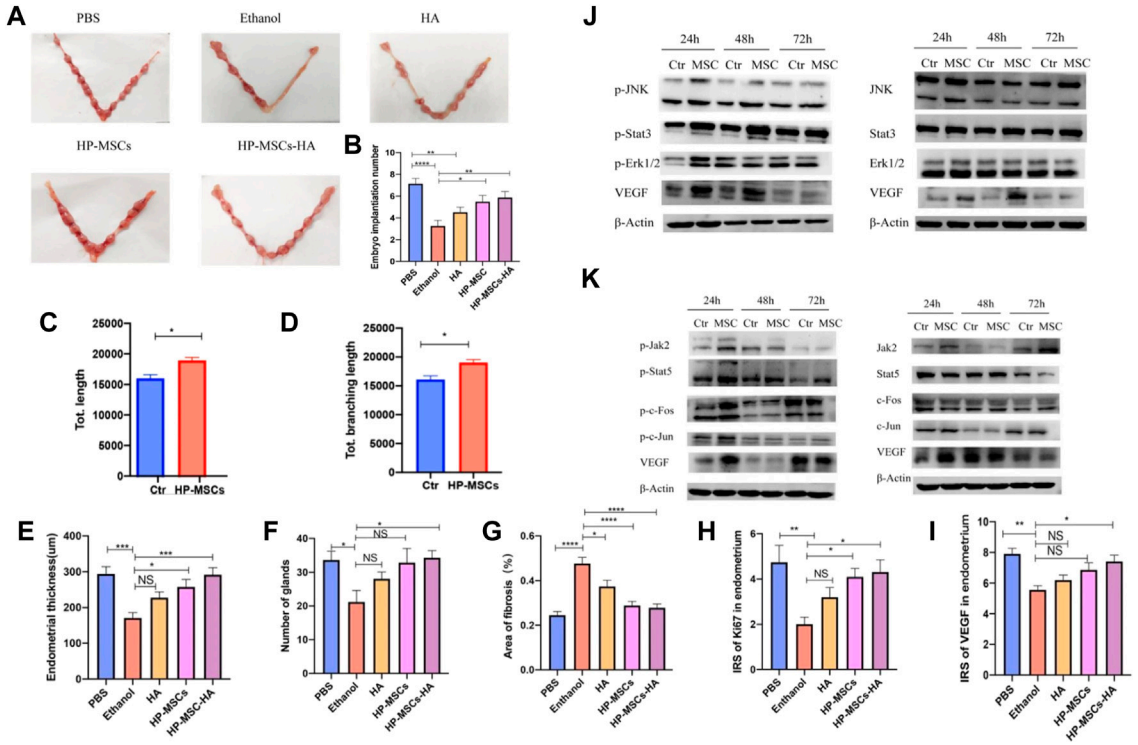

FIGURE 2 | (A,B) Evaluate the endometrial receptivity of the five mouse groups with different treatments by the number of implanted embryos. **(C,D)** Quantitative assay of tube formation assay and data were expressed as mean ± SEM. * indicates $p < 0.05$. **(E)** Average endometrial thickness and statistical analysis (±SEM) of the five groups. * indicates $p < 0.05$, ** indicates $p < 0.01$, *** indicates $p < 0.001$, n = 6. **(F)** Average gland number and statistical analysis (±SEM) of the five groups. * indicates $p < 0.05$, n = 6. **(G)** Average fibrosis area and statistical analysis (±SEM) of the five groups. The ratio of the fibrotic area = endometrial fibrotic area/endometrial area. * indicates $p < 0.05$, ** indicates $p < 0.01$, *** indicates $p < 0.001$, **** indicates $p < 0.0001$, n = 6. **(H)** Statistic analysis of IRS of Ki67 in the endometrium of the five groups. * indicates $p < 0.05$, ** indicates $p < 0.01$, n = 6. **(I)** Statistic analysis of IRS of VEGF in the endometrium of the five groups. * indicates $p < 0.05$, ** indicates $p < 0.01$, n = 6. **(J)** p-JNK, p-Stat3, p-Erk1/2, VEGF, and corresponding total protein western blot analysis at 24 h, 48 h, and 72 h, respectively, after culturing without and with HP-MSCs, respectively. **(K)** p-Jak2, p-Stat5, p-c-Fos, p-c-Jun, VEGF, and corresponding total protein western blot analysis at 24 h, 48 h, and 72 h, after culturing without and with HP-MSCs, respectively. * indicates $p < 0.05$, ** indicates $p < 0.01$, **** indicates $p < 0.0001$, n = 8. Reproduced with permission from ref (Lin et al., 2022). CC BY 4.0. Copyright 2022 The Author(s).

to prolong their retention time at the injury site to enhance the therapeutic effect. A bioengineered system based on decellularized porcine endometrial extracellular matrix (EndoECM) hydrogels (López-Martínez et al., 2021b) loaded with growth factors (GFs) was prepared. Proteomic analysis was performed to characterize the specific role of extracellular matrix proteins in tissue regeneration, followed by the repair effect of ECM hydrogels against endometrial injury in Asherman's syndrome (AS)/endometrial atrophy (EA) after the addition of GFs was investigated. The animal experiments showed that the model mice treated with GFs-ECM hydrogel showed a series of regenerative effects with an increased number of endometrial glands, high cell proliferation index, new blood vessel development, and higher pregnancy rate. Therefore, this system is expected to be used for treatments related to endometrial repair in reproductive medicine (López-Martínez et al., 2021a).

Synthetic Biomaterial-Based Hydrogels

Poloxamer is a class of water-soluble nonionic triblock copolymers with mild, non-toxic, and non-irritating properties approved by the FDA and included in the U.S. and European Pharmacopoeias. Its trade name is Pluronic. Poloxamer hydrogel is a synthetic thermosensitive hydrogel that undergoes a sol-gel transition at body temperature. Therefore, sol-state poloxamer has better fluidity, which is more convenient for developing and preparing injectable delivery systems. Studies have shown that poloxamer hydrogels are suitable for encapsulating cells or active factors, thereby promoting their release (Vashi et al., 2008). Likewise, adding heparin to the poloxamer hydrogel also plays a similar role to that mentioned above, enhancing the delivery system's affinity for growth factors or hormones and prolonging the half-life *in vivo*. In addition, temperature-sensitive hydrogels have attracted the attention of researchers due to their unique properties. Temperature-responsive hydrogels used in biomedical applications are usually liquid below physiological temperature and can rapidly form gels at physiological temperatures around specific tissues. Most intriguingly, this type of hydrogel can be dynamically adjusted to the morphology and size of the uterus to create a bio-scaffold with excellent support after injection into the uterine cavity (Han et al., 2016).

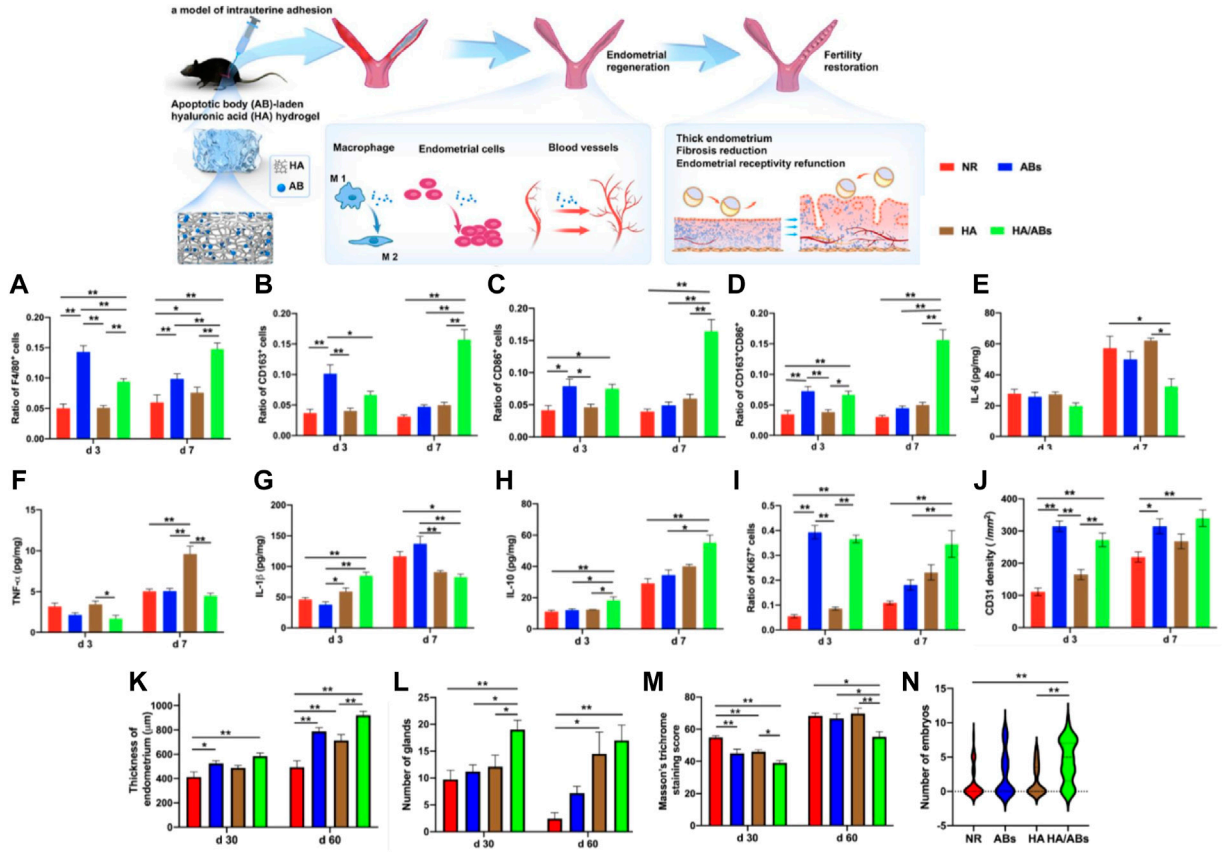

FIGURE 3 | An apoptotic body **(A,B)**-laden hyaluronic acid (HA) hydrogel was designed to deliver ABs *in situ* to treat IUA in a rodent model. Statistical analysis was performed to examine the expressions of F4/80 **(A)** (marker of macrophages), CD163 **(B)** (marker of M2 macrophages), CD86 **(C)** (marker of M1 macrophages) and concurrent expression of CD163 and CD86 **(D)** (n = 8). ELISA for IL-6 **(E)**, TNF-α **(F)**, IL-1β **(G)** and IL-10 **(H)** in uteri under different treatments (n = 4). Statistical analysis was performed to examine the expressions of Ki67 (e) (marker associated with cell proliferation) and CD31 (f) (marker of capillary vessels) (n = 8). The results in a-d, **(I,J)** were normalized to the total number of cells per view under a ×400 magnification and expressed as a ratio of the total number of cells positive for a marker to the total number of cells present. **(K)** Quantification of endometrial thickness at days 30 and 60 post-surgery using H&E staining (n = 10). **(L)** Quantification of endometrial glands at days 30 and 60 post-surgery using H&E staining (n = 10). **(M)** Masson's trichrome staining scores for uteri at days 30 and 60 after treatment (n = 10). **(N)** Violin plots showing the number of embryos per uterine horn following different treatments (n = 33 in the NR and ABs groups, n = 29 in the HA and HA/ABs groups). NR, natural repair without any treatment; ABs, injection of an AB solution only; HA, injection of HA only; HA/ABs, injection of the AB-laden HA hydrogel. $^{*}p < 0.05$ and $^{**}p < 0.01$. Reproduced with permission from ref (Xin et al., 2022). CC BY 4.0. Copyright 2021 The Author(s).

One study has prepared a temperature-sensitive hydrogel of poloxamer (HP) loaded with keratinocyte growth factor (KGF), modified with heparin to stabilize the growth factors and thus more easily control their release behavior. The rheological characterization indicates that the hydrogel system is suitable for intrauterine applications. Results from *in vivo* animal experiments showed that the HP hydrogel system significantly prolonged the residence time of KGF in the uterine cavity and promoted the proliferation and angiogenesis of endometrial epithelial cells (EEC), resulting in a better effect on the morphological and functional recovery of the injured uterus (**Figure 4**) (Xu et al., 2017a).

Subsequently, the team prepared mucoadhesive hydrogels loaded with KGF by adding ε-polylysine (EPL) as a functional excipient to a heparin-modified poloxamer matrix material to address two critical problems of short retention time and poor absorption of therapeutic agents or active factors in the damaged uterine cavity due to the rapid turnover of endometrial mucus. The rheological properties, adhesion, and KGF release behavior of HP hydrogels in the study were easily regulated by changing the doping amount of EPL in the formulation, which enabled KGF-EPL-HP hydrogels to promote the proliferation of endometrial epithelial cells and glands in a short time. As a result, the damaged endometrial morphology was well repaired, effectively solving the above two problems. By optimizing the matrix components, the research group made the prepared adhesive hydrogel system with great potential in endometrial repair (Xu et al., 2017b).

In subsequent studies, the researchers prepared a novel estrogen sustained-release system by loading 17β-estradiol (E_2) into heparin-modified poloxamer hydrogels. A rat injury model was established by simulating the scraping process. Then the prepared thermosensitive hydrogel was injected into the injured uterine cavity to investigate the repair effect of the endometrium.

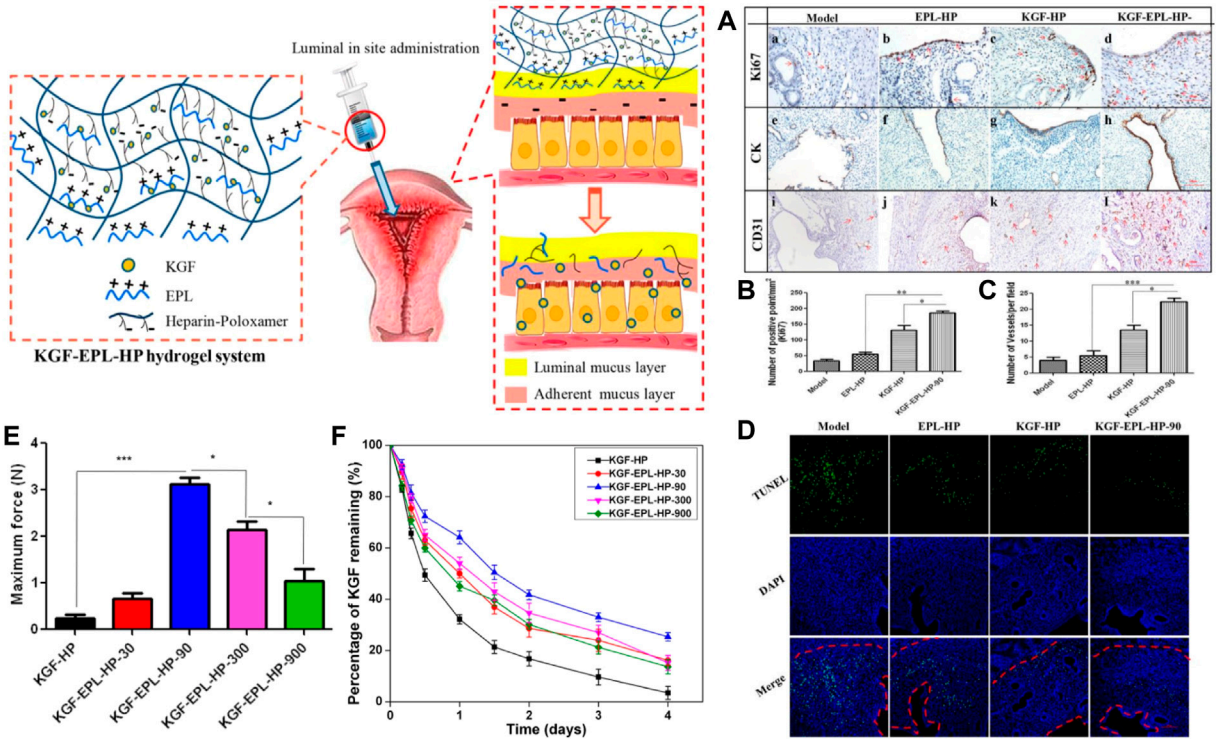

FIGURE 4 | Scheme of thermos-sensitive bioadhesive KGF-EPL-HP hydrogel for injured uterus. **(A)** Immunohistochemistry images of Ki67 (a–d), CK (e–h), and CD31 (i–l) staining for injured uterus on day 3 after treatments. Staining-positive cells were marked by red arrows (scale bar = 100 μm). **(B)** Quantitative analysis of number of Ki67-positive cells, and **(C)** number of vessels per field at day 3 after surgery. Original magnification: ×200 (*: $p < 0.05$; **: $p < 0.01$; ***: $p < 0.001$ n = 3). **(D)** TUNEL assays kit analysis of the injury uterus on 3 days after treatment. Red line: the border of the basal layer; blue: cell nuclei, DAPI; green: apoptosis cells. Original magnification: ×200, scale = 1 μm. Adhesive evaluation of KGF-EPL-HP hydrogel. **(E)** The adhesive force of KGF-EPL-HP hydrogels against gelatin substrate in comparison with HP hydrogels. **(F)** The remaining percentage of KGF on excised rabbit uterine mucosa for KGF-EPL-HP hydrogels with various EPL concentrations after continuous rinsing with PBS (*$p < 0.05$; ***$p < 0.001$; n = 3). Reproduced with permission from ref (Xu et al., 2017a). Copyright 2017 American Chemical Society.

The experimental results showed that E_2-HP hydrogel could effectively promote the proliferation of endometrium and significantly inhibit the apoptotic activity of the damaged area, which had a positive effect on endometrial regeneration. It was also demonstrated that E_2-HP hydrogels are closely associated with inhibiting endoplasmic reticulum stress signaling through activation of downstream signals PI3K/Akt & ERK1/2 and the upregulation of kisspeptin through activation of ERK1/2 & MAPKs p38 pathways in IUA recovery. E_2-HP hydrogel has emerged as a promising treatment for IUA (**Figure 5**) (Zhang et al., 2017; Zhang et al., 2020a).

As an ideal organic component, aloe was mixed with poloxamer to form a biofriendly hydrogel system in the study of Yao et al. (Baghersad et al., 2018), which is expected to be used to treat IUA with its ability that can promote wound healing (Kim et al., 2016; Singh et al., 2018). The researchers first prepared nanoparticulate decellularized uterus (uECMNPs) to encapsulate β-estradiol (E_2) (E_2@uECMNPs) to enhance the sustained-release effect of E_2. E_2@uECMNPs were then embedded into aloe/poloxamer hydrogels to make a nanocomposite temperature-sensitive hydrogel delivery system. The delivery system promoted the proliferation of endometrial stromal cells and reduced uterine fibrosis rates through stable and continuous delivery of E_2 to the site of intrauterine damage in concert with multiple components. *In situ* imaging and *in vivo* histological analysis data further confirmed that the E_2@uECMNPs-AP hydrogel exerted a good biological effect and exhibited excellent repairability, showing excellent application potential for the treatment of IUA (Yao et al., 2020).

Vitamin C can significantly affect the pluripotency, self-renewal, and differentiation of stem cells (D'Aniello et al., 2017). In Yang's study, Pluronic F-127/Vitamin C hydrogels loaded with bone marrow stromal cells (BMSCs) were prepared. The results demonstrated that vitamin C significantly promoted the survival and proliferation of BMSCs in the system and attenuated the biotoxic effects of PF127 hydrogel. Thickening of the endometrium increased glands, and decreased fibrotic areas were observed after transplantation of the hydrogel into the uterine cavity of IUA model rats, which effectively promoted the endometrium regeneration. In summary, heparin, aloe, and vitamin C have all been used to functionalize poloxamer hydrogels to improve the therapeutic effect of IUA, and promising research progress has been made (Yang et al., 2017).

Both exosomes and apoptotic bodies mentioned above (Xin et al., 2022) belong to a subgroup of extracellular vesicles.

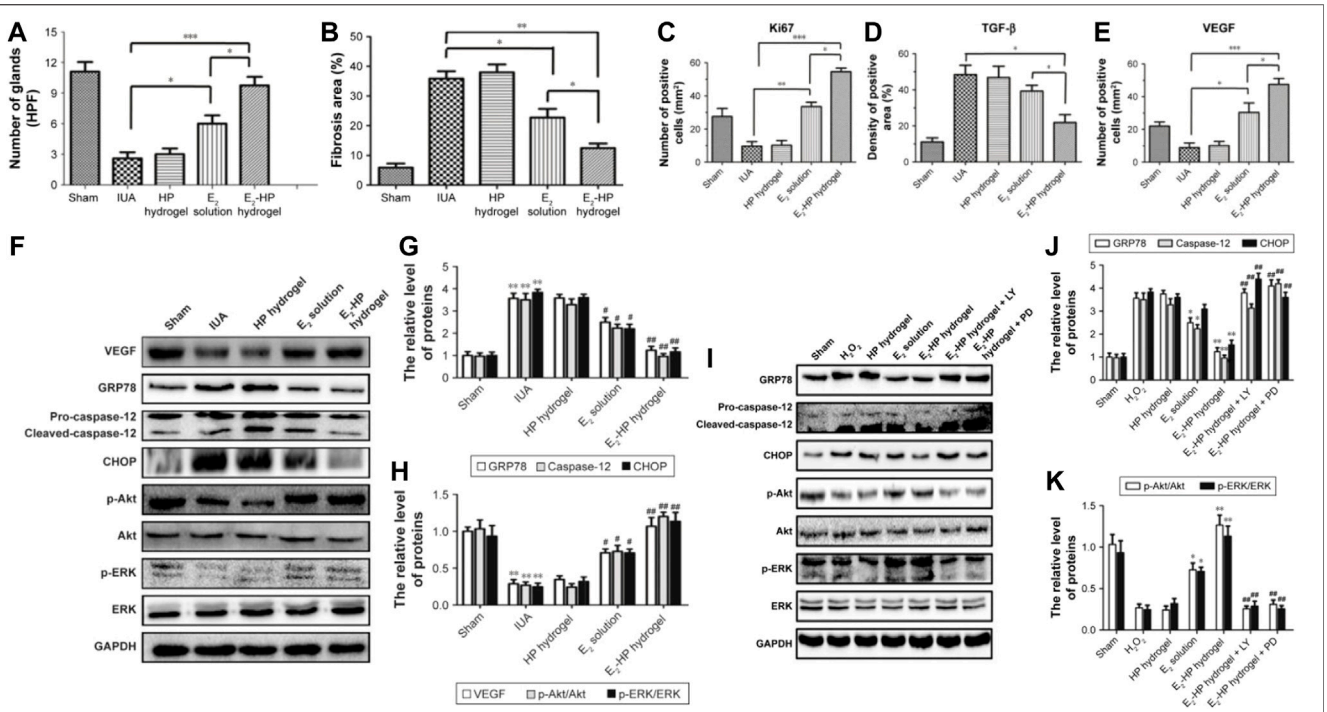

FIGURE 5 | Schematic diagram of E_2-HP hydrogel as an *in-situ* administration drug for the treatment of intrauterine adhesions. **(A)** Analysis of the number of glands in each group at 14 days after IUA. **(B)** Analysis of fibrosis area in endometrium in each group at 14 days after IUA. **(C)** Analysis of Ki67 positive cells of the immunohistochemistry results. **(D)** Analysis of TGF-β positive area of the immunohistochemistry results. **(E)** Analysis of VEGF-positive cells of the immunohistochemistry results. Data are presented as mean ± standard deviation; n = 5; *$p < 0.05$, **$p < 0.01$, and ***$p < 0.001$. E2-HP hydrogel inhibits ER stress and activates the Akt and ERK1/2 pathways in the IUA rats. Notes: **(F)** The protein expressions of VEGF, GRP78, caspase-12, CHOP, p-Akt, and p-ERK in each group were tested with Western blotting. GAPDH was used as the loading control and for band density normalization. **(G)** The optical density analysis of GRP78, caspase-12, and CHOP protein. **$p <$ 0.01 versus the Sham group and #$p < 0.05$ and ##$p < 0.01$ versus the IUA group. **(H)** The optical density analysis of VEGF, p-Akt, and p-ERK protein. **$p < 0.01$ versus the Sham group and #$p < 0.05$ and ##$p < 0.01$ versus the IUA group. The activation of Akt and ERK1/2 is crucial for the protective effect of E2-HP hydrogel in H2O2-induced ER stress in EECs. Notes: **(I)** The protein expressions of GRP78, caspase-12, CHOP, p-Akt, and p-ERK1/2 in ER stress-induced apoptosis in EECs treated with E2-HP hydrogel and different inhibitors. GAPDH was used as the loading control and for band density normalization. **(J)** The optical density analysis of GRP78, caspase-12, and CHOP protein. **(K)** The optical density analysis of p-AKT and p-ERK protein. *$p < 0.05$ and **$p < 0.01$ versus the H2O2 group and ##$p < 0.01$ versus the E2-HP hydrogel group. Data are presented as mean ± standard deviation; n = 3. Reproduced with permission from ref (Zhang et al., 2017). CC BY 4.0. Copyright 2017 The Author(s).

Although they differ in diameter and mode of production, both have been used in tissue damage repair and have made some positive progress. The complex microenvironment of the endometrium often makes the treatment less effective than desired. Lin et al. developed an exosome injectable antibacterial PEG hydrogel for microenvironmental protection to address this problem. The exosome hydrogel was formulated by dynamic coordination of Ag^+-S and fusion with adipose stem cell-derived exosomes (ADSC-exo). The system can promote the proliferation, migration, and tube formation of human umbilical vein endothelial cells (HUVEC) *in vitro*. And it can protect and improve the endometrial microenvironment *in vivo* for promoting angiogenesis and recovery of endometrial morphology and function while inhibiting local tissue fibrosis, thereby improving pregnancy outcomes. Although exosomes also have the disadvantage of not replicating *in vitro* compared to stem cells, nanoscale exosomes can easily pass through capillaries without the risk of immune rejection and tumorigenesis (Phinney and Pittenger, 2017; Zhang et al., 2020b). This study also provides a convenient, safe, and non-invasive approach for cell-free therapeutic strategies against IUA (**Figure 6**) (Lin et al., 2021).

In order to prevent uterine fibrosis after injury, Wang et al. prepared a hydrogel material that can inhibit the proliferation of fibroblasts. Poly (ethylene glycol)-b-poly (L-phenylalanine) block copolymer (PEBP) was synthesized by ring-opening polymerization (ROP) of L-phenylalanine N-carboxylic anhydride initiated by methoxy polyethylene glycol amine. Subsequently, injectable PEBP/PEG hydrogels were formed through π-π accumulation between PEBP macromolecules and hydrogen bonding between PEBP, PEG, and H_2O molecules. It was found that the PEBP/PEG hydrogel could sustainably release L-phenylalanine (L-Phe) through degradation, and L-Phe effectively inhibits uterine fibrosis and improves the success rate of embryo transfer by regulating the expression and interaction of transforming growth factor β1 (TGF-β1) and Muc-4. Therefore, this hydrogel material has potential applications in preventing uterine adhesions (**Figure 7**) (Wang et al., 2020a).

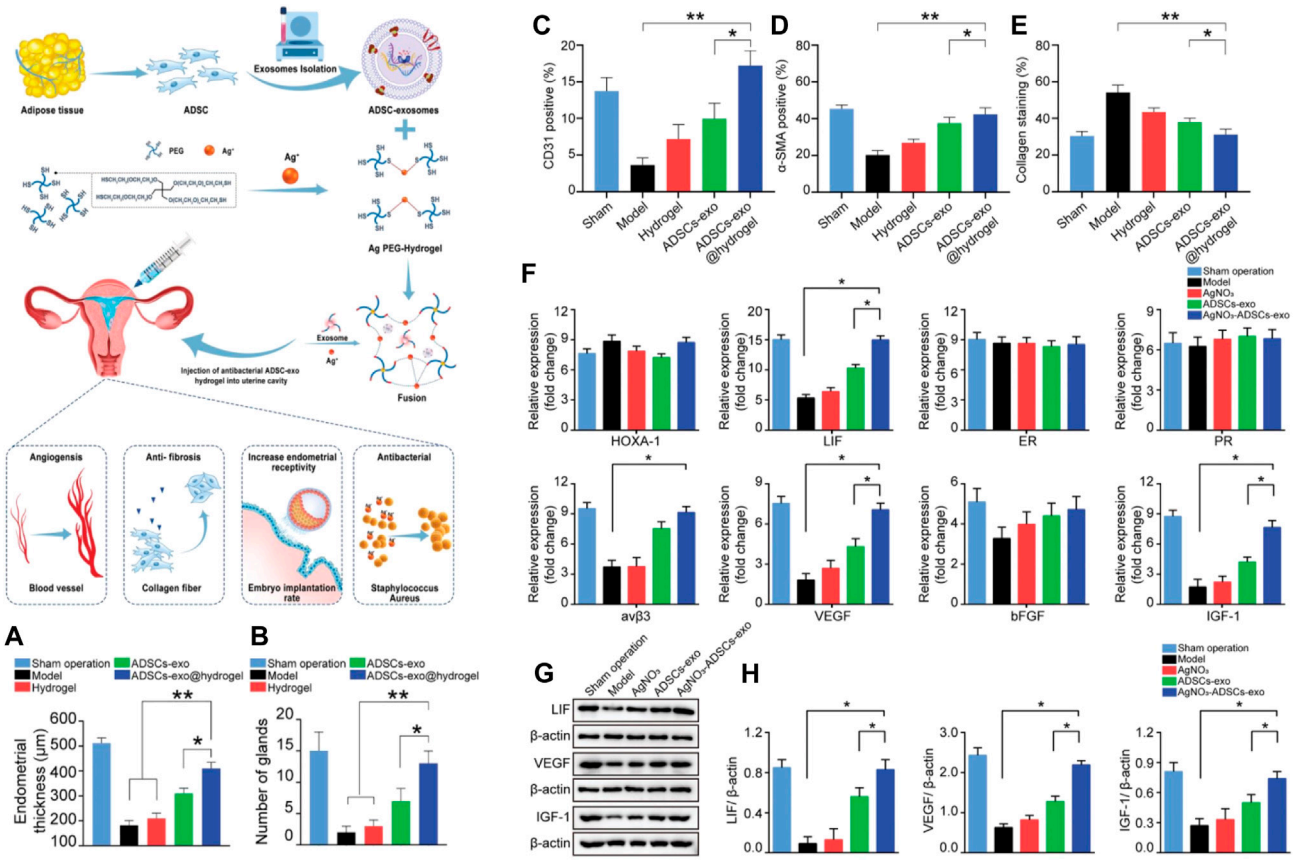

FIGURE 6 | Schematic overview of the development of an ADSC-exo hydrogel for endometrial regeneration. **(A)** Endometrial thicknesses in each group. **(B)** Numbers of glands in each group. Administration of ADSC-exos or AgNO3+ADSCs-exo promotes endometrial neovascularization, myometrial regeneration, and reduced endometrial collagen deposition. **(C–E)** Quantification of CD31, α-SMA, and collagen protein expression levels. The impact of ADSCs-exo and hydrogel transplantation on the expression of markers of endometrial receptivity and angiogenesis. **(F)** A qRT-PCR approach was used to assess the expression of markers of endometrial receptivity (HOXA-1, LIF, ER, PR, Integrin β3, IGF-1) and angiogenesis (VEGF, bFGF), with β-actin serving as a normalization control. **(G)** Western blotting was used to assess LIF, VEGF, and IGF-1 protein expression in each treatment group. **(H)** Western blotting data of the levels of LIF, VEGF, and IGF-1 in different treatment groups. Data are shown relative to internal reference controls. Data are means ± standard error, n = 5. $^{*}p < 0.05$, $^{**}p < 0.01$. Reproduced with permission from ref (Lin et al., 2021). Copyright 2021 Wiley-VCH GmbH.

Biocomposite Hydrogels

Natural hydrogels can usually interact with proteins or cells in specific or non-specific ways, enhancing the adhesion of the material in the uterine cavity. Thus, they affect the endometrial formation, cell growth, and phenotype maintenance. Still, their further application is often limited by disadvantages such as poor mechanical strength, uncontrolled degradation, risk of immunogenicity, and poor reproducible processing stability (Kirchhof et al., 2015; Rastogi and Kandasubramanian, 2019). Synthetic hydrogels can be prepared in large quantities, have more stable properties, and can be modified at the molecular level through polymerization, cross-linking, and functionalization. However, they cannot modulate intercellular responses, biorecognition, and cell-induced remodeling like native hydrogels. Therefore, in recent years, many researchers have combined the advantageous properties of various biomaterials to prepare composite hydrogels to obtain better repair effects (Lv et al., 2021).

Zhang et al. developed a thermo-responsive injectable hydrogel containing galactose modified xyloglucan (mXG) and hydroxybutyl chitosan (HBC) with good cytocompatibility and hemocompatibility. It has been shown the ability to promote skin wound healing and reduce scar formation in a rat trauma model. The synthesized hydrogel was found to be effective in preventing recurrent adhesions in a rat repeated injury-adhesion model. The conclusions of this study demonstrated the potential application of mXG/HBC composite hydrogel as an effective anti-adhesion system in the prevention and treatment of IUA-induced intrauterine adhesions (Zhang et al., 2018). In conclusion, several thermosensitive hydrogel delivery systems mentioned in the paper have made some progress in IUA treatment and expanded the ideas for developing stimuli-responsive hydrogels for endometrial repair in the future.

In another study, Kim et al. prepared a class of hyaluronic acid (HA)/fibrin composite hydrogels encapsulating decidualized endometrial stromal cells (dEMSCs), and a dose of thrombin was added to enhance gel formation and engraftment and can

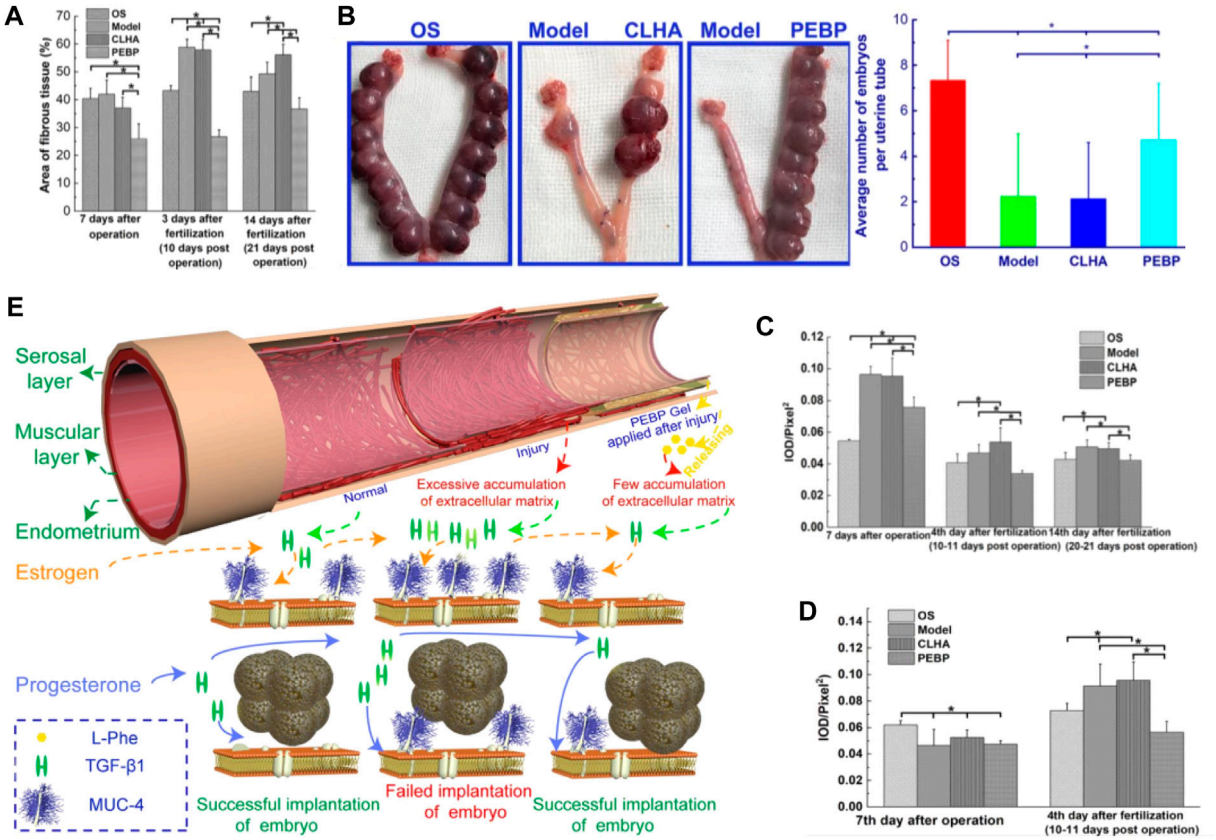

FIGURE 7 | (A) average area ratio of fibrotic tissue with different treatments in the uterine stromal layer; and **(B)** average number of embryos implanted in uteri with different treatments on day 14 of pregnancy. **(C)** average IOD of immunohistochemical images of TGF-β1 expressed at the uterine stromal layer. **(D)** average IOD of immunohistochemical images of Muc-4expressed at the surface of the uterine wall. **(E)** Mechanism of PEBP/PEG hydrogel on embryo implantation after uterine curettage, by regulating interactions between TGF-β1 and Muc-4 expression. Reproduced with permission from ref (Wang et al., 2020a). Copyright 2020 American Chemical Society.

effectively release adhesion molecules. The results confirmed that the composite hydrogel had a good anti-fibrotic effect and increased the thickness of the endometrium in a short period of time. The transferred embryos were successfully implanted and developed normally, resulting in a live birth of the offspring. This study proposes an innovative therapeutic strategy with the efficacy of rapidly restoring endometrial damage and also has therapeutic potential in intractable infertility or recurrent miscarriage (Kim et al., 2019).

Ji's research group used 3D printing technology to prepare a hydrogel scaffold loaded with human induced pluripotent stem cell-derived mesenchymal stem cells (hiMSC), and the 3D printing ink was made of a mixture of gelatin and sodium alginate. Compared to the direct local application of hiMSC, the hydrogel scaffold can significantly prolong the survival and action time of stem cells at the damaged site. *In vivo* animal experiments showed that the 3D printed hiMSC-loaded scaffold group promoted the recovery of endometrial tissue morphology and improved endometrial receptivity functional indicators. The damaged endometrium is well recovered (Ji et al., 2020). Feng et al. also developed a composite hydrogel containing different ratios of methacrylated gelatin (GelMA) and methacrylated collagen (ColMA) using 3D bioprinting technology and doped amniotic mesenchymal stem cells (AMSCs) in the hydrogel for the treatment of uterine adhesions. The hydrogels showed excellent anti-adhesive ability in *vivo* experiments and effectively prevented uterine adhesions in the IUA rat model (Feng et al., 2021). In addition, another research team used microfluidic droplet technology to prepare a new type of drug-loaded porous scaffold based on methacrylated gelatin and sodium alginate. The elasticity and mechanical properties of the scaffold have been improved, making it more suitable for the therapeutic repair of intrauterine injuries (Cai et al., 2019).

In addition, the methods for establishing animal endometrial injury models in the studies mentioned above are categorized and summarized. The first type is the mechanical injury method (scraping method), which usually involves repeated endometrial scraping through a surgical incision in the uterus after anesthesia until swelling and congestion to obtain an animal model of injury, and most studies have adopted this method (Xu et al., 2017a; Xu et al., 2017b; Yang et al., 2017; Zhang et al., 2017; Wang et al., 2020a; Zhang et al., 2020a; Wenbo et al., 2020; Yao et al., 2020; Xin et al., 2022). Some researchers have also

TABLE 1 | Summary of biomaterial-based hydrogels in repair of endometrial injury.

Active substance	Biomaterial	Biomaterial-based hydrogel features	Model	Mechanism	Effectiveness	References
Mesenchymal stem cell-secretome (MSC-Sec)	Cross-linked hyaluronic acid (HA) hydrogel	Biocompatibility, biodegradability, injectability, form-stability, low interfacial tension, adhesion properties and can improve the sustained-release effect of active substances	Murine uterus injury model	In research	Restoration of injured endometrial morphology and fertility	Liu et al. (2019)
The human placenta-derived mesenchymal stem cells (HP-MSCs)	Cross-linked hyaluronic acid (HA) hydrogel		Mice endometrium-injured model	Promoting the proliferation of human endometrial stromal cells by activating the JNK/Erk1/2-Stat3-VEGF pathway and the proliferation and migration of glandular cells through the Jak2-Stat5 and c-Fos-VEGF pathways	Reduced the fiber area, increased the endometrial thickness and the number of glands in the damaged endometrium, and improved embryo implantation rate	Lin et al. (2022)
Mesenchymal stem cell-derived apoptotic bodies (ABs)	Hyaluronic acid (HA) hydrogel		Murine endometrial acute damage model and rat IUA model	Decreasing the concentration of TNF-α & IL-1β and increasing the concentration of IL-10; the high expression of F4/80, CD163 and CD86; Increasing the number of Ki67 + cells and the increase in CD31 staining	Reduced fibrosis and promoted endometrial regeneration, resulting in fertility restoration	Xin et al. (2022)
Stromal cell-derived factor-1α (SDF-1α)	Chitosan-heparin hydrogel	Chitosan has good biocompatibility, biodegradability, and antibacterial activity, and heparin can enhance chitosan's affinity with growth factors and promote its gelation	Uterine injury rats model	Long-term recruitment of hematopoietic stem cells (HSCs) that secrete additional VEGF and down-regulate TGF-β1 cytokine expression	Endometrial thickness, number of glands, and fibrosis level in the experimental group were not statistically different from normal uterus	Wenbo et al. (2020)
Growth factors (GFs)	Decellularized porcine endometrial extracellular matrix (EndoECM)	Biocompatibility, gelation at physiological temperatures, and slow resorption	Mice endometrial damage model	Increasing the secretion levels of PDGFbb, bFGF, and IGF-1	Increasing the number of endometrial glands, high cell proliferation index, new blood vessel development, and higher pregnancy rate	López-Martínez et al. (2021a)
Keratinocyte growth factor (KGF)	Heparin-modified poloxamer (HP)	Low toxicity and biocompatibility, good gelation properties after heparinization, excellent affinity with growth factors & Good bioadhesion, rapid gelation, enhanced mechanical properties and prolonged the retention time of KGF in the uterine cavity with the addition of EPL.	Rat IUA model	Ki67 and CD31 staining were increased, and the expression of LC3-II and P62 was elevated. The underlying mechanism is closely related to the activation of autophagy	The proliferation of endometrial epithelial cells and angiogenesis were promoted. The morphology and function of the damaged uterus were restored	Xu et al. (2017a)
Keratinocyte growth factor (KGF)	Heparin-modified poloxamer (HP) & ε-polylysine (EPL) as functional excipient		Rat intrauterine mechanical injury model	Inhibition of apoptosis in the damaged uterus	The proliferation of endometrial epithelial cells and glands was significantly enhanced, as was angiogenesis of the regenerating endometrium	Xu et al. (2017b)

(Continued on following page)

TABLE 1 | (*Continued*) Summary of biomaterial-based hydrogels in repair of endometrial injury.

Active substance	Biomaterial	Biomaterial-based hydrogel features	Model	Mechanism	Effectiveness	References
17β-estradiol (E2)	Heparin-modified poloxamer (HP)		Rat IUA model	Improving the expression of kisspeptin via MAPKs p38 and ERK1/2 signal pathways & Activation of downstream signals PI3K/Akt and ERK1/2 inhibits endoplasmic reticulum stress signaling to play a protective role	Promoting endometrial proliferation and inhibiting apoptotic activity at the site of injury	(Zhang et al., 2020a), (Zhang et al., 2017)
β-estradiol (E2)	Aloe/Poloxamer	Bio-friendly, biomimetic and biodegradable properties, as well as being restorative, temperature sensitive, and low immunogenic	Rat IUA model	The levels of Ki67, cytokeratin, and estrogen receptor β were upregulated, while the expression of TGF-β1 and TNF-α was decreased	Promoting proliferation of endometrial mesenchymal cells, inhibiting their apoptosis, enhancing morphological recovery, and reducing the rate of uterine fibrosis	Yao et al. (2020)
Bone marrow stromal cells (BMSCs)	Pluronic F-127/ Vitamin C	Hybridized hydrogels have lower toxicity and ensure a longer survival time of BMSCs at the injury site	Rat IUA model	The expression of cytokeratin, von Willebrand Factor (vWF), was restored, and the secretion of interleukin-1β (IL-1β) was inhibited at a low level	Thicker endometrium, more glands, less fibrotic areas, endometrium shows better recovery	Yang et al. (2017)
Adipose stem cell-derived exosomes (ADSC-exo)	Thiolated polyethylene glycol (SH-PEG)	Injectable, self-healing, degradable, antimicrobial, and microenvironmental protection properties	Rat endometrial damage model	Significant increases in VEGF, LIF, avβ3, and IGF-1 expression	Promoting neovascularization and tissue regeneration while inhibiting local tissue fibrosis and restoring fertility	Lin et al. (2021)
L-phenylalanine (L-Phe)	Poly (ethylene glycol)-b-poly (L-phenylalanine) block copolymer (PEBP)/PEG	Hydrophilic, excellent slow release, easily adjustable viscosity and mechanical strength	Rat endometrial damage model	Regulating the expression and interaction of TGF-β1 and Muc-4	Preventing fibrosis and promoting pregnancy in damaged uterine tissue	Wang et al. (2020a)
	Galactose modified xyloglucan (mXG)/ hydroxybutyl chitosan (HBC)	Injectable, thermosensitive, cytocompatible, and hemocompatible	Rat repeated-injury model		Highly effective in preventing recurrent adhesions, promoting wound healing, and reducing scar formation	Zhang et al. (2018)
Decidualized endometrial stromal cells (dEMSCs)	Hyaluronic acid (HA)/ fibrin	Biocompatibility, sufficient mechanical support, promoting cell growth and engraftment	Murine uterine infertility (synechiae) model	Expression and secretion of desmin, CD44, PECAM, and IGF-1	Reducing fibrous tissue and increasing endometrial thickness, restoring fertility	Kim et al. (2019)
Human induced pluripotent stem cell-derived mesenchymal stem cells (hiMSC)	Gelatin/sodium alginate	Cytocompatibility, porous structure, enhanced mechanical properties, and structural stability	Rat IUA model		Effectively prevent intrauterine adhesions	Ji et al. (2020)

established *in vivo* models of endometrial injury by intrauterine injection of ethanol (Kim et al., 2019; López-Martínez et al., 2021a; Lin et al., 2021; Lin et al., 2022). In addition, Liu's group established a rat uterine injury model by using electrocoagulation, which is able to damage the endometrium and reduce angiogenesis, mimicking the pathological changes that lead to AS (Liu et al., 2019).

Current Limitations

In the available reports, the mechanical strength of some hydrogel materials is so poor that they cannot provide sufficient mechanical support and even shift in position after implantation (Wang et al., 2021). And *in situ* biomaterial-based hydrogels with non-cytotoxic degradation byproducts, minimal fibrosis, and associated foreign body reactions are also critical to the application. Precise control of material degradation *in vivo* is required to guide *in situ* tissue repair or regeneration (Abdulghani and Mitchell, 2019). Furthermore, the hydration of the hydrogel can make the sterilization process of the formulation difficult and time-consuming (Lima et al., 2020). Current hydrogel-based delivery systems for the treatment of endometrial diseases also rely primarily on the degradation and diffusion of materials to deliver therapeutic agents (Liu et al., 2019). This release method lacks specificity and controllability, making it difficult to achieve the desired therapeutic effect. Although some researchers have developed temperature-responsive hydrogel delivery systems, as mentioned above, the role of the temperature-regulated release of therapeutic agents is still quite limited. Despite the fact that some achievements have been achieved in the research on the *in situ* delivery of estrogen and other therapeutic drugs by hydrogels, which effectively overcome the potential risks such as breast hyperplasia caused by oral estrogen, most of the available research data are still at the stage of animal experiments and clinical progress is limited (Wang et al., 2020b).

Similarly, the treatment of IUA with hydrogel materials combined with stem cell therapy is still in the research and exploration stage, and good results have been achieved in animal experiments. But the safety issues of stem cell therapy, such as tumorigenic complications caused by stem cell implantation, as well as low cell survival rate and high cost, have limited the further clinical translation of research results. The future research and development trend should be to prepare a multifunctional hydrogel delivery system for repairing endometrial damage, which can not only provide sufficient support for the formation of the uterine cavity but also can accurately and efficiently respond to various exogenous or endogenous trigger modes at the same time, it can carry a variety of therapeutic agents with the stable and sustained release (Lin et al., 2020; Wang et al., 2021).

It is worth mentioning that it is difficult to make practical recommendations for the clinical treatment of human endometrium-related diseases due to the diversity of animal models, the limited number of studies, and the uniqueness of the endometrium. Other than that, research on endometrial regeneration based on stem cells or growth factors is in its infancy, and the ethical and technical issues involved in the context of human studies make it a long way to go (Keyhanvar et al., 2021).

CONCLUSION AND OUTLOOK

Hydrogel materials have received increasing attention in the field of endometrial repair due to their excellent water retention, biocompatibility, degradability, and controlled drug release properties, and early animal experiments have been performed to obtain more desirable therapeutic effects, showing great potential for clinical applications. Various types of hydrogels, including natural biomaterial-based, synthetic biomaterial-based, and biocomposite hydrogels, can be used as anti-adhesion physical barriers and can also be loaded with estrogen, stem cells, and various active factors (growth factors, exosomes) to build delivery systems for IUA treatment.

In conclusion, compared to cell delivery alone in stem cell therapy or a control group administering the active substance alone in an injury model, biomaterial-based hydrogels have many advantages as carrier materials for delivery systems: The hydrogels can provide sufficient dynamic mechanical support for the uterine cavity; their excellent adhesion and antimicrobial properties facilitate the regulation of the microenvironment at the site of endometrial injury and accelerate injury repair, and they have also been shown to enhance the sustained-release effect of cells or active substances and prolong the retention time in the uterine cavity. By promoting cell proliferation, differentiation, blood vessel formation, and regulating the intrauterine microenvironment to regulate the biological behavior of cells, it can more effectively enhance the repair of damaged endometrium, prevent the occurrence of adhesions, and improve the pregnancy rate.

The future development direction should focus on the role of hydrogels in repairing the endometrium and the exploration of therapeutic mechanisms. Under the premise of ensuring and optimizing safety, improving the bioactivity and biomimetic properties of hydrogels, and exploring the feasibility of the combined application of multiple therapeutic factors are crucial to accelerating the transition of the hydrogel delivery system from the experimental stage to the clinical translation. It can be foreseen that in the future, multi-disciplinary and multi-field resource integration and cross-cooperation will promote the vigorous development of hydrogel-based delivery systems in the field of repairing endometrial injury.

AUTHOR CONTRIBUTIONS

GC and ZH wrote this article and equally contributed to this work; WS, PL and JZ revised this article; LY and JC checked and review this article.

FUNDING

This work was supported by the Department of Science and Technology of Liaoning Province (2021-BS-110) and Shenyang Science and Technology Bureau (RC210239).

REFERENCES

Abdulghani, S., and Mitchell, G. (2019). Biomaterials for *In Situ* Tissue Regeneration: A Review. *Biomolecules* 9 (11), 750. doi:10.3390/biom9110750

Abudukeyoumu, A., Li, M. Q., and Xie, F. (2020). Transforming Growth Factor-B1 in Intrauterine Adhesion. *Am. J. Reprod. Immunol.* 84 (2), e13262. doi:10.1111/aji.13262

Almeida, G. H. D., Iglesia, R. P., Araujo, M. S., Carreira, A. C. O., Santos, E. X. D., Calomeno, C. V. A. Q., et al. (2021). *Uterine Tissue Engineering: Where We Stand and the Challenges Ahead.* Reviews: Tissue Engineering Part B.

Baghersad, S., Hajir Bahrami, S., Mohammadi, M. R., Mojtahedi, M. R. M., and Milan, P. B. (2018). Development of Biodegradable Electrospun Gelatin/aloe-Vera/poly(ε-caprolactone) H-ybrid N-anofibrous S-caffold for A-pplication as S-kin S-ubstitutes. *Mater. Sci. Eng. C* 93, 367–379. doi:10.1016/j.msec.2018.08.020

Bai, X., Liu, J., Cao, S., and Wang, L. (2019). Mechanisms of Endometrial Fibrosis and the Potential Application of Stem Cell Therapy. *Discov. Med.* 27 (150), 267–279.

Bozorgmehr, M., Gurung, S., Darzi, S., Nikoo, S., Kazemnejad, S., Zarnani, A.-H., et al. (2020). Endometrial and Menstrual Blood Mesenchymal Stem/stromal Cells: Biological Properties and Clinical Application. *Front. Cell Dev. Biol.* 8, 497. doi:10.3389/fcell.2020.00497

Brandon, V. S., Shahana, S. K., Omar, Z. F., Ali, K., and Nicholas, A. P. (2009). Hydrogels in Regenerative Medicine. *Adv. Mater.* 21 (32-33), 3307–3329. doi:10.1002/adma.200802106

Brock, C. K., Wallin, S. T., Ruiz, O. E., Samms, K. M., Mandal, A., Sumner, E. A., et al. (2019). Stem Cell Proliferation Is Induced by Apoptotic Bodies from Dying Cells during Epithelial Tissue Maintenance. *Nat. Commun.* 10 (1), 1–11. doi:10.1038/s41467-019-09010-6

Cai, Y., Wu, F., Yu, Y., Liu, Y., Shao, C., Gu, H., Li, M., and Zhao, Y. (2019). Porous Scaffolds from Droplet Microfluidics for Prevention of Intrauterine Adhesion. *Acta Biomater.* 84, 222–230. doi:10.1016/j.actbio.2018.11.016

Campo, H., Baptista, P. M., López-Pérez, N., Faus, A., Cervelló, I., and Simón, C. (2017). De- and Recellularization of the Pig Uterus: a Bioengineering Pilot Study. *Biol. reproduction* 96 (1), 34–45. doi:10.1095/biolre/bio143396

Can, S., Kirpinar, G., Dural, O., Karamustafaoglu, B. B., Tas, I. S., Yasa, C., et al. (2018). Efficacy of a New Crosslinked Hyaluronan Gel in the Prevention of Intrauterine Adhesions. *JSLS* 22 (4), e201800036. doi:10.4293/JSLS.2018.00036

Cenksoy, P., Ficicioglu, C., Yıldırım, G., and Yesiladali, M. (2013). Hysteroscopic Findings in Women with Recurrent IVF Failures and the Effect of Correction of Hysteroscopic Findings on Subsequent Pregnancy Rates. *Arch. Gynecol. Obstet.* 287 (2), 357–360. doi:10.1007/s00404-012-2627-5

Cervelló, I., Santamaría, X., Miyazaki, K., Maruyama, T., and Simón, C. (2015). Cell Therapy and Tissue Engineering from and toward the Uterus. *Seminars reproductive Med.* 33 (05), 366–372. doi:10.1055/s-0035-1559581

Cousins, F. L., Pandoy, R., Jin, S., and Gargett, C. E. (2021). The Elusive Endometrial Epithelial Stem/progenitor Cells. *Front. Cell Dev. Biol.* 9, 868. doi:10.3389/fcell.2021.640319

D'Aniello, C., Cermola, F., Patriarca, E. J., and Minchiotti, G. (2017). Vitamin C in Stem Cell Biology: Impact on Extracellular Matrix Homeostasis and Epigenetics. *Stem Cells Int.* 2017, 8936156. doi:10.1155/2017/8936156

Drury, J. L., and Mooney, D. J. (2003). Hydrogels for Tissue Engineering: Scaffold Design Variables and Applications. *Biomaterials* 24 (24), 4337–4351. doi:10.1016/s0142-9612(03)00340-5

El-Toukhy, T., Coomarasamy, A., Khairy, M., Sunkara, K., Seed, P., Khalaf, Y., et al. (2008). The Relationship between Endometrial Thickness and Outcome of Medicated Frozen Embryo Replacement Cycles. *Fertil. Steril.* 89 (4), 832–839. doi:10.1016/j.fertnstert.2007.04.031

Farnebo, S., Farnebo, L., Kim, M., Woon, C., Pham, H., and Chang, J. (2017). Optimized Repopulation of Tendon Hydrogel. *Hand (New York, N.Y.)* 12 (1), 68–77. doi:10.1177/1558944715628005

Fei, Z., Bin, Z., Xin, X., Fei, H., and Yuechong, C. (2019). Meta-analysis on the Use of Hyaluronic Acid Gel to Prevent Recurrence of Intrauterine Adhesion after Hysteroscopic Adhesiolysis. *Taiwan. J. Obstetrics Gynecol.* 58 (6), 731–736. doi:10.1016/j.tjog.2019.09.002

Fei, Z., Xin, X., Fei, H., and Yuechong, C. (2020). Meta-analysis of the Use of Hyaluronic Acid Gel to Prevent Intrauterine Adhesions after Miscarriage. *Eur. J. Obstetrics Gynecol. Reproductive Biol.* 244, 1–4. doi:10.1016/j.ejogrb.2019.10.018

Feng, M., Hu, S., Qin, W., Tang, Y., Guo, R., and Han, L. (2021). Bioprinting of a Blue Light-Cross-Linked Biodegradable Hydrogel Encapsulating Amniotic Mesenchymal Stem Cells for Intrauterine Adhesion Prevention. *ACS omega* 6 (36), 23067–23075. doi:10.1021/acsomega.1c02117

Feng, X., Liu, J., Xu, Y., Zhu, J., Chen, W., Feng, B., Pan, Q., Yu, J., Shi, X., Yang, J., Li, Y., Li, L., and Cao, H. (2020). Molecular Mechanism Underlying the Difference in Proliferation between Placenta-derived and Umbilical Cord-derived Mesenchymal Stem Cells. *J. Cell. Physiology* 235 (10), 6779–6793. doi:10.1002/jcp.29572

Gargett, C. E., Chan, R. W., and Schwab, K. E. (2008). Hormone and Growth Factor Signaling in Endometrial Renewal: Role of Stem/progenitor Cells. *Mol. Cell Endocrinol.* 288 (1-2), 22–29. doi:10.1016/j.mce.2008.02.026

Gargett, C. E., and Ye, L. (2012). Endometrial Reconstruction from Stem Cells. *Fertil. Steril.* 98 (1), 11–20. doi:10.1016/j.fertnstert.2012.05.004

Garry, R., Hart, R., Karthigasu, K. A., and Burke, C. (2009). A Re-appraisal of the Morphological Changes within the Endometrium during Menstruation: a Hysteroscopic, Histological and Scanning Electron Microscopic Study. *Hum. Reprod.* 24 (6), 1393–1401. doi:10.1093/humrep/dep036

Gharibeh, N., Aghebati-Maleki, L., Madani, J., Pourakbari, R., Yousefi, M., and Ahmadian Heris, J. (2022). Cell-based Therapy in Thin Endometrium and Asherman Syndrome. *Stem Cell Res. Ther.* 13 (1), 1–13. doi:10.1186/s13287-021-02698-8

Gurung, S., Werkmeister, J. A., and Gargett, C. E. (2015). Inhibition of Transforming Growth Factor-β Receptor Signaling Promotes Culture Expansion of Undifferentiated Human Endometrial Mesenchymal Stem/stromal Cells. *Sci. Rep.* 5 (1), 1–12. doi:10.1038/srep15042

Han, Y., Liu, S., Mao, H., Tian, L., and Ning, W. (2016). Synthesis of Novel Temperature- and pH-Sensitive ABA Triblock Copolymers P(DEAEMA-co-MEO2MA-co-OEGMA)-b-PEG-b-P(DEAEMA-co-MEO2MA-co-OEGMA): Micellization, Sol-Gel Transitions, and Sustained BSA Release. *Polymers* 8 (11), 367. doi:10.3390/polym8110367

Hennes, D. M. Z. B., Rosamilia, A., Werkmeister, J. A., Gargett, C. E., and Mukherjee, S. (2021). Endometrial SUSD2+ Mesenchymal Stem/Stromal Cells in Tissue Engineering: Advances in Novel Cellular Constructs for Pelvic Organ Prolapse. *Jpm* 11 (9), 840. doi:10.3390/jpm11090840

Hooker, A. B., de Leeuw, R. A., van de Ven, P. M., Brölmann, H. A. M., and Huirne, J. A. F. (2018). Reproductive Performance after the Application of Hyaluronic Acid Gel after Dilation and Curettage in Women Who Have Experienced at Least One Previous Curettage: Long-Term Results of a Multicenter Prospective Randomized Trial. *Fertil. Steril.* 110 (7), 1231–1238. doi:10.1016/j.fertnstert.2018.07.021

Hooker, A. B., Lemmers, M., Thurkow, A. L., Heymans, M. W., Opmeer, B. C., Brolmann, H. A. M., Mol, B. W., and Huirne, J. A. F. (2014). Systematic Review and Meta-Analysis of Intrauterine Adhesions after Miscarriage: Prevalence, Risk Factors and Long-Term Reproductive Outcome. *Hum. Reprod. update* 20 (2), 262–278. doi:10.1093/humupd/dmt045

Jabbour, H. N., Kelly, R. W., Fraser, H. M., and Critchley, H. O. D. (2006). Endocrine Regulation of Menstruation. *Endocr. Rev.* 27 (1), 17–46. doi:10.1210/er.2004-0021

Ji, W., Hou, B., Lin, W., Wang, L., Zheng, W., Li, W., Zheng, J., Wen, X., and He, P. (2020). 3D Bioprinting a Human iPSC-Derived MSC-Loaded Scaffold for Repair of the Uterine Endometrium. *Acta Biomater.* 116, 268–284. doi:10.1016/j.actbio.2020.09.012

Johary, J., Xue, M., Zhu, X., Xu, D., and Velu, P. P. (2014). Efficacy of Estrogen Therapy in Patients with Intrauterine Adhesions: Systematic Review. *J. Minim. invasive Gynecol.* 21 (1), 44–54. doi:10.1016/j.jmig.2013.07.018

Keyhanvar, N., Zarghami, N., Bleisinger, N., Hajipour, H., Fattahi, A., Nouri, M., et al. (2021). Cell-based Endometrial Regeneration: Current Status and Future Perspectives. *Cell Tissue Res.* 384 (2), 241–254. doi:10.1007/s00441-021-03419-6

Kim, D. K., Sim, B. R., and Khang, G. (2016). Nature-derived Aloe Vera Gel Blended Silk Fibroin Film Scaffolds for Cornea Endothelial Cell Regeneration and Transplantation. *ACS Appl. Mat. Interfaces* 8 (24), 15160–15168. doi:10.1021/acsami.6b04901

Kim, Y. Y., Park, K.-H., Kim, Y. J., Kim, M. S., Liu, H. C., Rosenwaks, Z., et al. (2019). Synergistic Regenerative Effects of Functionalized Endometrial Stromal

Cells with Hyaluronic Acid Hydrogel in a Murine Model of Uterine Damage. *Acta Biomater.* 89, 139–151. doi:10.1016/j.actbio.2019.03.032

Kirchhof, S., Goepferich, A. M., and Brandl, F. P. (2015). Hydrogels in Ophthalmic Applications. *Eur. J. Pharm. Biopharm.* 95, 227–238. doi:10.1016/j.ejpb.2015.05.016

Koliakos, G. G., Befani, C. D., Mikropoulos, D., Ziakas, N. G., and Konstas, A. G. P. (2008). Prooxidant-antioxidant Balance, Peroxide and Catalase Activity in the Aqueous Humour and Serum of Patients with Exfoliation Syndrome or Exfoliative Glaucoma. *Graefes Arch. Clin. Exp. Ophthalmol.* 246 (10), 1477–1483. doi:10.1007/s00417-008-0871-y

Kong, Y., Shao, Y., Ren, C., and Yang, G. (2021). Endometrial Stem/progenitor Cells and Their Roles in Immunity, Clinical Application, and Endometriosis. *Stem Cell Res. Ther.* 12 (1), 1–16. doi:10.1186/s13287-021-02526-z

Lima, C. S. A. d., Balogh, T. S., Varca, J. P. R. O., Varca, G. H. C., Lugão, A. B., A. Camacho-Cruz, L., Bucio, E., and Kadlubowski, S. S. (2020). An Updated Review of Macro, Micro, and Nanostructured Hydrogels for Biomedical and Pharmaceutical Applications. *Pharmaceutics* 12 (10), 970. doi:10.3390/pharmaceutics12100970

Lin, J., Wang, Z., Huang, J., Tang, S., Saiding, Q., Zhu, Q., et al. (2021). Microenvironment-Protected Exosome-Hydrogel for Facilitating Endometrial Regeneration, Fertility Restoration, and Live Birth of Offspring. *Small* 17 (11), 2007235. doi:10.1002/smll.202007235

Lin, X.-N., Zhou, F., Wei, M.-L., Yang, Y., Li, Y., Li, T. C., et al. (2015). Randomized, Controlled Trial Comparing the Efficacy of Intrauterine Balloon and Intrauterine Contraceptive Device in the Prevention of Adhesion Reformation after Hysteroscopic Adhesiolysis. *Fertil. Steril.* 104 (1), 235–240. doi:10.1016/j.fertnstert.2015.04.008

Lin, Y., Dong, S., Ye, X., Liu, J., Li, J., Zhang, Y., and Zhang, D. (2022). Synergistic Regenerative Therapy of Thin Endometrium by Human Placenta-Derived Mesenchymal Stem Cells Encapsulated within Hyaluronic Acid Hydrogels. *Stem Cell. Res. Ther.* 13 (1), 1–19. doi:10.1186/s13287-022-02717-2

Lin, Y., Dong, S., Zhao, W., Hu, K.-L., Liu, J., Wang, S., Tu, M., Du, B., and Zhang, D. (2020). Application of Hydrogel-Based Delivery System in Endometrial Repair. *ACS Appl. Bio Mat.* 3 (11), 7278–7290. doi:10.1021/acsabm.0c00971

Liu, F., Hu, S., Yang, H., Li, Z., Huang, K., Su, T., Wang, S., and Cheng, K. (2019). Hyaluronic Acid Hydrogel Integrated with Mesenchymal Stem Cell-Secretome to Treat Endometrial Injury in a Rat Model of Asherman's Syndrome. *Adv. Healthc. Mat.* 8 (14), 1900411. doi:10.1002/adhm.201900411

Liu, H., Xu, Y., Yi, N., and Yi, W. (2018). Efficacy and Safety of Hyaluronic Acid Gel for the Prevention of Intrauterine Adhesion: a Meta-Analysis of Randomized Clinical Trials. *Gynecol. Obstet. Invest.* 83 (3), 227–233. doi:10.1159/000486674

Liu, Y.-R., Liu, B., Yang, B.-P., Lan, Y., and Chi, Y.-G. (2022). Efficacy of Hyaluronic Acid on the Prevention of Intrauterine Adhesion and the Improvement of Fertility: A Meta-Analysis of Randomized Trials. *Complementary Ther. Clin. Pract.* 47, 101575. doi:10.1016/j.ctcp.2022.101575

López-Martínez, S., Campo, H., de Miguel-Gómez, L., Faus, A., Navarro, A. T., Díaz, A., and Cervelló, I. (2021). A Natural Xenogeneic Endometrial Extracellular Matrix Hydrogel toward Improving Current Human *In Vitro* Models and Future *In Vivo* Applications. *Front. Bioeng. Biotechnol.* 9, 156. doi:10.3389/fbioe.2021.639688

López-Martínez, S., Rodríguez-Eguren, A., de Miguel-Gómez, L., Francés-Herrero, E., Faus, A., Díaz, A., and Cervelló, I. (2021). Bioengineered Endometrial Hydrogels with Growth Factors Promote Tissue Regeneration and Restore Fertility in Murine Models. *Acta Biomater.* 135, 113–125. doi:10.1016/j.actbio.2021.08.025

Lv, H., Wu, B., Song, J., Wu, W., Cai, W., and Xu, J. (2021). Hydrogel, a Novel Therapeutic and Delivery Strategy, in the Treatment of Intrauterine Adhesions. *J. Mater. Chem. B.* 1. 1. doi:10.1039/d1tb01005k

Ma, J., Zhan, H., Li, W., Zhang, L., Yun, F., Wu, R., Lin, J., and Li, Y. (2021). Recent Trends in Therapeutic Strategies for Repairing Endometrial Tissue in Intrauterine Adhesion. *Biomater. Res.* 25 (1), 40–25. doi:10.1186/s40824-021-00242-6

Mao, X., Tao, Y., Cai, R., Zhang, J., Gao, H., Chen, Q., Kuang, Y., and Zhang, S. (2020). Cross-linked Hyaluronan Gel to Improve Pregnancy Rate of Women Patients with Moderate to Severe Intrauterine Adhesion Treated with IVF: a Randomized Controlled Trial. *Arch. Gynecol. Obstet.* 301 (1), 199–205. doi:10.1007/s00404-019-05368-6

Medina, C. B., Mehrotra, P., Arandjelovic, S., Perry, J. S. A., Guo, Y., Morioka, S., Barron, B., Walk, S. F., Ghesquière, B., Krupnick, A. S., Lorenz, U., and Ravichandran, K. S. (2020). Metabolites Released from Apoptotic Cells Act as Tissue Messengers. *Nature* 580 (7801), 130–135. doi:10.1038/s41586-020-2121-3

Mihm, M., Gangooly, S., and Muttukrishna, S. (2011). The Normal Menstrual Cycle in Women. *Anim. Reprod. Sci.* 124 (3-4), 229–236. doi:10.1016/j.anireprosci.2010.08.030

Milcovich, G., Lettieri, S., Antunes, F. E., Medronho, B., Fonseca, A. C., Coelho, J. F. J., Marizza, P., Perrone, F., Farra, R., Dapas, B., Grassi, G., Grassi, M., and Giordani, S. (2017). Recent Advances in Smart Biotechnology: Hydrogels and Nanocarriers for Tailored Bioactive Molecules Depot. *Adv. Colloid Interface Sci.* 249, 163–180. doi:10.1016/j.cis.2017.05.009

Olalekan, S. A., Burdette, J. E., Getsios, S., Woodruff, T. K., and Kim, J. J. (2017). Development of a Novel Human Recellularized Endometrium that Responds to a 28-day Hormone Treatment†. *Biol. reproduction* 96 (5), 971–981. doi:10.1093/biolre/iox039

Peppas, N. A., Hilt, J. Z., Khademhosseini, A., and Langer, R. (2006). Hydrogels in Biology and Medicine: from Molecular Principles to Bionanotechnology. *Adv. Mat.* 18 (11), 1345–1360. doi:10.1002/adma.200501612

Phinney, D. G., and Pittenger, M. F. (2017). Concise Review: MSC-Derived Exosomes for Cell-free Therapy. *Stem cells* 35 (4), 851–858. doi:10.1002/stem.2575

Rastogi, P., and Kandasubramanian, B. (2019). Review of Alginate-Based Hydrogel Bioprinting for Application in Tissue Engineering. *Biofabrication* 11 (4), 042001. doi:10.1088/1758-5090/ab331e

Rinaldi, L., Lisi, F., Floccari, A., Lisi, R., Pepe, G., and Fishel, S. (1996). Endometrial Thickness as a Predictor of Pregnancy after *In-Vitro* Fertilization but Not after Intracytoplasmic Sperm Injection. *Hum. Reprod.* 11 (7), 1538–1541. doi:10.1093/oxfordjournals.humrep.a019434

Robinson, J. K., Colimon, L. M. S., and Isaacson, K. B. (2008). Postoperative Adhesiolysis Therapy for Intrauterine Adhesions (Asherman's Syndrome). *Fertil. Steril.* 90 (2), 409–414. doi:10.1016/j.fertnstert.2007.06.034

Ryoo, H. D., Gorenc, T., and Steller, H. (2004). Apoptotic Cells Can Induce Compensatory Cell Proliferation through the JNK and the Wingless Signaling Pathways. *Dev. Cell.* 7 (4), 491–501. doi:10.1016/j.devcel.2004.08.019

Salamonsen, L. (2003). Tissue Injury and Repair in the Female Human Reproductive Tract. *Reproduction* 125 (3), 301–311. doi:10.1530/rep.0.1250301

Salazar, C. A., Isaacson, K., and Morris, S. (2017). A Comprehensive Review of Asherman's Syndrome: Causes, Symptoms and Treatment Options. *Curr. Opin. Obstetrics Gynecol.* 29 (4), 249–256. doi:10.1097/gco.0000000000000378

Singh, S., Gupta, A., and Gupta, B. (2018). Scar Free Healing Mediated by the Release of Aloe Vera and Manuka Honey from Dextran Bionanocomposite Wound Dressings. *Int. J. Biol. Macromol.* 120, 1581–1590. doi:10.1016/j.ijbiomac.2018.09.124

Song, Y. T., Liu, P. C., Tan, J., Zou, C. Y., Li, Q. J., Li-Ling, J., et al. (2021). Stem Cell-Based Therapy for Ameliorating Intrauterine Adhesion and Endometrium Injury. *Stem Cell Res. Ther.* 12 (1), 1–14. doi:10.1186/s13287-021-02620-2

Strassmann, B. I. (1996). Energy Economy in the Evolution of Menstruation. *Evol. Anthropol.* 5 (5), 157–164. doi:10.1002/(sici)1520-6505(1996)5:5<157::aid-evan4>3.0.co;2-c

Sun, H., Lu, J., Li, B., Chen, S., Xiao, X., Wang, J., Wang, J., and Wang, X. (2018). Partial Regeneration of Uterine Horns in Rats through Adipose-Derived Stem Cell Sheets†. *Biol. Reproduction* 99 (5), 1057–1069. doi:10.1093/biolre/ioy121

Tan, J., Li, P., Wang, Q., Li, Y., Li, X., Zhao, D., Xu, X., and Kong, L. (2016). Autologous Menstrual Blood-Derived Stromal Cells Transplantation for Severe Asherman's Syndrome. *Hum. Reprod.* 31 (12), 2723–2729. doi:10.1093/humrep/dew235

Thomas, H., Cowin, A., and Mills, S. (2017). The Importance of Pericytes in Healing: Wounds and Other Pathologies. *Ijms* 18 (6), 1129. doi:10.3390/ijms18061129

Thubert, T., Dussaux, C., Demoulin, G., Rivain, A.-L., Trichot, C., and Deffieux, X. (2015). Influence of Auto-Cross-Linked Hyaluronic Acid Gel on Pregnancy Rate and Hysteroscopic Outcomes Following Surgical Removal of Intra-uterine Adhesions. *Eur. J. Obstetrics Gynecol. Reproductive Biol.* 193, 65–69. doi:10.1016/j.ejogrb.2015.06.025

Vashi, A. V., Keramidaris, E., Abberton, K. M., Morrison, W. A., Wilson, J. L., O'Connor, A. J., Cooper-White, J. J., and Thompson, E. W. (2008). Adipose Differentiation of Bone Marrow-Derived Mesenchymal Stem Cells Using

Pluronic F-127 Hydrogel *In Vitro*. *Biomaterials* 29 (5), 573–579. doi:10.1016/j.biomaterials.2007.10.017

Wang, B., Feng, C., Dang, J., Zhu, Y., Yang, X., Zhang, T., Zhang, R., Li, J., Tang, J., Shen, C., Shen, L., Dong, J., and Zhang, X. (2020). Preparation of Fibroblast Suppressive Poly(ethylene Glycol)-B-Poly(l-phenylalanine)/Poly(ethylene Glycol) Hydrogel and its Application in Intrauterine Fibrosis Prevention. *ACS Biomater. Sci. Eng.* 7 (1), 311–321. doi:10.1021/acsbiomaterials.0c01390

Wang, J., Yang, C., Xie, Y., Chen, X., Jiang, T., Tian, J., and Lu, Y. (2021). Application of Bioactive Hydrogels for Functional Treatment of Intrauterine Adhesion. *Front. Bioeng. Biotechnol.* 9, 760943. doi:10.3389/fbioe.2021.760943

Wang, Z., Wu, J., Shi, X., Song, F., Gao, W., and Liu, S. (2020). Stereocomplexation of Poly(lactic Acid) and Chemical Crosslinking of Ethylene Glycol Dimethacrylate (EGDMA) Double-Crosslinked Temperature/pH Dual Responsive Hydrogels. *Polymers* 12 (10), 2204. doi:10.3390/polym12102204

Weissmann, B. (1955). The Transglycosylative Action of Testicular Hyaluronidase. *J. Biol. Chem.* 216 (2), 783–794. doi:10.1016/s0021-9258(19)81432-1

Wenbo, Q., Lijian, X., Shuangdan, Z., Jiahua, Z., Yanpeng, T., Xuejun, Q., Xianghua, H., and Jingkun, Z. (2020). Controlled Releasing of SDF-1α in Chitosan-Heparin Hydrogel for Endometrium Injury Healing in Rat Model. *Int. J. Biol. Macromol.* 143, 163–172. doi:10.1016/j.ijbiomac.2019.11.184

Wyatt, K. A., Filby, C. E., Davies-Tuck, M. L., Suke, S. G., Evans, J., and Gargett, C. E. (2021). Menstrual Fluid Endometrial Stem/progenitor Cell and Supernatant Protein Content: Cyclical Variation and Indicative Range. *Hum. Reprod.* 36 (8), 2215–2229. doi:10.1093/humrep/deab156

Xin, L., Wei, C., Tong, X., Dai, Y., Huang, D., Chen, J., Ma, L., and Zhang, S. (2022). *In Situ* delivery of Apoptotic Bodies Derived from Mesenchymal Stem Cells via a Hyaluronic Acid Hydrogel: A Therapy for Intrauterine Adhesions. *Bioact. Mater.* 12, 107–119. doi:10.1016/j.bioactmat.2021.10.025

Xu, H.-L., Xu, J., Shen, B.-X., Zhang, S.-S., Jin, B.-H., Zhu, Q.-Y., ZhuGe, D.-L., Wu, X.-Q., Xiao, J., and Zhao, Y.-Z. (2017). Dual Regulations of Thermosensitive Heparin-Poloxamer Hydrogel Using ε-Polylysine: Bioadhesivity and Controlled KGF Release for Enhancing Wound Healing of Endometrial Injury. *ACS Appl. Mat. Interfaces* 9 (35), 29580–29594. doi:10.1021/acsami.7b10211

Xu, H.-L., Xu, J., Zhang, S.-S., Zhu, Q.-Y., Jin, B.-H., ZhuGe, D.-L., Shen, B.-X., Wu, X.-Q., Xiao, J., and Zhao, Y.-Z. (2017). Temperature-sensitive Heparin-Modified Poloxamer Hydrogel with Affinity to KGF Facilitate the Morphologic and Functional Recovery of the Injured Rat Uterus. *Drug Deliv.* 24 (1), 867–881. doi:10.1080/10717544.2017.1333173

Xu, X., Lai, Y., and Hua, Z. C. (2019). Apoptosis and Apoptotic Body: Disease Message and Therapeutic Target Potentials. *Biosci. Rep.* 39 (1), BSR20180992. doi:10.1042/BSR20180992

Yang, H., Wu, S., Feng, R., Huang, J., Liu, L., Liu, F., et al. (2017). Vitamin C Plus Hydrogel Facilitates Bone Marrow Stromal Cell-Mediated Endometrium Regeneration in Rats. *Stem Cell Res. Ther.* 8 (1), 1–10. doi:10.1186/s13287-017-0718-8

Yao, Q., Zheng, Y.-W., Lan, Q.-H., Wang, L.-F., Huang, Z.-W., Chen, R., Yang, Y., Xu, H.-L., Kou, L., and Zhao, Y.-Z. (2020). Aloe/poloxamer Hydrogel as an Injectable β-estradiol Delivery Scaffold with Multi-Therapeutic Effects to Promote Endometrial Regeneration for Intrauterine Adhesion Treatment. *Eur. J. Pharm. Sci.* 148, 105316. doi:10.1016/j.ejps.2020.105316

Yoshimasa, Y., and Maruyama, T. (2021). Bioengineering of the Uterus. *Reprod. Sci.* 28 (6), 1596–1611. doi:10.1007/s43032-021-00503-8

Zhang, E., Guo, Q., Ji, F., Tian, X., Cui, J., Song, Y., Sun, H., Li, J., and Yao, F. (2018). Thermoresponsive Polysaccharide-Based Composite Hydrogel with Antibacterial and Healing-Promoting Activities for Preventing Recurrent Adhesion after Adhesiolysis. *Acta biomater.* 74, 439–453. doi:10.1016/j.actbio.2018.05.037

Zhang, S., Li, P., Yuan, Z., and Tan, J. (2019). Platelet-rich Plasma Improves Therapeutic Effects of Menstrual Blood-Derived Stromal Cells in Rat Model of Intrauterine Adhesion. *Stem Cell Res. Ther.* 10 (1), 61–12. doi:10.1186/s13287-019-1155-7

Zhang, S.-S., Xia, W.-T., Xu, J., Xu, H.-L., Lu, C.-T., Zhao, Y.-Z., et al. (2017). Three-dimensional Structure Micelles of Heparin-Poloxamer Improve the Therapeutic Effect of 17β-Estradiol on Endometrial Regeneration for Intrauterine Adhesions in a Rat Model. *Ijn* 12, 5643–5657. doi:10.2147/ijn.s137237

Zhang, S. S., Xu, X. X., Xiang, W. W., Zhang, H. H., Lin, H. L., Shen, L. E., Lin, Q., Lin, F., and Zhou, Z. Y. (2020). Using 17β-estradiol Heparin-poloxamer Thermosensitive Hydrogel to Enhance the Endometrial Regeneration and Functional Recovery of Intrauterine Adhesions in a Rat Model. *FASEB J.* 34 (1), 446–457. doi:10.1096/fj.201901603rr

Zhang, Y., Lin, X., Dai, Y., Hu, X., Zhu, H., Jiang, Y., et al. (2016). Endometrial Stem Cells Repair Injured Endometrium and Induce Angiogenesis via AKT and ERK Pathways. *Reproduction* 152 (5), 389–402. doi:10.1530/rep-16-0286

Zhang, Y., Wang, Y., Shao, L., Pan, X., Liang, C., Liu, B., Zhang, Y., Xie, W., Yan, B., Liu, F., Yu, X. y., and Li, Y. (2020). Knockout of Beta-2 Microglobulin Reduces Stem Cell-induced Immune Rejection and Enhances Ischaemic Hindlimb Repair via exosome/miR-24/Bim Pathway. *J. Cell. Mol. Medi* 24 (1), 695–710. doi:10.1111/jcmm.14778

Zhao, W., Jin, K., Li, J., Qiu, X., and Li, S. (2017). Delivery of Stromal Cell-Derived Factor 1α for *In Situ* Tissue Regeneration. *J. Biol. Eng.* 11 (1), 22–12. doi:10.1186/s13036-017-0058-3

Zheng, F., Xin, X., He, F., Liu, J., and Cui, Y. (2020). Meta-analysis on the Use of Hyaluronic Acid Gel to Prevent Intrauterine Adhesion after Intrauterine Operations. *Exp. Ther. Med.* 19 (4), 2672–2678. doi:10.3892/etm.2020.8483

Zhu, S.-F., Zhong, Z.-N., Fu, X.-F., Peng, D.-X., Lu, G.-H., Li, W.-H., Xu, H.-Y., Hu, H.-B., He, J.-M., Su, W.-Y., and He, Y.-L. (2013). Comparison of Cell Proliferation, Apoptosis, Cellular Morphology and Ultrastructure between Human Umbilical Cord and Placenta-Derived Mesenchymal Stem Cells. *Neurosci. Lett.* 541, 77–82. doi:10.1016/j.neulet.2013.03.018

Zhu, X., Péault, B., Yan, G., Sun, H., Hu, Y., and Ding, L. (2019). Stem Cells and Endometrial Regeneration: from Basic Research to Clinical Trial. *Cscr* 14 (4), 293–304. doi:10.2174/1574888x14666181205120110

Conflict of Interest: The authors declare that the research was conducted in the absence of any commercial or financial relationships that could be construed as a potential conflict of interest.

Publisher's Note: All claims expressed in this article are solely those of the authors and do not necessarily represent those of their affiliated organizations, or those of the publisher, the editors and the reviewers. Any product that may be evaluated in this article, or claim that may be made by its manufacturer, is not guaranteed or endorsed by the publisher.

frontiers | Frontiers in Bioengineering and Biotechnology

REVIEW
published: 22 June 2022
doi: 10.3389/fbioe.2022.921576

Advances in Barrier Membranes for Guided Bone Regeneration Techniques

Ze Yang[1†], Chang Wu[1†], Huixin Shi[2], Xinyu Luo[1], Hui Sun[1], Qiang Wang[1] and Dan Zhang[1*]*

[1]*Liaoning Provincial Key Laboratory of Oral Diseases, School and Hospital of Stomatology, China Medical University, Shenyang, China,* [2]*Department of Plastic Surgery, The First Affiliated Hospital of China Medical University, Shenyang, China*

Guided bone regeneration (GBR) is a widely used technique for alveolar bone augmentation. Among all the principal elements, barrier membrane is recognized as the key to the success of GBR. Ideal barrier membrane should have satisfactory biological and mechanical properties. According to their composition, barrier membranes can be divided into polymer membranes and non-polymer membranes. Polymer barrier membranes have become a research hotspot not only because they can control the physical and chemical characteristics of the membranes by regulating the synthesis conditions but also because their prices are relatively low. Still now the bone augment effect of barrier membrane used in clinical practice is more dependent on the body's own growth potential and the osteogenic effect is difficult to predict. Therefore, scholars have carried out many researches to explore new barrier membranes in order to improve the success rate of bone enhancement. The aim of this study is to collect and compare recent studies on optimizing barrier membranes. The characteristics and research progress of different types of barrier membranes were also discussed in detail.

Keywords: guided bone regeneration, barrier membrane, polymer, functional membrane, absorbable material

OPEN ACCESS

Edited by:
Jianshe Hu,
Northeastern University, China

Reviewed by:
Babak Akbari,
University of Tehran, Iran
Arun Prabhu Rameshbabu,
Harvard Medical School,
United States

***Correspondence:**
Qiang Wang
mfqwang@cmu.edu.cn
Dan Zhang
zdcmu888@outlook.com

[†]These authors have contributed equally to this work and share first authorship

Specialty section:
This article was submitted to Biomaterials, a section of the journal Frontiers in Bioengineering and Biotechnology

Received: *16 April 2022*
Accepted: *30 May 2022*
Published: *22 June 2022*

Citation:
Yang Z, Wu C, Shi H, Luo X, Sun H, Wang Q and Zhang D (2022) Advances in Barrier Membranes for Guided Bone Regeneration Techniques. Front. Bioeng. Biotechnol. 10:921576. doi: 10.3389/fbioe.2022.921576

1 INTRODUCTION

Alveolar bone defect is a common oral disease. Insufficient alveolar bone caused by trauma, tumor, periodontitis, and long-time tooth absence has gradually become a huge challenge for the medical application of subsequent implantation, orthodontic, periodontal and functional repair treatments. The absence of natural teeth will cause the loss of functional stimulation of alveolar bone, resulting in progressive, cumulative and irreversible bone resorption, and the alveolar bone cannot maintain the bone contour, nor can it obtain the effect of mucosal support (Cawood and Howell, 1988). There are many ways to improve the alveolar bone, including guided bone regeneration, cleavage of the alveolar crest, bone compression, maxillary sinus lifting, distraction osteogenesis and autologous mass bone grafting (Fu and Wang, 2011; Mohan et al., 2015; Danesh-Sani et al., 2016; Sakkas et al., 2017; Rachmiel et al., 2018). At present, GBR technology is recommended to be used before or during the same period of dental implantation to expand and retain alveolar bone. It has become a widely recognized method for repairing alveolar ridge defects and is the most common bone augmentation technology with the longest clinical application time. After 8 years of follow-up, Kim et al. (2020) found that the success rate of implants followed by GBR treatment was about 77.8%. GBR technology expands the indications of oral implantation, guarantees the biological, aesthetic effects after implantation and restoration as well as reduces the incidence of complications.

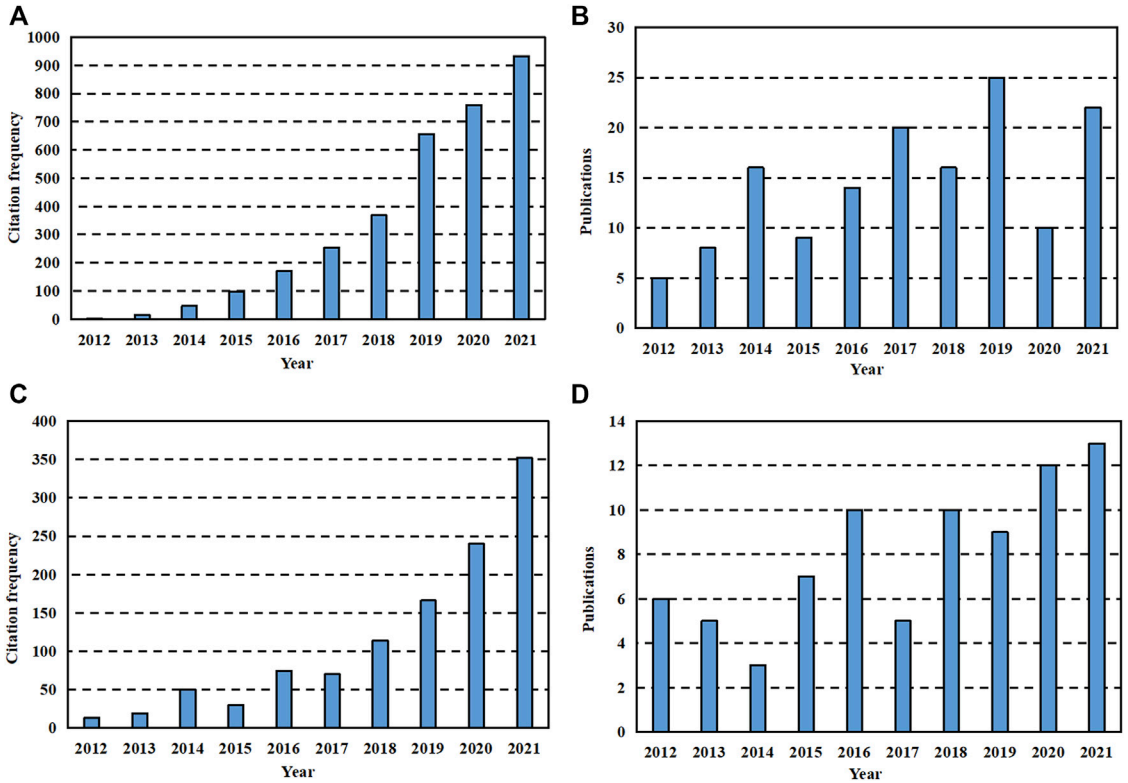

FIGURE 1 | Data search results for last 10 years. **(A)** The citation frequency of literature with "GBR" and "polymer" as keywords retrieved on Web of Science in recent 10 years. **(B)** The publication of literature with "GBR" and "polymer" as keywords searched on Web of Science in recent 10 years. **(C)** The sum of citation frequency of literature retrieved on Web of Science with "GBR" and "ceramic" as one group of keywords as well as "GBR "and "metal" as another group of keywords in recent 10 years. **(D)** The sum of the publication of literature retrieved with "GBR" and "ceramic" as one set of keywords and "GBR "and "metal" as another set of keywords on Web of Science in recent 10 years.

It is well-known that the essential substances in the composition of animals and plants, such as proteins and cellulose, are polymer compounds. The ubiquity in the biological community determines their special status in the field of medicine, so they are most commonly used as medical materials. Biomedical polymer materials have the advantages of designable structure, good biological activity, stable physical properties, wide sources and low price. Therefore, as shown in **Figure 1**, polymers are always hot spots in the development of GBR applications and show an increasing trend year by year. However, it is worth noting that polymers should have high polymer purity, clean production environment and little residue of polymerization additives due to the presence of monomer impurities. Besides, chemical and mechanical properties shall meet the requirements of medical design and function. Such as hardness, elasticity, mechanical strength and fatigue strength. Finally, the material needs to be compatible with other materials like human tissues so that the implanted material has no side effect on body fluids for long-time use. According to their different uses in the medical field, they can be divided into five categories: 1) Materials that are not in direct contact with the tissues of the organism. 2) Materials in contact with skin and mucous membranes (Goodier et al., 2018). 3) Materials in short-term contact with human tissues (Liu et al., 2018). 4) Materials implanted in the body for a long time (Williams, 2008). 5) Pharmaceutical polymers (Ekladious et al., 2019).

2 PERFORMANCE REQUIREMENTS OF BARRIER MEMBRANES IN GUIDED BONE REGENERATION TECHNIQUES

The principle of guided bone regeneration comes from guided tissue regeneration (GTR) in periodontium. The periodontal soft tissues such as epithelial cells and connective tissues proliferate and migrate relatively rapidly. GBR aims to insulate the soft tissues from the bone defect with a barrier membrane to provide a fairly closed environment for tissue growth. The cells with regenerative ability in the bone defect area proliferate and differentiate to the maximum extent to ensure the priority of osteogenesis and promote the formation of new bone (Elgali et al., 2017; Nowwarote et al., 2018). Selection of appropriate barrier membrane is the deciding factor in the success of guided bone regeneration. As seen in **Table 1**, ideal GBR barrier membrane should have good mechanical properties, including favorable space-making properties and clinical operability, favorable biological properties such as satisfactory biocompatibility, bioactive properties, tissue selectivity and antibacterial

TABLE 1 | Properties of ideal barrier membrane.

Properties	Purpose	Influencing Factor	Effect	References
Space-making properties	Provide a suitable space in which the regeneration of bone can take place	Plasticity	Adaptation to the bone defect	
		Stiffness	Withstand the compression of the soft tissue	
		Resistance of tear	Withstand the ambient pressure	Elgali et al. (2017)
		Thickness	Thicker: reduce soft tissue ingrowth	Benic et al. (2019)
		Stability of implant	Maintain the defect space	Moses et al. (2008)
		Implant site	Appropriate and effective	Hoornaert et al. (2016)
		Implant site	Steadfast and effective	
		Hold time	Meet the needs of periodontal tissue regeneration, 4~6w Meet the needs of bone tissue regeneration, 16~24w	
Clinical operability	Specific requirements conducive to surgical operation	Chemical properties	Cover the bone defect	
			Fit adjacent bone surface	
		Physical properties	Hard: cause the soft tissue cracking	Won et al. (2016), Aprile et al. (2020)
Biocompatibility	Regeneration of tissue	—	Osteopromotive	Won et al. (2016), Rakhmatia et al. (2013)
Bioactive properties	Positive effect on the regeneration of the bone defect	—	Membranes without this characteristic at present	Hoornaert et al. (2016)
Tissue selectivity	Promote bone regeneration and prevent the ingrowth of connective tissue	Porosity	Inhibition of soft tissue, promote bone tissue	Murphy et al. (2000), Sheikh et al. (2017a)
		Osteoconductivity	Allow osteogenitor cells to form new bone tissues	Abdelaziz et al. (2020), Wang and Boyapati (2006)
Antibacterial properties	Resistance to the bacterial invasion	—	Minimize the negative effects of exposure	Annibali et al. (2012)

properties. How to better improve the peri-implant bone volume and further increase the degree of osseointegration is one of the most important properties for GBR.

2.1 Space-Making Properties and Clinical Operability

Spatial maintenance of clinical GBR technology requires attention to maintain osteogenic space, so the barrier membrane materials need to have a series of corresponding characteristics to ensure the space maintenance effect (Won et al., 2016). Firstly, it is required to have appropriate plasticity, which can provide a specific spatial structure to promote the functional reconstruction of alveolar bone according to different defect areas. In addition, the barrier membrane needs to meet a specific strength requirement to withstand external pressure, so adequate rigidity and tear resistance are essential. Meanwhile, the thickness of the barrier membrane is different, which affects the space maintenance characteristics during the implantation process. The practice has shown that placing a thicker collagen membrane can reduce the ingrown soft tissue and promote bone formation (Elgali et al., 2017). In practice, whether the stability of the graft can be maintained determines the success of GBR to a certain extent. Therefore, minimizing the movement of the barrier membrane in the operative area can effectively maintain a stable three-dimensional reconstruction spatial structure. In addition, the appropriately placement of barrier membrane and the bone meal implantation will also affect the effect of bone increment after bone grafting (Benic et al., 2019). The barrier membrane applied to GBR plays a crucial role in forming new bone tissue at the implantation site. Some scholars believe that in GBR technology, the barrier membrane is required to last 4–6 weeks, which is the requirement of regeneration time of total periodontal tissue (Moses et al., 2008). Some scholars also suggest that ideal GBR membrane should maintain its barrier function for 16–24 weeks to meet the requirement of bone tissue regeneration time (Hoornaert et al., 2016).

From the perspective of clinical practicability, GBR barrier membrane needs to meet the specific requirements of convenient for surgical operation. The barrier membrane needs to be easy to cover the bone defect area and conform to the adjacent bone surface. In terms of physical properties, if the barrier membrane is too hard, it may interfere with tissue integration in the bone defect area or lead to soft tissue dehiscence (Won et al., 2016; Aprile et al., 2020).

2.2 Biocompatibility and Bioactive Properties

Barrier membrane for GBR needs to have good biocompatibility to achieve the effect of supporting tissue regeneration. Good biocompatibility requires that it has no negative effects on the prognosis of peripheral cell tissue, bone defect area, and the

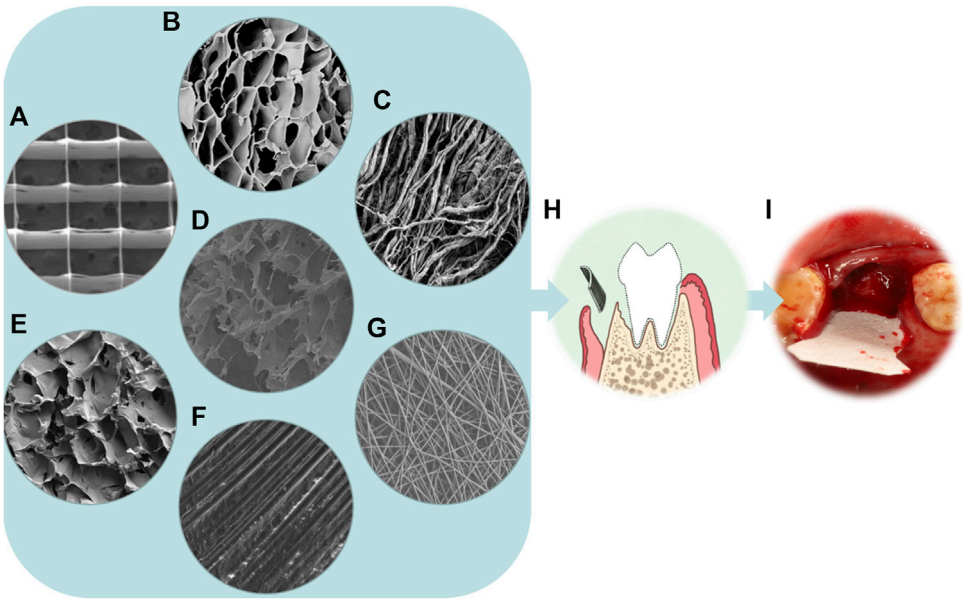

FIGURE 2 | From microscopy to reality of barrier membranes. **(A)** SEM micrograph of the PCL scaffold with the spacing of 500 μm (Dubey et al., 2020). **(B)** SEM micrograph of the γ-PGA/BC composite hydrogel (Dou et al., 2021). **(C)** SEM image of a rougher bottom layer with collagen strands of Bio-Gide (magnification×1,000) (Wu et al., 2018). **(D)** SEM image showing the morphology of the loose layer of an asymmetric porous chitosan membrane (magnification×2,000) (Ma et al., 2016). **(E)** SEM image showing the morphology of the loose cross-linked collagen layer of the aspirin-loaded chitosan nanoparticles contained in collagen-chitosan membrane (ACS-CCM) (Zhang et al., 2017). **(F)** SEM image of the dPTFE membrane (magnification×500) (Korzinskas et al., 2018). **(G)** Field emission scanning electron microscopy(FE-SEM) images of PLGA/PCL electrospinning membranes (magnification×1,000) (Qian et al., 2016). **(H)** Schematic illustration of the principle of GBR. **(I)** The implant placement procedure for BioGuide membrane.

patients' overall health (Rakhmatia et al., 2013; Won et al., 2016). The interaction between barrier membrane and tissue has a positive effect on the surrounding tissue, which further leads to the healing of the defect. If the barrier membrane is absorbable, it should have the ability to degrade or integrate into host tissues, reducing the potential incompatibility caused by the barrier membrane.

Bioactivity refers to the ability of biomaterials to produce chemical bonding with living bone which is an important indicator to measure biomaterials. In the application of GBR, it is mainly reflected in the osteogenic capacity of barrier membranes. First, the barrier membrane itself can evoke a local environment in the defect, which is conducive to the regeneration and differentiation of osteoblasts. The environment created by the membrane is also conducive to the formation and reconstruction of the molecular mechanism of coupled bone in the submembrane defect (Omar et al., 2019). In addition, membrane bioactivity can be improved by designing the membrane structure (Liu et al., 2021). In recent years, it has also become an important way to enhance the osteoinductive ability of membranes by adding some inorganic particles, growth factors, etc. Common additives *in vitro* experiments are Sr-CaP nanoparticles (Ye et al., 2019), octacalcium phosphate (OCP) (Wang Y. et al., 2019), bone morphogenetic protein (BMP) (Yin et al., 2017a) and so on. Common additives *in vivo* experiments are metformin (Met) (Ebrahimi et al., 2021), epigallocatechin-3-gallate (EGCG) (Chu et al., 2019), etc. Barrier membranes will not only have a passive role but can play an active role at the site of bone defect regeneration (Hoornaert et al., 2016).

2.3 Tissue Selectivity

One of the critical points of the tissue-selective GBR technique is to promote the regeneration of bone tissue in the bone defect area while preventing the peripheral junction of tissue growth. This requires the relevant performance of the barrier membrane to be guaranteed. In terms of selective tissue growth, the barrier membrane should allow the passage of oxygen, tissue fluid and related bioactive substances but prevent the growth of connective tissue cells and epithelial cells into the defect area. In addition, a certain porosity is required to allow cells to adapt to their surroundings, and to provide cells with fully permeate nutrients (Murphy et al., 2000). Appropriate pore size can inhibit the growth of soft tissue and facilitate the diffusion of substances beneficial to the growth of bone tissue (Sheikh et al., 2017a). The selective healing process of the tissue defect can be achieved in two general directions. One is to promote growth which stimulates the growth of the tissue around the bone defect area. The other is to prevent growth which prevents the growth and implantation of epithelial connective tissue cells (Iviglia et al., 2019).

Tissue integration between the barrier membrane and the adjacent bone contour ensures effective adsorption to grow, contributing to the relative seal between the natural bone and the implant material. Tissue integration accelerates the wound

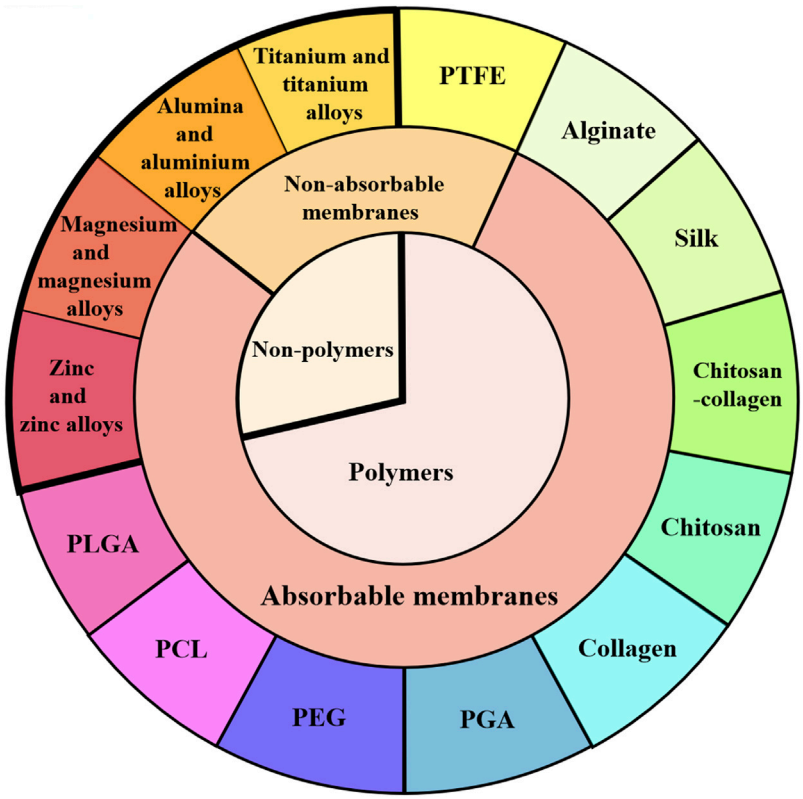

FIGURE 3 | Classification of barrier membranes. GBR barrier membranes are classified from polymer and non-polymer, absorbable and non-absorbable barrier membranes. Several typical barrier membranes in each classification are introduced in the text of this paper.

healing process in the surgical area and helps prevent the integration of non-osteogenic components such as fibrous connective tissue into the defect site. The ability to create a membrane space of the material is key to achieving tissue integration. Abdelaziz et al. (2020) proposed that the barrier membrane also needed to have good osteoconductivity. That is to say, the compatibility of the old barrier membrane or scaffold with osteoclasts allows osteogenic cells to grow from the edge of the existing bone to form a new bone tissue structure and achieve tissue integration of bone. GBR surgery requires good soft tissue sealing and long-term wound stability to protect the regenerative process (Wang and Boyapati, 2006).

2.4 Antibacterial Properties

Antibacterial property is also a heated topic in the study of barrier membrane modification by scholars nowadays. Bacterial infection has been a common headache in our daily life or clinics. Bacterial adhere on the surface of medical materials, resulting in infections or even failure of materials or surgery operation (Behzadi et al., 2017; Jensen et al., 2017). It has been verified that the adverse effects of barrier membrane exposure on surrounding tissues are mainly due to bacterial invasion. Inflammatory response caused by bacterial invasion can inhibit the growth of osteoblasts, thus affecting the effect of guided bone regeneration and even leading to the failure of surgery. Researchers hoped to ensure or improve bone regeneration by preventing bacterial invasion (Cao et al., 2019). One of the main challenges of GBR restoration is bacterial colonization on the membrane, constitutes to premature membrane degradation (Saarani et al., 2017). Therefore, timely treatment once membrane exposure occurs during the GBR process can minimize the negative effects of exposure (Annibali et al., 2012), which also reflects that tissue integration plays an important role in the success of GBR. Non-resorbable membranes with different pore sizes have been used for exposure experiments. It was found that the osteogenic effect of non-resorbable membranes with pore sizes smaller than the general diameter of bacteria had not been significantly reduced even if they were exposed (Barboza et al., 2010).

3 SPECIFIC TYPES OF BARRIER MEMBRANES

As shown in **Figure 2**, different types of barrier membranes can be applied to bone defects during the GBR procedure to play a certain role in osteogenesis. As shown in **Figure 3**, barrier membranes can be divided into two categories according to the composition, polymer membranes and non-polymer membranes. According to whether it is degradable or not, barrier membrane can be divided into absorbable membrane and non-absorbable membrane. Non-absorbable membranes are

still in a minority of the current barrier membrane studies. Judging from the mechanical properties of several common barrier membranes in **Table 2**, single-component polymers tend to have lower mechanical properties than composite polymers. Both mechanical and biological properties can affect the stability and effectiveness of the barrier membranes. Based on the biological characteristics of several common barrier membranes listed in **Table 3**, the barrier membranes meet the requirements for the cytotoxicity of surgical implant materials (grade 0–1). Among the rest, PLGA and collagen have class 1 cytotoxicity but are considered biosafe. Their inflammatory responses were within the acceptable range. In addition, it is worth noting that chitosan inflammatory responses are correlated with molecular weight.

3.1 Polymer Barrier Membranes

3.1.1 Poly(lactic-co-glycolic acid)(PLGA)

Polylactic acid (PLA) is a novel bio-based and renewable biodegradable material made from renewable plant resources such as straws like cereal husks and starchy crops like maize, sweet potato, and cassava. PLA is a good membrane material for treating bone defects. However, PLA membrane degrades rapidly, and the residue of PLA hydrolysis can cause local inflammation and abscess formation (Ovcharenko et al., 2020). Synthetic polymers of PLA have a higher potential to induce osteogenic differentiation and have been developed as an alternative to natural membranes (Jazayeri et al., 2017). PLGA consists of two monomers, lactic acid and hydroxyacetic acid, randomly polymerized. It is a degradable functional polymeric organic compound with good biocompatibility, non-toxicity, good capsule-forming and membrane-forming properties, which is widely used in pharmaceuticals, medical engineering materials and modern industries. The biodegradable synthetic barrier PLGA membrane generally consists of two layers: a dense layer that prevents invasion of soft tissue cells and the other is a thick microfibrous layer in which the blood clot is stabilized, allowing the blood clot to be stabilized osteoblasts to colonize the membrane. It has been suggested that the degradation rate of PLGA depends on the ratio of the two layers. Its general *in vivo* degradation time is 1–2months (Sun et al., 2017). Hoornaert et al. (2016) demonstrated that the bilayer PLGA membrane maintained structural integrity and barrier function for 16 weeks through *in vitro* and *in vivo* experiments. It was degraded by hydrolysis of polymer chains, which was easy to be applied with artificial bone filling particles for bone defect repair. They concluded that the bilayer PLGA membranes might be a safer and more predictable alternative to GBR. With the developing of PLGA barrier membranes, some composite PLGA material have come into use these years. Attapulgite (ATT) is a kind of natural clay material and an aluminum-magnesium silicate, which is widely distributed in China and the United States. ATT polymer composites have better mechanical durability than the corresponding pure polymers. Moreover, the hydrophilicity of the PLGA fiber membrane is improved with the addition of ATT, which can facilitate the penetration of hydrophilic nutrients and regulate cell response to the membrane surface. Xie X. et al. (2020) confirmed that electrospinning ATT doped PLGA fibrous scaffolds could induce the expression of osteogenic factors in bone marrow mesenchymal stem cells (BMSCs). By effectively promoting bone formation of alveolar bone defects, ATT doped PLGA was demonstrated to be an excellent barrier membrane material.

3.1.2 Polycaprolactone

PCL is a synthetic polymer known for its biocompatibility and excellent mechanical properties. Compared to PLGA, PCL has relatively lower cell affinity. However, with excellent mechanical properties, PCL has the advantage of preventing early fracture of the scaffold. It has been shown that adding silica nanoparticles (Si-NPs) into electrospun PCL membranes could greatly improve the mechanical and osteoconductive properties of the membranes (Castro et al., 2018). With good mechanical properties, PCL can be modified for other barrier membranes. For example, the PCL reticulation prepared by over melt electrowriting can not only delay hydrogel degradation and prevent soft tissue invasion, but also provide mechanical support for the regeneration and differentiation of progenitor cells (Dubey et al., 2020). The bioactivity of PCL was enhanced by mixing it with a natural silk fibroin polymer that has low immunogenicity and inherent bioactivity. It could promote bone regeneration not only in periodontal defects but also in other craniomaxillofacial regions. PCL can be modified by mixing with other materials through electrospinning technology. He et al. (2017) found that chitosan/PCL composite membrane significantly improved the ability of bone formation compared with PCL membrane.

3.1.3 Polyethylene Glycol

PEG is a biodegradable polymer with good biocompatibility. With good processability, PEG can be used as an ideal scaffold material and matrix material for other bone substitutes and blended with other polymers to make various new types of biological barrier membranes (Kim J. Y. et al., 2009; Jung et al., 2015). Wechsler et al. (2008) showed that PEG implantation maintained barrier function for up to 4 months *in vivo*. Some preclinical studies have found that PEG membranes have significant advantages for alveolar ridge bone augmentation in lateral ridge defects (Benic and Hämmerle, 2014). Jung et al. (2009a) used PEG membranes and collagen membranes for regeneration of peri-implant bone defects. They found that the PEG membrane group obtained more bone augmentation and could simplify clinical operation according to the shape of the membrane at the defect site. However, the postoperative exposure rate of PEG membranes (approximately 50%) was much higher than that of collagen membranes (12%) in their study. This may be due to the insufficient antimicrobial properties of the PGE membrane alone. Chitosan-based PEG can be synthesized by photochemical process to improve the thermal stability domain of PGE membrane, so that it has a strong inhibition effect on bacterial growth and reduce the membrane exposure rate (Sautrot-Ba et al., 2019).

3.1.4 Polyglycolic Acid

PGA is an aliphatic polyester polymer material with the least unit carbon count and the fastest degradation rate. Compared with the

TABLE 2 | Mechanical properties of barrier membranes.

Material	Processing method	Elastic modulus(MPa)	Tensile strength (MPa)	Elongation at break (%)	References
PLGA	Electrospinning	—	2.90(0.31)	—	Jazayeri et al. (2017), Zhao et al. (2008); Fu et al. (2017)
PCL	Solvent casting technique	26.32	19.84	627.58	Tsai et al. (2019), Lee et al. (2018)
PCL/Chitosan	Coaxial electrospinning	13.26 ± 2.79	4.23 ± 0.51	—	He et al. (2017), Shi et al. (2017)
Collagen	Bio-Gide is composed of porcine type I and type III collagen fibers	—	3.4–11.4	9.6–46.8	Elgali et al. (2017), Sheikh et al. (2016), Tolstunov et al. (2019), Ha et al. (2014), Taguchi et al. (2005), Bozkurt et al. (2014), Ortolani et al. (2015)
Silk	membrane casting of SF solution	15–30	610–690	4–16	Fenbo et al., 2019, Cao and Wang (2009)
PTFE	100% pure medical-grade bio-inert PTFE	—	4.3	301	Won et al. (2016), Ha et al. (2014), Carbonell et al. (2014)
Magnesium alloys	Smelting ingots casting	41–45	341	7.6	Rahman et al. (2020), Liu et al. (2019)
Titanium and titanium alloys	Selected laser melting	2.34 ± 0.48 (graded porous titanium) 110–117 (Titanium alloys)	67.63 ± 1.33 (graded porous titanium) 2.21–7.85 (3D-printing individualized titanium mesh) 930–1140 (Titanium alloys)	—	Rothamel et al. (2012), Xiong et al. (2020), Zhang et al. (2020)
Alumina and aluminium alloys	Electrospinning	—	264 ± 4 (coarse-grained alumina) 670 ± 160 (fine-grained alumina) 620 ± 40 (ultrafine-grained alumina)	—	Zhao et al. (2018)
PCL/PLGA	Solvent casting technique	305.33 ± 65.06	3.48 ± 0.16	—	Kim et al. (2009b), Qian et al. (2016)

mainstream like PLA, the current price of PGA is relatively high and its market supply is small. PGA has good biocompatibility, which can be degraded into water and carbon dioxide in the human body, so it is widely used in surgical sutures, fracture internal fixation, tissue engineering repair materials and drug control release system. For its good degradation performance and its degradation product, PGA is rarely applied as a separate barrier membrane but applied by copolymerizating with other materials. The principle is that PGA degrades firstly, leaving pores for the polymer, exposing the active components, increasing the humoral contact area and accelerating the polymer degradation. For instance, biodegradable polymer PGA was blended into the hydroxyapatite/poly-l-lactic acid scaffold fabricated by laser 3D printing to accelerate the degradation (Shuai et al., 2020). A lot of pores produced by the degradation of the scaffold promoted the exposure of HAP from the matrix, which not only activated the deposition of bone like apatite on scaffold but also accelerated apatite growth. Otherwise, the PGA fibers have a significant effect on the physical properties of the collagen scaffolds. *In vitro* cell culture experiments showed that with the incorporation of PGA fibers, the number of attached cells increased higher than that of the collagen sponge (Toosi et al., 2019).

3.1.5 Collagen

Collagen is the main component of extracellular matrix. With particular cell adhesion sites, collagen has excellent properties on regulating cell morphology, adhesion, growth and differentiation. As one of the most widely used barrier membranes (Sbricoli et al., 2020), collagen has good biocompatibility and comes from a wide range of sources (Wessing et al., 2018). Combined with growth factors, collagen membrane is one of the ideal pre-coating membranes, which can induce new bone formation. Compared with Teflon membrane, the surface of collagen membrane is more attractive to osteoblasts and stimulates their proliferation.

Although collagen membrane has good biocompatibility, it still has problems such as irregular degradation, excessive degradation rate, poor spatial stability leading to tissue regeneration damage (Sheikh et al., 2016; Elgali et al., 2017; Tolstunov et al., 2019), lacking osteogenic potential (Zhou L. et al., 2021) and uncontrollable permeability, which can easily cause surgical site collapse (Sheikh et al., 2017b). There are several available methods for improvement. One is the preparation of nanofiber scaffold materials by electrospinning technology, which can obtain good surface area, mechanical strength and biomimetic effect. The material has better performance than polymer fiber (Cai et al., 2010). Second, multi-layer superposition to obtain good mechanical properties. Li et al. (2019) improved the performance of acellular porcine small intestinal submucosa (SIS) by cladding the lyophilized technique. Multi-layer superposition enables the membrane with mechanical solid support. No significant degradation was observed for 4 weeks, while the degradation was complete 12 weeks after implantation, which met the requirements of GBR technology to provide at least 4–6 weeks barrier effect

TABLE 3 | Biological properties of barrier membranes.

Material	Cellular cytotoxicity class	Inflammatory reaction	Osteogenic effect	References
PLGA	1	Less macrophages and multi-nucleated giant cells	After 4 weeks, the defects weakly healed	Hoornaert et al. (2016), Li et al. (2016)
		Counts of granulocytes, plasmocytes and lymphocytes, always scored less 2	After 8 weeks, partial bone healing and a few bone spicules were observed	
PLGA/ATT	0	Cell proliferation on the PLGA/ATT was better than that on the PLGA on the 1st, 3rd, and 5th days	More obvious new bone formation, abundant thick bone trabeculae, and significant newly formed capillary vessels in the bone graft area	Xie et al. (2020b)
PCL	0	The presence of PCL further increased the proliferation rate	The PCL mesh infused with bioactive hydrogel facilitated the osteogenic differentiation and mineralization of MSCs	Dubey et al. (2020); Unagolla and Jayasuriya, (2019)
PEG	0	The semi-quantitative histological obsrvation: there was abnormal inflammation, infection or cellular change in the soft tissues	Well-vascularized hard tissue was apparent at all sites	Benic and Hämmerle (2014), Jung et al. (2009b)
			The regenerated bone was similar to the surrounding native bone	
PGA	0	The fibrous connective tissue began to form of the defect after 4 weeks	Histologically, a marked increase in bone formation was observed and bony bridging occurred at 12 weeks. Ct Scans revealed that overall bone regeneration within the defect was achieved at the initial time from 0 to 12 weeks	Lin et al. (2017), Toosi et al. (2019)
Collagen	0 or 1	Patient denied any pain or discomfort	Microscopic examination revealed predominately dense, lamellar bone with scant residual foci of acellular, basophilic graft material	Sbricoli et al. (2020), Açil et al. (2014), Soesilawati et al. (2021), Momen-Heravi et al. (2018)
Chitosan	0	Larger MW (>29.2 kDa) chitosans have anti-inflammatory activity	Autogenous bone showed a histo-morphometric tendency toward increased bone formation during the first month	Oktay et al. (2010), Chang et al. (2019), Ma et al. (2014)
		Smaller MW (≤29.2 kDa) chitosans have pro-inflammatory activity		
Chitosan-collagen	0	No inflammation and residual biomaterial particles were observed on the membrane surface or in the surrounding tissues	The CNC membranes induced significant expression of osteogenic genes in MSCs	Cai et al. (2010), Ma et al. (2016)
Silk	0 or 1	the *in vivo* inflammatory reaction and foreignbody response to silk membranes is similar to or less than collagen membranes	osteoblast-like MG63 cells could attach to, survive on, and proliferated on SF membrane	Yoo et al. (2016), Melke et al. (2016), Meinel et al. (2005)
PTFE	0	An inflammatory tissue reaction within the implantation beds of the PTFE membranes was showed at day 10 post-implantation	The mean bone loss at the proximal and distal margins of the Maxilla was 0.3 and 0.3 mm. The mean bone loss of proximal and distal mandible was-0.2 mm and-0.05 mm, respectively	Chang et al. (2019), Ye et al. (2011), Di carlo et al. (2021)
Magnesium and magnesium alloys	0	No inflammatory response was observed	The experimentally prepared bone defect showed a significant increase in the near distal length 2 months after surgery	Dutta et al. (2020)
Zinc and zinc alloys	0	Intracellular zinc is thereupon free to inhibit IKKβ and negatively regulate the inflammatory process	New bone formed mainly from the periphery of bone defect area to center, and Zn membrane with 300 μm pores manifested evident osteogenic capacity	Lin et al. (2017), Seo et al. (2010)
Titanium and titanium alloys	0	No signs of infection or inflammation appeared	The newly formed ridge dimensions were 6 mm horizontally and 10 mm vertically, with complete filling of the defect observed by CBCT	Amin et al. (2020), Willis et al. (2021), Xie et al. (2020a)
Alumina and aluminium alloys	0	At the highest dosage (50 μm^3 per cell) there was significant increase in the relative gene expression of IL-8, CCL2, CCL3 and CCL4 in Al_2O_3 group	The osteo-immune environment promoted by the 50 nm nano-porous structure was conducive to the osteo-differentiation of BMSCs	Jamieson et al. (2021), Chen et al. (2017)
	0	PRF regulates the inflammatory response, enhances the anti-infection ability, and	Enamel matrix derivative in a liquid carrier system increased alkaline phosphatase	

(Continued on following page)

TABLE 3 | (*Continued*) Biological properties of barrier membranes.

Material	Cellular cytotoxicity class	Inflammatory reaction	Osteogenic effect	References
Novel membranes loaded with drugs or growth factors		avoids immune rejection and cross infection	(ALP) mRNA levels 2.5-fold and collagen1alpha2 levels 1.7-fold at 3 days, as well as bone sialoprotein levels twofold at 14 days after inoculation	Miron et al. (2017), Zhang et al. (2017), Shiran et al. (2016), Al-Hamed et al. (2019)
PLGA/PCL	0	hBMSCs were able to proliferate on the porous layer of PLCL bilayer membrane as much as on control membrane though the hBMSCs on the compact layer were significantly less in number than on the control membranes	The highest ALP activity and extracellular calcium deposit were observed on the CS/PCL nanofibrous membrane	He et al. (2017), Abe et al. (2020), Qian et al. (2016)
			The expression of osteocalcin (OCN) and Runx2 were also significantly higher compared to the pure PCL nanofibrous membrane	

(Moses et al., 2008). Third, collagen cross-linking. Collagen is cross-linked physically or chemically to improve collagen's mechanical properties and stability used for GBR (Andrei et al., 2017). Fourth, collagen based composite scaffolds for bone regeneration are fabricated by the addition of different biological materials, such as bioceramic, carbon and polymer materials (Zhang et al., 2017). It has also been suggested that by concentrating collagen membranes, the barrier functions for up to 90 days. But it may lead to altered patterns of inflammatory tissue response (Gueldenpfennig et al., 2020).

Acellular dermal matrix (ADM) membrane is also a kind of collagen membrane. After removing cells in autologous or allogeneic skin tissue, the extracellular matrix with complete structure is retained, which can be used in repairing cartilage defects with type II collagen composite modification (Tiruvannamalai Annamalai et al., 2016). Studies have found that acellular matrix membrane can further promote the production of osteogenic chemokines by forming a local microenvironment conducive to the rapid recruitment of mesenchymal stem cells during bone remodeling. For example, C-X-C chemokine receptor type 4 (CXCR4) and monocyte chemoattractant protein-1 (MCP-1), etc. (Siddiqui et al., 2017; Jin et al., 2018). Momen-Heravi et al. (2018) applied ADM to repair peri-implant bone-cracking and found that new bone was formed around the bone defect area with fine effect of bone reconstruction.

Human amniotic membrane (HAM) is one of the oldest biomaterials used for wound healing in medicine, which consists of collagen and glycosaminoglycan (GAG) as main structural components (Rameshbabu et al., 2016). Similarly to HAM, chorionic membrane is four to five times thicker than HAM (Koob et al., 2015). HAM is a good source of growth factors (Grzywocz et al., 2014), and it is considered as a surgical waste (Fénelon et al., 2018), so it is a highly available and cost-efficient tissue that might be advantageous for bone regeneration. After conservation of extracellular matrix components in fresh and preserved HAM, Fenelon M et al. found that decellularization/lyophilization of HAM increased its mechanical properties and enhanced osteogenic differentiation of human bone marrow stromal cells (hBMSCs), which significantly increased early bone regeneration (Fenelon et al., 2020). Ghanmi et al. found that fresh acellular HAM promoted bone regeneration at the critical size of bone defect (Ghanmi et al., 2018). Besides creating a decellularized amnion/chorion membrane to improve the stiffness of this membrane (Koob et al., 2015), another possibility expected to further enhance the mechanical properties of HAM is to design a multilayered DL-HAM scaffold (Swim et al., 2019).

3.1.6 Chitosan

Chitosan, also known as deacetylchitin, is chemically known as polyglucosamine (1-4)-2-amino-B-D glucose. Chitosan has been widely used in bone tissue engineering in recent years because of its good permeability, antibacterial and immunomodulatory activity, and procoagulant wound healing properties (Ma et al., 2016; Tavelli et al., 2020). The porous scaffolds of chitosan reinforced with calcium phosphate can be used as a bone substitute for bone repair and dental fillings. Besides, chitosan can be degraded by lysozyme in organisms to generate natural metabolites, which are non-toxic and can be absorbed entirely by organisms. Therefore, it is superior to be used as a drug sustained-release agent and applied in controlled release system of drug and growth factors (Morris et al., 2010). Chitosan membrane was implanted subcutaneously in rats and was found to have the ability of maintaining barrier function for up to 6 weeks (Xu et al., 2012). The degradation rate, as well as the mechanical properties of chitosan membranes can be improved by changing their molecular weight and preparation methods. By electrostatic spinning technique, chitosan can be prepared into biofunctional composite with more rigid materials.

3.1.7 Chitosan-Collagen

The addition of chitosan to collagen scaffold material can change the cross-linking of collagen fibers and enhance the structure of the composite material. The scaffold has good bone conductivity, mechanical strength and biological stability (Martino et al., 2005).

Collagen electrospun nanofiber is superior to a solid wall in cell proliferation and differentiation. Therefore, chitosan reinforced collagen nanofiber membrane can be used as a natural biological composite polymer to prepare bioabsorbable membrane for GBR purposes. *In vivo* experiments showed that the fibrous structure of chitosan-collagen nanofibrous scaffold material membrane improved the osteogenic differentiation of bone marrow mesenchymal stem cells (MSCs). Lotfi et al. (2016) developed a chitosan-collagen nanofiber scaffold material. The marginal bone maturation effect was better than that of the bio-guide membrane covered group, with normal inflammatory response, indicating good bone conduction, mechanical strength and biocompatibility. Chitosan has osteogenic properties (Thein et al., 2008) and good tissue separation (Bumgardner et al., 2007). It also has a specific modification effect on collagen biomechanical properties.

3.1.8 Silk

Silk, a macromolecule produced by Cocoon (*Bombyx mori*) or Spider (*Nephila clavipes*), can be made into a variety of biomaterials, including membranes, porous scaffolders, gels, suture materials and non-woven webs after purified (Liu et al., 2013; Qi et al., 2017). It is worth mentioning that silk fibroin (SF), a structural protein of silk, has high biocompatibility and less foreign body reaction (Midha et al., 2016; Saleem et al., 2020; Luo et al., 2021). Compared with collagen membrane, SF, as a new biomedical material, has good biocompatibility as well as excellent mechanical properties, controllable degradation and plasticity, which has been widely used in the research of bone tissue engineering. Lee et al. (2014) prepared a thin silk membrane with fiber network structure by a simple separation method. The tensile strength of the silk membrane is similar to that of the collagen membrane in dry state, while higher than that of the collagen membrane in wet state. It was found that SF membranes showed good bone regeneration in the skull defect model with less inflammation and similar volume of bone regeneration was observed compared with collagen membranes (Kim et al., 2014; Song et al., 2014). Yoo et al. (2016) proved that osteoblast-like MG63 cells could attach to, survive on, and proliferated on SF membrane, as a hint of its suitableness for the bone regeneration process. Due to the low cost of SF membranes and zero risk of infection transmission from animal tissues, their clinical use should be encouraged as an alternative to collagen membranes widely used in GBR.

3.1.9 Alginate

Alginate is salt derivatives of alginic acid and constitute long chains of polysaccharides, which provides pliability and gelling adeptness to their structure. It has favorable biocompatibility and can be cross-linked to form hydrogels to form structures similar to the extracellular matrix. It can be coated directly on the surface of the bone defect area. The alginate membrane provides a sound barrier between the connective tissue and the bone defect area. The main defect of alginate barrier membrane is its poor mechanical properties. The membrane often collapses towards the bone defect area, leading to the reduction of osteogenic effect. Therefore, alginate is suitable to be used with other materials with particular strength to prepare composite membranes or improve processing technology to overcome its shortcomings further. Take an effective interaction between the sodium alginate chain and the nanosized hydroxyapatite for an example (D'Elía et al., 2020). Higher nanoscale hydroxyapatite concentrations increase the length and branching of the polymer network, which in turn reduces the water content in the structure. The viscosity and strength of fresh hydrogels are increased while the plasticity of the membranes was reduced.

3.1.10 Poly Tetra Fluoroethylene

PTFE is a macromolecular compound, which is one of the most widely used polymers in polymer non-absorbable barrier membranes. PTFE membrane has good biocompatibility and can effectively protect blood clots, so it is regarded as the gold standard of barrier function materials (Jazayeri et al., 2017). PTFE membrane should ensure good tissue tightness in the treatment process. Expanded PTFE (e-PTFE) is a polytetrafluoroethylene treated by expansion or stretching, which has the sealing property of polytetrafluoroethylene. At the same time, the plastic deformation of modified polytetrafluoroethylene occurs under long-term continuous load. However, bacteria are easy to invade through the pores of the membrane and cause postoperative complications. If it is exposed to the human oral environment before the end of treatment, it will lead to treatment failure. Due to the occurrence of postoperative complications of membrane exposure caused by its easy bacterial invasion, it is gradually replaced by a smaller pore size Dense PTFE (d-PTFE) membrane. But, because the porosity of the d-PTFE membrane is limited, so the blood supply to this area is limited. Commercially available non-resorbable barrier membranes are usually made of Teflon. It is biocompatible, which maintains its integrity during and after implantation. It can not only treat significant, drug-free bone defects and multiwall defects, but also can affect vertical enhancement (Caballé-Serrano et al., 2018). Different from the previous view that PTEE is a bioinert material, Korzinskas et al. (2018) found that the severity of proinflammatory and anti-inflammatory PTEE was equivalent to that of collagen membrane with good biocompatibility. It is not wholly a bioinert material, which can best support bone healing in the context of inducing bone regeneration.

3.1.11 Other Polymers

Some other polymers can also be used in the fabrication of barrier membranes. Hyaluronic acid (HA), a polyanionic natural polymer, is one of the main components of the hydrophilic polymer and extracellular matrix (Sudha and Rose, 2019). Hyaluronic acid membranes were widely used in the field of orthopedics due to the effectiveness in wound healing. Studies have indicated that HA membrane has an effect close to that of the collagen (Yilmaz et al., 2021). Furthermore, membranes based on HA derivatives hold great potential to stimulate mineralization for the periodontal regeneration (Federico et al., 2021), which can be investigated for periodontal barrier applications and used to achieve bone regeneration (Park et al., 2009). Ayanoğlu et al. (2015) conducted a study on the combined use of HA membrane and allograft on bone defects of rabbits.

Results indicated that the use of HA membranes alone or in combination with graft can promote bone healing.

Poly(3-hydroxybutyrate) (PHB) is a linear of naturally produced polyesters, unbranched homopolymer consisting of (R)-3-hydroxybutyric acid units, which stored in cells by prokaryotic microorganisms under the condition of nutritional imbalance (Valappil et al., 2007). It also has the characteristics of natural degradable materials and the advantages of synthetic degradable materials (Rodriguez-Contreras, 2019). Karahaliloğlu et al. (2015) fabricated NaOH treated PHB membranes, which showed increased proliferation of human osteoblasts for GBR applications. Partial bone regeneration can be observed in bifurcation defects in dogs by the application of rigid absorbable membranes made of hydroxyapatite and PHB (Reis et al., 2013). In addition, PHB not only degrades into non-toxic oligomers (Chiulan et al., 2017), but also has been found to have positive effects on mesenchymal stem cells (Voinova et al., 2019), which might be a suitable candidate for *in vivo* use in medical applications.

3.2 Non-Polymer Barrier Membranes

3.2.1 Magnesium and Magnesium Alloys

Compared with other orthopedic degradable materials, the local magnesium-rich environment generated by the degradation of magnesium-based materials can activate different signaling pathways through various signal mediations. The environment can stimulate bone regeneration, improve the adhesion rate of osteoblasts, inhibit the activity of osteoclasts and regulate the signal transduction of osteogenic cells. Magnesium alloy has relatively active chemical properties and is easily degraded and absorbed in the physiological environment. Its degradation can promote calcium deposition. The rate of osteogenesis is fast in the early stage of osteogenesis. Its bone-guiding property is better than titanium as well (Rahman et al., 2020). In addition, magnesium has Young's modulus similar to that of human bone, which can avoid stress shielding. Thereby the surrounding natural bone can be transferred to the defect and stimulating bone remodeling (Dutta et al., 2020). Different from titanium, magnesium alloy products can self-degrade after bone tissue repair and regeneration. It can promote bone tissue healing because magnesium ion is an essential element for the human body, which is convenient for clinical promotion. In addition, magnesium alloy does not interfere with CT and MRI imaging examination after surgery (Farraro et al., 2014), which facilitates the effect after implantation. Si et al. (2021) have studied a Mg-2.0Zn-1.0Gd alloy (wt%, MZG) membrane for biomedical use. The alloy material has a favorable plastic deformation ability. In order to improve the biological corrosion resistance and cytotoxicity *in vitro*, a biodegradable magnesium alloy GBR Mesh plate with 0.6 mm Ca-P coating was developed. Experiments indicate that MZG has excellent potential for clinical application as GBR membranes.

The degradation rates of magnesium alloy are too fast and the degradation *in vivo* produces hydrogen evolution reaction, causing increase in local PH. It affects the growth of the surrounding tissue, hemolysis, dissolved bone happens, even severely limited the application of magnesium alloy in clinic. Modification of magnesium alloys can be achieved by adding alloying elements as well as surface modification. Physical modification, such as modifying microstructural features, can effectively slow down the degradation of magnesium alloy *in vitro* and *in vivo*, reduce local hydrogen evolution and pH raise, which ulteriorly improves its biocompatibility (Wu et al., 2019; Saberi et al., 2021). Magnesium alloys can be modified by integrating with other materials such as collagen. Barbeck et al. (2020) embedded HF-treated magnesium-based meshes in a collagen membrane in order to combine the mechanical properties of degradable metal with the biocompatibility of collagen membrane. However, Steigmann et al. (2020) believed that even if the integration behavior of collagen membrane was comparable, pure magnesium membrane could still meet the requirements of biocompatibility.

3.2.2 Zinc and Zinc Alloys

As an essential trace element, Zinc involves in a variety of essential biological functions such as nucleic acid metabolism, signal transduction, apoptosis regulation and gene expression (Dermience et al., 2015; Lin et al., 2017). An vitro study showed that zinc degradation in saline solution did not have a large effect on the surrounding cultures and that the zinc corrosion rate was accelerated after 120 h due to passivation (Meng et al., 2018). Zinc is a clinically ideal material with an intermediate degradation rate between magnesium and iron. Zinc plays a crucial role in the growth and mineralization of bone tissue, which directly activates aminoacyl tRNA synthetase in osteoblasts (Seo et al., 2010) and stimulates cellular protein synthesis (Storrie and Stupp, 2005). In addition, zinc inhibits bone resorption by inhibiting the formation of osteoclast-like cells in bone marrow cells (Frederickson et al., 2005). Zinc also plays an essential role in the preservation of bone mass (Amin et al., 2020). Guo et al. (2020) concluded that microporous pure zinc membranes of 300 μm have superior MC3T3-E1 cytocompatibility *in vitro* and osteogenic capacity *in vivo*, which have potential bone regeneration applications in GBR membranes.

3.2.3 Titanium and Titanium Alloys

As a non-resorbable metal barrier membrane, titanium mesh can be used as a barrier membrane alone. It can also be used to strengthen absorbable collagen membrane and enhance polytetrafluoroethylene, etc. Good biomechanical properties of titanium membrane (Alagl and Madi, 2018) can effectively maintain osteogenic space and prevent the migration of epithelial and connective tissue cells. It has been widely used to reconstruct significant jaw defects and alveolar bone defects (Abdel-Hady Gepreel and Niinomi, 2012). Bai et al. (2019) found through 3D printing technology that the thickness and aperture of titanium mesh affected the amount of new bone under the titanium mesh. Appropriate pore size and thickness played a crucial role in promoting the growth of bone tissue. It has been concluded that 0.4 mm thickness titanium mesh not only carries enough strength but also has less stimulation to the mucosa and is more suitable for clinical use. Alagl and Madi (2018) combined a nano-bone graft and alloplastic with Ti-mesh for local Ridge Augmentation. It seems to be a clinically feasible method to repair soft tissue and complex tissue defects in a relatively short time so that suitable implants can be implanted in a short period.

3.2.4 Alumina and Aluminium Alloys

In physiological environment, alumina is an inert material matrix, which is non-absorbable and extremely hard. Al_2O_3 appeared to have no significant cytotoxic effect (Jamieson et al., 2021), however, aluminium is not considered to exhibit osteogenic properties and even recognized for having adverse effects on osteoblasts (Yang et al., 2018). To overcome these limitations, some composites have been developed from two or more materials to obtain the excellent properties of a single material. For instance, bioglass and hydroxyapatite-coated porous alumina scaffolds showed higher biocompatibility and osteointegration responses compared with pure alumina scaffolds (Camilo et al., 2017). In fact, alumina is more commonly used as a sandblasting coating in dentistry. The use of particles of different sizes to obtain regular roughness values results in changes in osteoblast behavior and binding to bone (Kim et al., 2006). It also stimulates calcium to flow out of the bones (Bushinsky et al., 1995). Studies showed that titanium aluminium vanadium (TiAIV) implants sandblasted with Al_2O_3 showed higher stability ratio (ISQ) and removal torque values than TiO_2 and SiO_2 at the end of the first and third months, and had a better effect on bone bonding (Yurttutan and Keskin, 2018).

4 FUNCTIONAL MEMBRANES

With the development of barrier membrane, absorbable functional membrane has received increasing attention these years. There are three main construction methods: 1) Loading antibacterial materials to reduce the repair failure rate caused by inflammation; 2) Loading bioactive factors to increase bone mass through their own osteogenesis and synergistic osteogenesis; 3) The multilayer structure is manufactured to meet different requirements of different contact surfaces such as implant surface, bone surface and epithelial tissue in bone regeneration.

4.1 Antibacterial Barrier Membranes

When loaded with antibiotics, growth factors and adhesion factors, the synthetic membrane can be used as a delivery device for specific preparations. To ensure the effectiveness of guided bone regeneration, it is necessary to reduce inflammatory response caused by bacterial invasion. First, antibiotics were added to the barrier membrane surface. Antibiotics in the barrier membrane can effectively reduce the risk of postoperative infection. Moreover, antibiotics can slow down collagen degradation. There are many antibacterial materials can be loaded onto the barrier membranes. PEG, superhydrophobic structural coating, biomembrane matrix-degrading enzyme coating, silver-releasing ion coating, titanium dioxide photoactive coating, chlorhexidine and other substances are widely used in the fabrication of antibacterial barrier membranes. Second, the application of structural drug-loaded sustained-release systems. At present, electrospinning technology, as a traditional textile industry applying polymer technology, is introduced as a novel production strategy for nanomimetic scaffolds in the field of tissue engineering. It is also a promising controllable drug delivery system, which allows the addition of therapeutic agents to the mesh eye of nonwoven nanofibers during electrospinning. Polymer nanoparticles, nanotubes, micelles, and lipid nanoparticles can be combined with electrospun nanofibers to improve the release profile, drug safety, loading efficiency and better functionality of the fibers. The commonly used therapeutic agents are aspirin (Ghavimi et al., 2020), azithromycin (Wang Z. et al., 2019), metronidazole (He et al., 2018), antibacterial peptide (Wei et al., 2018) and so on. In addition, composite encapsulating antibacterial agents can be prepared by cross-linking technology and may even be used as drug carriers in pH-responsive controlled release drug delivery systems (Mathew et al., 2017; Bi et al., 2019).

4.2 Bioactive Barrier Membranes

The main research hotspot of modern tissue engineered bone construction is how to control a variety of growth factors with different biological activities in time to play a role in different stages of bone healing and mimic the natural osteogenesis process. It is currently proved that the most important factors are osteogenic factors and angiogenic factors. In recent years, the commonly used pro-bone tissue growth factors include bone morphogenetic protein (BMP), vascular endothelial growth factor (VEGF), platelet-derived growth factor (PDGF), insulin-like growth factor (IGF), and transforming growth factor (TGF). BMP is one of the most widely used and studied growth factors for bone tissue engineering. During bone remodeling, signal analysis of the temporal and spatial expression of BMP genes showed that they were very similar to osteogenesis and fracture healing. BMP-2 is one of the relatively known bone formation effects among all growth factors, which has the ability to promote the directional differentiation and proliferation of mesenchymal stem cells into osteoblasts. It can be combined with a variety of carriers with different properties to compose various types of bioactive restorative materials. BMP-loaded carriers can be supramolecular hydrogels (Tan et al., 2019), core-shell nanofibers (da Silva et al., 2019), acellular collagen sponges (Sun T. et al., 2018), etc. The BMP-loaded barrier membrane can obtain site preservation after tooth extraction and obtain bone enhancement at the bone defect site. Among them, the amount of bone enhancement was proportional to the dose of recombinant human BMP-2 (rhBMP-2) (Sun Y.-K. et al., 2018). Thoma et al. (2018) demonstrated that rhBMP-2-loaded xenograft bone blocks showed little difference in results at 4 months compared with autologous bone blocks that were considered as the gold standard, though autologous bone blocks were more mineralized. However, in recent years, rhBMP-9 has shown better osteogenic differentiation ability compared with rhBMP-2 (Fujioka-Kobayashi et al., 2017). Another important growth factor, VEGF, is considered to be the most potent growth factor known to induce angiogenesis (Zhang et al., 2021). It not only affects the differentiation of osteoblasts, but also plays an important role in cartilage resorption and promoting the early and late chondroossification of angiogenesis. The combined use of VEGF and rhBMP-2 can increase angiogenesis and blood supply, promote the formation of new bone and solve the

problem of vertical bone regeneration in clinical work (Schorn et al., 2017). There is also TGF (Tan et al., 2021) similar to BMP synergistic osteogenesis. In addition to growth factors, some animal and plant active components such as BMP-2-related peptide P28 (Sun T. et al., 2018), amelogenin (EMD) (Miron et al., 2017) and Icariin (ICA) (Yin et al., 2017b) have also been applied in bone tissue engineering.

4.3 Structurally Layered Barrier Membranes

Multilayer barrier membranes have been designed to meet more complex requirements to endow the barrier membranes with more affluent properties. However, although the membranes are divided into multiple layers, they should still overall meet the primary purpose of GBR, so each layer should have different biological characteristics. For example, the pore size of the inner layer (loose layer) should be large enough to meet the specific requirements of the contact surface between barrier membrane and epithelial tissue, which can stabilize the blood clot and promote the integration of soft tissue in a double-layer membrane. The outer layer (dense layer) has a relatively small pore size to maintain the osteogenic space, block the entry of soft tissue cells in the same time and allow the stem cells and nutrients to pass through. In addition, there is a gap between the bilayer structure to facilitate tissue integration (Rothamel et al., 2012). Kim S.-H. et al. (2009) prepared a double-layer collagen membrane and implanted them in rats. They found that compared with the monolayer collagen membrane, the non-crosslinked collagen membrane bilayer technique could improve the bone resorption and bone strengthening effect of the embedded bone grafting technique. Tai et al. (2014) prepared and found a polyhydroxybutyrate-biphasic calcium phosphate/chitosan membrane that had the role of guiding bone regeneration barrier membranes in periodontal tissue engineering. The membrane developed by Sheikh et al. (2016) had one surface of polyether urethane (PEU), while the other side was hydroxy-terminated polydimethylsiloxane (PDMS) coated with PEU. The non-PDMS coated side adsorbed proteins, which could repair defects in periodontal tissue regeneration and attract growth factors, while the PDMS coated side acted as a barrier for gingival epithelial cells to prevent proliferation and migration of gingival epithelial cells into the defect gap through the soft tissue flap. PCL/PLGA scaffolds obtained biological and mechanical advantages during the mixing process, making up for their respective shortcomings (Kim J. Y. et al., 2009). Abe et al. (2020) made a double phase-out membrane by solid. The PLGA and PCL polymerization method of controlling the membrane degradation can reduce the cost of placing two or more than two membranes in the clinic and reduce the waste of membrane barrier materials.

5 COMMON PROCESSING TECHNIQUES FOR BARRIER MEMBRANES

The barrier membrane processing techniques include electrostatic spinning (Yin Y. et al., 2017), 3D printing (Bai et al., 2019), chemical crosslinking (Oryan et al., 2018), phase inversion (Fu et al., 2017) and other technologies. All kinds of preparation methods have different characteristics. Among them, electrospinning and 3D printing are the most widely used preparation technologies.

Electrospinning technology refers to a method in which polymer solution or melt produce jet stretching under the action of high-pressure electrostatic field force to obtain ultrafine fiber by solvent volatilization or melt curing. This technique can be used to prepare natural polymers such as collagen, SF, alginate; polymers such as PLGA, PCL, PEG, PGA, PTFE; inorganic materials such as alumina, zinc oxide; composite materials such as chitosan-collagen. The nanofibrous film it prepared has a very large specific surface area and a very high porosity (Henry et al., 2017). Compared with traditional materials, electrospun nanofiber scaffolds not only have good diversity and high parameter controllability, but also have unique advantages in personalized applications under different tissues and physiological conditions (Zhang et al., 2012). However, it is still difficult to conduct large-scale nanofiber production because of the slow electrospinning speed, low yield, and nanofiber with too small diameter cannot be obtained. The industrialization research of electrospinning industry should be strengthened in the future.

3D printing is a kind of fast forming technology, based on mathematical model documents (Trenfield et al., 2019). It uses metal powder, plastic and other adhesive materials to make products through heat sources such as laser. 3D printed granular bone graft could better maintain bone defects and support barrier membrane without corresponding clinical tests instead. The design of 3D printed custom titanium mesh avoids nerves and blood vessels, which is important for improving the precise reconstruction of GBR and providing enough space for implantation to reduce exposure rates (Zhou T. et al., 2021). In addition, 3D printing technology is also promising for polymers (Hwang et al., 2017). Park (Park et al., 2018) used 3D printing technology to print a three-dimensional PCL stent adapted to the bone defect area of the animal model and implanted it with β-tricalcium phosphate (β-TCP) powder which successfully maintained the physical space of the bone defect site and promoted the postoperative regeneration of healthy bone without an inflammatory or infectious response. However, while 3D printing solves the needs of personalization and precision in implantation, there are still some problems, such as higher cost, more complicated individual printing process and still deviation, etc.

6 PROSPECTS OF THE GBR TECHNIQUE

There are many shortcomings in current GBR technology. First, barrier failure may occur when applying membranes. One scenario is that the membrane is exposed to the oral environment due to poor soft tissue closure. Another circumstance is that the soft tissue is well sealed but the absorbable membrane degrades and loses the barrier protection function. Moreover, it relies mainly on the body's growth potential to repair the defect. If the activity and number of stem cells are insufficient, it will difficult to predict the osteogenic effect. Therefore, it is difficult to gain satisfactory osteogenic results, if the defect is large or the body is in poor condition.

With the fast development of GBR, further improvement on barrier membrane will become to one of the most important fields in bone regeneration. One is to improve the physical and chemical properties of the membrane to enhance the barrier function, such as the use of new processing methods, preparation of multilayer structure. The other is try to improve the ability of osteogenesis, such as loading drugs and various growth factors, combining osteogenesis and angiogenesis, further reducing the immune response and so on. By enhancing the use of growth factors in the barrier membrane, GBR will improve bone regeneration effects. If the bone mass and bone are stable, it is prospective that GBR could be extended to improve bone augmentation outside the mouth. For example, GBR may become the normally auxiliary means for repairing systemic tissue defect, such as the non-benign bone defect of diabetes and osteoporosis patients, even more extensive defect repair after injury.

AUTHOR CONTRIBUTIONS

QW and DZ contributed to conception and design of the study. ZY and CW wrote the manuscript. HS edited the manuscript. All authors contributed to manuscript revision, read, and approved the submitted version.

FUNDING

This work was supported by Liaoning Science and Technology Program (No. 2021-MS-185); The Innovation and Entrepreneurship Training Program for China Medical University (x202110159201); Shenyang Science and Technology Program (No. 19-112-4-029).

REFERENCES

Abdel-Hady Gepreel, M., and Niinomi, M. (2013). Biocompatibility of Ti-Alloys for Long-Term Implantation. *J. Mech. Behav. Biomed. Mater.* 20, 407–415. doi:10.1016/j.jmbbm.2012.11.014

Abdelaziz, D., Hefnawy, A., Al-Wakeel, E., El-Fallal, A., and El-Sherbiny, I. M. (2021). New Biodegradable Nanoparticles-In-Nanofibers Based Membranes for Guided Periodontal Tissue and Bone Regeneration with Enhanced Antibacterial Activity. *J. Adv. Res.* 28, 51–62. doi:10.1016/j.jare.2020.06.014

Abe, G. L., Sasaki, J.-I., Katata, C., Kohno, T., Tsuboi, R., Kitagawa, H., et al. (2020). Fabrication of Novel Poly(lactic Acid/caprolactone) Bilayer Membrane for GBR Application. *Dent. Mater.* 36 (5), 626–634. doi:10.1016/j.dental.2020.03.013

Açil, Y., Zhang, X., Nitsche, T., Möller, B., Gassling, V., Wiltfang, J., et al. (2014). Effects of Different Scaffolds on Rat Adipose Tissue Derived Stroma Cells. *J. Cranio-Maxillofacial Surg.* 42 (6), 825–834. doi:10.1016/j.jcms.2013.11.020

Al-Hamed, F. S., Mahri, M., Al-Waeli, H., Torres, J., Badran, Z., and Tamimi, F. (2019). Regenerative Effect of Platelet Concentrates in Oral and Craniofacial Regeneration. *Front. Cardiovasc. Med.* 6, 126. doi:10.3389/fcvm.2019.00126

Alagl, A. S., and Madi, M. (2018). Localized Ridge Augmentation in the Anterior Maxilla Using Titanium Mesh, an Alloplast, and a Nano-Bone Graft: a Case Report. *J. Int. Med. Res.* 46 (5), 2001–2007. doi:10.1177/0300060518758226

Amin, N., Clark, C. C. T., Taghizadeh, M., and Djafarnejad, S. (2020). Zinc Supplements and Bone Health: The Role of the RANKL-RANK axis as a Therapeutic Target. *J. Trace Elem. Med. Biol.* 57, 126417. doi:10.1016/j.jtemb.2019.126417

Andrei, M., Dinischiotu, A., Didilescu, A. C., Ionita, D., and Demetrescu, I. (2018). Periodontal Materials and Cell Biology for Guided Tissue and Bone Regeneration. *Ann. Anat. - Anatomischer Anzeiger* 216, 164–169. doi:10.1016/j.aanat.2017.11.007

Tiruvannamalai Annamalai, R., Mertz, D. R., Daley, E. L. H., and Stegemann, J. P. (2016). Collagen Type II Enhances Chondrogenic Differentiation in Agarose-Based Modular Microtissues. *Cytotherapy* 18 (2), 263–277. doi:10.1016/j.jcyt.2015.10.015

Annibali, S., Bignozzi, I., Sammartino, G., La Monaca, G., and Cristalli, M. P. (2012). Horizontal and Vertical Ridge Augmentation in Localized Alveolar Deficient Sites: a Retrospective Case Series. *Implant Dent.* 21 (3), 175–185. doi:10.1097/ID.0b013e31824ee3e9

Aprile, P., Letourneur, D., and Simon-Yarza, T. (2020). Membranes for Guided Bone Regeneration: A Road from Bench to Bedside. *Adv. Healthc. Mat.* 9 (19), 2000707. doi:10.1002/adhm.202000707

Ayanoglu, S., Esenyel, C. Z., Adanır, O., Dedeoğlu, S., İmren, Y., and Esen, T. (2015). Effects of Hyaluronic Acid (Hyalonect) on Callus Formation in Rabbits. *Acta Orthop. Traumatol. Turc* 49 (3), 319–325. doi:10.3944/AOTT.2015.14.0231

Bai, L., Ji, P., Li, X., Gao, H., Li, L., and Wang, C. (2019). Mechanical Characterization of 3D-Printed Individualized Ti-Mesh (Membrane) for Alveolar Bone Defects. *J. Healthc. Eng.* 2019, 1–13. doi:10.1155/2019/4231872

Barbeck, M., Kühnel, L., Witte, F., Pissarek, J., Precht, C., Xiong, X., et al. (2020). Degradation, Bone Regeneration and Tissue Response of an Innovative Volume Stable Magnesium-Supported GBR/GTR Barrier Membrane. *Ijms* 21 (9), 3098. doi:10.3390/ijms21093098

Barboza, E. P., Stutz, B., Ferreira, V. F., and Carvalho, W. (2010). Guided Bone Regeneration Using Nonexpanded Polytetrafluoroethylene Membranes in Preparation for Dental Implant Placements-A Report of 420 Cases. *Implant Dent.* 19 (1), 2–7. doi:10.1097/ID.0b013e3181cda72c

Behzadi, S., Luther, G. A., Harris, M. B., Farokhzad, O. C., and Mahmoudi, M. (2017). Nanomedicine for Safe Healing of Bone Trauma: Opportunities and Challenges. *Biomaterials* 146, 168–182. doi:10.1016/j.biomaterials.2017.09.005

Benic, G. I., Eisner, B. M., Jung, R. E., Basler, T., Schneider, D., and Hämmerle, C. H. F. (2019). Hard Tissue Changes after Guided Bone Regeneration of Peri-implant Defects Comparing Block versus Particulate Bone Substitutes: 6-month Results of a Randomized Controlled Clinical Trial. *Clin. Oral Impl Res.* 30 (10), 1016–1026. doi:10.1111/clr.13515

Benic, G. I., and Hämmerle, C. H. F. (20142000). Horizontal Bone Augmentation by Means of Guided Bone Regeneration. *Periodontol. 2000* 66 (1), 13–40. doi:10.1111/prd.12039

Bi, Y.-g., Lin, Z.-t., and Deng, S.-t. (2019). Fabrication and Characterization of Hydroxyapatite/sodium Alginate/chitosan Composite Microspheres for Drug Delivery and Bone Tissue Engineering. *Mater. Sci. Eng. C* 100, 576–583. doi:10.1016/j.msec.2019.03.040

Bozkurt, A., Apel, C., Sellhaus, B., van Neerven, S., Wessing, B., Hilgers, R.-D., et al. (2014). Differences in Degradation Behavior of Two Non-cross-linked Collagen Barrier Membranes: an in Vitroandin Vivostudy. *Clin. Oral Impl. Res.* 25 (12), 1403–1411. doi:10.1111/clr.12284

Bumgardner, J. D., Chesnutt, B. M., Yuan, Y., Yang, Y., Appleford, M., Oh, S., et al. (2007). The Integration of Chitosan-Coated Titanium in Bone: an *In Vivo* Study in Rabbits. *Implant Dent.* 16 (1), 66–79. doi:10.1097/ID.0b013e3180312011

Bushinsky, D. A., Sprague, S. M., Hallegot, P., Girod, C., Chabala, J. M., and Levi-Setti, R. (1995). Effects of Aluminum on Bone Surface Ion Composition. *J. Bone Min. Res.* 10 (12), 1988–1997. doi:10.1002/jbmr.5650101219

Caballé-Serrano, J., Munar-Frau, A., Ortiz-Puigpelat, O., Soto-Penaloza, D., Peñarrocha, M., and Hernández-Alfaro, F. (2018). On the Search of the Ideal Barrier Membrane for Guided Bone Regeneration. *J. Clin. Exp. Dent.* 10 (5), e477–e483. doi:10.4317/jced.54767

Cai, Y. Z., Wang, L. L., Cai, H. X., Qi, Y. Y., Zou, X. H., and Ouyang, H. W. (2010). Electrospun Nanofibrous Matrix Improves the Regeneration of Dense Cortical Bone. *J. Biomed. Mat. Res.* 95A (1), 49–57. doi:10.1002/jbm.a.32816

Camilo, C. C., Silveira, C. A. E., Faeda, R. S., de Almeida Rollo, J. M. D., de Moraes Purquerio, B., and Fortulan, C. A. (2017). Bone Response to Porous Alumina Implants Coated with Bioactive Materials, Observed Using Different Characterization Techniques. *J. Appl. Biomaterials Funct. Mater.* 15 (3), 223–235. doi:10.5301/jabfm.5000347

Cao, Y. B., Liu, C., Pan, W. L., Tu, Y., Li, C. J., and Hua, C. G. (2019). Research Progress on the Modification of Guided Bone Regeneration Membranes. *Hua Xi Kou Qiang Yi Xue Za Zhi* 37 (3), 325–329. Chinese[Article in Chinese]. doi:10.7518/hxkq.2019.03.019

Cao, Y., and Wang, B. (2009). Biodegradation of Silk Biomaterials. *Ijms* 10 (4), 1514–1524. doi:10.3390/ijms10041514

Carbonell, J. M., Martín, I. S., Santos, A., Pujol, A., Sanz-Moliner, J. D., and Nart, J. (2014). High-density Polytetrafluoroethylene Membranes in Guided Bone and Tissue Regeneration Procedures: a Literature Review. *Int. J. Oral Maxillofac. Surg.* 43 (1), 75–84. doi:10.1016/j.ijom.2013.05.017

Carlo Reis, E. C., Borges, A. P. B., del Carlo, R. J., Oliveira, P. M., Sepúlveda, R. V., Fernandes, N. A., et al. (2013). Guided Tissue Regeneration Using Rigid Absorbable Membranes in the Dog Model of Chronic Furcation Defect. *Acta Odontol. Scand.* 71 (3-4), 372–380. doi:10.3109/00016357.2012.680909

Castro, A. G. B., Diba, M., Kersten, M., Jansen, J. A., van den Beucken, J. J. J. P., and Yang, F. (2018). Development of a PCL-Silica Nanoparticles Composite Membrane for Guided Bone Regeneration. *Mater. Sci. Eng. C* 85, 154–161. doi:10.1016/j.msec.2017.12.023

Cawood, J. I., and Howell, R. A. (1988). A Classification of the Edentulous Jaws. *Int. J. Oral Maxillofac. Surg.* 17 (4), 232–236. doi:10.1016/s0901-5027(88)80047-x

Chang, S.-H., Lin, Y.-Y., Wu, G.-J., Huang, C.-H., and Tsai, G. J. (2019). Effect of Chitosan Molecular Weight on Anti-inflammatory Activity in the RAW 264.7 Macrophage Model. *Int. J. Biol. Macromol.* 131, 167–175. doi:10.1016/j.ijbiomac.2019.02.066

Chen, Z., Ni, S., Han, S., Crawford, R., Lu, S., Wei, F., et al. (2017). Nanoporous Microstructures Mediate Osteogenesis by Modulating the Osteo-Immune Response of Macrophages. *Nanoscale* 9 (2), 706–718. doi:10.1039/c6nr06421c

Chiulan, I., Frone, A., Brandabur, C., and Panaitescu, D. (2017). Recent Advances in 3D Printing of Aliphatic Polyesters. *Bioengineering* 5 (1), 2. doi:10.3390/bioengineering5010002

Chu, C., Wang, Y., Wang, Y., Yang, R., Liu, L., Rung, S., et al. (2019). Evaluation of Epigallocatechin-3-Gallate (EGCG) Modified Collagen in Guided Bone Regeneration (GBR) Surgery and Modulation of Macrophage Phenotype. *Mater. Sci. Eng. C* 99, 73–82. doi:10.1016/j.msec.2019.01.083co;2-f

D'Elía, N. L., Rial Silva, R., Sartuqui, J., Ercoli, D., Ruso, J., Messina, P., et al. (2020). Development and Characterisation of Bilayered Periosteum-Inspired Composite Membranes Based on Sodium Alginate-Hydroxyapatite Nanoparticles. *J. Colloid Interface Sci.* 572, 408–420. doi:10.1016/j.jcis.2020.03.086

da Silva, T. N., Gonçalves, R. P., Rocha, C. L., Archanjo, B. S., Barboza, C. A. G., Pierre, M. B. R., et al. (2019). Controlling Burst Effect with PLA/PVA Coaxial Electrospun Scaffolds Loaded with BMP-2 for Bone Guided Regeneration. *Mater. Sci. Eng. C* 97, 602–612. doi:10.1016/j.msec.2018.12.020

Danesh-Sani, S. A., Loomer, P. M., and Wallace, S. S. (2016). A Comprehensive Clinical Review of Maxillary Sinus Floor Elevation: Anatomy, Techniques, Biomaterials and Complications. *Br. J. Oral Maxillofac. Surg.* 54 (7), 724–730. doi:10.1016/j.bjoms.2016.05.008

Dermience, M., Lognay, G., Mathieu, F., and Goyens, P. (2015). Effects of Thirty Elements on Bone Metabolism. *J. Trace Elem. Med. Biol.* 32, 86–106. doi:10.1016/j.jtemb.2015.06.005

Di Carlo, S., Ciolfi, A., Grasso, E., Pranno, N., De Angelis, F., Di Gioia, C., et al. (2021). A Retrospective Analysis of Treatment Outcomes Following Guided Bone Regeneration at Sites Exhibiting Severe Alveolar Ridge Atrophy. *J. Craniofac Surg.* 32 (6), e572–e578. doi:10.1097/SCS.0000000000007735

Di Martino, A., Sittinger, M., and Risbud, M. V. (2005). Chitosan: a Versatile Biopolymer for Orthopaedic Tissue-Engineering. *Biomaterials* 26 (30), 5983–5990. doi:10.1016/j.biomaterials.2005.03.016

Dubey, N., Ferreira, J. A., Daghrery, A., Aytac, Z., Malda, J., Bhaduri, S. B., et al. (2020). Highly Tunable Bioactive Fiber-Reinforced Hydrogel for Guided Bone Regeneration. *Acta Biomater.* 113, 164–176. doi:10.1016/j.actbio.2020.06.011

Dutta, S., Gupta, S., and Roy, M. (2020). Recent Developments in Magnesium Metal-Matrix Composites for Biomedical Applications: A Review. *ACS Biomater. Sci. Eng.* 6 (9), 4748–4773. doi:10.1021/acsbiomaterials.0c00678

Ebrahimi, L., Farzin, A., Ghasemi, Y., Alizadeh, A., Goodarzi, A., Basiri, A., et al. (2021). Metformin-Loaded PCL/PVA Fibrous Scaffold Preseeded with Human Endometrial Stem Cells for Effective Guided Bone Regeneration Membranes. *ACS Biomater. Sci. Eng.* 7 (1), 222–231. doi:10.1021/acsbiomaterials.0c00958

Ekladious, I., Colson, Y. L., and Grinstaff, M. W. (2019). Polymer-drug Conjugate Therapeutics: Advances, Insights and Prospects. *Nat. Rev. Drug Discov.* 18 (4), 273–294. doi:10.1038/s41573-018-0005-0

Elgali, I., Omar, O., Dahlin, C., and Thomsen, P. (2017). Guided Bone Regeneration: Materials and Biological Mechanisms Revisited. *Eur. J. Oral Sci.* 125 (5), 315–337. doi:10.1111/eos.12364

Farraro, K. F., Kim, K. E., Woo, S. L.-Y., Flowers, J. R., and McCullough, M. B. (2014). Revolutionizing Orthopaedic Biomaterials: The Potential of Biodegradable and Bioresorbable Magnesium-Based Materials for Functional Tissue Engineering. *J. Biomechanics* 47 (9), 1979–1986. doi:10.1016/j.jbiomech.2013.12.003

Federico, S., Pitarresi, G., Palumbo, F. S., Fiorica, C., Yang, F., and Giammona, G. (2021). Hyaluronan Alkyl Derivatives-Based Electrospun Membranes for Potential Guided Bone Regeneration: Fabrication, Characterization and *In Vitro* Osteoinductive Properties. *Colloids Surfaces B Biointerfaces* 197, 111438. doi:10.1016/j.colsurfb.2020.111438

Fenbo, M., Xingyu, X., and Bin, T. (2019). Strontium Chondroitin Sulfate/silk Fibroin Blend Membrane Containing Microporous Structure Modulates Macrophage Responses for Guided Bone Regeneration. *Carbohydr. Polym.* 213, 266–275. doi:10.1016/j.carbpol.2019.02.068

Fénelon, M., Chassande, O., Kalisky, J., Gindraux, F., Brun, S., Bareille, R., et al. (2018). Human Amniotic Membrane for Guided Bone Regeneration of Calvarial Defects in Mice. *J. Mater Sci. Mater Med.* 29 (6), 78. doi:10.1007/s10856-018-6086-9

Fenelon, M., Etchebarne, M., Siadous, R., Grémare, A., Durand, M., Sentilhes, L., et al. (2020). Assessment of Fresh and Preserved Amniotic Membrane for Guided Bone Regeneration in Mice. *J. Biomed. Mater Res.* 108 (10), 2044–2056. doi:10.1002/jbm.a.36964

Frederickson, C. J., Koh, J.-Y., and Bush, A. I. (2005). The Neurobiology of Zinc in Health and Disease. *Nat. Rev. Neurosci.* 6 (6), 449–462. doi:10.1038/nrn1671

Fu, J. H., and Wang, H. L. (2011). Horizontal Bone Augmentation: the Decision Tree. *Int. J. Periodontics Restor. Dent.* 31 (4), 429–436. doi:10.4012/dmj.2011-028

Fu, L., Wang, Z., Dong, S., Cai, Y., Ni, Y., Zhang, T., et al. (2017). Bilayer Poly(Lactic-Co-Glycolic acid)/Nano-Hydroxyapatite Membrane with Barrier Function and Osteogenesis Promotion for Guided Bone Regeneration. *Materials* 10 (3), 257. doi:10.3390/ma10030257

Fujioka-Kobayashi, M., Schaler, B., Shirakata, Y., Nakamura, T., Noguchi, K., Zhang, Y., et al. (2017). Comparison of Two Porcine Collagen Membranes Combined with rhBMP-2 and rhBMP-9 on Osteoblast Behavior *In Vitro*. *Int. J. Oral Maxillofac. Implants* 32 (4), e221–e230. doi:10.11607/jomi.5652

Ghanmi, S., Trigui, M., Baya, W., Ellouz, Z., Elfeki, A., Charfi, S., et al. (2018). The Periosteum-like Effect of Fresh Human Amniotic Membrane on Bone Regeneration in a Rabbit Critical-Sized Defect Model. *Bone* 110, 392–404. doi:10.1016/j.bone.2018.03.004

Ghavimi, M. A., Bani Shahabadi, A., Jarolmasjed, S., Memar, M. Y., Maleki Dizaj, S., and Sharifi, S. (2020). Nanofibrous Asymmetric Collagen/curcumin Membrane Containing Aspirin-Loaded PLGA Nanoparticles for Guided Bone Regeneration. *Sci. Rep.* 10 (1), 18200. doi:10.1038/s41598-020-75454-2

Goodier, M. C., Ronkainen, S. D., and Hylwa, S. A. (2018). Rubber Accelerators in Medical Examination and Surgical Gloves. *Dermatitis* 29 (2), 66–76. doi:10.1097/DER.0000000000000342

Grzywocz, Z., Pius-Sadowska, E., Klos, P., Gryzik, M., Wasilewska, D., Aleksandrowicz, B., et al. (2014). Growth Factors and Their Receptors Derived from Human Amniotic Cells *In Vitro*. *Folia Histochem Cytobiol.* 52 (3), 163–170. doi:10.5603/FHC.2014.0019

Gueldenpfennig, T., Houshmand, A., Najman, S., Stojanovic, S., Korzinskas, T., Smeets, R., et al. (2020). The Condensation of Collagen Leads to an Extended Standing Time and a Decreased Pro-inflammatory Tissue Response to a Newly Developed Pericardium-Based Barrier Membrane for Guided Bone Regeneration. *Vivo* 34 (3), 985–1000. doi:10.21873/invivo.11867

Guo, H., Xia, D., Zheng, Y., Zhu, Y., Liu, Y., and Zhou, Y. (2020). A Pure Zinc Membrane with Degradability and Osteogenesis Promotion for Guided Bone Regeneration: *In Vitro* and *In Vivo* Studies. *Acta Biomater.* 106, 396–409. doi:10.1016/j.actbio.2020.02.024

Ha, Y.-Y., Park, Y.-W., Kweon, H., Jo, Y.-Y., and Kim, S.-G. (2014). Comparison of the Physical Properties and *In Vivo* Bioactivities of Silkworm-Cocoon-Derived Silk Membrane, Collagen Membrane, and Polytetrafluoroethylene Membrane

for Guided Bone Regeneration. *Macromol. Res.* 22 (9), 1018–1023. doi:10.1007/s13233-014-2138-2

He, Y., Jin, Y., Wang, X., Yao, S., Li, Y., Wu, Q., et al. (2018). An Antimicrobial Peptide-Loaded Gelatin/Chitosan Nanofibrous Membrane Fabricated by Sequential Layer-By-Layer Electrospinning and Electrospraying Techniques. *Nanomaterials* 8 (5), 327. doi:10.3390/nano8050327

He, Y., Wang, W., Tang, X., and Liu, X. (2017). Osteogenic Induction of Bone Marrow Mesenchymal Cells on Electrospun Polycaprolactone/chitosan Nanofibrous Membrane. *Dent. Mat. J.* 36 (3), 325–332. doi:10.4012/dmj.2016-203

Henry, J. J. D., Yu, J., Wang, A., Lee, R., Fang, J., and Li, S. (2017). Engineering the Mechanical and Biological Properties of Nanofibrous Vascular Grafts for *In Situ* Vascular Tissue Engineering. *Biofabrication* 9 (3), 035007. doi:10.1088/1758-5090/aa834b

Hoornaert, A., d'Arros, C., Heymann, M.-F., and Layrolle, P. (2016). Biocompatibility, Resorption and Biofunctionality of a New Synthetic Biodegradable Membrane for Guided Bone Regeneration. *Biomed. Mat.* 11 (4), 045012. doi:10.1088/1748-6041/11/4/045012

Hwang, K.-S., Choi, J.-W., Kim, J.-H., Chung, H., Jin, S., Shim, J.-H., et al. (2017). Comparative Efficacies of Collagen-Based 3D Printed PCL/PLGA/β-TCP Composite Block Bone Grafts and Biphasic Calcium Phosphate Bone Substitute for Bone Regeneration. *Materials* 10 (4), 421. doi:10.3390/ma10040421

Iviglia, G., Kargozar, S., and Baino, F. (2019). Biomaterials, Current Strategies, and Novel Nano-Technological Approaches for Periodontal Regeneration. *Jfb* 10 (1), 3. doi:10.3390/jfb10010003

Jamieson, S., Mawdesley, A., Deehan, D., Kirby, J., Holland, J., and Tyson-Capper, A. (2021). Inflammatory Responses to Metal Oxide Ceramic Nanopowders. *Sci. Rep.* 11 (1), 10531. doi:10.1038/s41598-021-89329-7

Jazayeri, H. E., Tahriri, M., Razavi, M., Khoshroo, K., Fahimipour, F., Dashtimoghadam, E., et al. (2017). A Current Overview of Materials and Strategies for Potential Use in Maxillofacial Tissue Regeneration. *Mater. Sci. Eng. C* 70 (Pt 1), 913–929. doi:10.1016/j.msec.2016.08.055

Jensen, L. K., Koch, J., Aalbaek, B., Moodley, A., Bjarnsholt, T., Kragh, K. N., et al. (2017). Early Implant-Associated Osteomyelitis Results in a Peri-Implanted Bacterial Reservoir. *APMIS* 125 (1), 38–45. doi:10.1111/apm.12597

Jin, W., Liang, X., Brooks, A., Futrega, K., Liu, X., Doran, M. R., et al. (2018). Modelling of the SDF-1/CXCR4 Regulated *In Vivo* Homing of Therapeutic Mesenchymal Stem/stromal Cells in Mice. *PeerJ* 6, e6072. doi:10.7717/peerj.6072

Jung, R. E., Hälg, G. A., Thoma, D. S., and Hämmerle, C. H. F. (2009a). A Randomized, Controlled Clinical Trial to Evaluate a New Membrane for Guided Bone Regeneration Around Dental Implants. *Clin. Oral Implants Res.* 20 (2), 162–168. doi:10.1111/j.1600-0501.2008.01634.x

Jung, R. E., Lecloux, G., Rompen, E., Ramel, C. F., Buser, D., and Hammerle, C. H. F. (2009b). A Feasibility Study Evaluating Anin Situformed Synthetic Biodegradable Membrane for Guided Bone Regeneration in Dogs. *Clin. Oral Implants Res.* 20 (2), 151–161. doi:10.1111/j.1600-0501.2008.01633.x

Jung, U.-W., Lee, I.-K., Park, J.-Y., Thoma, D. S., Hämmerle, C. H. F., and Jung, R. E. (2015). The Efficacy of BMP-2 Preloaded on Bone Substitute or Hydrogel for Bone Regeneration at Peri-Implant Defects in Dogs. *Clin. Oral Impl. Res.* 26 (12), 1456–1465. doi:10.1111/clr.12491

Karahaliloglu, Z., Ercan, B., Taylor, E. N., Chung, S., Denkbaş, E. B., and Webster, T. J. (2015). Antibacterial Nanostructured Polyhydroxybutyrate Membranes for Guided Bone Regeneration. *J. Biomed. Nanotechnol.* 11 (12), 2253–2263. doi:10.1166/jbn.2015.2106

Kim, J.-Y., Yang, B.-E., Ahn, J.-H., Park, S. O., and Shim, H.-W. (2014). Comparable Efficacy of Silk Fibroin with the Collagen Membranes for Guided Bone Regeneration in Rat Calvarial Defects. *J. Adv. Prosthodont* 6 (6), 539–546. doi:10.4047/jap.2014.6.6.539

Kim, J. Y., Yoon, J. J., Park, E. K., Kim, D. S., Kim, S.-Y., and Cho, D.-W. (2009a). Cell Adhesion and Proliferation Evaluation of SFF-Based Biodegradable Scaffolds Fabricated Using a Multi-Head Deposition System. *Biofabrication* 1 (1), 015002. doi:10.1088/1758-5082/1/1/015002

Kim, M.-J., Kim, C.-W., Lim, Y.-J., and Heo, S.-J. (2006). Microrough Titanium Surface Affects Biologic Response in MG63 Osteoblast-like Cells. *J. Biomed. Mat. Res.* 79A (4), 1023–1032. doi:10.1002/jbm.a.31040

Kim, O., Choi, J., Kim, B., and Seo, D. (2020). Long-term Success Rates of Implants with Guided Bone Regeneration or Bone Grafting. *Clin. Oral Impl Res.* 31, 230. doi:10.1111/clr.171_13644

Kim, S.-H., Kim, D.-Y., Kim, K.-H., Ku, Y., Rhyu, I.-C., and Lee, Y.-M. (2009b). The Efficacy of a Double-Layer Collagen Membrane Technique for Overlaying Block Grafts in a Rabbit Calvarium Model. *Clin. Oral Implants Res.* 20 (10), 1124–1132. doi:10.1111/j.1600-0501.2009.01744.x

Koob, T. J., Lim, J. J., Zabek, N., and Massee, M. (2015). Cytokines in Single Layer Amnion Allografts Compared to Multilayer Amnion/chorion Allografts for Wound Healing. *J. Biomed. Mat. Res.* 103 (5), 1133–1140. doi:10.1002/jbm.b.33265

Korzinskas, T., Jung, O., Smeets, R., Stojanovic, S., Najman, S., Glenske, K., et al. (2018). *In Vivo* Analysis of the Biocompatibility and Macrophage Response of a Non-resorbable PTFE Membrane for Guided Bone Regeneration. *Ijms* 19 (10), 2952. doi:10.3390/ijms19102952

Lee, S.-W., and Kim, S.-G., (2014). Membranes for the Guided Bone Regeneration. *Maxillofac. Plastic Reconstr. Surg.* 36 (6), 239–246. doi:10.14402/jkamprs.2014.36.6.239

Lee, S.-Y., Wu, S.-C., Chen, H., Tsai, L.-L., Tzeng, J.-J., Lin, C.-H., et al. (2018). Synthesis and Characterization of Polycaprolactone-Based Polyurethanes for the Fabrication of Elastic Guided Bone Regeneration Membrane. *BioMed Res. Int.* 2018, 1–13. doi:10.1155/2018/3240571

Li, B. W., Wu, W. Y., Tang, L., Zhang, Y., and Liu, Y. H. (2019). Barrier Effect of Improved Porcine Small Intestinal Submucosa Absorbable Membrane on Early Healing of Mandibular Defects in Rabbits. *Beijing Da Xue Xue Bao Yi Xue Ban.* 51 (5), 887–892. [Article in Chinese]. doi:10.19723/j.issn.1671-167X.2019.05.016

Li, H., Song, P., Qiao, T., Cui, Q., Song, X., and Zhang, B. (2016). A Quaternary Composite Fiber Membrane for Guided Tissue Regeneration. *Polym. Adv. Technol.* 27 (2), 178–184. doi:10.1002/pat.3616

Lin, P.-H., Sermersheim, M., Li, H., Lee, P., Steinberg, S., and Ma, J. (2017). Zinc in Wound Healing Modulation. *Nutrients* 10 (1), 16. doi:10.3390/nu10010016

Liu, D., Xu, G., Jamali, S. S., Zhao, Y., Chen, M., and Jurak, T. (2019). Fabrication of Biodegradable HA/Mg-Zn-Ca Composites and the Impact of Heterogeneous Microstructure on Mechanical Properties, *In Vitro* Degradation and Cytocompatibility. *Bioelectrochemistry* 129, 106–115. doi:10.1016/j.bioelechem.2019.05.001

Liu, F., Chen, Q., Liu, C., Ao, Q., Tian, X., Fan, J., et al. (2018). Natural Polymers for Organ 3D Bioprinting. *Polymers* 10 (11), 1278. doi:10.3390/polym10111278

Liu, S., Dong, C., Lu, G., Lu, Q., Li, Z., Kaplan, D. L., et al. (2013). Bilayered Vascular Grafts Based on Silk Proteins. *Acta Biomater.* 9 (11), 8991–9003. doi:10.1016/j.actbio.2013.06.045

Liu, W., Dong, X., Qin, H., Sui, L., and Wang, J. (2021). Three-dimensional Porous Reduced Graphene Oxide/hydroxyapatite Membrane for Guided Bone Regeneration. *Colloids Surfaces B Biointerfaces* 208, 112102. doi:10.1016/j.colsurfb.2021.112102

Lotfi, G., Shokrgozar, M. A., Mofid, R., Abbas, F. M., Ghanavati, F., Baghban, A. A., et al. (2016). Biological Evaluation (*In Vitro* and *In Vivo*) of Bilayered Collagenous Coated (Nano Electrospun and Solid Wall) Chitosan Membrane for Periodontal Guided Bone Regeneration. *Ann. Biomed. Eng.* 44 (7), 2132–2144. doi:10.1007/s10439-015-1516-z

Luo, D., Yao, C., Zhang, R., Zhao, R., Iqbal, M. Z., Mushtaq, A., et al. (2021). Silk Fibroin/Collagen Blended Membrane Fabricated via a Green Papermaking Method for Potential Guided Bone Regeneration Application: *In Vitro* and *In Vivo* Evaluation. *ACS Biomater. Sci. Eng.* 7 (12), 5788–5797. doi:10.1021/acsbiomaterials.1c01060

Ma, S., Adayi, A., Liu, Z., Li, M., Wu, M., Xiao, L., et al. (2016). Asymmetric Collagen/chitosan Membrane Containing Minocycline-Loaded Chitosan Nanoparticles for Guided Bone Regeneration. *Sci. Rep.* 6, 18–22. doi:10.1038/srep31822

Ma, S., Chen, Z., Qiao, F., Sun, Y., Yang, X., Deng, X., et al. (2014). Guided Bone Regeneration with Tripolyphosphate Cross-Linked Asymmetric Chitosan Membrane. *J. Dent.* 42 (12), 1603–1612. doi:10.1016/j.jdent.2014.08.015

Mathew, A., Vaquette, C., Hashimi, S., Rathnayake, I., Huygens, F., Hutmacher, D. W., et al. (2017). Antimicrobial and Immunomodulatory Surface-Functionalized Electrospun Membranes for Bone Regeneration. *Adv. Healthc. Mater* 6. doi:10.1002/adhm.201601345

Meinel, L., Hofmann, S., Karageorgiou, V., Kirker-Head, C., McCool, J., Gronowicz, G., et al. (2005). The Inflammatory Responses to Silk Films *In Vitro* and *In Vivo*. *Biomaterials* 26 (2), 147–155. doi:10.1016/j.biomaterials.2004.02.047

Melke, J., Midha, S., Ghosh, S., Ito, K., and Hofmann, S. (2016). Silk Fibroin as Biomaterial for Bone Tissue Engineering. *Acta Biomater.* 31, 1–16. doi:10.1016/j.actbio.2015.09.005

Meng, Y., Liu, L., Zhang, D., Dong, C., Yan, Y., Volinsky, A. A., et al. (2019). Initial Formation of Corrosion Products on Pure Zinc in Saline Solution. *Bioact. Mater.* 4 (1), 87–96. doi:10.1016/j.bioactmat.2018.08.003

Midha, S., Tripathi, R., Geng, H., Lee, P. D., and Ghosh, S. (2016). Elucidation of Differential Mineralisation on Native and Regenerated Silk Matrices. *Mater. Sci. Eng. C* 68, 663–674. doi:10.1016/j.msec.2016.06.041

Miron, R., Fujioka-Kobayashi, M., Buser, D., Zhang, Y., Bosshardt, D., and Sculean, A. (2017). Combination of Collagen Barrier Membrane with Enamel Matrix Derivative-Liquid Improves Osteoblast Adhesion and Differentiation. *Int. J. Oral Maxillofac. Implants* 32 (1), 196–203. doi:10.11607/jomi.5011

Mohan, N., Wolf, J., and Dym, H. (2015). Maxillary Sinus Augmentation. *Dent. Clin. N. Am.* 59 (2), 375–388. doi:10.1016/j.cden.2014.10.001

Momen-Heravi, F., Peters, S. M., Garfinkle, L., and Kang, P. (2018). Acellular Dermal Matrix as a Barrier for Guided Bone Regeneration of Dehiscence Defects Around Dental Implants: A Clinical and Histological Report. *Implant Dent.* 27 (4), 521–524. doi:10.1097/ID.0000000000000796

Morris, G. A., Kök, S. M., Harding, S. E., and Adams, G. G. (2010). Polysaccharide Drug Delivery Systems Based on Pectin and Chitosan. *Biotechnol. Genet. Eng. Rev.* 27, 257–284. doi:10.1080/02648725.2010.10648153

Moses, O., Vitrial, D., Aboodi, G., Sculean, A., Tal, H., Kozlovsky, A., et al. (2008). Biodegradation of Three Different Collagen Membranes in the Rat Calvarium: a Comparative Study. *J. Periodontology* 79 (5), 905–911. doi:10.1902/jop.2008.070361

Murphy, W. L., Kohn, D. H., and Mooney, D. J. (2000). Growth of Continuous Bonelike Mineral within Porous Poly(lactide-Co-Glycolide) Scaffoldsin Vitro. *J. Biomed. Mat. Res.* 50 (1), 50–58. doi:10.1002/(sici)1097-463610.1002/(sici)1097-4636(200004)50:1<50::aid-jbm8>3.0.co;2-f

Nowwarote, N., Chanjavanakul, P., Kongdecha, P., Clayhan, P., Chumprasert, S., Manokawinchoke, J., et al. (2018). Characterization of a Bioactive Jagged1-Coated Polycaprolactone-Based Membrane for Guided Tissue Regeneration. *Archives Oral Biol.* 88, 24–33. doi:10.1016/j.archoralbio.2018.01.007

Oktay, E., Demiralp, B., Demiralp, B., Senel, S., Cevdet Akman, A., Eratalay, K., et al. (2010). Effects of Platelet-Rich Plasma and Chitosan Combination on Bone Regeneration in Experimental Rabbit Cranial Defects. *J. Oral Implantol.* 36 (3), 175–184. doi:10.1563/AAID-JOI-D-09-00023

Omar, O., Elgali, I., Dahlin, C., and Thomsen, P. (2019). Barrier Membranes: More Than the Barrier Effect? *J. Clin. Periodontol.* 46 (Suppl. 21Suppl Suppl 21), 103–123. doi:10.1111/jcpe.13068

Ortolani, E., Quadrini, F., Bellisario, D., Santo, L., Polimeni, A., and Santarsiero, A. (2015). Mechanical Qualification of Collagen Membranes Used in Dentistry. *Ann. Ist. Super. Sanita* 51 (3), 229–235. doi:10.4415/ANN_15_03_11

Oryan, A., Kamali, A., Moshiri, A., Baharvand, H., and Daemi, H. (2018). Chemical Crosslinking of Biopolymeric Scaffolds: Current Knowledge and Future Directions of Crosslinked Engineered Bone Scaffolds. *Int. J. Biol. Macromol.* 107 (Pt A), 678–688. doi:10.1016/j.ijbiomac.2017.08.184

Ovcharenko, N., Greenwell, H., Katwal, D., Patel, A., Hill, M., Shumway, B., et al. (2020). A Comparison of the Effect of Barrier Membranes on Clinical and Histologic Hard and Soft Tissue Healing with Ridge Preservation. *Int. J. Periodontics Restor. Dent.* 40 (3), 365–371. doi:10.11607/prd.4120

Park, J. K., Yeom, J., Oh, E. J., Reddy, M., Kim, J. Y., Cho, D.-W., et al. (2009). Guided Bone Regeneration by Poly(lactic-Co-Glycolic Acid) Grafted Hyaluronic Acid Bi-layer Films for Periodontal Barrier Applications. *Acta Biomater.* 5 (9), 3394–3403. doi:10.1016/j.actbio.2009.05.019

Park, S., Lee, H.-J., Kim, K.-S., Lee, S., Lee, J.-T., Kim, S.-Y., et al. (2018). *In Vivo* Evaluation of 3D-Printed Polycaprolactone Scaffold Implantation Combined with β-TCP Powder for Alveolar Bone Augmentation in a Beagle Defect Model. *Materials* 11 (2), 238. doi:10.3390/ma11020238

Qi, Y., Wang, H., Wei, K., Yang, Y., Zheng, R.-Y., Kim, I., et al. (2017). A Review of Structure Construction of Silk Fibroin Biomaterials from Single Structures to Multi-Level Structures. *Ijms* 18 (3), 237. doi:10.3390/ijms18030237

Rachmiel, A., Emodi, O., Aizenbud, D., Rachmiel, D., and Shilo, D. (2018). Two-stage Reconstruction of the Severely Deficient Alveolar Ridge: Bone Graft Followed by Alveolar Distraction Osteogenesis. *Int. J. Oral Maxillofac. Surg.* 47 (1), 117–124. doi:10.1016/j.ijom.2017.07.007

Rahman, M., Dutta, N. K., and Roy Choudhury, N. (2020). Magnesium Alloys with Tunable Interfaces as Bone Implant Materials. *Front. Bioeng. Biotechnol.* 8, 564. doi:10.3389/fbioe.2020.00564

Rakhmatia, Y. D., Ayukawa, Y., Furuhashi, A., and Koyano, K. (2013). Current Barrier Membranes: Titanium Mesh and Other Membranes for Guided Bone Regeneration in Dental Applications. *J. Prosthodont. Res.* 57 (1), 3–14. doi:10.1016/j.jpor.2012.12.001

Rameshbabu, A. P., Ghosh, P., Subramani, E., Bankoti, K., Kapat, K., Datta, S., et al. (2016). Investigating the Potential of Human Placenta-Derived Extracellular Matrix Sponges Coupled with Amniotic Membrane-Derived Stem Cells for Osteochondral Tissue Engineering. *J. Mat. Chem. B* 4 (44), 613–625. doi:10.1039/c5tb02321a

Rodriguez-Contreras, A. (2019). Recent Advances in the Use of Polyhydroyalkanoates in Biomedicine. *Bioengineering* 6 (3), 82. doi:10.3390/bioengineering6030082

Rothamel, D., Schwarz, F., Fienitz, T., Smeets, R., Dreiseidler, T., Ritter, L., et al. (2012). Biocompatibility and Biodegradation of a Native Porcine Pericardium Membrane: Results of *In Vitro* and *In Vivo* Examinations. *Int. J. Oral Maxillofac. Implants* 27 (1), 146–154. doi:10.1016/j.ijom.2011.07.902

Saarani, N. N., Jamuna-Thevi, K., Shahab, N., Hermawan, H., and Saidin, S. (2017). Antibacterial Efficacy of Triple-Layered Poly(lactic-Co-Glycolic Acid)/nanoapatite/lauric Acid Guided Bone Regeneration Membrane on Periodontal Bacteria. *Dent. Mat. J.* 36 (3), 260–265. doi:10.4012/dmj.2016-177

Saberi, A., Bakhsheshi-Rad, H. R., Abazari, S., Ismail, A. F., Sharif, S., Ramakrishna, S., et al. (2021). A Comprehensive Review on Surface Modifications of Biodegradable Magnesium-Based Implant Alloy: Polymer Coatings Opportunities and Challenges. *Coatings* 11 (7), 747. doi:10.3390/coatings11070747

Sakkas, A., Wilde, F., Heufelder, M., Winter, K., and Schramm, A. (2017). Autogenous Bone Grafts in Oral Implantology-Is it Still a "gold Standard"? A Consecutive Review of 279 Patients with 456 Clinical Procedures. *Int. J. Implant Dent.* 3 (1), 23. doi:10.1186/s40729-017-0084-4

Saleem, M., Rasheed, S., and Yougen, C. (2020). Silk Fibroin/hydroxyapatite Scaffold: a Highly Compatible Material for Bone Regeneration. *Sci. Technol. Adv. Mater.* 21 (1), 242–266. doi:10.1080/14686996.2020.1748520

Sautrot-Ba, P., Razza, N., Breloy, L., Andaloussi, S. A., Chiappone, A., Sangermano, M., et al. (2019). Photoinduced Chitosan-PEG Hydrogels with Long-Term Antibacterial Properties. *J. Mat. Chem. B* 7 (42), 6526–6538. doi:10.1039/c9tb01170f

Sbricoli, L., Guazzo, R., Annunziata, M., Gobbato, L., Bressan, E., and Nastri, L. (2020). Selection of Collagen Membranes for Bone Regeneration: A Literature Review. *Materials* 13 (3), 786. doi:10.3390/ma13030786

Schorn, L., Sproll, C., Ommerborn, M., Naujoks, C., Kübler, N. R., and Depprich, R. (2017). Vertical Bone Regeneration Using rhBMP-2 and VEGF. *Head. Face Med.* 13 (1), 11. doi:10.1186/s13005-017-0146-0

Seo, H.-J., Cho, Y.-E., Kim, T., Shin, H.-I., and Kwun, I.-S. (2010). Zinc May Increase Bone Formation through Stimulating Cell Proliferation, Alkaline Phosphatase Activity and Collagen Synthesis in Osteoblastic MC3T3-E1 Cells. *Nutr. Res. Pract.* 4 (5), 356–361. doi:10.4162/nrp.2010.4.5.356

Sheikh, Z., Hamdan, N., Ikeda, Y., Grynpas, M., Ganss, B., and Glogauer, M. (2017a). Natural Graft Tissues and Synthetic Biomaterials for Periodontal and Alveolar Bone Reconstructive Applications: a Review. *Biomater. Res.* 21, 9–20. doi:10.1186/s40824-017-0095-5

Sheikh, Z., Khan, A. S., Roohpour, N., Glogauer, M., and Rehman, I. u. (2016). Protein Adsorption Capability on Polyurethane and Modified-Polyurethane Membrane for Periodontal Guided Tissue Regeneration Applications. *Mater. Sci. Eng. C* 68, 267–275. doi:10.1016/j.msec.2016.05.026

Sheikh, Z., Qureshi, J., Alshahrani, A. M., Nassar, H., Ikeda, Y., Glogauer, M., et al. (2017b). Collagen Based Barrier Membranes for Periodontal Guided Bone Regeneration Applications. *Odontology* 105 (1), 1–12. doi:10.1007/s10266-016-0267-0

Shi, C. N., Liu, J., Wang, F., and Hong-Yu, X. U. (2017). Preparation of OPG-PLA/CS Nanofibermembranes by Coaxial Electrospinning and its Characterization. *Chin. J. Conservative Dent.* 27, 141–144. [Article in Chinese]. doi:10.15956/j.cnki.chin.j.conserv.dent.2017.03.004

Shiran, G., Fan, Z., Mengting, L., Ting, H., and Lige, Z. (2016). Preparation of Hydroxyapatite/chitosan-Transforming Growth Factor-β Composite Coatings on Titanium Surfaces and its Effect on the Attachment and Proliferation of Osteoblasts. *Hua Xi Kou Qiang Yi Xue Za Zhi* 34 (3), 229–233. [Article in Chinese]. doi:10.7518/hxkq.2016.03.003

Shuai, C., Yang, W., Feng, P., Peng, S., and Pan, H. (2021). Accelerated Degradation of HAP/PLLA Bone Scaffold by PGA Blending Facilitates Bioactivity and Osteoconductivity. *Bioact. Mater.* 6 (2), 490–502. doi:10.1016/j.bioactmat.2020.09.001

Si, J., Shen, H., Miao, H., Tian, Y., Huang, H., Shi, J., et al. (2021). *In Vitro* and *In Vivo* Evaluations of Mg-Zn-Gd Alloy Membrane on Guided Bone Regeneration for Rabbit Calvarial Defect. *J. Magnesium Alloys* 9 (1), 281–291. doi:10.1016/j.jma.2020.09.013

Siddiqui, J. A., Johnson, J., Le Henaff, C., Bitel, C. L., Tamasi, J. A., and Partridge, N. C. (2017). Catabolic Effects of Human PTH (1-34) on Bone: Requirement of Monocyte Chemoattractant Protein-1 in Murine Model of Hyperparathyroidism. *Sci. Rep.* 7 (1), 15300. doi:10.1038/s41598-017-15563-7

Soesilawati, P., Rizqiawan, A., Roestamadji, R. I., Arrosyad, A. R., Firdauzy, M. A. B., and Abu Kasim, N. H. (2021). *In Vitro* Cell Proliferation Assay of Demineralized Dentin Material Membrane in Osteoblastic MC3T3-E1 Cells. *Ccide* 13, 443–449. doi:10.2147/CCIDE.S313184

Song, J. M., Shin, S. H., Kim, Y. D., Lee, J. Y., Baek, Y. J., Yoon, S. Y., et al. (2014). Comparative Study of Chitosan/fibroin-Hydroxyapatite and Collagen Membranes for Guided Bone Regeneration in Rat Calvarial Defects: Micro-computed Tomography Analysis. *Int. J. Oral Sci.* 6 (2), 87–93. doi:10.1038/ijos.2014.16

Steigmann, L., Jung, O., Kieferle, W., Stojanovic, S., Proehl, A., Görke, O., et al. (2020). Biocompatibility and Immune Response of a Newly Developed Volume-Stable Magnesium-Based Barrier Membrane in Combination with a PVD Coating for Guided Bone Regeneration (GBR). *Biomedicines* 8 (12), 636. doi:10.3390/biomedicines8120636

Storrie, H., and Stupp, S. (2005). Cellular Response to Zinc-Containing Organoapatite: an *In Vitro* Study of Proliferation, Alkaline Phosphatase Activity and Biomineralization. *Biomaterials* 26 (27), 5492–5499. doi:10.1016/j.biomaterials.2005.01.043

Sudha, P. N., and Rose, M. H. (2014). Beneficial Effects of Hyaluronic Acid. *Adv. Food Nutr. Res.* 72, 137–176. doi:10.1016/B978-0-12-800269-8.00009-9

Sun, T., Liu, M., Yao, S., Ji, Y., Shi, L., Tang, K., et al. (2018a). Guided Osteoporotic Bone Regeneration with Composite Scaffolds of Mineralized ECM/heparin Membrane Loaded with BMP2-Related Peptide. *Ijn* 13, 791–804. doi:10.2147/IJN.S152698

Sun, X., Xu, C., Wu, G., Ye, Q., and Wang, C. (2017). Poly(Lactic-co-Glycolic Acid): Applications and Future Prospects for Periodontal Tissue Regeneration. *Polymers* 9 (6), 189. doi:10.3390/polym9060189

Sun, Y.-K., Cha, J.-K., Thoma, D. S., Yoon, S.-R., Lee, J.-S., Choi, S.-H., et al. (2018b). Bone Regeneration of Peri-Implant Defects Using a Collagen Membrane as a Carrier for Recombinant Human Bone Morphogenetic Protein-2. *BioMed Res. Int.* 2018, 1–9. doi:10.1155/2018/5437361

Swim, M. M., Albertario, A., Iacobazzi, D., Caputo, M., and Ghorbel, M. T. (2019). Amnion-Based Scaffold with Enhanced Strength and Biocompatibility for *In Vivo* Vascular Repair. *Tissue Eng. Part A* 25 (7-8), 603–619. doi:10.1089/ten.TEA.2018.0175

Taguchi, Y., Amizuka, N., Nakadate, M., Ohnishi, H., Fujii, N., Oda, K., et al. (2005). A Histological Evaluation for Guided Bone Regeneration Induced by a Collagenous Membrane. *Biomaterials* 26 (31), 6158–6166. doi:10.1016/j.biomaterials.2005.03.023

Tai, H.-Y., Fu, E., Cheng, L.-P., and Don, T.-M. (2014). Fabrication of Asymmetric Membranes from Polyhydroxybutyrate and Biphasic Calcium Phosphate/chitosan for Guided Bone Regeneration. *J. Polym. Res.* 21 (5), 1–11. doi:10.1007/s10965-014-0421-8

Tan, J., Zhang, M., Hai, Z., Wu, C., Lin, J., Kuang, W., et al. (2019). Sustained Release of Two Bioactive Factors from Supramolecular Hydrogel Promotes Periodontal Bone Regeneration. *ACS Nano* 13 (5), 5616–5622. doi:10.1021/acsnano.9b00788

Tan, Y., Zhang, L., Rajoka, M. S. R., Mai, Z., Bahadur, A., Mehwish, H. M., et al. (2021). Jawbones Scaffold Constructed by TGF-B1 and BMP-2 Loaded Chitosan Microsphere Combining with Alg/HA/ICol for Osteogenic-Induced Differentiation. *Polymers* 13 (18), 3079. doi:10.3390/polym13183079

Tavelli, L., McGuire, M. K., Zucchelli, G., Rasperini, G., Feinberg, S. E., Wang, H. L., et al. (2020). Extracellular Matrix-based Scaffolding Technologies for Periodontal and Peri-implant Soft Tissue Regeneration. *J. Periodontol.* 91 (1), 17–25. doi:10.1002/JPER.19-0351

Thein-Han, W. W., Kitiyanant, Y., and Misra, R. D. K. (2008). Chitosan as Scaffold Matrix for Tissue Engineering. *Mater. Sci. Technol.* 24, 1062–1075. doi:10.1179/174328408X341753

Thoma, D. S., Payer, M., Jakse, N., Bienz, S. P., Hüsler, J., Schmidlin, P. R., et al. (2018). Randomized, Controlled Clinical Two-Centre Study Using Xenogeneic Block Grafts Loaded with Recombinant Human Bone Morphogenetic Protein-2 or Autogenous Bone Blocks for Lateral Ridge Augmentation. *J. Clin. Periodontol.* 45 (2), 265–276. doi:10.1111/jcpe.12841

Tolstunov, L., Hamrick, J. F. E., Broumand, V., Shilo, D., and Rachmiel, A. (2019). Bone Augmentation Techniques for Horizontal and Vertical Alveolar Ridge Deficiency in Oral Implantology. *Oral Maxillofac. Surg. Clin. N. Am.* 31 (2), 163–191. doi:10.1016/j.coms.2019.01.005

Toosi, S., Naderi-Meshkin, H., Kalalinia, F., HosseinKhani, H., Heirani-Tabasi, A., Havakhah, S., et al. (2019). Bone Defect Healing Is Induced by Collagen Sponge/polyglycolic Acid. *J. Mater Sci. Mater Med.* 30 (3), 33. doi:10.1007/s10856-019-6235-9

Trenfield, S. J., Awad, A., Madla, C. M., Hatton, G. B., Firth, J., Goyanes, A., et al. (2019). Shaping the Future: Recent Advances of 3D Printing in Drug Delivery and Healthcare. *Expert Opin. Drug Deliv.* 16 (10), 1081–1094. doi:10.1080/17425247.2019.1660318

Tsai, S.-W., Yu, W.-X., Hwang, P.-A., Hsu, Y.-W., and Hsu, F.-Y. (2019). Fabrication and Characteristics of PCL Membranes Containing Strontium-Substituted Hydroxyapatite Nanofibers for Guided Bone Regeneration. *Polymers* 11 (11), 1761. doi:10.3390/polym11111761

Unagolla, J. M., and Jayasuriya, A. C. (2019). Enhanced Cell Functions on Graphene Oxide Incorporated 3D Printed Polycaprolactone Scaffolds. *Mater. Sci. Eng. C* 102, 1–11. doi:10.1016/j.msec.2019.04.026

Valappil, S. P., Peiris, D., Langley, G. J., Herniman, J. M., Boccaccini, A. R., Bucke, C., et al. (2007). Polyhydroxyalkanoate (PHA) Biosynthesis from Structurally Unrelated Carbon Sources by a Newly Characterized Bacillus Spp. *J. Biotechnol.* 127 (3), 475–487. doi:10.1016/j.jbiotec.2006.07.015

Voinova, V., Bonartseva, G., and Bonartsev, A. (2019). Effect of Poly(3-Hydroxyalkanoates) as Natural Polymers on Mesenchymal Stem Cells. *Wjsc* 11 (10), 764–786. doi:10.4252/wjsc.v11.i10.764

Wang, H.-L., and Boyapati, L. (2006). "PASS" Principles for Predictable Bone Regeneration. *Implant Dent.* 15 (1), 8–17. doi:10.1097/01.id.0000204762.39826.0f

Wang, Y., Jiang, Y., Zhang, Y., Wen, S., Wang, Y., and Zhang, H. (2019a). Dual Functional Electrospun Core-Shell Nanofibers for Anti-infective Guided Bone Regeneration Membranes. *Mater. Sci. Eng. C* 98, 134–139. doi:10.1016/j.msec.2018.12.115

Wang, Z., Liang, R., Jiang, X., Xie, J., Cai, P., Chen, H., et al. (2019b). Electrospun PLGA/PCL/OCP Nanofiber Membranes Promote Osteogenic Differentiation of Mesenchymal Stem Cells (MSCs). *Mater. Sci. Eng. C* 104, 109796. doi:10.1016/j.msec.2019.109796

Wechsler, S., Fehr, D., Molenberg, A., Raeber, G., Schense, J. C., and Weber, F. E. (2008). A Novel, Tissue Occlusive Poly(ethylene Glycol) Hydrogel Material. *J. Biomed. Mat. Res.* 85A (2), 285–292. doi:10.1002/jbm.a.31477

Wei, Y., Chang, Y.-H., Liu, C.-J., and Chung, R.-J. (2018). Integrated Oxidized-Hyaluronic Acid/Collagen Hydrogel with β-TCP Using Proanthocyanidins as a Crosslinker for Drug Delivery. *Pharmaceutics* 10 (2), 37. doi:10.3390/pharmaceutics10020037

Wessing, B., Lettner, S., and Zechner, W. (2018). Guided Bone Regeneration with Collagen Membranes and Particulate Graft Materials: A Systematic Review and Meta-Analysis. *Int. J. Oral Maxillofac. Implants* 33 (1), 87–100. doi:10.11607/jomi.5461

Williams, D. F. (2008). On the Mechanisms of Biocompatibility. *Biomaterials* 29 (20), 2941–2953. doi:10.1016/j.biomaterials.2008.04.023

Willis, J., Li, S., Crean, S. J., and Barrak, F. N. (2021). Is Titanium Alloy Ti-6Al-4 V Cytotoxic to Gingival Fibroblasts-A Systematic Review. *Clin. Exp. Dent. Res.* 7 (6), 1037–1044. doi:10.1002/cre2.444

Won, J.-Y., Park, C.-Y., Bae, J.-H., Ahn, G., Kim, C., Lim, D.-H., et al. (2016). Evaluation of 3D Printed PCL/PLGA/β -TCP versus Collagen Membranes for

Guided Bone Regeneration in a Beagle Implant Model. *Biomed. Mat.* 11 (5), 055013. doi:10.1088/1748-6041/11/5/055013

Wu, T.-C., Joshi, S. S., Ho, Y.-H., Pantawane, M. V., Sinha, S., and Dahotre, N. B. (2021). Microstructure and Surface Texture Driven Improvement in *In-Vitro* Response of Laser Surface Processed AZ31B Magnesium Alloy. *J. Magnesium Alloys* 9, 1406–1418. doi:10.1016/j.jma.2020.11.002

Wu, W., Li, B., Liu, Y., Wang, X., and Tang, L. (20182018). Effect of Multilaminate Small Intestinal Submucosa as a Barrier Membrane on Bone Formation in a Rabbit Mandible Defect Model. *BioMed Res. Int.* 2018, 1-11. doi:10.1155/2018/3270293

Xie, X., Shi, X., Wang, S., Cao, L., Yang, C., and Ma, Z. (2020a). Effect of Attapulgite-Doped Electrospun Fibrous PLGA Scaffold on Pro-osteogenesis and Barrier Function in the Application of Guided Bone Regeneration. *Ijn* 15, 6761–6777. doi:10.2147/IJN.S244533

Xie, Y., Li, S., Zhang, T., Wang, C., and Cai, X. (2020b). Titanium Mesh for Bone Augmentation in Oral Implantology: Current Application and Progress. *Int. J. Oral Sci.* 12 (1), 37. doi:10.1038/s41368-020-00107-z

Xiong, Y.-Z., Gao, R.-N., Zhang, H., Dong, L.-L., Li, J.-T., and Li, X. (2020). Rationally Designed Functionally Graded Porous Ti6Al4V Scaffolds with High Strength and Toughness Built via Selective Laser Melting for Load-Bearing Orthopedic Applications. *J. Mech. Behav. Biomed. Mater.* 104, 103673. doi:10.1016/j.jmbbm.2020.103673

Xu, C., Lei, C., Meng, L., Wang, C., and Song, Y. (2012). Chitosan as a Barrier Membrane Material in Periodontal Tissue Regeneration. *J. Biomed. Mat. Res.* 100B (5), 1435–1443. doi:10.1002/jbm.b.32662

Yang, X., Zhang, J., Ji, Q., Wang, F., Song, M., and Li, Y. (2018). Autophagy Protects MC3T3-E1 Cells upon Aluminum-Induced Apoptosis. *Biol. Trace Elem. Res.* 185 (2), 433–439. doi:10.1007/s12011-018-1264-7

Ye, H., Zhu, J., Deng, D., Jin, S., Li, J., and Man, Y. (2019). Enhanced Osteogenesis and Angiogenesis by PCL/chitosan/Sr-doped Calcium Phosphate Electrospun Nanocomposite Membrane for Guided Bone Regeneration. *J. Biomaterials Sci. Polym. Ed.* 30 (16), 1505–1522. doi:10.1080/09205063.2019.1646628

Ye, J., Yao, Q., Anchun, M., Nie, J., Cui Ye, W., Liu, W., et al. (2011). Effects of an Antibacterial Membrane on Osteoblast-like Cells *In Vitro*. *Ijn* 6, 1853–1861. doi:10.2147/IJN.S17749

Yilmaz, C., Ersanli, S., Karabagli, M., Olgac, V., and Bolukbasi Balcioglu, N. (2021). May Autogenous Grafts Increase the Effectiveness of Hyalonect Membranes in Intraosseous Defects: An Experimental *In Vivo* Study. *Medicina* 57 (5), 430. doi:10.3390/medicina57050430

Yin, L., Wang, K., Lv, X., Sun, R., Yang, S., Yang, Y., et al. (2017a). The Fabrication of an ICA-SF/PLCL Nanofibrous Membrane by Coaxial Electrospinning and its Effect on Bone Regeneration *In Vitro* and *In Vivo*. *Sci. Rep.* 7 (1), 8616. doi:10.1038/s41598-017-07759-8

Yin, L., Yang, S., He, M., Chang, Y., Wang, K., Zhu, Y., et al. (2017b). Physicochemical and Biological Characteristics of BMP-2/igf-1-Loaded Three-Dimensional Coaxial Electrospun Fibrous Membranes for Bone Defect Repair. *J. Mater Sci. Mater Med.* 28 (6), 94. doi:10.1007/s10856-017-5898-3

Yin, Y., Pu, D., and Xiong, J. (2017c). Analysis of the Comprehensive Tensile Relationship in Electrospun Silk Fibroin/Polycaprolactone Nanofiber Membranes. *Membranes* 7 (4), 67. doi:10.3390/membranes7040067

Yoo, C.-K., Jeon, J.-Y., Kim, Y.-J., Kim, S.-G., and Hwang, K.-G. (2016). Cell Attachment and Proliferation of Osteoblast-like MG63 Cells on Silk Fibroin Membrane for Guided Bone Regeneration. *Maxillofac. Plast. Reconstr. Surg.* 38 (1), 17. doi:10.1186/s40902-016-0062-4

Yurttutan, M. E., and Keskin, A. (2018). Evaluation of the Effects of Different Sand Particles that Used in Dental Implant Roughened for Osseointegration. *BMC Oral Health* 18 (1), 47. doi:10.1186/s12903-018-0509-3

Zhang, C., Zhang, T., Geng, T., Wang, X., Lin, K., and Wang, P. (2021). Dental Implants Loaded with Bioactive Agents Promote Osseointegration in Osteoporosis: A Review. *Front. Bioeng. Biotechnol.* 9, 591796. doi:10.3389/fbioe.2021.591796

Zhang, D., Tong, A., Zhou, L., Fang, F., and Guo, G. (2012). Osteogenic Differentiation of Human Placenta-Derived Mesenchymal Stem Cells (PMSCs) on Electrospun Nanofiber Meshes. *Cytotechnology* 64 (6), 701–710. doi:10.1007/s10616-012-9450-5

Qian, Y., Zhang, F., Chen, H., Xu, Y., Yang, J., Zhou, X., et al. (2016). The Preosteoblast Response of Electrospinning PLGA/PCL Nanofibers: Effects of Biomimetic Architecture and Collagen I. *Ijn* 11, 4157–4171. doi:10.2147/IJN.S110577

Zhang, J., Ma, S., Liu, Z., Geng, H., Lu, X., Zhang, X., et al. (2017). Guided Bone Regeneration with Asymmetric Collagen-Chitosan Membranes Containing Aspirin-Loaded Chitosan Nanoparticles. *Ijn* 12, 8855–8866. doi:10.2147/IJN.S148179

Zhang, Y. S., Zhang, K., Chen, X. W., Mu, H. Z., Ding, W. W., Qin, M. L., et al. (2020). Mechanical Properties of 3D-Printed Titanium Mesh and its Biocompatibility *In Vitro*. *Shanghai Kou Qiang Yi Xue* 29 (3), 250–256. [Article in Chinese]. doi:10.19439/j.sjos.2020.03.005

Zhao, L., He, C., Gao, Y., Cen, L., Cui, L., and Cao, Y. (2008). Preparation and Cytocompatibility of PLGA Scaffolds with Controllable Fiber Morphology and Diameter Using Electrospinning Method. *J. Biomed. Mat. Res.* 87B (1), 26–34. doi:10.1002/jbm.b.31060

Zhao, M., Sun, Y., Zhang, J., and Zhang, Y. (2018). Novel Translucent and Strong Submicron Alumina Ceramics for Dental Restorations. *J. Dent. Res.* 97 (3), 289–295. doi:10.1177/0022034517733742

Zhou, L., Su, Y., Wang, J., Wang, J., Wang, X., and Liu, Q. (2021a). Effect of Exposure Rates with Customized versus Conventional Titanium Mesh on Guided Bone Regeneration: A Systematic Review and Meta-Analysis. *J. Oral Implantol.* doi:10.1563/aaid-joi-D-20-00200

Zhou, T., Chen, S., Ding, X., Hu, Z., Cen, L., and Zhang, X. (2021b). Fabrication and Characterization of Collagen/PVA Dual-Layer Membranes for Periodontal Bone Regeneration. *Front. Bioeng. Biotechnol.* 9, 630977. doi:10.3389/fbioe.2021.630977

Conflict of Interest: The authors declare that the research was conducted in the absence of any commercial or financial relationships that could be construed as a potential conflict of interest.

Publisher's Note: All claims expressed in this article are solely those of the authors and do not necessarily represent those of their affiliated organizations, or those of the publisher, the editors and the reviewers. Any product that may be evaluated in this article, or claim that may be made by its manufacturer, is not guaranteed or endorsed by the publisher.

frontiers | Frontiers in Bioengineering and Biotechnology

TYPE Review
PUBLISHED 22 July 2022
DOI 10.3389/fbioe.2022.941077

OPEN ACCESS

EDITED BY
Jianshe Hu,
Northeastern University, China

REVIEWED BY
Padmani Sandhu,
Chandigarh University, India
Angel León-Buitimea,
Universidad Autonoma de Nuevo Leon, Mexico
Nibedita Mahata,
National Institute of Technology, India

*CORRESPONDENCE
Shu Shen,
shenshu55@163.com

SPECIALTY SECTION
This article was submitted to Biomaterials, a section of the journal Frontiers in Bioengineering and Biotechnology

RECEIVED 11 May 2022
ACCEPTED 29 June 2022
PUBLISHED 22 July 2022

CITATION
Shao L, Shen S and Liu H (2022), Recent advances in PLGA micro/nanoparticle delivery systems as novel therapeutic approach for drug-resistant tuberculosis.
Front. Bioeng. Biotechnol. 10:941077.
doi: 10.3389/fbioe.2022.941077

Recent advances in PLGA micro/nanoparticle delivery systems as novel therapeutic approach for drug-resistant *tuberculosis*

Liqun Shao, Shu Shen* and Huan Liu

Department of Respiratory, Shenyang Tenth People's Hospital, Shenyang Chest Hospital, Shenyang, China

Tuberculosis is a severe infectious disease caused by *Mycobacterium tuberculosis* and is a significant public health concern globally. The World Health Organization (WHO) recommends a combination regimen of several drugs, such as rifampicin (RIF), isoniazid (INH), pyrazinamide (PZA), and ethambutol (ETB), to treat *tuberculosis*. However, these drugs have low plasma concentrations after oral administration and require multiple high doses, which may lead to the occurrence and development of drug-resistant *tuberculosis*. Micro/Nanotechnology drug delivery systems have considerable potential in treating drug-resistant *tuberculosis*, allowing the sustained release of the drug and delivery of the drug to a specific target. These system properties could improve drug bioavailability, reduce the dose and frequency of administration, and solve the problem of non-adherence to the prescribed therapy. This study systematically reviewed the recent advances in PLGA micro/nanoparticle delivery systems as a novel therapeutic approach for drug-resistant *tuberculosis*.

KEYWORDS

PLGA microparticles, PLGA nanoparticles, drug-resistant *tuberculosis*, *Mycobacterium tuberculosis*, combination therapy, inhalable therapy

Introduction

Human *tuberculosis* (TB) is one of the top 10 causes of death globally and the leading cause of death from a single infectious disease (Reid et al., 2019), which has become a global public health emergency (Figure 1). World Health Organization (WHO) estimates that approximately 9.9 million cases have contracted *tuberculosis* worldwide in 2020 (World Health Organization, 2021a), and there were 1.2 million deaths from *tuberculosis* in 2019 (World Health Organization, 2020). Pulmonary *tuberculosis* is the typical manifestation of *tuberculosis*, accounting for approximately 80% of *tuberculosis* cases (World Health Organization, 2020). WHO recommends a 2-month intensive regimen followed by an additional four to 6 months continuation regimen for *tuberculosis* treatment (Table 1). During the intensive treatment phase, patients are administered four anti-TB drugs daily, including rifampicin (RIF), isoniazid (INH), pyrazinamide (PZA), and ethambutol (ETB), while the continuation treatment phase requires daily RIF and INH (World Health Organization, 2010). Usually, poor patient adherence occurs

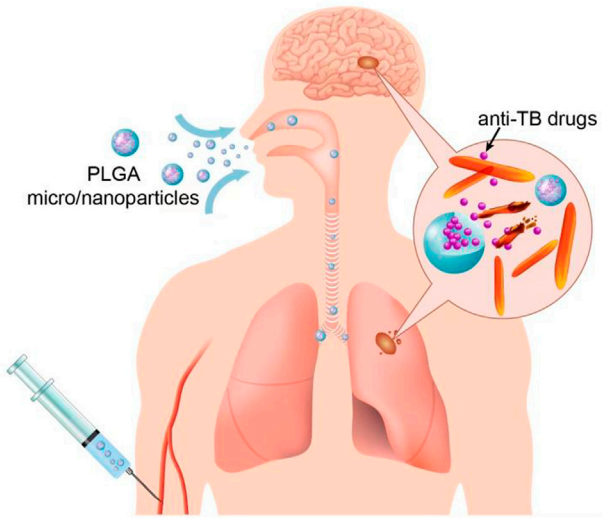

GRAPHICAL ABSTRACT

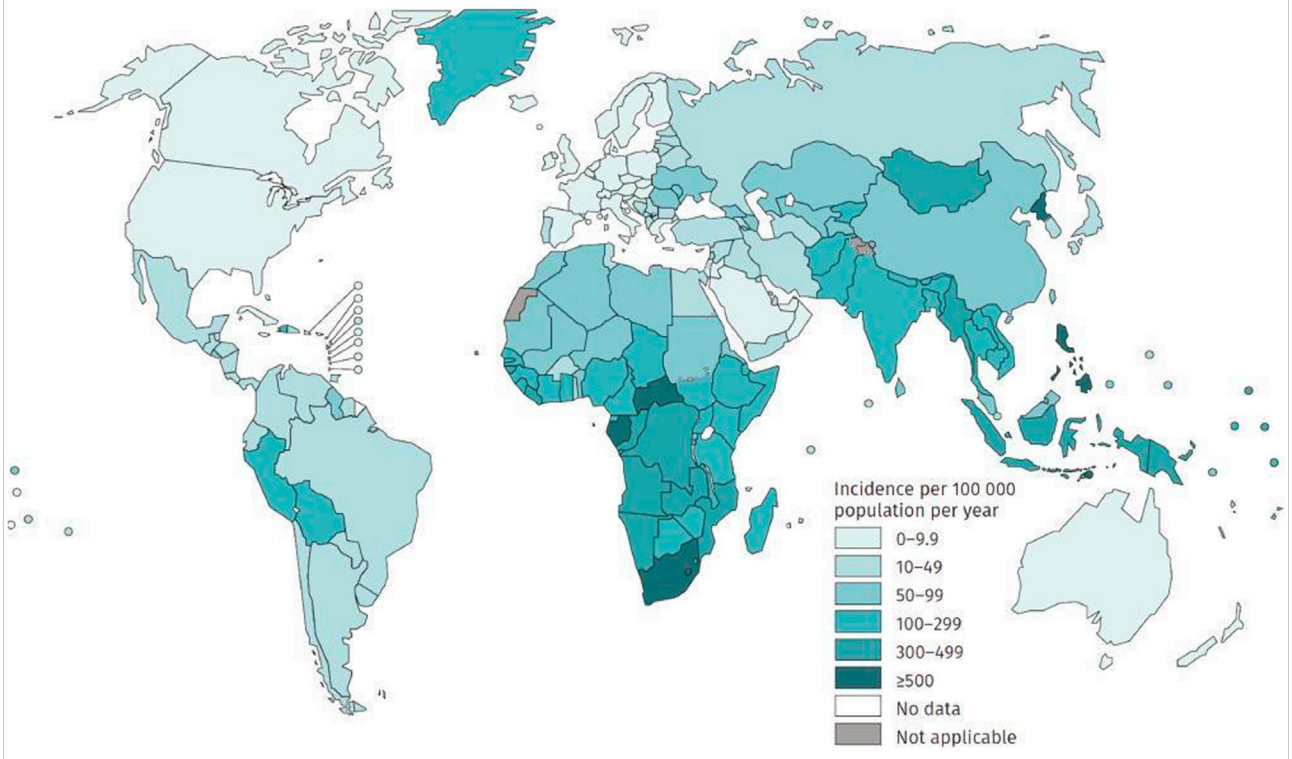

FIGURE 1
Estimated *tuberculosis* incidence rates, 2020 (excerpted from Global Tuberculosis Report, 2021; World Health Organization, Geneva).

under this administration, resulting in *drug-resistant tuberculosis* (DR-TB), including *multidrug-resistant tuberculosis* (MDR-TB) or *extensively drug-resistant tuberculosis* (XDR-TB) (World Health Organization, 2021b). *Drug-resistant tuberculosis* has become a significant public health concern in many countries (Figure 2). In recent years, the number of patients with *drug-resistant tuberculosis* has steadily increased globally (Lange et al., 2019). According to the WHO Tuberculosis Report 2019, there

TABLE 1 Regimen for treatment for *tuberculosis*.

	Under 50 kg	Over 50 kg
Intensive phase (2 months)		
RIF/INH/PYZ/ETB	4 tablets	5 tablets
Combination tablet 120/60/300/200 mg daily, 5 days per week		
Continuation phase (4–6 months)		
RIF/INH		
Combination tablet 150/100 mg	3 tablets	—
Combination tablet 300/150 mg	—	2 tablets

were nearly 5,00,000 new cases of rifampicin-resistant *tuberculosis* in the world in 2018, of which 78% were MDR-TB (World Health Organization, 2019a). Effectively controlling the epidemic of *drug-resistant tuberculosis* is still one of the significant challenges in the public health field of the world.

Various treatment approaches have been developed to combat this global emergence of *drug-resistant tuberculosis* (Patil et al., 2018). Recently, drug delivery methods which can deliver anti-tuberculosis drugs to specific sites in a controlled manner have received much attention. To make the anti-tuberculosis drug continuously released at the lesion site, the sustained-release system uses degradable polymers as the carrier comes into being, where the drug can be released for an extended period *via* a membrane or matrix-controlled diffusion (Kumar and Aeila, 2019; Jana et al., 2021). Such systems can reduce dose and frequency of administration to enhance patient compliance with treatment and control the distribution of drugs in tissues and the clearance rate in the blood to minimize the risk of toxicity and other side effects. The development of these advanced drug delivery systems provides an excellent alternative to addressing treatment failure due to patient non-adherence. Several micro/nanoparticles sized sustained-release systems have been designed for drug encapsulation to treat *tuberculosis* (Table 2).

Poly (lactic-co-glycolic acid) and poly (lactic-co-glycolic acid) micro/nanoparticles

Poly (lactic-co-glycolic acid) (PLGA) is one of the most successfully developed biodegradable polymers with a wide range of degradation times that can be tuned by its molecular weight and copolymer ratio. PLGA is soluble in common solvents and can be processed into virtually any shape and size. Therefore, PLGA polymers have been primarily tested as delivery vehicles for drugs, proteins, and other macromolecules

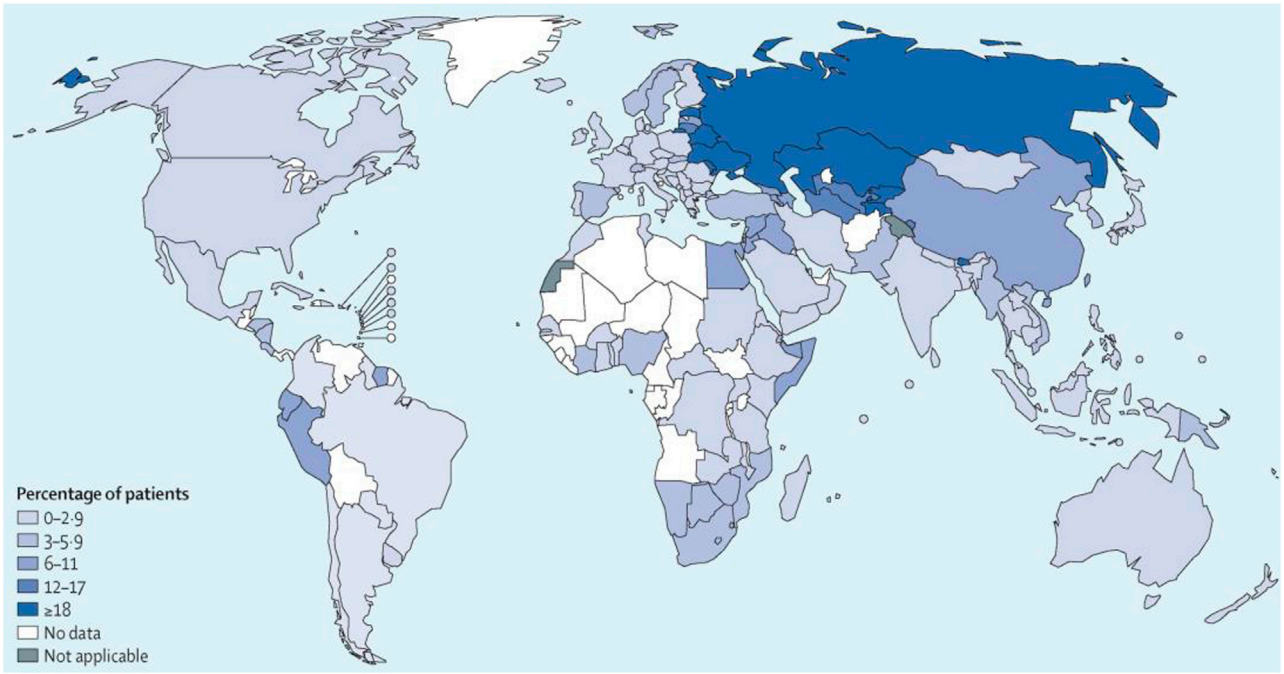

FIGURE 2
Percentages of patients with *multidrug-resistant tuberculosis* globally. Reproduced with permission from Lange et al. (2019). Copyright © 2019 Elsevier Ltd.

TABLE 2 Several micro/nanoparticles sized sustained-release systems for drug encapsulation to treat *tuberculosis*.

Type	Carrier	Drug	Size	Results	References
Microspheres	PLGA/PLA	Rapamycin without/with isoniazid and rifabutin	0.7–4.7 μm	Lung macrophages were better targeted when microsphere-based Nanoparticles were used.	Gupta et al. (2016)
Nanocapsules	Lipid	Tilmicosin	85–186 nm	Tilmicosin-loaded Lipid lipid-core nanocapsules Suggest more efficient treatment in comparison to the conventional Tilmicosin.	Al-Qushawi et al. (2016)
Nanoparticles	Lipid	Rifampicin	315 nm	The mannosylated Nanostructured lipid carriers (NLCS) showed efficient uptake by bone marrow derived macrophages. Further, rifampicin-loaded mannosylatedNLCS were more efficient in reducing mycobacteria's intracellular growth.	Vieira et al. (2017)
Microspheres	Polyamidoamine dendrimers	Rifampicin	~6 μm	The formulations could maintain drug plasma concentration above the minimal inhibitory concentration (mic) of an antibiotic for a more extended period	Rajabnezhad et al. (2016)
Nanoparticles	Graphene oxide	Ethambutol	59 nm	Sustained release of the drug resulted in better bioavailability. In addition, the designed formulation demonstrated high biocompatibility with mouse fibroblast cells.	Saifullah et al. (2017)
Micelles	PEG-PLA	Isoniazid/rifampicin	187.9 nm	Loaded micelles are less haemolytic and have lower MIC values for Mtb compared to free drug	Rani et al. (2018)
Nanocapsules	Chitosan	Bedaquiline	328 nm	The *in vitro* antimicrobial activity of the drug against TB strain H37Rv was still as effective as the free drug. Moreover, no cytotoxic effect on A549, hepg2 and THP-1 cell lines of bedaquiline-loaded nanocarriers was observed at the concentration needed to kill the bacteria.	De Matteis et al. (2018)
Micelles	Amphiphilic block copolypeptide	Bedaquiline	~250 nm	The encapsulated bedaquiline shows increased *in vitro* activity against *Mycobacterium tuberculosis* compared to free bedaquiline.	Soria-Carrera et al. (2019)
Nanoparticles	PCL	Ethambutol	280–300 nm	Nanoparticles reduced mycobacterial infection with the same efficacy observed in the case treated with ethambutol alone.	Helal-Neto et al. (2019)
Nanoparticles	Chitosan	Clofazimine	132–184 nm	Clofazimine nanoparticles were found to be 49.5 times superior in inhibition and anti-mycobacterial activity than free clofazimine.	Pawde et al. (2020)
Nanoparticles	Alginate	Rifampicin		The formulation is non-toxic and has no systemic toxicity after oral administration	Thomas et al. (2020)
Nanoparticles	Human serum albumin	Benzothiazinone	169 nm	Human serum albumin nanoparticle formulations demonstrated an enhanced efficacy compared to the unformulated drug in an *M. tuberculosis* infected macrophage model.	Patel et al. (2020)
Nanoparticles	Bovine serum albumin	Rifampicin	232 nm	Rifampicin-loaded bovine serum albumin nanoparticles demonstrated enhanced *in vitro* therapeutic efficacy compared to the free drug	Joshi and Prabhakar, (2021)
Micelles	Soluplus	Rifampicin	~107 nm	Rifampicin-loaded PMs enhanced (up to 2.5-fold) the *in vitro* drug microbicidal activity in Mtb-infected THP-1 macrophages versus a rifampicin solution	Grotz et al. (2019)
Nanoparticles	Phospholipid complex	Baicalein	~200 nm	Mucus-penetrative nanoparticles exhibited a higher diffusion rate in mucus, deeper penetration across the mucus layer, enhanced *in vitro* cellular uptake, increased drug distribution in airways, and superior local distribution and bioavailability compared to mucoadhesive nanoparticles.	Dong et al. (2020)

such as DNA, RNA, and peptides. In addition, the polymers chemical composition and molecular weight, and the physical properties of PLGA nanocarriers, such as size, shape, surface area to volume ratio, etc., can be "tuned" to obtain the desired release profile. With excellent biocompatibility, tunable degradation and release properties and high versatility have been approved for a variety of biomedical applications, PLGA is approved by Food and Drug Administration for human use and has been widely used in sustained-release drug delivery systems (Figure 3) and tissue engineering (Gentile et al., 2014; Mironov et al., 2017; Ding and Zhu, 2018; Lam et al., 2018; Lai et al., 2019; Park et al., 2019; Ghitman et al., 2020; Lagreca et al., 2020; Koerner et al., 2021).

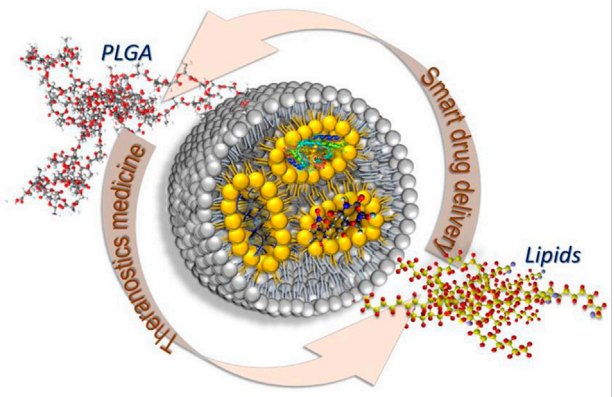

FIGURE 3
PLGA-lipid hybrid nanocarriers. Reproduced with permission from Ghitman et al. (2020). Copyright © 2020 the Authors.

PLGA particles are the most widely applied type of particles; the extensive use of PLGA micro/nanoparticle-based drug delivery systems is promising due to their higher efficiency and fewer adverse effects (Chereddy et al., 2016). Table 3 shows the current clinical trials/status of PLGA-based micro/nanoparticles therapy and diagnostics.

Poly (lactic-co-glycolic acid) micro/nanoparticles as novel therapeutic approaches for *drug-resistant tuberculosis*

In recent years, great efforts have been devoted to the development of PLGA Micro/nanoparticle delivery systems for treating *drug-resistant tuberculosis*, and the current research achievements have been listed in Table 4.

TABLE 3 Current clinical trials/status of PLGA-based micro/nanoparticles therapy and diagnostics.

Name	Carrier	Drug	Investigated applications	Company	Status	Ref
Pamorelin®	PLGA microsphere	Triptorelin	Prostate cancer	Ipsen Pharmaceuticals	Approved 1986	Jain et al. (2016)
Lupron Depot®	PLGA microsphere	Leuprolide acetate	Prostate cancer, Endometriosis Central precocious puberty	Takeda-Abbott Products	Approved 1989	Anselmo and itragotri, (2014)
Sandostatin Lar®	PLGA microsphere	Octreotide acetate	Endocrinology and Metabolism; Acromegaly	Novartis pharmaceuticals corp	Approved 1998	Zhong et al. (2018)
Trelstar®	PLGA microsphere	Triptorelin pamoate	Prostate cancer	Allergen DM	Approved 2000	Nkanga et al. (2020)
Arestin®	PLGA microsphere	Minocycline HCl	Infectious Diseases Periodontitis	Orapharma Inc.	Approved 2001	Molavi et al. (2020)
Eligard®	PLGA depot	Leuprolide acetate	Prostate cancer	Atrix Laboratories (Tolmar Therapeutics)	Approved 2002	Bobo et al. (2016)
Risperdal Consta®	PLGA microsphere	Risperidone	Neurologic Disorders antipsychotic	Janssen Pharmaceuticals Inc.	Approved 2003	Hrkach and Langer, (2020)
Vivitrol®	PLGA microsphere	Naltrexone	alcohol dependence opioid dependence	Alkermes Inc.	Approved 2006/2010	Dean (2005)
Ozurdex®	PLGA microsphere	Dexamethasone	Corticosteroid	Allergan Inc.	Approved 2009	Cao et al. (2019)
Bydureon®	PLGA microsphere	Exenatide	Type II diabetes	Amylin Pharmaceuticals	Approved 2012	Fineman et al. (2011)
Bydureon Bcise®	PLGA microsphere	Exenatide	Type II diabetes	AstraZeneca AB	Approved 2017	Rentzepis et al. (2018)
Signifor Lar®	PLGA microsphere	Pasireotide pamoate	Acromegaly	Novartis	Approved 2014	McKeage, (2015)
Zilretta®	PLGA microsphere	Triamcinolone	Osteoarthritis Other corticosteroid therapy	Flexion Therapeutics Inc.	Approved 2017	Chen et al. (2021)
Triptodur®	PLGA microsphere	Triptorelin pamoate	Central precocious puberty	Arbor	Approved 2017	Ghitman et al., 2020
Sublocade®	PLGA nanoparticles	Buprenorphine	Moderate to severe addiction to opioid drugs	Indivior Pharmaceuticals	Approved 2017	Chaurasiya et al. (2021)

TABLE 4 Current research achievements of PLGA Micro/nanoparticle delivery systems for treating drug-resistant *tuberculosis*

Carrier	Drug	Method	Size	Results	References
PLGA nanoparticles	Ethionamide	Solvent evaporation	286 nm	There was no significant drug-polymer interaction, and the ethionamide-loaded nanoparticles have no treatment-related toxic effect, which can release sustained for up to 15 days *in vitro*.	Kumar et al. (2011a)
PLGA nanoparticles	Ethionamide	Solvent evaporation	286 nm	When compared to the free drug, the ethionamide-loaded nanoparticles sustained the release of ethionamide for a longer period with significant improvement in pharmacokinetic parameters	Kumar et al. (2011b)
PLGA nanoparticles	Rifapentine	Premix membrane homogenization, solvent evaporation	150 nm	Rifapentine -loaded nps were more effective against *M. tuberculosis* than free RPT.	Liang et al. (2020)
PLGA nanoparticles	Isoniazid, Mycolic acids	Double emulsion solvent evaporation	~250 nm ~900 nm	The inclusion of mycolic acids in the nanoformulations resulted in their expression on the outer surface and a significant increase in phagocytic uptake of the nanoparticles	Lemmer et al. (2015)
PLGA nanoparticles	Moxifloxacin	Emulsion-evaporation	112 nm	Moxifloxacin-PEG-WSC nps presented striking prolongation in blood circulation, reduced protein binding, and long-drawn-out the blood circulation half-life with resultant reduced liver sequestration vis-à-vis MOX-PLGA nps.	Mustafa et al. (2017)
PLGA nanoparticles	Amikacin, Moxifloxacin	Emulsion evaporation	640 nm 312–365 nm	The release of alginate modified PLGA nanoparticles showed slower release in comparison with the non-modified PLGA nanoparticles. Furthermore, the anti-mycobacterial activity of the dually entrapped drug-loaded particles (moxifloxacin and amikacin) was higher compared to single drug-loaded nanoparticle formulations	Abdelghany et al. (2019)
PLGA nanoparticles	Clofazimine	Nanoprecipitation	311 nm	Clofazimine incorporation into the nps was advantageous to reduce drug cytotoxicity. The tfr-binding peptide-functionalized nps showed superior cell interaction and higher Clofazimine permeability compared to the non-functionalized nanoparticles	de Castro et al. (2021)
PLGA microparticles	Gatifloxacin	Solvent evaporation-extraction	40.3 μm, 1.4 μm	Gatifloxaci-loaded PLGA microparticles exhibited high encapsulation efficiency, adequate particle size for pulmonary administration, were rapidly phagocytosed by macrophages, and remained in their interior for at least 48 h	Marcianes et al. (2020)
PLGA microparticles	—	Double emulsion, solvent evaporation	2.2 μm	Drug-free PLGA microparticles could reduce the bacillary viability of THP-1 macrophages	Lawlor et al. (2016)
PLGA microparticles	Rifampicin, All-trans-Retinoic acid	Spray-drying	~2 μm	ATRA--PLGA microparticles treatments significantly decreased the bacterial burden in the lungs alongside a reduction in pulmonary pathology following just three doses administered intratracheally.	O'Connor et al. (2019)
PLGA microparticles	Isoniazid, Host defence peptides	Double emulsion-solvent evaporation	~5 μm	The Mucus-penetrating-microparticles dramatically increased (4.1fold) the particle transit through the mucus barrier, which does not adhere to lung mucus, disrupts the bacterial biofilm and provides uniform drug delivery to lungs after pulmonary delivery.	Sharma et al. (2020)
PLGA nanoparticles	Moxifloxacin	Multiple emulsion and solvent evaporation	299.66 nm	After 8 weeks of oral administration of nanoparticles, cfus in the lungs and spleen were reduced.	Vemuri et al. (2016)
PLGA nanoparticles	Econazole	Multiple emulsion and solvent evaporation	561 nm	After 8 weeks of oral administration of nanoparticles, cfus in the lungs and spleen were reduced.	Vemuri et al. (2016)
PLGA nanoparticles	Ethionamide	Multiple emulsion and solvent evaporation	364 nm	After 8 weeks of oral administration of nanoparticles, cfus in the lungs and spleen were reduced.	Vemuri et al. (2016)
PLGA nanoparticles	Thioridazine	Oil-in-water emulsion	211 nm	The thioridazine nanoparticles had no toxicity, and showed a significant therapeutic effect When combined with rifampicin	Vibe et al. (2016)
PLGA nanoparticles	Isoniazid, Moxifloxacin	single emulsion		An enhanced effect of the two drugs was achieved, when they were delivered inside the nanoparticles formulation achieved better antibacterial activity than the free mixture of the drugs	Moin et al. (2016)

(Continued on following page)

TABLE 4 (*Continued*) Current research achievements of PLGA Micro/nanoparticle delivery systems for treating drug-resistant *tuberculosis*

Carrier	Drug	Method	Size	Results	References
PLGA nanoparticles	Levofloxacin, BM2 aptamer	Double emulsification	273.9 nm	BM2- Levofloxacin nanoparticles could gathered accurately in the lesion tissues, and exhibited an excellent therapeutic effect after exposure to ultrasound.	Li et al. (2021)

Kumar et al. (2011a) developed ethionamide-loaded PLGA nanoparticles by solvent evaporation method to achieve prolonged drug release for the treatment of MDR-TB and improve patient compliance. *In vitro* release studies showed that ethionamide was sustainedly released for 15 days in various media. *In vivo* results showed that the ethionamide-loaded PLGA nanoparticles did not show any statistically significant treatment-related effects on weight gain and clinical signs. Likewise, no treatment-related toxic effects were found in haematology, clinical chemistry, and histopathology. The results demonstrate that orally safe ethionamide-loaded PLGA nanoparticles with sustained-release properties offer excellent potential for further preclinical and clinical studies. The authors also investigated ethionamide's pharmacokinetics and tissue distribution in mice (Kumar et al., 2011b). The sustained release of ethionamide in plasma for 6 days was detected for ethionamide-loaded PLGA nanoparticles compared to 6 h for free ethionamide. Furthermore, ethionamide was detected in organs (lungs, liver and spleen) for up to 5–7 days while maintaining drug levels above the MIC for 5 days, whereas free ethionamide was cleared within 12 h *in vivo* (Kumar et al., 2011b). Ethionamide-loaded PLGA nanoparticles showed significant improvement in pharmacokinetic parameters. Hence, the ethionamide-based PLGA nanoparticles have great potential for reducing the dosing frequency of ethionamide in treating MDR-TB. PLGA-based nanoparticles could also act as a sustained-release delivery vehicle for rifapentine to prolong drug release, alter pharmacokinetics, increase anti-tuberculosis activity, and reduce toxicity, allowing for low dose and frequency (Liang et al., 2020). Future studies on toxicity studies of drug-loaded nanoparticles and the chemotherapeutic potential of ethionamide-loaded nanoparticles against *Mycobacterium tuberculosis* (Mtb) in clinics should be performed.

It is well known that *tuberculosis* is a chronic infectious disease caused by *Mtb* (Khawbung et al., 2021). Resistant strains of *Mtb* cause a significant proportion of *drug-resistant tuberculosis* cases. There is an urgent need to develop new and innovative approaches for treatment. Lemmer et al. (2015) studied mycolic acids as a promising mycobacterial ligand for drug targeting using isoniazid PLGA nanoparticles. The results showed that the phagocytic uptake of mycobacterial acid-coated nanoparticles by mycobacterial-infected macrophages was significantly increased. Therefore, mycolic acid can be further explored as a potential target ligand for various nanoformulations to treat *tuberculosis* effectively.

Moxifloxacin (MOX) is an *Mtb* DNA gyrase inhibitor. Due to its strong hydrophilicity, MOX is cleared from the body within 24 h and requires repeated administration, leading to hepatotoxicity and acquisition of MOX-resistant *tuberculosis* associated with use. To overcome the limitations above, Mustafa et al. (2017) developed PLGA nanoparticles to act as an efficient carrier for the controlled delivery of MOX. The authors performed the affixation of polyethylene glycol (PEG) to MOX-PLGA nanoparticles and adsorption of water-soluble chitosan (WSC) to the particle surface to achieve a substantial extension in blood circulation. They investigated the *in vivo* pharmacokinetics and *in vivo* biodistribution after oral administration of the resulting surface-modified nanoparticles (MOX-PEG-WSC NPs), finding that the NPs surface charge was close to neutral +4.76 mV and was significantly affected by the WSC coating. MOX-PEG-WSC NPs significantly prolong blood circulation, reduce protein binding, and prolong blood circulation half-life compared with MOX-PLGA NPs. Therefore, these studies demonstrate that the MOX-PEG-WSC NPs exhibit sustained-release behaviour for controlled drug delivery and prolong the circulation time in the bloodstream for extended periods, thereby minimizing the frequency of dosing and avoiding the occurrence of MOX-resistant *tuberculosis*. Abdelghany et al. (2019) have entrapped amikacin and moxifloxacin into alginate modified-PLGA nanoparticles using two water-oil-water (w/o/w) emulsion strategies (Figure 4), targeting the treatment of MDR. The authors assessed the anti-mycobacterial activity of the resulting PLGA nanoparticles using *Mtb*-infected macrophages. The dually entrapped nanoparticles showed bacterial viability of 0.6% relative to the untreated group, compared to 6.49% for amikacin alone nanoparticles and 3.27% for moxifloxacin alone nanoparticles, revealing an enhanced inhibition of viable bacterial count due to the synergistic effect of moxifloxacin and amikacin in the PLGA nanoparticles (Abdelghany et al., 2019). The amikacin-moxifloxacin alginate entrapped PLGA nanoparticles have the potential to reduce the dose of these drugs, thereby improving patient compliance with treatment and potentially reducing adverse dose-related side effects. However, further *in vivo* studies are urgently required to confirm this prospect.

Clofazimine (CFZ) exhibits high activity against multidrug-resistant strains of *Mtb in vitro* (Nugraha et al., 2021; Mashele

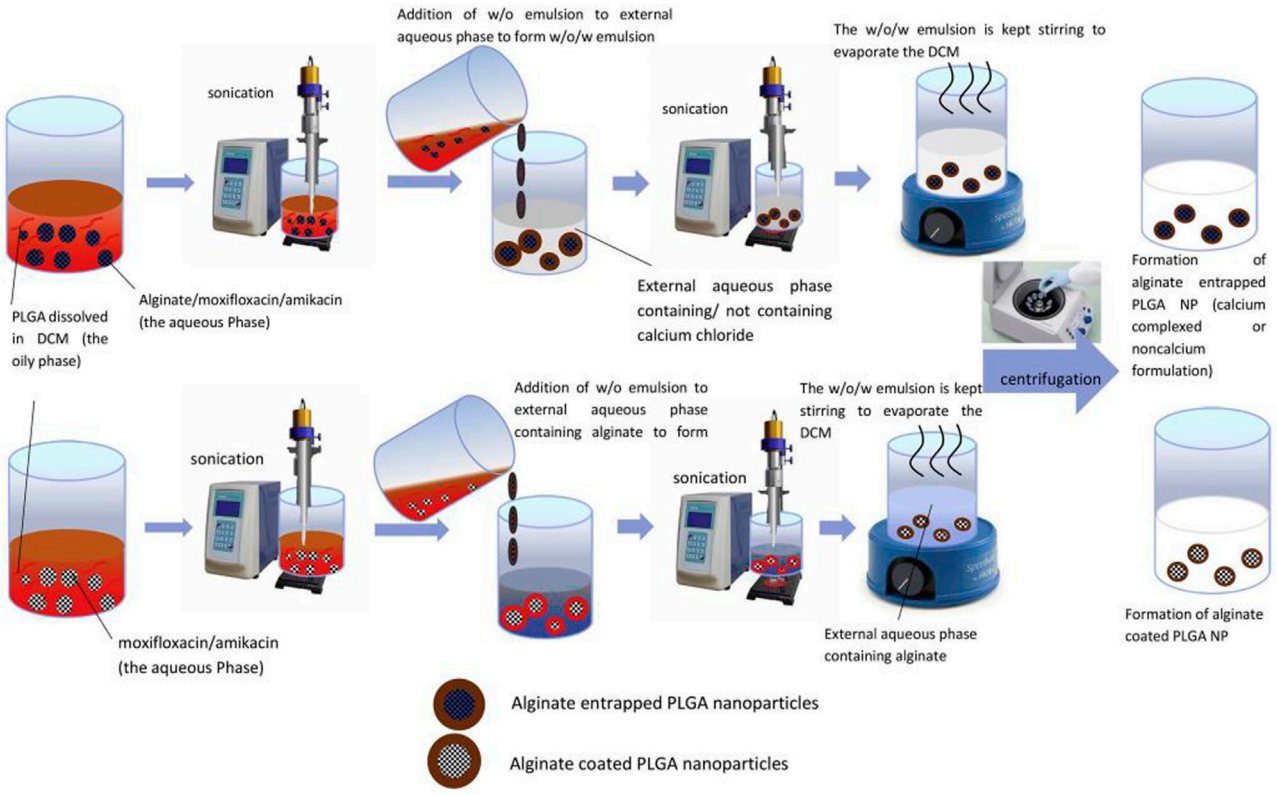

FIGURE 4
Schematic presentation of **(A)** alginate entrapped PLGA nanoparticles and **(B)** alginate coated PLGA nanoparticles. Reproduced with permission from Abdelghany et al. (2019). Copyright © 2019 Elsevier B. V.

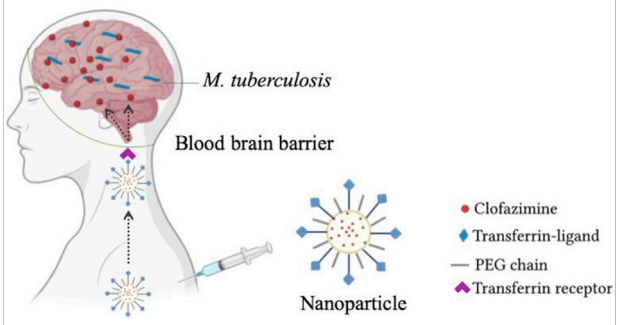

FIGURE 5
PLGA-PEG nanoparticles loaded with CFZ and functionalized with a transferrin receptor-binding peptide for brain drug delivery. Reproduced with permission from de Castro et al. (2021) Copyright © 2021 Elsevier B. V.

et al., 2022). However, its poor water solubility and high lipophilicity cause low and erratic drug bioavailability, high plasma protein binding and fatty tissue accumulation, limiting the therapeutic efficacy after oral administration (World Health Organization, 2019b). To solve this problem, de Castro et al. (2021) developed PLGA-PEG nanoparticles loaded with CFZ and functionalized with a transferrin receptor-binding peptide (Figure 5) to develop brain drug delivery to treat the central nervous system *tuberculosis*. *In vitro* studies in brain endothelial hCMEC/D3 cells showed that incorporating CFZ into nanoparticles significantly reduced drug cytotoxicity. TfR-binding peptide-functionalized nanoparticles exhibited better cellular interactions and higher CFZ permeability in hCMEC/D3 cell monolayers than non-functionalized NP controls. The functionalized PLGA-PEG nanoparticles demonstrate suitability for CFZ biological administration, suggested with low plasma protein binding, off-target biodistribution and precise delivery of CFZ towards the brain parenchyma.

Mtb can survive and replicate in alveolar macrophages (Ufimtseva et al., 2019), evading host defence mechanisms and developing the latent disease. Considering that phagocytes can localize and internalize foreign substances, such as polymeric particles, this fact could guide particles to the interior of macrophages, leading to an exciting approach to the treatment of intracellular infections affecting the mononuclear phagocytic system. Marcianes et al. (2020) developed a new biodegradable PLGA microparticle for pulmonary

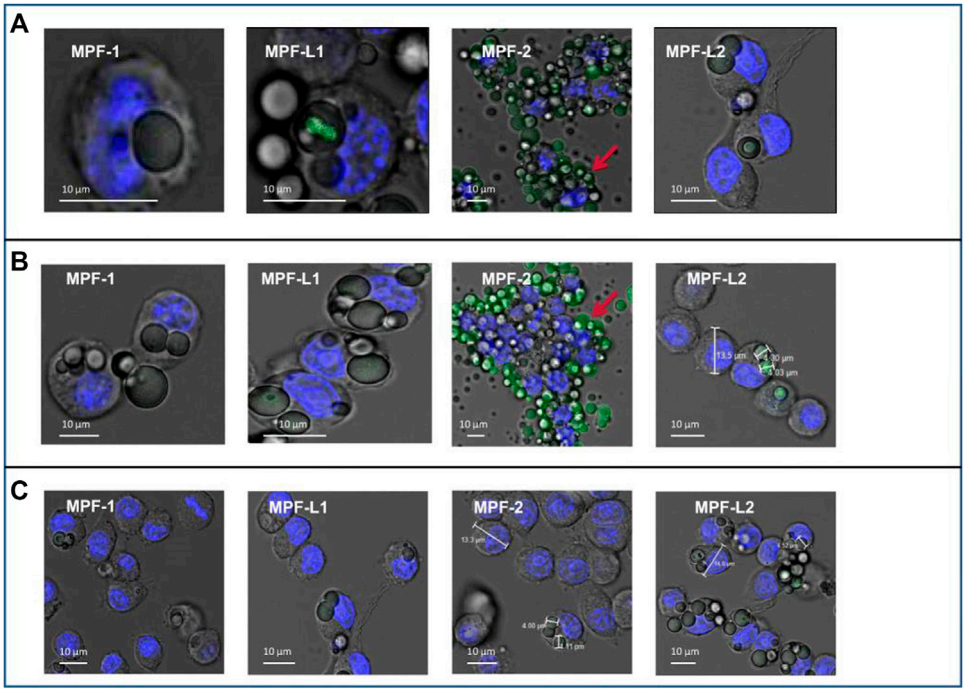

FIGURE 6
Confocal images of phagocytosis obtained at 3 h **(A)**, 5 h **(B)**, and 24 h **(C)**. MPF-1, fluorescein-loaded PLGA 502 MPs; MPF-2, fluorescein-loaded PLGA 502H MPs; MPF-L1, labrafil-modified fluorescein-loaded PLGA 502 MPs; MPF-L2, labrafil-modified fluorescein-loaded PLGA 502H MPs. Reproduced with permission from Marcianes et al. (2020). Copyright © 2022 Springer Nature Switzerland AG.

administration of gatifloxacin, using labrafil as a surface modifier to actively target alveolar macrophages, thereby allowing gain access of the drug to *Mtb*. Cell phagocytosis was studied in raw 264.7 mouse macrophage cell lines after incubating 3, 5, 24, and 48 h with the microparticles. The results showed that labrafil enhanced the uptake rate of PLGA 502H microparticles by macrophages (Figure 6). Gatifloxacin-loaded PLGA microparticles using PLGA 502H and labrafil exhibited high encapsulation efficiency (89.6% ± 0.2%), rapid phagocytosis by macrophages (3 h), and remained inside the cells for at least 48 h, resulting in a suitable carrier to potentially treat MDR-TB. These results are promising, but regarding future perspectives, further immunogenicity studies of the developed systems and phagocytosis in *Mtb*-infected macrophages should be conducted, and the safety of the formulations should be evaluated in an animal model of *tuberculosis*.

Pulmonary drug delivery systems are gaining popularity because of their ability to achieve high drug concentrations at the site of infection and minimize systemic toxicity for the treatment of various lung diseases, including *tuberculosis*. Lawlor et al. (2016) designed PLGA microparticles (MPs) carrying anti-tuberculosis drugs that human alveolar macrophages could successfully take up. They demonstrated how MPs affect macrophage function in *Mtb* infection by treating Mtb H37Ra or H37Rv-infected THP-1 macrophages with MPs. It was found that the activity of NF kappa B was increased in MPs-treated macrophages, although cytokine secretion was unaltered, and the induction of autophagy was demonstrated *via* the Confocal microscopy of immortalized murine bone marrow-derived macrophages expressing GFP-tagged LC3 (Figure 7). Inhibition of caspases did not influence the MP-induced restriction of bacillary growth, however, blockade of NF kappa B or autophagy with pharmacological inhibitors reversed this MP effect on macrophage function. These data support using the inhaled PLGA MP drug delivery system as a vehicle for immunotherapeutic agents and targeted drug delivery, exploiting the generation of inhaled vaccines and inhaled MDR-TB therapeutics.

O'Connor et al. (2019) prepared inhalable PLGA microparticles loaded with trans-Retinoic acid (ATRA) to establish the effect of targeted ATRA treatment on *Mtb* viability. The results showed that 70.5% ± 2.3% of encapsulated ATRA was targeted and delivered to the site of action within the alveolar macrophage, indicating the efficient cellular delivery of ATRA. Furthermore, the results of the BACT/ALERT® system and enumeration of colony-forming units showed a reduction in *Mtb* (H37Ra) growth in THP-1 derived

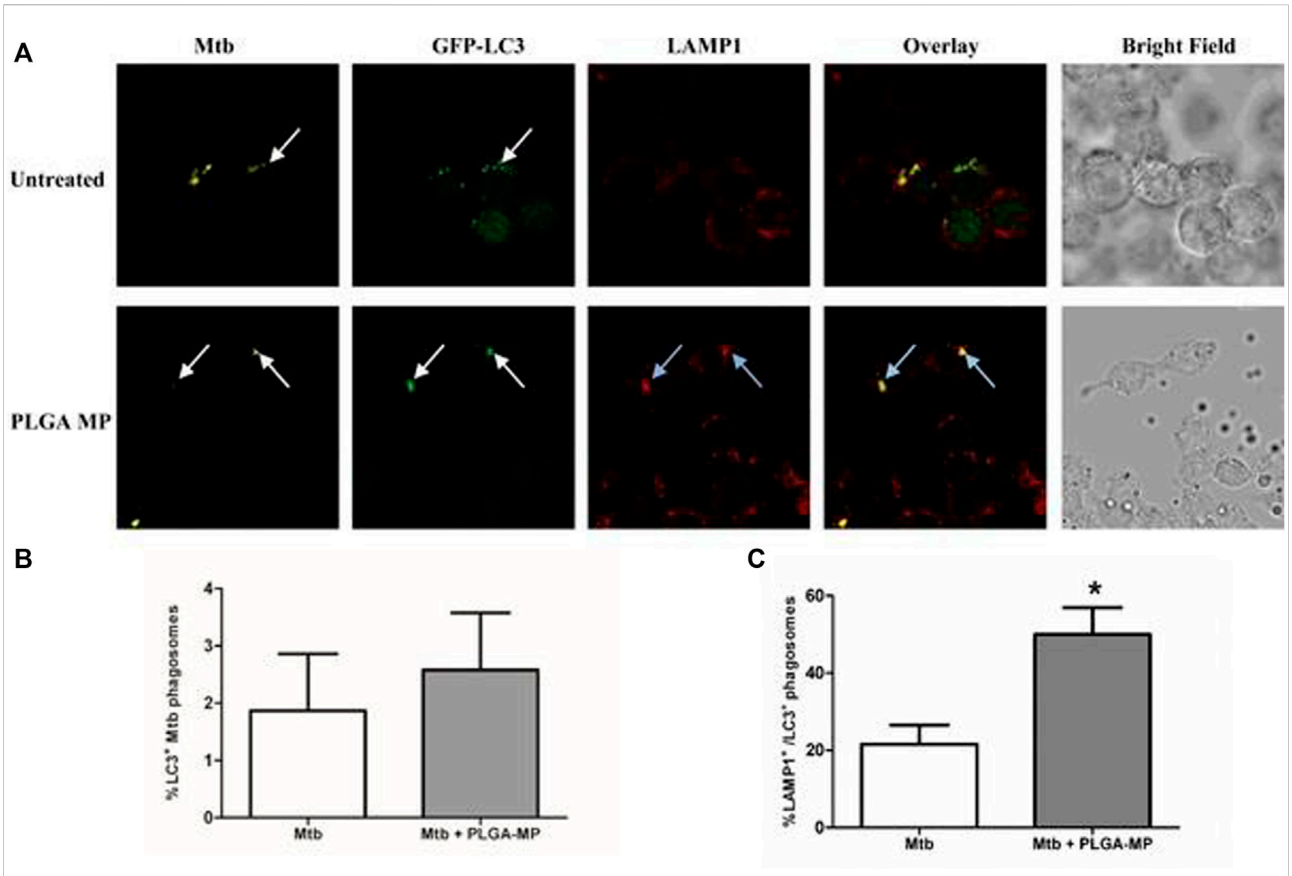

FIGURE 7
PLGA MPs trigger autophagic flux in Mtb-infected macrophages. **(A)** After a total of 24 h, infected macrophages were fixed and stained with anti-LAMP1_and anti-Mtb antibodies, and then observed by laser scanning confocal microscopy. The proportion of **(B)** LC3 positive Mtb phagosomes and **(C)** LC3 positive phagosomes which were also positive for LAMP1 were counted. Data represent the mean ± SEM of three independent experiments in which more than 100 phagosomes were counted for each condition. *$p < 0.05$. The white arrows indicate localization of Mtb phagosomes with GFP-LC3, blue arrows indicate co-localization of Mtb, GFP-LC3, and LAMP1. The results shown are the means of three independent experiments. Reproduced with permission from Lawlor et al. (2016). Copyright © 2016 the authors.

macrophages, confirming the good antibacterial effect of ATRA-loaded PLGA microparticles. The ATRA-loaded PLGA microparticles could also significantly decrease the bacterial burden in the lungs alongside a reduction in pulmonary pathology, as shown in the *in vivo* antibacterial assessment results in Mtb (H37Rv) strain infected BALB/c mice (Figure 8). This study is the first to treat *tuberculosis* with controlled release of ATRA *via* the pulmonary route *in vivo*, providing an alternative to traditional oral supplements that have been ineffective in clinical studies. It provides a new and tried strategy for treating *drug-resistant tuberculosis* and has broad clinical application prospects.

In *tuberculosis* treatment, antibiotics become less effective, and bacteria develop resistance over time due to the formation of some barriers around microorganisms, such as lung mucus and biofilms. Traditional respirable microparticles are mainly trapped in dense, chaotic networks of mucins and are rapidly cleared by mucociliary clearance. Therefore, if the anti-tuberculosis activity of drug-loaded inhalable polymer particles can synergize with the mucus-penetrating and biofilm-disrupting properties, it would be a significant advantage of anti-tuberculosis microparticles, helping to improve the therapeutic effect. Sharma et al. encapsulated IDR-1018 peptide with an anti-tuberculosis drug in N-acetyl cysteine (NAC) decorated porous PLGA microspheres (Sharma et al., 2020), developing Mucus-penetrating-microparticles (NAC/PLGA-MPP). The multiple tracking techniques showed that NAC coating on the porous PLGA microspheres significantly increased (4.1-fold) the passage of particles through the mucus barrier. The designed inhalable NAC/PLGA-MPP does not adhere to lung mucus, does not disrupt bacterial biofilms, and provides uniform drug delivery to the lungs after pulmonary delivery. The activity of the NAC/PLGA-MPP against Mtb in macrophage cultures and in mice model infected with a low-dose bacterial aerosol was evaluated. After 6 weeks of administration of the daily dose, the inhalation of

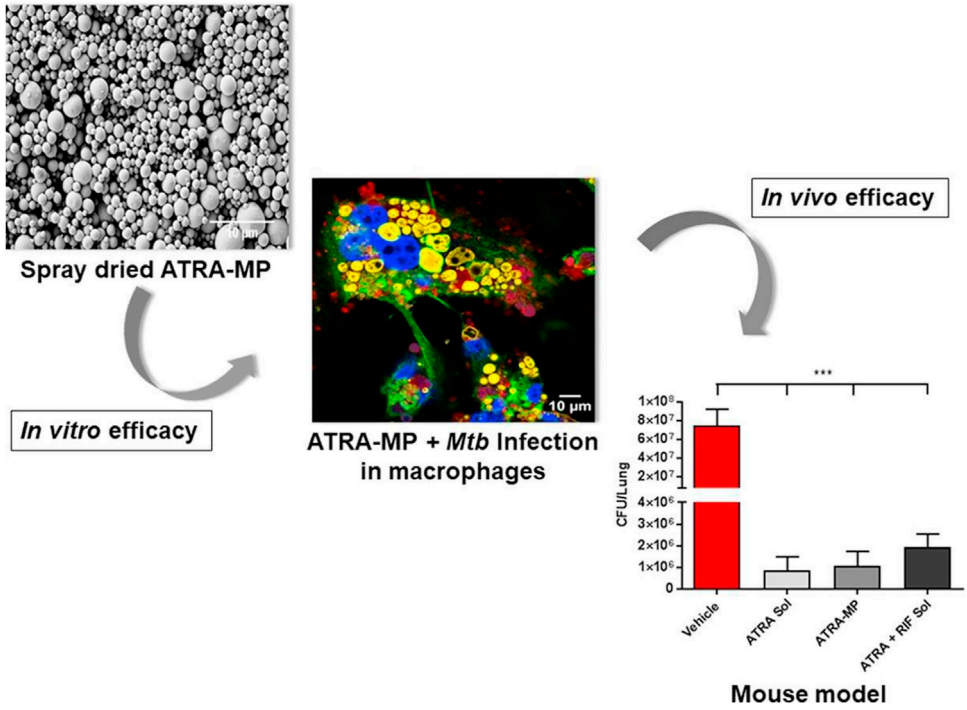

FIGURE 8
In vitro and *in vivo* efficacy of the inhalable PLGA microparticles loaded with trans-Retinoic acid (ATRA). Reproduced with permission from O'Connor et al. (2019). Copyright © 2018 Elsevier B. V.

NAC/PLGA-MPP encapsulated with IDR-1018 significantly reduced ($p < 0.05$) bacterial load and inflammation in the lungs in a mouse model of *tuberculosis*. The histopathological results also validate the compelling chemotherapeutic outcome of inhaled formulations (Figure 9). This data supports the potential of using mucus-penetrating inhalable drug delivery systems as a strategy for targeted pulmonary delivery, which may benefit *drug-resistant tuberculosis* treatment.

Combination therapy has been demonstrated as a potentially effective treatment for MDR-TB. Vemuri et al. (2016) encapsulated moxifloxacin (MOX), econazole (ECZ) and ethionamide (ETH) into PLGA nanoparticles to treat the MDR-TB infected mice. Eight weeks of oral administration of individual nanoformulations (PLGA-NP-ECZ/PLGA-NP-MOX/PLGA-NP-ETH) showed limited reduction of CFUs in lungs and spleen, while with 8 doses of a combination of the three nanoformulations (PLGA-NP-ECZ+PLGA-NPMOX+PLGA-NP-ETH) there was a significant reduction in CFUs in lungs as well as in spleen. Corroborating the results with histopathology revealed that the combination of 3-drugs loaded nanoparticles decreased lung congestion to 50%. This is the first report on the potential efficacy of a combination of ECZ, MOX and ETH nanoparticles against MDR-TB. Similar results were reported by Vibe et al. (2016) that when combined with rifampicin nanoparticles, the PLGA nanoparticles loaded with thioridazine gave a modest increase in the killing of both *Mycobacterium* Bovis BCG and *Mtb* in macrophages. The thioridazine nanoparticles showed a significant therapeutic effect combined with rifampicin in the zebrafish, enhancing embryo survival and reducing mycobacterial infection. The results show that thioridazine nanoparticle therapy can improve the antibacterial effect of rifampicin *in vivo*. Moin et al. (2016) also developed a dual drug conjugate PLGA nanoparticle using isoniazid (INH) and moxifloxacin (MOXI) to combat the multi-drug resistance exhibited by mycobacterial species. The drug-conjugate-loaded PLGA nanoparticles are rapidly hydrolyzed into individual parent molecules at the pH of macrophages and function with different mechanisms of action at the same site in macrophages, thereby preventing the development of drug resistance and the development of *tuberculosis*. From the results of the experimental work, it can be concluded that incorporating two or more drugs into *tuberculosis* with the same carrier and target can be an effective strategy against MDR-TB.

Sonodynamic antibacterial chemotherapy (SACT) combined with sonosensitizer-loaded nanoparticles with targeted therapeutic capabilities promises to eliminate bacteria to treat MDR-TB. Li et al. (2021) developed levofloxacin-loaded PLGA-PEG nanoparticles (BM2-LVFX-

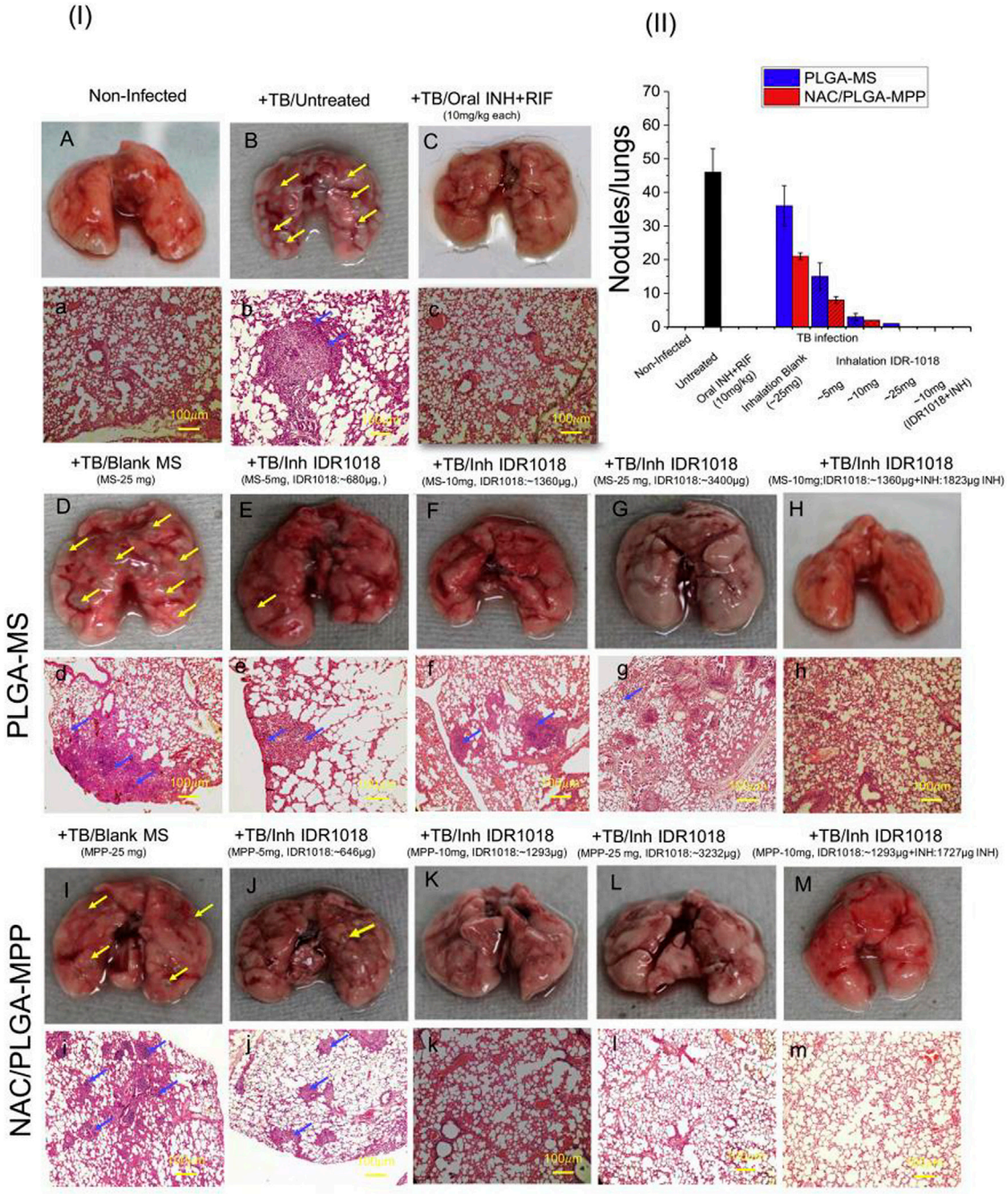

FIGURE 9
(I) Morphological and histopathological changes in the lungs of mice post Mtb infection and treatment. Representative images showing gross anatomic morphology of whole lungs of Balb/c mice infected with virulent Mtb (H37Rv) and treated with various formulations **(A–I,K–M)** (scale bar: 10 mm). Yellow arrowheads indicate grey-white coloured tubercular nodules (lesion). Histological sections of (**H,E**) stained lungs of normal, infected and treated mice **(a–h,j–m,l)**. Scale bar: 100 μm. Gross pathology photomicrograph showed granulomas (blue arrowheads) in the lungs (n = 6 animals/group). Graph show quantitative results of macroscopically detectable tubercular nodules per lung. (II) CFU counting in lungs from mice infected with Mtb. Tissue homogenates of each individual mouse were cultured in agar plates and CFU were counted and averaged. Reproduced with permission from Sharma et al. (2020). Copyright © 2020 Elsevier B. V.

NPs) with BM2 aptamer conjugated on the surface using cross-linking agents 1-ethyl-3-(3-dimethylaminopropyl) carbodiimide (EDC) and N-hydroxysuccinimide (NHS), to study the antibacterial activity underlying mechanisms of PLGA nanoparticles with targeted therapeutic function against *Bacillus* Calmette-Guérin bacteria (BCG, an *Mtb*

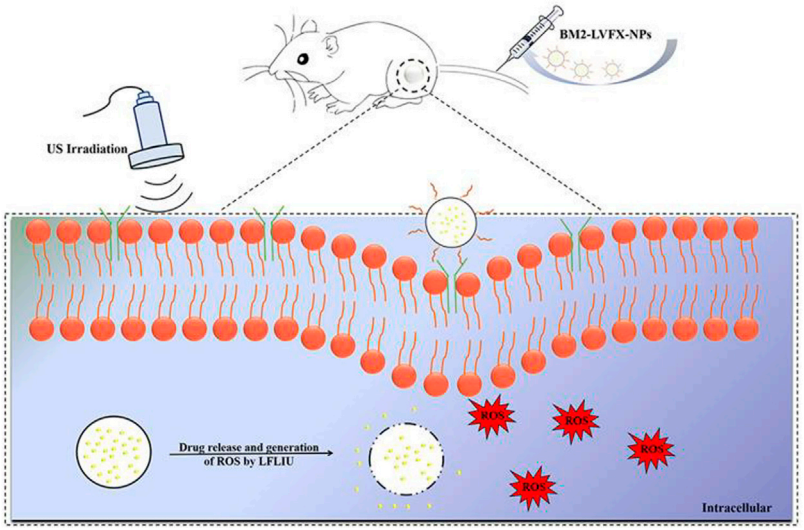

FIGURE 10
BM2-LVFX-NPs for sonodynamic antimicrobial chemotherapy for BCG infection. Reproduced with permission from Li et al. (2021). Copyright © 2021 the authors.

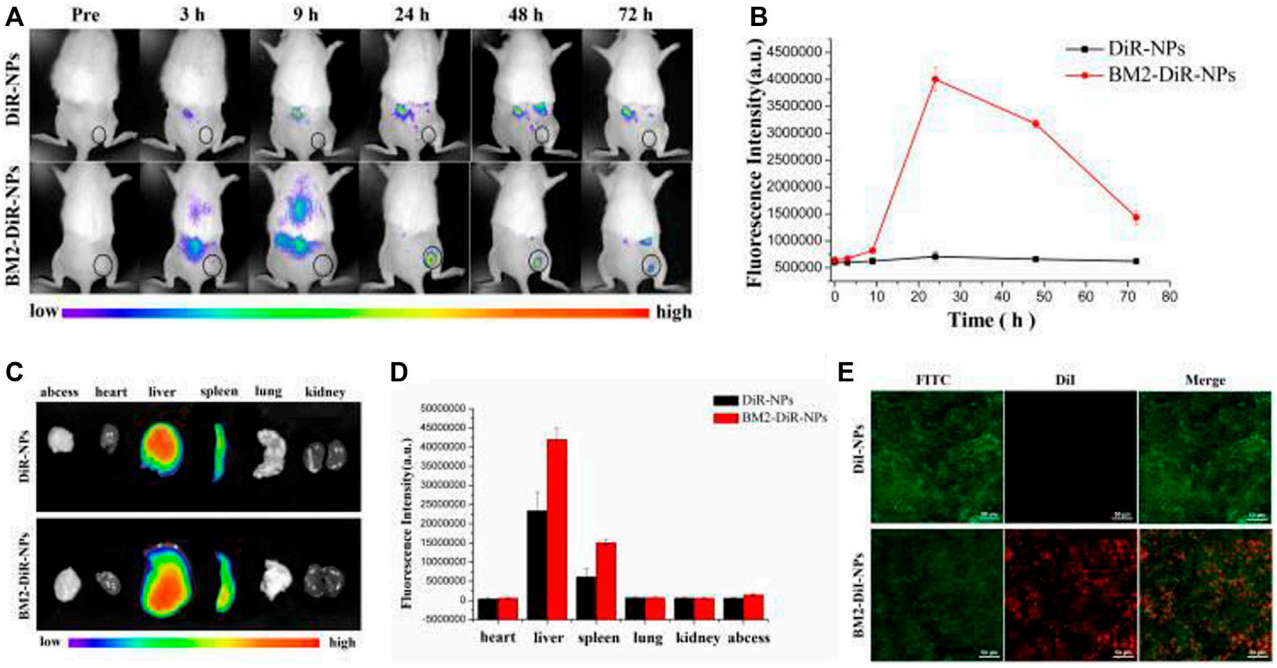

FIGURE 11
Targeting ability of BM2-modified nanoparticles *in vivo*. **(A)** Fluorescence images of a BCG-infected rat at 3, 9, 24, 48, and 72 h post injection of DiR-labelled nanoparticles. **(B)** Quantitative fluorescence intensity (n = 3) of abscess tissue at different time points. **(C)** Biodistribution of DiR-labeled nanoparticles in major organs extracted from rats at 72 h post injection. **(D)** Quantitative analysis of fluorescence intensity (n = 3) in major organs. **(E)** CLSM images of Frozen section of abscess tissues at 24 h post-injection of DiR-loaded nanoparticles. The scale bar is 50 μm. Reproduced with permission from Li et al. (2021). Copyright © 2021 the authors.

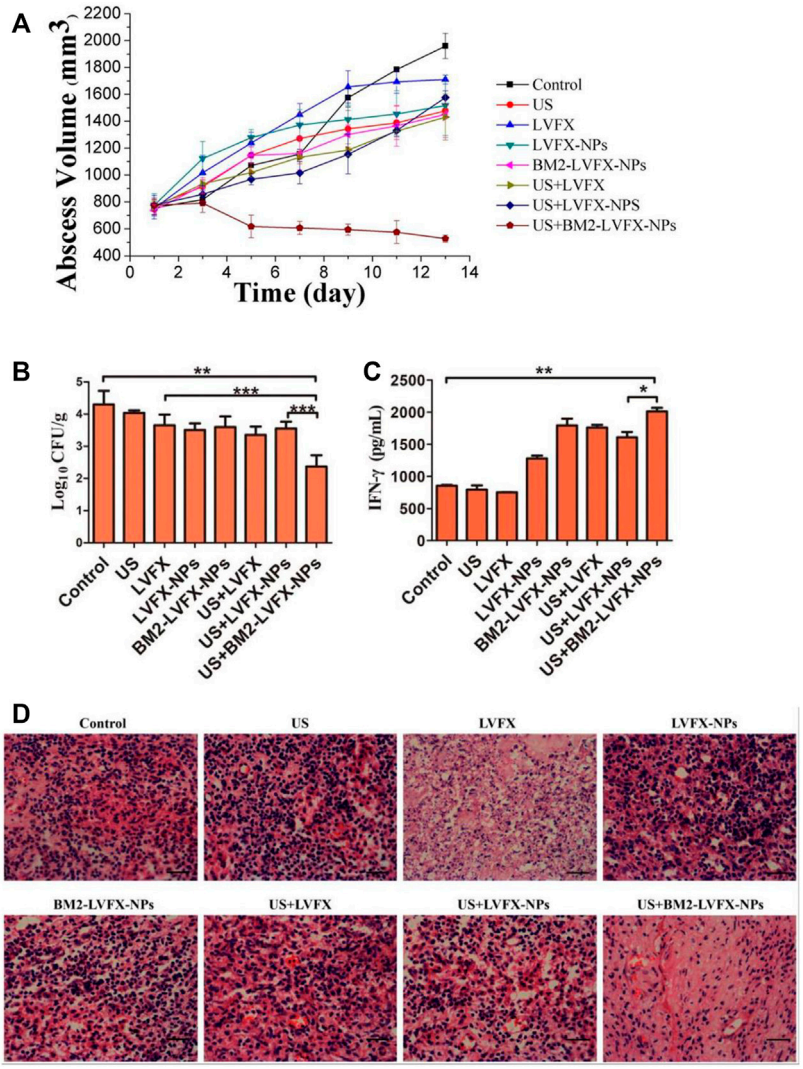

FIGURE 12
In vivo SACT efficacy of BM2-LVFX-NPs combined with ultrasound. **(A)** The time-dependent abscess volume curves of infected rats in each group. **(B)** Colony counting analysis (Log10 CFU) of bacterial cultures from the abscess tissue in the rats after a 14-day treatment. $^{**}p < 0.01$, $^{***}p < 0.001$. **(C)** Serum IFN-γ level of BCG-infected rats on Day 14 after treatment. **(D)** Histopathologic observation of the infected tissues of every group after being treated in various ways. The scale bar is 50 μm. Reproduced with permission from Li et al. (2021). Copyright © 2021 the authors.

model in the presence of ultrasound stimulations (Figure 10). PLGA nanoparticles were specifically recognized BCG *in vitro* and accurately accumulated in the lesion tissue (Figure 11), and the drugs with ultrasound-responsive properties loaded in PLGA nanoparticles were effectively released. Furthermore, PLGA nanoparticles exhibited significant SACT efficiency and higher ROS production levels, resulting in efficient bacterial elimination *in vitro*. Meanwhile, *in vivo* experiments, PLGA nanoparticles showed excellent ultrasound therapeutic effects in a BCG-infected rat model (Figure 12). The results show that PLGA nanoparticles containing levofloxacin can effectively transfer therapeutic drugs into cells and improve the bactericidal effect under ultrasound, which may be a targeted therapy strategy for *Mtb* infection with high biosafety.

Shortcomings and limitations

Despite recent advances in PLGA micro/nanoparticle drug delivery systems in *tuberculosis* treatment, many issues still need further addressed. First, it is not an easy task to develop a lyophilization process for dry powder of PLGA micro/nanoparticles, and it is necessary to ensure that the

lyophilized powder is easy to redisperse, avoiding aggregation and drug precipitation; Second, the total amount of biomaterial and lyoprotector to be inhaled over time should be evaluated in terms ofchronic lung toxicity. The total amount of materials and lyoprotectants, and thus nanomedicines for *tuberculosis* treatment, should be optimized to reduce the daily dose of excipients administered to patients. It is also necessary to emphasize the importance of reproducibility and stability (drug loading, encapsulation efficiency and physicochemical properties) in producing drug-loaded PLGA micro/nanoparticles during mass production. The lack of appropriate and specific regulatory guidelines on characterization, study design, and statistical analysis is a common obstacle to the clinical translation of nanoformulations. There is also a need to optimize shared practices to facilitate the translation of nanotechnology from experimental success to clinical practice. In addition, more *in vivo* data are needed. Only a few studies have shown that the PLGA micro/nanoparticles drug delivery system is effective in preclinical models of infected *tuberculosis*. This is a severe disadvantage as future clinical studies will depend on available preclinical data. The research on PLGA micro/nano drug delivery systems for the treatment of *tuberculosis* is still at an early stage, and more investment and capacity are required to make it possible to obtain commercially available micro/nano formulations.

Conclusion and prospect

Drug-resistant tuberculosis is a significant global disease with high morbidity and mortality and remains a major health problem. As current treatment strategies are inadequate, innovative strategies are needed to improve treatment and reduce mortality. The PLGA micro/nanoparticles can be loaded with single or combined drugs with additive/synergistic effects, allowing lower doses of drugs with reduced side effects while improving antituberculosis efficacy of first- and second-line antituberculosis drugs. PLGA micro/nanoparticles offer great potential for more efficient delivery of *tuberculosis* drugs to lesion sites to improve their efficacy, and the introduction of potent, novel and repurposed drugs will increase the effectiveness of such systems. Although the results obtained so far are too preliminary, it is still believed that PLGA micro/nanoparticles have great potential as a novel therapeutic approach for *drug-resistant tuberculosis* and reduce the risk of *drug-resistant tuberculosis* impacting human health. In order to promote the safe and extensive application of the drug-loaded PLGA micro/nanoparticles in the clinical treatment of *drug-resistant tuberculosis*, the following issues should be paid attention to in the future in-depth research: 1) A reliable animal model is necessarily required to examine the safety of PLGA micro/nanoparticles *in vivo* because the number of *in vivo* studies of these pharmaceutical formulations is minimal and requires careful study for human use; 2) Addressing the processing/manufacturing issues for large scale production at an affordable cost will be a fundamental issue in the future; 3) Furthermore, to further realize the progress and efficient delivery of nanomedicines in the lesion sites for precise drug delivery, active participation and cooperation in the fields of nanotechnology, biomedicine, bioengineering and computer analysis are required to make sure nano-drugs will not face any issues during application in clinical trials.

Author contributions

LS wrote this article; HL revised this article; SS checked and review this article.

Funding

This work was supported by the program of the Liaoning Natural Science Foundation (2019-ZD-0976).

Conflict of interest

The authors declare that the research was conducted in the absence of any commercial or financial relationships that could be construed as a potential conflict of interest.

Publisher's note

References

Abdelghany, S., Parumasivam, T., Pang, A., Roediger, B., Tang, P., Jahn, K., et al. (2019). Alginate modified-PLGA nanoparticles entrapping amikacin and moxifloxacin as a novel host-directed therapy for multidrug-resistant tuberculosis. *J. Drug Deliv. Sci. Technol.* 52, 642–651. doi:10.1016/j.jddst.2019.05.025

Al-Qushawi, A., Rassouli, A., Atyabi, F., Peighambari, S. M., Esfandyari-Manesh, M., Shams, G. R., et al. (2016). Preparation and characterization of three tilmicosin-loaded lipid nanoparticles: Physicochemical properties and *in-vitro* antibacterial activities. *Iran. J. Pharm. Res.* 15 (4), 663–676.

Anselmo, A. C., and Mitragotri, S. (2014). An overview of clinical and commercial impact of drug delivery systems. *J. Control. Release* 190, 15–28. doi:10.1016/j.jconrel.2014.03.053

Bobo, D., Robinson, K. J., Islam, J., Thurecht, K. J., and Corrie, S. R. (2016). Nanoparticle-based medicines: A review of FDA-approved materials and clinical trials to date. *Pharm. Res.* 33 (10), 2373–2387. doi:10.1007/s11095-016-1958-5

Cao, Y., Samy, K. E., Bernards, D. A., and Desai, T. A. (2019). Recent advances in intraocular sustained-release drug delivery devices. *Drug Discov. today* 24 (8), 1694–1700. doi:10.1016/j.drudis.2019.05.031

Chaurasiya, A., Patra, P., Thathireddy, P., and Gorajiya, A. (2021). "PLGA-based micro- and nano-particles," in *Micro-and nanotechnologies-based product development* (Boca Raton: CRC Press), 83–94. doi:10.1201/9781003043164-6

Chen, Y. C., Gad, S. F., Chobisa, D., Li, Y., and Yeo, Y. (2021). Local drug delivery systems for inflammatory diseases: Status quo, challenges, and opportunities. *J. Control. Release* 330, 438–460. doi:10.1016/j.jconrel.2020.12.025

Chereddy, K. K., Vandermeulen, G., and Préat, V. (2016). PLGA based drug delivery systems: Promising carriers for wound healing activity. *Wound Rep Reg* 24 (2), 223–236. doi:10.1111/wrr.12404

de Castro, R. R., do Carmo, F. A., Martins, C., Simon, A., de Sousa, V. P., Rodrigues, C. R., et al. (2021). Clofazimine functionalized polymeric nanoparticles for brain delivery in the tuberculosis treatment. *Int. J. Pharm.* 602, 120655. doi:10.1016/j.ijpharm.2021.120655

De Matteis, L., Jary, D., Lucía, A., García-Embid, S., Serrano-Sevilla, I., Pérez, D., et al. (2018). New active formulations against *M. tuberculosis*: Bedaquiline encapsulation in lipid nanoparticles and chitosan nanocapsules. *Chem. Eng. J.* 340, 181–191. doi:10.1016/j.cej.2017.12.110

Dean, R. L. (2005). The preclinical development of MedisorbÂ Naltrexone, a once a month long-acting injection, for the treatment of alcohol dependence. *Front. Biosci.* 10 (1), 643. doi:10.2741/1559

Ding, D., and Zhu, Q. (2018). Recent advances of PLGA micro/nanoparticles for the delivery of biomacromolecular therapeutics. *Mater. Sci. Eng. C* 92, 1041–1060. doi:10.1016/j.msec.2017.12.036

Dong, W., Ye, J., Zhou, J., Wang, W., Wang, H., Zheng, X., et al. (2020). Comparative study of mucoadhesive and mucus-penetrative nanoparticles based on phospholipid complex to overcome the mucus barrier for inhaled delivery of baicalein. *Acta Pharm. Sin. B* 10 (8), 1576–1585. doi:10.1016/j.apsb.2019.10.002

Fineman, M., Flanagan, S., Taylor, K., Aisporna, M., Shen, L. Z., Mace, K. F., et al. (2011). Pharmacokinetics and pharmacodynamics of exenatide extended-release after single and multiple dosing. *Clin. Pharmacokinet.* 50 (1), 65–74. doi:10.2165/11585880-000000000-00000

Gentile, P., Chiono, V., Carmagnola, I., and Hatton, P. (2014). An overview of poly(lactic-co-glycolic) acid (PLGA)-Based biomaterials for bone tissue engineering. *Int. J. Mol. Sci.* 15 (3), 3640–3659. doi:10.3390/ijms15033640

Ghitman, J., Biru, E. I., Stan, R., and Iovu, H. (2020). Review of hybrid PLGA nanoparticles: Future of smart drug delivery and theranostics medicine. *Mater. Des.* 193, 108805. doi:10.1016/j.matdes.2020.108805

Grotz, E., Tateosian, N. L., Salgueiro, J., Bernabeu, E., Gonzalez, L., Manca, M. L., et al. (2019). Pulmonary delivery of rifampicin-loaded soluplus micelles against *Mycobacterium tuberculosis*. *J. Drug Deliv. Sci. Technol.* 53, 101170. doi:10.1016/j.jddst.2019.101170

Gupta, A., Sharma, D., Meena, J., Pandya, S., Sachan, M., Kumar, S., et al. (2016). Preparation and preclinical evaluation of inhalable particles containing rapamycin and anti-tuberculosis agents for induction of autophagy. *Pharm. Res.* 33 (8), 1899–1912. doi:10.1007/s11095-016-1926-0

Helal-Neto, E., Rocha Pinto, S., Portilho, F. L., da Costa, M. D., Pereira, J. X., Nigro, F., et al. (2019). Development and biological evaluation of a new nanotheranostic for tuberculosis. *Drug Deliv. Transl. Res.* 9 (1), 97–105. doi:10.1007/s13346-018-0577-6

Hrkach, J., and Langer, R. (2020). From micro to nano: Evolution and impact of drug delivery in treating disease. *Drug Deliv. Transl. Res.* 10 (3), 567–570. doi:10.1007/s13346-020-00769-6

Jain, A., Kunduru, K. R., Basu, A., Mizrahi, B., Domb, A. J., and Khan, W. (2016). Injectable formulations of poly(lactic acid) and its copolymers in clinical use. *Adv. drug Deliv. Rev.* 107, 213–227. doi:10.1016/j.addr.2016.07.002

Jana, P., Shyam, M., Singh, S., Jayaprakash, V., and Dev, A. (2021). Biodegradable polymers in drug delivery and oral vaccination. *Eur. Polym. J.* 142, 110155. doi:10.1016/j.eurpolymj.2020.110155

Joshi, M., and Prabhakar, B. (2021). Development of respirable rifampicin loaded bovine serum albumin formulation for the treatment of pulmonary tuberculosis. *J. Drug Deliv. Sci. Technol.* 61, 102197. doi:10.1016/j.jddst.2020.102197

Khawbung, J. L., Nath, D., and Chakraborty, S. (2021). Drug resistant tuberculosis: A review. *Comp. Immunol. Microbiol. Infect. Dis.* 74, 101574. doi:10.1016/j.cimid.2020.101574

Koerner, J., Horvath, D., Herrmann, V. L., MacKerracher, A., Gander, B., Yagita, H., et al. (2021). PLGA-particle vaccine carrying TLR3/RIG-I ligand Riboxxim synergizes with immune checkpoint blockade for effective anti-cancer immunotherapy. *Nat. Commun.* 12 (1), 2935. doi:10.1038/s41467-021-23244-3

Kumar, A. R., and Aeila, A. S. S. (2019). Sustained release matrix type drug delivery system: An overview. *World J. Pharma Pharm. Sci.* 8 (12), 470–480. doi:10.20959/wjpps20201-15241

Kumar, G., Malhotra, S., Shafiq, N., Pandhi, P., Khuller, G. K., and Sharma, S. (2011a). In vitrophysicochemical characterization and short termin vivotolerability study of ethionamide loaded PLGA nanoparticles: Potentially effective agent for multidrug resistant tuberculosis. *J. Microencapsul.* 28 (8), 717–728. doi:10.3109/02652048.2011.615948

Kumar, G., Sharma, S., Shafiq, N., Pandhi, P., Khuller, G. K., and Malhotra, S. (2011b). Pharmacokinetics and tissue distribution studies of orally administered nanoparticles encapsulated ethionamide used as potential drug delivery system in management of multi-drug resistant tuberculosis. *Drug Deliv.* 18 (1), 65–73. doi:10.3109/10717544.2010.509367

Lagreca, E., Onesto, V., Di Natale, C., La Manna, S., Netti, P. A., and Vecchione, R. (2020). Recent advances in the formulation of PLGA microparticles for controlled drug delivery. *Prog. Biomater.* 9 (4), 153–174. doi:10.1007/s40204-020-00139-y

Lai, Y., Li, Y., Cao, H., Long, J., Wang, X., Li, L., et al. (2019). Osteogenic magnesium incorporated into PLGA/TCP porous scaffold by 3D printing for repairing challenging bone defect. *Biomaterials* 197, 207–219. doi:10.1016/j.biomaterials.2019.01.013

Lam, S. J., Wong, E. H. H., Boyer, C., and Qiao, G. G. (2018). Antimicrobial polymeric nanoparticles. *Prog. Polym. Sci.* 76, 40–64. doi:10.1016/j.progpolymsci.2017.07.007

Lange, C., Dheda, K., Chesov, D., Mandalakas, A. M., Udwadia, Z., and Horsburgh, C. R. (2019). Management of drug-resistant tuberculosis. *Lancet* 394 (10202), 953–966. doi:10.1016/s0140-6736(19)31882-3

Lawlor, C., O'Connor, G., O'Leary, S., Gallagher, P. J., Cryan, S. A., Keane, J., et al. (2016). Treatment of Mycobacterium tuberculosis-infected macrophages with poly(lactic-Co-glycolic acid) microparticles drives NFκB and autophagy dependent bacillary killing. *PLoS One* 11 (2), e0149167. doi:10.1371/journal.pone.0149167

Lemmer, Y., Kalombo, L., Pietersen, R. D., Jones, A. T., Semete-Makokotlela, B., Van Wyngaardt, S., et al. (2015). Mycolic acids, a promising mycobacterial ligand for targeting of nanoencapsulated drugs in tuberculosis. *J. Control. release* 211, 94–104. doi:10.1016/j.jconrel.2015.06.005

Li, G., Li, J., Hou, Y., Xie, S., Xu, J., Yang, M., et al. (2021). Levofloxacin-loaded nanosonosensitizer as a highly efficient therapy for Bacillus calmette-guérin infections based on bacteria-specific labeling and sonotheranostic strategy. *Int. J. Nanomedicine* 16, 6553–6573. doi:10.2147/ijn.s321631

Liang, Q., Xiang, H., Li, X., Luo, C., Ma, X., Zhao, W., et al. (2020). Development of rifapentine-loaded PLGA-based nanoparticles: *In vitro* characterisation and *in vivo* study in mice. *Int. J. Nanomedicine* 15, 7491–7507. doi:10.2147/ijn.s257758

Marcianes, P., Negro, S., Barcia, E., Montejo, C., and Fernández-Carballido, A. (2020). Potential active targeting of gatifloxacin to macrophages by means of surface-modified PLGA microparticles destined to treat tuberculosis. *AAPS PharmSciTech* 21 (1), 15. doi:10.1208/s12249-019-1552-3

Mashele, S. A., Steel, H. C., Matjokotja, M. T., Rasehlo, S. S., Anderson, R., and Cholo, M. C. (2022). Assessment of the efficacy of clofazimine alone and in combination with primary agents against *Mycobacterium tuberculosis in vitro*. *J. Glob. Antimicrob. Resist.* 29, 343–352. doi:10.1016/j.jgar.2022.03.008

McKeage, K. (2015). Pasireotide in acromegaly: A review. *Drugs* 75 (9), 1039–1048. doi:10.1007/s40265-015-0413-y

Mironov, A. V., Grigoryev, A. M., Krotova, L. I., Skaletsky, N. N., Popov, V. K., and Sevastianov, V. I. (2017). 3D printing of PLGA scaffolds for tissue engineering. *J. Biomed. Mat. Res.* 105 (1), 104–109. doi:10.1002/jbm.a.35871

Moin, A., Raizaday, A., Hussain, T., and Nagshubha, B. (2016). Development and optimization of dual drugs (Isoniazid and moxiflox-acin) loaded functional PLGA nanoparticles for the synergistic treatment of tuberculosis. *Curr. Drug Deliv.* 13 (7), 1034–1052. doi:10.2174/1567201813666160502124811

Molavi, F., Barzegar-Jalali, M., and Hamishehkar, H. (2020). Polyester based polymeric nano and microparticles for pharmaceutical purposes: A review on formulation approaches. *J. Control. Release* 320, 265–282. doi:10.1016/j.jconrel.2020.01.028

Mustafa, S., Devi, V. K., and Pai, R. S. (2017). Effect of PEG and water-soluble chitosan coating on moxifloxacin-loaded PLGA long-circulating nanoparticles. *Drug Deliv. Transl. Res.* 7 (1), 27–36. doi:10.1007/s13346-016-0326-7

Nkanga, C. I., Fisch, A., Rad-Malekshahi, M., Romic, M. D., Kittel, B., Ullrich, T., et al. (2020). Clinically established biodegradable long acting injectables: An industry perspective. *Adv. drug Deliv. Rev.* 167, 19–46. doi:10.1016/j.addr.2020.11.008

Nugraha, R. V., Yunivita, V., Santoso, P., Aarnoutse, R. E., and Ruslami, R. (2021). Clofazimine as a treatment for multidrug-resistant tuberculosis: A review. *Sci. Pharm.* 89 (2), 19. doi:10.3390/scipharm89020019

O'Connor, G., Krishnan, N., Fagan-Murphy, A., Cassidy, J., O'Leary, S., Robertson, B. D., et al. (2019). Inhalable poly(lactic-co-glycolic acid) (PLGA) microparticles encapsulating all-trans-Retinoic acid (ATRA) as a host-directed, adjunctive treatment for *Mycobacterium tuberculosis* infection. *Eur. J. Pharm. Biopharm.* 134, 153–165. doi:10.1016/j.ejpb.2018.10.020

Park, K., Skidmore, S., Hadar, J., Garner, J., Park, H., Otte, A., et al. (2019). Injectable, long-acting PLGA formulations: Analyzing PLGA and understanding microparticle formation. *J. Control. Release* 304, 125–134. doi:10.1016/j.jconrel.2019.05.003

Patel, A., Redinger, N., Richter, A., Woods, A., Neumann, P. R., Keegan, G., et al. (2020). *In vitro* and *in vivo* antitubercular activity of benzothiazinone-loaded human serum albumin nanocarriers designed for inhalation. *J. Control. Release* 328, 339–349. doi:10.1016/j.jconrel.2020.08.022

Patil, K., Bagade, S., Bonde, S., Sharma, S., and Saraogi, G. (2018). Recent therapeutic approaches for the management of tuberculosis: Challenges and opportunities. *Biomed. Pharmacother.* 99, 735–745. doi:10.1016/j.biopha.2018.01.115

Pawde, D. M., Viswanadh, M. K., Mehata, A. K., Sonkar, R., Haldiya, N. K., Poddar, S., et al. (2020). Mannose receptor targeted bioadhesive chitosan nanoparticles of clofazimine for effective therapy of tuberculosis. *Saudi Pharm. J.* 28 (12), 1616–1625. doi:10.1016/j.jsps.2020.10.008

Rajabnezhad, S., Casettari, L., Lam, J. K. W., Nomani, A., Torkamani, M. R., Palmieri, G. F., et al. (2016). Pulmonary delivery of rifampicin microspheres using lower generation polyamidoamine dendrimers as a carrier. *Powder Technol.* 291, 366–374. doi:10.1016/j.powtec.2015.12.037

Rani, S., Gothwal, A., Khan, I., Pachouri, P. K., Bhaskar, N., Gupta, U. D., et al. (2018). Smartly engineered PEGylated di-block nanopolymeric micelles: Duo delivery of isoniazid and rifampicin against *Mycobacterium tuberculosis*. *AAPS PharmSciTech* 19 (7), 3237–3248. doi:10.1208/s12249-018-1151-8

Reid, M. J. A., Arinaminpathy, N., Bloom, A., Bloom, B. R., Boehme, C., Chaisson, R., et al. (2019). Building a tuberculosis-free world: The Lancet Commission on tuberculosis. *Lancet* 393 (10178), 1331–1384. doi:10.1016/S0140-6736(19)30024-8

Rentzepis, P. J., Kurian, M. J., Carracher, A. M., and Close, K. L. (2018). Practical ways to achieve targets in diabetes care. *J. Diabetes* 10 (12), 911–915. doi:10.1111/1753-0407.12842

Saifullah, B., Chrzastek, A., Maitra, A., Naeemullah, B., Fakurazi, S., Bhakta, S., et al. (2017). Novel anti-tuberculosis nanodelivery formulation of ethambutol with graphene oxide. *Molecules* 22 (10), 1560. doi:10.3390/molecules22101560

Sharma, A., Vaghasiya, K., Gupta, P., Singh, A. K., Gupta, U. D., and Verma, R. K. (2020). Dynamic mucus penetrating microspheres for efficient pulmonary delivery and enhanced efficacy of host defence peptide (HDP) in experimental tuberculosis. *J. Control. release* 324, 17–33. doi:10.1016/j.jconrel.2020.05.013

Soria-Carrera, H., Lucía, A., Matteis, L., Aínsa, J. A., la Fuente, J. M., and Martín-Rapún, R. (2019). Polypeptidic micelles stabilized with sodium alginate enhance the activity of encapsulated bedaquiline. *Macromol. Biosci.* 19 (4), 1970012. doi:10.1002/mabi.201970012

Thomas, D., KurienThomas, K., and Latha, M. S. (2020). Preparation and evaluation of alginate nanoparticles prepared by green method for drug delivery applications. *Int. J. Biol. Macromol.* 154, 888–895. doi:10.1016/j.ijbiomac.2020.03.167

Ufimtseva, E., Eremeeva, N., Bayborodin, S., Umpeleva, T., Vakhrusheva, D., and Skornyakov, S. (2019). *Mycobacterium tuberculosis* with different virulence reside within intact phagosomes and inhibit phagolysosomal biogenesis in alveolar macrophages of patients with pulmonary tuberculosis. *Tuberculosis* 114, 77–90. doi:10.1016/j.tube.2018.12.002

Vemuri, N., K. Khuller, G., Prabhakar, T., Pal, N., Gupta, P., and Gupta, U. (2015). Nanoformulations of moxifloxacin, econozole and ethionamide as novel treatment regimens against MDR TB - an experimental study. *Curr. Nanosci.* 12 (1), 110–117. doi:10.2174/1573413711666150901203515

Vibe, C. B., Fenaroli, F., Pires, D., Wilson, S. R., Bogoeva, V., Kalluru, R., et al. (2016). Thioridazine in PLGA nanoparticles reduces toxicity and improves rifampicin therapy against mycobacterial infection in zebrafish. *Nanotoxicology* 10 (6), 680–688. doi:10.3109/17435390.2015.1107146

Vieira, A. C. C., Magalhães, J., Rocha, S., Cardoso, M. S., Santos, S. G., Borges, M., et al. (2017). Targeted macrophages delivery of rifampicin-loaded lipid nanoparticles to improve tuberculosis treatment. *Nanomedicine* 12 (24), 2721–2736. doi:10.2217/nnm-2017-0248

World Health Organization (2010). *Global tuberculosis report 2010*. Geneva: World Health Organization.

World Health Organization (2019a). *Global tuberculosis report 2019*. Geneva: World Health Organization.

World Health Organization (2020). *Global tuberculosis report 2020*. Geneva: World Health Organization.

World Health Organization (2021a). *Global tuberculosis report 2021*. Geneva: World Health Organization.

World Health Organization (2021b). *Rapid communication on updated guidance on the management of tuberculosis in children and adolescents*. Geneva: World Health Organization.

World Health Organization (2019b). *WHO consolidated guidelines on drug-resistant tuberculosis treatment*. Geneva: World Health Organization.

Zhong, H., Chan, G., Hu, Y., Hu, H., and Ouyang, D. (2018). A comprehensive map of FDA-approved pharmaceutical products. *Pharmaceutics* 10 (4), 263. doi:10.3390/pharmaceutics10040263

frontiers | Frontiers in Bioengineering and Biotechnology

TYPE Review
PUBLISHED 24 August 2022
DOI 10.3389/fbioe.2022.990145

OPEN ACCESS

EDITED BY
Mingqiang Li,
Third Affiliated Hospital of Sun Yat-sen University, China

REVIEWED BY
Vrinda Gote,
Inventprise Inc., United States
Han Lingyu,
Dalian Nationalities University, China
Tianqun Lang,
Shanghai Institute of Materia Medica (CAS), China

*CORRESPONDENCE
Tao Sun,
jianong@126.com
Liqun Yang,
yanglq@lnszjk.com.cn

SPECIALTY SECTION
This article was submitted to Biomaterials, a section of the journal Frontiers in Bioengineering and Biotechnology

RECEIVED 09 July 2022
ACCEPTED 05 August 2022
PUBLISHED 24 August 2022

CITATION
Jia Y, Chen S, Wang C, Sun T and Yang L (2022), Hyaluronic acid-based nano drug delivery systems for breast cancer treatment: Recent advances. *Front. Bioeng. Biotechnol.* 10:990145. doi: 10.3389/fbioe.2022.990145

Hyaluronic acid-based nano drug delivery systems for breast cancer treatment: Recent advances

Yufeng Jia[1], Siwen Chen[2,3], Chenyu Wang[4], Tao Sun[1]* and Liqun Yang[3]*

[1]Department of Breast Medicine, Liaoning Cancer Hospital, Cancer Hospital of China Medical University, Shenyang, China, [2]Center for Molecular Science and Engineering, College of Science, Northeastern University, Shenyang, China, [3]NHC Key Laboratory of Reproductive Health and Medical Genetics (China Medical University), Liaoning Research Institute of Family Planning (The Reproductive Hospital of China Medical University), Shenyang, China, [4]Department of Information Management, Cancer Hospital of China Medical University, Liaoning Cancer Hospital, Shenyang, China

Breast cancer (BC) is the most common malignancy among females worldwide, and high resistance to drugs and metastasis rates are the leading causes of death in BC patients. Releasing anti-cancer drugs precisely to the tumor site can improve the efficacy and reduce the side effects on the body. Natural polymers are attracting extensive interest as drug carriers in treating breast cancer. Hyaluronic acid (HA) is a natural polysaccharide with excellent biocompatibility, biodegradability, and non-immunogenicity and is a significant component of the extracellular matrix. The CD44 receptor of HA is overexpressed in breast cancer cells and can be targeted to breast tumors. Therefore, many researchers have developed nano drug delivery systems (NDDS) based on the CD44 receptor tumor-targeting properties of HA. This review examines the application of HA in NDDSs for breast cancer in recent years. Based on the structural composition of NDDSs, they are divided into HA NDDSs, Modified HA NDDSs, and HA hybrid NDDSs.

KEYWORDS

hyaluronic acid, breast cancer, anticancer drugs, nanoparticles, drug delivery system (DDS)

1 Introduction

Cancer is one of the significant causes of death in the world. Cancer can occur in many body areas, such as the liver, lungs, prostate, or breasts. Breast cancer is the most common cancer among women, accounting for nearly 30% of all cancers (Liyanage et al., 2019). According to statistics, there were 22,61,419 new breast cancer cases worldwide last year, along with the highest mortality rate of all types of cancer in women (684,996 deaths in 2020), seriously threatening the health status of women (Dubey et al., 2022). Although breast cancer is the most common type of cancer in women, it can be treated if detected and diagnosed in its early stages (Waks and Winer, 2019). However, if the cancer cells

metastasize and invade other tissues through the blood and lymphatic system, it becomes significantly more challenging to treat, increasing the mortality rate rapidly (Lou et al., 2016).

Chemotherapy is an effective way to treat breast cancer. This strategy involves treating breast cancer by using chemotherapeutic drugs to prevent the mitosis and growth of cancer cells (Sharma et al., 2010). So far, many anti-cancer drugs such as paclitaxel, Adriamycin, tamoxifen, docetaxel, and methotrexate have been approved for breast cancer treatment (Nomura, 1996; Perez, 1998; Colleoni et al., 2002; Smith et al., 2002; Jordan, 2014). Unfortunately, breast cancer is highly resistant to chemotherapy drugs, the poor solubility of chemotherapeutic drugs in the body, the short duration of circulation of drug molecules in the bloodstream, the limited choice of oncologic agents, and the potential severe drug side effects have greatly limited the role of chemotherapeutic drugs in the treatment of breast cancer (Luo et al., 2019). Furthermore, prolonged treatment can also cause multidrug resistance (MDR), leading to treatment failure and tumor relapse. Therefore, in recent years, nano drug delivery systems (NDDSs) based on nanotechnology have been extensively studied to overcome the shortcomings of chemotherapeutic drugs in breast cancer treatment.

Compared to conventional medical systems, NDDS has distinct advantages, including the ability to increase the solubility of anti-breast cancer drugs, control and prolong drug release, achieve targeted drug delivery by enhancing the permeability to the tumor and the enhanced permeability and retention effect (EPR) and reduce the side effects of drugs at other sites (Hu and Zhang, 2009). So far, a limited number of NDDSs have been approved by the Food and Drug Administration (FDA) for clinical use, such as Doxil, albumin-bound paclitaxel nanoparticles (Abraxane), poly (lactic acid) (PLA), micelles-based paclitaxel (Genxol), and paclitaxel-loaded liposomes (Weissig et al., 2014). Unfortunately, NDDS regimens with active targeting capabilities are under evaluation and have not yet been approved. The most significant obstacle encountered in developing NDDS is that the material must have good biocompatibility. Therefore, a series of naturally degradable polymers with excellent biocompatibility have received widespread interest (Lokeshwar et al., 2014; Wu et al., 2018; Narmani and Jafari, 2021).

Hyaluronic acid (HA) is a natural linear mucopolysaccharide composed of alternating repeats of D-glucuronic acid and nacetyl-D-glucosamine, the main component of the extracellular matrix (Fraser et al., 1997). The excellent hydrophilicity of HA reduces adsorption (corona) and permeation with proteins, thereby promoting the long-term circulation and stability of DDS composed of HA *in vivo* (Mizrahy et al., 2014). In addition, HA is an anionic polymer (pKa = 3–4) (Cadete and Alonso, 2016), enabling it to interact with cationic polymers, surfactants, and lipids to form a variety of nanostructures. In terms of composition, HA has carboxyl and hydroxyl groups and an N-acetyl group, offering unlimited potential for further modification (Burdick and Prestwich, 2011).

It is well known that the CD44 receptor is one of the many transmembrane glycoproteins that have great potential in achieving active targeting therapy. Meanwhile, CD44 is a primary receptor for HA (UNDERHILL, 1992). Standard CD44 (CD44s) is widely present in normal cells; HA binds to receptors and contributes to angiogenesis, wound healing, tissue hydration, and cell signaling in the extracellular matrix (Necas et al., 2008; Oh et al., 2010; Mattheolabakis et al., 2015; Wickens et al., 2017). CD44 is expressed at low levels on the surface in healthy cells, such as epithelial cells, hematopoietic cells, and neuronal cells (Huang and Chen, 2019). In contrast, variant CD44 (CD44v) is overexpressed on the surface of various cancer cells, including breast, squamous, ovarian, and colon carcinomas (Kim et al., 2018). Notably, CD44v has a higher affinity for HA than CD44s (Misra et al., 2011). In addition, HA has excellent hydrophilicity, good biocompatibility, biodegradability, and non-immunogenicity (Lapcık et al., 1998). The surface charge of HA-NDDSs is typically negative, which facilitates blocking the clearance of nano-carriers by the reticuloendothelial system (RES) (Xiao et al., 2011). In addition, nano-carriers are selectively transferred into cancer cells through the EPR effect and active targeting of CD44 receptors (Oh et al., 2010). Furthermore, HA has good biocompatibility, biodegradability, and non-immunogenicity. Therefore, HA-NDDSs have been extensively studied in the field of drug delivery.

We focus on the review of HA as NDDSs in breast cancer therapy in recent years, including HA NDDSs, Modified HA NDDSs, and HA nanohybrid NDDSs (Figure 1).

2 HA NDDSs

Chemotherapeutic agents used to treat breast cancer generally have disadvantages such as low water solubility, slow delivery, and non-specific biodistribution and targeting, hence restricting their clinical applications (Dheer et al., 2017).

HA with anti-cancer drugs provides better hydrophilicity and stability and improves drug absorption efficiency by targeting CD44 receptors while reducing the side effects of drugs on healthy cells (Yang et al., 2013; Tran et al., 2017). Table 1 summarizes NDDSs with HA-coated or modified nano-drug in recent years, including NDDSs drug type, size, drug loading capacity, etc.

Lapatinib (LPT) is an anti-cancer drug approved to treat advanced HER2 + breast cancer (Castellino et al., 2012). Agrawal et al. prepared LPT-HA-NCs by HA encapsulating nanocrystalline LPT to enhance the therapeutic efficacy and reduce drug side effects in triple-negative breast cancer (TNBC). It was shown that the anti-cancer activity of LPT-HA-NCs was superior to that of LPT-NCs and free LPT through the active targeting ability of CD44 receptor, which is

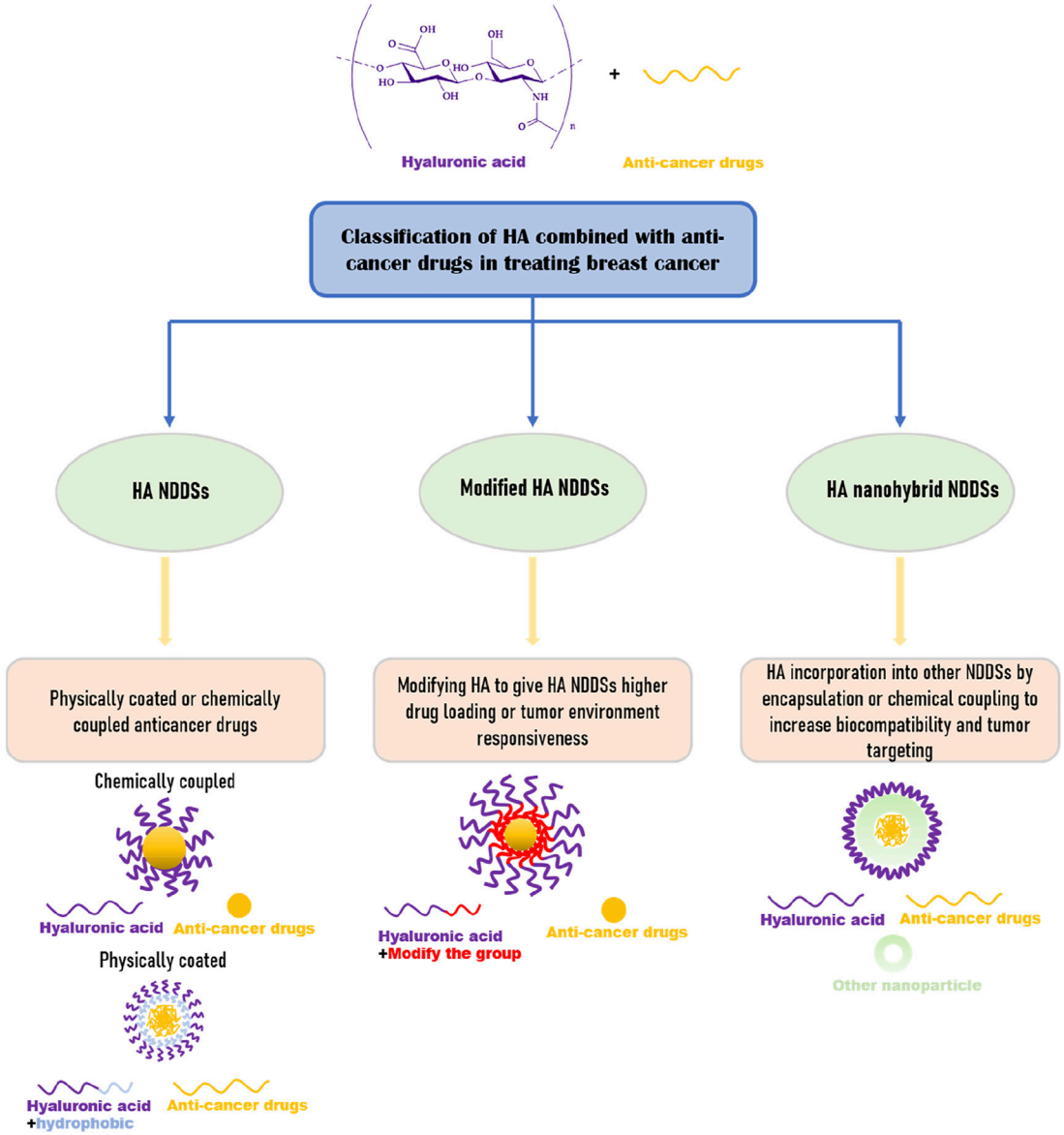

FIGURE 1
Classification of hyaluronic acid NDDSs in breast cancer.

characteristic of HA, and had lower toxic side effects. LPH-HA-NCs showed 83.32% tumor reduction after 28 days of anti-tumor treatment and effectively inhibited lung metastasis. LPH-HA-NCs at low doses exhibit significant therapeutic effects, thereby suggesting a strategy for minimizing the dose for the treatment of TNBC (Agrawal et al., 2018).

Curcumin (Cur) is one of the dietary polyphenolic compounds with anti-cancer effects (Hong et al., 2017). To improve the surface hydrophilicity of curcumin nanocrystals (Cur-NC) and increase the drug release time, Ji et al. modified the surface of Cur-NC using HA to prepare HA@Cur-NCs. According to the data, HA@Cur-NCs significantly improved the bioavailability of Cur compared to free drugs and Cur-NC, prolonged the retention time of Cur *in vivo*, and showed better anti-cancer effects in mice loaded with 4t1 with negligible systemic side effects. HA@Cur-NCs provide a new alternative for the future clinical treatment of breast cancer (Ji et al., 2020).

According to previous studies, chronic inflammation is closely related to carcinogenesis (Arias et al., 2007). Anti-inflammatory drugs are emerging as new candidates in the treatment and prevention of cancer. Naproxen (NAP) is a well-known non-steroidal anti-inflammatory drug, and its

TABLE 1 Characteristics of HA NDDSs.

Component	Formulation	Therapeutics	Size (nm)	%DLC	Indication	Status	References
Lapatinib-HA-NCs	Nanoparticle	Lapatinib	288.8 ± 17.4 PDI: 0.272 ± 0.022	—	MDA-MB-231 4T1	*In vivo*	Agrawal et al. (2018)
HA@ Curcumin -NC	Nanoparticle	Curcumin	161.85 ± 1.70 PDI: 0.25 ± 0.02	—	MDA-MB-231 4T1	*In vivo*	Ji et al. (2020)
HA- Cationic naproxen P-NPs	Nanoparticle	Naproxen	297.0 ± 6 PDI: 0.113 ± 0.017	HA adsorption: 46%	MCF-7 HepG2	*In vitro*	Espinosa-Cano et al. (2021)
HA- Shikonin -Lip	Liposome	Shikonin	173 ± 5 PDI: 0.14 ± 0.02	3.3 ± 0.1	MDA-MB-231	*In vivo*	Meng et al. (2022)
HA-Lip-17-hydroxy-jolkinolide B	Liposome	17-hydroxy-jolkinolide B	130.8 ± 1.9	3.6 ± 0.1	4T1	*In vivo*	Liu et al. (2021)
HA nanohydrogel of quercetin	Nanogels	Quercetin Everolimus	211.3 ± 5.3 PDI: 0.1 ± 0.014	~12.09	MCF-7	*In vitro*	Quagliariello et al. (2017)
HA-ionic-triphenylphosphonium - Doxorubicin	Nanoparticle	Doxorubicin	~257 PDI:0.096	TTP-DOX:31.4	MCF-7/ADR	*In vivo*	Liu et al. (2018a)

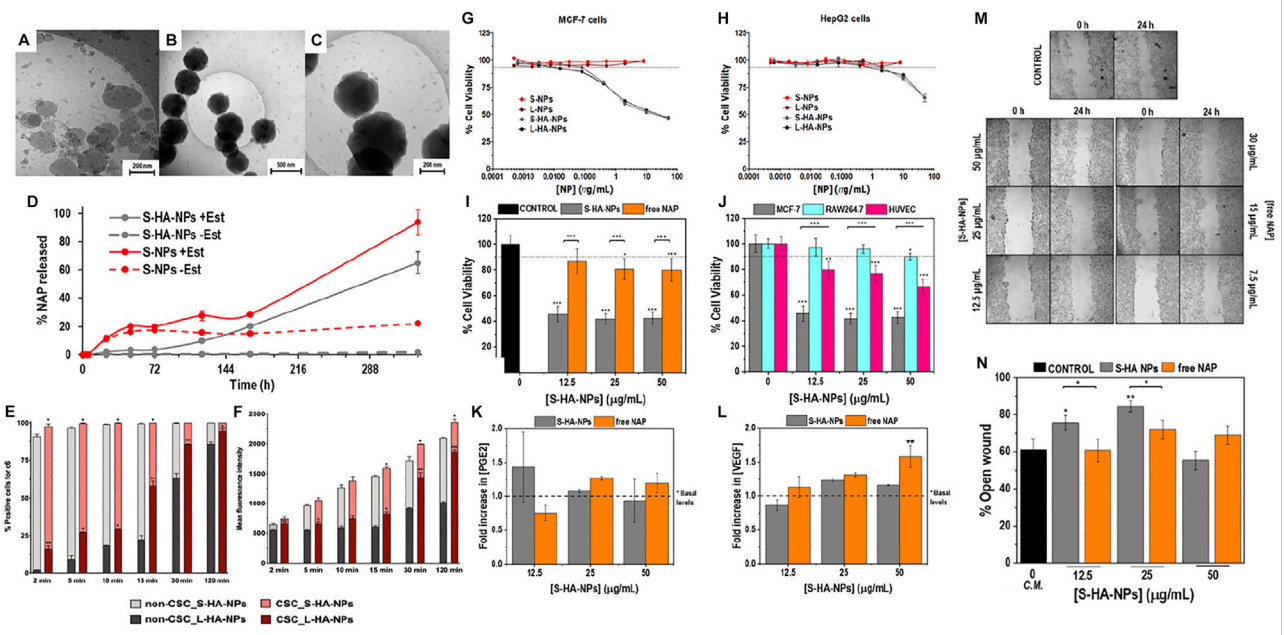

FIGURE 2
(A) Uncoated NPs, without HA covering **(B)** HA-NPs at low magnification, **(C)** HA-NPs at higher magnification. **(D)** Naproxen release kinetics from HA-coated or uncoated NPs. **(E)** Percentage of positive cells for c6 and **(F)** the mean fluorescence intensity per cell (t-student, *$p < 0.05$, **$p < 0.01$, ***$p < 0.001$). *In vitro* cytotoxicity of HA-NPs in cells with differential expression of CD44. **(G)** Percentage of cell viability of MCF-7 cells (high expression of CD44) after 72 h of treatment with different concentrations. **(H)** Cell viability experiments in HepG2 cells (low expression of CD44) using the same NPs. Cell viability assays by Alamar Blue in MCF-7, RAW264.7 and HUVEC cells treated with S-HA-NPs. **(I)** Percentage of viable MCF-7 cells relative to control (culture media of MCF-7 cells) after 72 h of treatment with different concentrations. **(J)** Percentage of cell viability in respect to controls (cells treated with culture media) after 72 h of treatment with different concentrations of S-HA-NPs(Statistical analysis was performed by one-way ANOVA test with *$p < 0.01$, **$p < 0.05$ and ***$p < 0.001$). ELISA quantification of **(K)** PGE2 and **(L)*** VEGF released by MCF-7 cells after 72 h of treatment (Statistical analysis was performed by one-way ANOVA test with **$p < 0.05$). Wound healing assay in S-HA-NPs or free NAP treated MCF-7 cells. Effect of different concentrations of S-HA-NPs or free NAP on MCF-7 migration *in vitro*: **(M)** Inverted microscope images (20-fold magnification) of the wound at the beginning of the assay (0 h) and 24 h post-scratching and **(N)** Percentage of open wound after 24 h of treatment when compared to the original wound size (Statistical analysis was performed by one-way ANOVA with *$p < 0.01$ and **$p < 0.05$). Reproduced with permission from ref (Liu et al., 2018a). CC BY 4.0. Copyright 2021 The Authors.

derivatives have been well demonstrated for treating breast cancer (Deb et al., 2014). Espinosa-Cano et al. synthesized HA-NPs from cationic NAP-bearing polymeric NPs (NPs) with excellent anti-inflammatory ability by electrostatically imparting HA coatings. Based on data analysis, the drug release from NPs with HA coating was more stable and linear in the study of NAP release kinetics. Furthermore, regarding the CD44-targeted cellular uptake ability, smaller NPs were shown to be internalized more rapidly in MCF-7 cancer cells than medium to larger NPs. For both types of NPs, regardless of size, faster and more intense internalization of HA-NPs in $CD44^{+}$ CSC, hence CD44-HA interactions can be considered an excellent vehicle to improve the efficiency of anti-cancer drugs against CSC. Cytotoxicity and scratch assays demonstrated that HA-NPs not only had a significant targeting effect on RAW264.7, HUVEC, and MCF-7 in terms of toxicity but also had a better inhibitory effect on MCF-7 than free NAP. The system also allowed a reduced dose of NAP for pro-apoptotic and anti-migration activity. Overall, HA-NPs can potentially improve the treatment of advanced breast cancer (Espinosa-Cano et al., 2021) (Figure 2).

Reactive oxygen species (ROS) is a significant indicator for regulating biological functions (Perillo et al., 2020). ROS level in cancer cells is higher than that in healthy cells, which ROS can realize to promote tumor proliferation and metastasis. One of the ways chemotherapeutic drugs induce apoptosis in cancer cells is to enhance oxidative stress in cells by increasing intracellular ROS levels (Yang et al., 2018a). Therefore ROS inducers that effectively cause apoptosis of cancer cells through oxidative stress can be potential candidates for cancer chemotherapy. Shikonin (SHK) is a bioactive natural naphthoquinone isolated from the roots of Lithospermum erythrorhizon, which has demonstrated good bioactivity in cancer therapy and anti-inflammation and wound healing (Guo et al., 2019). Meng et al. utilized hyaluronic acid encapsulated SNK liposomes to obtain HA-SHK-Lip to treat triple-negative breast cancer (TNBC). As a result, the internalization ability and retention time of HA-SHK-Lip in MDA-MB-231 cells was significantly higher than free SHK and SHK-Lip. HA-SHK-Lip effectively increased intracellular oxidative stress by effectively upregulating ROS levels in MDA-MB-231 cells and decreasing intracellular GSH (53.6% in the control group) through ROS caused apoptosis and thus exhibited excellent anti-tumor ability. This study provides an effective therapeutic strategy to combat TNBC by enhancing cellular oxidative stress (Meng et al., 2022).

Recently, an active anticancer substance, 17-hydroxy-jolkinolide B (HJB), a diterpenoid from the roots of *Euphorbia* Fischer Diana Steud, has attracted the interest of researchers. In clinical cancer therapy, low water solubility and bioavailability are the main factors limiting its application (Jian et al., 2018a; Jian et al., 2018b). Liu et al. first studied the effect of HJB on breast cancer inhibition. The HJB liposomes were encapsulated with HA by electrostatic adsorption to obtain HA-Lip-HJB, aiming to improve its hydrophilicity and bioavailability and enhance tumor targeting *in vivo*. The results showed that HA-Lip-HJB significantly improved the delivery of liposomes in 4T1 cells in response to the CD44 receptor. In addition, HA-Lip-HJB could inhibit the 4T1 cell migration of cancer cells by regulating EMT progression. Meanwhile, in tumor suppression tests, *in vitro* 3D tumor spheroids decreased in size to 5.9% of the original size after 9 days, and *in vivo* tumor suppression was finally 75.6% after 15 days, which was higher than that of free HJB and Lip-HJB, evidencing the excellent anti-tumor ability of HA-Lip-HJB. It could also inhibit the migration and colonization of tumor cells in the lung. Therefore, the HA-Lip-HJB prepared by the research group provides a potential strategy for treating metastatic breast cancer (Liu et al., 2021).

Quercetin is a natural candidate for novel anti-inflammatory and anti-cancer agents; recently, it has attracted attention for its anti-tumor activity (İkizler et al., 2007). Everolimus is an oral rapamycin analog used to treat breast cancer (Royce and Osman, 2015). In 2017, Quagliariello et al. prepared a HA nanogel based on CD44-targeted loaded quercetin for co-administration with everolimus derivatives against hormone-responsive human breast cancer cells MCF7. The objective was to combine natural molecules with chemotherapy to reduce drug doses, thereby reducing side effects and improving treatment outcomes (Nam et al., 2016). In the research, the nano-carriers had good biosafety, and the CD44-mediated endocytosis of the nanohydrogels in human breast cancer cells MCF-7 showed significant internalization of up to 24 h incubation and exhibited higher cytotoxicity than free quercetin against human breast cancer cells MCF-7. In addition, the nano-carriers had good biosafety and could significantly internalize within 24 h of incubation due to CD44-mediated endocytosis of the nanohydrogels in human breast cancer cells MCF-7. Furthermore, the quercetin-loaded HA nanogels exhibited higher cytotoxicity than free quercetin against human breast cancer cells MCF-7. According to the data, the combination of everolimus and quercetin hyaluronic acid hydrogel produced a highly synergistic effect on MCF-7 cells, showing a good inhibition of MCF-7 cells by low concentration administration (10 nM everolimus, 2 mg/ml quercetin HA) with fewer toxic side effects (approximately 60% reduction in the IC50 of everolimus at 72 h). This combination therapy has a profound future in treating breast cancer (Quagliariello et al., 2017).

Adriamycin (DOX) has also been studied to be modified and coupled with HA to form NDDSs for drug delivery targeting breast cancer. Liu et al. used triphenylphosphine (TPP) to bind with HA through ionic bonding, to form a supramolecular self-assembled structure HA-ionic-TPP-DOX between TPP-DOX and HA. HA-ionic-TPP-DOX possessed the ability to target mitochondria inside breast cancer cells through the

TABLE 2 Characteristics of modified HA NDDSs.

Component	Formulation	Therapeutics	Size (nm)	%DLC	Indication	Status	References
HA-poly caprolactone	Polymersome	Doxorubicin	146.2 ± 9.6	3.6 ± 0.4	4 T1 MCF-7	*In vivo*	Shahriari et al. (2019)
DOX-HA-polylactic acid	Nanoparticle	Doxorubicin	123.9 ± 3.3 PDI: 0.191 ± 0.030	DLE: 71.7 ± 3.8	4T1	*In vivo*	Deng et al. (2018)
Dox/HA-ss- ibuprofen	Micelles	Doxorubicin	~120 PDI:0.2	—	4T1	*In vivo*	Chai et al. (2020)
DTX/HA-cys-docosahexaenoic acid/chlorin e6	Nanoparticle	Docetaxel	181.4 ± 1.8 PDI: 0.241 ± 0.039	—	MCF-7	*In vivo*	Wang et al. (2021a)
HA-DTX-Dendron	Dendronized polymer	Docetaxel	122 ± 4 PDI:0.174	—	MDA-MB-231	*In vivo*	Wang et al. (2021b)
SFN/M-HA-SS-n-Tetradecanethiol	Nanoparticle	Sulforaphane	85.90 ± 3.49 PDI: 0.13 ± 0.01	DLE: 33.64 ± 1.33	MDA-MB-231	*In vivo*	Gu et al. (2021)
HA-DOX-cisplatin	Micelles	Doxorubicin, Cisplatin	~80	—	4 T1	*In vivo*	Yu et al. (2020)
α1-acid glycoprotein-HA NPs	Nanoparticle	Doxorubicin	352 ± 22	—	MCF-7, MDA-MB-231	*In vitro*	Omar et al. (2022)

CD44 receptor targeting of HA and the property of TPP to accumulate inside mitochondria. HA-ionic-TPP-DOX in MCF-7 cells can accumulate more DOX in mitochondria, increasing reactive oxygen species (ROS) levels and decreasing mitochondrial membrane potential, resulting in superior anti-tumor effects in MCF-7/ADR cells in zebrafish. In conclusion, HA-ionic-TPP-DOX is promising in treating breast cancer (Liu et al., 2018a).

3 Modified HA NDDSs

By modifying the hydrophilic HA surface with hydrophobic tips (polymers or small molecules) and obtaining amphiphilic NDDSs by self-assembly (Ondreas et al., 2021). These NDDSs have a core-shell structure, with a hydrophilic shell to increase the stability of NDDSs in water for prolonged circulation and a hydrophobic core for drug encapsulation and sustained release. HA has excellent hydrophilic and CD44 receptor targeting properties without triggering the "accelerated blood clearance (ABC) phenomenon (Zhang et al., 2016). Table 2 presents the Modified HA NDDSs prepared by other polymers or small molecules modified HA in recent years.

Recently, Shahriari et al. developed a novel hyaluronic acid-polycaprolactone (HA-PCL) nanopolymer, encapsulated doxorubicin (DOX) in HA-PCL, and studied the therapeutic index and biodistribution of HA-PCL-DOX for a 4T1 metastatic mouse breast cancer model. The obtained results confirmed that HA-PCL-DOX has a higher uptake rate than PEG-PCL-DOX and free DOX in 2 cell types (4T1 and MCF-7), owing to the targeting of the CD44 receptor. In addition, HA-PCL-DOX was shown to be non-significantly toxic to mice organs and to have optimal tumor suppression, effectively prolonging the survival rate of mice. Accordingly, HA-PCL may be considered a potential ideal candidate for DOX delivery in breast cancer treatment (Shahriari et al., 2019).

Efficient delivery of drugs to tumor cells and eventual complete elimination of the tumor is the ultimate purpose of cancer treatment. Unfortunately, due to high interstitial fluid pressure and the multilayered character of tumor cells, anti-cancer drugs are challenging to deliver inside tumors (Jain, 1990; Heldin et al., 2004). The tumor penetrating peptide-iRGD facilitates the penetration of anti-cancer drugs and NDDSs into tumor tissue and can inhibit tumor metastasis (Sugahara et al., 2010; Sugahara et al., 2015). In order to enhance the effectiveness of NDDSs in breast cancer treatment, a DOX-loaded HA-PLA (DOX-HA-PLA) NDDS combined with an iRGD drug delivery system was developed by Deng et al. Their group studied the inhibitory effect of the combined system on the growth and metastasis of breast cancer. The results indicated that DOX-HA-PLA eliminated the ABC phenomenon compared to DOX-PLA and the ability to be taken up by 4T1 cells through specific HA-CD44 interactions. *In vivo* and tumor penetration studies showed significantly better tumor accumulation and lung distribution of DOX-HA-PLA compared to DOX-PLA controls. When co-administered with iGRD, DOX-HA-PLA accumulation at tumor and lung metastasis sites was dramatically increased. The combined administration remarkably enhanced the tumor suppressive effect and survival time of the mice, and no significant lung metastasis was observed. The combined delivery strategy of DOX-HA-PLA and iGRD enhances DOX inhibition of breast cancer tumor growth and metastasis, providing a promising new strategy for breast cancer treatment (Deng et al., 2018).

Precursor drug-polymer micelles (PMs) can improve the aqueous solubility and bioavailability of anticancer drugs (Biswas et al., 2016). However, the lack of tumor targeting and environmentally responsive drug release have limited

their further clinical application (Yin et al., 2018). PMs can be used to realize combination therapy by co-delivery different drugs (Ha et al., 2018). Therefore, preparing PMs-NDDSs with targeting ability is a potential therapeutic strategy to treat breast cancer.

Glutathione (GSH) is an antioxidant widely found in mammals. GSH levels are higher in tumor cells than in extracellular and normal cells (Liu, 2019). Therefore, redox sensitivity has been extensively studied as a stimulating condition for drug release (Akita et al., 2013). In 2020, Chai et al. synthesized a hyaluronic acid-ibuprofen prodrug (HA-ss-BF) with a redox response by binding ibuprofen (BF) to HA *via* disulfide bonds. HA-ss-BF could be a drug delivery carrier for DOX by self-assembly (DOX/HA-ss-BF). *In vitro*, DOX/HA-ss-BF showed excellent inhibition of metastasis (48h, ~9.42%) and improved cell uptake through CD44 receptor mediation. In addition, HA-ss-BF effectively down-regulated the biological levels of COX-2 in 4T1 cells by CD44 receptor- and redox-response-triggered BF release. *In vivo*, DOX/HA-ss-BF showed excellent biosafety and remained capable of rapid accumulation at tumor sites *via* HA-CD44 interactions. In addition, Dox/HA-ss-BF had a good suppressive effect on 4T1 tumor growth (15d, ~58.9%) and metastasis by reducing intracellular COX-2 levels through BF release and the obstruction of tumor growth *in situ* by DOX. DOX/HA-ss-BF shows potential for effective treatment of metastatic breast cancer and offers a novel direction for targeted combination drug delivery for breast cancer treatment (Chai et al., 2020).

In another study, HA was surface modified with docosahexaenoic acid (DHA) and chlorin e6 (Ce6) *via* disulfide bonding to obtain amphiphilic HA derivatives HA-cys-DHA/Ce6 (CHD) for encapsulation of doxorubicin (DTX) for targeted treatment of breast cancer to achieve combined chemotherapy and photodynamic therapy (PDT), and *in vivo* fluorescence imaging by Ce6 to provide aid in tumor diagnosis and treatment. DTX/CHD nanoparticles increased the uptake of MCF-7 cells through the CD44 receptor, thus reducing side effects and realizing redox response in tumor cells to enable the release of DTX and Ce6. Meanwhile, DTX and Ce6 exerted favorable anti-tumor effects under the action of NIR light. The combination therapy of chemotherapy and PDT was realized (Wang et al., 2021a).

In addition to the preparation of NDDSs using linear HA polymers, NDDSs obtained by coupling glycodendrons with HA to obtain dendronized polymers can further improve the drug-carrier interactions and effectively enhance the drug delivery efficiency (Zhang et al., 2020a). Wang et al. used HA-DTX coupling as a design idea, linking DTX to HA by a tetrapeptide with proteinase B response (GFLG) and a disulfide bond linking the glycoside to HA to obtain the branched and functional nanostructures HA-DTX-Dendron (HADD). Studies showed that the presence of glycodendrons enhanced the stability of HADD and promoted the accumulation in breast cancer tumors. The stimulatory response of GFLG and disulfide bonds in breast cancer cells increased the rate of DTX release, enabling HADD to demonstrate excellent anti-breast cancer tumor efficacy (Wang et al., 2021b).

The synthesis of GSH-responsive amphiphilic conjugates mostly requires tedious steps. More importantly, these amphiphilic conjugates are not morphologically stable enough after being highly diluted by liquids (Owen et al., 2012). Biomineralization provides a novel strategy for designing simple and stable GSH-responsive amphiphilic conjugates. Calcium phosphate (CaP), a mineral component with good biocompatibility, can be used to mineralize amphiphilic coupled nano-carriers. CaP mineralized nano-carriers can remain stable in a typical human environment (pH 7.4), but tumor-specific drug release can be realized in the weakly acidic tumor cell environment (pH 5–6.5) (Han et al., 2013). Gu et al. based amphiphilic hyaluronic acid-SS-tetradecyl conjugates (HA-SS-TA), mineralized by CaP to obtain M-HA-SS-TA for the delivery of sulforaphane (SFN) with anticancer efficacy for the suppression of breast cancer stem cells (BCSC). M-HA-SS-TA had excellent targeting ability to tumors *via* CD44 receptors and could release SFN rapidly to tumor ecological niche based on pH and redox responses. Therefore, SFN/M-HA-SS-TA exhibited better suppression of BCSC *in vitro* and *in vivo* compared to free SFN. Overall, M-HA-SS-TA provides a new strategy for both the preparation of amphiphilic nanoparticles and the treatment of breast cancer (Gu et al., 2021).

In another facile strategy for preparing a pH-sensitive HA-based anti-breast cancer drug delivery system, HA-DOX-CDDP dual drug-loaded micelles were synthesized by cross-linking cisplatin (CDDP) with HA chelation and loading DOX by electron interaction. The pH sensitivity of HA-DOX-CDDP resulted in its significantly enhanced drug release efficiency under acidic conditions. In *in vitro* cell uptake studies, HA-DOX-CDDP showed a differentiated targeting effect on 3T3 and 4T1 cells and, in addition, showed higher internalization compared to the free drug (DOX + CDDP) and HA pretreatment groups. Therefore, HA-DOX-CDDP showed a better internalization effect as well as CD44 targeting. Moreover, HA-DOX-CDDP showed enhanced drug penetration in 3D 4T1 cell cultures. HA-DOX-CDDP has the best *in vivo* tumor suppression effect compared to other experimental groups while ensuring lower toxicity to systemic tissues and organs. Compared with the free drug group, mice treated with HA-DOX-CDDP tumor sections showed increased PARP expression and decreased survivin expression with sound anti-tumor effects (Yu et al., 2020) (Figures 3, 4).

The phenomenon of multidrug resistance (MDR) evasion is a capability possessed by most NDDSs but is powerless against the metastasis of inflammatory tumors (Vyas et al., 2014). The anti-inflammatory protein α1-acid glycoprotein (AGP) can suppress the expression of pro-inflammatory

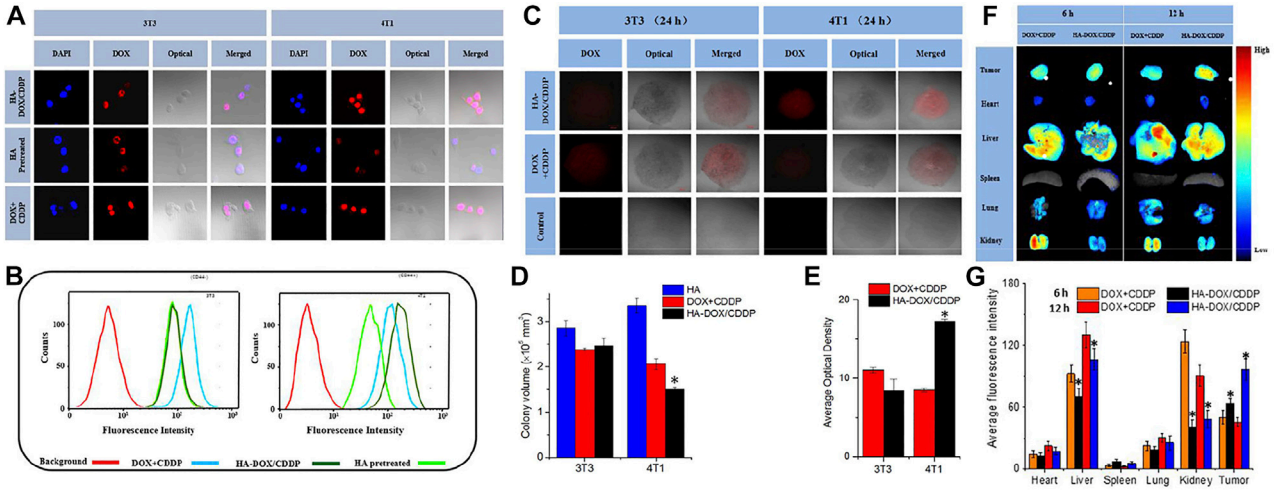

FIGURE 3
In vitro cellular uptake and intracellular DOX release in 3T3 and 4T1 cells. **(A)** Confocal laser scattering microscopy and **(B)** FCM analysis were performed on 3T3 and 4T1 cells following HA pretreatment, and treatment with free DOX + CDDP and HA-DOX-CDDP. *In vitro* multicellular spheroids in 3D suspension cultures. **(C)** Confocal laser scattering microscopy of 4T1 and 3T3 cell spheroids treated with HA, DOX + CDDP, and HA-DOX-CDDP for 24 h. **(D)** Colony volume and **(E)** fluorescence density analyses of 4T1 and 3T3 cell spheroids treated with HA, DOX + CDDP, and HA-DOX-CDDP for 24 h (*$p < 0.05$ compared with the DOX + CDDP group). *In vivo* DOX biodistribution. **(F)** *Ex vivo* fluorescence images of isolated organs and tumors at 6 or 12 h post-injection. **(G)** Semi-quantitative analysis of the mean fluorescence intensity in isolated organs and tumors at 6 or 12 h post-injection. Data are presented as the mean ± SD ($n = 3$) (*$p < 0.05$ compared with the DOX + CDDP group). Reproduced with permission from ref (Owen et al., 2012). CC BY 4.0. Copyright 2020 The Authors.

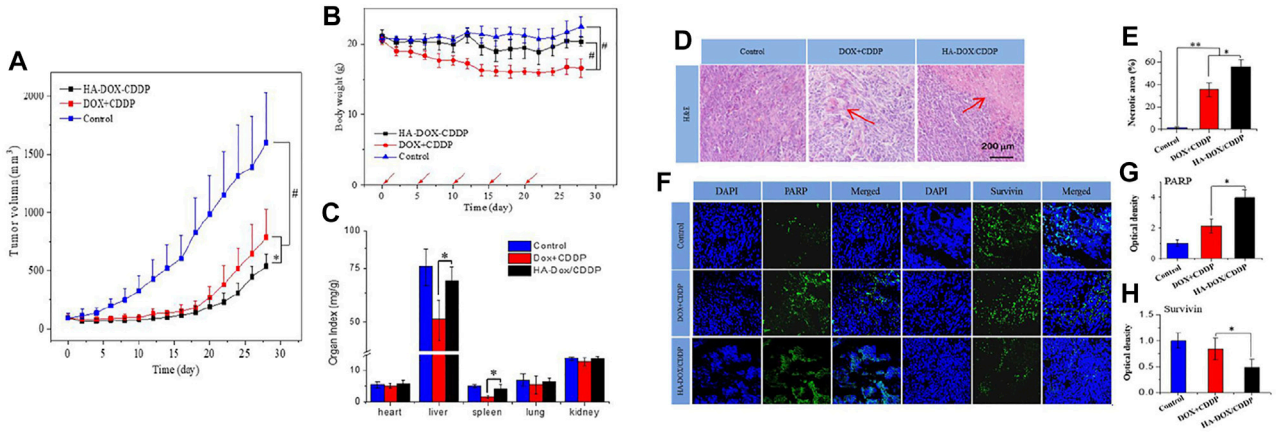

FIGURE 4
In vivo safety and antitumor efficacies. **(A)** Tumor volumes and **(B)** body weights of 4T1-xenografted mice after treatment with NS as the control, DOX + CDDP, or HA-DOX-CDDP. Red arrows showed the tail-veil injection time. **(C)** Organ coefficients of isolated organs in NS, DOX + CDDP, or HA-DOX-CDDP treated groups (*$p < 0.05$, #$p < 0.001$). Histopathology and immunofluorescence analyses. **(D)** Histopathological (H&E) analyses and **(E)** necrotic areas in H&E-stained tumor sections from 4T1-xenografted mice following treatment with NS as the control, DOX + CDDP, or HA-DOX-CDDP. Red arrows indicated the necrotic area. **(F)** Immunohistochemical (PARP and survivin) analyses of tumor tissue sections following treatment with NS as the control, DOX + CDDP, or HA-DOX-CDDP. **(G)** Relative optical densities of tumor sections showing PARP immunofluorescence. **(H)** Relative optical densities of tumor sections showing survivin immunofluorescence (Data are presented as the mean ± SD ($n = 5$). *$p < 0.05$, **$p < 0.01$). Reproduced with permission from ref (Owen et al., 2012). CC BY 4.0. Copyright 2020 The Authors.

factors such as TNF-α and interleukins (IL-6) in the tumor microenvironment (Landskron et al., 2014). Therefore, Omar et al. prepared AGP-HA NPs by combining AGP and HA NPs for targeted delivery of DOX to suppress the growth and migration of tumor cells. The results showed that AGP-HA NPs could effectively inhibit the tumor migration of MCF-7

TABLE 3 Characteristics of HA hybrid NDDSs.

Component	Formulation	Therapeutics	Size (nm)	%DLC	Indication	Status	References
Mesoporous silica nanoparticle-HA-Curcumin	Nanoparticle	Curcumin	75–110	14.76	MDA-MB-231	*In vivo*	Ghosh et al. (2021)
Biodegradable mesoporous silica nanoparticle, HA	Nanoparticle	Doxorubicin, IR780	69.15 ± 3.4	DOX:1.1 ± 0.3 IR780: 9.4 ± 1.8	MCF-7	*In vivo*	Zhan et al. (2021)
Gold nanorods-HA- Folate-DOX	Nanoparticle	Doxorubicin	70.9 ± 1.4	7.1	MCF-7	*In vivo*	Xu et al. (2017)
AuNC@Bovine serum albumin-PTX-Indocyanine green@HA-NO_3 、	Nanoparticle	Paclitaxel, Indocyanine green	195.6 ± 3.2 PDI:0.181 ± 0.012	PTX: 2.97% ± 0.05	4T1	*In vivo*	Liu et al. (2018b)
Cu(II)-Quercetin-Dextran-aldehyde/superparamagnetic iron oxide nanoparticle@HA	Nanoparticle	Quercetin, Cu(II)	—	0.3 ± 0.02 mg/ml	MDA-MB-231, HCC1395	*In vivo*	Cheng et al. (2021)
HA-graphene oxide-Metformin	Nanoparticle	Metformin	673.4 PDI: 0.235	—	MDA-MB-231	*In vitro*	Basu et al. (2021)
HA- carbon dots @p-4-Carboxybenzaladehyde-DOX	Nanoparticle	Doxorubicin	38.61 ± 14.30 PDI: 0.214	22.15%	4T1	*In vivo*	Li et al. (2020)
(DOX/levulan (5-aminolevulinic acid -AHCS/HA^{HER2})	Nanocomplexe	Doxorubicin levulan (5-aminolevulinic acid	~140	ALA:29.38% DOX:11.47%	MCF-7	*In vitro*	Wang et al. (2019a)
NP^{HER2}(DOX/Cisplatin)	Nanoparticle	Doxorubicin, Cisplatin	~162	DOX: 20.55 CDDP:9.53	MCF-7	*In vitro*	Wang et al. (2019b)
Dox,miR34a/Chitosan - linoleic acid/HA	Nanoparticle	Doxorubicin	180 ± 8.3 PDI: 0.082 ± 0.03	13.5 ± 1.20	MCF-7/A	*In vivo*	Yang et al. (2021)
17α-Methyltestosterone/ HA–chitosan–lipoic acid	Nanoparticle	17α-Methyltestosterone	280 ± 0.045 PDI: 0.327 ± 0.002	10.30	BT-20, MCF-7	*In vitro*	Rezaei et al. (2020)
HA-Zein-Honokiol	Nanoparticle	Honokiol	~200	DLE:88.1%~93.6	4T1	*In vivo*	Zhang et al. (2020b)
HA-DOX/Poly (L-histidine)/R848	Nanoparticle	Doxorubicin, R848	~200 PDI: 0.215	DOX: ~6.5 R848:22.8	4T1	*In vivo*	Liu et al. (2018c)
Polypyrrole@Camptothecin-HA-IRDye800CW	Nanoparticle	Camptothecin Photothermal therapy (PTT)	86 ± 9.2	CPT-HA:2.2	4T1	*In vivo*	Sun et al. (2019)
HA/Polyethyleneimine	Nanoparticle	Docetaxel α-napthtoflavone	193.6 ± 3.1 PDI:0.169	DTX:1.14 ± 0.18 ANF: 1.56 ± 0.20	MCF-7/1B1	*In vitro*	Zhang et al. (2019)
Hyaluronic Acid-Based Conjugate/ D-α-Tocopheryl Poly (ethylene glycol) 1000 Succinate	Micelles	Doxorubicin, Quercetin	201.2 ± 2.36 329.83 ± 2.24	D-MM: 8.81 Q-MM: 2.46	MDA-MB-231/ MDR1	*In vivo*	Liu et al. (2020)
HA-D-α-tocopherol succinate-(4-carboxybutyl)triphenyl phosphonium bromide/LPT	Nanoparticle	Lapatinib	207 ± 3 PDI: 0.19 ± 0.03	DLE:84%	MDA-MB-231	*In vivo*	Lee and Cho, (2018)
E-selectin binding peptide-polyethene glycol-1-octadecylamine-HA-PTX/PTX	Micelles	Paclitaxel	102.6 ± 7.9 PDI:0.169	31.5	4TI	*In vivo*	Han et al. (2017)
TMX- Papain -HA-ss-lithocholic acid	Nanoparticle	Tamoxifen	367.5 PDI: 0.116	—	MCF-7	*In vivo*	Batool et al. (2020)
Cur@ZIF-8@HA	Nanoparticle	Curcumin	184.1 ± 13.2	9.6	4T1	*In vivo*	Yu et al. (2021)

cells by suppressing inflammation. In addition, AGP-HA NPs could effectively deliver DOX to the nucleus of MDA-MB-231 cells and inhibit cell proliferation and induce apoptosis. In summary, AGP-HA NPs inhibit the ability of inflammation to attenuate breast cancer cell migration, providing a promising nanotherapeutic platform for the treatment of breast cancer (Omar et al., 2022).

4 HA hybrid NDDSs

In order to improve the effectiveness of breast cancer treatment, it is necessary to give some other advantages to NDDSs composed of HA, including high drug loading, more precise targeting, and more effective inhibition of cancer cell growth and metastasis, etc. The development of HA hybrid

NDDSs composed of HA and other substances offers the possibility of better treatment of breast cancer. In recent years, HA hybrid NDDSs composed of HA in combination with other substances (both organic and inorganic) are shown in Table 3.

4.1 HA hybrid with inorganic mineral

4.1.1 Mesoporous silica

Mesoporous silica (MSN) has received widespread attention as an alternative material for synthesizing NDDS due to its large specific surface area, adjustable particle and pore size, excellent biocompatibility, and high drug encapsulation efficiency (Gao et al., 2020). Recently, Ghosh et al. bonded MSN and HA to synthesize HA-MSN nanohybrid NDDS, which combined CD44 receptor targeting ability and high drug delivery efficiency. By loading nanohybrid with curcumin (MSN-HA-C), the effect of MSN-HA-C in inhibiting triple-negative breast tumors was studied. The results showed that MSN-HA-C effectively inhibited the growth and migration of triple-negative breast cancer tumors in mice through induction of ROS, cell cycle arrest, and regulation of NF-κB and Bax-mediated apoptotic pathways. Compared with free curcumin, it has more efficient bioavailability and cellular uptake (Ghosh et al., 2021). In addition, Zhan et al. prepared bMID NPs with chemotherapeutic and photothermal therapeutic capabilities by equipping DOX and photothermal initiator IR780 based on HA and MSN. MID NPs could accumulate at the tumor site through CD44 receptors and effectively enhance the circulation time of the drug *in vivo* (Yue et al., 2013). bMID NPs showed an increased survival rate in mice compared to the free drug DOX and IR780 groups and favorable inhibition of breast cancer tumors by chemotherapy and photothermal therapy. Thus bMID NPs provide novel nanoplatforms for breast cancer treatment (Zhan et al., 2021).

4.1.2 Gold nanoparticles

Gold nanorods (GNRs) are promising nanomaterials in biomedicine. Au NRs are frequently used for photothermal therapy (PTT) in the treatment of breast cancer due to the strong surface plasmon resonance absorption in the near-infrared spectral region (NIR) while converting NIR to heat with an efficiency close to 100% (Wang et al., 2011; Maestro et al., 2014). Furthermore, rod-shaped nanoparticles exhibit better *in vivo* circulation time and aggregation at the tumor site compared to spherical ones (Chauhan et al., 2011; Barua et al., 2013). However, the non-specific delivery of GNRs limits their application in PTT. To maximize the PTT effectiveness of GNRs in breast cancer cells, it is essential to improve the targeted delivery capacity and *in vivo* circulation duration of Au NRs. In 2017, Xu et al. developed a pH and NIR dual-responsive nanoplatform GNRs-HA-FA-DOX based on HA and GNRs for actively targeted chemotherapy and synergistic photothermal treatment of breast cancer. HA was modified by folic acid (FA), used to modify GNRs, and carried DOX through an unstable hydrazone bond with a pH response. The results showed that trifunctionalized HA increased the morphological stability of GNRs-HA-FA-DOX, increased tumor targeting, and prolonged *in vivo* circulation time, where the addition of FA further promoted the endocytosis of GNRs and DOX by MCF-7 cells compared to the CD44 targeting of HA. *In vitro* and *in vivo*, GNRs-HA-FA-DOX showed excellent chemotherapy/PTT synergism, outperforming chemotherapy or PTT alone. *In vivo* studies, mouse tumors were eliminated after 20 d of treatment, with no recurrence and severe side effects. In conclusion, GNRs-HA-FA-DOX shows excellent potential in breast cancer treatment, maximizes the effect of combined chemotherapy/photothermal treatment, and provides new ideas for designing multifunctional nanocarriers (Xu et al., 2017).

Cancer diagnosis is another issue besides treatment, and combining diagnosis with a treatment simultaneously is the future trend in treating cancer (Khandelia et al., 2015). While most NDDSs designed to treat breast cancer lack diagnostic functions, some imaging functions need to be given to monitor and evaluate the treatment effect. In recent years, gold nanoclusters have been increasing attention for applications such as fluorescence imaging and diagnostics (Zhang et al., 2015a; Zhou et al., 2016). In a previous study, Xie et al. synthesized a highly fluorescent gold nanocluster (AuNC@BSA) with red emissions at 640 nm through the biomineralization of bovine serum albumin (BSA) (Xie et al., 2009). Moreover, the BSA coating retained the capability of AuNC@BSA surface modification and had the potential as a drug carrier. On this basis, Liu et al. introduced HA into AuNC@BSA by cationic cross-linking (AuNC@CBSA@HA), followed by loading PTX, indocyanine green (ICG), and NO donors to construct a diagnostic nanoplatforms for combined chemotherapy/photothermal treatment AuNC@CBSA-PTX-ICG@HA-NO, and studied the suppressive effect of the nanoplatforms on breast cancer tumor growth and metastasis. The addition of HA shielded the positive charge effect of AuNC@CBSA, which effectively prolonged the non-specific toxicity and circulation time of nanoparticles *in vivo* and endowed the active targeting of CD44 receptor of nanoparticles as well as increased the penetration of nanoparticles while degrading at tumor sites. Besides, the nanoparticles showed significantly enhanced penetration ability for breast cancer cells by the synergistic effect of hyaluronidase degradation and NO regulation of the tumor microenvironment. Under the effect of combined treatment by delivering PTX and ICG, AuNC@CBSA-PTX-ICG@HA-NO3 exhibited excellent inhibition of *in situ* breast cancer tumor growth (~95.3%) and lung metastasis (~88.4%), providing an efficient potential strategy for the treatment of breast cancer (Liu et al., 2018b).

4.1.3 Superparamagnetic iron oxide nanoparticle

Superparamagnetic iron oxide nanoparticles (SPIONs) are generally used in cancer treatment and diagnosis, with biodegradability and excellent magnetic properties (Kandasamy and Maity, 2015). SPIONs can achieve targeting capabilities in drug delivery utilizing magnetism and antibody attachment (Laurent and Mahmoudi, 2011). By combining HA and SPION(IO), Cheng et al. prepared a CuQDA/IO@HA nanoparticle loaded with dextran aldehyde (DA)-modified quercetin (Q)-Cu(II) complex with dual targeting function (HA-CD44 and magnetic navigation). CuQDA/IO@HA showed significantly higher internalization efficiency in BRCA mutant TNBC HCC1395 cells than in the non-targeted experimental group in the presence of CD44 receptor and magnetic navigation. In addition, CuQDA/IO@HA exhibited low toxicity to triple-negative breast cancer cells MDA-MB-231 (without BRCA mutation) while exhibiting high toxicity to HCC1395 cells, demonstrating the high specificity of the nanoparticles. In the mutant BRCA1 mice model, the dual targeting function increased the accumulation of CuQDA/IO@HA at tumor sites, reduced systemic toxicity, induced substantial DNA damage *via* Cu(II), and inhibited poly (ADP-ribose) polymerase (PARP), increased double-strand breaks (DSBs) accumulation and inhibited tumor growth. CuQDA/IO@HA provides a novel chemotherapy-free, drug-free regimen for breast cancer treatment through Cu(II)-induced DNA damage in breast cancer cells and further inhibition of DNA repair by quercetin (Cheng et al., 2021).

4.1.4 Graphene oxide

Graphene oxide (GO), an oxidized derivative of graphene, has been widely used as a carrier to deliver drugs due to its high specific surface area and easy functionalization (Depan et al., 2011). Recently, GO has been shown to have an inhibitory effect on the metastasis of TNBC cells (Basu et al., 2018). Basu et al. modified metformin-loaded GO by PEG-PLGA and attached polymer nanoparticles to HA to obtain HA-GO-Met nanoparticles with cellular targeting of TNBC. In particular, HA provided CD44 receptor targeting to improve the uptake of breast cancer cells, while GO offered a higher efficiency encapsulation platform for the drug. The experimental data demonstrated that HA-GO-Met nanoparticles induced apoptosis, suppressed migration and reduced stem cells in MDAMB-231 cells by limiting the translocation of nuclear transcription factor NFkB-p65 in the nucleus and targeting miR-10b in a 4T1 murine mammary carcinoma model, with excellent anti-cancer effects without significant toxicity to normal cells. To summarize, the HA-GO-Met nanoparticles provide a new avenue for treating TNBC as a promising drug delivery platform to suppress the development of breast cancer cells (Basu et al., 2021).

4.1.5 Carbon dots

Carbon dots (CDs) are novel nanomaterials with favorable biocompatibility and potential for surface modification (Singh et al., 2017). In recent years, CDs have received growing interest as drug delivery vehicles in cancer therapy (Panwar et al., 2019). Unfortunately, CDs cannot bind specifically to tumors; therefore, they cannot independently perform the task of effective drug delivery to tumor cells. Li et al. provided a facile strategy to construct a CD44-targeted carbon-site drug delivery system by a one-step method utilizing HA and loading DOX *via* a pH-responsive linker (HA-CD@p-CBA-DOX). The presence of HA conferred better structural stability and hemocompatibility to HA-CD@p-CBA-DOX and showed high cytotoxicity against 4T1 cells through CD44 receptor targeting and acid-sensitive DOX release. HA-CD@p-CBA-DOX exhibited excellent antitumor effects compared to free DOX without significant side effects. These results suggest that HA-CD@p-CBA-DOX deserves further study as a promising novel nano-drug delivery system for breast cancer treatment (Li et al., 2020).

4.2 HA hybrid with organic polymers

4.2.1 Natural polymers

Chitosan (CS) is one of the most commonly used natural biopolymers with good biocompatibility and degradability (Elieh-Ali-Komi and Hamblin, 2016). CS and its derivatives are self-positively charged, so they are usually assembled with negatively charged polymers to form nanocomplexes, and HA is suitable for the need for a negative charge (Srivastava and Purwar, 2017). Based on these advantages, Wang et al. developed multifunctional polysaccharide-based nanocomplexes by employing a layer-by-layer (LbL) self-assembly method using an anionic aldehyde-functionalized hyaluronic acid (AHA), cationic hydroxyethyl chitosan (HECS) and targeting ligand human epithelial growth factor receptor 2 (HER2) antibody-decorated AHA (HA^{HER2}) to prepare multifunctional polysaccharide-based nanocomplexes, and to chemically couple DOX and the photosensitizing prodrug 5-aminolevulinic acid (ALA) to AHA *via* Schiff base bonding to synthesize DOX/ALA- AHCS/HA^{HER2} nanocomplexes. The nanocomplex significantly enhanced the uptake of breast cancer MCF-7 cells through the active targeting of CD44 and HER2 antibodies. Furthermore, ALA in the nanocomplex could be effectively converted into endogenous photosensitizer PpIX in MCF-7 cells and achieve pH-responsive rapid release of DOX in the acidic microenvironment of cancer cells. Combining chemotherapy and photodynamic therapy (PDT) could effectively kill breast cancer MCF-7 cells (Wang et al., 2019a). Although this chemotherapy/PDT combination showed sound anti-cancer effects, the nanocomplexes showed unsatisfactory stability under PDT and limited tissue penetration

by excitation light, limiting the application of nanopolymers. Using CDDP instead of ALA, CDDP molecules were inserted into the nanopolymer by chelating with AHA carboxyl groups to obtain the new NP ^{HER2} (DOX/CDDP) nanopolymer. The introduction of CDDP by cross-linking improves the stability of nanoparticles, but the combination of CDDP and DOX can achieve excellent anti-tumor ability without the need for an external excitation light source, completely overcoming the previous drawbacks. The experimental results showed that NPHER2 (DOX/CDDP) uptake by MCF-7 cells was significantly enhanced by the active targeting of CD44 and HER2 receptors. Due to the micro-acidic environment inside cancer cells, DOX and CDDP acidic pH-sensitive release significantly increased the mortality rate of breast cancer MCF-7 cells. The synergistic treatment of DOX/CDDP exhibited higher toxicity to breast cancer MCF-7 cells compared to DOX release alone. In summary, *in vitro* trials demonstrated the potential of NP^{HER2} (DOX/CDDP) for the treatment of breast cancer tumors, and this novel nanoplatform is expected to be further used for synergistic combination chemotherapy in breast cancer (Wang et al., 2019b).

Besides the efficiency of breast cancer suppression can be improved by combining multiple drugs for chemotherapy, the introduction of MicroRNA34a (miR34a) to reverse the resistance of breast cancer (BCa) cells and treat with chemotherapeutic drugs has also been studied. Yang et al. introduced miR34a and DOX into conjugated linoleic acid (CLA)-modified CS NPs and modified HA on the surface to obtain a novel targeting nanosystem (CCMDH NPs). CCMDH NPs increase the targeting of breast cancer cells through CD44 receptor action and utilize the miR34a to reverse Dox resistance in BCa to enhance DOX anti-tumor effects. The experimental data showed that CCmDHNPs suppressed and facilitated apoptosis by modulating protein expression of B-cell lymphoma-2 (Bcl-2) and poly (ADP-ribose) polymerase (PARP), producing sound inhibitory effects on xenograft tumors in nude mice, as well as effectively suppressed invasion, metastasis, and adhesion of breast cancer cells by regulating the levels of E-cadherin, N-cadherin, MMP2, CD44, and Snail molecules. CCmDHNPs have shown good inhibitory effects on the growth and migration of anti-DOX metastatic BCa tumors, providing an effective and novel therapeutic strategy for breast cancer treatment (Yang et al., 2021).

Hormone therapy also plays a vital role in treating breast cancer, and testosterone is an essential drug for hormone-sensitive metastatic breast cancer (Boni et al., 2014). Rezaei et al. designed a hyaluronic acid-chitosan-lipoic acid nanoparticle (HACSLA-NPs) with CD44 receptor targeting and reduction-responsive drug release, loaded with 17α-Methyltestosterone (MT). The effect of nanoparticles on breast cancer cells was evaluated. In the presence of glutathione, MT could achieve rapid release. Additionally, MT/HACSLA-NPs exhibited better targeting and good inhibition of BT-20 breast cancer cells compared to MT/CSLA-NPs. MT/HACSLA-NPs provide a novel and simple strategy for testosterone inhibition of breast cancer progression (Rezaei et al., 2020). Zeatin is a natural amphiphilic protein contained in corn, with the advantages of good biocompatibility, biodegradability, low cost, and easy availability. Zeatin nanoparticles are widely used to encapsulate and deliver various bioactive molecules. (Chen et al., 2019). Meanwhile, the complexes/or couplings composed of maize protein and other natural materials are simple to prepare and have good physical and chemical stability, which provide the possibility to prepare advanced zein nano delivery systems (Luo and Wang, 2014). Studies have shown that honokiol (HNK) can inhibit the growth and metastasis of various tumors, but its poor hydrophilicity and low bioavailability have significantly limited its use in cancer treatment. (Zhang et al., 2015b; Banik et al., 2019). Zhang et al. combined zein and HA and loaded HNK to prepare hydrophilic HA-coated HNK-loaded zein nanoparticles (HA-Zein-HNK). With CD44 receptor-mediated endocytosis, HA-Zein-HNK had efficient 4T1 cell endocytic uptake, antiproliferative and pro-apoptotic abilities *in vitro*. In addition, HA-Zein-HNK upregulated E-calmodulin expression in breast cancer cells and simultaneously downregulated Vimentin expression, significantly attenuating the invasion and migration of 4T1 cells. In the 4T1 tumor-bearing mice model, HA-Zein-HNK demonstrated a superior ability to suppress tumor growth and metastasis without significant systemic toxicity during treatment. HA-Zein-HNK provides a novel and promising strategy for preparing simple and efficient nanoparticles from natural material complexes to treat breast cancer (Zhang et al., 2020b).

4.2.2 Synthetic polymers

Poly (amino acid) and its derivatives have good biocompatibility, biodegradability, and ease of modification. Through hydrophobic, electrostatic phase, and hydrogen bonding interactions, these nano micelles generally exhibit high hydrophobic drug loading capacity or high hydrophilic ability to modify hydrophobic segments. More importantly, these micelles have pH-sensitive drug release capability to ensure precise drug release in tumor tissues (Xu et al., 2015). Liu et al. used L-histidine (PHIS) to encapsulate the antitumor immunomodulator R848 to prepare PHIS/R848 nanocores (PHIS/R848) and synthesized HA-DOX prodrugs through hydrazone bonds to coat them on the surface of PHIS/R848, to obtain HA-DOX/PHIS/R848 nanoparticles with dual pH sensitivity. In the tumor microenvironment (pH~6.5), PHIS/R848 released R848 to induce macrophage activation and cytokine secretion to achieve immunomodulation; moreover, at pH 5.5 (pH of endo/lysosomes), the breakage of hydrazone bond allowed the rapid release of DOX to achieve toxic effects on cells. The results indicated that PHIS/R848 had

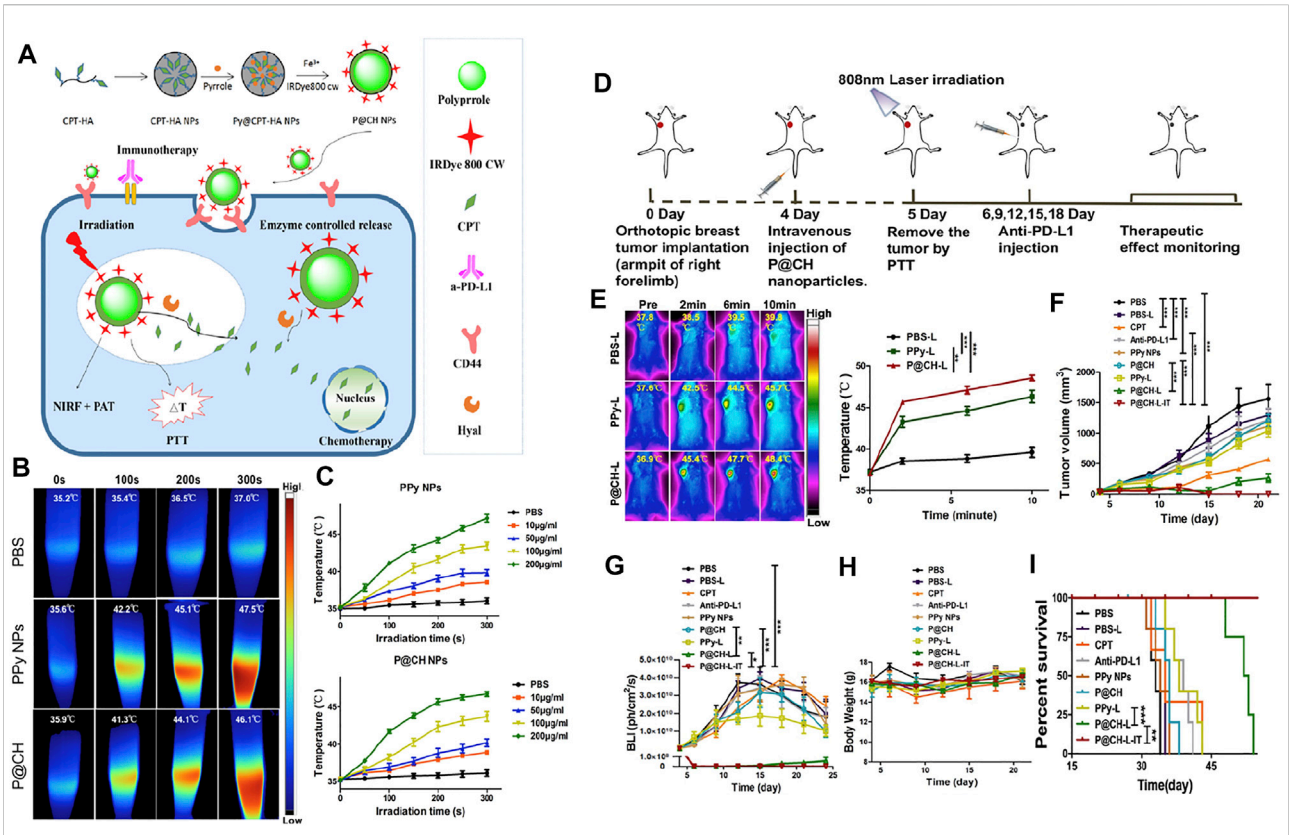

FIGURE 5
(A) Schematic illustration of the formation and functions of P@CH nanoparticles. **(B)** NIR thermal imaging before and after NIR irradiation on PBS, PPy NPs, and P@CH NPs plus laser irradiation. **(C)** Monitoring the increase of temperature with prolonged irradiation time over a series of concentrations of PPy NPs, and P@CH NPs (n = 3). **(D)** Scheme showing the experimental design to evaluate the therapeutic effect. **(E)** Infrared thermal images of the tumor-bearing mice at 24 h post-injection of PBS, PPy NPs, and P@CH NPs *via* the tail vein, before and after NIR laser light irradiation (1.5 W/cm2, 10 min), and the increase of temperature at tumor sites at different time points. **(F)** Tumor volume measurement for different treatment groups. **(G)** Quantification of the BLI signal of tumors after different treatments. **(H)** The body weight of 4T1 tumor-bearing mice with different treatments was measured. **(I)** Survival analysis of orthotopic 4T1 breast cancer mice with different treatments (n = 5) (**p < 0.01). Immune-memory effects induced by P@CH-L-IT combination treatment. Reproduced with permission from ref (Chen et al., 2019). CC BY 4.0. Copyright 2019 The Authors.

the same superior immunomodulatory ability as free R848, and HA-DOX could significantly inhibit the growth of breast cancer cells (MCF-7 and 4T1) mediated by CD44 receptors. The pH-ordered response of HA-DOX/PHIS/R848 resulted in the efficient release of R848 and DOX to target breast cancer cells. In 4T1 tumor-bearing mice, HA-DOX/PHIS/R848 exhibited excellent tumor targeting ability and significantly enhanced tumor suppressive activity in synergy with immunomodulation and chemotherapy, effectively inhibiting breast tumor growth. HA-DO X/PHIS/R848 combined with immunotherapy and chemotherapy showed great potential in breast cancer treatment (Liu et al., 2018c).

Polypyrrole (PPy) has been innovatively applied to photothermal therapy for cancer due to its good biocompatibility and efficient photothermal conversion ability (Yang et al., 2012). Camptothecin (CPT) is a potent anticancer natural compound extracted from the bark of Camptotheca acuminata, which exerts antitumor activity by inhibiting DNA topoisomerase I (Topo I) (Tai et al., 2019). Sun et al. prepared a novel targeted PPy@CPT-HA-IRDye800CW (P@CH) nanoparticle with synergistic chemotherapy/photothermal therapy and PAI/FMI dual-modality imaging capability based on PPy and HA. P@CH NPs have a favorable PTT effect and can reach 46.1°C after 300 s of 808 nm NIR light irradiation. In the *in vivo* combination of photothermal therapy and immunotherapy against tumors, the P@CH + laser irradiation + anti-PD-L1 (P@CH-L-IT) group had surprising results compared to other experimental groups, where 4T1-fluc tumor bearing mice with *in situ* breast cancer tumors were completely eliminated and did not recur throughout the 24-day observation period, with mice surviving over 60 days, much longer than other treatment groups. In the tumor metastasis trial observation, all treatment groups had several pulmonary metastatic nodules, except for the P@CH-L-IT combination treatment group. In addition, the P@

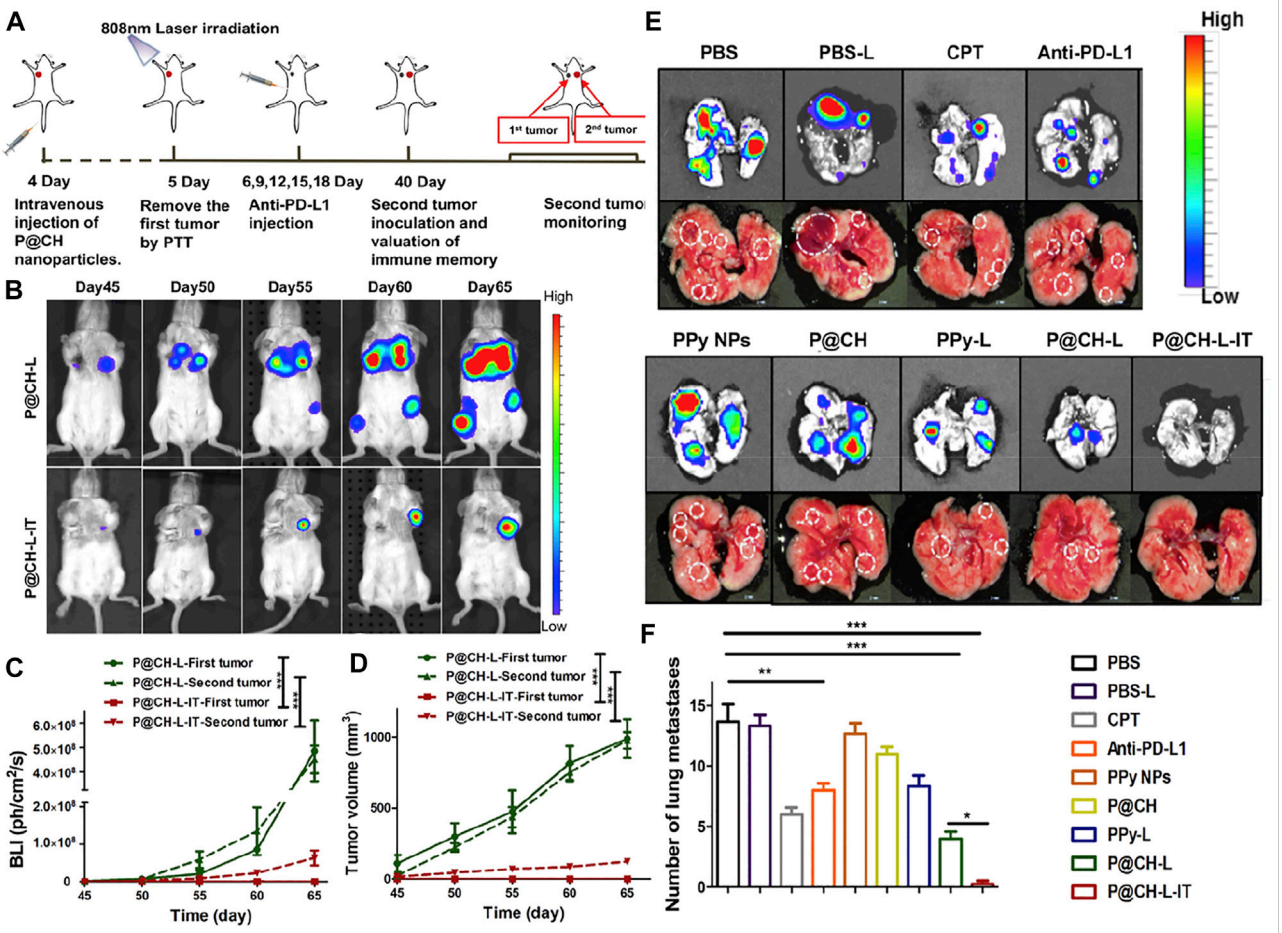

FIGURE 6
(A) Scheme showing the rechallenge experimental design to evaluate the immune-memory effect. **(B)** The dynamic BLI images of rechallenged mice from the P@CH-L and P@CH-L-IT groups (n = 5) for 65 continuous days. **(C)** Quantification of the BLI signal intensity of rechallenged tumors. **(D)** Tumor volume measurement of second rechallenged tumors and first tumors in two groups. Chemo-photothermal therapy in combination with immune checkpoint blockade therapy prevented lung metastases. **(E)** Representative BLI images and white-light pictures showing the lung metastases. **(F)** The number of lung metastasis nodules of different groups (n = 3). Reproduced with permission from ref (Chen et al., 2019). CC BY 4.0. Copyright 2019 The Authors.

CH-L-IT group activated a systemic anti-tumor immune response to suppress lung metastasis and tumor recurrence in the long term. The combined therapy of P@CH-L-IT has an excellent effect on treating and preventing breast cancer recurrence. More excitingly, the PAI/FMI imaging properties of P@CH can be further used for image-guided chemoradiotherapy of breast tumors. This potential therapeutic strategy opens up a new path and direction for the clinical management of breast cancer and other malignant tumors. (Sun et al., 2019) (Figures 5, 6).

Polyethyleneimine (PEI), a cationic polymer, has been extensively studied as an anticancer drug delivery carrier (Fahira et al., 2022). α-naphthoflavone (ANF) is a CYP1B1 inhibitor that can reduce the multidrug resistance (MDR) of cancer cells to DTX by inhibiting the expression of CYP1B1 (Cui et al., 2015). Zhang et al. modified PEI with PLGA followed by wrapping HA outer layer by loading ANF and DTX to obtain HA/PEI NPs. Notably, HA/PEI NPs could effectively promote endocytosis of breast cancer cells by binding to CD44 receptors on the surface of breast cancer cells, thereby increasing the enrichment of ANF in breast cancer cells. The inhibitory effect of ANF on CYP1B1 expression increased the bioavailability of DTX and thereby enhanced the apoptosis-inducing ability of DTX. HA/PEI NPs effectively overcome the CYP1B1-mediated MDR in breast cancer and provide a promising strategy for the treatment of MDR breast cancer (Zhang et al., 2019).

D-α-tocopheryl polyethylene glycol succinate (TPGS or Vitamin E TPGS) is approved by the FDA as a safe adjuvant. TPGS has the characteristics of excellent biocompatibility,

improving drug solubility and permeability, and inhibiting the activity of ATP-dependent P-glycoprotein, so it is widely used in the delivery system of anticancer drugs (Guo et al., 2013; Yang et al., 2018b). Liu et al. prepared HA-based reduction-sensitive couples (HA-SS-DOCA) through previous work and synthesized mixed micelles together with TPGS, and used the mixed micelles to load DOX (D-MM) and quercetin (QU) (Q-MM) (Deng et al., 2017). Through the combined effect of Q-MM/Q-MM on MDA-MB-231/MDR1 cells, reducing the efflux of DOX by down-regulating the expression of P-glycoprotein can accelerate the mitochondrial apoptotic pathway and promote DOX-induced apoptosis. This combined treatment strategy improved tumor targeting in MDA-MB-231/MDR1 tumor-bearing mice and effectively inhibited tumor growth without serious side effects. In this study, the combination of DOX and QU effectively improved the bioavailability of DOX and reduced the toxic side effects, providing a novel strategy for chemotherapeutic drugs and chemotherapeutic drugs to reverse tumor MDR (Liu et al., 2020).

4.3 HA hybrid with organic molecule compounds

D-α-tocopherol succinate (TS) is a vitamin derivative with nontoxicity and good biocompatibility. Due to the poor water solubility of TS, it can be used as the hydrophobic core of self-assembled nanoparticles (Liang et al., 2015). In addition, TS induces apoptosis of malignant tumor cells through a reactive oxygen species (ROS)-dependent mechanism, which can synergize with chemotherapeutic drugs (Liang et al., 2015). Lee et al. designed to graft TS onto the HA backbone to prepare HA-TS amphiphilic nanoparticles, followed by introducing TPP as a mitochondrial targeting agent into HA-TS, and finally encapsulated lapatinib (LPT) to obtain HA-TS-TPP/LPT NPs for the treatment of breast cancer. HA-TS-TPP/LPT could effectively target tumors in MDA-MB-231 tumor-bearing mice through the EPR effect and CD44 receptor effect, and the cationic property and lipophilicity of TPP enhanced the intracellular accumulation of nanoparticles. In addition, after the nanoparticles were endocytosed by breast cancer cells, the mitochondrial targeting of TPP and the mitochondrial destruction capability of TS combined with LPT to produce killing effects on breast cancer cells, effectively improving the anti-cancer efficiency and anti-cancer activity of LPT. HA-TS-TPP/LPT showed promising effects in treating breast cancer in animal models, providing a possibility for further clinical research (Lee and Cho, 2018).

E-selectin (CD62E) is an inducible transmembrane adhesion protein expressed on endothelial cells activated by cytokines such as TNF-α and IL1-β during inflammation and tumors (Kang et al., 2016). In addition, E-selectin can target dividing microvascular endothelial cells that generate active blood vessels in tumor vasculature. Hence E-selectin can be used to modify nanoparticles to increase the uptake of dividing microvascular endothelial cells (Shamay et al., 2015). Han et al. applied E-selectin-binding peptide (Esbp) to treat breast cancer. The synthetic Esbp-polyethylene glycol-1-octadecylamine (Esbp-PEG-OA) divided microvascular endothelial cell-targeting ligand for amphiphilic HA-coupled prodrug micelles (HA-PTX). Esbp-PEG-OA and HA-PTX were self-assembled in an aqueous environment containing free DOX to obtain novel anticancer micelles (Esbp-HA-PTX/PTX). The experimental results showed that through the targeting of E-selectin and CD44 receptors, Esbp-HA-PTX exhibited both good targeting and excellent levels of cellular internalization on HUVEC and 4T1 cells *in vitro* and higher cytotoxicity compared to PTX solution. *In vivo*, Esbp-HA-PTX/PTX exhibited prolonged cycling time and excellent dual-cell targeting ability. More importantly, Esbp-HA-PTX/PTX exhibited excellent capability to inhibit tumor proliferation and metastasis without significant toxic side effects based on the suppression of intra-tumor microvasculature and tumor cell growth. Overall, Esbp-HA-PTX/PTX micelles provide a compelling new strategy for multicellular targeted breast cancer treatment (Han et al., 2017).

Among the treatments for breast cancer, endocrine therapy (anti-estrogen) is considered one of the preferable treatment modalities due to its low morbidity and mortality (Lumachi et al., 2011). Tamoxifen (TMX) is the preferred drug for anti-estrogen therapy for metastatic and advanced breast cancer, but long-term oral administration of TMX has significant side effects on the body (Hard et al., 1993). To overcome this challenging problem, we developed a self-emulsifying drug delivery system (SEDDS) for targeted delivery of TMX to the intestinal lymphatic system, reducing toxic side effects and increasing the bioavailability of TMX (Trevaskis et al., 2008). Batool et al. synthesized TMX-PAP-HA-SS-LCA SNEDDS using papain modification of S-protected hyaluronic acid-lithocholic acid co-block polymer carbodiimide containing TMX for suppression of breast tumors. Compared with the pure TMX experimental group, the mucus permeability of TMX-PAP-HA-SS-LCA was significantly improved, therefore enhancing cellular uptake. Additionally, TMX-PAP-HA-SS-LCA exhibited good compatibility with macrophages at different concentrations of TMX and had a lower drug release concentration on MCF-7 cells (IC_{50} = 5.98 ± 0.9 μg/ml, 24 h; 5.48 ± 1.4 μg/ml, 48 h) with targeting potential and antiproliferative solid activity. TMX-PAP-HA-SS-LCA improves the bioavailability of TMX through enhanced mucosal permeation without significant systemic toxicity, providing a novel and feasible strategy for endocrine therapy to inhibit the growth of breast tumors (Batool et al., 2020).

Among metal-organic frameworks (MOFs), zeolitic imidazolate framework-8 nanoparticle (ZIF-8) is frequently used as drug delivery carriers with good biocompatibility and ph-responsive degradability (Kida et al., 2013; Chen et al., 2020).

Yu et al. loaded curcumin (Cur) into ZIF-8 (Cur@ZIF-8), prepared Cur@ZIF-8@HA nanoparticles by electrostatic interaction with HA, and applied it to breast cancer treatment. Benefiting from the excellent biocompatibility of HA and the active targeting ability of the CD44 receptor, Cur@ZIF8@HA showed a significant enhancement of biocompatibility and 4T1 cell uptake compared to Cur@ZIF-8. In addition, in 4T1 cells, Cur@ZIF8@HA could effectively induce apoptosis through LDH release, cell cycle arrest, and ROS overproduction. *In vivo*, tumor growth and lung metastasis could be effectively inhibited by 4T1 cell targeting of Cur@ZIF8@HA and the release of Cur in response to acidic pH. Cur@ZIF-8@HA showed excellent potential in breast cancer therapy and combining HA and MOF to prepare nanoparticles provides a new direction for developing anti-breast cancer drug delivery systems (Yu et al., 2021).

5 Clinical studies of nanomedicine in HA

HA has been extensively studied as a targeting ligand in the preclinical stage. HA-based NDDSs have shown enhanced anticancer activity and a higher safety profile than conventional regimens for cancer treatment. The classification of HA conjugates as new chemical entities (NCE) is one of the barriers to their treatment of cancer. Various anticancer drugs combined with HA for targeted therapy (e.g., irinotecan, DOX, 5FU, and MTX) have been studied in clinical trials. HA-irinotecan was shown to be biosafety and well-tolerated without reducing irinotecan drug activity in a phase 1 clinical trial of 12 patients (Brown, 2008). In another phase 2 clinical trial designed for 41 patients, the advantages of HA nanoformulations in progression-free survival and safety were demonstrated (Gibbs et al., 2011). In 2014, Alchemia Oncology initiated a study using HA-irinotecan in phase 2, a single-arm trial of FOLF(HA)iri in combination with cetuximab in second-line patients with KRAS wild-type metastatic colorectal cancer not treated with irinotecan (NCT02216487). The objective of the study was to confirm the safety and efficacy of FOLF(HA)iri plus cetuximab as a second-line treatment for patients with primary metastatic colorectal cancer treated with irinotecan.

6 Summary and prospective outlook

In recent decades, nanotechnology has been dramatically developed in cancer therapy. Presently, NDDSs play a critical role in the targeted delivery of breast cancer treatment, which can realize high accumulation and release of anticancer drugs at the tumor site to improve the therapeutic efficiency of drugs while reducing the toxic side effects on the normal tissues and organs of the human body, which not only overcomes the limitations of traditional drugs for breast cancer treatment but also has the potential to reduce the cost of conventional treatment, thereby solving a significant obstacle in breast cancer treatment.

Improving tumor-specific targeting is one of the critical factors for NDDSs to improve the efficacy of treating breast tumors. HA can target overexpressing breast cancer cells CD44 receptor, which is suitable as a potential target for breast cancer-targeting NDDSs. In addition, HA has good biocompatibility and excellent hydrophilicity, which provides advantages such as better hydrophilicity and long internal circulation time for inorganic or organic nanoparticles, including hydrophobic anticancer drugs. Therefore, HA is highly suitable for clinical application in breast cancer treatment.

In this review, we have discussed recent advances in treating breast cancer with HA-containing NDDSs. In recent years, many studies have shown that nano-delivery systems with HA can effectively target breast cancer cells *via* passive EPR and active CD44 receptor-mediated endocytosis, providing a simple and efficient way to target breast cancer cells for drug delivery actively. More excitingly, HA can be easily modified due to its wealthy chemical groups and can be combined with other inorganic or organic compounds to give HA NDDSs other advantages, such as increased drug loading, enhanced targeting, and some synergistic therapies. The HA NDDSs section of the review summarizes the progress of research on HA as a hydrophilic fraction for encapsulation or coupling of chemotherapeutic drugs, which directly enriches chemotherapeutic drugs at breast tumors through CD44 targeting, improving drug utilization and reducing systemic toxicity. In order to enhance the drug loading capacity and functionalization of HA NDDSs, researchers developed Modified HA NDDSs, which were further modified to confer higher drug loading capacity and tumor environment-sensitive drug release, significantly improving the anti-cancer effects of HA NDDSs. Many substances have anticancer potential, but their application is greatly limited because they do not possess the ability to target breast tumors or have poor biocompatibility on their own. HA nanohybrid NDDSs section summarizes the application of HA as an increase in the targeting ability or increased biocompatibility of other NDDSs, and the introduction of HA has dramatically broadened the choice of nano drugs in the treatment of breast cancer. They are resulting in Modified HA NDDSs and HA nanohybrid NDDSs with excellent performance for treating, preventing, and diagnosing breast cancer.

Unfortunately, until now, artificial mouse xenograft cancer models have been widely used due to the lack of suitable animal models, thereby having the disadvantage of not being able to mimic the different mutations carried by multiple cancer cells in human tumors, resulting in the inability to accurately mimic the immune landscape of *in situ* tumors (Sun et al., 2020). Although the development of HA-based drug carriers offers potential new clinical options for treating and preventing breast cancer, clinical

studies demonstrating the efficacy of HA NDDSs in treating breast cancer are still lacking. In addition, in previous studies, there were discrepancies between preclinical and clinical experimental results of nano drugs, and nano drugs did not produce the same effects in humans as they did in rodents (Youn and Bae, 2018). However, the future work is still auspicious as more researchers from various disciplines (including physiology, pathology, oncology, material science, etc.) continue to develop superior NDDSs for better treatment of breast cancer in the clinic.

Nanomedicine is an emerging approach to cancer treatment, and a growing number of researchers continue to develop NDDSs with superior properties that offer more promising options for the treatment of breast cancer. Among these, HA-containing NDDSs are typically biocompatible and show significant potential for drug delivery and breast cancer tumor targeting. Although clinical data are lacking in breast cancer, HA has demonstrated its potential for clinical utilization in several clinical trials. These data provide strong evidence for continued research into the use of HA for future clinical breast cancer treatment.

Author contributions

YJ and SC wrote this article; CW revised this article; LY and TS checked and review this article.

Conflict of interest

The authors declare that the research was conducted in the absence of any commercial or financial relationships that could be construed as a potential conflict of interest.

Publisher's note

References

Agrawal, S., Dwivedi, M., Ahmad, H., Chadchan, S. B., Arya, A., Sikandar, R., et al. (2018). CD44 Targeting Hyaluronic Acid Coated Lapatinib Nanocrystals Foster the Efficacy against Triple-Negative Breast Cancer. *Nanomedicine Nanotechnol. Biol. Med.* 14 (2), 327–337. doi:10.1016/j.nano.2017.10.010

Akita, H., Ishiba, R., Hatakeyama, H., Tanaka, H., Sato, Y., Tange, K., et al. (2013). A Neutral Envelope-Type Nanoparticle Containing pH-Responsive and SS-Cleavable Lipid-Like Material as a Carrier for Plasmid DNA. *Adv. Healthc. Mater.* 2 (8), 1120–1125. doi:10.1002/adhm.201200431

Arias, J.-I., Aller, M.-A., and Arias, J. (2007). Cancer Cell: Using Inflammation to Invade the Host. *Mol. Cancer* 6 (1), 29–10. doi:10.1186/1476-4598-6-29

Banik, K., Ranaware, A. M., Deshpande, V., Nalawade, S. P., Padmavathi, G., Bordoloi, D., et al. (2019). Honokiol for Cancer Therapeutics: A Traditional Medicine that Can Modulate Multiple Oncogenic Targets. *Pharmacol. Res.* 144, 192–209. doi:10.1016/j.phrs.2019.04.004

Barua, S., Yoo, J.-W., Kolhar, P., Wakankar, A., Gokarn, Y. R., and Mitragotri, S. (2013). Particle Shape Enhances Specificity of Antibody-Displaying Nanoparticles. *Proc. Natl. Acad. Sci. U. S. A.* 110 (9), 3270–3275. doi:10.1073/pnas.1216893110

Basu, A., Upadhyay, P., Ghosh, A., Bose, A., Gupta, P., Chattopadhyay, S., et al. (2021). Hyaluronic Acid Engrafted Metformin Loaded Graphene Oxide Nanoparticle as CD44 Targeted Anti-cancer Therapy for Triple Negative Breast Cancer. *Biochimica Biophysica Acta - General Subj.* 1865 (3), 129841. doi:10.1016/j.bbagen.2020.129841

Basu, A., Upadhyay, P., Ghosh, A., Chattopadhyay, D., and Adhikary, A. (2018). Folic-Acid-Adorned PEGylated Graphene Oxide Interferes with the Cell Migration of Triple Negative Breast Cancer Cell Line, MDAMB-231 by Targeting miR-21/PTEN Axis through NFκB. *ACS Biomater. Sci. Eng.* 5 (1), 373–389. doi:10.1021/acsbiomaterials.8b01088

Batool, A., Arshad, R., Razzaq, S., Nousheen, K., Kiani, M. H., and Shahnaz, G. (2020). Formulation and Evaluation of Hyaluronic Acid-Based Mucoadhesive Self Nanoemulsifying Drug Delivery System (SNEDDS) of Tamoxifen for Targeting Breast Cancer. *Int. J. Biol. Macromol.* 152, 503–515. doi:10.1016/j.ijbiomac.2020.02.275

Biswas, S., Kumari, P., Lakhani, P. M., and Ghosh, B. (2016). Recent Advances in Polymeric Micelles for Anti-cancer Drug Delivery. *Eur. J. Pharm. Sci.* 83, 184–202. doi:10.1016/j.ejps.2015.12.031

Boni, C., Pagano, M., Panebianco, M., Bologna, A., Sierra, N. M. A., Gnoni, R., et al. (2014). Therapeutic Activity of Testosterone in Metastatic Breast Cancer. *Anticancer Res.* 34 (3), 1287–1290.

Brown, T. J. (2008). The Development of Hyaluronan as a Drug Transporter and Excipient for Chemotherapeutic Drugs. *Curr. Pharm. Biotechnol.* 9 (4), 253–260. doi:10.2174/138920108785161514

Burdick, J. A., and Prestwich, G. D. (2011). Hyaluronic Acid Hydrogels for Biomedical Applications. *Adv. Mat.* 23 (12), H41–H56. doi:10.1002/adma.201003963

Cadete, A., and Alonso, M. J. (2016). Targeting Cancer with Hyaluronic Acid-Based Nanocarriers: Recent Advances and Translational Perspectives. *Nanomedicine* 11 (17), 2341–2357. doi:10.2217/nnm-2016-0117

Castellino, S., O'Mara, M., Koch, K., Borts, D. J., Bowers, G. D., and MacLauchlin, C. (2012). Human Metabolism of Lapatinib, a Dual Kinase Inhibitor: Implications for Hepatotoxicity. *Drug Metab. Dispos.* 40 (1), 139–150. doi:10.1124/dmd.111.040949

Chai, Z., Teng, C., Yang, L., Ren, L., Yuan, Z., Xu, S., et al. (2020). Doxorubicin Delivered by Redox-Responsive Hyaluronic Acid–Ibuprofen Prodrug Micelles for Treatment of Metastatic Breast Cancer. *Carbohydr. Polym.* 245, 116527. doi:10.1016/j.carbpol.2020.116527

Chauhan, V. P., Popović, Z., Chen, O., Cui, J., Fukumura, D., Bawendi, M. G., et al. (2011). Fluorescent Nanorods and Nanospheres for Real-time *In Vivo* Probing of Nanoparticle Shape-dependent Tumor Penetration. *Angew. Chem. Int. Ed. Engl.* 123 (48), 11619–11622. doi:10.1002/ange.201104449

Chen, S., Han, Y., Huang, J., Dai, L., Du, J., McClements, D. J., et al. (2019). Fabrication and Characterization of Layer-By-Layer Composite Nanoparticles Based on Zein and Hyaluronic Acid for Codelivery of Curcumin and Quercetagetin. *ACS Appl. Mat. Interfaces* 11 (18), 16922–16933. doi:10.1021/acsami.9b02529

Chen, X., Tong, R., Liu, B., Liu, H., Feng, X., Ding, S., et al. (2020). Duo of (–)-Epigallocatechin-3-Gallate and Doxorubicin Loaded by Polydopamine Coating ZIF-8 in the Regulation of Autophagy for Chemo-Photothermal Synergistic Therapy. *Biomater. Sci.* 8 (5), 1380–1393. doi:10.1039/c9bm01614g

Cheng, H.-W., Chiang, C.-S., Ho, H.-Y., Chou, S.-H., Lai, Y.-H., Shyu, W.-C., et al. (2021). Dextran-modified Quercetin-Cu (II)/hyaluronic Acid Nanomedicine with Natural Poly (ADP-Ribose) Polymerase Inhibitor and Dual Targeting for Programmed Synthetic Lethal Therapy in Triple-Negative Breast Cancer. *J. Control. Release* 329, 136–147. doi:10.1016/j.jconrel.2020.11.061

Colleoni, M., Rocca, A., Sandri, M., Zorzino, L., Masci, G., Nole, F., et al. (2002). Low-dose Oral Methotrexate and Cyclophosphamide in Metastatic Breast Cancer: Antitumor Activity and Correlation with Vascular Endothelial Growth Factor Levels. *Ann. Oncol.* 13 (1), 73–80. doi:10.1093/annonc/mdf013

Cui, J., Meng, Q., Zhang, X., Cui, Q., Zhou, W., and Li, S. (2015). Design and Synthesis of New α-naphthoflavones as Cytochrome P450 (CYP) 1B1 Inhibitors to Overcome Docetaxel-Resistance Associated with CYP1B1 Overexpression. *J. Med. Chem.* 58 (8), 3534–3547. doi:10.1021/acs.jmedchem.5b00265

Deb, J., Majumder, J., Bhattacharyya, S., and Jana, S. S. (2014). A Novel Naproxen Derivative Capable of Displaying Anti-cancer and Anti-migratory Properties against Human Breast Cancer Cells. *BMC cancer* 14 (1), 567–568. doi:10.1186/1471-2407-14-567

Deng, B., Xia, M., Qian, J., Li, R., Li, L., Shen, J., et al. (2017). Calcium Phosphate-Reinforced Reduction-Sensitive Hyaluronic Acid Micelles for Delivering Paclitaxel in Cancer Therapy. *Mol. Pharm.* 14 (6), 1938–1949. doi:10.1021/acs.molpharmaceut.7b00025

Deng, C., Xu, X., Tashi, D., Wu, Y., Su, B., and Zhang, Q. (2018). Co-administration of Biocompatible Self-Assembled Polylactic Acid–Hyaluronic Acid Block Copolymer Nanoparticles with Tumor-Penetrating Peptide-iRGD for Metastatic Breast Cancer Therapy. *J. Mat. Chem. B* 6 (19), 3163–3180. doi:10.1039/c8tb00319j

Depan, D., Shah, J., and Misra, R. (2011). Controlled Release of Drug from Folate-Decorated and Graphene Mediated Drug Delivery System: Synthesis, Loading Efficiency, and Drug Release Response. *Mater. Sci. Eng. C* 31 (7), 1305–1312. doi:10.1016/j.msec.2011.04.010

Dheer, D., Arora, D., Jaglan, S., Rawal, R. K., and Shankar, R. (2017). Polysaccharides Based Nanomaterials for Targeted Anti-cancer Drug Delivery. *J. drug Target.* 25 (1), 1–16. doi:10.3109/1061186x.2016.1172589

Dubey, S. K., Bhatt, T., Agrawal, M., Saha, R. N., Saraf, S., Saraf, S., et al. (2022). Application of Chitosan Modified Nanocarriers in Breast Cancer. *Int. J. Biol. Macromol.* 194, 521–538. doi:10.1016/j.ijbiomac.2021.11.095

Elieh-Ali-Komi, D., and Hamblin, M. R. (2016). Chitin and Chitosan: Production and Application of Versatile Biomedical Nanomaterials. *Int. J. Adv. Res.* 4 (3), 411–427.

Espinosa-Cano, E., Huerta-Madroñal, M., Cámara-Sánchez, P., Seras-Franzoso, J., Schwartz, S., Jr, Abasolo, I., et al. (2021). Hyaluronic Acid (HA)-coated Naproxen-Nanoparticles Selectively Target Breast Cancer Stem Cells through COX-independent Pathways. *Mater. Sci. Eng. C* 124, 112024. doi:10.1016/j.msec.2021.112024

Fahira, A. I., Amalia, R., Barliana, M. I., Gatera, V. A., and Abdulah, R. (2022). Polyethyleneimine (PEI) as a Polymer-Based Co-delivery System for Breast Cancer Therapy. *Breast Cancer Targets Ther.* 14, 71–83. doi:10.2147/bctt.s350403

Fraser, J. R. E., Laurent, T. C., and Laurent, U. (1997). Hyaluronan: its Nature, Distribution, Functions and Turnover. *J. Intern. Med.* 242 (1), 27–33. doi:10.1046/j.1365-2796.1997.00170.x

Gao, Y., Gao, D., Shen, J., and Wang, Q. (2020). A Review of Mesoporous Silica Nanoparticle Delivery Systems in Chemo-Based Combination Cancer Therapies. *Front. Chem.* 8, 598722. doi:10.3389/fchem.2020.598722

Ghosh, S., Dutta, S., Sarkar, A., Kundu, M., and Sil, P. C. (2021). Targeted Delivery of Curcumin in Breast Cancer Cells via Hyaluronic Acid Modified Mesoporous Silica Nanoparticle to Enhance Anticancer Efficiency. *Colloids Surfaces B Biointerfaces* 197, 111404. doi:10.1016/j.colsurfb.2020.111404

Gibbs, P., Clingan, P. R., Ganju, V., Strickland, A. H., Wong, S. S., Tebbutt, N. C., et al. (2011). Hyaluronan-Irinotecan Improves Progression-free Survival in 5-fluorouracil Refractory Patients with Metastatic Colorectal Cancer: a Randomized Phase II Trial. *Cancer Chemother. Pharmacol.* 67 (1), 153–163. doi:10.1007/s00280-010-1303-3

Gu, H.-f., Ren, F., Mao, X.-y., and Du, M. (2021). Mineralized and GSH-Responsive Hyaluronic Acid Based Nano-Carriers for Potentiating Repressive Effects of Sulforaphane on Breast Cancer Stem Cells-like Properties. *Carbohydr. Polym.* 269, 118294. doi:10.1016/j.carbpol.2021.118294

Guo, C., He, J., Song, X., Tan, L., Wang, M., Jiang, P., et al. (2019). Pharmacological Properties and Derivatives of Shikonin—A Review in Recent Years. *Pharmacol. Res.* 149, 104463. doi:10.1016/j.phrs.2019.104463

Guo, Y., Luo, J., Tan, S., Otieno, B. O., and Zhang, Z. (2013). The Applications of Vitamin E TPGS in Drug Delivery. *Eur. J. Pharm. Sci.* 49 (2), 175–186. doi:10.1016/j.ejps.2013.02.006

Ha, W., Zhao, X.-b., Chen, X.-y., Jiang, K., and Shi, Y.-p. (2018). Prodrug-based Cascade Self-Assembly Strategy for Precisely Controlled Combination Drug Therapy. *ACS Appl. Mat. Interfaces* 10 (25), 21149–21159. doi:10.1021/acsami.8b05170

Han, H. S., Lee, J., Kim, H. R., Chae, S. Y., Kim, M., Saravanakumar, G., et al. (2013). Robust PEGylated Hyaluronic Acid Nanoparticles as the Carrier of Doxorubicin: Mineralization and its Effect on Tumor Targetability *In Vivo*. *J. Control. Release* 168 (2), 105–114. doi:10.1016/j.jconrel.2013.02.022

Han, X., Dong, X., Li, J., Wang, M., Luo, L., Li, Z., et al. (2017). Free Paclitaxel-Loaded E-Selectin Binding Peptide Modified Micelle Self-Assembled from Hyaluronic Acid-Paclitaxel Conjugate Inhibit Breast Cancer Metastasis in a Murine Model. *Int. J. Pharm.* 528 (1-2), 33–46. doi:10.1016/j.ijpharm.2017.05.063

Hard, G. C., Iatropoulos, M. J., Jordan, K., Radi, L., Kaltenberg, O. P., Imondi, A. R., et al. (1993). Major Difference in the Hepatocarcinogenicity and DNA Adduct Forming Ability between Toremifene and Tamoxifen in Female Crl: CD (BR) Rats. *Cancer Res.* 53 (19), 4534–4541.

Heldin, C.-H., Rubin, K., Pietras, K., and Östman, A. (2004). High Interstitial Fluid Pressure—An Obstacle in Cancer Therapy. *Nat. Rev. Cancer* 4 (10), 806–813. doi:10.1038/nrc1456

Hong, J., Liu, Y., Xiao, Y., Yang, X., Su, W., Zhang, M., et al. (2017). High Drug Payload Curcumin Nanosuspensions Stabilized by mPEG-DSPE and SPC: *In Vitro* and *In Vivo* Evaluation. *Drug Deliv.* 24 (1), 109–120. doi:10.1080/10717544.2016.1233589

Hu, C.-M. J., and Zhang, L. (2009). Therapeutic Nanoparticles to Combat Cancer Drug Resistance. *Curr. Drug Metab.* 10 (8), 836–841. doi:10.2174/138920009790274540

Huang, G., and Chen, J. (2019). Preparation and Applications of Hyaluronic Acid and its Derivatives. *Int. J. Biol. Macromol.* 125, 478–484. doi:10.1016/j.ijbiomac.2018.12.074

İkizler, M., Erkasap, N., Dernek, S., Kural, T., and Kaygisiz, Z. (2007). Dietary Polyphenol Quercetin Protects Rat Hearts during Reperfusion: Enhanced Antioxidant Capacity with Chronic Treatment. *Anadolu Kardiyol. Derg.* 7 (4), 404–410.

Jain, R. K. (1990). Vascular and Interstitial Barriers to Delivery of Therapeutic Agents in Tumors. *Cancer metast. Rev.* 9 (3), 253–266. doi:10.1007/bf00046364

Ji, P., Wang, L., Chen, Y., Wang, S., Wu, Z., and Qi, X. (2020). Hyaluronic Acid Hydrophilic Surface Rehabilitating Curcumin Nanocrystals for Targeted Breast Cancer Treatment with Prolonged Biodistribution. *Biomater. Sci.* 8 (1), 462–472. doi:10.1039/c9bm01605h

Jian, B., Zhang, H., Han, C., and Liu, J. (2018). Anti-cancer Activities of Diterpenoids Derived from Euphorbia Fischeriana Steud. *Molecules* 23 (2), 387. doi:10.3390/molecules23020387

Jian, B., Zhang, H., and Liu, J. (2018). Structural Diversity and Biological Activities of Diterpenoids Derived from Euphorbia Fischeriana Steud. *Molecules* 23 (4), 935. doi:10.3390/molecules23040935

Jordan, V. C. (2014). Tamoxifen as the First Targeted Long-Term Adjuvant Therapy for Breast Cancer. *Endocrine-related cancer* 21 (3), R235–R246. doi:10.1530/erc-14-0092

Kandasamy, G., and Maity, D. (2015). Recent Advances in Superparamagnetic Iron Oxide Nanoparticles (SPIONs) for *In Vitro* and *In Vivo* Cancer Nanotheranostics. *Int. J. Pharm.* 496 (2), 191–218. doi:10.1016/j.ijpharm.2015.10.058

Kang, S., Blache, C. A., Bajana, S., Hasan, N., Kamal, M., Morita, Y., et al. (2016). The Effect of Soluble E-Selectin on Tumor Progression and Metastasis. *BMC cancer* 16 (1), 331–413. doi:10.1186/s12885-016-2366-2

Khandelia, R., Bhandari, S., Pan, U. N., Ghosh, S. S., and Chattopadhyay, A. (2015). Gold Nanocluster Embedded Albumin Nanoparticles for Two-photon Imaging of Cancer Cells Accompanying Drug Delivery. *Small* 11 (33), 4075–4081. doi:10.1002/smll.201500216

Kida, K., Okita, M., Fujita, K., Tanaka, S., and Miyake, Y. (2013). Formation of High Crystalline ZIF-8 in an Aqueous Solution. *CrystEngComm* 15 (9), 1794–1801. doi:10.1039/c2ce26847g

Kim, J. H., Moon, M. J., Kim, D. Y., Heo, S. H., and Jeong, Y. Y. (2018). Hyaluronic Acid-Based Nanomaterials for Cancer Therapy. *Polymers* 10 (10), 1133. doi:10.3390/polym10101133

Landskron, G., De la Fuente, M., Thuwajit, P., Thuwajit, C., and Hermoso, M. A. (2014). Chronic Inflammation and Cytokines in the Tumor Microenvironment. *J. Immunol. Res.* 2014, 149185. doi:10.1155/2014/149185

Lapcık, L., Jr, Lapcık, L., De Smedt, S., Demeester, J., and Chabrecek, P. (1998). Hyaluronan: Preparation, Structure, Properties, and Applications. *Chem. Rev.* 98 (8), 2663–2684. doi:10.1021/cr941199z

Laurent, S., and Mahmoudi, M. (2011). Superparamagnetic Iron Oxide Nanoparticles: Promises for Diagnosis and Treatment of Cancer. *Int. J. Mol. Epidemiol. Genet.* 2 (4), 367–390.

Lee, S. Y., and Cho, H.-J. (2018). Mitochondria Targeting and Destabilizing Hyaluronic Acid Derivative-Based Nanoparticles for the Delivery of Lapatinib to Triple-Negative Breast Cancer. *Biomacromolecules* 20 (2), 835–845. doi:10.1021/acs.biomac.8b01449

Li, J., Li, M., Tian, L., Qiu, Y., Yu, Q., Wang, X., et al. (2020). Facile Strategy by Hyaluronic Acid Functional Carbon Dot-Doxorubicin Nanoparticles for CD44 Targeted Drug Delivery and Enhanced Breast Cancer Therapy. *Int. J. Pharm.* 578, 119122. doi:10.1016/j.ijpharm.2020.119122

Liang, D., Wang, A.-t., Yang, Z.-z., Liu, Y.-j., and Qi, X.-r. (2015). Enhance Cancer Cell Recognition and Overcome Drug Resistance Using Hyaluronic Acid and α-tocopheryl Succinate Based Multifunctional Nanoparticles. *Mol. Pharm.* 12 (6), 2189–2202. doi:10.1021/acs.molpharmaceut.5b00129

Liu, D., Zhang, Q., Wang, J., Guan, S., Cai, D., and Liu, J. (2021). Inhibition of Growth and Metastasis of Breast Cancer by Targeted Delivery of 17-Hydroxy-Jolkinolide B via Hyaluronic Acid-Coated Liposomes. *Carbohydr. Polym.* 257, 117572. doi:10.1016/j.carbpol.2020.117572

Liu, H.-n., Guo, N.-n., Guo, W.-w., Huang-Fu, M.-y., Vakili, M. R., Chen, J.-j., et al. (2018). Delivery of Mitochondriotropic Doxorubicin Derivatives Using Self-Assembling Hyaluronic Acid Nanocarriers in Doxorubicin-Resistant Breast Cancer. *Acta Pharmacol. Sin.* 39 (10), 1681–1692. doi:10.1038/aps.2018.9

Liu, P. (2019). *Redox-and pH-Responsive Polymeric Nanocarriers, Stimuli Responsive Polymeric Nanocarriers for Drug Delivery Applications*. Elsevier, 3–36.

Liu, R., Xiao, W., Hu, C., Xie, R., and Gao, H. (2018). Theranostic Size-Reducible and No Donor Conjugated Gold Nanocluster Fabricated Hyaluronic Acid Nanoparticle with Optimal Size for Combinational Treatment of Breast Cancer and Lung Metastasis. *J. Control. release* 278, 127–139. doi:10.1016/j.jconrel.2018.04.005

Liu, S., Li, R., Qian, J., Sun, J., Li, G., Shen, J., et al. (2020). Combination Therapy of Doxorubicin and Quercetin on Multidrug-Resistant Breast Cancer and Their Sequential Delivery by Reduction-Sensitive Hyaluronic Acid-Based Conjugate/d-α-Tocopheryl Poly (Ethylene Glycol) 1000 Succinate Mixed Micelles. *Mol. Pharm.* 17 (4), 1415–1427. doi:10.1021/acs.molpharmaceut.0c00138

Liu, Y., Qiao, L., Zhang, S., Wan, G., Chen, B., Zhou, P., et al. (2018). Dual pH-Responsive Multifunctional Nanoparticles for Targeted Treatment of Breast Cancer by Combining Immunotherapy and Chemotherapy. *Acta Biomater.* 66, 310–324. doi:10.1016/j.actbio.2017.11.010

Liyanage, P. Y., Hettiarachchi, S. D., Zhou, Y., Ouhtit, A., Seven, E. S., Oztan, C. Y., et al. (2019). Nanoparticle-mediated Targeted Drug Delivery for Breast Cancer Treatment. *Biochimica Biophysica Acta - Rev. Cancer* 1871 (2), 419–433. doi:10.1016/j.bbcan.2019.04.006

Lokeshwar, V. B., Mirza, S., and Jordan, A. (2014). Targeting Hyaluronic Acid Family for Cancer Chemoprevention and Therapy. *Adv. Cancer Res.* 123, 35–65. doi:10.1016/b978-0-12-800092-2.00002-2

Lou, C., Xiao, M., Cheng, S., Lu, X., Jia, S., Ren, Y., et al. (2016). MiR-485-3p and miR-485-5p Suppress Breast Cancer Cell Metastasis by Inhibiting PGC-1α Expression. *Cell. Death Dis.* 7, e2159. doi:10.1038/cddis.2016.27

Lumachi, F., Luisetto, G., Mm Basso, S., Basso, U., Brunello, A., and Camozzi, V. (2011). Endocrine Therapy of Breast Cancer. *Curr. Med. Chem.* 18 (4), 513–522. doi:10.2174/092986711794480177

Luo, Y., and Wang, Q. (2014). Zein-based Micro-and Nano-particles for Drug and Nutrient Delivery: A Review. *J. Appl. Polym. Sci.* 131 (16). doi:10.1002/app.40696

Luo, Z., Dai, Y., and Gao, H. (2019). Development and Application of Hyaluronic Acid in Tumor Targeting Drug Delivery. *Acta Pharm. Sin. B* 9 (6), 1099–1112. doi:10.1016/j.apsb.2019.06.004

Maestro, L. M., Haro-González, P., Sánchez-Iglesias, A., Liz-Marzán, L. M., Garcia Sole, J., and Jaque, D. (2014). Quantum Dot Thermometry Evaluation of Geometry Dependent Heating Efficiency in Gold Nanoparticles. *Langmuir* 30 (6), 1650–1658. doi:10.1021/la403435v

Mattheolabakis, G., Milane, L., Singh, A., and Amiji, M. M. (2015). Hyaluronic Acid Targeting of CD44 for Cancer Therapy: from Receptor Biology to Nanomedicine. *J. drug Target.* 23 (7-8), 605–618. doi:10.3109/1061186x.2015.1052072

Meng, L., Ren, J., Liu, Z., and Zhao, Y. (2022). Hyaluronic Acid-Coated Shikonin Liposomes for the Treatment of Triple-Negative Breast Cancer via Targeting Tumor Cells and Amplification of Oxidative Stress. *J. Drug Deliv. Sci. Technol.* 70, 103193. doi:10.1016/j.jddst.2022.103193

Misra, S., Heldin, P., Hascall, V. C., Karamanos, N. K., Skandalis, S. S., Markwald, R. R., et al. (2011). Hyaluronan–CD44 Interactions as Potential Targets for Cancer Therapy. *FEBS J.* 278 (9), 1429–1443. doi:10.1111/j.1742-4658.2011.08071.x

Mizrahy, S., Goldsmith, M., Leviatan-Ben-Arye, S., Kisin-Finfer, E., Redy, O., Srinivasan, S., et al. (2014). Tumor Targeting Profiling of Hyaluronan-Coated Lipid Based-Nanoparticles. *Nanoscale* 6 (7), 3742–3752. doi:10.1039/c3nr06102g

Nam, J.-S., Sharma, A. R., Nguyen, L. T., Chakraborty, C., Sharma, G., and Lee, S.-S. (2016). Application of Bioactive Quercetin in Oncotherapy: from Nutrition to Nanomedicine. *Molecules* 21 (1), 108. doi:10.3390/molecules21010108

Narmani, A., and Jafari, S. M. (2021). Chitosan-based Nanodelivery Systems for Cancer Therapy: Recent Advances. *Carbohydr. Polym.* 272, 118464. doi:10.1016/j.carbpol.2021.118464

Necas, J., Bartosikova, L., Brauner, P., and Kolar, J. (2008). Hyaluronic Acid (Hyaluronan): a Review. *Veterinarni Med.* 53 (8), 397–411. doi:10.17221/1930-vetmed

Nomura, Y. (1996). Adriamycin--breast Cancer, Gan to Kagaku Ryoho. *Cancer & Chemother.* 23 (14), 1911–1915.

Oh, E. J., Park, K., Kim, K. S., Kim, J., Yang, J.-A., Kong, J.-H., et al. (2010). Target Specific and Long-Acting Delivery of Protein, Peptide, and Nucleotide Therapeutics Using Hyaluronic Acid Derivatives. *J. Control. Release* 141 (1), 2–12. doi:10.1016/j.jconrel.2009.09.010

Omar, H., Fardous, R., Alhindi, Y. M., Aodah, A. H., Alyami, M., Alsuabeyl, M. S., et al. (2022). α1-Acid Glycoprotein-Decorated Hyaluronic Acid Nanoparticles for Suppressing Metastasis and Overcoming Drug Resistance Breast Cancer. *Biomedicines* 10 (2), 414. doi:10.3390/biomedicines10020414

Ondreas, F., Dusankova, M., Sita, J., Cepa, M., Stepan, J., Belsky, P., et al. (2021). Self-assembly of Hydrophobically Modified Hyaluronic Acid. *Appl. Surf. Sci.* 546, 149161. doi:10.1016/j.apsusc.2021.149161

Owen, S. C., Chan, D. P., and Shoichet, M. S. (2012). Polymeric Micelle Stability. *Nano today* 7 (1), 53–65. doi:10.1016/j.nantod.2012.01.002

Panwar, N., Soehartono, A. M., Chan, K. K., Zeng, S., Xu, G., Qu, J., et al. (2019). Nanocarbons for Biology and Medicine: Sensing, Imaging, and Drug Delivery. *Chem. Rev.* 119 (16), 9559–9656. doi:10.1021/acs.chemrev.9b00099

Perez, E. A. (1998). Paclitaxel in Breast Cancer. *Oncol.* 3 (6), 373–389. doi:10.1634/theoncologist.3-6-373

Perillo, B., Di Donato, M., Pezone, A., Di Zazzo, E., Giovannelli, P., Galasso, G., et al. (2020). ROS in Cancer Therapy: The Bright Side of the Moon. *Exp. Mol. Med.* 52 (2), 192–203. doi:10.1038/s12276-020-0384-2

Quagliariello, V., Iaffaioli, R. V., Armenia, E., Clemente, O., Barbarisi, M., Nasti, G., et al. (2017). Hyaluronic Acid Nanohydrogel Loaded with Quercetin Alone or in Combination to a Macrolide Derivative of Rapamycin RAD001 (Everolimus) as a New Treatment for Hormone-responsive Human Breast Cancer. *J. Cell. Physiol.* 232 (8), 2063–2074. doi:10.1002/jcp.25587

Rezaei, S., Kashanian, S., Bahrami, Y., Cruz, L. J., and Motiei, M. (2020). Redox-sensitive and Hyaluronic Acid-Functionalized Nanoparticles for Improving Breast Cancer Treatment by Cytoplasmic 17α-Methyltestosterone Delivery. *Molecules* 25 (5), 1181. doi:10.3390/molecules25051181

Royce, M. E., and Osman, D. (2015). *Everolimus in the Treatment of Metastatic Breast Cancer, Breast Cancer: Basic and Clinical Research 9*. London: BCBCR, S29268.

Shahriari, M., Taghdisi, S. M., Abnous, K., Ramezani, M., and Alibolandi, M. (2019). Synthesis of Hyaluronic Acid-Based Polymersomes for Doxorubicin Delivery to Metastatic Breast Cancer. *Int. J. Pharm.* 572, 118835. doi:10.1016/j.ijpharm.2019.118835

Shamay, Y., Raviv, L., Golan, M., Voronov, E., Apte, R. N., and David, A. (2015). Inhibition of Primary and Metastatic Tumors in Mice by E-Selectin-Targeted Polymer–Drug Conjugates. *J. Control. Release* 217, 102–112. doi:10.1016/j.jconrel.2015.08.029

Sharma, G. N., Dave, R., Sanadya, J., Sharma, P., and Sharma, K. (2010). Various Types and Management of Breast Cancer: an Overview. *J. Adv. Pharm. Technol. Res.* 1 (2), 109–126.

Singh, S., Mishra, A., Kumari, R., Sinha, K. K., Singh, M. K., and Das, P. (2017). Carbon Dots Assisted Formation of DNA Hydrogel for Sustained Release of Drug. *Carbon* 114, 169–176. doi:10.1016/j.carbon.2016.12.020

Smith, I. C., Heys, S. D., Hutcheon, A. W., Miller, I. D., Payne, S., Gilbert, F. J., et al. (2002). Neoadjuvant Chemotherapy in Breast Cancer: Significantly Enhanced Response with Docetaxel. *J. Clin. Oncol.* 20 (6), 1456–1466. doi:10.1200/jco.2002.20.6.1456

Srivastava, C. M., and Purwar, R. (2017). Chitosan-finished Antheraea Mylitta Silk Fibroin Nonwoven Composite Films for Wound Dressing. *J. Appl. Polym. Sci.* 134 (1). doi:10.1002/app.44341

Sugahara, K. N., Braun, G. B., de Mendoza, T. H., Kotamraju, V. R., French, R. P., Lowy, A. M., et al. (2015). Tumor-penetrating iRGD Peptide Inhibits Metastasis. *Mol. cancer Ther.* 14 (1), 120–128. doi:10.1158/1535-7163.mct-14-0366

Sugahara, K. N., Teesalu, T., Karmali, P. P., Kotamraju, V. R., Agemy, L., Greenwald, D. R., et al. (2010). Coadministration of a Tumor-Penetrating Peptide Enhances the Efficacy of Cancer Drugs. *science* 328 (5981), 1031–1035. doi:10.1126/science.1183057

Sun, D., Zhou, S., and Gao, W. (2020). What Went Wrong with Anticancer Nanomedicine Design and How to Make it Right. *ACS Nano* 14 (10), 12281–12290. doi:10.1021/acsnano.9b09713

Sun, W., Du, Y., Liang, X., Yu, C., Fang, J., Lu, W., et al. (2019). Synergistic Triple-Combination Therapy with Hyaluronic Acid-Shelled PPy/CPT Nanoparticles Results in Tumor Regression and Prevents Tumor Recurrence and Metastasis in

4T1 Breast Cancer. *Biomaterials* 217, 119264. doi:10.1016/j.biomaterials.2019.119264

Tai, C.-J., Liu, C.-H., Pan, Y.-C., Wong, S. H., Tai, C.-J., Richardson, C. D., et al. (2019). Chemovirotherapeutic Treatment Using Camptothecin Enhances Oncolytic Measles Virus-Mediated Killing of Breast Cancer Cells. *Sci. Rep.* 9 (1), 6767. doi:10.1038/s41598-019-43047-3

Tran, S., DeGiovanni, P.-J., Piel, B., and Rai, P. (2017). Cancer Nanomedicine: a Review of Recent Success in Drug Delivery. *Clin. Transl. Med.* 6 (1), 44–21. doi:10.1186/s40169-017-0175-0

Trevaskis, N. L., Charman, W. N., and Porter, C. J. (2008). Lipid-based Delivery Systems and Intestinal Lymphatic Drug Transport: a Mechanistic Update. *Adv. drug Deliv. Rev.* 60 (6), 702–716. doi:10.1016/j.addr.2007.09.007

Underhill, C. (1992). CD44: the Hyaluronan Receptor. *J. Cell. Sci.* 103 (2), 293–298. doi:10.1242/jcs.103.2.293

Vyas, D., Laput, G., and Vyas, A. K. (2014). Chemotherapy-enhanced Inflammation May Lead to the Failure of Therapy and Metastasis. *Onco. Targets. Ther.* 7, 1015–1023. doi:10.2147/ott.s60114

Waks, A. G., and Winer, E. P. (2019). Breast Cancer Treatment: A Review. *JAMA* 321 (3), 288–300. doi:10.1001/jama.2018.19323

Wang, L., Liu, Y., Li, W., Jiang, X., Ji, Y., Wu, X., et al. (2011). Selective Targeting of Gold Nanorods at the Mitochondria of Cancer Cells: Implications for Cancer Therapy. *Nano Lett.* 11 (2), 772–780. doi:10.1021/nl103992v

Wang, R., Yang, H., Khan, A. R., Yang, X., Xu, J., Ji, J., et al. (2021). Redox-responsive Hyaluronic Acid-Based Nanoparticles for Targeted Photodynamic Therapy/chemotherapy against Breast Cancer. *J. Colloid Interface Sci.* 598, 213–228. doi:10.1016/j.jcis.2021.04.056

Wang, W., Zhang, X., Li, Z., Pan, D., Zhu, H., Gu, Z., et al. (2021). Dendronized Hyaluronic Acid-Docetaxel Conjugate as a Stimuli-Responsive Nano-Agent for Breast Cancer Therapy. *Carbohydr. Polym.* 267, 118160. doi:10.1016/j.carbpol.2021.118160

Wang, Y., Qian, J., Yang, M., Xu, W., Wang, J., Hou, G., et al. (2019). Doxorubicin/cisplatin Co-loaded Hyaluronic Acid/chitosan-Based Nanoparticles for *In Vitro* Synergistic Combination Chemotherapy of Breast Cancer. *Carbohydr. Polym.* 225, 115206. doi:10.1016/j.carbpol.2019.115206

Wang, Y., Yang, M., Qian, J., Xu, W., Wang, J., Hou, G., et al. (2019). Sequentially Self-Assembled Polysaccharide-Based Nanocomplexes for Combined Chemotherapy and Photodynamic Therapy of Breast Cancer. *Carbohydr. Polym.* 203, 203–213. doi:10.1016/j.carbpol.2018.09.035

Weissig, V., Pettinger, T. K., and Murdock, N. (2014). Nanopharmaceuticals (Part 1): Products on the Market. *Int. J. Nanomedicine* 9, 4357–4373. doi:10.2147/ijn.s46900

Wickens, J. M., Alsaab, H. O., Kesharwani, P., Bhise, K., Amin, M. C. I. M., Tekade, R. K., et al. (2017). Recent Advances in Hyaluronic Acid-Decorated Nanocarriers for Targeted Cancer Therapy. *Drug Discov. today* 22 (4), 665–680. doi:10.1016/j.drudis.2016.12.009

Wu, P., Liu, Q., Wang, Q., Qian, H., Yu, L., Liu, B., et al. (2018). Novel Silk Fibroin Nanoparticles Incorporated Silk Fibroin Hydrogel for Inhibition of Cancer Stem Cells and Tumor Growth. *Int. J. Nanomedicine* 13, 5405–5418. doi:10.2147/ijn.s166104

Xiao, K., Li, Y., Luo, J., Lee, J. S., Xiao, W., Gonik, A. M., et al. (2011). The Effect of Surface Charge on *In Vivo* Biodistribution of PEG-Oligocholic Acid Based Micellar Nanoparticles. *Biomaterials* 32 (13), 3435–3446. doi:10.1016/j.biomaterials.2011.01.021

Xie, J., Zheng, Y., and Ying, J. Y. (2009). Protein-directed Synthesis of Highly Fluorescent Gold Nanoclusters. *J. Am. Chem. Soc.* 131 (3), 888–889. doi:10.1021/ja806804u

Xu, H., Yao, Q., Cai, C., Gou, J., Zhang, Y., Zhong, H., et al. (2015). Amphiphilic Poly (Amino Acid) Based Micelles Applied to Drug Delivery: The *In Vitro* and *In Vivo* Challenges and the Corresponding Potential Strategies. *J. Control. Release* 199, 84–97. doi:10.1016/j.jconrel.2014.12.012

Xu, W., Qian, J., Hou, G., Suo, A., Wang, Y., Wang, J., et al. (2017). Hyaluronic Acid-Functionalized Gold Nanorods with pH/NIR Dual-Responsive Drug Release for Synergetic Targeted Photothermal Chemotherapy of Breast Cancer. *ACS Appl. Mat. Interfaces* 9 (42), 36533–36547. doi:10.1021/acsami.7b08700

Yang, C., Liu, Y., He, Y., Du, Y., Wang, W., Shi, X., et al. (2013). The Use of HA Oligosaccharide-Loaded Nanoparticles to Breach the Endogenous Hyaluronan Glycocalyx for Breast Cancer Therapy. *Biomaterials* 34 (28), 6829–6838. doi:10.1016/j.biomaterials.2013.05.036

Yang, C., Wu, T., Qi, Y., and Zhang, Z. (2018). Recent Advances in the Application of Vitamin E TPGS for Drug Delivery. *Theranostics* 8 (2), 464–485. doi:10.7150/thno.22711

Yang, H., Villani, R. M., Wang, H., Simpson, M. J., Roberts, M. S., Tang, M., et al. (2018). The Role of Cellular Reactive Oxygen Species in Cancer Chemotherapy. *J. Exp. Clin. Cancer Res.* 37 (1), 266–310. doi:10.1186/s13046-018-0909-x

Yang, K., Xu, H., Cheng, L., Sun, C., Wang, J., and Liu, Z. (2012). *In Vitro* and *In Vivo* Near-infrared Photothermal Therapy of Cancer Using Polypyrrole Organic Nanoparticles. *Adv. Mat.* 24 (41), 5586–5592. doi:10.1002/adma.201202625

Yang, X., Shang, P., Ji, J., Malichewe, C., Yao, Z., Liao, J., et al. (2021). Hyaluronic Acid-Modified Nanoparticles Self-Assembled from Linoleic Acid-Conjugated Chitosan for the Codelivery of miR34a and Doxorubicin in Resistant Breast Cancer. *Mol. Pharm.* 19 (1), 2–17.

Yin, T., Wang, Y., Chu, X., Fu, Y., Wang, L., Zhou, J., et al. (2018). Free Adriamycin-Loaded pH/reduction Dual-Responsive Hyaluronic Acid–Adriamycin Prodrug Micelles for Efficient Cancer Therapy. *ACS Appl. Mat. Interfaces* 10 (42), 35693–35704. doi:10.1021/acsami.8b09342

Youn, Y. S., and Bae, Y. H. (2018). Perspectives on the Past, Present, and Future of Cancer Nanomedicine. *Adv. Drug Deliv. Rev.* 130, 3–11. doi:10.1016/j.addr.2018.05.008

Yu, S., Wang, S., Xie, Z., Yu, S., Li, L., Xiao, H., et al. (2021). Hyaluronic Acid Coating on the Surface of Curcumin-Loaded ZIF-8 Nanoparticles for Improved Breast Cancer Therapy: An *In Vitro* and *In Vivo* Study. *Colloids Surfaces B Biointerfaces* 203, 111759. doi:10.1016/j.colsurfb.2021.111759

Yu, T., Li, Y., Gu, X., and Li, Q. (2020). Development of a Hyaluronic Acid-Based Nanocarrier Incorporating Doxorubicin and Cisplatin as a pH-Sensitive and CD44-Targeted Anti-breast Cancer Drug Delivery System. *Front. Pharmacol.* 11, 532457. doi:10.3389/fphar.2020.532457

Yue, C., Liu, P., Zheng, M., Zhao, P., Wang, Y., Ma, Y., et al. (2013). IR-780 Dye Loaded Tumor Targeting Theranostic Nanoparticles for NIR Imaging and Photothermal Therapy. *Biomaterials* 34 (28), 6853–6861. doi:10.1016/j.biomaterials.2013.05.071

Zhan, W., Li, H., Guo, Y., Yang, L., Pang, L., and Zhang, C. (2021). Hyaluronic Acid Functionalized Biodegradable Mesoporous Silica Nanocomposites for Efficient Photothermal and Chemotherapy in Breast Cancer. *Nanotechnology* 32 (16), 165703. doi:10.1088/1361-6528/abda74

Zhang, C., Li, C., Liu, Y., Zhang, J., Bao, C., Liang, S., et al. (2015). Gold Nanoclusters-based Nanoprobes for Simultaneous Fluorescence Imaging and Targeted Photodynamic Therapy with Superior Penetration and Retention Behavior in Tumors. *Adv. Funct. Mat.* 25 (8), 1314–1325. doi:10.1002/adfm.201403095

Zhang, J., Song, J., Liang, X., Yin, Y., Zuo, T., Chen, D., et al. (2019). Hyaluronic Acid-Modified Cationic Nanoparticles Overcome Enzyme CYP1B1-Mediated Breast Cancer Multidrug Resistance. *Nanomedicine* 14 (4), 447–464. doi:10.2217/nnm-2018-0244

Zhang, Q., Deng, C., Fu, Y., Sun, X., Gong, T., and Zhang, Z. (2016). Repeated Administration of Hyaluronic Acid Coated Liposomes with Improved Pharmacokinetics and Reduced Immune Response. *Mol. Pharm.* 13 (6), 1800–1808. doi:10.1021/acs.molpharmaceut.5b00952

Zhang, Q., Wang, J., Liu, D., Zhu, W., Guan, S., Fan, L., et al. (2020). Targeted Delivery of Honokiol by Zein/hyaluronic Acid Core-Shell Nanoparticles to Suppress Breast Cancer Growth and Metastasis. *Carbohydr. Polym.* 240, 116325. doi:10.1016/j.carbpol.2020.116325

Zhang, X., Wu, Y., Li, Z., Wang, W., Wu, Y., Pan, D., et al. (2020). Glycodendron/pyropheophorbide-a (Ppa)-Functionalized Hyaluronic Acid as a Nanosystem for Tumor Photodynamic Therapy. *Carbohydr. Polym.* 247, 116749. doi:10.1016/j.carbpol.2020.116749

Zhang, Y., Chen, T., Yuan, P., Tian, R., Hu, W., Tang, Y., et al. (2015). Encapsulation of Honokiol into Self-Assembled Pectin Nanoparticles for Drug Delivery to HepG2 Cells. *Carbohydr. Polym.* 133, 31–38. doi:10.1016/j.carbpol.2015.06.102

Zhou, F., Feng, B., Yu, H., Wang, D., Wang, T., Liu, J., et al. (2016). Cisplatin Prodrug-Conjugated Gold Nanocluster for Fluorescence Imaging and Targeted Therapy of the Breast Cancer. *Theranostics* 6 (5), 679–687. doi:10.7150/thno.14556

Glossary

AGP α1-acid glycoprotein
AHA Anionic aldehyde-functionalized hyaluronic acid
ALA 5-aminolevulinic acid
ANF α-naphthoflavone
BC Breast cancer
BCSC Breast cancer stem cells
Bcl-2 B-cell lymphoma-2
BSA Bovine serum albumin
BF Ibuprofen
CaP Calcium phosphate
CDDP Cisplatin
CDs Carbon dots
CS Chitosan
Ce6 Chlorin e6
CLA Conjugated linoleic acid
CPT Camptothecin
Cur Curcumin
DA Dextran aldehyde
DHA Docosahexaenoic acid
DSBs Double-strand breaks
DOX,DTX Adriamycin, Doxorubicin
EPR Enhanced permeability and retention effect
FA Folic acid
FDA Food and Drug Administration
GO Graphene oxide
GNRs Gold nanorods
GSH Glutathione
HA Hyaluronic acid
HJB 17-hydroxy-jolkinolide B
HER2 Human epidermal growth factor receptor 2
HNK Honokiol
IL-6 Interleukins
LPT Lapatinib
MDR Multidrug resistance
MOFs Metal-organic frameworks
miR34a MicroRNA34a
MSN Mesoporous silica
MT 17α-Methyltestosteron
NAP Naproxen
NDDS Nano drug delivery systems
PARP Poly (ADP-ribose) polymerase
PEG Polyethylene glycol
PEI Polyethyleneimine
PDT Photodynamic therapy
PHIS L-histidin
PTT Photothermal therapy
PPy Polypyrrole
ROS Reactive oxygen species
SEDDS self-emulsifying drug delivery system
SFN Sulforaphane
SHK Shikonin
SPIONs Superparamagnetic iron oxide nanoparticles
TNBC Triple-negative breast cancer
TMX Tamoxifen
TPGS or Vitamin E TPGS D-α-tocopheryl polyethylene glycol succinate
TPP Riphenylphosphine
TS D-α-tocopherol succinate
ZIF-8 Framework-8 nanoparticle

frontiers | Frontiers in Bioengineering and Biotechnology

TYPE Review
PUBLISHED 06 September 2022
DOI 10.3389/fbioe.2022.968482

OPEN ACCESS

EDITED BY
Jianshe Hu,
Northeastern University, China

REVIEWED BY
Chengjin Ye,
Texas Biomedical Research Institute, United States
Wanhua Xie,
Shenyang Medical College, China

*CORRESPONDENCE
Yongping Lu,
valensu423@163.com
Jing Chen,
chenj@sj-hospital.org

SPECIALTY SECTION
This article was submitted to Biomaterials, a section of the journal Frontiers in Bioengineering and Biotechnology

RECEIVED 14 June 2022
ACCEPTED 09 August 2022
PUBLISHED 06 September 2022

CITATION
Lin M, Lu Y and Chen J (2022), Tissue-engineered repair material for pelvic floor dysfunction.
Front. Bioeng. Biotechnol. 10:968482.
doi: 10.3389/fbioe.2022.968482

Tissue-engineered repair material for pelvic floor dysfunction

Meina Lin[1], Yongping Lu[1]* and Jing Chen[2]*

[1]NHC Key Laboratory of Reproductive Health and Medical Genetics (China Medical University) and Liaoning Key Laboratory of Reproductive Health, Liaoning Research Institute of Family Planning (The Affiliated Reproductive Hospital of China Medical University), Shenyang, China, [2]Department of Obstetrics and Gynecology, Shengjing Hospital of China Medical University, Shenyang, China

Pelvic floor dysfunction (PFD) is a highly prevalent urogynecology disorder affecting many women worldwide, with symptoms including pelvic organ prolapse (POP), stress urinary incontinence (SUI), fecal incontinence, and overactive bladder syndrome (OAB). At present, the clinical treatments of PFD are still conservative and symptom-based, including non-surgical treatment and surgery. Surgical repair is an effective and durable treatment for PFD, and synthetic and biological materials can be used to enforce or reinforce the diseased tissue. However, synthetic materials such as polypropylene patches caused a series of complications such as mesh erosion, exposure, pain, and inflammation. The poor mechanical properties and high degradation speed of the biomaterial meshes resulted in poor anatomical reduction effect and limitation to clinical application. Therefore, the current treatment options are suboptimal. Recently, tissue-engineered repair material (TERM) has been applied to repair PFD and could markedly improve the prognosis of POP and SUI repair surgery in animal models. We review the directions and progression of TERM in POP and SUI repair. Adipose-derived stem cells (ADSCs) and endometrial mesenchymal stem cells (eMSCs) appear to be suitable cell types for scaffold seeding and clinical implantation. The multidisciplinary therapy approach to tissue engineering is a promising direction for tissue repair. More and longer follow-up studies are needed before determining cell types and materials for PFD repair.

KEYWORDS

pelvic floor dysfunction, tissue-engineered repair material, mesenchymal stem cells, scaffolds, pelvic organ prolapses, stress urine incontinence

Introduction

Pelvic floor dysfunction (PFD) is a highly prevalent urogynecology disorder, affecting about 30%~50% of middle-aged and elderly women. The main manifestations of PFD are pelvic organ prolapse (POP), stress urinary incontinence (SUI), fecal incontinence, and overactive bladder syndrome (OAB). POP and SUI mostly occur in parous women and are caused by childbirth-associated pelvic floor injury. The prevalence of PFD varies in different geographical regions. It is estimated that one in three and one in nine women are affected by SUI and POP, respectively, and POP and SUI may coexist in up to 80% of

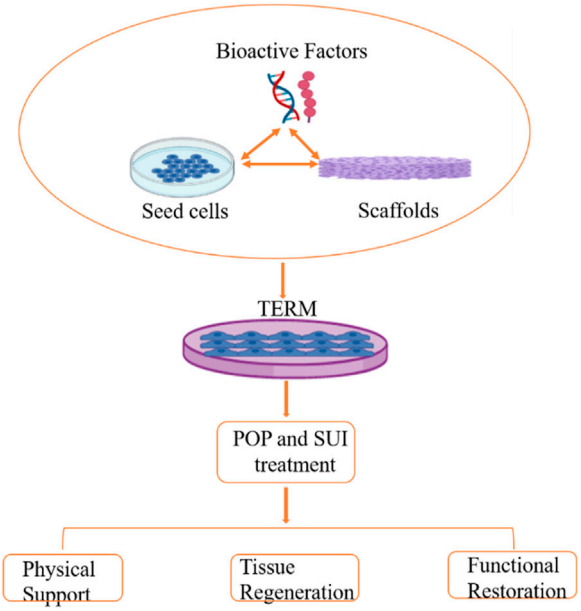

GRAPHICAL ABSTRACT

women with prolapse (Farmer et al., 2020). Studies have predicted that the number of women with at least one PFD will increase by 55.8% from 2010 to 2050 (Wu et al., 2009).

At present, the clinical treatments of PFD are still conservative and symptom-based, including non-surgical treatment and surgery. Non-surgical treatment mainly consists of a manual approach, stimulation, or relaxation technique (Quaghebeur et al., 2021). Surgery was considered to be the most effective and durable treatment, which includes autologous tissue repair and synthetic mesh implantation. In general, autologous tissue repair showed good integration within host tissues, a minimal to moderate inflammatory response, and a moderate degree of collagen production and underwent a degree of remodeling over the long term, but a high recurrence rate (Gigliobianco et al., 2015; Lo et al., 2015). Polypropylene patches are the most used synthetic meshes in implantation surgery, which offer several advantages including lack of transmission of infectious diseases, ease of availability, sustainable tensile strength, and good mechanical properties. However, its nondegradable nature and poor histocompatibility caused a series of problems such as mesh erosion, exposure, pain, infection, pronounced inflammation, massive cell infiltration, and collagen production, and these led to the withdrawal of transvaginal polypropylene mesh from the market and its banning in some countries (Elmer et al., 2009; Gigliobianco et al., 2015). Biomaterial meshes have been used recently for their good histocompatibility, but the poor mechanical properties and high degradation speed resulted in poor anatomical reduction effect and limitation to clinical application. Therefore, the current treatment options are suboptimal, and alternative methods are needed to promote the repair of PFD.

The defects of the pelvic floor support, which are due to the interaction between the muscles and connective tissues within the pelvis, are the main pathophysiology of PFD. They are mainly manifested as altered elastin/collagen metabolism and connective tissue abnormalities (Jin et al., 2016a), such as (1) the interruption in elastin homeostasis caused by abnormal degradation/synthesis of elastin and (2) the changes in the total content and the ratio of subtypes of collagen and the deficient crosslinking of collagens. Therefore, the goal of PFD therapy is to support weakened tissue of the pelvic floor and promote tissue remodeling, thus achieving the effect of improving pelvic floor functions.

Tissue-engineered repair material (TERM) is a multidisciplinary therapy approach that seeks to use a combination of cells, materials, and sometimes additional genes, drugs, or growth factors, to regenerate diseased tissues. The purpose of the cell component, gene, and growth factor is to accelerate repair and promote regeneration of damaged or lost tissue, while the material provides physical support and niches to deliver cells, drugs, and growth factors to the tissue, which, in turn, provides a platform to control the local pharmacokinetics of growth factors and the proliferation and differentiation of transplanted stem cells (Mangir et al., 2019; Zhao et al., 2021). Using TERM for PFD treatment has obvious advantages: first, the scaffolds can support weakened tissue and will not cause so many complications for its degradable nature and good histocompatibility; second, the seeding cells will drive tissue

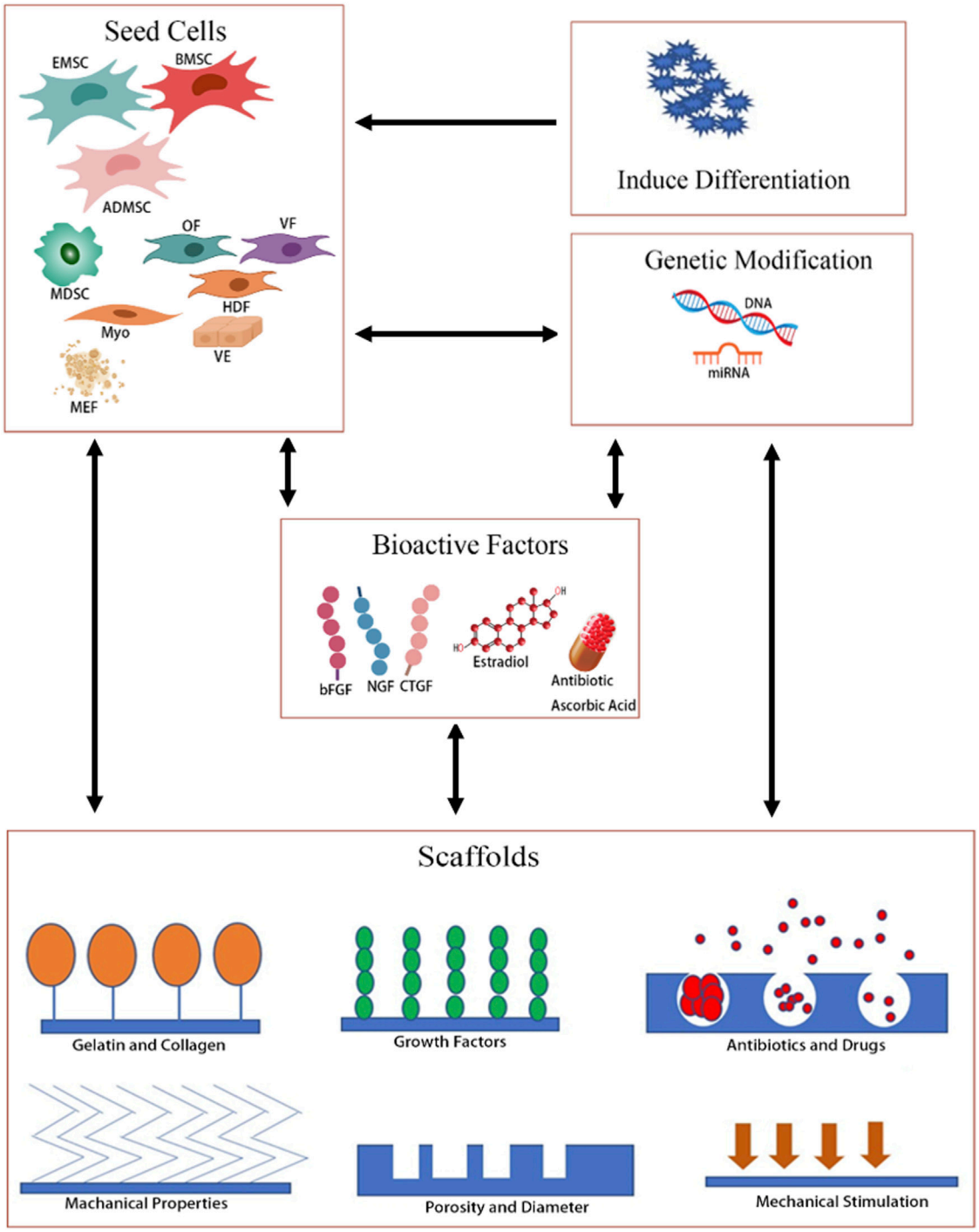

FIGURE 1
Overview of TERMs of different strategies for PFD. OF, oral fibroblast; VF, vaginal fibroblast; HDF, human dermal fibroblast; VE, vaginal epithelial; Myo, myoblasts; MFF, muscle fiber fragment.

remodeling, ultimately providing a permanent repair; third, the bioactive factors, such as growth factors, drugs, and estrogen can speed up repair and improve the microenvironment. So, TERM is a promising treatment for PFD. However, the choice of cells and scaffolds is crucial to the success of TERM. Therefore, different scaffolds and cells have been studied to create a TERM for the

TABLE 1 Advantages and disadvantages of different seed cells and scaffolds.

Seed cell	Advantage	Disadvantage
ADSCs	(1) Adipose tissue is readily available in large quantities during single liposuction and without general anesthesia	N/A
	(2) Easy to culture and expand *in vitro*, self-renewal and multilineage differentiation ability, and proliferative efficiency	
	(3) Low donor morbidity and surgical interference	
	(4) Good compatibility with biological materials	
eMSCs	(1) Excellent regenerative capacity in the endometrial lining	N/A
	(2) Easily obtained from menstrual blood or endometrial biopsies, even from the post-menopausal uterus	
	(3) Procurement method is minimally invasive, with minimum pain and morbidity, without anesthesia	
	(4) Easy to culture and expand *in vitro*, self-renewal and multilineage differentiation ability, and high proliferative capacity *in vitro*	
	(5) Can be purified using a unique marker SUSD2	
	(6) A83-01 can maintain clonogenic SUSD2^{+}eMSCs and prevent spontaneous fibroblast differentiation	
	(7) EMSCs could reduce the foreign body reaction to the degradable mesh	
BMSC	(1) Easy to culture and expand *in vitro*, self-renewal and multilineage differentiation ability, and high proliferative capacity *in vitro*	(1) The procurement method is invasive, with pain and need for general anesthesia
	(2) BMSCs are used in the repair of various diseases and injuries with good efficacy	(2) Relatively scarce number and low cell yields, especially cannot be easily expanded in the middle-aged people
MDSC	(1) Could form myotubes	Acquisition requires surgical anesthesia and invasive operation, resulting in pain and low cell yield
	(2) Could improve the function of urination in rats with intrinsic sphincter deficiency and increase the expression of myosin and α-SMA.	
Fibroblasts	(1) Similar to the nature of the cells in the damaged tissue, it can repair the damaged tissue	Acquisition requires surgical anesthesia and invasive operation, resulting in pain and low cell yield
Scaffold		
PLA	(1) Mimics the architecture of native fascia tissues and integrates well into native tissues	(1) Too brittle and degrades very slowly *in vivo*
	(2) Produces better extracellular matrix components	(2) Acidity and high crystallinity of its byproduct degradation often triggered inflammatory reactions
	(3) With good cell infiltration, neovascularization, and macrophage type 2 response	
PCL	(1) Good thermal stability, good biocompatibility, and low immunogenicity	Hydrophobicity of PCL impedes cell adhesion and limits the degradation rate
	(2) Easy to process and surface modifications	
PLGA	(1) Good biocompatibility and controllable biodegradability	Limited mechanical properties
	(2) Can be combined with a variety of materials	

treatment of PFD. So, we reviewed the research results of TERM applied in PFD treatment and drew the structure diagram of TERM (Figure 1).

Seed cells

Seed cells are the premise of tissue engineering; they could be obtained from a wide range of sources, including autologous, allogeneic, and heterologous tissues. Stem cells and differentiated cells have been reported as the seed cells for pelvic floor repair. Mesenchymal stem cells (MSCs) are the most widely used stem cells, including adipose-derived stem cells (ADSCs), bone marrow-derived mesenchymal stem cells (BMSCs), endometrial mesenchymal stem cells (eMSCs), and muscle-derived stem cells (MDSCs). The differentiated cells include fibroblasts, myoblasts, and smooth muscle cells. Among them, ADSCs and eMSCs are the most promising cells for experimental research and clinical treatment of PFD (Table 1).

ADSCs are considered beneficial for PFD treatment by *in vitro* and *in vivo* studies because ADSCs can be obtained in large quantities during single liposuction and without general anesthesia and are easy to culture and expand *in vitro* (Chen H. et al., 2021a; Wang et al., 2021). ADSCs not only exhibit self-renewal and multilineage differentiation, but they also have confirmed proliferative efficiency and low donor morbidity (Sterodimas et al., 2010). In addition, there is a relatively low occurrence of surgical interference in collecting them as compared with other derived stem cells. Some studies suggested that ADSCs have equal or superior therapeutic

potential compared to BMSCs. ADSCs were used to treat SUI in many clinical trials by urethral injection showing better results and minimal side effects and complications (Barakat et al., 2020). Roman et al. (2014) showed that hADSCs appear to be suitable cell types to combine with biodegradable scaffolds for the treatment of SUI and POP.

eMSCs are a rare population of perivascular MSCs in the endometrial layer of the uterus and are another ideal source of autologous therapeutic cells for the treatment of POP using novel tissue engineering approaches for the following reasons: (1) eMSCs exhibit excellent regenerative capacity in the endometrial lining following menstruation and high proliferative capacity *in vitro*. (2) They can be easily obtained from menstrual blood or endometrial biopsies, even from the post-menopausal uterus; the procurement method is minimally invasive, without the need for an anesthetic, resulting in minimum pain and morbidity. (3) eMSCs can be purified using a unique marker, SUSD2 (Masuda et al., 2012). (4) A small molecule TGF-β receptor inhibitor (A83-01) can maintain clonogenic SUSD2^{+}eMSCs and prevents spontaneous fibroblast differentiation during culture expansion (Gurung et al., 2015). (5) eMSCs could reduce the foreign body reaction to the degradable mesh by modulating inflammatory cytokine secretion and changing the ratio of M1/M2 of macrophages (Darzi et al., 2018).

BMSCs are among the best characterized of all stem cells studied so far, with great differentiation ability and the ability to secrete factors beneficial to tissue repair. BMSCs are used in the repair of various diseases and injuries with good efficacy in many studies. Among them, the treatment of PFD by BMSCs was also studied *in vitro* and *in vivo* and the results showing good repair effects, whether through local cell injection or tissue engineering combined with biological scaffolds (Jin et al., 2016a; Jin et al., 2016b; Zhao et al., 2017; Zhao et al., 2018; Zhao et al., 2021). However, BMSCs carry disadvantages such as painful isolation procedures, the need for general anesthesia, relatively scarce numbers, and low cell yields, and they, especially, cannot be easily expanded in middle-aged people. So these shortcomings limited the clinical use of BMSCs.

MDSCs are isolated from muscle biopsies and differentiated *in vitro* and *in vivo* into skeletal myotubes, osteoblasts, chondrocytes, neural cells, and smooth muscle cells. There are only small studies investigating PFD treatment using MDSCs with or without scaffolds. The clinical study showed that the quality of life in patients with SUI improved significantly 2–4 years after the MDSC injection procedure (Stangel-Wojcikiewicz et al., 2014; Stangel-Wojcikiewicz et al., 2016). *In vitro* studies demonstrated that urethral striated muscle-derived stem/progenitor cells (uMDSCs) could form myotubes when treated with micro-energy acoustic pulses or low-intensity extracorporeal shock waves (Wang B. et al., 2018a; Cui et al., 2019). Animal experiments showed that MDSC injection improved the function of urination in rats with intrinsic sphincter deficiency and increased the expression of myosin and α-smooth muscle actin (α-SMA) (Cui et al., 2018). However, the acquisition of MDSCs requires surgical anesthesia and invasive operation, resulting in pain and low cell yield, which limits its clinical application.

Additionally, some other differentiated cells were also used for repairing damaged tissue due to PFD, such as vaginal fibroblasts, epithelial cells, smooth muscle cells, and human oral fibroblasts. However, the use of these differentiated cells in tissue engineering repair is significantly less than that of MSCs, for MSCs have a particular advantage over differentiated cells.

Scaffolds

The ideal scaffolds for tissue engineering should meet the following conditions: (1) the scaffolds should be biocompatible, integrate well into the patient's tissues, and reflect the properties of the tissues into which it is implanted. (2) The property of scaffolds should be stable, with proper porosity and pore size, conducive to cell adhesion, proliferation, no toxicity, and no immunity. (3) The scaffolds should be strong enough to provide structural support and remain relatively elastic to cope with the forces experienced with routine events such as coughing or sneezing and become reversibly stronger at higher strain, similar to the native healthy fascia. (4) Materials proposed for grafts should degrade *in vivo*, provoke an acute inflammatory response, undergo tissue remodeling, allow cell permeability, and exhibit mechanical robustness at the point of implantation (Gigliobianco et al., 2015). PFD is a chronic disorder with no optimal standards for the repair or treatment; an ideal mesh would be desirable for degradable biomaterials to last 6–12 months to ensure sufficient tissue re-organization with desired stiffness. The scaffolds in TERM for PFD were mainly synthetic materials in a large number of *in vitro* and *in vivo* studies, and they are all FDA-approved materials, such as poly-L-lactic acid (PLA), polyglycolide (PGA), poly lactic-co-glycolic acid (PLGA), and polycaprolactone (PCL). Different materials have their own advantages and disadvantages, and they had been reported in the study of PFD treatment by combining with different cells (Table 1).

PLA scaffold mimics the architecture of native fascia tissues, produces better extracellular matrix components for cell attachment and proliferation *in vitro*, and integrates well in native tissue with good cell infiltration, neovascularization, and macrophage type 2 (M2) response (Roman et al., 2019). However, PLA is too brittle and degrades very slowly *in vivo*, and the acidity and high crystallinity of its degradation byproducts often triggered inflammatory reactions. Relatively few studies were reported on the effect of PLA or PLA-added cells on PFD (Mangir et al., 2016; Roman et al., 2016; Mangir et al., 2019).

PCL is an FDA-approved polyester with excellent thermal stability, good biocompatibility, and low immunogenicity, it is

easy to process and susceptible to surface modifications, and it has been widely used as biomaterials for tissue engineering purposes, including pelvic meshes (Siddiqui et al., 2018). However, the hydrophobicity of PCL impedes cell adhesion and limits the degradation rate. So many PCL composites were studied for PFD treatment, such as PCL/PLA, PCL/PGA, PCL/PEG (Ren et al., 2022), PLGA/PCL (Vashaghian et al., 2017; Vashaghian et al., 2019; Chen YP. et al., 2021b), and UPy-PCL(Hympanova et al., 2018), and the results showed that PCL/PEG and PLGA/PCL were better than the others, the degradation rate of PCL/PLA and PCL/PGA were too high, and UPy-PCL had a high failure rate.

PLGA scaffold is approved by the FDA (U.S. Food and Drug Administration, United States)/EMA (European Medicines Agency) and extensively explored. PLGA holds a prominent position in a variety of tissue repairs due to its biocompatibility and controllable biodegradability. PLGA scaffold has been successfully applied in pelvic floor repair (Oe et al., 2022) and bladder replacement alone (Salem et al., 2020) (Rocha et al., 2022) or PLGA-based composites, such as PLGA-NPs (Jin et al., 2016a; Jin et al., 2016b), PLGA/PCL (Qian et al., 2016; Vashaghian et al., 2016), PLGA-MPEG (Jangö et al., 2017), and PLACL/gelatin (Mukherjee et al., 2019). Among them, PLGA/PCL has been studied the most in the treatment of pelvic floor repair.

In addition, other scaffolds are also used for PFD repair, such as PGA, PLTG, PU, and PLCL/Fg (Hou et al., 2014; Wu et al., 2016; Wang et al., 2017; Wang X. et al., 2018b; Masudi and Abdelrahman, 2021). However, the relevant studies are limited. PGA is beneficial to using as sling material for SUI treatment because of its low stiffness.

Bioactive factors

The appropriate microenvironment for tissue regeneration is another key factor of an ideal tissue engineering scaffold. So some bioactive factors were added to scaffolds to induce stem cell proliferation and differentiation, promote cell–material interaction, enhance mechanical and biological properties, and antisepsis, etc. PFD-related factors include basic fibroblast growth factor (bFGF), nerve growth factor (NGF), connective tissue growth factor (CTGF), estrogen, 17-β-estradiol, ascorbic acid, ascorbate-2-phosphate, and antibiotics. Jin et al. demonstrated that bFGF significantly promoted the production of collagen and elastin from elastin-expressing BMSCs *in vitro* and *in vivo*, and co-injection of PLGA-loaded bFGF NP and elastin-expressing BMSCs into the PFD rats significantly improved the outcome of urodynamic tests (Jin et al., 2016a). *In situ* gel-forming bulking agent, containing NGF and bFGF, provided regeneration of damaged nerves and smooth muscles and enhanced biological function around the urethra (Oh et al., 2015). The solid PCL-CTGF mesh delivering rMSC demonstrated improved biomechanical properties and no complications after implantation in a rat model of a weakened vaginal wall after 8–24 weeks (Hansen et al., 2020). Studies have shown that estrogen released from PLA mesh promotes more ECM production involving collagen I, collagen III, and elastin and doubled new blood vessel formation in the chorioallantoic membrane (Mangir et al., 2019). Shafaat et al. (2018) reported that 17-β-estradiol-releasing PU scaffolds showed increased ultimate tensile strength and produced more ECM and blood vessels. However, the controversial therapeutic effect of estrogen was also reported (Wu et al., 2020). Ascorbic acid and ascorbate-2-phosphate in the PLA scaffold could increase its hydrophilicity and strength and promote the production of collagen from human dermal fibroblasts (Mangir et al., 2016). Ren et al. (2022) coated the PCL/PEG composite meshes with azithromycin and elicited the antibacterial properties of the meshes; the results showed that it is effective in suppressing the growth of *S. aureus* bacteria and will be supporting cell attachment and proliferation.

The cross-talk between scaffolds and cells

Cell therapy using MSCs and surgery with synthetic polymer scaffolds alone could somewhat improve the PFD symptoms, and cell-based tissue engineering has even more dramatic therapeutic effects. So, how and why therapeutic cells together with scaffolds enhance therapeutic outcomes is the key factor. From a clinical perspective, the cross-talk between scaffolds and cells may be imperative for enhancing the therapeutic effect of PFD (Mukherjee et al., 2019).

The cell–biomaterial interactions between eMSCs and nanofiber meshes of PLACL/gelatin *in vitro* and *in vivo* were evaluated by Mukherjee et al. (2019), and the results showed: (1) mesh properties influence eMSC size, proliferation rate, adhesion, migration, structure, and expression of F-actin and vinculin protein *in vitro*. PLACL/gelatin nanofiber meshes provide suitable scaffolding where cells can interact with the mesh, as well as with each other and the host cells. (2) PLACL/gelatin significantly enhanced eMSC retention and infiltration properties *in vivo*. Many clinical trials of cell therapies suggested that mere injection of therapeutic cells is not sufficient to cure diseases (Galipeau and Sensebe 2018). One reason is that there are no enough cells in the damaged site, so retention of MSCs in the transplantation site is a key factor for cellular infiltration and tissue integration. (3) eMSCs control ECM formation and degradation of nanofiber meshes *in vivo*, allowing time for tissue strengthening before the scaffold fully disappears. (4) eMSCs influence the macrophage-based foreign body response to nanofiber meshes *in vivo*. Wang X. et al.

TABLE 2 TERM implants for PFD *in vitro* and *in vivo* (2015–2022).

Scaffold	Cell	Additive/ treatment factor	Application	Main outcome
PGA	ADMSCs	5-Azacytidine	TE slings cultured *in vitro* and used in the SUI rat model	TE slings promoted collagen production, integrated better with the urethral sphincter, and rescued the urine controlling ability and the LPP of the rat model Wang et al. (2016)
PGA	ADMSCs		TE slings cultured *in vitro*	TE sling demonstrated matured form at 12 weeks, with gradually increased mechanical properties and collagen fibers and myoblast expression over time Wang et al. (2017)
PLACL/gelatin nanofiber meshes	SUSD2+ eMSC		Foreign body response of $SUSD^{2+}$eMSCPLACL/gelatin meshes in the mice model	eMSCs impacted the degradation rate and tissue integration of PLACL/gelatin mesh and PLACL/gelatin nanofiber meshes enable entrapment of eMSCs for up to 6 weeks promoting substantial cellular infiltration of host anti-inflammatory macrophages Mukherjee et al. (2019)
PLA	ADSCs		Cell-impregnated scaffolds developed *in vitro* for the repair of SUI and POP	ADSCs attached well and increased in number and metabolic activity; ultimate tensile (UT) strength, UT strain, and YM of scaffolds increased; collagen I, collagen III, and elastin were produced at acceptable levels. Wang et al. (2018b)
PLA	ADMSCs and OF	Intermittent stress	*In vitro* TERM for POP and SUI	Both cells attached and proliferated well on PLA, increased biomechanical properties of scaffolds, and produced more elastin under restrained conditions. Under unstrained conditions, ADSCs on PLA produced more total collagen and a denser homogenous ECM than OF Roman et al. (2014)
PLA	ADMSCs	Estradiol	ADSCs seeded on estradiol-releasing scaffolds	PLA-estradiol scaffolds increased ECM production and stimulate angiogenesis (Mangir et al., 2019)
PLA	HDF	AA/A2P	PLA-AA/A2P scaffolds were co-cultured with fibroblasts	PLA-AA/A2P scaffolds increased hydrophilicity and strength and promoted collagen production of HDF Mangir et al. (2016)
PLA	hADMSCs		Construct scaffolds that mimic the 3D architecture of human fascia	PLA-aligned scaffolds showed increased bulk density, Young's modulus, and UTS, promoted the production of collagen, and maintained the strength and stiffness without changes after 2 weeks of culture *in vitro*
PLA/PU	ADMSCs	Dynamic loading	Cell-impregnated sling *in vitro* for SUI	PLA/Z1 improved the interaction of the scaffolds with cells, reduction in material strength, and the ability of cells to penetrate the scaffolds Hillary et al. (2016)
PLGA	BMSCs	bFGF/mirRNA-29a-3p inhibition	BMSCs- mirRNA-29a-3p + PLGA- bFGF for PFD rats	MirRNA-29a-3p + PLGA-bFGF promoted elastin production of BMSCs, rescued the void volume, bladder void pressure, and LPP Jin et al. (2016b)
PLGA	BMSCs	bFGF + elastin-BMSCs	Elastin-BMSCs and PLGA-bFGF to the pelvis of PFD rats	PLGA-bFGF induced prolonged production of collagen and elastin from elastin–BMSCs, and PLGA-bFGF + elastin–BMSCs improved the urodynamic tests
MPEG-PLGA	MEF		MFF seeded on MPEG-PLGA scaffold for the rat abdominal wall defect model	Cells originating from the MFF influence the histological and biomechanical properties of the native tissue Jango et al. (2015). MPEG-PLGA + MFF explants showed higher stiffness and strength, with no sign of an inflammatory or foreign-body response
PCL	rMSC	bFGF/CTGF	PCL-CTGF-rMSC used on a rat model of PFD	PCL-CTGF-rMSC mesh showed increased biomechanical properties, collagen production, and without complications after 8 and 24 weeks Hansen et al. (2020)
PCL/PEG	ADSCs	Azithromycin	PCL/PEG–azithromycin mesh *in vitro*	PCL/PEG–azithromycin mesh showed anti-infectious properties and supported cell attachment and proliferation after pre-released for 14 days Ren et al. (2022)
PCL/PLGA	Fibroblasts		Effect of PCL/PLGA scaffolds on fibroblasts	Gentle cyclic straining of human fibroblasts on PCL/PLGA scaffolds enhances the regenerative potential
P (LLA-CL)-collagen 1 nanoyarn	Myoblasts from PSCs		Fabricate a novel nanoyarn for the treatment of SUI as a sling	P (LLA-CL)-collagen1 sling promoted the proliferation, infiltration, and production of collagen and elastin
PU	hADMSCs	17-β-estradiol	Developing scaffolds for POP and SUI	

(Continued on following page)

TABLE 2 (*Continued*) TERM implants for PFD *in vitro* and *in vivo* (2015–2022).

Scaffold	Cell	Additive/ treatment factor	Application	Main outcome
				PU-17-β-estradiol scaffolds increased the ultimate tensile strength and promoted ECM production and angiogenic formation Shafaat et al. (2018)
PLCL	VE/SC		TE-based treatment for vaginal defects	VE/SC attached and maintained viability on scPLCL Sartoneva et al. (2018)
PCL/PLGA	VF		Effect of fiber diameter on scaffolds and cells *in vitro*	Fiber diameter affects cell behavior, ECM deposition, and the mechanical properties of the matrices but did not affect the ultimate tensile strength Vashaghian et al. (2016)
PTLG	ADSCs		Cell-impregnated scaffolds for repair of SUI and POP	ADSCs attached well and increased in number and metabolic activity; ultimate tensile (UT) strength, UT strain, and YM of scaffolds increased; collagen I, collagen III, and elastin were produced at acceptable levels. Wang et al. (2018b)

(2018b) reported that the addition of ADSCs onto both PLA and PLTG scaffolds led to a significant increase in stiffness and maximum stress of the scaffolds. A similar phenomenon was also observed in other experiments using human oral fibroblasts (OFs) and the hADSC effects on PLA scaffold (Roman et al., 2014). Significant temporal changes in tensile properties and clear differences in collagen organization with time between eMSC-seeded and -unseeded scaffolds were observed (Edwards et al., 2015). PLA combined with PU greatly improved the interaction of cells with this material (Hillary et al., 2016).

So, the cross-talk between scaffolds and cells is of great significance in tissue engineering. The scaffolds could provide support for cell growth, promote cell proliferation, and prevent cell migration. At the same time, the cells can affect the property of the biomaterials, such as stiffness, elasticity, and degradation rate, especially for PFD, it would be desirable for degradable biomaterials to last 6–12 months until new tissue of desired stiffness has been regenerated, so regulating the degradation of biomaterials is the key to TERM for PFD (Hillary et al., 2016).

Tissue-engineered repair material for stress urinary incontinence

SUI is the involuntary urine leakage associated with increased intra-abdominal pressure on the bladder during activities, such as coughing, laughing, sneezing, exercising, impact movements, or squatting (Wallace et al., 2019). The urine leakage of SUI happens in the absence of detrusor contraction. The pathophysiology of SUI is not well known and multifactorial, including pregnancies with subsequent vaginal deliveries, nerve damage, intrinsic sphincteric deficiency (ISD), body mass index (BMI), advancing age, hormonal changes, and smoking. The current treatment options mainly include conservative, pharmacological, and surgical treatments, and the efficacy is generally unsatisfactory. TERM has provided a variety of opportunities to restore the damaged sphincter function in patients with SUI (Table 2).

The suburethral sling implantation is the mainstay of surgical treatment for SUI. However, these approaches only supply passive support for the urethral lumen without restoring the damaged sphincter function. Also, tissue rejection, urethral erosion, and infection are the major problems and headaches of the currently used slings. Ying Wang tried to explore the possibility of generating a sling complex *in vitro* by seeding ADSCs onto PGA under constant strain; the results showed that the ADSC-PGA construct appeared as a sling-like structure with a cord-like shape during the first 4 weeks of *in vitro* culture, and the ADSC-PGA sling exhibited to be relatively thicker, smoother, much thinner, and mature at 12 weeks and had gradually increased stress/strain curves, max load, and Young's modulus values over time. The collagen fibers and myoblasts' expression increased in a time-dependent manner (Wang et al., 2017). A tissue-engineered sling was constructed by seeding GFP-transfected ADSCs on PGA fibers, and with the induction of 5-azacytidine for 4 weeks, the sling was then implanted in the SUI rat model established by the vaginal balloon dilatation method and bilateral ovariectomy. LPP increased significantly and reached nearly close to baseline normal levels, 2 months after implantation. ADSCs promote more collagen matrix formation and are integrated better with the urethral sphincter (Wang et al., 2016). To find materials with more appropriate mechanical properties for a sling, which can also support cell integration, scaffolds of different materials were compared; the results showed that PU Z1 and PU Z3 coped well with dynamic strain and maintained their elasticity after 7 days of sustained cyclical distention (Hillary et al., 2016). PLA is superior at supporting cellular interactions and new matrix production,

but the mechanical properties changed after only 7 days of dynamic strain. PU/PLA was weaker and stiffer than PU or PPL but significantly improved the interaction of the scaffolds with cells and promoted the total collagen expression of hADSCs cultured on the scaffolds, suggesting that a combination of materials could be more suitable for successful implantation and longer survival for the management of SUI. Zhang et al. (2016) fabricated a novel electrospun nanoyarn with higher porosity, larger pore size, and aligned fibers/yarns than the nanofiber scaffold. A tissue-engineered sling was formed by seeding myoblasts on nanoyarn, and the myoblasts proliferated greatly on the nanoyarn scaffold and infiltrated deeply into it after 7 days; nanoyarn myoblasts produced more type 1 and 3 collagen and elastin and improved muscular tissue development, suggesting myoblast–nanoyarn sling could be a promising tissue-engineered sling for SUI.

Bulking agents are another common treatment for SUI, which allows minimally invasive treatment and low medical expenses. However, the migration and/or degradation of the injected bulking agents shortened the lasting of long-term effectiveness in the therapeutic period. An alternative approach based on cells/bioactive molecules and biodegradable biomaterials can induce the regeneration of target tissues and improve the sphincter function. Oh et al. (2015) developed an injectable bioactive bulking agent for the SUI rat model by loading dual growth factor (NGF and bFGF) *in situ* hydrogel/PCL bead mixture, and the results showed that the PCL beads were located stably at the applied site without migration. The sequential release of the growth factors from the bulking agent promoted the regeneration of damaged nerves and smooth muscles and thus enhanced biological function around the urethra. Jin et al. (2016a) formulated the bFGF-loaded PLGA nanoparticle (bFGF-loaded PLGA NPs) system to achieve the sustained release of bFGF and employed this system in elastin–over-expressing BMSC culture *in vitro* and in the rat vaginal distention translational model *in vivo*. The results showed that bFGF-loaded PLGA NPs could markedly stimulate the differentiation of elastin–over-expressing BMSCs to fibroblasts and then produce more collagen and elastin *in vitro* and *in vivo*. Also, the combination using of a bFGF-loaded PLGA NP system and elastin–over-expressing BMSCs in the rat model could alleviate the PFD symptoms, reverse the decreased void volume and bladder void pressure, and rescue the decreased peak bladder pressure. In another study, Jin et al. (2016b) demonstrated that inhibition of miR-29a-3p in BMSCs along with bFGF-PLGA-NP injection can markedly increase the expression and secretion of elastin, which consequently largely improved the urodynamic parameters and urodynamics and promoted the therapeutic effect of BMSCs on PFD rats.

Tissue-engineered repair material for pelvic organ prolapse

POP is defined as the descent of one or more of the pelvic organs (vaginal wall, bladder, uterus, and vaginal apex) from their natural positions in the pelvis because of the weakening of the pelvic floor and the organ support structure (Iglesia and Smithling 2017). POP mainly results from pregnancy/vaginal birth, which is due to the strain, overstretching, and tearing of the pelvic floor ligaments, muscles, and connective tissues (Wallace et al., 2019). Surgery treatment with synthetic meshes is the main method for POP therapy, but the surgical outcomes do not meet patients' needs. Many studies demonstrated that TERM consisting of cells/drugs/growth factors/biodegradable scaffolds could improve the therapeutic effect (Table 2).

Jango et al. (2015) employed MPEG-PLGA (methoxypolyethyleneglycol polylactic-co-glycolic acid) scaffold seeded with autologous muscle fiber fragments (MFFs) to treat a rat abdominal wall defect model; the results demonstrated that MPEG-PLGA scaffold is a safe carrier for MFFs, and MFFs affect the regenerative repair process, but the MPEG-PLGA+MFF group showed a trend toward higher stiffness in the physiologically more important low stiffness zone, which is not ideal from a clinical point of view. An estradiol-releasing electrospun PLA mesh containing different concentrations of estradiol was designed, and the results showed that ADMSCs cultured on estradiol-releasing PLA meshes produced more ECM and formed more new blood vessels and outgrew the pro-angiogenic cells (Mangir et al., 2019). Meanwhile, the estradiol-releasing PLA mesh with ADMSCs was more elastic and stronger than control PLA meshes. PU scaffolds with 17-β-estradiol significantly increased the ultimate tensile strength of scaffolds, and hADMSCs on estradiol-releasing PU scaffolds showed more ECM production, higher angiogenic potential, and good cellular infiltration and tissue integration (Shafaat et al., 2018). Ascorbic acid (AA) and ascorbate-2-phosphate (A2P) containing PLA scaffolds were significantly more hydrophilic and stronger than PLA scaffolds and had approximately two times higher UTS, strain, and YM values than pure PLA. Human dermal fibroblasts seeded on AA or A2P containing PLA scaffolds produced more collagen (Mangir et al., 2016). Four different PLA scaffolds with various degrees of fiber alignment were constructed to mimic the three-dimensional architecture of human fascia, and the results showed that the bulk density, Young's modulus, and UTS were significantly increased from PLA-random to PLA-aligned scaffolds, and ADSCs grew well on scaffolds with aligned fibers, produced the largest amount of total collagen, and maintained the strength and stiffness without changes after 2 weeks of culture *in vitro* (Roman et al., 2016). The scPLCL is a potential scaffold material for vaginal tissue engineering, vaginal epithelial (VE), and stromal cells (SCs) that attached and

maintained viability on scPLCL (Sartoneva et al., 2018). The comparison of PLGA/PCL films with different fiber diameters suggested that the fiber diameter affects cell behavior, mechanical properties, and cellular infiltration ECM deposition (Vashaghian et al., 2016).

Conclusion

The clinical experience and studies *in vitro* or *in vivo* suggest that tissue engineering technology can provide successful outcomes when used in the surgical management of pelvic floor disorders. These data provide valuable evidence for clinical application in the urogynecological setting. However, different cells, scaffolds, or cell-combined scaffolds have their own advantages and disadvantages, which can produce different therapeutic effects on PFD. The question is which is most desirable? Therefore, more studies with longer follow-up are needed to select the most effective and safe cells and materials for PFD repair.

Author contributions

ML contributed to the literature search and drafting of the manuscript; YL contributed to drawing pictures and making tables; and JC designed and reviewed the manuscript. All the authors reviewed the manuscript and approved it for publication.

Funding

This research was supported by the following funding schemes: Scientific Research Funds Project of Higher Education Institutions of Liaoning Province, under No. LJKZ0791 and the Young and Middle-Aged Science and Technology Innovation Talents Support Program of Shenyang, under No. RC210454.

Conflict of interest

The authors declare that the research was conducted in the absence of any commercial or financial relationships that could be construed as a potential conflict of interest.

Publisher's note

All claims expressed in this article are solely those of the authors and do not necessarily represent those of their affiliated organizations, or those of the publisher, the editors, and the reviewers. Any product that may be evaluated in this article, or claim that may be made by its manufacturer, is not guaranteed or endorsed by the publisher.

References

Barakat, B., Franke, K., Schakaki, S., Hijazi, S., Hasselhof, V., and Vogeli, T. A. (2020). Stem cell applications in regenerative medicine for stress urinary incontinence: A review of effectiveness based on clinical trials. *Arab. J. Urol.* 18, 194–205. doi:10.1080/2090598x.2020.1750864

Chen, H., Li, Z., Lin, M., Lv, X., Wang, J., Wei, Q., et al. (2021a). MicroRNA-124-3p affects myogenic differentiation of adipose-derived stem cells by targeting Caveolin-1 during pelvic floor dysfunction in Sprague Dawley rats. *Ann. Transl. Med.* 9, 161. doi:10.21037/atm-20-8212

Chen, Y. P., Lo, T. S., Lin, Y. T., Chien, Y. H., Lu, C. J., and Liu, S. J. (2021b). Fabrication of drug-eluting polycaprolactone/poly(lactic-co-glycolic acid) prolapse mats using solution-extrusion 3D printing and coaxial electrospinning techniques. *Polym. (Basel)* 13, 2295. doi:10.3390/polym13142295

Cui, K., Kang, N., Banie, L., Zhou, T., Liu, T., Wang, B., et al. (2019). Microenergy acoustic pulses induced myogenesis of urethral striated muscle stem/progenitor cells. *Transl. Androl. Urol.* 8, 489–500. doi:10.21037/tau.2019.08.18

Cui, L., Meng, Q., Wen, J., Gao, Z., Yan, Z., Tian, Y., et al. (2018). A functional comparison of treatment of intrinsic sphincter deficiency with muscle-derived and adipose tissue-derived stem cells. *IUBMB Life* 70, 976–984. doi:10.1002/iub.1896

Darzi, S., Deane, J. A., Nold, C. A., Edwards, S. E., Gough, D. J., Mukherjee, S., et al. (2018). Endometrial mesenchymal stem/stromal cells modulate the macrophage response to implanted polyamide/gelatin composite mesh in immunocompromised and immunocompetent mice. *Sci. Rep.* 8, 6554. doi:10.1038/s41598-018-24919-6

Edwards, S. L., Ulrich, D., White, J. F., Su, K., Rosamilia, A., Ramshaw, J. A., et al. (2015). Temporal changes in the biomechanical properties of endometrial mesenchymal stem cell seeded scaffolds in a rat model. *Acta Biomater.* 13, 286–294. doi:10.1016/j.actbio.2014.10.043

Elmer, C., Blomgren, B., Falconer, C., Zhang, A., and Altman, D. (2009). Histological inflammatory response to transvaginal polypropylene mesh for pelvic reconstructive surgery. *J. Urol.* 181, 1189–1195. doi:10.1016/j.juro.2008.11.030

Farmer, Z. L., Dominguez-Robles, J., Mancinelli, C., Larraneta, E., and Lamprou, D. A. (2020). Urogynecological surgical mesh implants: New trends in materials, manufacturing and therapeutic approaches. *Int. J. Pharm. X.* 585, 119512. doi:10.1016/j.ijpharm.2020.119512

Galipeau, J., and Sensebe, L. (2018). Mesenchymal stromal cells: Clinical challenges and therapeutic opportunities. *Cell Stem Cell* 22, 824–833. doi:10.1016/j.stem.2018.05.004

Gigliobianco, G., Regueros, S. R., Osman, N. I., Bissoli, J., Bullock, A. J., Chapple, C. R., et al. (2015). Biomaterials for pelvic floor reconstructive surgery: How can we do better? *Biomed. Res. Int.* 2015, 1–20. doi:10.1155/2015/968087

Gurung, S., Werkmeister, J. A., and Gargett, C. E. (2015). Inhibition of transforming growth factor-beta receptor signaling promotes culture expansion of undifferentiated human endometrial mesenchymal stem/stromal cells. *Sci. Rep.* 5, 15042. doi:10.1038/srep15042

Hansen, S. G., Taskin, M. B., Chen, M., Wogensen, L., Vinge Nygaard, J., and Axelsen, S. M. (2020). Electrospun nanofiber mesh with fibroblast growth factor and stem cells for pelvic floor repair. *J. Biomed. Mat. Res.* 108, 48–55. doi:10.1002/jbm.b.34364

Hillary, C. J., Roman, S., Bullock, A. J., Green, N. H., Chapple, C. R., and MacNeil, S. (2016). Developing repair materials for stress urinary incontinence to withstand dynamic distension. *PLoS One* 11, e0149971. doi:10.1371/journal.pone.0149971

Hou, M., Wu, Q., Dai, M., Xu, P., Gu, C., Jia, X., et al. (2014). Fabrication of electrospun thermoplastic polyurethane blended poly (l-lactide-co-e-caprolactone) microyarn scaffolds for engineering of female pelvic-floor tissue. *Biomed. Mat.* 10, 015005. doi:10.1088/1748-6041/10/1/015005

Hympanova, L., Mori da Cunha, M., Rynkevic, R., Wach, R. A., Olejnik, A. K., Dankers, P. Y. W., et al. (2018). Experimental reconstruction of an abdominal wall defect with electrospun polycaprolactone-ureidopyrimidinone mesh conserves

compliance yet may have insufficient strength. *J. Mech. Behav. Biomed. Mat.* 88, 431–441. doi:10.1016/j.jmbbm.2018.08.026

Iglesia, C. B., and Smithling, K. R. (2017). Pelvic organ prolapse. *Am. Fam. Physician* 96, 179–185.

Jango, H., Gras, S., Christensen, L., and Lose, G. (2015). Muscle fragments on a scaffold in rats: A potential regenerative strategy in urogynecology. *Int. Urogynecol. J.* 26, 1843–1851. doi:10.1007/s00192-015-2782-x

Jangö, H., Gräs, S., Christensen, L., and Lose, G. (2017). Tissue-engineering with muscle fiber fragments improves the strength of a weak abdominal wall in rats. *Int. Urogynecol J.* 28, 223–229. doi:10.1007/s00192-016-3091-8

Jin, M., Chen, Y., Zhou, Y., Mei, Y., Liu, W., Pan, C., et al. (2016a). Transplantation of bone marrow-derived mesenchymal stem cells expressing elastin alleviates pelvic floor dysfunction. *Stem Cell Res. Ther.* 7, 51. doi:10.1186/s13287-016-0308-1

Jin, M., Wu, Y., Wang, J., Ye, W., Wang, L., Yin, P., et al. (2016b). MicroRNA-29 facilitates transplantation of bone marrow-derived mesenchymal stem cells to alleviate pelvic floor dysfunction by repressing elastin. *Stem Cell Res. Ther.* 7, 167. doi:10.1186/s13287-016-0428-7

Lo, T. S., Pue, L. B., Hung, T. H., Wu, P. Y., and Tan, Y. L. (2015). Long-term outcome of native tissue reconstructive vaginal surgery for advanced pelvic organ prolapse at 86 months: Hysterectomy versus hysteropexy. *J. Obstet. Gynaecol. Res.* 41, 1099–1107. doi:10.1111/jog.12678

Mangir, N., Bullock, A. J., Roman, S., Osman, N., Chapple, C., and MacNeil, S. (2016). Production of ascorbic acid releasing biomaterials for pelvic floor repair. *Acta Biomater.* 29, 188–197. doi:10.1016/j.actbio.2015.10.019

Mangir, N., Hillary, C. J., Chapple, C. R., and MacNeil, S. (2019). Oestradiol-releasing biodegradable mesh stimulates collagen production and angiogenesis: An approach to improving biomaterial integration in pelvic floor repair. *Eur. Urol. Focus* 5, 280–289. doi:10.1016/j.euf.2017.05.004

Masuda, H., Anwar, S. S., Buhring, H. J., Rao, J. R., and Gargett, C. E. (2012). A novel marker of human endometrial mesenchymal stem-like cells. *Cell Transpl.* 21, 2201–2214. doi:10.3727/096368911x637362

Masudi, S. T., and Abdelrahman, A. (2021). Evaluating tissue-engineered repair material for pelvic floor dysfunction: A comparison of *in vivo* response to meshes implanted in rats. *Int. Urogynecol J.* doi:10.1007/s00192-022-05143-3

Mukherjee, S., Darzi, S., Rosamilia, A., Kadam, V., Truong, Y., Werkmeister, J. A., et al. (2019). Blended nanostructured degradable mesh with endometrial mesenchymal stem cells promotes tissue integration and anti-inflammatory response *in vivo* for pelvic floor application. *Biomacromolecules* 20, 454–468. doi:10.1021/acs.biomac.8b01661

Oe, Y., Ogino, S., Kobayashi, M., Kojima, H., Terukina, T., Kanazawa, T., et al. (2022). Testosterone sustained release microspheres for the treatment of fecal incontinence. *J. Pharm. Sci.* 111, 2322–2329. doi:10.1016/j.xphs.2022.03.008

Oh, S. H., Bae, J. W., Kang, J. G., Kim, I. G., Son, J. Y., Lee, J. Y., et al. (2015). Dual growth factor-loaded *in situ* gel-forming bulking agent: Passive and bioactive effects for the treatment of urinary incontinence. *J. Mat. Sci. Mat. Med.* 26, 33. doi:10.1007/s10856-014-5365-3

Qian, Y., Chen, H., Xu, Y., Yang, J., Zhou, X., Zhang, F., et al. (2016). The preosteoblast response of electrospinning PLGA/PCL nanofibers: Effects of biomimetic architecture and collagen I. *Int. J. Nanomed.* 11, 4157–4171. doi:10.2147/ijn.s110577

Quaghebeur, J., Petros, P., Wyndaele, J. J., and De Wachter, S. (2021). Pelvic-floor function, dysfunction, and treatment. *Eur. J. Obstet. Gynecol. Reprod. Biol. X.* 265, 143–149. doi:10.1016/j.ejogrb.2021.08.026

Ren, J., Murray, R., Wong, C. S., Qin, J., Chen, M., Totsika, M., et al. (2022). Development of 3D Printed Biodegradable Mesh with Antimicrobial Properties for Pelvic Organ Prolapse. *Polym. (Basel)* 14, 763. doi:10.3390/polym14040763

Rocha, C. V., Goncalves, V., da Silva, M. C., Banobre-Lopez, M., and Gallo, J. (2022). PLGA-based composites for various biomedical applications. *Int. J. Mol. Sci.* 23, 2034. doi:10.3390/ijms23042034

Roman, S., Mangera, A., Osman, N. I., Bullock, A. J., Chapple, C. R., and MacNeil, S. (2014). Developing a tissue engineered repair material for treatment of stress urinary incontinence and pelvic organ prolapse-which cell source? *Neurourol. Urodyn.* 33, 531–537. doi:10.1002/nau.22443

Roman, S., Mangir, N., Bissoli, J., Chapple, C. R., and MacNeil, S. (2016). Biodegradable scaffolds designed to mimic fascia-like properties for the treatment of pelvic organ prolapse and stress urinary incontinence. *J. Biomater. Appl.* 30, 1578–1588. doi:10.1177/0885328216633373

Roman, S., Mangir, N., and MacNeil, S. (2019). Designing new synthetic materials for use in the pelvic floor: What is the problem with the existing polypropylene materials? *Curr. Opin. Urol.* 29, 407–413. doi:10.1097/mou.0000000000000623

Salem, S. A., Rashidbenam, Z., Jasman, M. H., Ho, C. C. K., Sagap, I., Singh, R., et al. (2020). Incorporation of smooth muscle cells derived from human adipose stem cells on poly(lactic-co-glycolic acid) scaffold for the reconstruction of subtotally resected urinary bladder in athymic rats. *Tissue Eng. Regen. Med.* 17, 553–563. doi:10.1007/s13770-020-00271-7

Sartoneva, R., Kuismanen, K., Juntunen, M., Karjalainen, S., Hannula, M., Kyllonen, L., et al. (2018). Porous poly- l -lactide-co-ε-caprolactone scaffold: A novel biomaterial for vaginal tissue engineering. *R. Soc. open Sci.* 5, 180811. doi:10.1098/rsos.180811

Shafaat, S., Mangir, N., Regureos, S. R., Chapple, C. R., and MacNeil, S. (2018). Demonstration of improved tissue integration and angiogenesis with an elastic, estradiol releasing polyurethane material designed for use in pelvic floor repair. *Neurourol. Urodyn.* 37, 716–725. doi:10.1002/nau.23510

Siddiqui, N., Asawa, S., Birru, B., Baadhe, R., and Rao, S. (2018). PCL-based composite scaffold matrices for tissue engineering applications. *Mol. Biotechnol.* 60, 506–532. doi:10.1007/s12033-018-0084-5

Stangel-Wojcikiewicz, K., Jarocha, D., Piwowar, M., Jach, R., Uhl, T., Basta, A., et al. (2014). Autologous muscle-derived cells for the treatment of female stress urinary incontinence: A 2-year follow-up of a polish investigation. *Neurourol. Urodyn.* 33, 324–330. doi:10.1002/nau.22404

Stangel-Wojcikiewicz, K., Piwowar, M., Jach, R., Majka, M., and Basta, A. (2016). Quality of life assessment in female patients 2 and 4 years after muscle-derived cell transplants for stress urinary incontinence treatment. *Ginekol. Pol.* 87, 183–189. doi:10.17772/gp/61330

Sterodimas, A., de Faria, J., Nicaretta, B., and Pitanguy, I. (2010). Tissue engineering with adipose-derived stem cells (ADSCs): Current and future applications. *J. Plast. Reconstr. Aesthet. Surg.* 63, 1886–1892. doi:10.1016/j.bjps.2009.10.028

Vashaghian, M., Diedrich, C. M., Zandieh-Doulabi, B., Werner, A., Smit, T. H., and Roovers, J. P. (2019). Gentle cyclic straining of human fibroblasts on electrospun scaffolds enhances their regenerative potential. *Acta Biomater.* 84, 159–168. doi:10.1016/j.actbio.2018.11.034

Vashaghian, M., Ruiz-Zapata, A. M., Kerkhof, M. H., Zandieh-Doulabi, B., Werner, A., Roovers, J. P., et al. (2017). Toward a new generation of pelvic floor implants with electrospun nanofibrous matrices: A feasibility study. *Neurourol. Urodyn.* 36, 565–573. doi:10.1002/nau.22969

Vashaghian, M., Zandieh-Doulabi, B., Roovers, J. P., and Smit, T. H. (2016). Electrospun matrices for pelvic floor repair: Effect of fiber diameter on mechanical properties and cell behavior. *Tissue Eng. Part A* 22, 1305–1316. doi:10.1089/ten.tea.2016.0194

Wallace, S. L., Miller, L. D., and Mishra, K. (2019). Pelvic floor physical therapy in the treatment of pelvic floor dysfunction in women. *Curr. Opin. Obstet. Gynecol.* 31, 485–493. doi:10.1097/gco.0000000000000584

Wang, B., Zhou, J., Banie, L., Reed-Maldonado, A. B., Ning, H., Lu, Z., et al. (2018a). Low-intensity extracorporeal shock wave therapy promotes myogenesis through PERK/ATF4 pathway. *Neurourol. Urodyn.* 37, 699–707. doi:10.1002/nau.23380

Wang, X., Chen, Y., Fan, Z., and Hua, K. (2018b). Comparing different tissue-engineered repair materials for the treatment of pelvic organ prolapse and urinary incontinence: Which material is better? *Int. Urogynecol. J.* 29, 131–138. doi:10.1007/s00192-017-3406-4

Wang, X., Chen, Y., Fan, Z., and Hua, K. (2021). Evaluating tissue-engineered repair material for pelvic floor dysfunction: a comparison of in vivo response to meshes implanted in rats *Int. Urogynecol. J.* 33, 2143–2150. doi:10.1007/s00192-021-05008-1

Wang, Y., Shi, G. W., Wang, J. H., Cao, N. L., and Fu, Q. (2016). Adipose-derived stem cells seeded on polyglycolic acid for the treatment of stress urinary incontinence. *World J. Urol.* 34, 1447–1455. doi:10.1007/s00345-015-1757-3

Wang, Y., Wang, W., Wang, X., Wang, Y., Wang, J., Fu, Q., et al. (2017). Tissue-engineered sling with adipose-derived stem cells under static mechanical strain. *Exp. Ther. Med.* 14, 1337–1342. doi:10.3892/etm.2017.4705

Wu, J. M., Hundley, A. F., Fulton, R. G., and Myers, E. R. (2009). Forecasting the prevalence of pelvic floor disorders in U.S. Women: 2010 to 2050. *Obstetrics Gynecol.* 114, 1278–1283. doi:10.1097/aog.0b013e3181c2ce96

Wu, X., Jia, Y., Sun, X., and Wang, J. (2020). Tissue engineering in female pelvic floor reconstruction. *Eng. Life Sci.* 20, 275–286. doi:10.1002/elsc.202000003

Wu, X., Wang, Y., Zhu, C., Tong, X., Yang, M., Yang, L., et al. (2016). Preclinical animal study and human clinical trial data of co-electrospun poly(L-lactide-co-caprolactone) and fibrinogen mesh for anterior pelvic floor reconstruction. *Int. J. Nanomed.* 11, 389–397. doi:10.2147/ijn.s88803

Zhang, K., Guo, X., Li, Y., Fu, Q., Mo, X., Nelson, K., et al. (2016). Electrospun nanoyarn seeded with myoblasts induced from placental stem cells for the application of stress urinary incontinence sling: An *in vitro* study. *Colloids Surfaces B Biointerfaces* 144, 21–32. doi:10.1016/j.colsurfb.2016.03.083

Zhao, B., Hu, M., Wu, H., Ren, C., Chen, J., Zhang, X., et al. (2018). Peroxisome proliferator-activated receptor-gamma and its related pathway in bone marrow mesenchymal stem cell differentiation co-cultured with mechanically stretched ligament fibroblasts. *Int. J. Mol. Med.* 42, 219–227. doi:10.3892/ijmm.2018.3578

Zhao, B., Hu, M., Wu, H., Ren, C., Wang, J., and Cui, S. (2017). Tenascin-C expression and its associated pathway in BMSCs following co-culture with mechanically stretched ligament fibroblasts. *Mol. Med. Rep.* 15, 2465–2472. doi:10.3892/mmr.2017.6329

Zhao, B., Sun, Q., Fan, Y., Hu, X., Li, L., Wang, J., et al. (2021). Transplantation of bone marrow-derived mesenchymal stem cells with silencing of microRNA-138 relieves pelvic organ prolapse through the FBLN5/IL-1β/elastin pathway. *Aging (Albany NY)* 13, 3045–3059. doi:10.18632/aging.202465

frontiers | Frontiers in Bioengineering and Biotechnology

TYPE Original Research
PUBLISHED 30 September 2022
DOI 10.3389/fbioe.2022.1021218

OPEN ACCESS

EDITED BY
Liqun Yang,
China Medical University, China

REVIEWED BY
Lu Cao,
Fudan University, China
Liu Tong,
Zhejiang University of Technology, China
Chenyang Zhao,
Shenzhen University, China

*CORRESPONDENCE
Qing Liu,
qliu@ametcorp.com
Guannan Wang,
chemwangguannan@gmail.com

†These authors have contributed equally to this work

SPECIALTY SECTION
This article was submitted to Biomaterials, a section of the journal Frontiers in Bioengineering and Biotechnology

RECEIVED 17 August 2022
ACCEPTED 12 September 2022
PUBLISHED 30 September 2022

CITATION
Fan T, Qin J, Meng X, Li J, Liu Q and Wang G (2022), Biodegradable membrane of poly(l-lactide acid-dioxanone-glycolide) and stereocomplex poly(lactide) with enhanced crystallization and biocompatibility.
Front. Bioeng. Biotechnol. 10:1021218.
doi: 10.3389/fbioe.2022.1021218

Biodegradable membrane of poly(l-lactide acid-dioxanone-glycolide) and stereocomplex poly(lactide) with enhanced crystallization and biocompatibility

Tiantang Fan[1†], Jingwen Qin[2†], Xiao Meng[3], Jiafeng Li[4], Qing Liu[2*] and Guannan Wang[1*]

[1]College of Medical Engineering & the Key Laboratory for Medical Functional Nanomaterials, Jining Medical University, Jining, China, [2]The Institute for Translational Nanomedicine, Shanghai East Hospital, The Institute for Biomedical Engineering & Nano Science, Tongji University School of Medicine, Shanghai, China, [3]College of Materials Science and Engineering, North China Electric Power University, Beijing, China, [4]China Coal Research Institute, Beijing, China

The membranes of poly(l-lactide acid-p-dioxanone-glycolide) (PLPG) with stereocomplex poly(lactic acid) (sc-PLA) were prepared by the solution blending way. It was observed that sc-PLA significantly heightened the crystallizing behavior of PLLA segments of the PLPG matrix. The crystallizing behavior displayed that the temperature of crystallization shifted to a higher range than that of PLPG. Moreover, the half-time of crystallization sharply decreased in value as the sc-PLA content increased in value on account of the pre-eminent nucleation ability of sc-PLA. TGA results revealed the thermal stability of the samples with the increase of sc-PLA compared to PLPG. Meanwhile, enzymatic degradation results indicated that the mass loss rate of the membrane decreased with the introduction of sc-PLA, but the overall degradation ability was still greater than that of PLLA. In the meantime, the biological experiment indicated that the membrane possessed low cytotoxicity.

KEYWORDS

poly(l-lactide), stereocomplex poly(lactic acid), crystallization, biodegradability, biocompatibility

1 Introduction

Poly(l-lactide) (PLLA) has gained interest in tissue engineering and orthopedics fields owing to its mechanical properties, biodegradability, and easy processability (Liu et al., 2017; Ziemba et al., 2018; Shamsah et al., 2020). However, PLLA still has disadvantages, such as poor toughness and a slow degradation rate, that restrain its applications on a large scale (Vilay et al., 2011; Li et al., 2020a). Consequently, several researchers are trying to modify the structure for PLLA to enhance both properties simultaneously (Fasolino

et al., 2017; Yang et al., 2018; Li et al., 2020b). Chemical modification methods are employed to strengthen the performance of polymers. Ring-opening polymerization has significant advantages, such as simple operation, mature technology, controllable product structure, and molecular weight, compared with the other chemical modification methods (Nikovia et al., 2019). Poly (p-dioxanone) (PPDO) has excellent mechanical strength, distinguished biodegradability, and biocompatibility, which are widely useful in surgical suturing, cardiovascular applications, and tissue engineering (Schattmann et al., 2017). Moreover, poly(lactic-co-glycolic acid) (PLGA) is another popular biomedical degradable polymer material, which can regulate the comprehensive properties by changing the ratio of LLA to GA and is widely employed in tissue engineering (Yoo and Won, 2020; Song et al., 2022). Hence, biodegradable PLLA-PDO-GA (PLPG) copolymers were prepared by ring-opening polymerization. Adding GA and PDO improves the performance of PLLA; however, GA and PDO interrupt the regularity of PLLA segments compromising the crystallization ability of the polymers. Consequently, it is indispensable to find out the enhancement mechanism to expand the practical applications of PLPG polymers.

Recently, several studies have reported blending PLLA with inorganic or organic materials to enhance the crystallization ability of PLLA (Chen et al., 2014; Tao et al., 2018; Purnama et al., 2021). Generally, the inorganic or organic materials reduce the energy barrier or surface-free energy barrier, thereby enhancing the crystallization kinetics of the materials. Wang and Qiu (2012) reported that the overall isothermal melt crystallization rates of PLLA/graphene oxide were greater than that of PLLA. Furthermore, Zhang et al. (2016) demonstrated that the talcum powder (Talc) and multiamide compound (TMC) could heighten the crystallizing ability of PLLA. However, the aforementioned inorganic materials still have defects such as easy migration and difficult degradation. Consequently, some organic materials are exploited to accelerate the crystallization ability of PLLA. Notably, stereocomplex poly(lactic acid) (sc-PLA) is extensively employed in biomedical fields due to its excellent mechanical properties and biocompatibility. Additionally, the melting temperature (T_m) of sc-PLA is significantly higher than that of PLLA by 50°C; hence, the additional sc-PLA could remain in PLLA during its melting state. Previous studies have shown that sc-PLA could significantly enhance the crystallization ability of PLLA polymers. Furthermore, Fan et al. (2020) reported that sc-PLA would significantly strengthen the kinetic crystallizability of the PLLA segments in poly(TMC-b-(LLA-ran-GA)), and the crystallization half-time ($t_{0.5}$) decreased from 12.3 to 3.7 min as sc-PLA increased from 3% to 20% at 120°C.

In the present study, a series of PLPG/sc-PLA (P/s) blends were prepared and a thermal process was designed to generate a "standard state" to examine the efficiency of nucleation. The influence of different sc-PLA content on the crystallization ability of PLLA and biocompatibility of PLPG copolymers was analyzed. Moreover, the enhanced mechanism was investigated to control the mechanical performances and biocompatibility of the PLPG polymers. We believe that the P/s membrane materials are expected to be used in skin trauma, bone tissue engineering, and so on.

2 Materials and methods

2.1 Materials

LLA, GA, and PDO were supplied by Daigang Biomaterial Co., Ltd. (China, >99%). Stannous octoate [$Sn(Oct)_2$] was obtained from Adamas Reagent Co., Ltd. (Shanghai, China). Proteinase K with white powder was obtained from Solarbio (China). All the experiment reagents were used as received. Sc-PLA was prepared by the solution blending method according to the published literature (Fan et al., 2019). Briefly, PLLA was dissolved in dichloromethane (CH_2Cl_2). When PLLA was completely dissolved, PDLA was added to the aforementioned solution at a mass ratio of 50:50. After stirring for 6 h, the mixture solution was placed at room temperature. Finally, sc-PLA was obtained after the solution was completely volatilized.

2.2 Preparation of the PLPG copolymers

The PLPG polymers with 6.0×10^5 g/mol and polydispersity values (PDI) of 1.38 were prepared by ROP. The molar ratio of LLA, GA, and PDO was set as 90: 5: 5 (Fan et al., 2020). Briefly, the right contents of LLA, GA, and PDO were put into a silanized tube using $Sn(Oct)_2$. The tube was sintered under a vacuum after degassing and polymerization was accomplished at 135°C for 72 h. The obtained polymers were treated with CH_2Cl_2 and ethanol. Finally, the PLPG copolymers were dried at 50°C in a vacuum while keeping the mass constant. The yield of the PLPG copolymers was about 85%.

2.3 Preparation of the P/s membrane

The polymer membranes were prepared to employ the solution-casting method at room temperature. The various concentrations of sc-PLA in the samples were obtained by dissolving PLPG and sc-PLA solution of chloroform and 1,1,1,3,3,3-hexafluoro-2-propanol and stirred for about 6 h. Then, the solution was evaporated and the membrane was dried at 37°C in a vacuum drying oven for 24 h until the mass was constant. The weight ratio of sc-PLA to PLPG was 5, 10, 15, and 20 wt%, respectively. The membrane with χ wt% sc-PLA was named P/s-χ.

2.4 Characterizations

2.4.1 Crystal structure and crystallization behavior

The X-ray diffraction (XRD) patterns of the samples were recorded by using the Bruker D8 advanced X-ray diffractometer with 40 kV and 25 mA. The diffractogram of the samples was gained from 5° to 35° using the Cu Kα radiation (4°/minute).

2.4.2 Thermal behavior

DSC (Mettler Toledo, Switzerland) at N_2 was used to display the thermal properties of the samples. Briefly, 4–8 mg of the samples was heated to about 230°C at 20°C/min first. Later, the samples were incubated for 3 min to clear off the thermal history and then cooled down to 20°C quickly. Finally, the sample was reheated to 230°C at 10°C/min to study the melting behavior. Furthermore, for non-isothermal crystallization, 4–8 mg of the membrane was heated to 230°C at 20°C/min and then maintained for 3 min. The temperature was dropped gradually to room temperature at 3°C/min. Additionally, the sample was heated to about 230°C and maintained for about 5 min. Then, the samples were cooled down to 155°C and kept for 10 min to generate sc-PLA completely. Finally, the samples were quickly quenched to 100, 105, 110, 115, 120, 125, and 130°C and held for about 30 min to examine the isothermal crystallization behavior of the samples.

2.4.3 Enzymatic degradation

The square samples with dimensions 5 × 5 × 0.1 mm were analyzed for enzymatic degradation by treating them with protease K at different time intervals. Briefly, the samples were soaked in the proteinase K-tris buffer solution (3 ml, 0.05 M, pH = 8.5) and their weight before and after soaking was recorded. The activity of proteinase K was evaluated by changing the solution every 2 days. The samples were rinsed with distilled water three times at a scheduled time. In the end, the membranes were placed in the drying oven (37°C) until the mass was constant.

2.4.4 Thermal degradation behavior

Thermogravimetric analysis (Hengjiu, Beijing) was employed to reveal the kinetics of thermal degradation. In brief, the membrane was heated to 500°C at 10, 15, 20, and 25°C/min, respectively.

2.4.5 Cytotoxicity assay

The cytotoxicity of the samples was investigated on the human adipose-derived stem cells (hADSCs) using cell culture experiments. hADSCs were obtained from the GMP Laboratory of Stem Cell Transformation, medicine industry base (Shanghai East Hospital). The protocol for processing human tissues and cells was ratified by the Ethics Committee (Tongji University School of Medicine, Tongji University Affiliated East Hospital, and Jining Medical University). Adipose tissue donors signed informed consent and voluntarily donated samples. The viability was assessed by employing live/dead staining assay. Specifically, hADSCs (3×10^4 cells/mL) were seeded into 96-cell culture plates that had leach liquors of the membrane at 37°C atmospheres under a medium (5% CO_2). Furthermore, hADSCs were colored by calcein-AM and propidium iodide (PI) for 30 min after incubation for 1, 2, and 3 days. In the end, fluorescent staining was captured by using a fluorescence microscope (LEICA). The proliferation of hADSCs was quantified by the cell counting kit-8 (CCK-8) assays. hADSCs (3×10^4 cells/mL) were cultured in 96-cell culture plates that contained the membrane leach liquor. Later, the CCK-8 solution was introduced into each well in the dark at the predetermined time. The absorbancy of the membrane was acquired by using a multimode reader at 450 nm.

The hADSCs grown in the leach liquor of the membrane were fixed with paraformaldehyde (4%) for about 10 min and permeated by the Triton X-100 solution (0.5%) for about 5 min. hADSCs were washed with PBS and colored to observe the actin cytoskeleton by the prepared RBITC-labeled phalloidin working reagents for about half hour in the dark conditions. Later, DAPI (5 μg/ml) was implied to detect the nuclear staining. Finally, fluorescent staining was performed by using the fluorescence microscope.

3 Results and discussion

3.1 Thermal properties and crystal structures

The crystallization behavior of polymer materials reflects their crystallization ability and the kinetics of the molecular chains in the polymers. Figure 1A shows the DSC curve of the second heating of the samples and after quenching from 230°C. Table 1 shows the thermal performance parameters such as cold crystallization temperature (T_{cc}), melting point (T_m), and melting enthalpy (ΔH_m). The gradual decrease in the temperature with the increase in the sc-PLA content was detected. Furthermore, T_{cc} of the P/s-5 was 134.3°C; however, as the additional amount of sc-PLA reached 20 wt%, T_{cc} of the P/s-20 decreased to 127.4°C. Meanwhile, a melting peak at about 159°C corresponding to T_m of PLLA in the PLPG polymers was detected. Moreover, due to the addition of sc-PLA in the PLPG polymers, a new melting peak appeared at about 212°C, corresponding to T_m of sc-PLA (Deng et al., 2021). Compared with the PLPG matrix, PLLA in the P/s was almost unchanged, while ΔH_{m-hc} increased gradually with the increase in the sc-PLA content. ΔH_{m-hc} of the PLPG matrix was 8.9 J/g with a corresponding crystallinity (X_{c-hc}) of 9.5%. ΔH_{m-hc} of the P/s-15 was 17.5 J/g with a corresponding X_{c-hc} of 18.6%. X_{c-hc} of the P/s-20 was slightly lower than that of P/s-15 (Table 1),

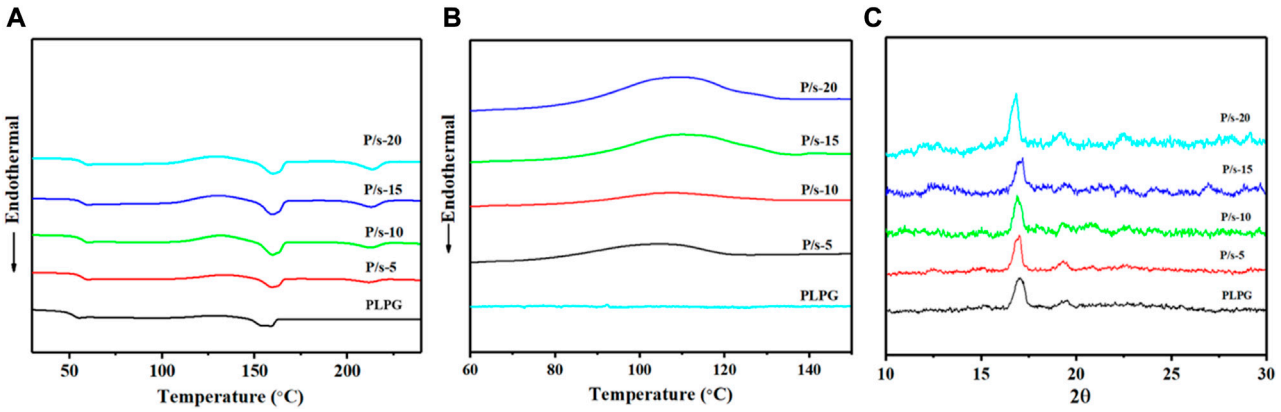

FIGURE 1
(A) Melting curves from 25°C to 230°C at 10°C/min. **(B)** Non-isothermal crystallization curves. **(C)** WAXD profile of the membrane at 3°C/min.

TABLE 1 Thermal property parameters of the PLPG polymers and P/s membranes.

Membrane	T_{cc} (°C)	T_{m1} (°C)	ΔH_{m-hc} (J/g)	X_{c-hc} (%)	T_{m2} (°C)	ΔH_{m-cs} (J/g)	X_{c-sc} (%)
PLPG	—	158.5	8.9	9.5	—	—	—
P/s-5	134.3	159.2	9.7	10.3	211.4	2.8	1.8
P/s-10	131.3	159.3	16.1	17.1	212.5	5.1	3.3
P/s-15	129.1	159.2	17.5	18.6	212.9	6.8	4.4
P/s-20	127.4	159.5	16.7	17.7	213.5	8.2	5.3

T_{m1} and T_{m2} are the melting points of PLLA and sc-PLA in the samples, respectively. ΔH_{m-hc} and ΔH_{m-sc} are the melting enthalpies of PLLA and sc-PLA in the samples, respectively. X_{c-hc} and X_{c-sc} are the crystallinity of PLLA and sc-PLA in the samples, respectively. $X_c=(\Delta H_m/\Delta H_m^{\infty})\times 100\%$, and ΔH_m^{∞} of PLLA and sc-PLA are 94 J/g and 155 J/g (Li et al., 2016), respectively.

suggesting that too much sc-PLA would hinder the migration of PLLA segments and weaken the crystallization ability of PLLA segments in the PLPG polymers. Meanwhile, ΔH_{m-sc} of sc-PLA of the P/s membrane increased gradually as the content of sc-PLA increased. ΔH_{m-sc} of sc-PLA in the P/s-5 was 2.8 J/g with a corresponding X_{c-sc} of 1.8%. Furthermore, as the content of sc-PLA increased to 20 wt%, ΔH_{m-sc} of sc-PLA in the P/s-20 was 8.2 J/g, and X_{c-sc} of sc-PLA was 5.3%. The aforementioned results indicated that adding sc-PLA can effectively improve the crystallization ability of PLLA segments of PLPG polymers.

Furthermore, the non-isothermal crystallization behavior was tested to assess the impact of sc-PLA in enhancing kinetic crystallizability of the PLLA segments of PLPG polymers. Figure 1B shows crystallization temperature (T_c), crystallization enthalpy (ΔH_c), and crystallinity (X_c) at the cooling rate of 3°C/min. The crystallization and melting behavior of the samples exhibited dependence on the sc-PLA content in the polymer. Moreover, the crystallization peak of PLLA segments in PLPG polymers cannot be detected, suggesting that the crystallization ability of PLLA was negligible at the cooling rate of 3°C/min. Conversely, the crystallization peak was detected with the introduction of sc-PLA, and T_c shifted to a higher temperature with increased sc-PLA. The results implied that the induction of sc-PLA strengthened the crystallization ability of PLLA segments of PLPG polymers. The results suggested that sc-PLA provided enough heterogeneous nucleation sites and reduced the energy barrier for nucleation, thus heightening the kinetic crystallizability of PLLA segments of PLPG polymers.

Additionally, the crystal structures of the samples that cooled from 230 to 25°C at 3°C/min were analyzed by XRD (Figure 1C), and the crystallization peaks of PLLA and sc-PLA in the blends were detected. The crystallization peaks at about 14.7°, 16.8°, 19.3°, and 22.4° could be assigned to the crystals of PLLA of PLPG polymers corresponding to the (010), (200)/(110), (203), and (210) crystal grids, respectively (Jiang et al., 2015; Park and Hong, 2021). The crystallization peaks of sc-PLA were 11.8°, 20.6°, and 24°. The aforementioned results displayed that adding sc-PLA would effectively heighten the crystallization ability of the PLLA segment of PLPG polymers.

The isothermal crystallization was measured by DSC, and the enhancement impact of adding sc-PLA on the crystallization ability of PLLA segments of PLPG polymers was evaluated (Figure 2). T_c of the isothermal crystallization was selected

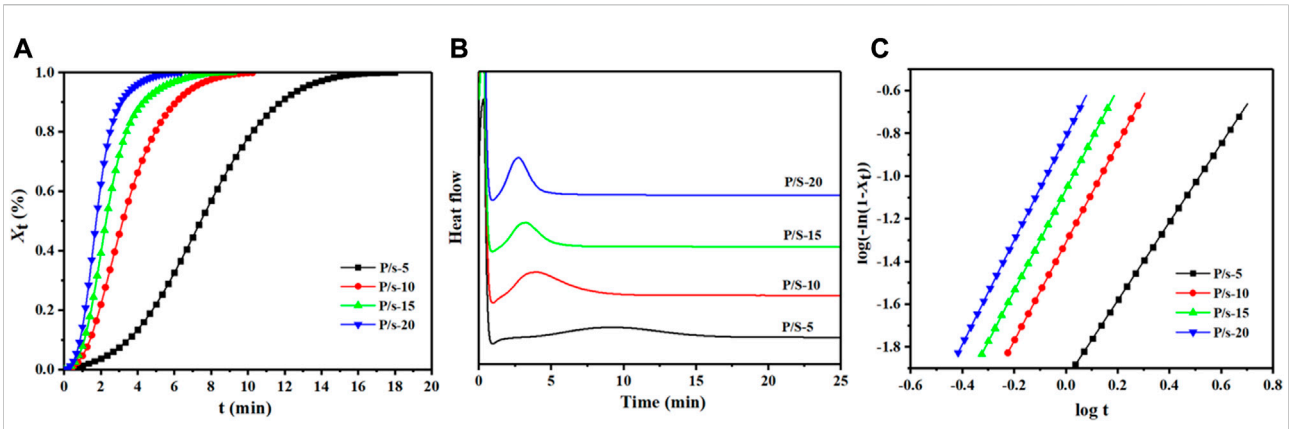

FIGURE 2
(A) DSC heat flow at 125°C, **(B)** X_t from DSC at 125°C, and **(C)** plots of log[-ln (1-X_t)] *versus* log *t* at 125°C.

from 100°C to 125°C. The relative degree of crystallinity (X_t) was calculated by the following equation (Cartier et al., 1997):

$$X_t = \frac{\int_0^t \left(\frac{dH}{dt}\right) dt}{\int_0^\infty \left(\frac{dH}{dt}\right) dt} = \frac{\Delta H_t}{\Delta H_\infty}.$$

Here dH/dt was the enthalpy change rate, ΔH_t was the heat enthalpy, and ΔH_∞ was the total heat enthalpy calculated. A broad exothermal peak for the samples with lower sc-PLA content was detected, suggesting an influence of the content of sc-PLA on crystallization (Figures 2A,B). Furthermore, with an increase in the sc-PLA content, the exothermal peaks became narrow by degrees and X_t decreased, indicating a strengthening of the crystallization ability. The crystallinity curves were of S-shape, and there was an obvious induction period in the early stage. In addition, with the increase in the sc-PLA content, the crystallinity conversion rate compared with the initial stage increased, suggesting that sc-PLA could be defined as a heterogeneous nucleation site to reduce the free energy barrier. Furthermore, as the content of sc-PLA increased, the number of nucleation sites was increased, resulting in an enhanced crystallization rate of PLLA segments of the P/s membranes. These results indicated that sc-PLA had an obvious enhancing impact on the overall crystallization rate of PLLA segments of PLPG polymers. $t_{0.5}$ was calculated at X_t = 50% (Supplementary Table S1). $t_{0.5}$ decreased with the introduction of sc-PLA as T_c was below 120°C, which could be due to a lower subcooling degree and more flexibility in the molecular chain movement, leading to a hard arrangement in the lattice. In the P/s-5, $t_{0.5}$ decreased from 10.8 to 5.2 min, which corresponded to T_c of 100°C and 115°C, respectively. As T_c was above 120°C, $t_{0.5}$ increased from 5.2 min to 7.4 min. Meanwhile, as the content of sc-PLA increased, $t_{0.5}$ decreased under the same T_c. These results showed that the introduction of sc-PLA could significantly enhance the crystallization ability of PLLA segments in PLPG polymers. In addition, the isothermal crystallization process of the P/s samples was also calculated by the Avrami equation (Lu et al., 2021).

$$\log\left[-\ln\left(1 - X_t\right)\right] = \log k + n \log t.$$

Here n was the Avrami index and k was the overall crystallization rate. n and k can be acquired by plotting log [–ln (1-X_t)] versus log t, which is the slope and intercept, respectively. Lorenzo et al. pointed out that X_t (3%–20%) was selected to evaluate the values of n and k (Arnaldo et al., 2007). The overall crystallization kinetics in the primary crystallization range was entirely denoted using the Avrami equation (Figure 2C). The n values of P/s samples oscillated between 2.0 and 3.0 (Supplementary Table S1), corresponding to the crystal growth mechanism of three-dimensional spherulites.

3.2 Thermal degradation behavior

The thermal degradation behavior of P/s membranes influenced by adding sc-PLA was examined by TGA at 10°C/min (Figure 3A). All the samples were observed to be stable below 200°C, and single-stage thermal degradation could be detected as the heating temperature reached 400°C. Meanwhile, adding sc-PLA enhanced the thermostability of the P/s membranes compared to that of PLPG copolymers. The P/s-20 had better thermal stability than the other membranes, and the temperature of the maximum mass loss rate (T_P) was about 314°C. This may be due to the following reasons. First, the thermal stability of sc-PLA was higher than that of PLLA. Meanwhile, the PLLA segments in PLPG and PDLA segments in sc-PLA could form the stereocomplex effect, which made the molecular chain bind closer and enhanced the intermolecular force.

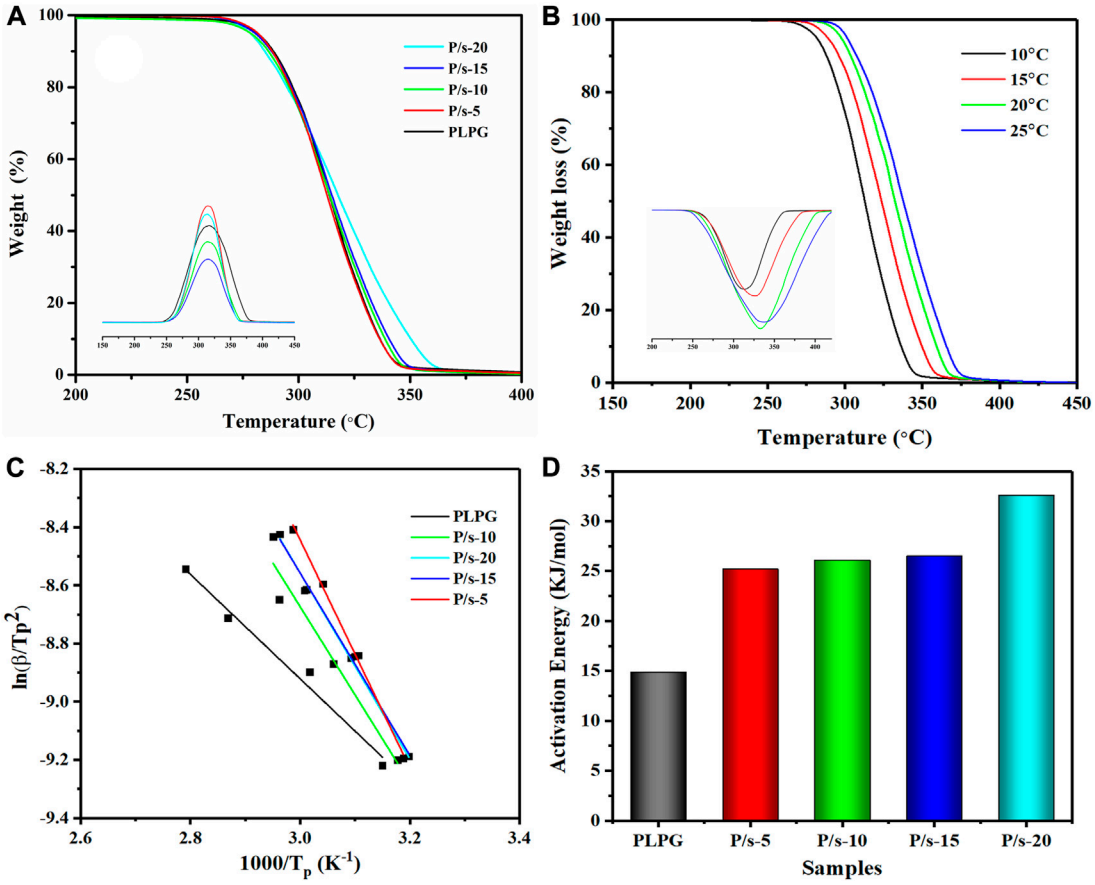

FIGURE 3
(A) TGA and DTG of the P/s membrane at 10°C/min, **(B)** TGA and DTG of the P/s-20 at 10, 15, 20, and 25°C/min, **(C)** Kissinger method that was applied to the experimental data, and **(D)** apparent E_a data.

At the same time, the Kissinger method was applied to analyze the kinetics of thermal degradation of the P/s membrane (Figure 3B). The TGA plots moved to the higher temperature region with a heating rate up to 25°C due to the requirement of the specific temperature in a shorter time and release gaseous products faster. The values are calculated using the following equation (Monika and Katiyar, 2017):

$$ln\frac{\beta}{T_P^2} = -\frac{E_a}{R}*\frac{1}{T_P} + ln\frac{AR}{E}.$$

Here, β was the heating rate. A was the pre-exponential factor. R was the gas constant. Figures 3C,D show the smooth linear fitted lines, indicating that the kinetics of thermal decomposition could be described by the Kissinger method. Furthermore, thermal degradation activation energy (E_a) gradually increased with the increase of the sc-PLA content. E_a of PLPG was about 14.9 kJ/mol. When the content of sc-PLA was increased to 20 wt%, E_a of P/s-20 increased to about 32.6 kJ/mol (Figure 3D). This is due to the higher thermal stability than that of PLLA. Further addition of sc-PLA accelerated the crystallization ability of PLLA of PLPG polymers, thus leading to the higher PLLA content in the P/s membranes.

3.3 Preparation and enhancement mechanism

A series of controlled P/s membranes was prepared using the solution blending methods (Scheme 1). Epitaxial nucleation and chemical mechanisms are often applied to explain the enhancement of nucleating materials (Hall et al., 2014; Xu et al., 2022). The epitaxial crystallization of polymers that grow on organic materials is usually applied to manifest the crystallization behaviors of PLLA (Takenaka et al., 2004). Meanwhile, sc-PLA and the PLPG matrix have similar crystal structures, and sc-PLA heightened the crystallization of the second crystalline phase by weakening the free energy of

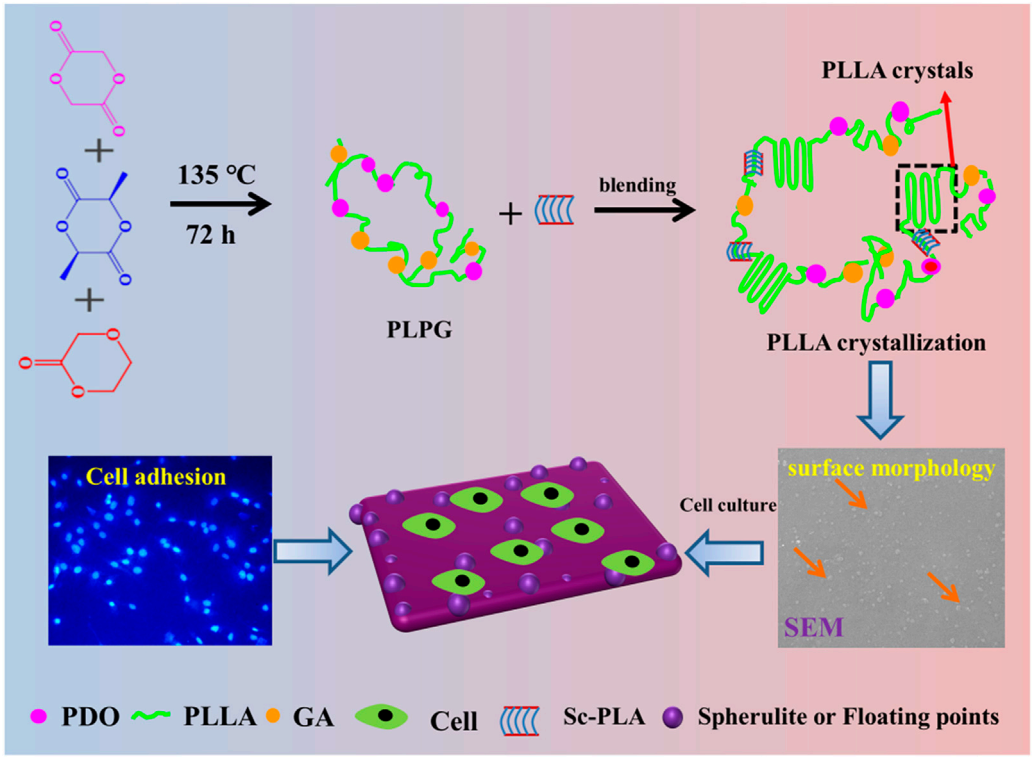

SCHEME 1
Schematic illustration of the preparation and enhancement mechanism of crystallization and improvement of cell adhesion of the P/s membranes used as biodegradable materials.

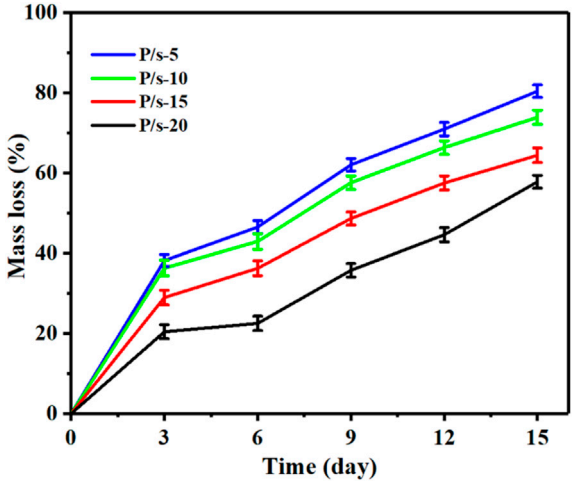

FIGURE 4
Mass loss of the membrane by enzymatic degradation for 15 days.

activation (Scheme 1). With the increase of sc-PLA contents, more spherical crystals appeared on the surface of P/s membranes, thus generating many floating points, which were beneficial to improve the ability of cell adhesion and growth. So the P/s samples would possess good biocompatibility and biodegradability.

3.4 Enzymatic degradation behavior

Enzyme degradation performance is an important index for evaluating completely degradable biomedical polymer materials. Figure 4 shows the influence of adding sc-PLA on the degradation performance of the P/s membrane by the protease K degradation experiment. The mass loss of the samples was calculated by the following equation:

$$\text{Mass loss } (\%) = \frac{(M_i - M_d)}{M_i} * 100.$$

Here, M_i and M_d were the initial weight and dry weight of the membrane, respectively.

It can be observed that the mass loss of the samples showed a linear trend of increase with the extension of the enzyme degradation time (Figure 4). The samples showed a linear trend of increase with the extension of the enzyme degradation time. Moreover, with the increase of sc-PLA

10.3389/fbioe.2022.1021218

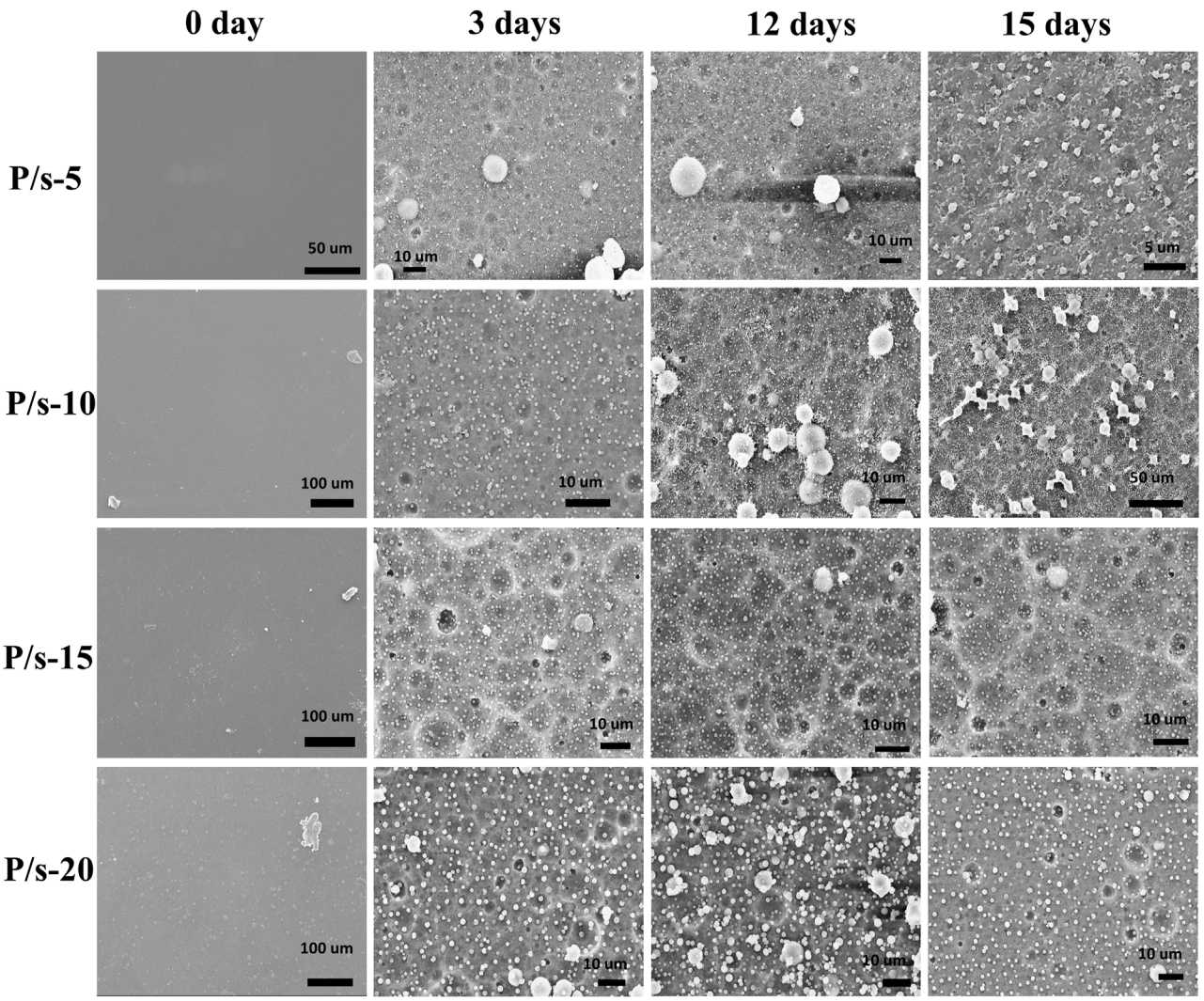

FIGURE 5
Surface morphology of the membranes during enzymatic degradation for 15 days.

contents, the mass loss of the P/s membrane decreased gradually. The mass loss of the P/s-15 and P/s-20 membranes was greatly reduced and calculated to be 64.45% and 57.84%, respectively. Only the amorphous regions of PLLA could be degraded by proteinase K. Adding sc-PLA enhanced the crystallization ability of PLLA segments of PLPG polymers, thus improving X_c of PLPG polymers. Furthermore, since the stereocomplex structure is not easily degraded by proteinase K, the enzymatic degradation of sc-PLA was less efficient than that of PLLA. Therefore, with the increase of sc-PLA content, the mass loss of the P/s membrane decreased.

Generally, the protease K degradation mechanism follows surface erosion degradation, and protease K has a high degree of selectivity to the degraded materials (Reeve et al., 1994). Moreover, protease K can degrade the amorphous region but not the crystalline region of PLLA materials. This is mainly due to the complex and larger structure of protease K, which cannot enter the interior of the polymer material. Therefore, protease K could only be adsorbed over the surface of the polymer material, causing breakage of the molecular chain on the polymer surface, and finally exposing the interiors of the polymer material for further degradation. The changes in the surface morphology of the samples during enzymatic degradation after 15 days were detected (Figure 5). The surface of the initial membrane was smooth, and a few irregular spherulites were observed on the surface of the membrane. When the degradation time lasted 3 days, the amorphous areas of the membranes were gradually eroded by the action of protease K. Hence, the surface appeared uneven with a little of pits. Furthermore, the amorphous region around the spherulite was eroded by protease K, while the

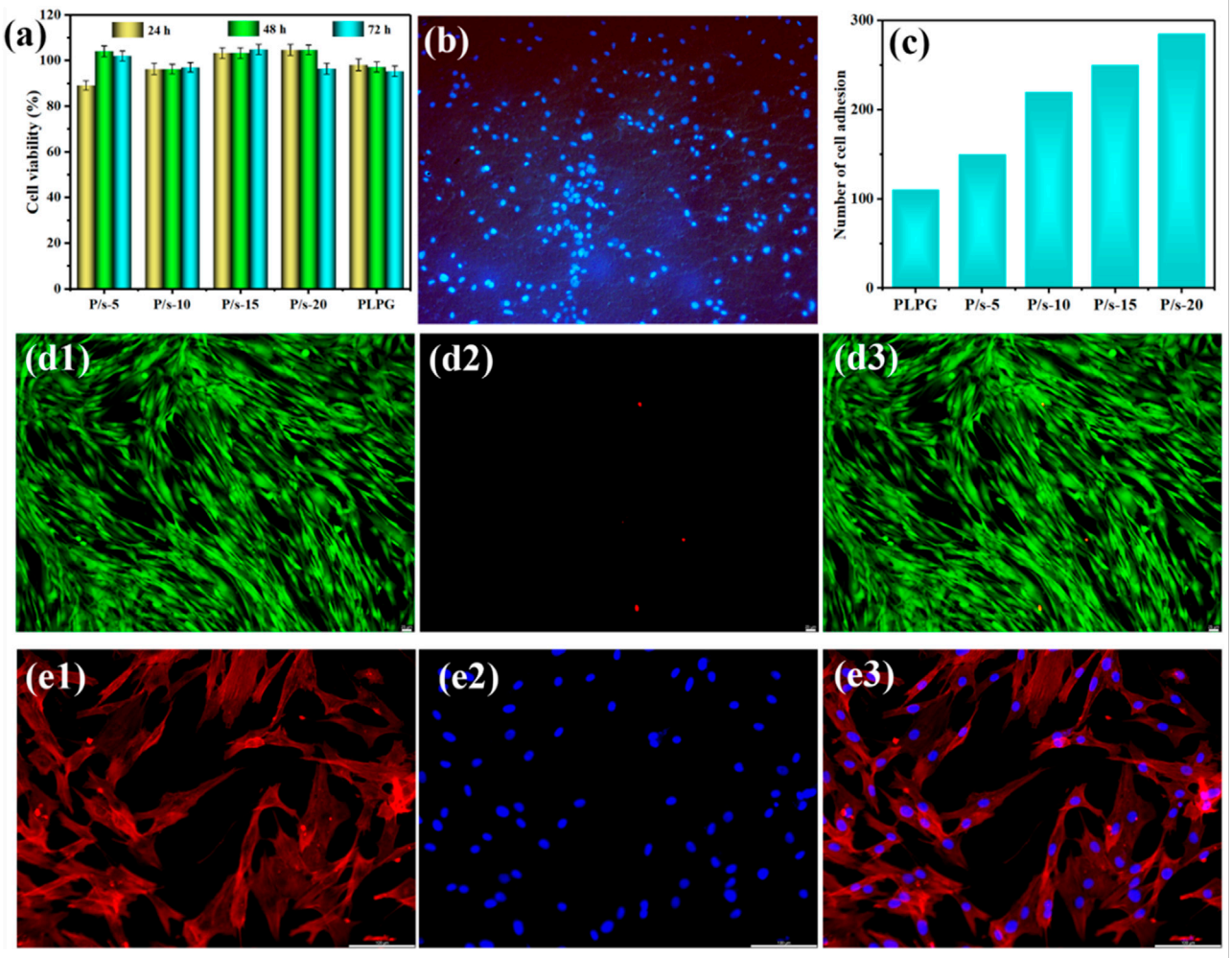

FIGURE 6
(A) CCK-8 assay of hADSCs for 24, 48, and 72 h, **(B)** cell adhesion on the surface of P/s-10 for 4 h (× 10), **(C)** number of cell adhesions on the surface of the samples for 4 h, **(d1–d3)** live/dead cell viability of the P/s-10 blends for 48 h (× 20), and **(e1–e3)** representative immunofluorescence microscopy images of the P/s-10 blends for 48 h (× 20).

spherulite could not be degraded and gradually fell off the surface during the degradation process. The increase in the degradation time of protease K to 15 days resulted in a large number of spherulites, and almost no amorphous areas on the surface of the membrane was detected. The enzymatic degradation after 15 days showed further reduction in the amorphous area and increased appearance of granular structures on the surface of the samples.

3.5 *In vitro* cellular assay

Figure 6 shows the cytotoxicity of hADSCs co-cultured with the samples. The cell viabilities of the samples analyzed by CCK-8 were all above 90%, and the cell viability increased with the extension of culture time to 72 h (Figure 6A). The cells could better adhere to the surface after being co-cultured with the P/s-10 membranes for 4 h (Figure 6B). Moreover, the number of cell adhesions increased by degrees as the sc-PLA content increased (Figure 6C).

The cytotoxicity of membranes was examined by live/dead staining (Figure 6d1–d3). The green and red fluorescences were the live cells and dead cells, respectively. All the membranes cultured for 48 h had low cytotoxicity with few dead cells (Figure 6d1–d3). Furthermore, the cell nucleus was stained with red color and the cytoplasm was stained with blue color for immunofluorescence microscopy images. It can be attributed that with the increase of sc-PLA, the surface of P/s membranes gradually became rough (Figure 4), which was consistent with the published literature (Li et al., 2020b). Figure 6(e1–e3) shows that the hADSCs co-cultured with the sample extract were well-

distributed in shape and slender filamentous pseudopods, while the large number of straight actin stress fibers were observed to be well organized. Therefore, the aforementioned results revealed that the P/s blends possessed good biocompatibility.

4 Conclusion

Sc-PLA showed a dramatically improving effect on the crystallization ability of PLLA segments of PLPG polymers. The non-isothermal and isothermal crystallization results indicated that the crystallization behavior of the membranes obviously heightened owing to the nucleation density, and the crystallization acceleration became more prominent. The enzymatic degradation behavior showed that as the sc-PLA content increased, the weight loss of the membranes decreased by degrees and was still greater than that of PLLA polymers. Meanwhile, the biological experiments indicated that the P/s membranes had good cytocompatibility. Therefore, the aforementioned results demonstrated a significant enhancing impact of sc-PLA on the crystallization behavior of PLLA segments of PLPG polymers, and the P/s membranes possessed good cytocompatibility.

Data availability statement

The original contributions presented in the study are included in the article/Supplementary Material; further inquiries can be directed to the corresponding authors.

Author contributions

TF and JQ contributed to the conception and design of the study and wrote the first draft of the manuscript. XM and JL organized the database and performed the statistical analysis. GW and QL contributed to manuscript revision and read and approved the submitted version.

Funding

This work was supported by the Natural Science Foundation of Shandong Province (No. ZR2021QC205), the Scientific Research Foundation of Jining Medical University (No. 600768001), and the scientific research and innovation team of Jining Medical University (No. 102425001).

Conflict of interest

The authors declare that the research was conducted in the absence of any commercial or financial relationships that could be construed as a potential conflict of interest.

Publisher's note

All claims expressed in this article are solely those of the authors and do not necessarily represent those of their affiliated organizations, or those of the publisher, the editors, and the reviewers. Any product that may be evaluated in this article, or claim that may be made by its manufacturer, is not guaranteed or endorsed by the publisher.

Supplementary material

The Supplementary Material for this article can be found online at: https://www.frontiersin.org/articles/10.3389/fbioe.2022.1021218/full#supplementary-material

References

Arnaldo, T., Maria, L., Julio, A., and Alejandro, J. (2007). DSC isothermal polymer crystallization kinetics measurements and the use of the Avrami equation to fit the data: Guidelines to avoid common problems. *Polym. Test.* 26, 222–231. doi:10.1016/j.polymertesting.2006.10.005

Cartier, L., Okihara, T., and Lotz, B. (1997). Triangular polymer single crystals: Stereocomplexes, twins, and frustrated structures. *Macromolecules* 30, 6313–6322. doi:10.1021/ma9707998

Chen, C., Chen, L., Cao, L., Yu, L., and Ding, J. (2014). Effects of L-lactide and D, L-lactide in poly(lactide-co-glycolide)-poly(ethylene glycol)-poly(lactide-co-glycolide) on the bulk states of triblock copolymers, and their thermogellation and biodegradation in water. *RSC Adv.* 4, 8789–8798. doi:10.1039/c3ra47494a

Deng, S., Yao, J., Bai, H., Xiu, H., Zhang, Q., and Fu, Q. (2021). A generalizable strategy toward highly tough and heat-resistant stereocomplex-type polylactide/elastomer blends with substantially enhanced melt processability. *Polymer* 224, 123736. doi:10.1016/j.polymer.2021.123736

Fan, T., Qin, J., Lin, S., Ye, W., Li, J., Zhang, Q., et al. (2019). Enhancement of the crystallization and biocompatibility of poly(TMC-*b*-(LLA-*ran*-GA)) by poly(lactide) stereocomplex. *CrystEngComm* 21, 6269–6280. doi:10.1039/c9ce01291e

Fan, T., Qin, J., Lin, S., Ye, W., Liu, Q., Fan, Z., et al. (2020). Enhancing crystallization behavior for optimized performances of poly(TMC-b-(LLA-ran-GA)) by PDLA/PLLA stereocomplex crystallization. *Polym. Adv. Technol.* 31, 1675–1687. doi:10.1002/pat.4895

Fasolino, I., Bonadies, I., Ambrosio, L., Raucci, M., Carfagna, C., Caso, F., et al. (2017). Eumelanin coated PLA electrospun micro fibers as bioinspired cradle for SH-SY5Y neuroblastoma cells growth and maturation. *ACS Appl. Mat. Interfaces* 9, 40070–40076. doi:10.1021/acsami.7b13257

Hall, K., Percec, S., Shinoda, W., and Klein, M. (2014). Chain-end modification: A starting point for controlling polymer crystal nucleation. *Macromolecules* 54, 1599–1610. doi:10.1021/acs.macromol.0c02398

Jiang, L., Lv, P., Ma, P., Bai, H., Dong, W., and Chen, M. (2015). Stereocomplexation kinetics of enantiomeric poly(L-lactide)/poly(D-lactide) blends seeded by nanocrystalline cellulose. *RSC Adv.* 5, 71115–71119. doi:10.1039/c5ra12586c

Li, J., Chen, Q., Zhang, Q., Fan, T., Gong, L., Ye, W., et al. (2020a). Improving mechanical properties and biocompatibilities by highly oriented long chain branching poly(lactic acid) with bionic surface structures. *ACS Appl. Mat. Interfaces* 12, 14365–14375. doi:10.1021/acsami.9b20264

Li, J., Zhang, Q., Fan, T., Gong, L., Ye, W., Fan, Z., et al. (2020b). Crystallization and biocompatibility enhancement of 3D-printed poly(L-lactide) vascular stents with long chain branching structures. *CrystEngComm* 22, 728–739. doi:10.1039/c9ce01477b

Li, W., Chen, X., Ma, Yan., and Fan, Z. (2016). The accelerating effect of the star-shaped poly(D-lactide)-block-poly(L-lactide) stereoblock copolymer on PLLA melt crystallization. *CrystEngComm* 18, 1242–1250. doi:10.1039/c5ce02124c

Liu, P., Chen, X., and Ye, H. (2017). Enhancing stereocomplexation ability of polylactide by coalescing from its inclusion complex with urea. *Polymers* 9, 592. doi:10.3390/polym9110592

Lu, H., Ma, R., Chang, R., and Tian, Y. (2021). Evaluation of starch retrogradation by infrared spectroscopy. *Food Hydrocoll.* 120, 106975. doi:10.1016/j.foodhyd.2021.106975

Monika, D., and Katiyar, V. (2017). Thermal degradation kinetics of polylactic acid/acid fabricated cellulose nanocrystal based bionanocomposites. *Int. J. Biol. Macromol.* 104, 827–836. doi:10.1016/j.ijbiomac.2017.06.039

Nikovia, C., Sougioltzoupoulou, E., Rigas, V., and Pitsikalis, M. (2019). Macromolecular brushes based on poly(L-lactide) and poly(ε-caprolactone) single and double macromonomers via ROMP. Synthesis, characterization and thermal properties. *Polymers* 11, 1606. doi:10.3390/polym11101606

Park, H., and Hong, C. (2021). Relationship between the stereocomplex crystallization behavior and mechanical properties of PLLA/PDLA blends. *Polymers* 13, 1851. doi:10.3390/polym13111851

Purnama, P., Samsuri, M., and Iswaldi, I. (2021). Properties enhancement of high molecular weight polylactide using stereocomplex polylactide as a nucleating agent. *Polymers* 13, 1725. doi:10.3390/polym13111725

Reeve, M., McCarthy, S., Downey, M., and Gross, R. A. (1994). Polylactide stereochemistry: Effect on enzymic degradability. *Macromolecules* 27, 825–831. doi:10.1021/ma00081a030

Schattmann, P., Neffe, A., Ahmad, B., Williams, G., Bele, G., Vanneaux, V., et al. (2017). RGD constructs with physical anchor groups as polymer co-electrospinnable cell adhesives. *Polym. Adv. Technol.* 28, 1312–1317. doi:10.1002/pat.3963

Shamsah, A., Cartmell, S., Richardson, S., and Bosworth, L. (2020). Tissue engineering the annulus fibrosus using 3D rings of electrospun PCL:PLLA angle-ply nanofiber sheets. *Front. Bioeng. Biotechnol.* 7, 437. doi:10.3389/fbioe.2019.00437

Song, X., Liu, X., Ma, Y., Zhu, Q., and Bi, M. (2022). Synthesis of Ce/Gd@HA/PLGA scaffolds contributing to bone repair and MRI enhancement. *Front. Bioeng. Biotechnol.* 10, 834226. doi:10.3389/fbioe.2022.834226

Takenaka, Y., Miyaji, H., Hoshino, A., Tracz, A., Jeszka, J., and Kucinska, I. (2004). Interface structure of epitaxial polyethylene crystal grown on Hopg and MoS_2 substrates. *Macromolecules* 37, 9667–9669. doi:10.1021/ma0485080

Tao, G., ZhAng, Z., Li, L., Bao, R., Liu, Z., Xie, B., et al. (2018). Tailoring crystalline morphology by high-efficiency nucleating fiber: Toward high-performance poly(L-lactide) biocomposites. *ACS Appl. Mat. Interfaces* 10, 20044–20054. doi:10.1021/acsami.8b04907

Vilay, V., Mariatti, M., Ahmad, Z., Pasomsouk, K., and Todo, M. (2011). Effect of PEO-PPO-PEO copolymer on the mechanical and thermal properties and morphological behavior of biodegradable poly (L-lactic acid) (PLLA) and poly (butylene succinate-co-L-lactate) (PBSL) blends. *Polym. Adv. Technol.* 22, 1786–1793. doi:10.1002/pat.1672

Wang, H., and Qiu, Z. (2012). Crystallization kinetics and morphology of biodegradable poly(l-lactic acid)/graphene oxide nanocomposites: Influences of graphene oxide loading and crystallization temperature. *Thermochim. Acta* 527, 40–46. doi:10.1016/j.tca.2011.10.004

Xu, Y., Martinez, R., Guthertz, N., Heath, G., Manfield, L., Breeze, A., et al. (2022). Tuning the rate of aggregation of hIAPP into amyloid using small-molecule modulators of assembly. *Nat. Commun.* 13, 1040. doi:10.1038/s41467-022-28660-7

Yang, D., Liu, W., Zhu, H., Wu, G., Chen, S., Wang, X., et al. (2018). Toward super-tough poly(l-lactide) via constructing pseudo-cross-link network in toughening phase Anchored by stereocomplex crystallites at the interface. *ACS Appl. Mat. Interfaces* 10, 26594–26603. doi:10.1021/acsami.8b06343

Yoo, J., and Won, Y. (2020). Phenomenology of the initial burst release of drugs from PLGA microparticles. *ACS Biomater. Sci. Eng.* 6, 6053–6062. doi:10.1021/acsbiomaterials.0c01228

Zhang, X., Meng, L., Li, G., Liang, N., Zhang, J., Zhu, Z., et al. (2016). Effect of nucleating agents on the crystallization behavior and heat resistance of poly(L-lactide). *J. Appl. Polym. Sci.* 42999. doi:10.1002/app.42999

Ziemba, A., Lane, K., San Segundo, I., D'Amato, A., Mason, A., Sexton, R., et al. (2018). Poly-l-lactic acid-co-poly(pentadecalactone) electrospun fibers result in greater neurite outgrowth of chick dorsal root ganglia *in vitro* compared to poly-l-lactic acid fibers. *ACS Biomater. Sci. Eng.* 4, 1491–1497. doi:10.1021/acsbiomaterials.8b00013

frontiers | Frontiers in Bioengineering and Biotechnology

TYPE Review
PUBLISHED 24 November 2022
DOI 10.3389/fbioe.2022.1042128

OPEN ACCESS

EDITED BY
Jianshe Hu,
Northeastern University, China

REVIEWED BY
Pranothi Mulinti,
Cipla USA, United States
Lifeng Shen,
Sir Run Run Shaw Hospital, China
Qiang Ao,
Sichuan University, China

*CORRESPONDENCE
A. Liang,
Aliang123123@163.com

SPECIALTY SECTION
This article was submitted to Biomaterials, a section of the journal Frontiers in Bioengineering and Biotechnology

RECEIVED 12 September 2022
ACCEPTED 14 November 2022
PUBLISHED 24 November 2022

CITATION
Liu Y, Li X and Liang A (2022), Current research progress of local drug delivery systems based on biodegradable polymers in treating chronic osteomyelitis.
Front. Bioeng. Biotechnol. 10:1042128.
doi: 10.3389/fbioe.2022.1042128

Current research progress of local drug delivery systems based on biodegradable polymers in treating chronic osteomyelitis

Yixiu Liu[1,2], Xu Li[1,2] and A. Liang[1,2]*

[1]Department of Orthopaedics, The Central Hospital Affiliated to Shenyang Medical College, Shenyang, China, [2]Shenyang Clinical Research Center for Hand and Foot, Shenyang, China

Chronic osteomyelitis is one of the most challenging diseases in orthopedic treatment. It is usually treated with intravenous antibiotics and debridement in clinical practice, which also brings systemic drug side effects and bone defects. The local drug delivery system of antibiotics has the characteristics of targeted slow release to the lesion site, replacing systemic antibiotics and reducing the toxic and side effects of drugs. It can also increase the local drug concentration, achieve sound bacteriostatic effects, and promote bone healing and formation. Currently, PMMA beads are used in treating chronic osteomyelitis at home and abroad, but the chain beads need to be removed after a second operation, inconveniences patients. Biodegradable materials have been extensively studied as optimal options for antibiotic encapsulation and delivery, bringing new hope for treating chronic osteomyelitis. This article reviews the research progress of local drug delivery systems based on biodegradable polymers, including natural and synthetic ones, in treating chronic osteomyelitis.

KEYWORDS

chronic osteomyelitis, local drug delivery systems, synthetic biodegradable polymers, natural biodegradable polymers, micro/nanoparticles

1 Introduction

Chronic osteomyelitis is a severe infectious disease in bone tissue that easily occurs in vertebrae, feet of diabetes patients, and penetrating bone injury caused by trauma or surgery. It is usually caused by aerobic or anaerobic bacteria, mycobacterium, and fungi. After entering the human body, most bacteria adhere to the surface of necrotic soft tissue and bone tissue and form a biofilm that protects bacteria, significantly enhancing bacterial resistance and making it difficult for bacteria to be removed entirely. Therefore, chronic osteomyelitis is difficult to cure and becomes a major challenge for orthopedic surgery (Lew and Waldvogel, 2004). The incidence of chronic osteomyelitis has increased significantly with improved diagnosis and an aging population (Pollard et al., 2006; Trampuz and Zimmerli, 2006). The cost of treating implant-related chronic osteomyelitis in US hospitals is estimated to reach 1.62 billion US dollars by 2020 (Kurtz et al., 2012), bringing a heavy economic burden to patients and society. In addition, infection in ulcers of the chronic diabetic foot may lead to diabetic foot osteomyelitis, increasing mortality and amputation risk (Demetriou et al., 2013;

Panagopoulos et al., 2015), which has been challenging for physicians and patients due to the limitation of recurrent and persistent infections.

The primary treatment of chronic osteomyelitis is complete debridement followed by long-term antimicrobial therapy (Walter et al., 2012; Zimmerli and Sendi, 2017). Debridement is a functional and practical approach to eradicating the infection in complicated chronic osteomyelitis (Inzana et al., 2016); it can reduce most bacteria in the infected area and optimize the soft tissues and vascular function in the surroundings. It is well known that systemic and local delivery of antibiotics could eradicate remaining bacteria. However, voids created during the deep debridement in bone tissue require bone grafts to fill, possibly causing further infection (Zhou et al., 2018a). In addition, long-term systemic administration of antibiotics is expensive and often causes systemic adverse effects such as nephrotoxicity and gastrointestinal discomfort (Huang et al., 2019). Oral or intravenous antibiotic therapy under ischemia is difficult to achieve adequate local antibiotic concentrations due to vascular damage to the infected bone; limited biofilm penetration makes managing chronic osteomyelitis more complex (Cobb et al., 2020). Therefore, antibiotic therapy focuses on utilizing topical delivery systems to achieve high concentrations of antibiotics at the infection site while avoiding side effects from systemic administration (Zhang et al., 2010), which plays an essential role in symptom relief and treating chronic osteomyelitis (Ahluwalia et al., 2021).

The application of bone cement loaded with antibiotics has been demonstrated as an efficient and commonly used strategy for treating infectious osteomyelitis due to the following advantages: 1) effective infection suppression in the early stage, 2) noticeable reduction in the incidence of recurrent infection, 3) decreasing the occurrence of pathological fracture caused by internal reinforcement, 4) suitable for bone regeneration (Dzyuba et al., 2016; Mauffrey et al., 2016; Wang et al., 2021). The most widely used bone cement material is poly(methyl methacrylate) (PMMA) beads with mixed antibiotics before surgery (Gogia et al., 2009), it offers high concentrations of antibiotics at the lesion site without causing hypersensitivity reactions (Lalidou et al., 2014) and is the gold standard of local delivery therapy for osteomyelitis (Mohanty et al., 2003). However, PMMA is non-biodegradable and requires removal *via* a second surgery (Mills et al., 2018); the stability of mixed antibiotics would be affected by the heat released during the preparation of PMMA beads (Nandi et al., 2009). Therefore, significant efforts have been devoted to developing biodegradable materials to prepare the local antibiotic delivery system for treating osteomyelitis (Nandi et al., 2009; Wassif et al., 2021).

2 Biodegradable polymers

As an essential branch of biodegradable materials, biodegradable polymers, including natural and synthetic polymers (Englert et al., 2018; Samadian et al., 2020; Guo et al., 2021; Jung et al., 2022), are of great importance in drug delivery and tissue engineering due to their excellent biocompatibility or low toxicity and biodegradation. Natural biodegradable polymers (collagen, chitosan, and silk protein), and synthetic polymers, such as poly-lactic acid (PLA), poly(lactic-co-glycolic) acid (PLGA), poly(ε-caprolactone) (PCL), and poly(trimethylene carbonate) (PTMC), offer great potential in designing delivery systems for local delivery of antimicrobial agents to the infected sites.

2.1 Natural biodegradable polymers

Natural polymers from nature are often used in biomedical applications because of their biodegradability, high biocompatibility, and low non-toxicity (Bhatia, 2016; Kaur et al., 2018; George et al., 2019). Among them, collagen, chitosan, and silk protein appear as sensible biomaterials for treating osteomyelitis (Dorati et al., 2017; Zhang et al., 2021; Zhang et al., 2022) due to their ability to promote cell adhesion and growth (O'brien, 2011).

2.1.1 Collagen

Collagen, a natural protein in the extracellular matrix of bone, has become an ideal biomaterial for scaffolding material due to its high biocompatibility (Meyer, 2019). The antibiotics-loaded collagen has been extensively investigated in treating osteomyelitis, including acute and chronic ones. No removal of the resulting systems was required compared to PMMA (Atan et al., 2018) due to the excellent biodegradation behaviors.

Promising progress has been made in using collagen as an antibiotic delivery matrix to treat osteomyelitis. The commercially available antibiotic-loaded collagen sponge products have been developed (Table 1). The collagen matrix is processed into a sponge-like shape to increase the rate of collagen degradation and the level of antibiotic release, resulting in a better therapeutic effect. Some researchers have investigated the efficacy, evidence quality, and the *in vivo* pharmacokinetics of commercially available antibiotic-loaded collagen sponges in the clinical management of chronic osteomyelitis (Van Vugt et al., 2018). The results showed inadequate evidence quality and level of the included studies and high bias risk in these studies, making it challenging to guide any clinical decision. Hence, more convincing evidence is required for applying antibiotic-loaded collagen sponges in treating chronic osteomyelitis.

In addition, more mature delivery systems include gentamicin-containing collagen implants (GCCI), which have also progressed in preventing bone infections, and clinical research results have been reported one after another. Zawadzki et al. (2017) evaluated the efficacy of the GCCI in treating 103 patients with craniofacial and osteomyelitis, 54 patients received GCCI intraoperatively, and 49 were

TABLE 1 Commercially available antibiotic-loaded collagen sponges.

Brand name	Antibiotics	Concentration (mg per 1 × 1 × 0.5 cm)	Collagen; origin
Septocoll	Gentamicin-sulfate/gentamicin-crobefate	1.2 mg gentamicin, 1.5 mg sulfate, 4.4 mg crobefate	Type I; equine
Sulmycin	Gentamicin-sulfate	1.43 mg gentamicin, 2.0 mg sulfate	Type I; equine or bovine

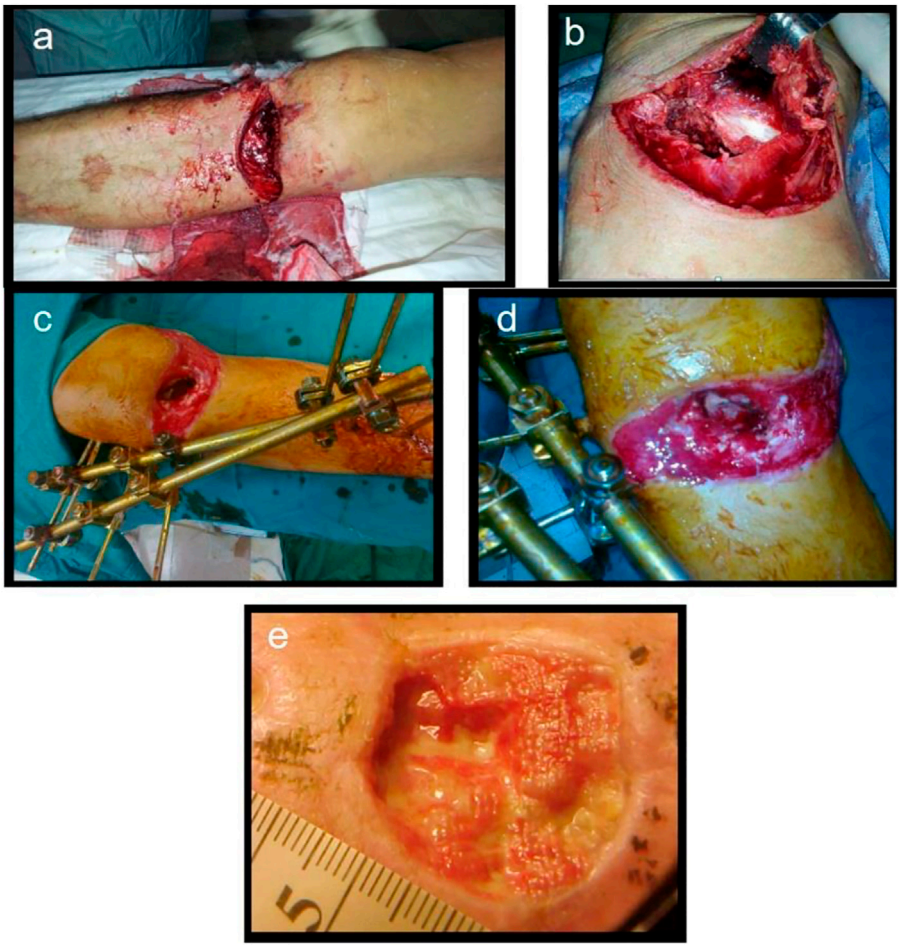

FIGURE 1
Open fracture of the proximal tibial metaphysis **(A)**, massive soft tissue injuries, periosteal stripping **(B)**, external fixator with knee spanning, bone defect visible **(C)**, Collatamp G filling the bone defect **(D)**, remaining skin defect, secondary epitelisation **(E)**. Reproduced with permission from Lupescu et al. (2016). Copyright Trans Tech Publications Ltd.

treated according to standard procedures as a control group. The study found that the course of postoperative antibiotic treatment and hospitalization was shorter, and the incidence of local complications was lower in GCCI patients, indicating a promotion for applying GCCI in treating osteomyelitis. In addition, Collatamp G, as one kind of GCCI, is a collagen-based sponge consisting of 280 mg collagen and 200 mg gentamicin, showing high treatment efficiency in post-traumatic bone infections (Deshmukh et al., 2016). Lupescu et al. (2016) described the clinical results after using Collatamp G, and the results are shown in Figure 1. The positive outcome for bone healing and infection control suggests that Collatamp G is a biomaterial that can address the abovementioned issues in treating bone infections.

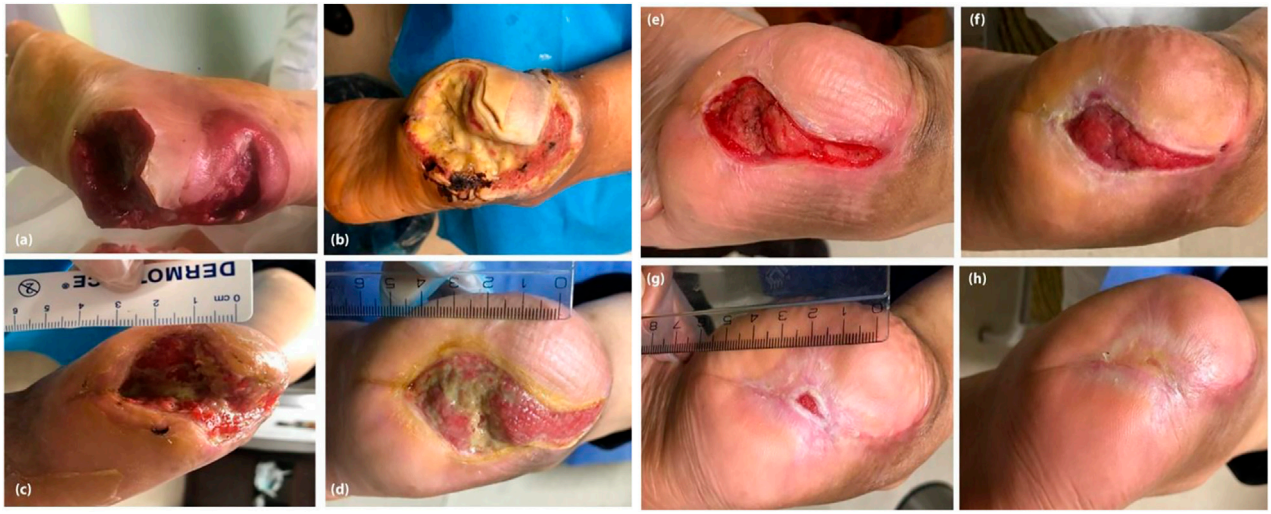

FIGURE 2
The patient before treatment **(A)**, 1 month **(B)**, 2 months **(C)**, 3 months **(D)**, 4 months **(E)**, 5 months **(F)**, 6 months **(G)**, and 7 months **(H)** after treatment. Reproduced with permission from Nilforoushzadeh et al. (2021). Copyright © 2020 The Authors.

A practical clinical case recently reported by Nilforoushzadeh et al. (2021). A type 2 diabetic patient with diabetic foot ulcer (DFU)-associated osteomyelitis were treated with a combination therapy of trichloroacetic acid, calcium alginate and foam dressings, human autologous fibroblast injection, and a fibroblast cell-seeded collagen scaffold. After treatment, the wound area was reduced by 90% (Figure 2), showing that the combination therapy positively affected DFU-induced osteomyelitis and could significantly reduce the risk of amputation in DFU patients. Although combination therapy is effective on DFU, some limitations must be solved: 1) the high cost of this combination therapy leads to difficulty in large-scale clinical promotion 2) an excellent cell bank is required on a large scale. 3) The preparation of the dressing was also tricky.

Recently, a new strategy has been developed to treat osteomyelitis by combining topical antibiotic delivery with a heparinized nano-hydroxyapatite/collagen bone substitute (Padrão et al., 2021). This work prepared particles of heparinized nano-hydroxyapatite/collagen biocomposites to load with vancomycin for treating osteomyelitis. After administration, the infection would be eradicated by the high concentrations of vancomycin provided by this system, and bone regeneration would be induced due to the regenerative scaffold role of the particles after antibiotic release. The study showed that the nano-hydroxyapatite/collagen particles could release high concentrations of vancomycin for 19 days above the MIC, which could completely inhibit the growth of MRSA and thus did not produce biofilm formation. Adjusting the sintering temperature enables the material to have a larger actual surface area with more binding sites, thus increasing vancomycin adsorption and further release. Moreover, the nano-hydroxyapatite/collagen biocomposites have good biocompatibility and no cytotoxic effect. Considering these results, the vancomycin-loaded nano-hydroxyapatite/collagen biocomposite was shown to be sufficient to resist bone infection and create a suitable environment for forming new bone in the defect area, offering a promising solution for the treatment of osteomyelitis. Sheehy et al. (2018) also explored the anti-infective effect of the collagen/hydroxyapatite antibiotic delivery system, using the commercially available antibiotic-eluting fleece Septocoll as the control group to evaluate the therapeutic effect on an animal model of chronic osteomyelitis. After 8 weeks of treatment, most of the rabbits in the blank group were still infected, while the infection rate was lower in both the antibiotic-eluting stent and the control groups. The results demonstrate that implantation of an antibiotic-loaded collagen-based material after debridement could enhance the bacterial clearance at the lesion site and improves the therapeutic effect of chronic osteomyelitis.

2.1.2 Chitosan

Chitosan (CS) is a natural polymer from chitin. In addition to its biological properties (Li et al., 2020; Wang et al., 2020; Aranaz et al., 2021), such as biodegradability, biocompatibility, tissue engineering ability, and antibacterial activity, it also possesses chemical properties. It has been widely studied as a topical drug delivery vehicle for treating osteomyelitis *in vitro* and animal models (Wells et al., 2018; Sarwar et al., 2020).

The drug delivery systems based on CS present essential potential in treating infectious injuries. (Boles et al., 2018). The

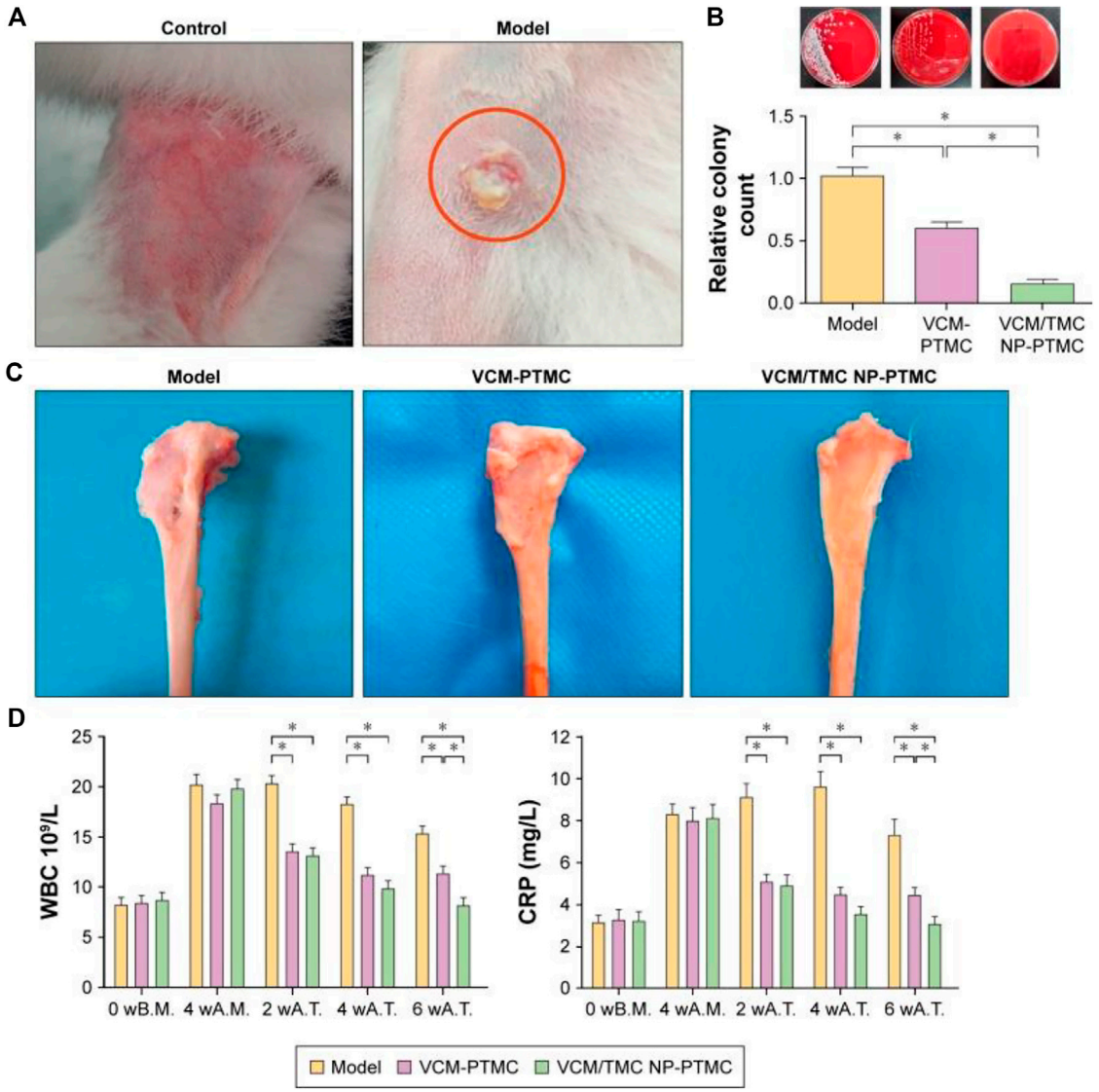

FIGURE 3
The antibacterial activity of VCM-PTMC and VCM/TMC-loaded PTMC nanoparticles. **(A)** The appearance of the rabbit legs at the fourth week after infection with *Staphylococcus aureus*. **(B)** A typical photograph of bacterial colonies forming on sheep blood agar plates and the number of bacterial colonies in the tibia marrow counted following overnight incubation. **(C)** Typical photographs of the tibia underwent 8 weeks of treatment with VCM-PTMC and VCM/TMC-loaded PTMC. **(D)** The results of WBC and CRP estimations in the rabbit serum at the time before modeling, fourth week after infection, fourth week after treatment, and eighth week after treatment. *$p < 0.05$. Reproduced with permission from Zhang et al. (2017). Copyright © 2017 The Authors.

CS-polycaprolactone blend sponge can also be prepared to treat chronic osteomyelitis as a drug delivery system. The composite sponge can simultaneously load and adjust ciprofloxacin hydrochloride and ibuprofen release behavior, presenting a dual antimicrobial and anti-inflammatory activity to enhance the treatment therapy of chronic osteomyelitis. (Wei et al., 2019). The treatment effect of calcium sulfate-based drug delivery systems for chronic osteomyelitis could be improved by CS coating, which can affect the cell affinity and antibiotic elution *via* its deacetylation degree. Therefore, CS/calcium sulfate composite can release high concentrations of antibiotics and promote osteoblast adhesion, proliferation, and bone mineralization (Beenken et al., 2014).

In addition, some studies on chitosan and its derivative-based delivery systems have made some progress in repairing bone defects and promoting bone healing. These delivery systems can potentially be used in treating osteomyelitis when supplemented with antibiotic delivery. It has been reported that CS derivatives

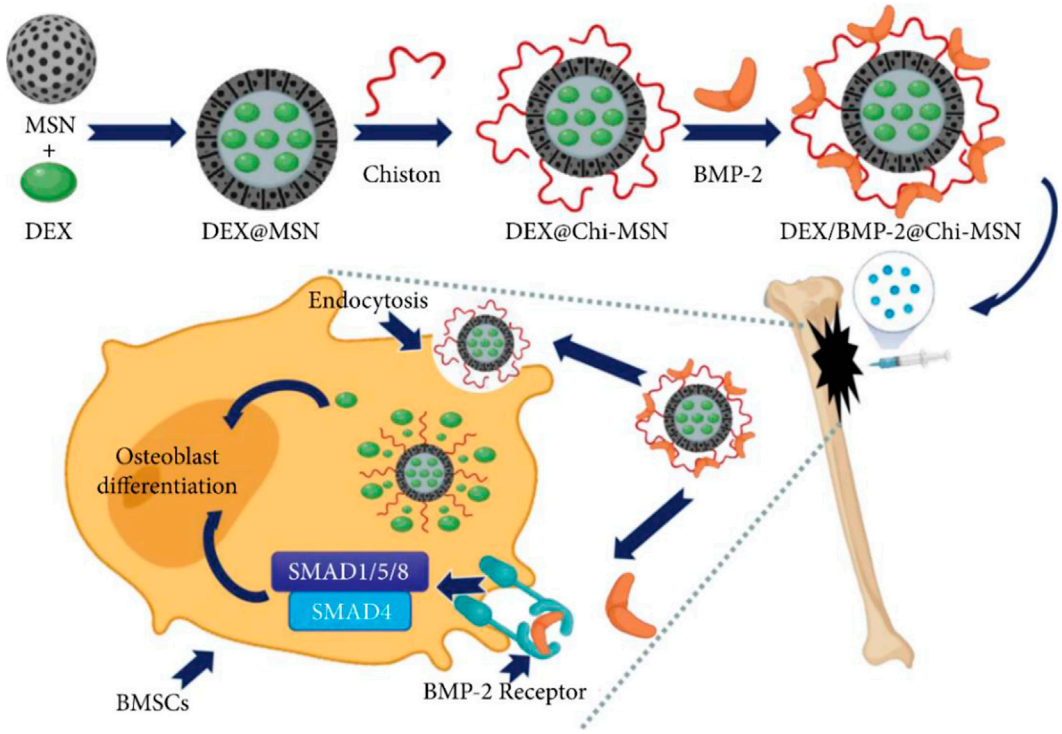

FIGURE 4
Mesoporous Silica Nanoparticle-Chitosan-Loaded BMP-2 in the Repair of Bone Defect in Chronic Osteomyelitis. Reproduced with permission from Yi et al. (2022). Copyright © 2022 The Authors.

have unique biological properties that can improve the therapeutic effect of osteomyelitis and promote bone regeneration. CS derivatives have been found to have excellent efficiency in drug delivery for osteomyelitis treatment, as reported in various studies (Tao et al., 2021). N-trimethyl chitosan (TMC) is a derivative of CS, which is water-soluble and can be used to prepare highly efficient delivery systems of antibiotics. Zhang et al. (2017) reported that vancomycin-loaded N-trimethyl chitosan nanoparticles exhibited good biodegradability, cytocompatibility, and antibacterial properties. Vancomycin (VCM) showed smooth and sustained release kinetics, and no initial burst was observed, which benefited from polytrimethylene carbonate (PTMC) in the nano-drug delivery system. The surface erosion degradation mechanism of PTMC provided a sound sustained-release barrier to achieve long-acting sustained-release of antibiotics. In this drug delivery system, the active regulatory proteins, which are primarily adsorbed on the scaffold by positive charges, can promote the adhesion and proliferation of osteoblasts (Figure 3). The above advantages are crucial for promoting bone healing and repair, making this system a promising candidate for treating chronic osteomyelitis.

The release and delivery of bone morphogenetic protein 2 (BMP-2) are critical for improving the clinical efficacy of bone healing and repair. To transfer BMP-2 to the target area, Yi et al. (2022) constructed a novel nano-delivery system (Chi-MSN) composed of mesoporous silica nanoparticles (MSN) and chitosan. The study reported that the Chi-MSN system could effectively reduce drug loss and deliver BMP-2 to the lesion site due to its stable and pH-responsive properties. In addition, Chi-MSN can better penetrate cells, thus better enhancing cell viability and reducing apoptosis. In the *in vivo* experiments, the defect in bone tissue was better repaired in the Chi-MSN group, as indicated by the increased number and thickness of trabecular bone in this group (Figure 4). Therefore, the Chi-MSN delivery system may be a promising candidate for future bone repair in chronic osteomyelitis.

The lack of effective delivery methods limits the high-concentration release of VCM in irregular bone tissue, resulting in suboptimal infection therapy. Recently, chitosan-based thermosensitive hydrogel loading VCM nanoparticles (VCM-NPs/Gel) have been designed and prepared to simultaneously prevent infection and repair fractures, showing activity against *Staphylococcus aureus* due to the sustained release of VCM for more than 26 days, promoting osteoblast proliferation. Furthermore, the release mechanism of VCM-NPs/Gel was the diffusion and degradation of the hydrogel matrix, which together maintained the stable release of VCM.

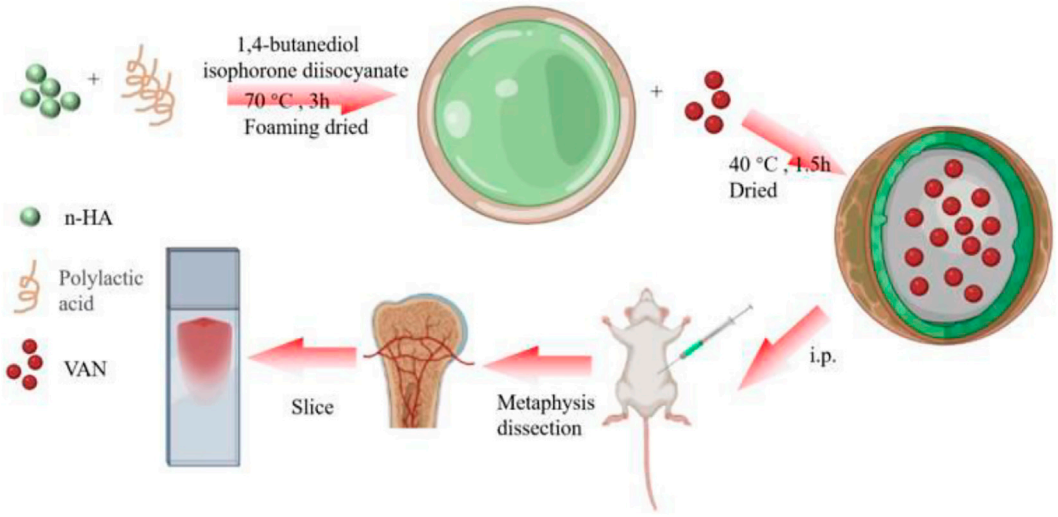

FIGURE 5
nHA-PLA-VAN system assembling and study strategy. Reproduced with permission from Lv et al. (2022). Copyright © 2022 The Authors.

The results *in vivo* showed that the investigated system had prominent anti-infective properties and accelerated bone repair and regeneration during osteomyelitis treatment, showing great potential as an effective strategy for treating osteomyelitis (Tao et al., 2020).

2.1.3 Silk protein

Like chitosan and collagen, silk protein such as that produced by silkworms and spiders also has a comprehensive source. It also has more robust mechanical properties, excellent biocompatibility, and low immunogenic response (Zapata et al., 2022). Furthermore, it can be processed into various structures, such as hydrogels, fibers, membranes, microspheres, and nanospheres (Altman et al., 2003; Koh et al., 2015; Mottaghitalab et al., 2015), making it more suitable for orthopedic applications. For example, the vancomycin-loaded silk nanospheres could effectively clear the bacteria from the infection site (Hassani Besheli et al., 2017; Mulinti et al., 2021). Silk protein incorporated with HA has also been demonstrated to be a strategy for cell proliferation and adhesion to enhance the growth of bone (Saleem et al., 2020).

2.2 Synthetic biodegradable polymers

The properties of synthetic biodegradable polymers can be precisely tailored to the needs of the application, including physical and mechanical properties, as well as biodegradability, which facilitates adjustment of the release rate of therapeutic agents such as antibiotics for better therapeutic effects. In addition, the performance of different synthetic batches of polymers is also more stable and reliable, suitable for mass production and clinical applications. Among the synthetic biodegradable polymers, polylactic acid (PLA), poly(lactic-co-glycolic acid) acid (PLGA), poly(ε-caprolactone) (PCL), and poly(trimethylene carbonate) (PTMC), and drug delivery systems constructed with them as carrier materials play an essential role in the treatment of chronic osteomyelitis.

2.2.1 Polylactic acid

Polylactic acid (PLA) has good biocompatibility, biodegradability, a wide range of mechanical and physical properties, and low immunogenicity and has been approved by the Food and Drug Administration. Therefore, PLA has been the focus of numerous preclinical and clinical trials, especially in drug delivery and bone tissue engineering (Tyler et al., 2016; Liu et al., 2020).

The acidic products generated in the degradation process of PLA can easily induce an inflammatory response. To overcome the problems caused by acidic degradation products, PLA is usually combined with hydroxyapatite (HA) to form a composite material. Lv et al. (2022) prepared a nanodevice based on nHA-PLA to deliver vancomycin (VAN) in treating chronic osteomyelitis (Figure 5). This study found that nHA-PLA showed good biocompatibility and degradability. It could effectively release VAN into the lesion and deliver it to the bone marrow tissue, thereby better inhibiting bacteria and inflammatory reactions. Meanwhile, the sound osteoconductive and osteoinductive effects of nHA-PLA-VAN help promote osteoblasts' adhesion and proliferation, thereby achieving a better repair of bone defects. In a model of chronic osteomyelitis, nHA-PLA-VAN was found to be effective in

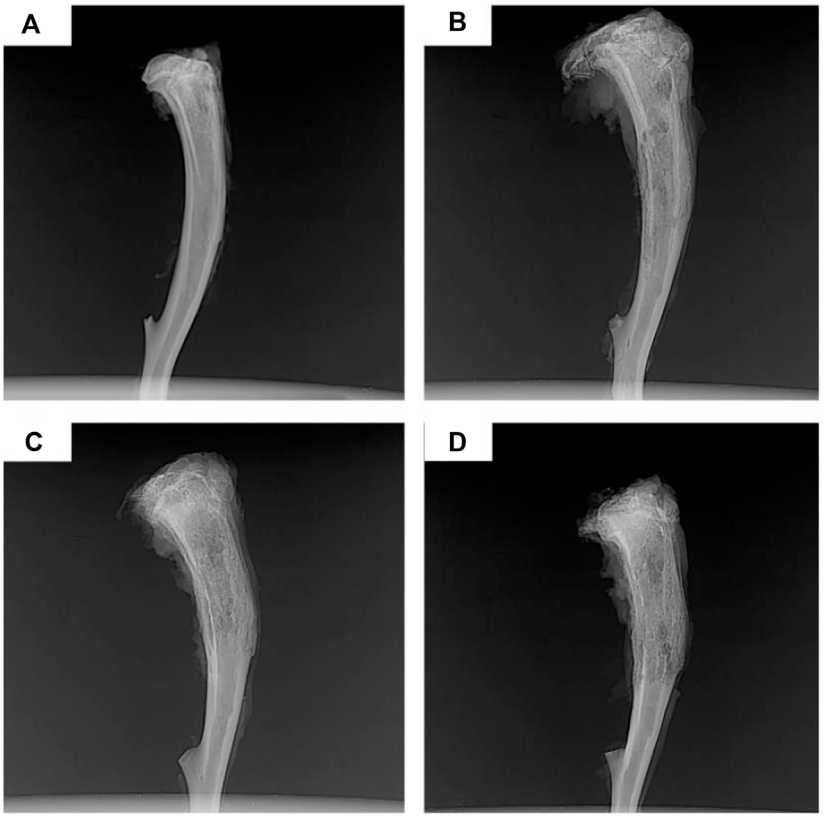

FIGURE 6
X-rays of chronic-osteomyelitis-model rats after 4 weeks of treatments: **(A)** Ciprofloxacin-PLGC system, **(B)** pure ciprofloxacin, **(C)** blank PLGC, and **(D)** no treatment. Reproduced with permission from Liu et al. (2020). Copyright © 2020 The Authors.

reducing inflammatory reactions, promoting the construction of medullary cancellous bone, and helping restore the biomechanical properties of bone. Therefore, nHA-PLA nanodevice loading vancomycin has great potential in treating chronic osteomyelitis. A similar observation was also found in the work of Zhao (Zhao et al., 2019). They developed local drug delivery beads of ofloxacin, consisting of poly(sebacic anhydride) (PSA) and poly-D, L-lactide (PDLLA), for treating chronic osteomyelitis. The delivery system with 90 wt% PDLLA produced a prominent inhibition effect against bacteria *Staphylococcus aureus*, *Escherichia coli*, and *Pseudomonas aeruginosa* within 89 days. Drug release in the local bone of rabbits showed that the mean concentration of ofloxacin was 20.1 ± 10.3 μg/g over 8 weeks, and the mean concentration in plasma was 35.6 ± 18.8 ng/ml. Radiography, bacterial culture, and histology showed an excellent therapy of osteomyelitis in rabbits, suggesting that PSA/PLA mixtures as antibiotic carriers may help treat chronic osteomyelitis and prevent bone infections (Chen et al., 2007).

Recently, PLA and PCL (PLC) copolymers have been investigated for bone repair and drug delivery (Sang et al., 2018; Mendibil et al., 2019). Biodegradable scaffolds of PLC composited with calcium phosphate (CaP) were prepared for delivery of the antibiotic moxifloxacin hydrochloride (MOX) (Radwan et al., 2021). The resulting scaffolds showed sustained release of MOX for 6 weeks and maintained cell proliferation and differentiation, thereby reducing inflammation and sequestrum formation in the bones caused by chronic osteomyelitis. The results indicate that PLC/CaP scaffolds are favorable candidates for chronic osteomyelitis therapy and suggest further clinical trials.

2.2.2 Poly-(lactic-co-glycolic acid)

Poly-(lactic-co-glycolic acid) (PLGA) is the copolymer of lactic acid (LA) and glycolic acid (GA), which is one of the most accepted materials for controlled drug delivery and bone tissue engineering (Lagreca et al., 2020; Jin et al., 2021) and has been approved by Food and Drug Administration (FDA) in the clinic because of its excellent biodegradability and biocompatibility.

Currently, treating chronic osteomyelitis presents a significant challenge to clinical orthopedics. Combining PLGA and antibiotics provides a new option for treating chronic

osteomyelitis. PLGA microspheres can improve the encapsulation rate of antibiotics, alleviate the initial burst release, reduce the cumulative release of drugs, prolong the action time of drugs (Yang et al., 2017; Li et al., 2022), and improve the antibacterial activity *in vitro* and *in vivo* (Cevher et al., 2007; Posadowska et al., 2015).

Novel inorganic-organic composites are potential materials for treating chronic osteomyelitis or infected bone defects. Mistry et al. (2022) reported the efficacy of antibiotic-loaded PLGA/biphasic calcium phosphate composite bone cement in treating experimental osteomyelitis. Compared with PMMA cement, PLGA composite cement showed superior cytocompatibility and coagulation activity, enabling faster and better sepsis control and promoting bone regeneration, indicating that PLGA cement is a promising carrier of the antibiotic-loaded delivery system for treating chronic osteomyelitis without the removal of cement. Cheng's group prepared vancomycin-loaded bioactive glass (MBG)/PLGA scaffolds for bone tissue engineering (Cheng et al., 2018). Compared with pure PLGA scaffolds, MBG/PLGA scaffolds exhibited better cytocompatibility and osteoblast differentiation properties. Vancomycin-loaded MBG/PLGA scaffolds exhibited good release properties and biocompatibility, which can sustainably release vancomycin for more than 8 weeks *in vitro*, inhibiting biofilm formation without adversely affecting cells. Gatifloxacin-loaded PLGA and β-tricalcium phosphate composite also demonstrated sufficient *in vitro* bactericidal activity and could significantly reduce inflammation within the debridement area, accompanied by osteoconduction and vascularization (Tamazawa et al., 2011; Kimishima et al., 2016). Likewise, the composites of gatifloxacin (GLFX)-loaded PLGA and hydroxyapatite (HA) (Makiishi et al., 2017) could maintain sufficient bactericidal activities from 3 h to 10 days. After 4-week implantation in bone defects of osteomyelitis, the inflammation was significantly reduced ($p < 0.05$), and the formation of new bone can be found (Makiishi et al., 2017), as compared to the debridement group. These findings show that PLGA composites could control bacterial infection and support bone regeneration for osteomyelitis treatment.

In addition to the above, to avoid the side effects caused by systemic antibiotic therapy for treating osteomyelitis, a novel sol-gel drug delivery system was developed consisting of polyethylene glycol monomethyl ether (mPEG) and PLGA, which offered several advantages, such as easy preparation, high encapsulation efficiency, zero-order release, injectable and *in situ* gelling in lesion sits. The implantation of teicoplanin-containing mPEG-PLGA hydrogel is effective in treating rabbit osteomyelitis and may have great promise as a therapeutic strategy for chronic osteomyelitis (Peng et al., 2010).

2.2.3 Poly(ε-caprolactone)

Poly(ε-caprolactone) (PCL) is a well-known biodegradable polymer with good biocompatibility. Research on PCL and its applications in drug delivery and other medical fields have recently received extensive attention.

While treating chronic osteomyelitis, insufficient antibiotics concentration at the infected lesions discounted the treatment therapy, so significant effort has been devoted to novel delivery systems to achieve sustained high concentrations without accompanying systemic side effects; for example, a rifampicin-loaded 3D-printed PCL scaffold was developed to treat osteomyelitis (Lee et al., 2020). The growth inhibitory activity against the representative pathogenic bacteria of osteomyelitis confirmed the excellent therapeutic effect. Maiti et al. (2018) developed a vancomycin-loaded PCL chip to treat MRSA-infected osteomyelitis, which can eliminate and recover bone, suggesting the efficacy of sustained release. The findings reported by Wei et al. (2018) also suggested that vancomycin-loaded PCL membranes have great potential in effectively controlling bone infection and promoting bone regeneration.

Blending can improve the properties of the parent materials and is an effective strategy to achieve desired target properties. PCL has the advantages of low toxicity, good mechanical strength, and controlled release properties. However, it lacks cellular recognition signals, while natural polymers possess cell-affinity sites, which can compensate for PCL's lack of cell-affinity. Therefore, blending natural polymers and PCL will provide a better biomaterial for treating chronic osteomyelitis. Pawar and Srivastava (2019) prepared mixed sponges of PCL and chitosan to control ciprofloxacin hydrochloride and ibuprofen to treat chronic osteomyelitis, concluding that sponges are promising candidates for chronic osteomyelitis management after surgical debridement due to the ideal release profiles and potential antibacterial and anti-inflammatory activities. The 3D-printed PCL/alginate scaffolds containing antibiotics (Lee et al., 2022) were also demonstrated as a novel osteomyelitis treatment inhibiting biofilm formation and bacterial activity.

PLGC-based delivery systems loaded with ciprofloxacin are capable of maintaining sustained release of antibiotics for up to 30 days with sufficient concentrations to sustain long-term antimicrobial activity.

The PLGC-based and ciprofloxacin-loaded delivery system maintained sustained release of antibiotics for up to 30 days with sufficient concentrations to maintain long-term antibacterial activity.

Although PLGA-based antibiotic delivery systems are promising candidates for treating chronic osteomyelitis, the higher glass-transition temperature hinders the implantation of matrix PLGA-based delivery systems into the bone marrow cavity. The introduction of PCL structure into the PLGA chain endows better flexibility to the resulting copolymer poly(d, l-lactide-co-glycolide-co-ε-caprolactone) (PLGC). PLGC-based delivery systems loaded with ciprofloxacin are capable of maintaining sustained release of antibiotics for up to 30 days with sufficient concentrations to sustain long-term antimicrobial activity (Liu and Bai, 2020). In a rat model of chronic

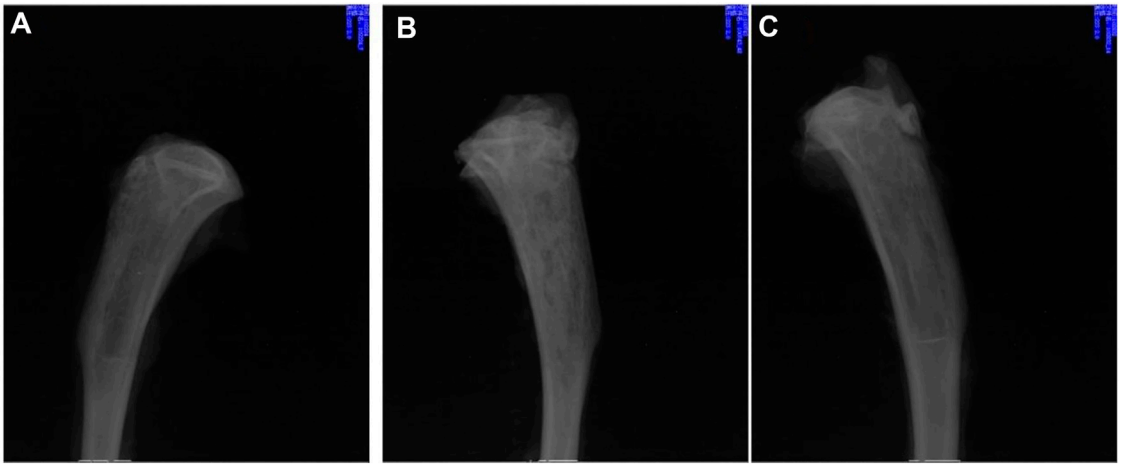

FIGURE 7
X-rays of chronic-osteomyelitis-mode. Treatment group (treated with ciprofloxacin-loaded PTMC implants) **(A)**, control group (treated with PTMC implants without ciprofloxacin) **(B)**, and blank group (no treatment) **(C)** after 28 days of treatments. Reproduced with permission from Liu et al. (2022). Copyright © 2022 The Authors.

osteomyelitis, the significant antibacterial effect of the PLGC/ciprofloxacin system was confirmed by the returned normal structure of proximal and middle tibiae (Figure 6), indicating that the PLGC-based local antibiotic delivery system is a suitable candidate for treating chronic osteomyelitis.

In a study, three-dimensional (3D)-printed antibiotic-loaded biodegradable scaffolds made of PCL/PLGA/tobramycin were reported for the first time for the treatment of chronic osteomyelitis (Shim et al., 2015), which was shown to be effective in antibacterial activity against *S. aureus* and *E. coli* and non-toxic to the proliferation of MG63 cells. The anti-inflammatory effect of PCL/PLGA/tobramycin scaffolds was further confirmed by gene expression (TNF-α, IL-6) in RAW 264.7 cells. In a rat model of chronic osteomyelitis, the tobramycin-loaded PCL/PLGA scaffold significantly reduced the infection-induced edema and inflammation. It promoted new bone formation after 8 weeks of implantation. The above findings suggest that 3D printed PCL/PLGA/tobramycin scaffolds can eradicate osteomyelitis and promote bone regeneration, showing great potential as local antibiotics delivery system in treating osteomyelitis. Moreover, the drug delivery systems are prepared from the composites of PCL with inorganics, such as calcium sulfate (Gupta et al., 2009; Yaprakci et al., 2013; Zhou et al., 2018b; Kyriacou et al., 2020) and calcium phosphate (Miyai et al., 2008; Kundu et al., 2012; Makarov et al., 2014; Kamboj et al., 2019) have modified drug release behavior that can continuously release sufficient concentrations of antibiotics and simultaneously promote bone regeneration, also demonstrating an efficient strategy in treating chronic osteomyelitis.

2.2.4 Poly(trimethylene carbonate)

The above reports have confirmed that aliphatic polyesters, such as PLA, PLGA, PCL and their copolymers, or composites formed by blending with inorganic materials have great potential as a matrix for delivery systems in the field of bone tissue repair. However, studies have shown that aliphatic polyesters produce acidic degradation products during the degradation process, which can lead to sterile inflammation, bacterial growth at bone lesions, and bone resorption or bone loss (Gunatillake et al., 2003; Böstman et al., 2005; Reich et al., 2020). Hence, further investigation of alternative materials without acidic degradation products is required. Poly(trimethylene carbonate) (PTMC) is a possible candidate material with good biocompatibility and controllable degradation rate without acidic degradation products (Yang et al., 2015; Yang et al., 2016; Hou et al., 2017; Hou et al., 2019; Wuyuntana et al., 2019; Hou et al., 2020; Cai et al., 2021; Hou et al., 2021; Hou et al., 2022), which may provide sustained high antibiotic release rates. As expected, gentamicin-loaded PTMC discs (Neut et al., 2009), ciprofloxacin-loaded PTMC implants (Liu et al., 2022), and vancomycin-loaded PTMC nanoparticles (Zhang et al., 2017) show characteristics of antibiotic-controlled release and biofilm inhibition (Figure 7). Hence, PTMC is also a promising potential carrier for local antibiotic delivery systems in treating osteomyelitis.

The synthetic polymers above include aliphatic polyesters and aliphatic polycarbonates, and their excellent biocompatibility and low toxicity have been confirmed in previous reports (Dubois et al., 1999; Suriano et al., 2011; Tempelaar et al., 2013; Mespouille et al., 2014; Ghosh et al.,

2019). And their degradation products, after being degraded *in vivo* are non-toxic and can be absorbed by the body or excreted with metabolism (Brannigan and Dove, 2017; Xu et al., 2020). However, the degradation products of polyester materials can cause a decrease in the pH of the local microenvironment and are prone to cause sterile inflammation (Srivastava et al., 2020). This problem also needs to be considered and solved in practical applications.

3 Future perspectives

In summary, the local drug delivery system based on the degradable polymer has potential clinical applications in treating osteomyelitis. Despite this, much work is still desired in the properties of the biodegradable polymeric carriers, the kinetics of antibiotic release, and the further development of current systems. For example, in terms of the composition of the carrier, composite materials have more advantages, which can make up for the deficiencies of various materials and exert their respective advantages. Since about 65% nano-HA and 35% collagen in human bone tissue, researchers tend to use inorganic-organic combinations such as adding calcium phosphate to polymers and using Ca^{2+} to promote bone defect repair; In terms of material selection, since the acidic degradation products produced by polyester are harmful to local tissue growth, the reduction of local pH may also affect the biological activity of antibiotics, and drug delivery systems based on biodegradable polycarbonate may be more suitable for the chronic osteomyelitis treatment; The shape of local drug delivery systems is often composed of microspheres and nanoparticles, which can provide larger surface area to increase the drug loading capacity. In addition to ensuring sufficient effective concentration, another research focus is to match the degradation rate of biodegradable polymers with the growth rate of bone tissue to realize bone tissue regeneration. The local antibiotic delivery system based on biodegradable polymers is a promising strategy for treating osteomyelitis. Good results have been achieved in many animal models and a small number of clinical trials.

The future development direction will combine different biomaterials to complement their advantages and disadvantages. The developed new composite material carrier should have biodegradability, good biocompatibility, and low toxicity and be able to tune the release kinetics of antibiotics by tailoring the performance parameters of the carrier materials to achieve a long-lasting and stable release process. Furthermore, the focus should be placed on studying the pharmacokinetics and pharmacodynamics of novel antibiotic delivery systems *in vivo*. Moreover, fluorescence technology for antibiotic labeling could be attempted for visualization study. The final development direction is to reduce the cost of treatment of osteomyelitis, enhance treatment efficacy, and improve patient compliance.

4 Conclusion

This review discusses the research progress of biodegradable polymer-based drug delivery systems for treating chronic osteomyelitis. In conclusion, it is imperative to design new antibiotic-loaded local delivery systems with desirable properties for treating chronic osteomyelitis early and after debridement. The biodegradability, biocompatibility, and drug release properties of the polymer-carriers are essential to ensure that the drug delivery system can provide a microenvironment and mechanical support for the regeneration of new bone tissue during healing while at the same time avoiding long-term systemic therapy. Other biodegradable polymer-based antibiotic delivery systems are still in primary or preclinical research, except for collagen-based antibiotic delivery systems. There is a long distance to achieve actual practice in the clinic. The joint efforts of the multidisciplinary integration of biomedical polymer science, orthopedics, pharmacy, and clinical medicine are urgently required to accelerate this process.

Author contributions

YL wrote this article; XL revised this article; AL checked and reviewed this article.

Funding

This work was supported by the Shenyang Science and Technology Bureau (No. 21-173-9-29).

Conflict of interest

The authors declare that the research was conducted in the absence of any commercial or financial relationships that could be construed as a potential conflict of interest.

Publisher's note

References

Ahluwalia, R., Lázaro-Martínez, J. L., Reichert, I., and Maffulli, N. (2021). Advances in pharmacotherapy for diabetic foot osteomyelitis. *Expert Opin. Pharmacother.* 22 (16), 2281–2291. doi:10.1080/14656566.2021.1954159

Altman, G. H., Diaz, F., Jakuba, C., Calabro, T., Horan, R. L., Chen, J., et al. (2003). Silk-based biomaterials. *Biomaterials* 24 (3), 401–416. doi:10.1016/s0142-9612(02)00353-8

Aranaz, I., Alcántara, A. R., Civera, M. C., Arias, C., Elorza, B., Heras Caballero, A., et al. (2021). Chitosan: An overview of its properties and applications. *Polymers* 13 (19), 3256. doi:10.3390/polym13193256

Atan, A. A., Bajuri, M. Y., Ali, A. M., Rehir, R., and Rashid, A. (2018). The effects of gentamicin-impregnated collagen sponge versus gentamicin-impregnated polymethylmethacrylate beads in patients with osteomyelitis. *Asian J. Pharm. Clin. Res.* 11 (12), 241–246. doi:10.22159/ajpcr.2018.v11i12.26910

Beenken, K. E., Smith, J. K., Skinner, R. A., Mclaren, S. G., Bellamy, W., Gruenwald, M. J., et al. (2014). Chitosan coating to enhance the therapeutic efficacy of calcium sulfate-based antibiotic therapy in the treatment of chronic osteomyelitis. *J. Biomater. Appl.* 29 (4), 514–523. doi:10.1177/0885328214535452

Bhatia, S. (2016). *Natural polymer drug delivery systems: Nanoparticles, plants, and algae*. Springer.

Boles, L. R., Awais, R., Beenken, K. E., Smeltzer, M. S., Haggard, W. O., and Jessica, A. J. (2018). Local delivery of amikacin and vancomycin from chitosan sponges prevent polymicrobial implant-associated biofilm. *Mil. Med.* 183 (1), 459–465. doi:10.1093/milmed/usx161

Böstman, O., Laitinen, O. M., Tynninen, O., Salminen, S. T., and Pihlajamäki, H. (2005). Tissue restoration after resorption of polyglycolide and poly-laevo-lactic acid screws. *J. Bone Jt. Surg. Br. volume* 87 (11), 1575–1580. doi:10.1302/0301-620x.87b11.16520

Brannigan, R. P., and Dove, A. P. (2017). Synthesis, properties and biomedical applications of hydrolytically degradable materials based on aliphatic polyesters and polycarbonates. *Biomater. Sci.* 5 (1), 9–21. doi:10.1039/c6bm00584e

Cai, G. Y., Hou, Z. P., Li, P., Sun, W., Guo, J., Yang, L. Q., et al. (2021). More precise control of the *in vitro* enzymatic degradation via ternary self-blending of high/medium/low molecular weight poly(trimethylene carbonate). *Front. Mat.* 8. doi:10.3389/fmats.2021.733535

Cevher, E., Orhan, Z., Şensoy, D., Ahiskali, R., Kan, P. L., Sağirli, O., et al. (2007). Sodium fusidate-poly (D, L-lactide-co-glycolide) microspheres: Preparation, characterisation and *in vivo* evaluation of their effectiveness in the treatment of chronic osteomyelitis. *J. Microencapsul.* 24 (6), 577–595. doi:10.1080/02652040701472584

Chen, L., Wang, H., Wang, J., Chen, M., and Shang, L. (2007). Ofloxacin-delivery system of a polyanhydride and polylactide blend used in the treatment of bone infection. *J. Biomed. Mat. Res.* 83 (2), 589–595. doi:10.1002/jbm.b.30832

Cheng, T., Qu, H., Zhang, G., and Zhang, X. (2018). Osteogenic and antibacterial properties of vancomycin-laden mesoporous bioglass/PLGA composite scaffolds for bone regeneration in infected bone defects. *Artif. Cells Nanomed. Biotechnol.* 46 (8), 1935–1947. doi:10.1080/21691401.2017.1396997

Cobb, L. H., McCabe, E. M., and Priddy, L. B. (2020). Therapeutics and delivery vehicles for local treatment of osteomyelitis. *J. Orthop. Res.* 38 (10), 2091–2103. doi:10.1002/jor.24689

Demetriou, M., Papanas, N., Panopoulou, M., Papatheodorou, K., Bounovas, A., and Maltezos, E. (2013). Tissue and swab culture in diabetic foot infections: Neuropathic versus neuroischemic ulcers. *Int. J. Low. Extrem. wounds* 12 (2), 87–93. doi:10.1177/1534734613481975

Deshmukh, S. N., Dive, A. M., Moharil, R., and Munde, P. (2016). Enigmatic insight into collagen. *J. Oral Maxillofac. Pathol.* 20 (2), 276. doi:10.4103/0973-029x.185932

Dorati, R., DeTrizio, A., Modena, T., Conti, B., Benazzo, F., Gastaldi, G., et al. (2017). Biodegradable scaffolds for bone regeneration combined with drug-delivery systems in osteomyelitis therapy. *Pharmaceuticals* 10 (4), 96. doi:10.3390/ph10040096

Dubois, P., Krishnan, M., and Narayan, R. (1999). Aliphatic polyester-grafted starch-like polysaccharides by ring-opening polymerization. *Polymer* 40 (11), 3091–3100. doi:10.1016/s0032-3861(98)00110-4

Dzyuba, G., Reznik, L., Erofeev, S., and Odarchenko, D. (2016). Efficiency of local cement reinforcing antibacterial implants in surgical treatment of long bones chronic osteomyelitis. *Khirurgiia* 5, 31–36. doi:10.17116/hirurgia2016531-36

Englert, C., Brendel, J. C., Majdanski, T. C., Yildirim, T., Schubert, S., Gottschaldt, M., et al. (2018). Pharmapolymers in the 21st century: Synthetic polymers in drug delivery applications. *Prog. Polym. Sci.* 87, 107–164. doi:10.1016/j.progpolymsci.2018.07.005

George, A., Shah, P. A., and Shrivastav, P. S. (2019). Natural biodegradable polymers based nano-formulations for drug delivery: A review. *Int. J. Pharm.* 561, 244–264. doi:10.1016/j.ijpharm.2019.03.011

Ghosh, T., Borkotoky, S. S., and Katiyar, V. (2019). Green composites based on aliphatic and aromatic polyester: Opportunities and application. *Adv. Sustain. Polym.*, 249–275.

Gogia, J. S., Meehan, J. P., Di Cesare, P. E., and Jamali, A. A. (2009). *Local antibiotic therapy in osteomyelitis, Seminars in plastic surgery*. Thieme Medical Publishers, 100–107.

Gunatillake, P. A., Adhikari, R., and Gadegaard, N. (2003). Biodegradable synthetic polymers for tissue engineering. *Eur. Cell. Mat.* 5 (1), 1–16. doi:10.22203/ecm.v005a01

Guo, L., Liang, Z., Yang, L., Du, W., Yu, T., Tang, H., et al. (2021). The role of natural polymers in bone tissue engineering. *J. Control. Release* 338, 571–582. doi:10.1016/j.jconrel.2021.08.055

Gupta, H., Anand, A., Pundir, R., Pandian, C., and Saraf, S. (2009). Fabrication of cefuroxime-impregnated calcium sulfate: Polycaprolactone composite implant for osteomyelitis. *Asian J. Pharm.* 3 (3), 227. doi:10.4103/0973-8398.56303

Hassani Besheli, N., Mottaghitalab, F., Eslami, M., Gholami, M., Kundu, S. C., Kaplan, D. L., et al. (2017). Sustainable release of vancomycin from silk fibroin nanoparticles for treating severe bone infection in rat tibia osteomyelitis model. *ACS Appl. Mat. Interfaces* 9 (6), 5128–5138. doi:10.1021/acsami.6b14912

Hou, Z., Chen, S., Hu, W., Guo, J., Li, P., Hu, J., et al. (2022). Long-term *in vivo* degradation behavior of poly (trimethylene carbonate-co-2, 2′-dimethyltrimethylene carbonate). *Eur. Polym. J.* 177, 111442. doi:10.1016/j.eurpolymj.2022.111442

Hou, Z., Chen, S., Li, Z., Chen, Z., Hu, J., Guo, J., et al. (2021). Controllable degradation of poly (trimethylene carbonate) via self-blending with different molecular weights. *Polym. Degrad. Stab.* 189, 109596. doi:10.1016/j.polymdegradstab.2021.109596

Hou, Z., Hu, J., Li, J., Zhang, W., Li, M., Guo, J., et al. (2017). The *in vitro* enzymatic degradation of cross-linked poly(trimethylene carbonate) networks. *Polym. (Basel)* 9 (11), 605. doi:10.3390/polym9110605

Hou, Z. P., Li, P., Guo, J., Wang, J. W., Hu, J. S., and Yang, L. Q. (2020). The effect of molecular weight on thermal properties and degradation behavior of copolymers based on TMC and DTC. *Polym. Degrad. Stab.* 175, 109128. doi:10.1016/j.polymdegradstab.2020.109128

Hou, Z. P., Zhang, W., Guo, J., Chen, Z. P., Hu, J. S., and Yang, L. Q. (2019). The *in vitro* enzymatic degradation of poly(trimethylene carbonate-co-2, 2 ′-dimethyltrimethylene carbonate). *Eur. Polym. J.* 112, 51–59. doi:10.1016/j.eurpolymj.2018.12.027

Huang, C.-Y., Hsieh, R. W., Yen, H.-T., Hsu, T.-C., Chen, C.-Y., Chen, Y.-C., et al. (2019). Short-versus long-course antibiotics in osteomyelitis: A systematic review and meta-analysis. *Int. J. Antimicrob. agents* 53 (3), 246–260. doi:10.1016/j.ijantimicag.2019.01.007

Inzana, J. A., Schwarz, E. M., Kates, S. L., and Awad, H. A. (2016). Biomaterials approaches to treating implant-associated osteomyelitis. *Biomaterials* 81, 58–71. doi:10.1016/j.biomaterials.2015.12.012

Jin, S., Xia, X., Huang, J., Yuan, C., Zuo, Y., Li, Y., et al. (2021). Recent advances in PLGA-based biomaterials for bone tissue regeneration. *Acta Biomater.* 127, 56–79. doi:10.1016/j.actbio.2021.03.067

Jung, K., Corrigan, N., Wong, E. H., and Boyer, C. (2022). Bioactive synthetic polymers. *Adv. Mater.* 34 (2), 2105063. doi:10.1002/adma.202105063

Kamboj, N., Rodríguez, M. A., Rahmani, R., Prashanth, K. G., and Hussainova, I. (2019). *Bioceramic scaffolds by additive manufacturing for controlled delivery of the antibiotic vancomycin*.

Kaur, M., Mehta, A., and Gupta, R. (2018). *Biomedical applications of synthetic and natural biodegradable polymers, Green and sustainable advanced materials*. Scrivener Publishing LLC, 281–310.

Kimishima, K., Matsuno, T., Makiishi, J., Tamazawa, G., Sogo, Y., Ito, A., et al. (2016). Effects of gatifloxaine content in gatifloxacine-loaded PLGA and β-tricalcium phosphate composites on efficacy in treating osteomyelitis. *Odontology* 104 (1), 105–113. doi:10.1007/s10266-014-0187-9

Koh, L.-D., Cheng, Y., Teng, C.-P., Khin, Y.-W., Loh, X.-J., Tee, S.-Y., et al. (2015). Structures, mechanical properties and applications of silk fibroin materials. *Prog. Polym. Sci.* 46, 86–110. doi:10.1016/j.progpolymsci.2015.02.001

Kundu, B., Nandi, S. K., Roy, S., Dandapat, N., Soundrapandian, C., Datta, S., et al. (2012). Systematic approach to treat chronic osteomyelitis through ceftriaxone–sulbactam impregnated porous β-tri calcium phosphate localized delivery system. *Ceram. Int.* 38 (2), 1533–1548. doi:10.1016/j.ceramint.2011.09.038

Kurtz, S. M., Lau, E., Watson, H., Schmier, J. K., and Parvizi, J. (2012). Economic burden of periprosthetic joint infection in the United States. *J. arthroplasty* 27 (8), 61–65. e1. doi:10.1016/j.arth.2012.02.022

Kyriacou, H., Kamaraj, A., and Khan, W. S. (2020). Developments in antibiotic-eluting scaffolds for the treatment of osteomyelitis. *Appl. Sci.* 10 (7), 2244. doi:10.3390/app10072244

Lagreca, E., Onesto, V., Di Natale, C., La Manna, S., Netti, P. A., and Vecchione, R. (2020). Recent advances in the formulation of PLGA microparticles for controlled drug delivery. *Prog. Biomater.* 9 (4), 153–174. doi:10.1007/s40204-020-00139-y

Lalidou, F., Kolios, G., and Drosos, G. I. (2014). Bone infections and bone graft substitutes for local antibiotic therapy. *Surg. Technol. Int.* 24, 353–362.

Lee, J.-H., Baik, J.-M., Yu, Y.-S., Kim, J. H., Ahn, C. B., Son, K. H., et al. (2020). Development of a heat labile antibiotic eluting 3D printed scaffold for the treatment of osteomyelitis. *Sci. Rep.* 10 (1), 7554–7558. doi:10.1038/s41598-020-64573-5

Lee, J.-H., Park, J.-K., Son, K.-H., and Lee, J.-W. (2022). PCL/Sodium-Alginate based 3D-printed dual drug delivery system with antibacterial activity for osteomyelitis therapy. *Gels* 8 (3), 163. doi:10.3390/gels8030163

Lew, D. P., and Waldvogel, F. A. (2004). Osteomyelitis. *Lancet* 364 (9431), 369–379. doi:10.1016/s0140-6736(04)16727-5

Li, Q., Dunn, E., Grandmaison, E., and Goosen, M. F. (2020). *Applications and properties of chitosan, Applications of chitin and chitosan*. Boca Raton, FL: CRC Press, 3–29.

Li, S., Shi, X., Xu, B., Wang, J., Li, P., Wang, X., et al. (2022). *In vitro* drug release and antibacterial activity evaluation of silk fibroin coated vancomycin hydrochloride loaded poly (lactic-co-glycolic acid)(PLGA) sustained release microspheres. *J. Biomater. Appl.* 36 (9), 1676–1688. doi:10.1177/08853282211064098

Liu, S., Qin, S., He, M., Zhou, D., Qin, Q., and Wang, H. (2020). Current applications of poly (lactic acid) composites in tissue engineering and drug delivery. *Compos. Part B Eng.* 199, 108238. doi:10.1016/j.compositesb.2020.108238

Liu, Y., and Bai, X. (2020). *In vitro* and *in vivo* evaluation of a ciprofloxacin delivery system based on poly (DLLA-co-GA-co-CL) for treatment of chronic osteomyelitis. *J. Appl. Biomaterials Funct. Mater.* 18, 228080002097572. doi:10.1177/2280800020975727

Liu, Y. X., Liang, A., Li, X., Ma, Z. H., and Zhang, D. (2022). Efficacy evaluation of ciprofloxacin-loaded poly (trimethylene carbonate) implants in the treatment of chronic osteomyelitis. *Front. Bioeng. Biotechnol.* 10, 864041. doi:10.3389/fbioe.2022.864041

Lupescu, O., Nagea, M., Patru, C., Dimitriu, A., Ciurea, N., Lupescu, D., et al. (2016). Treatment of chronic bone infections using the collagen based haemostatic-Collatamp G. *Key Eng. Mater.*, 133–138. doi:10.4028/www.scientific.net/KEM.695.133

Lv, X.-F., Zhou, D.-M., Sun, X.-H., and Zhao, Z. (2022). Nano sized hydroxyapatite-polylactic acid-vancomycin in alleviation of chronic osteomyelitis. *Drug Des. Dev. Ther.* 16, 1983–1993. doi:10.2147/DDDT.S356257

Maiti, P., Senapati, S., and Saraf, S. (2018). Inhibition of chronic osteomyelitis using sustained release of drug from biodegradable polymeric chip. *Clin. Oncol.* 3, 1406.

Makarov, C., Cohen, V., Raz-Pasteur, A., and Gotman, I. (2014). *In vitro* elution of vancomycin from biodegradable osteoconductive calcium phosphate–polycaprolactone composite beads for treatment of osteomyelitis. *Eur. J. Pharm. Sci.* 62, 49–56. doi:10.1016/j.ejps.2014.05.008

Makiishi, J., Matsuno, T., Ito, A., Sogo, Y., and Satoh, T. (2017). *in vitro*/*in vivo* evaluation of the efficacy of gatifloxacine-loaded PLGA and hydroxyapatite composite for treating osteomyelitis. *Dent. Mat. J.* 36 (6), 714–723. doi:10.4012/dmj.2016-338

Mauffrey, C., Butler, N., and Hake, M. E. (2016). Fabrication of an interlocked antibiotic/cement-coated carbon fiber nail for the treatment of long bone osteomyelitis. *J. Orthop. Trauma* 30, S23–S24. doi:10.1097/bot.0000000000000587

Mendibil, X., Ortiz, R., Sáenz de Viteri, V., Ugartemendia, J. M., Sarasua, J.-R., and Quintana, I. (2019). High throughput manufacturing of bio-resorbable micro-porous scaffolds made of poly (L-lactide-co-ε-caprolactone) by micro-extrusion for soft tissue engineering applications. *Polymers* 12 (1), 34. doi:10.3390/polym12010034

Mespouille, L., Coulembier, O., Kawalec, M., Dove, A. P., and Dubois, P. (2014). Implementation of metal-free ring-opening polymerization in the preparation of aliphatic polycarbonate materials. *Prog. Polym. Sci.* 39 (6), 1144–1164. doi:10.1016/j.progpolymsci.2014.02.003

Meyer, M. (2019). Processing of collagen based biomaterials and the resulting materials properties. *Biomed. Eng. OnLine* 18 (1), 24–74. doi:10.1186/s12938-019-0647-0

Mills, D. K., Jammalamadaka, U., Tappa, K., and Weisman, J. (2018). Studies on the cytocompatibility, mechanical and antimicrobial properties of 3D printed poly (methyl methacrylate) beads. *Bioact. Mater.* 3 (2), 157–166. doi:10.1016/j.bioactmat.2018.01.006

Mistry, S., Roy, R., Jha, A. K., Pandit, N., Das, S., Burman, S., et al. (2022). Treatment of long bone infection by a biodegradable bone cement releasing antibiotics in human. *J. Control. Release* 346, 180–192. doi:10.1016/j.jconrel.2022.04.018

Miyai, T., Ito, A., Tamazawa, G., Matsuno, T., Sogo, Y., Nakamura, C., et al. (2008). Antibiotic-loaded poly-ε-caprolactone and porous β-tricalcium phosphate composite for treating osteomyelitis. *Biomaterials* 29 (3), 350–358. doi:10.1016/j.biomaterials.2007.09.040

Mohanty, S., Kumar, M., and Murthy, N. (2003). Use of antibiotic-loaded polymethyl methacrylate beads in the management of musculoskeletal sepsis—A retrospective study. *J. Orthop. Surg. (Hong. Kong).* 11 (1), 73–79. doi:10.1177/230949900301100115

Mottaghitalab, F., Hosseinkhani, H., Shokrgozar, M. A., Mao, C., Yang, M., and Farokhi, M. (2015). Silk as a potential candidate for bone tissue engineering. *J. Control. Release* 215, 112–128. doi:10.1016/j.jconrel.2015.07.031

Mulinti, P., Shreffler, J., Hasan, R., Dea, M., and Brooks, A. E. (2021). Infection responsive smart delivery of antibiotics using recombinant spider silk nanospheres. *Pharmaceutics* 13 (9), 1358. doi:10.3390/pharmaceutics13091358

Nandi, S. K., Mukherjee, P., Roy, S., Kundu, B., De, D. K., and Basu, D. (2009). Local antibiotic delivery systems for the treatment of osteomyelitis–A review. *Mater. Sci. Eng. C* 29 (8), 2478–2485. doi:10.1016/j.msec.2009.07.014

Neut, D., Kluin, O. S., Crielaard, B. J., van der Mei, H. C., Busscher, H. J., and Grijpma, D. W. (2009). A biodegradable antibiotic delivery system based on poly-(trimethylene carbonate) for the treatment of osteomyelitis. *Acta Orthop.* 80 (5), 514–519. doi:10.3109/17453670903350040

Nilforoushzadeh, M. A., Heidari-Kharaji, M., Zare, M., Zare, S., Baiat Tork, B., and Jaffary, F. (2021). Combination therapy of trichloroacetic acid, human autologous fibroblast injection and fibroblast seeded microfibrous collagen scaffold as a novel treatment for osteomyelitis diabetic foot ulcer. *J. Diabetes Investig.* 12 (6), 1112–1117. doi:10.1111/jdi.13454

O'brien, F. J. (2011). Biomaterials & scaffolds for tissue engineering. *Mater. today* 14 (3), 88–95. doi:10.1016/s1369-7021(11)70058-x

Padrão, T., Coelho, C. C., Costa, P., Alegrete, N., Monteiro, F. J., and Sousa, S. R. (2021). Combining local antibiotic delivery with heparinized nanohydroxyapatite/collagen bone substitute: A novel strategy for osteomyelitis treatment. *Mater. Sci. Eng. C* 119, 111329. doi:10.1016/j.msec.2020.111329

Panagopoulos, P., Drosos, G., Maltezos, E., and Papanas, N. (2015). Local antibiotic delivery systems in diabetic foot osteomyelitis: Time for one step beyond. *Int. J. Low. Extrem. wounds* 14 (1), 87–91. doi:10.1177/1534734614566937

Pawar, V., and Srivastava, R. (2019). Chitosan-polycaprolactone blend sponges for management of chronic osteomyelitis: A preliminary characterization and *in vitro* evaluation. *Int. J. Pharm.* 568, 118553. doi:10.1016/j.ijpharm.2019.118553

Peng, K.-T., Chen, C.-F., Chu, I.-M., Li, Y.-M., Hsu, W.-H., Hsu, R. W.-W., et al. (2010). Treatment of osteomyelitis with teicoplanin-encapsulated biodegradable thermosensitive hydrogel nanoparticles. *Biomaterials* 31 (19), 5227–5236. doi:10.1016/j.biomaterials.2010.03.027

Pollard, T., Newman, J., Barlow, N., Price, J., and Willett, K. (2006). Deep wound infection after proximal femoral fracture: Consequences and costs. *J. Hosp. Infect.* 63 (2), 133–139. doi:10.1016/j.jhin.2006.01.015

Posadowska, U., Brzychczy-Włoch, M., and Pamuła, E. (2015). Gentamicin loaded PLGA nanoparticles as local drug delivery system for the osteomyelitis treatment. *Acta Bioeng. Biomech.* 17 (3), 41–48.

Radwan, N. H., Nasr, M., Ishak, R. A., and Awad, G. A. (2021). Moxifloxacin-loaded *in situ* synthesized Bioceramic/Poly (L-lactide-co-ε-caprolactone) composite scaffolds for treatment of osteomyelitis and orthopedic regeneration. *Int. J. Pharm.* 602, 120662. doi:10.1016/j.ijpharm.2021.120662

Reich, K. M., Viitanen, P., Apu, E. H., Tangl, S., and Ashammakhi, N. (2020). The effect of diclofenac sodium-loaded poly(lactide-co-glycolide) rods on bone formation and inflammation: A histological and histomorphometric study in the femora of rats. *Micromachines* 11 (12), 1098. doi:10.3390/mi11121098

Saleem, M., Rasheed, S., and Yougen, C. (2020). Silk fibroin/hydroxyapatite scaffold: A highly compatible material for bone regeneration. *Sci. Technol. Adv. Mater.* 21 (1), 242–266. doi:10.1080/14686996.2020.1748520

Samadian, H., Maleki, H., Allahyari, Z., and Jaymand, M. (2020). Natural polymers-based light-induced hydrogels: Promising biomaterials for biomedical applications. *Coord. Chem. Rev.* 420, 213432. doi:10.1016/j.ccr.2020.213432

Sang, Q., Li, H., Williams, G., Wu, H., and Zhu, L.-M. (2018). Core-shell poly (lactide-co-ε-caprolactone)-gelatin fiber scaffolds as pH-sensitive drug delivery systems. *J. Biomater. Appl.* 32 (8), 1105–1118. doi:10.1177/0885328217749962

Sarwar, M. S., Huang, Q., Ghaffar, A., Abid, M. A., Zafar, M. S., Khurshid, Z., et al. (2020). A smart drug delivery system based on biodegradable chitosan/poly (allylamine hydrochloride) blend films. *Pharmaceutics* 12 (2), 131. doi:10.3390/pharmaceutics12020131

Sheehy, E., von Deimling, C., Moriarty, S. K. F., and O'Brien, F. (2018). Evaluation of the capacity of an antibiotic-eluting scaffold to treat infection in a rabbit model of chronic osteomyelitis. *Orthop. proc.* 100-B (SUPP_14), 45.

Shim, J.-H., Kim, M.-J., Park, J. Y., Pati, R. G., Yun, Y.-P., Kim, S. E., et al. (2015). Three-dimensional printing of antibiotics-loaded poly-ε-caprolactone/poly (lactic-co-glycolic acid) scaffolds for treatment of chronic osteomyelitis. *Tissue Eng. Regen. Med.* 12 (5), 283–293. doi:10.1007/s13770-015-0014-6

Srivastava, A., Ahuja, R., Bhati, P., Singh, S., Chauhan, P., Vashisth, P., et al. (2020). Fabrication and characterization of PLLA/Mg composite tube as the potential bioresorbable/biodegradable stent (BRS). *Materialia* 10, 100661. doi:10.1016/j.mtla.2020.100661

Suriano, F., Coulembier, O., Hedrick, J. L., and Dubois, P. (2011). Functionalized cyclic carbonates: From synthesis and metal-free catalyzed ring-opening polymerization to applications. *Polym. Chem.* 2 (3), 528–533. doi:10.1039/c0py00211a

Tamazawa, G., Ito, A., Miyai, T., Matsuno, T., Kitahara, K., Sogo, Y., et al. (2011). Gatifloxacine-loaded PLGA and β-tricalcium phosphate composite for treating osteomyelitis. *Dent. Mat. J.* 30, 264–273. doi:10.4012/dmj.2010-098

Tao, F., Ma, S., Tao, H., Jin, L., Luo, Y., Zheng, J., et al. (2021). Chitosan-based drug delivery systems: From synthesis strategy to osteomyelitis treatment–A review. *Carbohydr. Polym.* 251, 117063. doi:10.1016/j.carbpol.2020.117063

Tao, J., Zhang, Y., Shen, A., Yang, Y., Diao, L., Wang, L., et al. (2020). Injectable chitosan-based thermosensitive hydrogel/nanoparticle-loaded system for local delivery of vancomycin in the treatment of osteomyelitis< . *Int. J. Nanomedicine* 15, 5855–5871. doi:10.2147/ijn.s247088

Tempelaar, S., Mespouille, L., Coulembier, O., Dubois, P., and Dove, A. P. (2013). Synthesis and post-polymerisation modifications of aliphatic poly (carbonate) s prepared by ring-opening polymerisation. *Chem. Soc. Rev.* 42 (3), 1312–1336. doi:10.1039/c2cs35268k

Trampuz, A., and Zimmerli, W. (2006). Diagnosis and treatment of infections associated with fracture-fixation devices. *Injury* 37 (2), S59–S66. doi:10.1016/j.injury.2006.04.010

Tyler, B., Gullotti, D., Mangraviti, A., Utsuki, T., and Brem, H. (2016). Polylactic acid (PLA) controlled delivery carriers for biomedical applications. *Adv. drug Deliv. Rev.* 107, 163–175. doi:10.1016/j.addr.2016.06.018

Van Vugt, T., Walraven, J., Geurts, J., and Arts, J. (2018). Antibiotic-loaded collagen sponges in clinical treatment of chronic osteomyelitis: A systematic review. *J. Bone Jt. Surg.* 100 (24), 2153–2161. doi:10.2106/jbjs.17.01140

Walter, G., Kemmerer, M., Kappler, C., and Hoffmann, R. (2012). Treatment algorithms for chronic osteomyelitis. *Dtsch. Arztebl. Int.* 109 (14), 257–264. doi:10.3238/arztebl.2012.0257

Wang, G., Luo, W., Zhou, Y., Zhu, Z., Zhao, Z., Liu, S., et al. (2021). Custom-made antibiotic cement-coated nail for the treatment of infected bone defect. *BioMed Res. Int.* 2021, 1–12. doi:10.1155/2021/6693906

Wang, W., Xue, C., and Mao, X. (2020). Chitosan: Structural modification, biological activity and application. *Int. J. Biol. Macromol.* 164, 4532–4546. doi:10.1016/j.ijbiomac.2020.09.042

Wassif, R. K., Elkayal, M., Shamma, R. N., and Elkheshen, S. A. (2021). Recent advances in the local antibiotics delivery systems for management of osteomyelitis. *Drug Deliv.* 28 (1), 2392–2414. doi:10.1080/10717544.2021.1998246

Wei, J., Wang, Y., Jiang, J., Yan, Y., Fan, D., Yang, X., et al. (2019). Development of an antibacterial bone graft by immobilization of levofloxacin hydrochloride-loaded mesoporous silica microspheres on a porous scaffold surface. *J. Biomed. Nanotechnol.* 15 (5), 1097–1105. doi:10.1166/jbn.2019.2743

Wei, S., Jian, C., Xu, F., Bao, T., Lan, S., Wu, G., et al. (2018). Vancomycin–impregnated electrospun polycaprolactone (PCL) membrane for the treatment of infected bone defects: An animal study. *J. Biomater. Appl.* 32 (9), 1187–1196. doi:10.1177/0885328218754462

Wells, C. M., Beenken, K. E., Smeltzer, M. S., Courtney, H. S., Jennings, J. A., and Haggard, W. O. (2018). Ciprofloxacin and rifampin dual antibiotic-loaded biopolymer chitosan sponge for bacterial inhibition. *Mil. Med.* 183 (1), 433–444. doi:10.1093/milmed/usx150

Wuyuntana, L., Lingyan, Z., Wei, Z., Yuan, X., and Liqun, Y. (2019). Factors i nfluencing the enzymatic hydrolysis performance of polytrimethylene carbonate *in vitro* and their action rules. *Tissue Eng. Res. China* 23 (06), 945–950.

Xu, Y., Zhou, F., Zhou, D., Mo, J., Hu, H., Lin, L., et al. (2020). Degradation behaviors of biodegradable aliphatic polyesters and polycarbonates. *J. Biobased Mat. Bioenergy* 14 (2), 155–168. doi:10.1166/jbmb.2020.1958

Yang, H., Hao, Y., Liu, Q., Mi, Z., Wang, Z., Zhu, L., et al. (2017). Preparation and *in vitro* study of hydrochloric norvancomycin encapsulated poly (d, l-lactide-co-glycolide, PLGA) microspheres for potential use in osteomyelitis. *Artif. cells, nanomedicine, Biotechnol.* 45 (7), 1326–1330.

Yangand Gu, Z. (2016). The *in vitro* and *in vivo* degradation of cross-linked poly(trimethylene carbonate)-based networks. *Polym. (Basel)* 8 (4), 151. doi:10.3390/polym8040151

Yang, L.Q., Li, J.X., Zhang, W., Jin, Y., Zhang, J.Z., Liu, Y., Yi, D.X., Li, M., Guo, J., and Gu, Z.W. (2015). The degradation of poly(trimethylene carbonate) implants: The role of molecular weight and enzymes. *Polymer Degradation and Stability* 122, 77–87. doi:10.1016/j.polymdegradstab.2015.10.016

Yaprakci, V., Erdemli, O., Kayabolen, A., Tezcaner, A., Bozkurt, F., and Keskin, D. (2013). *In vitro*/*in vivo* comparison of cefuroxime release from poly (ε-caprolactone)–calcium sulfate implants for osteomyelitis treatment. *Biotechnol. Appl. Biochem.* 60 (6), 603–616. doi:10.1002/bab.1118

Yi, M., Nie, Y., Zhang, C., and Shen, B. (2022). Application of mesoporous silica nanoparticle-chitosan-loaded BMP-2 in the repair of bone defect in chronic osteomyelitis. *J. Immunol. Res.* 2022, 1–11. doi:10.1155/2022/4450196

Zapata, D., Higgs, J., Wittholt, H., Chittimalli, K., Brooks, A. E., and Mulinti, P. (2022). Nanotechnology in the diagnosis and treatment of osteomyelitis. *Pharmaceutics* 14 (8), 1563. doi:10.3390/pharmaceutics14081563

Zawadzki, P. J., Perkowski, K., Kotlarski, M., Pietruczuk-Padzik, A., and Chomicz, L. (2017). Comparative study on usefulness of gentamycin-containing collagen implants in the treatment of patients with osteitis and osteomyelitis of the craniofacial skeleton. *Ann. Agric. Environ. Med.* 24 (2), 299–302. doi:10.5604/12321966.1235182

Zhang, H., Cheng, J., and Ao, Q. (2021). Preparation of alginate-based biomaterials and their applications in biomedicine. *Mar. Drugs* 19 (5), 264. doi:10.3390/md19050264

Zhang, H., Wu, X., Quan, L., and Ao, Q. (2022). Characteristics of marine biomaterials and their applications in biomedicine. *Mar. Drugs* 20 (6), 372. doi:10.3390/md20060372

Zhang, X., Jia, W., Gu, Y., Xiao, W., Liu, X., Wang, D., et al. (2010). Teicoplanin-loaded borate bioactive glass implants for treating chronic bone infection in a rabbit tibia osteomyelitis model. *Biomaterials* 31 (22), 5865–5874. doi:10.1016/j.biomaterials.2010.04.005

Zhang, Y., Liang, R.-j., Xu, J.-j., Shen, L.-f., Gao, J.-q., Wang, X.-p., et al. (2017). Efficient induction of antimicrobial activity with vancomycin nanoparticle-loaded poly (trimethylene carbonate) localized drug delivery system. *Int. J. Nanomedicine* 12, 1201–1214. doi:10.2147/ijn.s127715

Zhao, X., Han, Y., Zhu, T., Feng, N., Sun, Y., Song, Z., et al. (2019). Electrospun polylactide-Nano-hydroxyapatiteVancomycin composite scaffolds for advanced Osteomyelitis therapy. *J. Biomed. Nanotechnol.* 15 (6), 1213–1222. doi:10.1166/jbn.2019.2773

Zhou, J., Zhou, X., Wang, J., Zhou, H., and Dong, J. (2018). Treatment of osteomyelitis defects by a vancomycin-loaded gelatin/β-tricalcium phosphate composite scaffold. *bone & Jt. Res.* 7 (1), 46–57. doi:10.1302/2046-3758.71.bjr-2017-0129.r2

Zhou, Z., Yao, Q., Li, L., Zhang, X., Wei, B., Yuan, L., et al. (2018). Antimicrobial activity of 3D-printed poly (ε-caprolactone)(PCL) composite scaffolds presenting vancomycin-loaded polylactic acid-glycolic acid (PLGA) microspheres. *Med. Sci. Monit.* 24, 6934–6945. doi:10.12659/msm.911770

Zimmerli, W., and Sendi, P. (2017). Orthopaedic biofilm infections. *Apmis* 125 (4), 353–364. doi:10.1111/apm.12687

frontiers | Frontiers in Bioengineering and Biotechnology

TYPE Review
PUBLISHED 25 November 2022
DOI 10.3389/fbioe.2022.1060026

OPEN ACCESS

EDITED BY
Mingqiang Li,
Third Affiliated Hospital of Sun Yat-sen University, China

REVIEWED BY
Yuzhen Wang,
People's Liberation Army General Hospital, China
Zhiyu Li,
Shandong University, China
Qiang Ao,
Sichuan University, China

*CORRESPONDENCE
Liqun Yang,
yanglq@lnszjk.com.cn
Chenchao Wang,
wangchenchao@139.com

SPECIALTY SECTION
This article was submitted to Biomaterials, a section of the journal Frontiers in Bioengineering and Biotechnology

RECEIVED 02 October 2022
ACCEPTED 14 November 2022
PUBLISHED 25 November 2022

CITATION
Ren S, Guo S, Yang L and Wang C (2022), Effect of composite biodegradable biomaterials on wound healing in diabetes.
Front. Bioeng. Biotechnol. 10:1060026. doi: 10.3389/fbioe.2022.1060026

Effect of composite biodegradable biomaterials on wound healing in diabetes

Sihang Ren[1,2,3,4], Shuaichen Guo[3], Liqun Yang[1]* and Chenchao Wang[2]*

[1]NHC Key Laboratory of Reproductive Health and Medical Genetics (Liaoning Research Institute of Family Planning), The Affiliated Reproductive Hospital of China Medical University, Shenyang, China, [2]Department of Plastic Surgery, The First Hospital of China Medical University, Shenyang, China, [3]The First Clinical College of China Medical University China Medical University, Shenyang, China, [4]Department of Plastic Surgery, The Second Hospital of Dalian Medical University, Dalian, China

The repair of diabetic wounds has always been a job that doctors could not tackle quickly in plastic surgery. To solve this problem, it has become an important direction to use biocompatible biodegradable biomaterials as scaffolds or dressing loaded with a variety of active substances or cells, to construct a wound repair system integrating materials, cells, and growth factors. In terms of wound healing, composite biodegradable biomaterials show strong biocompatibility and the ability to promote wound healing. This review describes the multifaceted integration of biomaterials with drugs, stem cells, and active agents. In wounds, stem cells and their secreted exosomes regulate immune responses and inflammation. They promote angiogenesis, accelerate skin cell proliferation and re-epithelialization, and regulate collagen remodeling that inhibits scar hyperplasia. In the process of continuous combination with new materials, a series of materials that can be well matched with active ingredients such as cells or drugs are derived for precise delivery and controlled release of drugs. The ultimate goal of material development is clinical transformation. At present, the types of materials for clinical application are still relatively single, and the bottleneck is that the functions of emerging materials have not yet reached a stable and effective degree. The development of biomaterials that can be further translated into clinical practice will become the focus of research.

KEYWORDS

biodegradable biomaterials, diabetic wound, drug delivery systems (DDS), mesenchymal stem cells (MSCs), exosomes

1 Introduction

Diabetes (DM) is a chronic disease that is difficult to treat. It is estimated that the global number of patients will reach 592 million by 2035 (Guariguata et al., 2014). Foot ulcers affect 6.3% of diabetes patients in the world (Zhang P. et al., 2017), and the national health service of the United Kingdom spent 580 million pounds every year to treat patients with related diseases (Kerr et al., 2019). In addition, foot ulcers significantly impact patients' quality of life, leading to more pain, less vitality, and social function

limitations (Meaume et al., 2017). With the increase in the prevalence of diabetes, wounds with poor healing or nonhealing have become a serious global health problem. Hyperglycemia can impair wound healing through different mechanisms.

Hypoxia is a major cause of diabetic wound damage caused by two factors: limited oxygen supply and high oxygen consumption in the wound. Neurological sensory loss may aggravate traumatic tissue loss, while epithelium delays wound healing due to cell proliferation and resistance to growth factors (Tuhin et al., 2017). The imbalance between angiogenic factors and vascular inhibitory factors leads to the limitation of feeding sources (Gadelkarim et al., 2018). The high oxygen consumption of activated inflammatory cells makes this dilemma even more difficult. In this environment, the functions of various wound healing-related cells, such as keratinocytes, fibroblasts, and vascular endothelial cells, are inhibited (Bai et al., 2020). Studies have shown that diabetes wounds have higher activity of matrix metalloproteinases (MMPs) than healthy wounds (Louiselle et al., 2021). Therefore, collagen fibers are destroyed faster than their secretion, delaying the formation of sufficient granulation tissue (Pan et al., 2022). The lack of nutrition in the wound is more serious, and the main culprit is bacterial colonization (Amirrah et al., 2020).

The standard treatment of diabetes wounds includes wound cleaning, revascularization, infection control, blood sugar control, foot care, and limb lifting. However, these treatments are often insufficient to ensure good wound healing, and even after standardized treatment, patients still face the possibility of amputation (Shettigar and Murali, 2020). Unfortunately, the simple application of biomaterials is still difficult to achieve absolute benefits for wound healing and even produce slight adverse effects due to the characteristic of their degradation products. The idea of wound healing with biomaterials as the core and additional active ingredients is advanced and desirable. Therefore, the idea of using mesenchymal stem cells, various drugs, and active factors combined with biodegradable biopolymer materials to treat refractory wounds came into being. Through a comprehensive literature search of published and ongoing studies, we aim to provide an overview of the experimental basis, scientific background, and possible clinical applications, to clarify the therapeutic role of composite degradable biomaterials combined with multiple preparation methods in diabetic wound healing.

2 Clinical strategies for diabetes wound treatment

In the healing treatment of diabetes wound, the core problem is that the time axis of wound repair is disturbed, which makes the wound healing process fall into the inflammatory stage, and the vascularization is damaged, hypoxia, immune cell dysfunction, and then induce the inactive tissue to provide a suitable environment for bacterial growth and biofilm formation. And then aggravate the inflammatory reaction, and inhibit ECM deposition and tissue repair. And ultimately lead to wound nonhealing, amputation, and even life-threatening (Saghazadeh et al., 2018). The treatment of diabetes wound needs to consider many factors. In general, it can be broadly divided into systemic treatment and local treatment. In addition to actively treating the primary disease, the systemic treatment also needs to adjust the nutritional structure and improve the nutritional status; The local treatment gives priority to the repair of local wounds, and the etiological treatment can be carried out from the four stages of wound repair. In clinical practice, the early treatment and the optimization of local dressings are emphasized to effectively treat the infection, biofilm formation, and excessive keratinized inactive tissues of the wound (Figure 1).

2.1 Surgical management: Debridement

The main management guidelines of European, Canadian and American organizations and the International Working Group on diabetes foot regard CSWD of DFU as the standard treatment method. Using sharp treatment tools such as scalpel, forceps, and spatula to remove the inactive tissue and aging and nonfunctional cells of the wound surface (Rayman et al., 2020; Schaper et al., 2020), it is not clear how much this can improve the bacterial load, but it is meaningful in removing biofilm (Wolcott et al., 2010) and controlling infection. In addition, hyperkeratosis is a special feature of diabetes-related foot ulcers, which is associated with sensory loss and chronic repetitive trauma and can also be treated by sharp debridement. Removal of hyperkeratosis is associated with a decrease in plantar pressure, which may contribute to healing (Nube et al., 2021). Patients with non-ischemic diabetes-related foot ulcers are provided with CSWD once a week, which is the main way to remove inactive tissues to promote healing. Another clinical study focuses on the treatment of diabetic foot wounds and forms a series of diagnosis and treatment processes. Doctors will meet patients at the wound care center or bedside. According to the patient's wound condition, wound screening, debridement, wound care advice, and education will be provided gradually. Through the establishment of this effective path, the amputation rate of diabetes feet was greatly reduced. The study emphasized the necessity of early, long-term and standardized debridement (Hsu et al., 2015).

2.2 Intensive care: Speed dating model

It is composed of Surgeons (mainly vascular surgeons and podiatrists) and supported by endocrinologists, diabetes

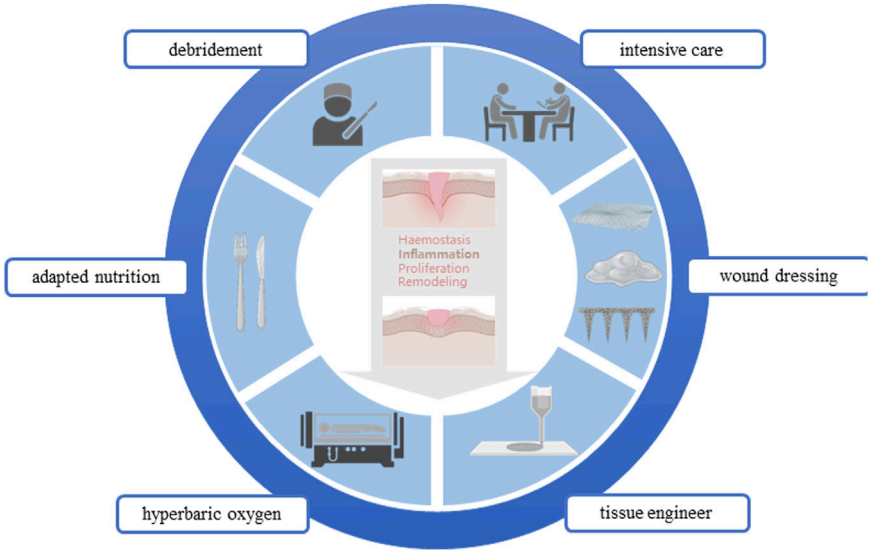

FIGURE 1
Clinical strategies for diabetic wounds.

educators, nutritionists, infectious disease doctors, nurses, and clinical psychologists to form a rapid access rapid discipline team. It adopts a double-blind approach to conduct an overall assessment of the patient's mental health, compliance programs, diet, and blood glucose monitoring. This method may reduce the incidence of leg amputation (Everett and Mathioudakis, 2018).

2.3 Adapted nutrition

The guidelines of the International Working Group on diabetes feet (IWGDF) in 2019 pointed out that "do not use interventions aimed at correcting the nutritional status of patients with diabetes feet (including supplementation of protein, vitamins and trace elements, and use of drugs to promote angiogenesis to treat diabetic foot ulcers. The aim is to improve healing rather than the best standard of care" (Basiri et al., 2020). Vitamins and minerals play an important role in wound healing, and if people lack these factors, their wound healing will be affected (Moore et al., 2020; Bechara et al., 2021). Vitamin C supplementation at the usual supplementation dose (up to 1,000 mg per day) is also considered safe because it is water-soluble and excess intake will be excreted from the urine (Bechara et al., 2021). Vitamin C supplementation is beneficial for patients with foot ulcers (Afzali et al., 2019). Vitamin D (Halschou-Jensen et al., 2021) and complex vitamin B may also be effective for the healing of foot ulcers. Both methods are relatively safe but should be performed under dietary and/or medical supervision. In addition, zinc, magnesium, omega-3, vitamin D, and probiotics have obvious benefits in wound recovery. Genistein supplementation will be a potential therapeutic nutrient that can prevent and treat delayed wound healing by regulating inflammation and oxidative stress during the inflammatory phase (Eo et al., 2016). In the treatment of complications of diabetes, oleopicroside can reverse apoptosis, regenerate tissue, restore histological tissue and reduce oxidative stress (Zheng et al., 2021). Arginine, glutamine, and β- Hydroxyl-β- Methyl butyrate may improve the healing of patients with diabetic foot ulcers (Armstrong et al., 2014). Supplementation of adult diabetes mice with standardized fermented papaya preparation (FPP) can improve skin wound healing results (Dickerson et al., 2012). These preparations may also be able to achieve rapid healing of diabetes wounds by combining with effective drug delivery systems (DDS).

2.4 Sterile confinement: Wound dressing

A case report of nonhealing of the wound of a patient with type 2 diabetes 7 months after cardiac surgery was carried out in Italy. In the report, the patient used the NPWT method to treat the wound for a long time after infection with MSSA, but the effect was poor. After diagnosis and treatment by the wound care team, a dressing combined with bacteria and true bacteria was selected as the healing trigger, because this dressing can interrupt the circulation of chronic or long-term inflammation. The sternal wound improved after the appropriate dressing regimen was applied. The improvement observed with sorbet was not detected in the first 7 months of NPWT (Caruso et al., 2018). Researchers

believe that this wound-healing environment can greatly improve the prognosis (Castiello et al., 2019). However, at present, there are still few functional dressings applied to the human body, and the clinical transformation is difficult. In this regard, biomaterials become important players. Section 4 of this article focuses on the role of antibacterial biomaterials in wound healing.

2.5 Hyperbaric oxygen therapy

Systemic hyperbaric oxygen therapy (HBOT) has been proposed as a drug treatment for diabeti foot ulcers (Doctor et al., 1992). HBOT has been shown to have antibacterial effects and increase oxygenation of hypoxic wound tissues (Löndahl et al., 2010). This enhances the killing ability of neutrophils, stimulates angiogenesis, and enhances the activity of fibroblasts and collagen synthesis. In addition, hyperbaric oxygen enhances wound healing in diabetes by promoting fibroblast proliferation and endothelial cell angiogenesis (Huang et al., 2020). In the past 20 years, many clinical trials have proved that HBOT can promote the healing of diabetes wounds (Mutluoglu, 2018). HBOT is to treat patients with 100% oxygen above atmospheric pressure. This is provided either in a unit (single-person) chamber that is normally compressed with oxygen or in a multi-position chamber (multi-person) that is compressed with air, where oxygen is delivered by a mask or mask. Bring the effect of improving leukocyte function, improving ischemia-reperfusion injury, and neovascularization due to the increase of local growth factors and the release of autologous progenitor cells (Thom, 2011). However, hyperbaric oxygen also has its unavoidable harm. Including various forms of barotrauma, central nervous system (CNS), and pulmonary oxygen toxicity, as well as ocular side effects, and claustrophobia (Thom, 2011; Heyboer et al., 2017). In response, researchers have introduced dressings rich in oxygen or other effective gases to inhibit the growth of anaerobic bacteria or provide more positive effects on the tissue. This effective effect does not need to be mobilized and may be achieved only by topical dressings or stents.

2.6 Skin tissue engineering

It may be difficult to achieve the healing of the wound by simply supplementary treatment. The development of tissue engineering, bioengineered skin substitutes, and genetic growth factors have made great progress in the treatment of chronic skin ulcers in recent years (Morimoto et al., 2015). At present, there are few reports of skin tissue engineering materials applied in the clinic, but it must be said that this will be the inevitable trend in wound repair (Gholian et al., 2022). Bioengineered skin substitutes for DW include amniotic membrane, autologous stem cell therapy, fibroblast-derived dermis, and porcine small intestinal submucosa (PSIs). The biological activity of PSIs includes GF, such as TGF-β, vascular endothelial growth factor (VEGF), and FGF, which limit the destructive movement of MMPs and promote angiogenesis to help neovascular development (Tallapaneni et al., 2021).

Some studies used bioengineered skin for control experiments, including 880 subjects. Bioengineered skin (BS) has significant advantages in effectiveness and safety, and the risk of infection is significantly reduced (Teng et al., 2010). Another study used degradable gelatin dressings (applied as DDS of bFGF in clinical trials) to load PrP to treat diabetic wounds. A total of 30 patients were included in the study. This combination therapy may be an alternative to bioengineered skin substitutes containing live cells and lead to substantial progress in chronic skin wound management (Morimoto et al., 2015). Collagen dressings can serve as skin substitutes for natural extracellular matrix (ECM) to guide the complex cellular interactions necessary to promote the migration of keratinocytes and fibroblasts (Amirrah et al., 2020). The engineered skin grafts with matrix blood vessel cells encapsulated by fibrin collagen hydrogel also have good effects on the wounds of patients with diabetes. It is hoped that the grafts can be truly applied to the clinic through multi-center clinical trials. Among them, scaffolds composed of a combination of type I collagen and fibrin can improve mechanical properties and enhance the ability of SVF microvascular formation (Nilforoushzadeh et al., 2020). Next, the treatment method incorporating stem cells has also become a new research hotspot. Placenta-derived mesenchymal stem cells were isolated from human donor placentas and cultured in electrospun gelatin nanofiber scaffolds (GNs). The results showed that the implantation of HPD-MSCs in GNS could accelerate wound healing of DFU patients (Meamar et al., 2021). The gradual promotion of clinical practice can better promote the development of basic research, and clinical application is also the ultimate goal. Therefore, it is necessary to provide more directions for clinical trials through multi-faceted biocompatibility verification. The following summary will focus on the application of biodegradable materials in diabetes wounds through the addition of various factors based on biodegradable materials.

It is worth noting that, during the wound healing process, the dressing protects the injury and contributes to the recovery of dermal and epidermal tissues. As per the sophisticated definition of tissue engineering described at a National Science Foundation workshop, scaffolds are the best materials for restoring, maintaining, and improving tissue function (Chaudhari et al., 2016). In other words, dressings are more likely to provide a conducive environment for healing, while scaffolds are more likely to serve as a connection and storage of active ingredients.

3 Biodegradable biomaterials

The targeted delivery of drugs has been a focus topic in recent years. During systemic administration, the ineffective vasculature tissue of the wound can effectively deliver drugs, and the half-life of the drug itself and the unpredictable wound environment make it difficult for the drug to act accurately (Wang et al., 2019). Therefore, for the treatment of diabetes wounds, it seems to be more inclined to local action. Although there is still great controversy about carrying antibacterial drugs for local action, although it can reduce the dosage, it is difficult to ignore the impact on the local microenvironment (Bhise et al., 2011).

As an ideal dressing, it should have the following characteristics (Vuerstaek et al., 2006; Chong et al., 2007; Boateng et al., 2008; Das and Baker, 2016) for diabetes wound:

- Liquid balance: it can not only absorb excessive wound exudation but also maintain the moist environment of the wound;
- Avoid further wound damage;
- Prevention and control of bacteria present or colonization;
- Eliminate dead space;
- Debridement of necrotic tissue;
- Does not affect the activity of surrounding tissues;
- Do not cause an allergic reaction or shed substances that can cause foreign body reaction;
- Convenient replacement, no pain, low price;
- Transparent, easy to observe and monitor the wound condition;
- The tensile strength is in the range of 0.7–18 mPa (Samadian et al., 2020);
- It can contain endogenous cells or active factors and promote cell proliferation, differentiation, and migration, to promote wound healing (Chereddy et al., 2016).

Combined with the above theoretical support, researchers are committed to developing biomaterials closer to ideal dressings for wound repair in diabetes patients. The development of different materials also provides us with more alternative directions.

3.1 Classification and characteristics of degradable biomaterials

Biodegradable biomaterials can be mainly divided into two categories: natural polymers and synthetic polymers. Natural polymers are easy to obtain and have strong biocompatibility, but their physical and chemical properties are not controlled and their types are limited (Zhang et al., 2021; Zhang et al., 2022). However, synthetic polymers, due to their high controllability, effectively make up for this defect of natural materials. We summarized the table for specific material classification and characteristics of each material (Table 1). However, no matter what kind of material, its characteristics are mostly reflected in its good basis as a wound dressing, such as degradability, biocompatibility, and mechanical properties. However, the disadvantages of various basic materials used for wound healing are also obvious. For example, synthetic polymers lack the ability of cell recognition, so it is less likely to be used alone (Vogt et al., 2021). Therefore, to vantage the advantages and avoid the disadvantages of materials, researchers hope to mix materials using materials to achieve the optimization of materials.

First of all, composite materials themselves can guide wound healing. Various cells and active factors involved in the process of wound healing are affected by physical signals, mechanical signals, chemical signals, inorganic signals, and other ways of the materials themselves, thus changing the behavior of cells (Castaño et al., 2018). In other words, materials mainly interfere with the internal factors of the wound itself.

After that, the ability of the material itself entered a “threshold” state, and the effect of material processing and changes on wound healing was not significantly improved. Combined with the basic principle of wound healing, researchers focused on external factors that may be involved in wound healing. For example, by improving the properties of the materials or the proportions of various components of the composite materials, we can find the drug delivery system (DDS) most suitable for carrying exogenous drugs, or by innovating the processing technology of the materials, we can improve the internal structure of the materials, to achieve greater cell adhesion.

However, the exertion of the characteristics of the materials themselves is still the most serious issue. Through the literature summary, we summarized and sorted out the second table, which sorted out the combination methods, main functions, and mechanisms of composite materials after combination (Table 2). The combination of natural materials and synthetic materials needs to consider the synthesis efficiency of natural materials and the maintenance of physical and chemical properties after synthesis. Although the mixing of multiple synthetic materials is controllable, most of the required manufacturing processes are complex, and it is difficult to ensure that the biological compatibility after synthesis can still maintain the efficacy of a single polymer.

3.2 Development and changes of degradable biomaterials

Biodegradable biomaterials have gradually changed from the initial covering to the cell culture matrix with bionic function. Biomaterials can not only become scaffolds or dressings for

TABLE 1 Classification and characteristics of biomaterials.

Source	Classification	Ingredient	Preparation procedure	Advantages	Disadvantages	References
Natural polymers	protein-based	collagen	Hydrogel, nanofiber scaffold, sponge, etc	Easy to get, excellent biocompatibility	Suitable for wounds with less exudation; Contraindicated for patients with third-degree burns and allergic patients	Tang et al. (2018)
		silk fibroin	3D scaffolds, nanofibers, films, etc	biocompatibility, biodegradability, flexibility, adherence, absorption of exudates, minimal inflammatory reaction	Degradation is slow and may cause sensitization	Kundu et al. (2013)
		gelatin	films, sponge	excellent biocompatibility	Do not apply to the wound with more exudation	Xiao et al. (2021)
	polysaccharides	agarose	films	Water expansion capacity (4–5 times) and tensile strength (30–50 MPa)	Poor biomechanical properties	Taghipour et al. (2020)
		alginate	Film, sponge, hydrogel, etc	Stop the bleeding. Water absorption; Antibacterial; Can be combined with laser therapy	It is porous and non-adhesive. It needs to be protected and secured with secondary dressing	Taghipour et al. (2020)
		hyaluronic acid	Hydrogels, scaffolds, etc	No scar healing, good angiogenesis effect, nerve repair effect, can be modified to simulate the effect of ECM	Poor adhesion, poor stability *in vivo*	Kim et al. (2021)
		chitosan	Bandages, ointments, films, sponges, hydrogels, etc	Hemostatic, antibacterial, simple method of blending with other effective substances	Contraindicated with strong oxidants	Muxika et al. (2017)
Syntheitc polymers	polyesters	PLA	Scaffolds, nanoparticles, etc	Strong mechanical properties, strong absorbability, good air permeability	Acidic products may cause local foreign body reactions	Hajikhani et al. (2021)
		PGA	Thin films, nanofiber scaffolds	Hydrophilic, biocompatible, biodegradable and non-toxic	It has no tissue adhesion ability or wound healing effect, and is often used in combination with fibrin glue	Zha et al. (2022), Kouketsu et al. (2021)
		PLGA	Nanofibers, membranes, microspheres, hydrogels, nanoparticles	Easy degradation, possibility of adjusting surface and physicochemical properties, continuous drug release	Low drug loading and high material strength may induce local irritant reaction	Chereddy et al. (2016)
		PHB	Nanofibers, nanoparticles, scaffolds	Good mechanical properties, can be degraded in the ideal time range, insoluble in water	Poor antibacterial effect	Sanhueza et al. (2021), Avossa et al. (2021)
		PCL	Nanofibers, nanoparticles, scaffolds	Poly (ε-caprolactone) (PCL) is biocompatible and biodegradable polymer which can be electrospun easily at low voltages and is able to provide required scaffold mechanical resistance in aqueous environments.The cell affinity, stability and strength of nanofibers were improved	Higher processing conditions; It is not effective on its own	Croisier et al. (2014)
	Polyanhydrides	poly (sebacic acid)	Hydrogels, scaffolds, etc	Stable batch to batch consistency; Easy to customize	Lack of cell recognition; Difficult to apply independently	Vogt et al. (2021)
		polyamino acids	Nanofibers, hydrogels, etc	Strong biocompatibility, bacteriostatic, hemostasis, drug delivery, good film forming effect	The preparation process is demanding and the synthesis is difficult	Shen et al. (2021), Ji et al. (2022)
	phosphorous based polymers	polyphosphates	Hydrogel, hydrocolloid, etc	Hemostasis, providing energy for cell proliferation, and effectively enriched in the wound site	The preparation process is demanding and the synthesis is difficult	Al-Musawi et al. (2020)
	Others	polyurethane	Foam, hydrogel, film, etc	It has adjustable hard and soft chain segments and modifiable chain extenders	The biocompatibility is relatively poor	Lutzke et al. (2016)

TABLE 2 Composite material combination and wound healing mechanism.

Complex method	Ingredient	Function	Mechanism	References
Natural-Natural	Col-CS	hemostasis	The binding affinity of CS was increased	Tripathi et al. (2021)
	Col-SF	Moisturizing; The biodegradability is controllable; The synergistic effect on cell viability was improved	inflammation stage: ↑IL-6, IL-1β, TGF-β1, TGF-βR2↑; MSC + Col + SF→Blood vessels mature↑, Cell adhesion (>60%)	Naomi et al. (2020)
	CS-Col-alginate (CCA)	Good water absorption; Good mechanical properties; Good cell compatibility; The seawater intrusion can be prevented for 4 h	EGF, bFGF, TGF-β and CD31↑	Xie et al. (2018)
	Col-CS + IGF1	The 3D structure has a large number of pores, which is conducive to cell adhesion, proliferation, and liquid exchange	Erk1/2 mediates IGF-1-induced proliferation and migration of BMSC	Xia Y. et al. (2020)
	Gel-cellulose-bFGF	Improved biocompatibility (Gel and bFGF were fixed by hydrogen bond) Oxygen was permeated and water vapor was controlled to evaporate and absorb wound exudate	Composite material specific ↓ Mir-29b-3p level, targeting Akt/GSK-3β/β-catenin pathway to regulate the biological function of endothelial cells	Yu et al. (2020)
	CS-alginate-Velvet antler blood peptide	Heat sensitivity, antioxidant properties, antibacterial properties, safety, sustained drug release, and the dressing locks water and provides oxygen to the wound	PI3K/Akt/mTOR pathway SIRT1/NF-kB pathway	Hao et al. (2022)
Natural-Synthetic	PCL-Col-ZnO-VEGF fibrous	Antibacterial, angiogenesis, cell proliferation	TGF-β, CD31 ↑	Li P. et al. (2021)
	PHB-Gel-OSA-Col	OSA: osthole amine - for antibacterial Composite material is stable to enzymatic degradation	promote the regeneration of dermal papilla layer and hair follicle	Kandhasamy et al. (2017)
	nCur-PVA-Col	Cytotoxicity ↓; Fibroblast adhesion and proliferation ↑	During the stages of skin repair and remodeling, Tgf-β ↑, collagen maturates	Leng et al. (2020)
	PVA/Alginate hydrogel	Moisturizing, anti oxidation and slow release	regulation PI3K/Akt pathway	Chen G. et al. (2020)
	PCL-HA Nanofiber scaffold	Significantly enhanced cell infiltration	It is affected by the changes of cell adhesion receptor-integrin β1 and the formation and distribution of neotins Tgf-β/MMP-2 pathway for cell motility	Qian et al. (2015)
	VMT-PCL	Promoting angiogenesis	HIF-1α pathway VEGF,SDF-1α,eNOs↑ Col III, FN, bFGF↑(PCL/5%VMT) M2↑	Huang et al. (2022)
	PCL-CA-CSThree-layer nanoscaffolds	Mimics the extracellular matrix	PCL/CA→YAP→Notch pathway Proteomics of differential expression of ribosome-related proteins and metabolic pathway-related proteins	Lin et al. (2021)
	PCL-Gel Nanofiber scaffold	Promote the adhesion, proliferation and migration of human keratinocytes (HaCaTs) and HUVECs; Promote angiogenesis, collagen deposition, re-epithelialization	Activating epithelial-mesenchymal transition (EMT) and endothelial-mesenchymal transition (EndMT)	Lv et al. (2017)
	SF-PCL	The ability to regulate macrophage polarization	The ability of noncovalent binding to IL-4 to regulate macrophage polarization The effect of promoting macrophage polarization in the early stage can significantly inhibit the degree of late foreign body reaction MARK, PI3K, JKN and Nf-Kb pathways regulate macrophage polarization	Qian et al. (2018)
Synthetic-Synthetic	HAP-ZrO2-GO-PLA	Rough surface: cell adhesion ↑	Go surface coordination keeps oxygen-containing groups that interact with the surrounding environment highly active	Al-Wafi et al. (2021)
	PHBV-HMK nanofibers	HMK has strong biocompatibility PHBV has strong mechanical strength and antibacterial property	HMK promoted cell proliferation	Ye et al. (2020)

wound healing but also create a favorable environment for cell growth. This change has promoted the progress of materials science.

3.2.1 Temporary wound cover

The original intention of designing the wound dressing was simply to cover the wound with a shielding "cloth" instinctively for protection of the wound Gauze can absorb exudation, keep the environment moist, and can be made into sterilized products by simple methods, but its shielding ability is poor, and dressing change is often accompanied by pain or secondary damage (Jones, 2006). Given this situation, a transparent elastic dressing made of polyurethane was derived to shield bacteria and allow gas exchange, but it cannot be absorbed when too many exudates. Foam dressings seem to perfectly solve this problem, but excessive water absorption is difficult to achieve drug delivery (Vermeulen et al., 2005). As a cross-linked three-dimensional network structure, the hydrogel has variable morphology and adjustable swelling. However, its permeability to gas limits its use on infectious wounds. Therefore, it is unwise to use hydrogel dressing alone for diabetes wounds (Annabi et al., 2014). The hydrogel made of alginate has both antibacterial and water absorption. Hydrogel dressings made of gelatin, pectin, or hydroxymethyl cellulose seem to have a similar effect. The dressings at this stage are mostly used to supplement or provide temporary solutions after problems occur according to clinical needs.

3.2.2 Regenerated scaffold or environment

No matter how comprehensive the cover is, it can not replace the lost tissue. Therefore, new biomaterials will focus on the establishment of bioactive scaffolds for the wound. Fiber scaffolds affect cell arrangement, shape, and function by mimicking ECM fiber organization. The main form of simulated ECM is a hydrogel, which shows good thermal stability, controllable biodegradation, good swelling, and smooth surface morphology (Thangavel et al., 2017). *In vivo* wound closure examination using STZ-induced mice showed that the full-layer wound wrapped with a chitosan sponge containing TMC nanoparticles healed faster than that of ordinary chitosan wound dressings. The biological activity of TMC nanoparticles is a good antibacterial effect, thus improving the wound healing of diabetes injury (Xia G. et al., 2020). These bioactive scaffolds or the enclosed environment formed between the wound and the dressing can solve the problem that temporary ECM is difficult to generate due to the presence of too many MMPs (Griffin et al., 2015).

3.2.3 Restore the natural structure of ECM

As mentioned above, collagen and hyaluronic acid are components of natural ECM and have good histocompatibility and biodegradability *in vivo*. Studies have shown that scaffolds bound to extracellular matrix (ECM) proteins can regulate cell behavior and improve wound healing. However, most brackets that contain the ECM cannot capture the dynamic functions of the ECM. The collagen fiber structure in ECM can be simulated by electrospinning technology (Kim et al., 2017). Nanofiber scaffolds mimic the compositional transition of ECM during wound healing and may have great potential to promote skin regeneration through dynamic regulation of the microenvironment (Zhao et al., 2016; Sun et al., 2021).

The dressing developed according to this idea has good cell compatibility with keratinocytes and fibroblasts and enhances their cell proliferation and migration ability *in vitro*. The supportive nanoscale matrix mimicking ECM promotes increased collagen deposition in the wound bed, thereby accelerating the complete healing process through massive tissue regeneration and functional recovery (Nanditha and Kumar, 2022). Through the electrospinning method, researchers have manufactured polylactic acid glycolic acid/collagen nanoscale mats, and functionalized the surface with wound healing peptides, loaded chitosan nanoparticles and micron-sized particles to form an extracellular matrix (ECM) - like structure with bionic functions (Yin et al., 2020). The researchers also found that iPSCs-derived fibroblasts ("post IPSF") can promote angiogenesis by producing more ECM than IPSF precursor cells (somatic precursor - "IPSF precursor"), and their ECM has the characteristics of fetal ECM. This initial state of ECM recovery, with higher cell content, higher vascular endothelial growth factor (VEGF), and higher interleukin-1 receptor antagonist (IL-1ra) (Santarella et al., 2020).

3.2.4 Promote cell proliferation, differentiation, and migration

The pore diameter of the sponge material can be from 50 μ M to mm, which is conducive to cell infiltration, migration, and signal transduction (Katoh et al., 2004). The results showed that the sponge scaffolds made of collagen could promote the adhesion, migration, and proliferation of fibroblasts and keratinocytes cultured on its surface. However, the collagen from lactating animals is degraded rapidly and may also cause transgenic diseases (Chandika et al., 2015; Ramanathan et al., 2017). Adding glycosaminoglycan (GAG) to the hydrogel can also promote cell infiltration and proliferation (Kirker et al., 2002). Surface plasma treatment can improve the hydrophilicity of materials, thus playing a similar role (Chandrasekaran et al., 2011). Studies have shown that hFDSPC-CM can pass through TGF- β/Smad signaling pathway promotes the proliferation and migration of cells (keratinocytes and fibroblasts) in the wound surface of diabetic mice and realizes the wound healing of diabetes mice by combining with HA (Xin et al., 2021).

3.2.5 Promote angiogenesis

Although collagen is a widely used wound healing material, its angiogenic ability is poor and its explanation speed is fast.

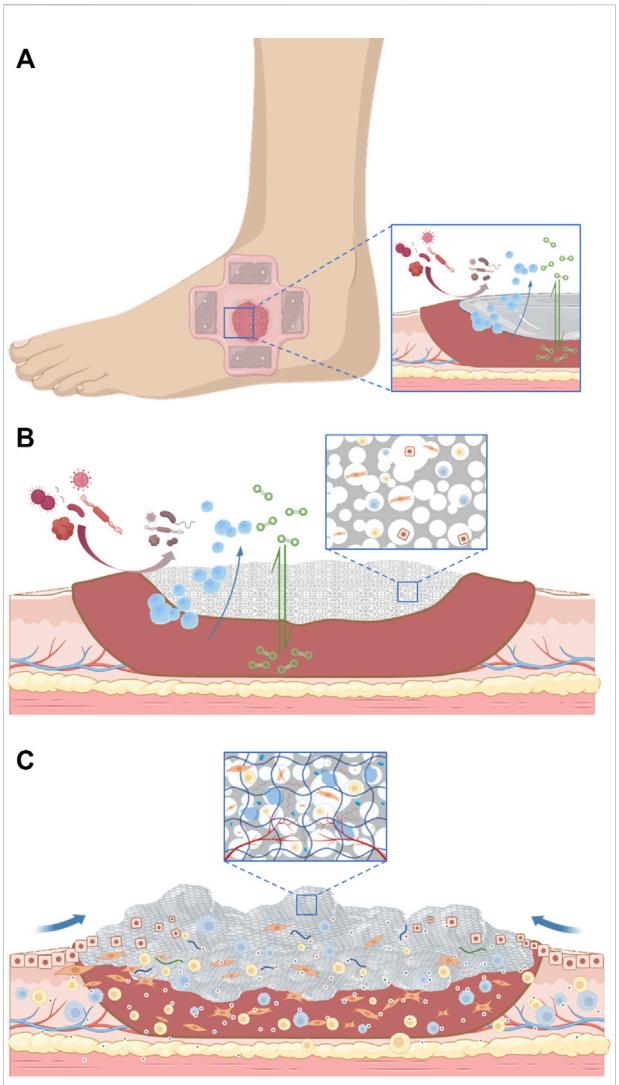

FIGURE 2
(A). The initial action of the dressing applied to the wound. **(B)**. The dressing serves as a scaffold for tissue regeneration. **(C)**. Dressings are gradually becoming biomimetic.

Therefore, fibrin-based hydrogels were designed to effectively promote angiogenesis and cell recruitment (Zeng et al., 2015; Chung et al., 2016). Or electrospinning using these natural proteins to improve their angiogenic ability (Xu et al., 2019). Recent studies have found that a 3D short fiber sponge provides an oxygen-rich environment for cell growth, which is conducive to the 3D proliferation and growth of HUVECs, stimulates the expression of VEGF, and well promotes the angiogenesis of HUVECs (Li Y. et al., 2021). But the promotion of angiogenesis and cell function may be concomitant.

3.2.6 Sterilization characteristics

One of the main characteristics of a diabetes wound is the complex infection of the wound. Chitosan has unique advantages in dealing with this problem. It has been found that chitosan not only promotes cell adhesion and migration but also has a bactericidal ability (Miguel et al., 2014). The concentration of 188 g/ml enables the hydrogel given to chitosan to inhibit the growth of bacteria, and the electrospun chitosan material has a similar effect. The collagen sponge with anti-infective bioactive molecules also effectively restored the normal function of fibroblasts and keratinocytes in infectious wounds (Ramanathan et al., 2017). The latest research shows that glycopeptide hydrogel accelerates the reconstruction of full-thickness diabetes and scalded skin infected by methicillin-resistant *Staphylococcus aureus* (MRSA) by coordinating a large number of M2-type macrophages, reducing inflammation and promoting angiogenesis (Liu W. et al., 2022). We summarize the evolution of wound dressing function through a set of figures (Figure 2).

3.3 Flexible applications of biodegradable biomaterials

After improving the composite and modification of biomaterials themselves, we hope that biomaterials can realize the exogenous supplement of missing active ingredients, at the same time, maximize the activity of endogenous cells and growth factors, and on this basis, carry some drugs or inorganic substances, to realize the flexible application of biomaterials based wound healing materials. As mentioned in the second part, there are some extremely effective methods in clinical application, but they are accompanied by serious problems, such as systemic adverse reactions of hyperbaric oxygen chamber therapy or the uniformity of wound dressing. The flexible application of biodegradable biomaterials provides a supplement to this shortcoming in clinical practice. Therefore, according to the characteristics of diabetic wounds, we expect biomaterials to be antibacterial, anti-inflammatory, pro-angiogenic, and restore appropriate environmental conditions for wound healing.

3.3.1 Purpose of active ingredient accumulation

The three elements of tissue repair and reconstruction include scaffolds, cells, and growth factors. Whether it is the repair of bone defects (Ren S. et al., 2022) or the healing of skin wounds, these three factors are inseparable. Therefore, based on degradable biomaterials, adding cells and growth factors can meet the environment and requirements of tissue regeneration to the greatest extent.

In addition, in a large number of studies, degradable biomaterials loaded different drugs to achieve targeted drug delivery. In addition to the improvement of medication, it is more important to promote some drugs with short half-lives to protect their activity *in vivo*. In addition, the presence of a large number of proteases in the microenvironment of diabetes

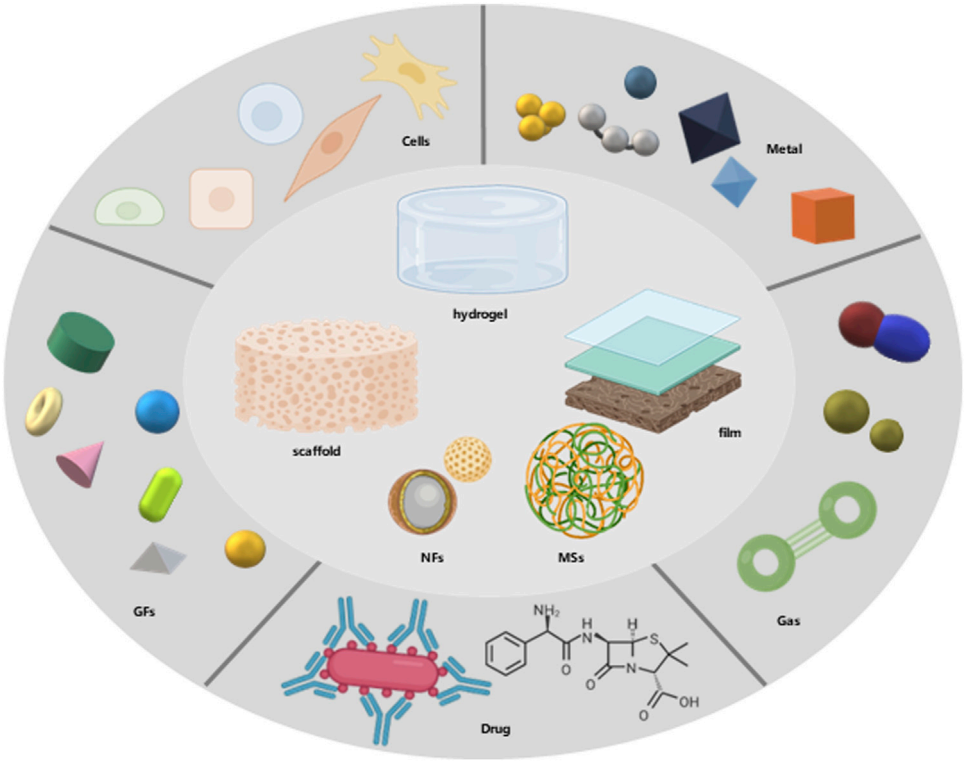

FIGURE 3
The combination of composite biodegradable biomaterials.

wounds leads to the degradation of GFS, which further hinders angiogenesis and diabetes wound healing. Some studies have shown that ECM simulation and immune regulation can be achieved through the modification of the material itself (Liu W. et al., 2022), to achieve the antibacterial effect. However, the healing of diabetes wounds does not depend solely on the antibacterial effect.

Admittedly, what we need to prove is that each accumulated component has a synergistic effect, not an opposite effect. The cytotoxicity of chemosynthetic drugs may affect the activity of cells and cell components, while the preparation process and mode of action of scaffold materials may not necessarily reach the ideal state. However, by observing the accumulation of time, environmental assessment at different stages, and the changes in the microenvironment *in vivo*, we hope to truly achieve the most ideal environment for wound healing, and even make use of some specific environments, such as diabetes, to respond to pH or temperature, to accumulate effective ingredients and make adjustable personalized wound healing materials.

3.3.2 Functional enhancement of biodegradable biomaterials

The application research of degradable biomaterials is always inseparable from material-based property modification. Of course, new basic materials are emerging constantly. The current research focus is to combine materials with various drugs, cells or ions, and other components that have positive effects on wound healing to simulate the optimal and ideal conditions for wound healing (Figure 3). As mentioned above, we should focus on the functional improvement of wound dressings and skin tissue engineering. The local oxygen-rich environment and drug-loading conditions are particularly important for functional improvement.

3.3.2.1 Loading drugs

The most important means to combat chronic wounds related to diabetes is to use drugs for intervention. Through the mastery and application of the properties of biomaterials, various drugs can be carried and released, form a drug delivery system (DDS) based on degradable biomaterials, and make the pharmacological effect play a better level. However, the research in recent years tends to apply more known drugs in other fields, and develop more combinations of materials through the modification of natural extracts. Because biomaterials themselves can achieve the partial antibacterial effect through modification, it seems that the local antibacterial drug carrier is conservative for the

antibacterial effect of wounds (Garin et al., 2021; Zhou et al., 2022).

3.3.2.1.1 Anti-diabetes drugs. PLGA and metformin were dissolved in 1,1,1,3,3,3-hexafluoro-2-propanol (HFIP) and spun into nanofiber membranes by electrospinning. The metformin in PLGA could be slowly and persistently released for more than 3 weeks due to the stable degradation performance of PLGA, thus promoting the healing of diabetes wounds (Lee et al., 2014). Similarly, to achieve the sustained release of metformin, cam et al. Manufactured bacterial cellulose gelatin nanofibers co-loaded with glibenclamide and metformin (Alven et al., 2022). Core-shell nanofiber bioactive insulin-loaded PLGA scaffolds can also be used to repair wounds in diabetic rats. Mechanical analysis of the insulin-loaded nanofibers showed that the elongation at break was 164.3% ± 27.2%, and the tensile strength was about 2.87 ± 0.07 MPa, which was similar to human natural skin. PLGA and insulin obtained scaffolds by coaxial electrospinning, and insulin was continuously released for 4 weeks. Nanofiber core-shell insulin-loaded scaffolds reduced the content of type I collagen *in vitro* and increased the growth factor in vivo-β, which can prolong the release of insulin and promote the healing of diabetes wounds (Lee et al., 2020b). The pioglitazone-loaded PVP-PCL nanofiber pad showed an initial rapid release of the drug in type I diabetes mice, followed by a sustained release mode. The sustained release of pioglitazone and its good cytocompatibility led to an accelerated wound-healing process (Cam et al., 2020). *In vitro*, the lira (Yu et al., 2020) reversed the inhibitory effect of high glucose (Hg)-induced endothelial cells on proliferation, migration, tube differentiation, and VEGF secretion. In the mechanism study, the lira was found to specifically reduce the level of mir-29b-3p and target Akt/GSK-3 β/β- The catenin pathway regulates the biological function of endothelial cells.

3.3.2.1.2 Antibiotics. Continuous topical use of antibiotics can avoid wound infection and related bacterial colonization. Therefore, the method of adding antibiotics to local dressings and making them sustained release has a positive effect on wound healing (Lee et al., 2020a). Local use of DCH to treat wound infection is a common clinical method. Because the local concentration and treatment cycle are difficult to control, the side effects are large in the clinical application process. DCH-encapsulated polylactide (DCH/PLA) nanofibers were prepared by electrospinning. Among them, the rate of DCH release can be controlled within 3d-2w, which can specifically fight against E. coli and S. aureus, thus promoting wound healing (Cui et al., 2019). Gentamicin-loaded collagen sponges also have similar effects (Lipsky et al., 2012). Vancomycin-loaded N-trimethyl chitosan nanoparticles (VCM/TMC NPs), as a potential drug delivery system, have high intracellular penetration and effective intracellular antibacterial activity (Fukushima 2016; Zhang Y. et al., 2017). Ahmed et al. (2018) reported that calcium alginate-ba lyophilized sheets combined with ciprofloxacin were used for wound management of diabetes patients with microbial infection to inhibit and prevent reinfection caused by Gram-positive and Gram-negative bacteria. Loading the antibiotic ciprofloxacin into the wafer can be used to treat diabetes injury caused by bacterial infection, and it shows good cytocompatibility with human keratinocytes. Another hydrogel loaded with fusidic acid has excellent flexibility and elasticity based on rapid film formation, and produces high drug release. The FFH loaded with sodium fusidate with the weight ratio of sodium fusidate/PVP/PVA/propylene glycol/ethanol/water of 1/2/12/3/8/74 can rapidly form a corresponding dry film at the wound site and can be stable at 45°C for 6 months (Kim et al., 2015). There are also studies using PVA foam-loaded methylene blue and gentian violet for anti-local infection treatment (Coutts et al., 2014). In the future, we should implement appropriate local dressings according to the results of bacterial culture and drug sensitivity tests of the wound.

3.3.2.1.3 New trials of drugs for the treatment of other diseases. PLLA basedoaded electrospun fiber membrane, which is coated with dimethylglyoglycine-loaded mesoporous silica nanoparticles, promotes the proliferation, migration, and angiogenesis-related gene expression of human umbilical vein endothelial cells (Ren et al., 2018).

Through electrostatic interaction, chitosan, heparin, and poly (γ- Glutamic acid). Hydrogels have a good swelling ability and show typical viscoelasticity and good mechanical properties in rheological tests. The fibroblast proliferation test showed that the hydrogel had cell compatibility. Its ability to promote healing is attributed to the wound healing function of chitosan loading superoxide dismutase by promoting cell proliferation and by reducing ROS production in the wound bed (Zhang L. et al., 2018).

Neurotensin (NT), also known as neurotensin, is named because it has an obvious antihypertensive effect and exists in nerve tissue. It is easy to separate from other peptide hormones due to its specific vascular effect and blood pressure lowering effect. The main problem of the neuropeptide problem is the short half-life and low bioactive concentration in the peptide-rich wound environment. Moura et al. (2014) reported the application of chitosan-based foam loaded with neurotensin in wound healing of diabetes. This material can increase the migration of fibroblasts and the expression and deposition of collagen (COL1A1, COL1A2, and COL3A1), to promote wound healing. The *in vitro* drug release curve of neurotensin-loaded PLGA cellulose nanocrystalline nanofiber membrane indicates that neurotensin is continuously released from the nanofiber membrane and the full-thickness wound healing of diabetes rats is faster (Zheng et al., 2018).

Ginkgolide B (GB), a natural product extracted from Ginkgo biloba leaves, has been used to treat cerebrovascular and

cardiovascular diseases, mainly due to its antioxidant, anti-inflammatory, and proliferative effects. Through the combination of high molecular weight hyaluronic acid and ginkgolide B, anti-inflammatory and angiogenesis can be achieved. However, at present, only the comparison with ordinary dressings has been achieved, and its effectiveness cannot be evaluated (Wang L. et al., 2022).

Diosmin is a drug for enhancing venous tension and a vasoprotective agent. For the lymphatic system, it can increase the speed of lymphatic drainage and the contraction of lymphatic vessels, improve lymphatic reflux and reduce edema. A composite wafer was obtained using sodium alginate: gelatin with 1.5%/1.5% w/w, and Diosmin was continuously released within 8 h. Complete epithelial regeneration, well-organized dermis, well-formed granulation tissue, and mature collagen bundles were observed in the treated rats, and the stability of diosmin nanocrystals was maintained at the same time (Atia et al., 2019).

Hyaluronic acid (HA)/poly (lactic acid co glycolic acid, PLGA) core/shell fiber matrix loaded epigallocatechin-3-O-gallate (EGCG) (HA/PLGA) was fabricated by coaxial electrospinning. HA/PLGA-E core/fiber matrix is composed of randomly oriented submicron fibers with a 3D porous network structure. EGCG was uniformly dispersed in the shell and sustained uniformly for 4 weeks. In streptozotocin-induced diabetes rats, this novel composite enhanced re-epithelialization/neovascularization and increased collagen deposition (Shin et al., 2016).

3.3.2.2 Loading cells

3.3.2.2.1 Provide appropriate ECM for stem cells. The microenvironment change induced by diabetes hurts the wound repair function of mesenchymal stem cells. Therefore, there are studies to counteract the influence caused by the microenvironment of diabetes by increasing photobiological regulation (PBM) and enabling mesenchymal stem cells to play a repair role (Fridoni et al., 2019). PBM can synergize with ADSC to jointly regulate the inflammatory response, increase wound strength and wound closure rate, and significantly reduce CFU (Ebrahimpour-Malekshah et al., 2020).

Lipolysis of dermal adipocytes contributes to wound healing by regulating inflammatory macrophage infiltration. In addition to mobilizing lipid reserves, the wound environment also induces changes in the plasticity of adipocyte cells, making adipocytes at the edge of the wound become wound bed myofibroblasts that generate ECM during the proliferation phase of repair (Shook et al., 2020).

The initial attempt was to collect allogeneic adipose stem cells (ASCs) from the inguinal fat of normal rats, create ASC sheets using cell sheet technology, and transplant them to the full-thickness skin defect of diabetes obese rats. A variety of angiogenic growth factors (VEGF, HGF, TGF- β 1. IGF-I, EGF, and KGF) accelerate wound healing by promoting angiogenesis (Kato et al., 2015).

However, it is difficult to obtain and prepare large-scale stem cell sheets alone. Due to the repulsive force between cells and the binding force between cells and the substrate, it is difficult for stem cells on the wound surface to act effectively. By using soluble cell adhesion molecule (CAM) to engineer and transform cells, a powerful cell sheet is formed, which makes it possible to obtain a unique method of large-scale hADSC sheet (Na et al., 2018). This kind of stem cell sheet made by the photothermal principle also provides a new idea for the combination of materials and stem cells.

Oxygen tension is an important regulator of stem cells, controlling their homing and implantation in injured tissues. The underlying mechanism is the transient increase of reactive oxygen species/nitrogen species based on HBOT. Although a temporary increase in oxidative stress at the wound site may have deleterious effects, these active substances act as important signaling molecules to activate hypoxia-inducible factor (HIF) -1 when oxygen levels fall to normal levels. Subsequently, VEGF is activated, thereby recruiting endothelial progenitor cells and activating important antioxidant defense. The obtained results showed that the combination of MSC with HBOT improved collagen synthesis and increased neovascularization and epithelialization in the wound bed, supporting its therapeutic application (Peña-Villalobos et al., 2018).

The sprayable gel hydrogel is easy form a thick film on the wound surface after being crosslinked by blue light. The simulated neutrophil nanoparticles composed of GOx and CPO dual enzyme systems are encapsulated in zif-8 nanoparticles, which can effectively reduce the glucose concentration around the wound of diabetes and produce HClO to inhibit bacterial growth. In addition, the generated HClO plays a role in inhibiting scar formation to ensure efficient treatment of diabetes wounds, the wounds almost recover, and no scar formation on day 21 (Liu C. et al., 2022).

3.3.2.2.2 Promote the function of stem cells. Mesenchymal stem cells stimulate cell migration, neovascularization, epithelial regeneration, and new wound bed formation and maturation (Kuo et al., 2011). In addition, they can also reduce the inflammatory response, enhance wound contraction, and can improve healing (Hu et al., 2018). The excised wounds of diabetes treated with HUC MSCs showed enhanced microvessel density and vascular synthesis ability, which were caused by IGF and TGF- β Upregulation (Moon et al., 2017). TGF- β It plays an important role in the whole wound healing process, mainly by recruiting inflammatory cells to the wound area from the early stage until the late stage of epithelial regeneration, involving the production and remodeling of ECM and the migration and differentiation of fibroblasts and keratinocytes to influence the proliferation stage (Pakyari et al., 2013).

Polyethersulfone nanofibers loaded with human cord blood-derived CD34 + cells (hereinafter referred to as CD34 + cells) homing in the wound site after systemic administration and significantly accelerating wound closure. Wound bed NF- κ B and its downstream effector molecule TNF- α, IL-1β And the sustained pro-inflammatory activity of IL-6 decreased. In addition, improved granulation tissue formation increased collagen deposition and myofibroblasts, and decreased MMP-1 expression was observed (Kanji et al., 2019).

Gellan ha sponge hydrogels loaded with hASCs were pre-cultured in selected standard neurogenic conditioned media and found to be able to generate structures that control angiogenesis and inflammation and stimulate new innervation (da Silva et al., 2017). Wound tissue wrapped in ADSC-loaded silk fibroin chitosan film is almost redeveloped at a position close to normal tissue, and this process seems to depend on the similarity between ADSC and skin stem cells (Wu et al., 2018).

Kaisang et al. (2017) reported that injectable Pluronic F-127 hydrogel encapsulated with adipose stem cells (ADSC) as a drug delivery system to enhance the healing of diabetic wounds. Compared with untreated wounds, vascular endothelial growth factor, messenger RNA expression level of key angiogenic growth factor, transforming growth factor in ADSCs-pluronic-f127 hydrogel treated wounds- β1 and key wound healing GF levels were enhanced.

Fibrinogen and collagen I, respectively, was incorporated into the shell and core of nanofibers to mimic the sequential appearance of fibrinogen and collagen I during wound healing. This biomimetic coaxial scaffold significantly promotes the immunoregulatory paracrine of ASC. Incubation of macrophages with ASC conditioned medium confirmed the enhanced immune regulation of ASC on biomimetic coaxial scaffolds by enhanced M1 to M2 polarization of macrophages (Sun et al., 2021).

3.3.2.2.3 Promote the delivery of stem cells in a 3D environment. ADSCs cultured in a 3D environment has a higher level of proangiogenic ability (Im et al., 2021). Therefore, some studies have designed 3D nanofiber scaffolds, whose size, depth, and shape can be adjusted to adapt to different wound conditions. BMSCs were loaded on the nanofiber scaffolds. The 3D scaffolds loaded with BMSCs could enhance the formation of granulation tissue, promote angiogenesis and promote the deposition of collagen. In addition, this scaffold inhibits the formation of M1-type macrophages and the pro-inflammatory cytokines IL-6 and TNF- α. And promotes the formation of M2-type macrophages and the expression of anti-inflammatory cytokines IL-4 (Chen S. et al., 2020).

Using the electrochemical deposition method to load hADSCs onto collagen, the composite biomaterials formed have high tensile strength, high porosity, excellent biocompatibility, and cell proliferation ability (Edwards et al., 2018). In addition, a human epidermal growth factor curcumin bandage bio couple (EGF curb) loaded with MSCs (MSCs EGF curb) was used at the injured site for wound healing in diabetes. Culturing MSCs on EGF curb enhanced the viability of MSCs and their association with pluripotency and self-renewal (OCT ¾, Sox2 and Nanog). *In vivo* experiments have found that this new type of MSC-loaded dressing can significantly enhance wound closure by increasing granulation tissue formation, collagen deposition, and angiogenesis (Mohanty and Pradhan, 2020).

As a kind of biocompatible dressing, PDMS has a certain clinical value. It has a certain strength and can maintain 3D structure during cell spreading. However, its hydrophobicity and permeability are poor, so it is not feasible to be used for wound repair. However, some studies have made PDMS into a material with a 3D concave surface by photolithography. When this material is used alone, wound healing has not proved. However, after ADSC is added, its 3D structure can make ADSC in a spherical state for a long time (7d), which enhances its ability of proliferation and migration, increases the expression of therapeutic growth factors, and thus significantly improve wound healing (Jeong et al., 2022).

3.3.2.2.4 Promote the action of active components in cells. Cell components are the root of wound regeneration. After wound formation, different epidermal stem cells recruited from different skin regions need to cooperate with other cell types (including fibroblasts and immune cells) to ensure effective and synergistic wound healing. This process depends on the activation, migration, and plasticity of these cell components during tissue repair (Dekoninck and Blanpain, 2019). Only using cells to act on the wound has a certain effect, but the activity of stem cells is low, and the ability of proliferation, differentiation, and migration is inhibited. And biomaterials can provide an improved microenvironment and three-dimensional growth scaffolds for them, and try their best to simulate the physiological state.

The soluble growth factors and cytokines released by MSCs are combined with the curcumin complex bandage designed previously (Fromer et al., 2018), and EGF that constitutes the bandage can also help maintain MSC proliferation, stemness, and self-renewal. The synergistic effect of MSC and curcumin allows the complex bandage that can promote wound healing to be upgraded again (Mohanty and Pradhan, 2020). The long-term effect needs to be achieved by the slow release of the active ingredient, which combines the collagen binding domain (CBD) with SDF-1 α And VEGF were specifically fused, and the sustained release of the two recombinant proteins from the collagen scaffolds was successfully observed. Meanwhile, when cbd-vegf and cbd-sdf-1 α When CO modified scaffolds were implanted into the skin wound model of diabetes rats, they not only showed synergistic effects in promoting angiogenesis, but also reduced inflammation in the short term (Hu Y. et al., 2021).

3.3.2.3 Loading active factor

At first, researchers used the modified double lotion method to prepare recombinant human epidermal growth factor (rhEGF) nanoparticles with poly (lactic acid co glycolic acid) as the carrier. The diameter of rhEGF nanoparticles is about 193.5 nm (diameter), and the particle size distribution is uniform and dispersible. The encapsulation efficiency was 85.6% and the release of rhEGF lasted for 24 h. The composite can promote fibroblast proliferation, and its controlled release enhances the effect of rhEGF to stimulate cell proliferation and shorten wound healing time (Chu et al., 2010).

Effects of sponge based wound dressings made of HA and collagen and encapsulated *in vivo* with epidermal growth factor (EGF). EGF loaded sponge wound dressings promoted epithelialization to a greater exten (Kondo et al., 2012). By gathering (ε-The amine terminated block copolymer composed of caprolactone [PCL] and poly (ethylene glycol) [peg] and PCL was electrospun into biocompatible nanofibers with functional amine groups on the surface through peg linker. Surface chemical binding of EGF to nanofibers. When human primary keratinocytes were cultured on EGF conjugated nanofibers, the expression of specific genes was significantly increased. Immunohistochemical staining results showed that EGF receptor (EGFR) was highly expressed in the EGF nanofiber group (Choi et al., 2008). Recombinant human epidermal growth factor (rhEGF) - bound polyurethane foam (PUF) is time and concentration dependent and accelerates wound healing by promoting wound contraction, epithelial regeneration, collagen deposition and the formation of skin appendages (Pyun et al., 2015). Recently, the nanostructured lipid carrier gel formulation of recombinant human thrombomodulin improved wound healing in diabetes by local administration (Hsueh et al., 2021).

Poly (ether) carbamate polydimethylsiloxane/fibrin scaffolds loaded with VEGF and bFGF (scaffolds/GF loaded NPs) poly (lactic acid co glycolic acid) (PLGA) nanoparticles, the application of scaffolds on full-thickness dorsal skin wounds significantly accelerated wound closure on day 15 (Losi et al., 2013). Another material of rhEGF loaded poly (lactic acid co glycolic acid) (PLGA)–alginate microspheres (MS) showed a statistically significant reduction in wound area on days 7 and 11 in the *in vivo* experiment, which was completely re epithelialized by day 11 and the inflammatory process subsided earlier (Gainza et al., 2013). Chitosan and hyaluronic acid are made into composite sponges, which are loaded with fibrin nanoparticles containing VEGF. After evaluating the characteristics of the material itself such as porosity, expansion rate, biodegradability, mechanical properties and hemostatic ability, researchers found that VEGF can be released in high concentration within 3 days after the attachment of the material and induce angiogenesis (Mohandas et al., 2015). Similar studies also included PLGA nanofibers encapsulated with PDGF, vancomycin and gentamicin 115. While the administration of VEGF encapsulated in PLGA nanoparticles (PLGA-VEGF NPs) will promote rapid healing due to the sustained and combined effects of VEGF and lactate (Chereddy et al., 2015).

The prepared PVA solution was mixed with CTGF solution to obtain a 6% w/v PVA solution containing 0.1% w/w CTGF. For PLA shells, a 10% PLLA solution was prepared in a DCM/DMF (1:9 ratio) mixed solvent system. The electrospun pva-pla hybrid membrane coated with connective tissue growth factor prepared by electrospinning showed high cell proliferation and migration ability of fibroblasts, keratinocytes and epithelial cells with potential angiogenesis (Augustine et al., 2019).

In addition, nanofiber biodegradable drug loaded films with sustained release of recombinant human platelet-derived growth factor (rhPDGF BB) to repair diabetes wounds have been developed. RhPDGF BB and polylactic acid co glycolic acid (PLGA) were mixed in hexafluoroisopropanol, and then the solution was electrospinned into biodegradable membranes to equip nanofiber membranes. Based on the formation of Schiff base bond, ODEX/HA-AMP/PRP hydrogel was prepared by mixing oxidized dextran (ODEX), ha-amp modified by antimicrobial peptide and PRP under physiological conditions, which has obvious bacteriostatic circle. It has significant antibacterial activity against *Staphylococcus aureus* and *Pseudomonas aeruginosa*, and inhibits proinflammatory factors (TNF-α, IL-1β and IL-6), enhancing anti-inflammatory factor (TGF- β1) And the production of vascular endothelial growth factor (VEGF) (Wei et al., 2021).

Polylactic acid glycolic acid/collagen nano-scale dressing, and surface functionalization with wound healing peptide, loaded chitosan nano and micro scale particles to form extracellular matrix (ECM)-like structure with bionic function. The developed dressings have good cell compatibility with keratinocytes and fibroblasts and enhance their cell proliferation and migration ability *in vitro*. Experiments in streptozotocin induced diabetes mouse model showed that bioactive peptides released by chitosan particles could shorten the inflammatory phase and promote neovascularization. The supportive nanoscale matrix promotes increased collagen deposition in the wound bed, thereby accelerating the complete healing process through massive tissue regeneration and functional recovery. The results showed that the nanoscale mat rich in nano/particles showed the potential as an effective wound repair dressing for diabetes wounds (Nanditha and Kumar, 2022).

Horseradish peroxidase (HRP) catalyzed spray gelatin gel (GH) loaded two types of chemokines [i.e., macrophage inflammatory protein 3A (MIP-3a) and interleukin-8 (IL-8)] by *in situ* crosslinking. IL-8, MIP-3 without affecting GH swelling rate and mechanical stiffness α Release from GH and maintain biological activity, and finally significantly promote wound healing in diabetes by stimulating collagen deposition and neovascularization/re-epithelialization (Wei et al., 2021).

The antioxidant thermoresponsive hydrogel is composed of poly (poly (ethylene citrate co-n-isopropyl acrylamide) (PPCN) through sequential polycondensation and free radical polymerization. SDF-1 is blocked by gel of ppcn + SDF-1 solution above its lower critical solution temperature (LCST), and its release and biological activity are measured. Finally, under the action of accelerated granulation tissue formation, epithelial maturation, and the highest density of perfusion vessels, The repair of 6 mm diameter wounds in mice was completed in 24 days (Zhu et al., 2016).

Heparin-bound epidermal growth factor (HB-EGF) has a positive effect on wound contraction, epithelial regeneration and collagen deposition due to its affinity for heparin-bound growth factor. In the highly sulfated heparin-like polysaccharide 2-N, 6O sulfated chitosan (26SCS)- doped poly (lactic acid co glycolic acid) scaffolds (S-PLGA), 26scs has strong scavenging activity against superoxide radicals. *In vivo* experiments, the sustained release of HB-EGF induced by 26scs and the migration of glial forming cells after ROS removal can also be observed (Zhang X. et al., 2018).

Chitosan, silk fibroin, and PRP (CBPGCTS-SF@PRP) The composing self-healing and injectable hydrogels can protect PrP from enzymatic hydrolysis, sustainably release PrP, and enhance the chemotaxis of mesenchymal stem cells (Qian et al., 2020).

A natural polysaccharide-based hydrogel matrix was prepared using green algae sulfide polysaccharides, chitosan, dopamine (DPA), and silver nanoparticles (Ag NPs). Human umbilical cord mesenchymal stem cells lyophilized powder (HUC MSCs) was loaded into hydrogels to develop a new type of wound healing material for chronic diabetes (UC-DPA-Ag@hUC-MSCs). The resulting hydrogel has sufficient mechanical properties, swelling ability, adhesion, antioxidant, antibacterial ability, and the ability to promote cell proliferation and migration. The *in vivo* wound healing of the wound model of type II diabetes mice showed that HUC MSCs loaded with UC DPA Ag hydrogel could effectively accelerate wound healing. This advanced hydrogel provides a simple and effective method for chronic wound management in diabetes (Ren Y. et al., 2022).

Injectable BG/sodium alginate (BG/SA) hydrogel loaded with MMP9 SINP can significantly accelerate the healing process of full-thickness resected wounds in diabetes rats by reducing MMP-9 expression, improving collagen synthesis and enhancing wound angiogenesis. Injectable bioglass/sodium alginate (B/SA) hydrogel loaded with MMP9 SINP significantly accelerated the healing process of full-thickness excised wounds in diabetes rats by reducing the expression of MMP-9, improving the accumulation of collagen and enhancing angiogenesis in the wounds (Li et al., 2022).

3.3.2.4 Loading ions

3.3.2.4.1 Ag^{+}. Silver nanoparticles have strong wound-healing potential due to their well-known antibacterial activity. The mixed solution of polyethylene glycol (PEG) and chitosan reduces silver nitrate to convert silver ions into silver nanoparticles (Ag NPs), to obtain chitosan peg prepolymer containing Ag NPs. After that, the prepolymer solution is crosslinked by glutaraldehyde to form a hydrogel. The hydrogel impregnated with Ag NPs has higher porosity, higher swelling degree and, higher water vapor conversion rate (WVTR). In addition, Ag NPs have the antibacterial and antioxidant abilities, so the obtained polymer is beneficial to the wound healing of diabetes (Masood et al., 2019). Chitosan dextran hydrogel loaded with Ag nanoparticles also has a broad-spectrum antibacterial effect, promoting granulation tissue formation, fibroblast migration and angiogenesis (Shi et al., 2019).

A wound dressing composed of chitosan, crosslinked gelatin/polyvinylpyrrolidone, and embedded silver nanoparticles were prepared by solution casting method. The films were characterized by FTIR, SEM and TGA. Glutaraldehyde (0.5%) was used for cross-linking of membrane modules, and was associated with a 7-fold improvement in mechanical properties, 28% hydrolysis stability, 3-fold reduction in thickness and morphological roughness. This developed membrane can serve as a promising and cost-effective system to combat severe diabetes and burn wound infections (El-Aassar et al., 2021).

In addition, the combination of nanosilver, chitosan, and hyaluronic acid has also been reported, and its antibacterial mechanism has been studied in depth: ①nAg damages the bacterial cell wall and interferes with the proteins involved in the formation of membrane potential; ②The proton gradient necessary for electron transfer to establish oxidative phosphorylation is disrupted; ③Membrane damage and permeability change. Due to the in-depth discussion of the above mechanisms, the clinical status of anionic antibacterial dressing was established (Anisha et al., 2013).

The preparation of biocompatible and multifunctional self-assembled hydrogels using polymer nanoparticle interactions is a simple and universal approach for effective chronic wound treatment. Mixed silver lignin nanoparticles play two roles: ① structural role, acting as a cross-linking node in the hydrogel and giving it shear thinning (the ability to flow under the applied shear stress) and self-healing characteristics; ② Function: it has strong antibacterial and antioxidant activities. Thiolated hyaluronic acid and Ag@LigNPs The nanocomposite hydrogel produced by *in situ* self-assembly of can simultaneously inhibit the main factors of wound chronicity, i.e., overexpressed harmful proteolytic enzymes and oxidase, and high bacterial loaded (Pérez-Rafael et al., 2021).

3.3.2.4.2 Cu^{2+}. Cu ion is a basic element with a long history of use in humans (Gopal et al., 2014). It is involved in many processes related to wound healing, including the induction of vascular endothelial growth factor, angiogenesis, and the

expression and stabilization of extracellular skin proteins such as keratin and collagen (Marelli et al., 2015). Cu ion is also a well-known antibacterial agent, which can promote healing by reducing the possibility of wound infection (Amna et al., 2014). The increase in nonphysiological concentrations of copper ions may be toxic because these ions interfere with the homeostasis of other metals, disrupt DNA, and generate reactive oxygen species that may adversely affect proteins, lipids, and nucleic acids. However, if copper ions are slowly released from the warehouse placed at the desired location, the toxicity may be mitigated (Guo et al., 2013). Metal-organic frameworks (MOFs), also known as porous coordination polymers, are crystalline porous materials composed of inorganic metal ions or clusters connected by polydentate organic ligands (Lu et al., 2014). The citric acid saline gel can be safely absorbed in the thermal response of oxidation resistance. On the basis of the above research, Xiao et al. (2017) Developed a composite scaffold combining copper ions with a basic framework and made a hydrogel.

Firstly, poly (ethylene citrate) acrylate prepolymer (PPcac) was prepared by polycondensation of citric acid, PEG and glycerol 1,3-diglycidyl diacrylate. Subsequently, PPcac was reacted with pre purified NIPAM by radical polymerization overnight, using AIBN as a radical initiator. The reaction product PPCN was obtained by precipitation and purification with ether. Copper acetate monohydrate (0.15 g, 0.75 mmol) dissolved in distilled water (2 ml) was added dropwise to h3btc (0.11 g, 0.5 mmol) dissolved in ethanol (2 ml), and then stirred at room temperature for 20 min to form a gel-like dark Turquoise suspension. The suspension was then centrifuged and the precipitate was washed twice with ethanol/water (1:1, V/V) solution to obtain purified HKUST-1. Hkust-1nps were added to PPCN solution (100 mg/ml) and the copper concentration was 0.1 M under vortex at room temperature. The solution was directly placed on the QFDE sample tray, heated to solid at 45°C, and then rapidly frozen. Further functional validation found that h-hkust-1 hydrogel can protect nanoparticles from decomposition and slowly release copper ions, thereby reducing apoptosis and cytotoxicity, enhancing dermal cell migration, and improving wound closure rate (Xiao et al., 2017).

3.3.2.4.3 Ce^{2+}. Cerium is a rare Earth element, which is widely used in industrial fields such as catalysts, fuel additives, and colored components incorporated into glass. Ce^{4+} and CeO2 show high antibacterial activity. Silver, copper, zinc, and gallium have been incorporated into a bioactive glass (BG) to give it antibacterial ability. Direct contact with BG may adhere to the wound and cause adverse reactions such as wound tearing. BG-loaded hydrogels can avoid adverse reactions caused by BG alone (Cheng et al., 2021). Photo cross linkable and biodegradable gelatin methacrylate (gel MA) as the framework of hydrogel, loaded with cerium containing bioactive glass nanoparticles, can significantly reduce the colony number of *Staphylococcus aureus* and *Escherichia coli*. *In vivo* experiments verified its role in promoting wound healing (Chen et al., 2021).

Diabetes wounds have extremely complex microenvironments of hyperglycemia, hypoxia, and high reactive oxygen species (ROS). Based on the co-assembly of CE-driven special double ligands (alendronate and 2-methylimidazole) and glucose oxidase (GOx), a glucose/ROS cascade responsive nanoenzyme was developed (CHA@GOx) Yes, for wound treatment of diabetes. It has superoxide dismutase and catalase mimetic activities and can effectively remove excess ROS. In particular, it can catalyze the excessive hydrogen peroxide produced by glucose oxidation reaction to generate oxygen, regulate the oxygen balance of the wound, reduce the toxic and side effects of GOx, and achieve the purpose of synergetic repair of diabetes wounds. *In vitro* experiments showed that, CHA@GOx It contributes to the migration of mouse fibroblasts and promotes the formation of human umbilical vein endothelial cell tubes. *In vivo* experiments, it can induce angiogenesis, collagen deposition, and epithelial reformation (Yu et al., 2022).

3.3.2.4.4 Zn^{2+}. Microporous and flexible chitosan-based hydrogel composite bandages loaded with ZnO nanoparticles showed improved blood coagulation, controllable degradation, swellingand good antibacterial activity. The 80% porosity can absorb a large amount of exudate and improve cell viability, thus promoting wound healing while inhibiting bacteria (Kumar et al., 2012).

After methacrylation of simulated natural glycosaminoglycans κ- When carrageenan (Kama) is used as the hydrogel matrix, polydopamine of different concentrations is loaded to improve the mechanical, antibacterial and cellular properties. L-glutamic acid promotes wound healing. The composite material has good elasticity and adhesion as a whole, and can effectively coagulate blood. It also ensures that the viability of incubated cells is still 95% after 3 days. *In vivo* experiments found that it accelerated wound healing by promoting granulation tissue proliferation (Tavakoli et al., 2020).

Epigallocatechingallate (EGCG) modified zinc oxide quantum dots hydrogel (ZnO-EGCG@H), it is used to treat the delayed wound of diabetes. EGCG was successfully combined with ZnO quantum dots through phenol hydroxyl groups and formed a coordination bond with Zn atoms on ZnO quantum dots. Then, the obtained ZnO EGCG was packaged in hydrogels as a dual-purpose nano reagent to promote angiogenesis and epithelial regeneration by enhancing the expression of VEGF and EGF. In addition, hydrogel, as an excellent drug delivery system, provides continuous water and high local concentration of ZnO EGCG, enabling ZnO-EGCG@H By reducing inflammatory factors (TNF-α, IL-6) and the production of various antibacterial mechanisms including ROS to accelerate the wound healing of diabetes and provide ideal biomaterials for the wound treatment of diabetes. ZnO-EGCG@H After 15 days

of treatment, the lesion closure rate of the rats was 96.3%, which was significantly better than that of the control group (65.4%). The safety experiment shows that, ZnO-EGCG@H It has reassuring biocompatibility and is harmless to important organs (Yin et al., 2022).

Researchers have developed a new healing hydrogel based on histidine, a natural dietary essential amino acid that is important for tissue formation. Amino acids are crosslinked with zinc ions (Zn^{2+}) and sodium alginate (SA) through dynamic coordination bonds and hydrogen bonds respectively to form histidine-SA-Zn^{2+} (HSZH) hydrogels with good injectability, adhesion and biocompatibility and antibacterial properties. The application of this double dynamic bond crosslinked hydrogel accelerated the migration and angiogenesis of skin related cells *in vitro*. *In vivo* experiments, the wound was completely repaired within about 13 days, while the healing process of the control group took about 27 days. This weakly crosslinked material based on tissue-friendly small molecules can cure wounds more effectively than the highly crosslinked material based on long-chain polymers (Yao et al., 2022b).

3.3.2.5 Loading gas

3.3.2.5.1 NO. Since 1987, the role of no *in vivo* has been gradually clarified, especially its ability to control cell proliferation and apoptosis, promote angiogenesis induced by growth factors and promote wound healing (Miller and Megson, 2007). However, this feature depends on the site and concentration of no generation. Current research shows that the surface flux of no is 0.5–4.1 × 10^{-10} mol cm^{-2} min^{-1}. However, due to the extreme reactivity, short half-life and short diffusion distance of no, artificial application is very difficult (He et al., 2019). A particle based no release material has been developed, which can produce physiologically relevant levels of no for a long time without any toxic and side effects (Lautner et al., 2016). The NO donors-nitroso-n-acetyl-d-penicillamine (SNAP) was encapsulated in 50:50 (PLGA) and microspheres were prepared using oil in water solid lotion solvent evaporation method. Snap was slowly released for more than 10 days, while release continued for more than 4 weeks by using ester terminated PLGA (Mw = 38,000–54000). The presence of copper ions and/or ascorbate in the solution is effective for decomposing the released no donor and obtaining sustained no release. It was also demonstrated that light could be used to induce the microspheres to release no rapidly within several hours. These new microsphere formulations can be used for site-specific administration and treatment of diseases related to dysfunction of endogenous NO production. The microparticles reported here can eventually be injected into many locations in the body or incorporated into creams or hydrogels to generate wound healing patches that can be used to treat various types of wounds, including ulcers related to diabetes (Lautner et al., 2016).

Gelatin methacrylate (gelma) has been proven to be a highly cell friendly, cell adhesive, and inexpensive biopolymer for various tissue engineering and wound healing applications. In this study, the nitric oxide (no) donor SNAP was incorporated into the highly porous gelMA hydrogel patch to improve cell proliferation, promote rapid cell migration and promote wound healing in diabetes (Zahid et al., 2021).

A new type of porous metal organic framework (MOF) microneedle (MN) patch can realize the delivery of photothermally responsive nitric oxide (no) to promote the wound healing of diabetes. Since the copper-benzene-1,3,5-tricarboxylic acid copper (HKUST-1) MOF that can carry no is encapsulated by graphene oxide (go), the resulting NO@HKUST-1 @Go microparticles (NHGS) can promote the controlled release of no molecules in the near infrared ray (NIR) photothermal response. When these NHGS are embedded in porous pegda-mns, the porous structure, larger specific surface area and sufficient mechanical strength of the integrated MNS can promote more accurate and deeper delivery of no molecules to the wound site (Yao et al., 2022a).

3.3.2.5.2 O_2. Hyperbaric oxygen therapy is a commonly used chronic wound treatment method in clinic at present. The oxygen concentration in the body is increased through the whole-body treatment of hyperbaric oxygen chamber. There are studies on hyperbaric oxygen therapy for systemic application, combined with WJ-MSCs based on IM (a commercial wound care device, integramatrix wound dressing, which provides the ECM for cell invasion and capillary growth), to promote wound healing in diabetes mice *in vivo* experiments (Peña-Villalobos et al., 2018). However, due to the low vascular density around the chronic wound and slow local blood circulation, the treatment effect is not satisfactory, and there may be concurrent problems such as oxygen poisoning. Therefore, scientists think of local oxygen therapy by local administration. Some studies have used frozen gel technology to make it by adding calcium peroxide (CPO) to the antioxidant polyurethane (PUAO) scaffolds. PUAO-CPO frozen gel attenuated ROS and showed sustained oxygen release over a period of 10 days. *In vitro* analysis showed that they could maintain H9c2 cardiomyocytes under hypoxia, and the cell viability was significantly better than that of common polyurethane (PU) scaffolds. In addition, *in vivo* studies using an ischemic flap model showed that oxygen releasing frozen gel scaffolds were able to prevent tissue necrosis for up to 9 days. This approach can be used to develop oxygen releasing biomaterials with sustained oxygen delivery and reduced production of residual ROS and free radicals due to ischemia or oxygen production (Shiekh et al., 2018). After that, there were studies using 7%PCL +2% sodium percarbonate (SPC) at 19 kv voltage and 50 μ L flow rate, and found that O_2 in the electrospun sheet can be sustained for up to 10 days, and the cells seeded on

the SPC can express higher levels of HIF-1 at the gene and protein levels α. *In vivo* experiments, it shows a strong angiogenic effect and forms a relatively dense ECM (Zehra et al., 2020).

However, it seems that the oxygen release in 9–10 days is still insufficient, so scientists based on the oxygen release microspheres (ORM) and the oxygen generation system of injectable, rapid gel and reactive oxygen species (ROS) scavenging hydrogel (Ross gel) (Guan et al., 2021). The microspheres rapidly released enough oxygen to support the cells to survive under hypoxia and maintain oxygen release for at least 2 weeks. Unlike most current oxygen production systems that first release toxic H_2O_2 into the tissue environment and then release oxygen through its decomposition, the designed ORM directly releases oxygen, clears ROS, and avoids its damaging effect on cells. The continuous oxygenation of released oxygen to skin cells promotes the survival, migration and paracrine of skin cells and the formation of endothelial lumen under hypoxia *in vitro*. In addition, after effectively increasing intracellular oxygen content and adenosine triphosphate content, extracellular signal regulated kinase 1 and heme oxygenase 1 signaling (ERK 1/2 and HO-1) were activated. Meanwhile, *in vivo* experiments, it was found that sustained oxygenation and ROS clearance in diabetes wounds stimulated the expression of angiogenic growth factors and angiogenesis (Guan et al., 2021).

4 Biomaterials development towards intelligence

We expect that the accumulation of single active ingredients can achieve synergistic effect, but most attempts are contrary to our expectations. More attempts have been made to design more intelligent composite materials.

4.1 PH sensitivity

PH responsive hydrogels were prepared by Schiff base crosslinking using phenyl boron modified chitosan (CSPBA), polyvinyl alcohol (PVVA) and benzaldehyde terminated peg, and insulin and fibroblasts were encapsulated into the hydrogels at pH = 7.4. When the pH decreases, the Schiff base is unstable, and the phenyl boron group preferentially binds to glucose. In addition, in high-level glucose water, the modulus of the hydrogel decreases, which means that insulin molecules are released through the swollen hydrogel matrix. Due to the acidic environment and high glucose level in the wound area of diabetes, this intelligent responsiveness is what we want to see (Zhao et al., 2017).

Traumatic multidrug resistant (MDR) bacterial infection is a fatal threat to the public. To combat MDR bacteria, a bifunctional pH sensitive hydrogel based on peptide DP7 (VQWRIRVAVIRK) and oxidized dextran (DP7-ODEX hydrogel) was developed. As an antimicrobial peptide, DP7 can synergize with many antibiotics. When ceftazidime was added to DP7-ODEX hydrogel, it showed obvious advantages in MDR inhibition of *Pseudomonas aeruginosa*. This hydrogel made of the bifunctional peptide DP7 can kill multidrug-resistant bacteria colonizing the wound bed and promote scar free wound healing (Wu et al., 2022).

Under alkaline conditions, graphene is reduced to graphene oxide (pGO) by PDA, and pGO is dispersed in chitosan CS/silk fibroin SF. After double crosslinking, pGO gel is obtained. The pGO in the gel can clear excessive ROS and promote wound regeneration through physiological and electrical signal transmission that promotes cell growth (Tang et al., 2019).

Gini flat cross linked chitosan (CHT)/gelatin (GEL) scaffolds were fabricated by lyophilization and loaded with platelet rich plasma (PRP). Human dermal fibroblasts were seeded on the scaffolds, and then polychromatic light in the NIR was applied to the scaffolds to activate platelets and stimulate fibroblasts (photoactivation, PAC). Thus, fibroblasts were chemically and physically stimulated by PRP and light, respectively. It was found that the expression of laminin and collagen 4 was up-regulated, and the angiogenesis related PDGF and VEGF were also significantly increased under the action of PRP and light (Koyuncu et al., 2022). However, this complex system also means that biomaterials have also changed from single to complex, from the combination of simple biomaterials and some ingredients that promote wound healing to a bionic system that strives to restore the normal wound healing mode (Bulutoglu et al., 2022). Nano ZnO was loaded into the hydrogel to kill microorganisms. Paeoniflorin encapsulated micelles with ROS responsive properties were immobilized on the framework of hydrogels by Schiff base bonds for low pH and ROS stimulated angiogenic activity. The continuous responsiveness of the novel hydrogel can intelligently rescue the harmful microenvironment in refractory wounds. This highly biocompatible hydrogel significantly promotes the healing of chronic infected diabetes wounds *in vitro* and through continuous hemostatic, microbial killing and angiogenic activities. This microenvironment responsive hydrogel loaded with nzno and PF encapsulated micelles has great potential as a site-specific dual response delivery platform for the treatment of refractory, chronic infected diabetes wounds (Guo et al., 2022). Cellulose nanofibers (CNFs) obtain pH responsiveness through acro amino hyperbranched polyamines ($HBP\text{-}NH_2$) and simultaneously load indocyanine green (ICG) to achieve temperature responsiveness. In addition, the 3D cage structure of the material itself provides high loading capacity of doxorubicin and ICG, thus achieving multi responsive composite materials (Zhao et al., 2021). The introduction of exogenous factors such as visible light and heat has broadened the design idea of wound dressing (Yanina et al., 2017).

4.2 Optical responsiveness

New glycerol monoester based thermosensitive matrix as wound management system. First, an appropriate portion of glycerol monooleate (GMO) and glycerol monostearate (GMS) were mixed to provide a thermoresponsive matrix (gmo-gms, GG). Subsequently, in order to improve the photothermal response and antibacterial properties, silver nanoparticles (Ag)–modified reduced graphene oxide (RGO) nanocomposites (RGO Ag) were added to the GG matrix to obtain (GG RGO Ag). According to the systematic study of uninfected, infected and diabetes wound models, the phase transition of GG RGO Ag can be triggered by applying NIR laser to release Ag for sterilization as required. More importantly, this smart GG substrate can also promote the production of vascular endothelial growth factor protein, thus serving as a multi effect wound management system defined by NIR(Jin et al., 2021).

Graphene quantum dots modified luminescent porous silicon material has become a new dressing. The luminescent porous silicon carrying EGF and insulin was embedded in the chitosan film. Under the effect of fluorescence resonance energy transfer, the dressing was red, H2O2 triggered Si oxidation, and at the same time, the drug was released, while the PL of gqds was restored, and the dressing was blue. *In vitro* and *in vivo* results showed that smart dressing enhanced cell proliferation and migration and significantly cured diabetes wounds (Cui et al., 2021).

And exogenous speed limiting intervention measures can better realize the intellectualization of dressing. PLGA is used as a scaffold to encapsulate Mxene nanosheets and mesoporous silica nanoparticles containing VEGF. After that, dopamine hyaluronic acid hydrogel is used as a shell to realize photothermal conversion through NIR, so as to release an appropriate amount of VEGF from the Mxene nanofiber skeleton to promote angiogenesis. DA generates H_2S to induce macrophage polarization. The thermal effect of NIR itself promotes local blood circulation, and multiple effects combine to achieve controllable release of effective substances, thereby promoting wound healing (Jin et al., 2022).

Biocompatible Cu_3SnS_4 NFs nanosheets are prepared by a simple and low-cost manufacturing process. These NFs can be activated by visible light, leading to visible light mediated photocatalytic production of a large amount of reactive oxygen species (ROS). In addition, plasma Cu_3SNS_4 NFs exhibited strong NIR absorption and high photothermal conversion efficiency of 55.7%. The novel combination promotes endothelial cell angiogenesis and collagen deposition, thus accelerating wound healing. In addition, their inherent local surface plasmon resonance effect makes them active substrates for surface enhanced Raman scattering (SERS) imaging and SERS labeled bacterial detection (Yang et al., 2022).

4.3 Internal environment responsiveness

The stable and uniform distribution of polydopamine reduced graphene oxide enables the scaffolds to have stable electrical and mechanical properties even after long-term immersion. Due to its unique biomimetic structure and tissue affinity, the scaffold further acts as an “electronic skin,” transmitting endogenous bioelectricity by absorbing wound exudates, and promoting the treatment of diabetes wounds (Wang J. et al., 2022). Injectable sodium alginate/Bioglass (SA/BG) composite hydrogel is used to carry SA microparticles containing cell conditioned medium (CM) (SA-CM), including pirfenidone (PFD) polylactic acid (PLGA) microspheres. This multilayer injectable gel system delivers bioactive molecules in sequence. 1-3d regulates host inflammatory response, 2-7d promotes vascularization and granulation tissue formation, 8-20d releases PFD, and prevents regenerative skin fibrosis and scar formation (Ma et al., 2020).

Another custom dressing was derived from antibacterial nanoparticles containing recombinant human type III collagen (rh Col III) (PDA@AgNPs), first released PDA@AgNPs Rapidly kill *Staphylococcus aureus* and *Escherichia coli*, and subsequently, customized rh col III was used to promote the proliferation and migration of fibroblasts and endothelial cells (Hu C. et al., 2021). The composite material based on rh col III and naproxen (nAP) is composed of polylactic acid (PLGA) nanoparticles combined with hyaluronic acid (HA) microneedles (MN). It can also deliver effective drugs in order according to the wound conditions. It is worth mentioning that rh col III is synthesized based on Gly483-Pro512 fragment and has strong cell adhesion (Long et al., 2022).

4.4 Temperature responsiveness

A recombinant fusion protein, which contains a rage (vRAGE) binding domain linked to elastin like polypeptide (ELP), can self assemble into a coacervate at about 30–31°C. The size of the condensed layer is related to the concentration and temperature, and the range is 500–1600 nm. VRAGE-ELP reversed several age-mediated changes in cultured human umbilical vein endothelial cells, including a decrease in the number of viable cells, an increase in the level of reactive oxygen species (ROS), and an increase in the expression of the pro-inflammatory marker intercellular adhesion molecule-1 (ICAM-1). vRAGE-ELP can stably exist for 7 days *in vitro*. This coagulation system that locally delivers competitive ages inhibitors has the potential to treat diabetes wounds (Kang et al., 2021).

A temperature resistant (−20–60°C) antibacterial hydrogel dressing consists of polyacrylamide, gelatin and ε- Poly lysine is assembled. Due to the binary solvent system of water/glycerol (Gly), the resulting hydrogel (G-PAGL) showed good heat

resistance and freezing resistance, and showed long-lasting and extensive antibacterial activity against Gram-positive and Gram-negative bacteria. It is satisfactory that the double network (DN) G-PAGL hydrogel dressing can effectively promote the healing of DFUs by accelerating collagen deposition, promoting angiogenesis and inhibiting bacterial growth (Liu et al., 2021).

5 Application and analysis of composite biomaterials used in clinical trials

Refer to https://clincialtrials.gov by taking wounds and different types of materials (hydrogels, scaffolds, films, nanofibers) as the search keywords. It is not difficult to see that the number of relevant clinical studies is small compared with basic research, and the quality of published articles is also mixed. The purpose of basic research is ultimately to apply the research results to the clinic. Therefore, finding a suitable clinical transformation path is also a problem that researchers must consider.

5.1 Status of clinical trials

Most of the clinical research on biomaterials is concentrated in the past 5 years, which depends on the progress of basic research. However, the conclusions obtained in the basic research may not be directly applicable to the human body.

5.1.1 Fundamental deviation of basic research

The biocompatibility and effectiveness of some classic degradable biomaterials have been confirmed in clinical trials, but the next development has experienced a cliff like stagnation. One of the important reasons is that the application of biomaterials has transitioned from a single material to a new stage: composite biomaterials. As we have analyzed in the previous article, biomaterials can be combined with stem cells, active factors and other substances, which is recognized in the academic field, but it cannot be smoothly carried out in clinical transformation due to ethics, diversity of ingredient sources and other reasons.

In addition, most of the animal models selected for basic research are rodents, which have the advantages of wide sources, mature model preparation methods and easy feeding. However, the biggest problem is that its wound healing mechanism is different from that of humans. This problem may fundamentally negate the results of basic research. To solve this problem, scientists used rubber rings to prevent skin contraction to brake the wound. After that, large mammals such as pigs were used for preclinical trials. However, there are still some clinical trials that fail to achieve the desired results in human body, which makes the clinical transformation work stagnate. However, preclinical trials in mammals and primates can still reduce the risk of clinical trials to a certain extent.

5.1.2 Feasibility of basic research

There is no doubt that the ultimate goal of basic research is to apply it to clinical practice. Therefore, in the basic research, the design of the experimental scheme should take the clinical application as the ultimate goal. In order to be convenient, quick and easy to operate, comprehensively study and judge the factors affecting ethics, economy and psychology, and design the experimental scheme with strong transformation ability. Otherwise, it will be of little help to clinical work. The basic research team should communicate closely with the clinic and conduct targeted basic research for the purpose of clinical transformation in combination with the actual clinical needs.

Basic research still focuses on confirmatory research, which verifies the effectiveness and safety of materials through the development of materials and observation of wound healing. However, as a basic research, the verification of material safety and effectiveness is far from enough. We have to figure out which behaviors, which signals, or which pathways are affected by the design and development of various materials. Only by fundamentally clarifying the mechanism can this material be brought to the clinic.

5.1.3 Complexity of clinical situation

For basic research, there are mature models and methods to construct wound healing model system and verify the effectiveness of biomaterials *in vivo* and *in vitro*. However, the complexity of clinical wound is not only due to its location, area and wound environment, but also due to other factors. The patient's economic ability and many personal conditions, including compliance, are different. It needs to combine various factors to promote the final clinical transformation. From the current clinical research and the publication of high-quality articles, it can be seen that simple operation methods and the intervention of finished product manufacturing companies are the keys to the success of clinical trials. As far as the materials themselves are concerned, the most teams use film materials for clinical research, which may be due to strong operability and good patient compliance. The number of cases included in the current clinical study is generally small, mostly ranging from 20 to 50. In addition to the limitations of the clinical trial itself on the situation of the subjects, the conservative psychology of the subjects and the ability to bear unexpected situations are uncontrollable. In one study, 100 people were included as subjects, but the trial had to be terminated due to too many lost visits. Such cases can be found everywhere. In addition, the protocols, results, endpoint values and follow-up time of different clinical trials are different, and the lack of standardization makes it more difficult to compare the collected data and different types

of treatments (Chereddy et al., 2016; Nilforoushzadeh et al., 2017).

5.2 Solution

The standardization and rational use of biodegradable biomaterials will be an inevitable trend. Therefore, solving the existing problems is the best way to promote the development of this field.

5.2.1 Develop uniform standards

Under the guidance of the industry association, an expert technical committee and a technical alliance shall be established, and a unified technical standard shall be formulated. Relevant basic research shall be evaluated according to the unified standard, so as to ensure the effectiveness and repeatability of experimental data while ensuring innovation, so that the data can be summarized horizontally and vertically, and the accuracy of data can be rapidly improved, so as to accelerate the transformation of results into clinical practice.

5.2.2 Support work

The funds generated in the process of scientific research should not become the burden of scientific research personnel. After the project design and scheme pass the review, different funds should be provided. In particular, the government can provide funds through insurance, risk investment and other channels to fully guarantee the product quality, medical application safety and accelerate the transformation to clinical practice.

5.2.3 Early enterprise involvement

An important part of promoting clinical transformation is related drug and device enterprises that commercialize and popularize the results. In the early stage of R & D, enterprises are introduced to share and dilute risks, and accelerate the progress of R & D and industrial transformation.

5.2.4 Improve the process system

Promote the rapid advancement of legislative and regulatory procedures through various channels, such as academicians' suggestions and NPC deputies' proposals. Improve relevant laws and regulations, accelerate the training of review professionals, and then improve the review speed, so as to form scientific management in this field.

We believe that biomaterials are an excellent direction for wound repair, but the choice of specific programs still needs to be discussed. The combination of biological materials with active ingredients should not be blunt, and the imposition of cells or cellular components on the material does not necessarily work perfectly. For example, loading cells with material results in a decrease in cell loading and the number of adherent cells is affected by factors such as surface area and hydrophilicity of the material surface, which is not worth the loss. In the development and utilization of biomaterials, more attention should be paid to the interaction between materials and cells.

6 Expansion of research ideas and future research directions

OxOBand is composed of antioxidant polyurethane (PUAO) as a highly porous frozen gel with continuous oxygen release characteristics, supplemented by adipose stem cells (ADSCs) exosomes. Exosomes engulfed by cells enhanced the migration of human keratinocytes and fibroblasts and increased the survival rate of human neuroblastoma cells under hyperglycemic conditions. Compared with untreated diabetes control wounds, oxoband promoted faster wound closure, enhanced collagen deposition, faster epithelial regeneration, increased neovascularization, and reduced oxidative stress within 2 weeks. This dressing promotes the development of mature epithelial structures, and the morphology of hair follicles and epidermis is similar to that of healthy skin (Shiekh et al., 2020). This method will change the passive to active, so that the cells become "hungry" and take what they want from the materials we provide. Although this sounds like a difficult goal to achieve, it is still a better research direction.

However, whether it is the application of exosomes or various cell active ingredients, the most important thing is to improve its utilization rate while clarifying its effectiveness. Most of the cells and drugs exist in the form of fluids, and the rational use of biomaterials should provide an appropriate "refuge" for the effective substances that are difficult to exist stably for a long time, so that they will not be attacked by the immune system and will not be cleaved due to the unfriendliness of the environment, but will be released at a suitable time to play their due role.

In addition, compared with the use of toxic oxidative cross-linking initiators (such as sodium periodate and silver nitrate) traditionally used, the current research is more inclined to the use of effective extracts in natural ingredients. For example, the natural polyphenol compound tannic acid (TA) achieves near instantaneous (<25 s) hydrogen bond mediated citrate gel. Mussel-based biological adhesives combine antioxidant, anti-inflammatory, and antibacterial activities (3A-TCMBAs). *In vivo* evaluation in the infected full-thickness skin wound model and the rat skin incision model showed that 3A-TCMBAs + NIR treatment could promote wound closure and collagen deposition, increase the collagen I/III ratio at the wound site, and inhibit the expression of pro-inflammatory cytokines. In the early stage, the wound promotes angiogenesis, and in the later stage, the remodeling and degradation of ECM are triggered by platelet endothelial cell adhesion factor-1 to promote scar-free healing of the wound (Wu et al., 2023). This study seems to suggest the development direction of biomaterials in the wound in the future.

There is a relatively clear time window and natural process for wound healing. In different periods, different cells, growth factors, and extracellular matrix play different roles. For example, fibroblasts act as the main component of ECM during the formation of granulation tissue. However, if the process of fibroblasts transforming into myofibroblasts is out of control at the later stage of wound healing, the next pathological process may be induced: hypertrophic scar. Therefore, the superposition of simple effective ingredients may not play a perfect role, but more importantly, it can restore the ability of normal wound healing while treating the effects of some pathological factors (such as infection, biofilm formation, and vascular degeneration) on the wound (Zhang X. et al., 2018). Although external intervention is important, restoring the original healing mode may be a supplement to the normal physiological process.

Despite the remarkable achievements, the treatment of diabetes-related chronic wounds is still very challenging due to the complexity and diversity of etiology and pathogenesis. At present, the bottleneck that is still difficult to break through lies in the difference in animal models. There is a great difference in the process of skin healing between mice and humans, but the mouse model is still difficult to replace (Wang L. et al., 2022). Therefore, establishing a mouse animal model with less difference is the key to the transformation of the experiment. In addition, the diversity of basic research proves the urgency of clinical needs. However, there are still few studies that can enter the clinical transformation stage. It is the ultimate goal of each study to translate the results of basic research into clinical practice. As we gradually master the pathogenesis and pathological process, we still hope to solve the problem of diabetes wounds through the treatment of the disease itself, improve the speed and quality of wound healing, to protect the lives of patients, and prevent the occurrence of adverse consequences such as amputation.

7 Conclusion

The research between biomaterials and diabetic wounds should be more and more in-depth. However, integrating the above points, there should be a complete idea about the design and utilization aspects of biomaterials. First of all, the selected materials must have excellent biocompatibility. Then, after the pathological conditions of the wound are clarified, these problems should be targeted for direct or indirect regulation, and the microscopic mechanism should be explored under the premise of clear macroscopic effects. The other aspect is to screen suitable materials after analyzing the pathological mechanism of the wound, which seems to be more in line with medical thinking. No matter which idea is chosen, it is certain that the highly adjustable nature of biodegradable biomaterials combined with effective active ingredients can achieve a positive effect in promoting diabetic wound healing. However, for medical researchers, how to apply them more appropriately in clinical practice is another greater challenge.

Author contributions

SR was responsible for the project design, data collection, results in analysis, manuscript preparation, and literature search. SG was responsible for the literature search and preparation of the manuscript. LY was responsible for the project design, data analysis, the content of the article, and funding collection. CW was responsible for the project design, manuscript preparation, and funding collection.

Funding

This work was sponsored by the Natural Science Foundation of Liaoning Province (2022-YGJC-69) and the support program for excellent young scholars of China Medical University, the National Natural Science Foundation of China (grant/award no. 51872332) and Basic Research Project of the Education Department of Liaoning Province (grant/award no. LJKZ0740).

Conflict of interest

The authors declare that the research was conducted in the absence of any commercial or financial relationships that could be construed as a potential conflict of interest.

Publisher's note

All claims expressed in this article are solely those of the authors and do not necessarily represent those of their affiliated organizations, or those of the publisher, the editors and the reviewers. Any product that may be evaluated in this article, or claim that may be made by its manufacturer, is not guaranteed or endorsed by the publisher.

References

Afzali, H., Jafari Kashi, A. H., Momen-Heravi, M., Razzaghi, R., Amirani, E., Bahmani, F., et al. (2019). The effects of magnesium and vitamin E co-supplementation on wound healing and metabolic status in patients with diabetic foot ulcer: A randomized, double-blind, placebo-controlled trial. *Wound Repair Regen.* 27 (3), 277–284. doi:10.1111/wrr.12701

Ahmed, A., Getti, G., and Boateng, J. (2018). Ciprofloxacin-loaded calcium alginate wafers prepared by freeze-drying technique for potential healing of chronic diabetic foot ulcers. *Drug Deliv. Transl. Res.* 8 (6), 1751–1768. doi:10.1007/s13346-017-0445-9

Al-Musawi, S., Albukhaty, S., Al-Karagoly, H., Sulaiman, G. M., Alwahibi, M. S., Dewir, Y. H., et al. (2020). Antibacterial activity of honey/chitosan nanofibers loaded with capsaicin and gold nanoparticles for wound dressing. *Molecules* 25 (20), 4770. doi:10.3390/molecules25204770

Al-Wafi, R., Mansour, S. F., AlHammad, M. S., and Ahmed, M. K. (2021). Biological response, antibacterial properties of ZrO(2)/hydroxyapatite/graphene oxide encapsulated into nanofibrous scaffolds of polylactic acid for wound healing applications. *Int. J. Pharm. X.* 601, 120517. doi:10.1016/j.ijpharm.2021.120517

Alven, S., Peter, S., Mbese, Z., and Aderibigbe, B. A. (2022). Polymer-based wound dressing materials loaded with bioactive agents: Potential materials for the treatment of diabetic wounds. *Polym. (Basel)* 14 (4), 724. doi:10.3390/polym14040724

Amirrah, I, N., Mohd Razip Wee, M. F., Tabata, Y., Idrus, R. B. H., Nordin, A., and Fauzi, M. B. (2020). Antibacterial-integrated collagen wound dressing for diabetes-related foot ulcers: An evidence-based review of clinical studies. *Polym. (Basel)* 12 (9), 2168. doi:10.3390/polym12092168

Amna, T., Hassan, M. S., Yang, J., Khil, M. S., Song, K. D., Oh, J. D., et al. (2014). Virgin olive oil blended polyurethane micro/nanofibers ornamented with copper oxide nanocrystals for biomedical applications. *Int. J. Nanomedicine* 9, 891–898. doi:10.2147/ijn.s54113

Anisha, B. S., Biswas, R., Chennazhi, K. P., and Jayakumar, R. (2013). Chitosan-hyaluronic acid/nano silver composite sponges for drug resistant bacteria infected diabetic wounds. *Int. J. Biol. Macromol.* 62, 310–320. doi:10.1016/j.ijbiomac.2013.09.011

Annabi, N., Tamayol, A., Uquillas, J. A., Akbari, M., Bertassoni, L. E., Cha, C., et al. (2014). 25th anniversary article: Rational design and applications of hydrogels in regenerative medicine. *Adv. Mat.* 26 (1), 85–124. doi:10.1002/adma.201303233

Armstrong, D. G., Hanft, J. R., Driver, V. R., Smith, A. P., Lazaro-Martinez, J. L., Reyzelman, A. M., et al. (2014). Effect of oral nutritional supplementation on wound healing in diabetic foot ulcers: A prospective randomized controlled trial. *Diabet. Med.* 31 (9), 1069–1077. doi:10.1111/dme.12509

Atia, N. M., Hazzah, H. A., Gaafar, P. M. E., and Abdallah, O. Y. (2019). Diosmin nanocrystal-loaded wafers for treatment of diabetic ulcer: *In vitro* and *in vivo* evaluation. *J. Pharm. Sci.* 108 (5), 1857–1871. doi:10.1016/j.xphs.2018.12.019

Augustine, R., Zahid, A. A., Hasan, A., Wang, M., and Webster, T. J. (2019). <p>CTGF loaded electrospun dual porous core-shell membrane for diabetic wound healing</p>. *Int. J. Nanomedicine* 14, 8573–8588. doi:10.2147/ijn.s224047

Avossa, J., Pota, G., Vitiello, G., Macagnano, A., Zanfardino, A., Di Napoli, M., et al. (2021). Multifunctional mats by antimicrobial nanoparticles decoration for bioinspired smart wound dressing solutions. *Mater. Sci. Eng. C* 123, 111954. doi:10.1016/j.msec.2021.111954

Bai, Q., Han, K., Dong, K., Zheng, C., Zhang, Y., Long, Q., et al. (2020). Potential applications of nanomaterials and technology for diabetic wound healing. *Int. J. Nanomedicine* 15, 9717–9743. doi:10.2147/ijn.s276001

Basiri, R., Spicer, M. T., Levenson, C. W., Ormsbee, M. J., Ledermann, T., and Arjmandi, B. H. (2020). Nutritional supplementation concurrent with nutrition education accelerates the wound healing process in patients with diabetic foot ulcers. *Biomedicines* 8 (8), 263. doi:10.3390/biomedicines8080263

Bechara, N., Gunton, J. E., Flood, V., Hng, T. M., and McGloin, C. (2021). Associations between nutrients and foot ulceration in diabetes: A systematic review. *Nutrients* 13 (8), 2576. doi:10.3390/nu13082576

Bhise, N. S., Shmueli, R. B., Sunshine, J. C., Tzeng, S. Y., and Green, J. J. (2011). Drug delivery strategies for therapeutic angiogenesis and antiangiogenesis. *Expert Opin. Drug Deliv.* 8 (4), 485–504. doi:10.1517/17425247.2011.558082

Boateng, J. S., Matthews, K. H., Stevens, H. N., and Eccleston, G. M. (2008). Wound healing dressings and drug delivery systems: A review. *J. Pharm. Sci.* 97 (8), 2892–2923. doi:10.1002/jps.21210

Bulutoglu, B., Acun, A., Deng, S. L., Mert, S., Lupon, E., Lellouch, A. G., et al. (2022). Combinatorial use of therapeutic ELP-based micelle particles in tissue engineering. *Adv. Healthc. Mat.* 11 (13), e2102795. doi:10.1002/adhm.202102795

Cam, M. E., Yildiz, S., Alenezi, H., Cesur, S., Ozcan, G. S., Erdemir, G., et al. (2020). Evaluation of burst release and sustained release of pioglitazone-loaded fibrous mats on diabetic wound healing: An *in vitro* and *in vivo* comparison study. *J. R. Soc. Interface* 17 (162), 20190712. doi:10.1098/rsif.2019.0712

Caruso, R., Magon, A., Baroni, I., Dellafiore, F., Arrigoni, C., Pittella, F., et al. (2018). Health literacy in type 2 diabetes patients: A systematic review of systematic reviews. *Acta Diabetol.* 55 (1), 1–12. doi:10.1007/s00592-017-1071-1

Castaño, O., Pérez-Amodio, S., Navarro-Requena, C., Mateos-Timoneda, M., and Engel, E. (2018). Instructive microenvironments in skin wound healing: Biomaterials as signal releasing platforms. *Adv. Drug Deliv. Rev.* 129, 95–117. doi:10.1016/j.addr.2018.03.012

Castiello, G., Ghizzardi, G., Dellafiore, F., Turrini, F., and Caruso, R. (2019). Treating a non-healing postoperative sternal wound in a woman with type 2 diabetes mellitus: A case report. *Int. Wound J.* 16 (3), 713–715. doi:10.1111/iwj.13085

Chandika, P., Ko, S. C., Oh, G. W., Heo, S. Y., Nguyen, V. T., Jeon, Y. J., et al. (2015). Fish collagen/alginate/chitooligosaccharides integrated scaffold for skin tissue regeneration application. *Int. J. Biol. Macromol.* 81, 504–513. doi:10.1016/j.ijbiomac.2015.08.038

Chandrasekaran, A. R., Venugopal, J., Sundarrajan, S., and Ramakrishna, S. (2011). Fabrication of a nanofibrous scaffold with improved bioactivity for culture of human dermal fibroblasts for skin regeneration. *Biomed. Mat.* 6 (1), 015001. doi:10.1088/1748-6041/6/1/015001

Chaudhari, A. A., Vig, K., Baganizi, D. R., Sahu, R., Dixit, S., Dennis, V., et al. (2016). Future prospects for scaffolding methods and biomaterials in skin tissue engineering: A review. *Int. J. Mol. Sci.* 17 (12), 1974. doi:10.3390/ijms17121974

Chen, G., He, L., Zhang, P., Zhang, J., Mei, X., Wang, D., et al. (2020). Encapsulation of green tea polyphenol nanospheres in PVA/alginate hydrogel for promoting wound healing of diabetic rats by regulating PI3K/AKT pathway. *Mater. Sci. Eng. C* 110, 110686. doi:10.1016/j.msec.2020.110686

Chen, S., Wang, H., Su, Y., John, J. V., McCarthy, A., Wong, S. L., et al. (2020). Mesenchymal stem cell-laden, personalized 3D scaffolds with controlled structure and fiber alignment promote diabetic wound healing. *Acta Biomater.* 108, 153–167. doi:10.1016/j.actbio.2020.03.035

Chen, Y. H., Rao, Z. F., Liu, Y. J., Liu, X. S., Liu, Y. F., Xu, L. J., et al. (2021). Multifunctional injectable hydrogel loaded with cerium-containing bioactive glass nanoparticles for diabetic wound healing. *Biomolecules* 11 (5), 702. doi:10.3390/biom11050702

Cheng, H., Shi, Z., Yue, K., Huang, X., Xu, Y., Gao, C., et al. (2021). Sprayable hydrogel dressing accelerates wound healing with combined reactive oxygen species-scavenging and antibacterial abilities. *Acta Biomater.* 124, 219–232. doi:10.1016/j.actbio.2021.02.002

Chereddy, K. K., Lopes, A., Koussoroplis, S., Payen, V., Moia, C., Zhu, H., et al. (2015). Combined effects of PLGA and vascular endothelial growth factor promote the healing of non-diabetic and diabetic wounds. *Nanomedicine Nanotechnol. Biol. Med.* 11 (8), 1975–1984. doi:10.1016/j.nano.2015.07.006

Chereddy, K. K., Vandermeulen, G., and Preat, V. (2016). PLGA based drug delivery systems: Promising carriers for wound healing activity. *Wound Repair Regen.* 24 (2), 223–236. doi:10.1111/wrr.12404

Choi, J. S., Leong, K. W., and Yoo, H. S. (2008). *In vivo* wound healing of diabetic ulcers using electrospun nanofibers immobilized with human epidermal growth factor (EGF). *Biomaterials* 29 (5), 587–596. doi:10.1016/j.biomaterials.2007.10.012

Chong, E. J., Phan, T. T., Lim, I. J., Zhang, Y. Z., Bay, B. H., Ramakrishna, S., et al. (2007). Evaluation of electrospun PCL/gelatin nanofibrous scaffold for wound healing and layered dermal reconstitution. *Acta Biomater.* 3 (3), 321–330. doi:10.1016/j.actbio.2007.01.002

Chu, Y., Yu, D., Wang, P., Xu, J., Li, D., and Ding, M. (2010). Nanotechnology promotes the full-thickness diabetic wound healing effect of recombinant human epidermal growth factor in diabetic rats. *Wound Repair Regen.* 18 (5), 499–505. doi:10.1111/j.1524-475x.2010.00612.x

Chung, E., Rybalko, V. Y., Hsieh, P. L., Leal, S. L., Samano, M. A., Willauer, A. N., et al. (2016). Fibrin-based stem cell containing scaffold improves the dynamics of burn wound healing. *Wound Repair Regen.* 24 (5), 810–819. doi:10.1111/wrr.12459

Coutts, P. M., Ryan, J., and Sibbald, R. G. (2014). Case series of lower-extremity chronic wounds managed with an antibacterial foam dressing bound with gentian violet and methylene blue. *Adv. Skin. Wound Care* 27 (3), 9–13. doi:10.1097/01.asw.0000443270.71030.71

Croisier, F., Atanasova, G., Poumay, Y., and Jérôme, C. (2014). Polysaccharide-coated PCL nanofibers for wound dressing applications. *Adv. Healthc. Mat.* 3 (12), 2032–2039. doi:10.1002/adhm.201400380

Cui, S., Sun, X., Li, K., Gou, D., Zhou, Y., Hu, J., et al. (2019). Polylactide nanofibers delivering doxycycline for chronic wound treatment. *Mater. Sci. Eng. C* 104, 109745. doi:10.1016/j.msec.2019.109745

Cui, Y., Duan, W., Jin, Y., Wo, F., Xi, F., and Wu, J. (2021). Graphene quantum dot-decorated luminescent porous silicon dressing for theranostics of diabetic wounds. *Acta Biomater.* 131, 544–554. doi:10.1016/j.actbio.2021.07.018

da Silva, L. P., Santos, T. C., Rodrigues, D. B., Pirraco, R. P., Cerqueira, M. T., Reis, R. L., et al. (2017). Stem cell-containing hyaluronic acid-based spongy hydrogels for integrated diabetic wound healing. *J. Invest. Dermatol.* 137 (7), 1541–1551. doi:10.1016/j.jid.2017.02.976

Das, S., and Baker, A. B. (2016). Biomaterials and nanotherapeutics for enhancing skin wound healing. *Front. Bioeng. Biotechnol.* 4, 82. doi:10.3389/fbioe.2016.00082

Dekoninck, S., and Blanpain, C. (2019). Stem cell dynamics, migration and plasticity during wound healing. *Nat. Cell Biol.* 21 (1), 18–24. doi:10.1038/s41556-018-0237-6

Dickerson, R., Deshpande, B., Gnyawali, U., Lynch, D., Gordillo, G. M., Schuster, D., et al. (2012). Correction of aberrant NADPH oxidase activity in blood-derived mononuclear cells from type II diabetes mellitus patients by a naturally fermented papaya preparation. *Antioxid. Redox Signal.* 17 (3), 485–491. doi:10.1089/ars.2011.4292

Doctor, N., Pandya, S., and Supe, A. (1992). Hyperbaric oxygen therapy in diabetic foot. *J. Postgrad. Med.* 38 (3), 112111–4, 111.

Ebrahimpour-Malekshah, R., Amini, A., Zare, F., Mostafavinia, A., Davoody, S., Deravi, N., et al. (2020). Combined therapy of photobiomodulation and adipose-derived stem cells synergistically improve healing in an ischemic, infected and delayed healing wound model in rats with type 1 diabetes mellitus. *BMJ Open Diabetes Res. Care* 8 (1), e001033. doi:10.1136/bmjdrc-2019-001033

Edwards, N., Feliers, D., Zhao, Q., Stone, R., Christy, R., and Cheng, X. (2018). An electrochemically deposited collagen wound matrix combined with adipose-derived stem cells improves cutaneous wound healing in a mouse model of type 2 diabetes. *J. Biomater. Appl.* 33 (4), 553–565. doi:10.1177/0885328218803754

El-Aassar, M. R., Ibrahim, O. M., Fouda, M. M. G., Fakhry, H., Ajarem, J., Maodaa, S. N., et al. (2021). Wound dressing of chitosan-based-crosslinked gelatin/polyvinyl pyrrolidone embedded silver nanoparticles, for targeting multidrug resistance microbes. *Carbohydr. Polym.* 255, 117484. doi:10.1016/j.carbpol.2020.117484

Eo, H., Lee, H. J., and Lim, Y. (2016). Ameliorative effect of dietary genistein on diabetes induced hyper-inflammation and oxidative stress during early stage of wound healing in alloxan induced diabetic mice. *Biochem. Biophys. Res. Commun.* 478 (3), 1021–1027. doi:10.1016/j.bbrc.2016.07.039

Everett, E., and Mathioudakis, N. (2018). Update on management of diabetic foot ulcers. *Ann. N. Y. Acad. Sci.* 1411 (1), 153–165. doi:10.1111/nyas.13569

Fridoni, M., Kouhkheil, R., Abdollhifar, M. A., Amini, A., Ghatrehsamani, M., Ghoreishi, S. K., et al. (2019). Improvement in infected wound healing in type 1 diabetic rat by the synergistic effect of photobiomodulation therapy and conditioned medium. *J. Cell. Biochem.* 120 (6), 9906–9916. doi:10.1002/jcb.28273

Fromer, M. W., Chang, S., Hagaman, A. L. R., Koko, K. R., Nolan, R. S., Zhang, P., et al. (2018). The endothelial cell secretome as a novel treatment to prime adipose-derived stem cells for improved wound healing in diabetes. *J. Vasc. Surg.* 68 (1), 234–244. doi:10.1016/j.jvs.2017.05.094

Fukushima, K. (2016). Poly(trimethylene carbonate)-based polymers engineered for biodegradable functional biomaterials. *Biomater. Sci.* 4 (1), 9–24. doi:10.1039/c5bm00123d

Gadelkarim, M., Abushouk, A. I., Ghanem, E., Hamaad, A. M., Saad, A. M., and Abdel-Daim, M. M. (2018). Adipose-derived stem cells: Effectiveness and advances in delivery in diabetic wound healing. *Biomed. Pharmacother.* 107, 625–633. doi:10.1016/j.biopha.2018.08.013

Gainza, G., Aguirre, J. J., Pedraz, J. L., Hernández, R. M., and Igartua, M. (2013). rhEGF-loaded PLGA-Alginate microspheres enhance the healing of full-thickness excisional wounds in diabetised Wistar rats. *Eur. J. Pharm. Sci.* 50 (3-4), 243–252. doi:10.1016/j.ejps.2013.07.003

Garin, C., Alejo, T., Perez-Laguna, V., Prieto, M., Mendoza, G., Arruebo, M., et al. (2021). Chalcogenide nanoparticles and organic photosensitizers for synergetic antimicrobial photodynamic therapy. *J. Mat. Chem. B* 9 (31), 6246–6259. doi:10.1039/d1tb00972a

Gholian, S., Pishgahi, A., Shakouri, S. K., Eslamian, F., Yousefi, M., Kheiraddin, B. P., et al. (2022). Use of autologous conditioned serum dressings in hard-to-heal wounds: A randomised prospective clinical trial. *J. Wound Care* 31 (1), 68–77. doi:10.12968/jowc.2022.31.1.68

Gopal, A., Kant, V., Gopalakrishnan, A., Tandan, S. K., and Kumar, D. (2014). Chitosan-based copper nanocomposite accelerates healing in excision wound model in rats. *Eur. J. Pharmacol.* 731, 8–19. doi:10.1016/j.ejphar.2014.02.033

Griffin, D. R., Weaver, W. M., Scumpia, P. O., Di Carlo, D., and Segura, T. (2015). Accelerated wound healing by injectable microporous gel scaffolds assembled from annealed building blocks. *Nat. Mat.* 14 (7), 737–744. doi:10.1038/nmat4294

Guan, Y., Niu, H., Liu, Z., Dang, Y., Shen, J., Zayed, M., et al. (2021). Sustained oxygenation accelerates diabetic wound healing by promoting epithelialization and angiogenesis and decreasing inflammation. *Sci. Adv.* 7 (35), eabj0153. doi:10.1126/sciadv.abj0153

Guariguata, L., Whiting, D. R., Hambleton, I., Beagley, J., Linnenkamp, U., and Shaw, J. E. (2014). Global estimates of diabetes prevalence for 2013 and projections for 2035. *Diabetes Res. Clin. Pract.* 103 (2), 137–149. doi:10.1016/j.diabres.2013.11.002

Guo, C., Wu, Y., Li, W., Wang, Y., and Kong, Q. (2022). Development of a microenvironment-responsive hydrogel promoting chronically infected diabetic wound healing through sequential hemostatic, antibacterial, and angiogenic activities. *ACS Appl. Mat. Interfaces* 14 (27), 30480–30492. doi:10.1021/acsami.2c02725

Guo, L., Panderi, I., Yan, D. D., Szulak, K., Li, Y., Chen, Y. T., et al. (2013). A comparative study of hollow copper sulfide nanoparticles and hollow gold nanospheres on degradability and toxicity. *ACS Nano* 7 (10), 8780–8793. doi:10.1021/nn403202w

Hajikhani, M., Emam-Djomeh, Z., and Askari, G. (2021). Fabrication and characterization of mucoadhesive bioplastic patch via coaxial polylactic acid (PLA) based electrospun nanofibers with antimicrobial and wound healing application. *Int. J. Biol. Macromol.* 172, 143–153. doi:10.1016/j.ijbiomac.2021.01.051

Halschou-Jensen, P. M., Sauer, J., Bouchelouche, P., Fabrin, J., Brorson, S., and Ohrt-Nissen, S. (2021). Improved healing of diabetic foot ulcers after high-dose vitamin D: A randomized double-blinded clinical trial. *Int. J. Low. Extrem. Wounds*, 15347346211020268. doi:10.1177/15347346211020268

Hao, M., Peng, X., Sun, S., Ding, C., and Liu, W. (2022). Chitosan/sodium alginate/velvet antler blood peptides hydrogel promoted wound healing by regulating PI3K/AKT/mTOR and SIRT1/NF-κB pathways. *Front. Pharmacol.* 13, 913408. doi:10.3389/fphar.2022.913408

He, M., Sun, L., Fu, X., McDonough, S. P., and Chu, C. C. (2019). Biodegradable amino acid-based poly(ester amine) with tunable immunomodulating properties and their *in vitro* and *in vivo* wound healing studies in diabetic rats' wounds. *Acta Biomater.* 84, 114–132. doi:10.1016/j.actbio.2018.11.053

Heyboer, M., 3rd, Sharma, D. W. S., and McCulloch, N. (2017). Hyperbaric oxygen therapy: Side effects defined and quantified. *Adv. Wound Care (New. Rochelle.* 6 (6), 210–224. doi:10.1089/wound.2016.0718

Hsu, C. R., Chang, C. C., Chen, Y. T., Lin, W. N., and Chen, M. Y. (2015). Organization of wound healing services: The impact on lowering the diabetes foot amputation rate in a ten-year review and the importance of early debridement. *Diabetes Res. Clin. Pract.* 109 (1), 77–84. doi:10.1016/j.diabres.2015.04.026

Hsueh, Y. S., Shyong, Y. J., Yu, H. C., Jheng, S. J., Lin, S. W., Wu, H. L., et al. (2021). Nanostructured lipid carrier gel formulation of recombinant human thrombomodulin improve diabetic wound healing by topical administration. *Pharmaceutics* 13 (9), 1386. doi:10.3390/pharmaceutics13091386

Hu, C., Liu, W., Long, L., Wang, Z., Yuan, Y., Zhang, W., et al. (2021). Microenvironment-responsive multifunctional hydrogels with spatiotemporal sequential release of tailored recombinant human collagen type III for the rapid repair of infected chronic diabetic wounds. *J. Mat. Chem. B* 9 (47), 9684–9699. doi:10.1039/d1tb02170b

Hu, M. S., Borrelli, M. R., Lorenz, H. P., Longaker, M. T., and Wan, D. C. (2018). Mesenchymal stromal cells and cutaneous wound healing: A comprehensive review of the background, role, and therapeutic potential. *Stem Cells Int.* 2018, 6901983. doi:10.1155/2018/6901983

Hu, Y., Tao, R., Chen, L., Xiong, Y., Xue, H., Hu, L., et al. (2021). Exosomes derived from pioglitazone-pretreated MSCs accelerate diabetic wound healing through enhancing angiogenesis. *J. Nanobiotechnology* 19 (1), 150. doi:10.1186/s12951-021-00894-5

Huang, X., Liang, P., Jiang, B., Zhang, P., Yu, W., Duan, M., et al. (2020). Hyperbaric oxygen potentiates diabetic wound healing by promoting fibroblast cell proliferation and endothelial cell angiogenesis. *Life Sci.* 259, 118246. doi:10.1016/j.lfs.2020.118246

Huang, X., Wang, Q., Mao, R., Wang, Z., Shen, S. G. F., Mou, J., et al. (2022). Two-dimensional nanovermiculite and polycaprolactone electrospun fibers composite scaffolds promoting diabetic wound healing. *J. Nanobiotechnology* 20 (1), 343. doi:10.1186/s12951-022-01556-w

Im, G.-B., Kim, S.-W., and Bhang, S. H. (2021). Fortifying the angiogenic efficacy of adipose derived stem cell spheroids using spheroid compaction. *J. Industrial Eng. Chem.* 93, 228–236. doi:10.1016/j.jiec.2020.09.027

Jeong, G. J., Im, G. B., Lee, T. J., Kim, S. W., Jeon, H. R., Lee, D. H., et al. (2022). Development of a stem cell spheroid-laden patch with high retention at skin wound site. *Bioeng. Transl. Med.* 7 (2), e10279. doi:10.1002/btm2.10279

Ji, Y., Song, W., Xu, L., Yu, D. G., and Annie Bligh, S. W. (2022). A review on electrospun poly(amino acid) nanofibers and their applications of hemostasis and wound healing. *Biomolecules* 12 (6), 794. doi:10.3390/biom12060794

Jin, L., Cheng, H., Xie, X., Chen, X., Tian, G., Zhu, Z., et al. (2021). Dual-effective chronic wounds management system through a monoglyceride binary blend matrix based thermal-responsive phase-transition substrate. *Adv. Healthc. Mat.* 10 (8), e2001966. doi:10.1002/adhm.202001966

Jin, L., Guo, X., Gao, D., Liu, Y., Ni, J., Zhang, Z., et al. (2022). An NIR photothermal-responsive hybrid hydrogel for enhanced wound healing. *Bioact. Mat.* 16, 162–172. doi:10.1016/j.bioactmat.2022.03.006

Jones, V. J. (2006). The use of gauze: Will it ever change? *Int. Wound J.* 3 (2), 79–88. doi:10.1111/j.1742-4801.2006.00215.x

Kaisang, L., Siyu, W., Lijun, F., Daoyan, P., Xian, C. J., and Jie, S. (2017). Adipose-derived stem cells seeded in Pluronic F-127 hydrogel promotes diabetic wound healing. *J. Surg. Res.* 217, 63–74. doi:10.1016/j.jss.2017.04.032

Kandhasamy, S., Perumal, S., Madhan, B., Umamaheswari, N., Banday, J. A., Perumal, P. T., et al. (2017). Synthesis and fabrication of collagen-coated ostholamide electrospun nanofiber scaffold for wound healing. *ACS Appl. Mat. Interfaces* 9 (10), 8556–8568. doi:10.1021/acsami.6b16488

Kang, H. J., Kumar, S., D'Elia, A., Dash, B., Nanda, V., Hsia, H. C., et al. (2021). Self-assembled elastin-like polypeptide fusion protein coacervates as competitive inhibitors of advanced glycation end-products enhance diabetic wound healing. *J. Control. Release* 333, 176–187. doi:10.1016/j.jconrel.2021.03.032

Kanji, S., Das, M., Joseph, M., Aggarwal, R., Sharma, S. M., Ostrowski, M., et al. (2019). Nanofiber-expanded human CD34(+) cells heal cutaneous wounds in streptozotocin-induced diabetic mice. *Sci. Rep.* 9 (1), 8415. doi:10.1038/s41598-019-44932-7

Kato, Y., Iwata, T., Morikawa, S., Yamato, M., Okano, T., and Uchigata, Y. (2015). Allogeneic transplantation of an adipose-derived stem cell sheet combined with artificial skin accelerates wound healing in a rat wound model of type 2 diabetes and obesity. *Diabetes* 64 (8), 2723–2734. doi:10.2337/db14-1133

Katoh, K., Tanabe, T., and Yamauchi, K. (2004). Novel approach to fabricate keratin sponge scaffolds with controlled pore size and porosity. *Biomaterials* 25 (18), 4255–4262. doi:10.1016/j.biomaterials.2003.11.018

Kerr, M., Barron, E., Chadwick, P., Evans, T., Kong, W. M., Rayman, G., et al. (2019). The cost of diabetic foot ulcers and amputations to the National Health Service in England. *Diabet. Med.* 36 (8), 995–1002. doi:10.1111/dme.13973

Kim, B. J., Cheong, H., Choi, E. S., Yun, S. H., Choi, B. H., Park, K. S., et al. (2017). Accelerated skin wound healing using electrospun nanofibrous mats blended with mussel adhesive protein and polycaprolactone. *J. Biomed. Mat. Res. A* 105 (1), 218–225. doi:10.1002/jbm.a.35903

Kim, D. W., Kim, K. S., Seo, Y. G., Lee, B. J., Park, Y. J., Youn, Y. S., et al. (2015). Novel sodium fusidate-loaded film-forming hydrogel with easy application and excellent wound healing. *Int. J. Pharm. X.* 495 (1), 67–74. doi:10.1016/j.ijpharm.2015.08.082

Kim, J., Kim, S., Son, D., and Shin, M. (2021). Phenol-hyaluronic acid conjugates: Correlation of oxidative crosslinking pathway and adhesiveness. *Polym. (Basel)* 13 (18), 3130. doi:10.3390/polym13183130

Kirker, K. R., Luo, Y., Nielson, J. H., Shelby, J., and Prestwich, G. D. (2002). Glycosaminoglycan hydrogel films as bio-interactive dressings for wound healing. *Biomaterials* 23 (17), 3661–3671. doi:10.1016/s0142-9612(02)00100-x

Kondo, S., Niiyama, H., Yu, A., and Kuroyanagi, Y. (2012). Evaluation of a wound dressing composed of hyaluronic acid and collagen sponge containing epidermal growth factor in diabetic mice. *J. Biomaterials Sci. Polym. Ed.* 23 (13), 1729–1740. doi:10.1163/092050611x597799

Kouketsu, A., Shimizu, Y., Nogami, S., Yamada-Fujiwara, M., Nagai, H., Yamauchi, K., et al. (2021). Wound healing effect of autologous fibrin glue and polyglycolic acid sheets in a rat back skin defect model. *Transfus. Apher. Sci.* 60 (4), 103144. doi:10.1016/j.transci.2021.103144

Koyuncu, A., Koç, S., Akdere Ö, E., Çakmak, A. S., and Gümüşderelioğlu, M. (2022). Investigation of the synergistic effect of platelet-rich plasma and polychromatic light on human dermal fibroblasts seeded chitosan/gelatin scaffolds for wound healing. *J. Photochem. Photobiol. B Biol.* 232, 112476. doi:10.1016/j.jphotobiol.2022.112476

Kumar, P. T., Lakshmanan, V. K., Biswas, R., Nair, S. V., and Jayakumar, R. (2012). Synthesis and biological evaluation of chitin hydrogel/nano ZnO composite bandage as antibacterial wound dressing. *J. Biomed. Nanotechnol.* 8 (6), 891–900. doi:10.1166/jbn.2012.1461

Kundu, B., Rajkhowa, R., Kundu, S. C., and Wang, X. (2013). Silk fibroin biomaterials for tissue regenerations. *Adv. Drug Deliv. Rev.* 65 (4), 457–470. doi:10.1016/j.addr.2012.09.043

Kuo, Y. R., Wang, C. T., Cheng, J. T., Wang, F. S., Chiang, Y. C., and Wang, C. J. (2011). Bone marrow-derived mesenchymal stem cells enhanced diabetic wound healing through recruitment of tissue regeneration in a rat model of streptozotocin-induced diabetes. *Plastic Reconstr. Surg.* 128 (4), 872–880. doi:10.1097/prs.0b013e3182174329

Lautner, G., Meyerhoff, M. E., and Schwendeman, S. P. (2016). Biodegradable poly(lactic-co-glycolic acid) microspheres loaded with S-nitroso-N-acetyl-D-penicillamine for controlled nitric oxide delivery. *J. Control. Release* 225, 133–139. doi:10.1016/j.jconrel.2015.12.056

Lee, C. H., Hsieh, M. J., Chang, S. H., Lin, Y. H., Liu, S. J., Lin, T. Y., et al. (2014). Enhancement of diabetic wound repair using biodegradable nanofibrous metformin-eluting membranes: *In vitro* and *in vivo*. *ACS Appl. Mat. Interfaces* 6 (6), 3979–3986. doi:10.1021/am405329g

Lee, C. H., Hung, K. C., Hsieh, M. J., Chang, S. H., Juang, J. H., Hsieh, I. C., et al. (2020a). Core-shell insulin-loaded nanofibrous scaffolds for repairing diabetic wounds. *Nanomedicine Nanotechnol. Biol. Med.* 24, 102123. doi:10.1016/j.nano.2019.102123

Lee, C. H., Liu, K. S., Cheng, C. W., Chan, E. C., Hung, K. C., Hsieh, M. J., et al. (2020b). Codelivery of sustainable antimicrobial agents and platelet-derived growth factor via biodegradable nanofibers for repair of diabetic infectious wounds. *ACS Infect. Dis.* 6 (10), 2688–2697. doi:10.1021/acsinfecdis.0c00321

Leng, Q., Li, Y., Pang, X., Wang, B., Wu, Z., Lu, Y., et al. (2020). Curcumin nanoparticles incorporated in PVA/collagen composite films promote wound healing. *Drug Deliv. (Lond).* 27 (1), 1676–1685. doi:10.1080/10717544.2020.1853280

Li, P., Ruan, L., Wang, R., Liu, T., Song, G., Gao, X., et al. (2021). Electrospun scaffold of collagen and polycaprolactone containing ZnO quantum dots for skin wound regeneration. *J. Bionic Eng.* 18 (6), 1378–1390. doi:10.1007/s42235-021-00115-7

Li, Y., Wang, J., Qian, D., Chen, L., Mo, X., Wang, L., et al. (2021). Electrospun fibrous sponge via short fiber for mimicking 3D ECM. *J. Nanobiotechnology* 19 (1), 131. doi:10.1186/s12951-021-00878-5

Li, Y., Zhang, X., He, D., Ma, Z., Xue, K., and Li, H. (2022). 45S5 Bioglass® works synergistically with siRNA to downregulate the expression of matrix metalloproteinase-9 in diabetic wounds. *Acta Biomater.* 145, 372–389. doi:10.1016/j.actbio.2022.04.010

Lin, Z., Zhao, C., Lei, Z., Zhang, Y., Huang, R., Lin, B., et al. (2021). Epidermal stem cells maintain stemness via a biomimetic micro/nanofiber scaffold that promotes wound healing by activating the Notch signaling pathway. *Stem Cell Res. Ther.* 12 (1), 341. doi:10.1186/s13287-021-02418-2

Lipsky, B. A., Kuss, M., Edmonds, M., Reyzelman, A., and Sigal, F. (2012). Topical application of a gentamicin-collagen sponge combined with systemic antibiotic therapy for the treatment of diabetic foot infections of moderate severity: A randomized, controlled, multicenter clinical trial. *J. Am. Podiatr. Med. Assoc.* 102 (3), 223–232. doi:10.7547/1020223

Liu, C., Zeng, H., Chen, Z., Ge, Z., Wang, B., Liu, B., et al. (2022). Sprayable methacrylic anhydride-modified gelatin hydrogel combined with bionic neutrophils nanoparticles for scar-free wound healing of diabetes mellitus. *Int. J. Biol. Macromol.* 202, 418–430. doi:10.1016/j.ijbiomac.2022.01.083

Liu, H., Li, Z., Zhao, Y., Feng, Y., Zvyagin, A. V., Wang, J., et al. (2021). Novel diabetic foot wound dressing based on multifunctional hydrogels with extensive temperature-tolerant, durable, adhesive, and intrinsic antibacterial properties. *ACS Appl. Mat. Interfaces* 13 (23), 26770–26781. doi:10.1021/acsami.1c05514

Liu, W., Gao, R., Yang, C., Feng, Z., Ou-Yang, W., Pan, X., et al. (2022). ECM-mimetic immunomodulatory hydrogel for methicillin-resistant Staphylococcus aureus-infected chronic skin wound healing. *Sci. Adv.* 8 (27), eabn7006. doi:10.1126/sciadv.abn7006

Löndahl, M., Katzman, P., Nilsson, A., and Hammarlund, C. (2010). Hyperbaric oxygen therapy facilitates healing of chronic foot ulcers in patients with diabetes. *Diabetes Care* 33 (5), 998–1003. doi:10.2337/dc09-1754

Long, L. Y., Liu, W., Li, L., Hu, C., He, S., Lu, L., et al. (2022). Dissolving microneedle-encapsulated drug-loaded nanoparticles and recombinant humanized collagen type III for the treatment of chronic wound via anti-inflammation and enhanced cell proliferation and angiogenesis. *Nanoscale* 14 (4), 1285–1295. doi:10.1039/d1nr07708b

Losi, P., Briganti, E., Errico, C., Lisella, A., Sanguinetti, E., Chiellini, F., et al. (2013). Fibrin-based scaffold incorporating VEGF- and bFGF-loaded nanoparticles stimulates wound healing in diabetic mice. *Acta Biomater.* 9 (8), 7814–7821. doi:10.1016/j.actbio.2013.04.019

Louiselle, A. E., Niemiec, S. M., Zgheib, C., and Liechty, K. W. (2021). Macrophage polarization and diabetic wound healing. *Transl. Res.* 236, 109–116. doi:10.1016/j.trsl.2021.05.006

Lu, W., Wei, Z., Gu, Z. Y., Liu, T. F., Park, J., Park, J., et al. (2014). Tuning the structure and function of metal-organic frameworks via linker design. *Chem. Soc. Rev.* 43 (16), 5561–5593. doi:10.1039/c4cs00003j

Lutzke, A., Neufeld, B. H., Neufeld, M. J., and Reynolds, M. M. (2016). Nitric oxide release from a biodegradable cysteine-based polyphosphazene. *J. Mat. Chem. B* 4 (11), 1987–1998. doi:10.1039/c6tb00037a

Lv, F., Wang, J., Xu, P., Han, Y., Ma, H., Xu, H., et al. (2017). A conducive bioceramic/polymer composite biomaterial for diabetic wound healing. *Acta Biomater.* 60, 128–143. doi:10.1016/j.actbio.2017.07.020

Ma, Z., Song, W., He, Y., and Li, H. (2020). Multilayer injectable hydrogel system sequentially delivers bioactive substances for each wound healing stage. *ACS Appl. Mat. Interfaces* 12 (26), 29787–29806. doi:10.1021/acsami.0c06360

Marelli, B., Le Nihouannen, D., Hacking, S. A., Tran, S., Li, J., Murshed, M., et al. (2015). Newly identified interfibrillar collagen crosslinking suppresses cell proliferation and remodelling. *Biomaterials* 54, 126–135. doi:10.1016/j.biomaterials.2015.03.018

Masood, N., Ahmed, R., Tariq, M., Ahmed, Z., Masoud, M. S., Ali, I., et al. (2019). Silver nanoparticle impregnated chitosan-PEG hydrogel enhances wound healing in diabetes induced rabbits. *Int. J. Pharm. X.* 559, 23–36. doi:10.1016/j.ijpharm.2019.01.019

Meamar, R., Ghasemi-Mobarakeh, L., Norouzi, M. R., Siavash, M., Hamblin, M. R., and Fesharaki, M. (2021). Improved wound healing of diabetic foot ulcers using human placenta-derived mesenchymal stem cells in gelatin electrospun nanofibrous scaffolds plus a platelet-rich plasma gel: A randomized clinical trial. *Int. Immunopharmacol.* 101, 108282. doi:10.1016/j.intimp.2021.108282

Meaume, S., Dompmartin, A., Lok, C., Lazareth, I., Sigal, M., Truchetet, F., et al. (2017). Quality of life in patients with leg ulcers: Results from CHALLENGE, a double-blind randomised controlled trial. *J. Wound Care* 26 (7), 368–379. doi:10.12968/jowc.2017.26.7.368

Miguel, S. P., Ribeiro, M. P., Brancal, H., Coutinho, P., and Correia, I. J. (2014). Thermoresponsive chitosan-agarose hydrogel for skin regeneration. *Carbohydr. Polym.* 111, 366–373. doi:10.1016/j.carbpol.2014.04.093

Miller, M. R., and Megson, I. L. (2007). Recent developments in nitric oxide donor drugs. *Br. J. Pharmacol.* 151 (3), 305–321. doi:10.1038/sj.bjp.0707224

Mohandas, A., Anisha, B. S., Chennazhi, K. P., and Jayakumar, R. (2015). Chitosan-hyaluronic acid/VEGF loaded fibrin nanoparticles composite sponges for enhancing angiogenesis in wounds. *Colloids Surfaces B Biointerfaces* 127, 105–113. doi:10.1016/j.colsurfb.2015.01.024

Mohanty, C., and Pradhan, J. (2020). A human epidermal growth factor-curcumin bandage bioconjugate loaded with mesenchymal stem cell for *in vivo* diabetic wound healing. *Mater. Sci. Eng. C* 111, 110751. doi:10.1016/j.msec.2020.110751

Moon, K. C., Lee, J. S., Han, S. K., Lee, H. W., and Dhong, E. S. (2017). Effects of human umbilical cord blood-derived mesenchymal stromal cells and dermal fibroblasts on diabetic wound healing. *Cytotherapy* 19 (7), 821–828. doi:10.1016/j.jcyt.2017.03.074

Moore, Z. E., Corcoran, M. A., and Patton, D. (2020). Nutritional interventions for treating foot ulcers in people with diabetes. *Cochrane Database Syst. Rev.* 7 (7), Cd011378. doi:10.1002/14651858.CD011378.pub2

Morimoto, N., Kakudo, N., Matsui, M., Ogura, T., Hara, T., Suzuki, K., et al. (2015). Exploratory clinical trial of combination wound therapy with a gelatin sheet and platelet-rich plasma in patients with chronic skin ulcers: Study protocol. *BMJ Open* 5 (5), e007733. doi:10.1136/bmjopen-2015-007733

Moura, L. I., Dias, A. M., Leal, E. C., Carvalho, L., de Sousa, H. C., and Carvalho, E. (2014). Chitosan-based dressings loaded with neurotensin--an efficient strategy to improve early diabetic wound healing. *Acta Biomater.* 10 (2), 843–857. doi:10.1016/j.actbio.2013.09.040

Mutluoglu, M. (2018). Comment on Santema et al. Hyperbaric Oxygen Therapy in the Treatment of Ischemic Lower-Extremity Ulcers in Patients With Diabetes: Results of the DAMO(2)CLES Multicenter Randomized Clinical Trial. Diabetes Care 2018;41:112-119. *Diabetes Care* 41 (4), e61. doi:10.2337/dc17-2440

Muxika, A., Etxabide, A., Uranga, J., Guerrero, P., and de la Caba, K. (2017). Chitosan as a bioactive polymer: Processing, properties and applications. *Int. J. Biol. Macromol.* 105 (2), 1358–1368. doi:10.1016/j.ijbiomac.2017.07.087

Na, J., Song, S. Y., Kim, J. D., Han, M., Heo, J. S., Yang, C. E., et al. (2018). Protein-engineered large area adipose-derived stem cell sheets for wound healing. *Sci. Rep.* 8 (1), 15869. doi:10.1038/s41598-018-34119-x

Nanditha, C. K., and Kumar, G. S. V. (2022). Bioactive peptides laden nano and micro-sized particles enriched ECM inspired dressing for skin regeneration in diabetic wounds. *Mat. Today Bio* 14, 100235. doi:10.1016/j.mtbio.2022.100235

Naomi, R., Ratanavaraporn, J., and Fauzi, M. B. (2020). Comprehensive review of hybrid collagen and silk fibroin for cutaneous wound healing. *Mater. (Basel)* 13 (14), 3097. doi:10.3390/ma13143097

Nilforoushzadeh, M. A., Sisakht, M. M., Amirkhani, M. A., Seifalian, A. M., Banafshe, H. R., Verdi, J., et al. (2020). Engineered skin graft with stromal vascular fraction cells encapsulated in fibrin-collagen hydrogel: A clinical study for diabetic wound healing. *J. Tissue Eng. Regen. Med.* 14 (3), 424–440. doi:10.1002/term.3003

Nilforoushzadeh, M. A., Sisakht, M. M., Seifalian, A. M., Amirkhani, M. A., Banafshe, H. R., Verdi, J., et al. (2017). Regenerative medicine applications in wound care. *Curr. Stem Cell Res. Ther.* 12 (8), 658–674. doi:10.2174/1574888x12666170929123842

Nube, V. L., Alison, J. A., and Twigg, S. M. (2021). Frequency of sharp wound debridement in the management of diabetes-related foot ulcers: Exploring current practice. *J. Foot Ankle Res.* 14 (1), 52. doi:10.1186/s13047-021-00489-1

Pakyari, M., Farrokhi, A., Maharlooei, M. K., and Ghahary, A. (2013). Critical role of transforming growth factor beta in different phases of wound healing. *Adv. Wound Care (New. Rochelle.* 2 (5), 215–224. doi:10.1089/wound.2012.0406

Pan, S., Guan, Y., Ma, Y., Cui, Q., Tang, Z., Li, J., et al. (2022). Advanced glycation end products correlate with breast cancer metastasis by activating RAGE/TLR4 signaling. *BMJ Open Diabetes Res. Care* 10 (2), e002697. doi:10.1136/bmjdrc-2021-002697

Peña-Villalobos, I., Casanova-Maldonado, I., Lois, P., Prieto, C., Pizarro, C., Lattus, J., et al. (2018). Hyperbaric oxygen increases stem cell proliferation, angiogenesis and wound-healing ability of WJ-MSCs in diabetic mice. *Front. Physiol.* 9, 995. doi:10.3389/fphys.2018.00995

Pérez-Rafael, S., Ivanova, K., Stefanov, I., Puiggalí, J., Del Valle, L. J., Todorova, K., et al. (2021). Nanoparticle-driven self-assembling injectable hydrogels provide a multi-factorial approach for chronic wound treatment. *Acta Biomater.* 134, 131–143. doi:10.1016/j.actbio.2021.07.020

Pyun, D. G., Choi, H. J., Yoon, H. S., Thambi, T., and Lee, D. S. (2015). Polyurethane foam containing rhEGF as a dressing material for healing diabetic wounds: Synthesis, characterization, *in vitro* and *in vivo* studies. *Colloids Surfaces B Biointerfaces* 135, 699–706. doi:10.1016/j.colsurfb.2015.08.029

Qian, Y., Li, L., Jiang, C., Xu, W., Lv, Y., Zhong, L., et al. (2015). The effect of hyaluronan on the motility of skin dermal fibroblasts in nanofibrous scaffolds. *Int. J. Biol. Macromol.* 79, 133–143. doi:10.1016/j.ijbiomac.2015.04.059

Qian, Y., Li, L., Song, Y., Dong, L., Chen, P., Li, X., et al. (2018). Surface modification of nanofibrous matrices via layer-by-layer functionalized silk assembly for mitigating the foreign body reaction. *Biomaterials* 164, 22–37. doi:10.1016/j.biomaterials.2018.02.038

Qian, Z., Wang, H., Bai, Y., Wang, Y., Tao, L., Wei, Y., et al. (2020). Improving chronic diabetic wound healing through an injectable and self-healing hydrogel with platelet-rich plasma release. *ACS Appl. Mat. Interfaces* 12 (50), 55659–55674. doi:10.1021/acsami.0c17142

Ramanathan, G., Singaravelu, S., Muthukumar, T., Thyagarajan, S., Perumal, P. T., and Sivagnanam, U. T. (2017). Design and characterization of 3D hybrid collagen matrixes as a dermal substitute in skin tissue engineering. *Mater. Sci. Eng. C* 72, 359–370. doi:10.1016/j.msec.2016.11.095

Rayman, G., Vas, P., Dhatariya, K., Driver, V., Hartemann, A., Londahl, M., et al. (2020). IWGDF guidance on use of interventions to enhance the healing of chronic ulcers of the foot in diabetes. *Diabetes. Metab. Res. Rev.* 36 (1), 75–83. doi:10.1002/dmrr.2700

Ren, S., Wang, C., and Guo, S. (2022). Review of the role of mesenchymal stem cells and exosomes derived from mesenchymal stem cells in the treatment of orthopedic disease. *Med. Sci. Monit.* 28, e935937. doi:10.12659/msm.935937

Ren, X., Han, Y., Wang, J., Jiang, Y., Yi, Z., Xu, H., et al. (2018). An aligned porous electrospun fibrous membrane with controlled drug delivery - an efficient strategy to accelerate diabetic wound healing with improved angiogenesis. *Acta Biomater.* 70, 140–153. doi:10.1016/j.actbio.2018.02.010

Ren, Y., Aierken, A., Zhao, L., Lin, Z., Jiang, J., Li, B., et al. (2022). hUC-MSCs lyophilized powder loaded polysaccharide ulvan driven functional hydrogel for chronic diabetic wound healing. *Carbohydr. Polym.* 288, 119404. doi:10.1016/j.carbpol.2022.119404

Saghazadeh, S., Rinoldi, C., Schot, M., Kashaf, S. S., Sharifi, F., Jalilian, E., et al. (2018). Drug delivery systems and materials for wound healing applications. *Adv. Drug Deliv. Rev.* 127, 138–166. doi:10.1016/j.addr.2018.04.008

Samadian, H., Zamiri, S., Ehterami, A., Farzamfar, S., Vaez, A., Khastar, H., et al. (2020). Electrospun cellulose acetate/gelatin nanofibrous wound dressing containing berberine for diabetic foot ulcer healing: *In vitro* and *in vivo* studies. *Sci. Rep.* 10 (1), 8312. doi:10.1038/s41598-020-65268-7

Sanhueza, C., Hermosilla, J., Bugallo-Casal, A., Da Silva-Candal, A., Taboada, C., Millán, R., et al. (2021). One-step electrospun scaffold of dual-sized gelatin/poly-3-hydroxybutyrate nano/microfibers for skin regeneration in diabetic wound. *Mater. Sci. Eng. C* 119, 111602. doi:10.1016/j.msec.2020.111602

Santarella, F., Sridharan, R., Marinkovic, M., Do Amaral, R., Cavanagh, B., Smith, A., et al. (2020). Scaffolds functionalized with matrix from induced pluripotent stem cell fibroblasts for diabetic wound healing. *Adv. Healthc. Mat.* 9 (16), e2000307. doi:10.1002/adhm.202000307

Schaper, N. C., van Netten, J. J., Apelqvist, J., Bus, S. A., Hinchliffe, R. J., Lipsky, B. A., et al. (2020). Practical Guidelines on the prevention and management of diabetic foot disease (IWGDF 2019 update). *Diabetes. Metab. Res. Rev.* 36 (1), e3266. doi:10.1002/dmrr.3266

Shen, J., Zhou, Z., Chen, D., Wang, Y., He, Y., Wang, D., et al. (2021). Poly(aspartic acid) based self-healing hydrogels with antibacterial and light-emitting properties for wound repair. *Colloids Surfaces B Biointerfaces* 200, 111568. doi:10.1016/j.colsurfb.2021.111568

Shettigar, K., and Murali, T. S. (2020). Virulence factors and clonal diversity of *Staphylococcus aureus* in colonization and wound infection with emphasis on diabetic foot infection. *Eur. J. Clin. Microbiol. Infect. Dis.* 39 (12), 2235–2246. doi:10.1007/s10096-020-03984-8

Shi, G., Chen, W., Zhang, Y., Dai, X., Zhang, X., and Wu, Z. (2019). An antifouling hydrogel containing silver nanoparticles for modulating the therapeutic immune response in chronic wound healing. *Langmuir* 35 (5), 1837–1845. doi:10.1021/acs.langmuir.8b01834

Shiekh, P. A., Singh, A., and Kumar, A. (2020). Exosome laden oxygen releasing antioxidant and antibacterial cryogel wound dressing OxOBand alleviate diabetic and infectious wound healing. *Biomaterials* 249, 120020. doi:10.1016/j.biomaterials.2020.120020

Shiekh, P. A., Singh, A., and Kumar, A. (2018). Oxygen-releasing antioxidant cryogel scaffolds with sustained oxygen delivery for tissue engineering applications. *ACS Appl. Mat. Interfaces* 10 (22), 18458–18469. doi:10.1021/acsami.8b01736

Shin, Y. C., Shin, D. M., Lee, E. J., Lee, J. H., Kim, J. E., Song, S. H., et al. (2016). Hyaluronic acid/PLGA core/shell fiber matrices loaded with EGCG beneficial to diabetic wound healing. *Adv. Healthc. Mat.* 5 (23), 3035–3045. doi:10.1002/adhm.201600658

Shook, B. A., Wasko, R. R., Mano, O., Rutenberg-Schoenberg, M., Rudolph, M. C., Zirak, B., et al. (2020). Dermal adipocyte lipolysis and myofibroblast conversion are required for efficient skin repair. *Cell Stem Cell* 26 (6), 880–895.e6. doi:10.1016/j.stem.2020.03.013

Sun, L., Li, J., Gao, W., Shi, M., Tang, F., Fu, X., et al. (2021). Coaxial nanofibrous scaffolds mimicking the extracellular matrix transition in the wound healing process promoting skin regeneration through enhancing immunomodulation. *J. Mat. Chem. B* 9 (5), 1395–1405. doi:10.1039/d0tb01933j

Taghipour, Y. D., Hokmabad, V. R., Del Bakhshayesh, A. R., Asadi, N., Salehi, R., and Nasrabadi, H. T. (2020). The application of hydrogels based on natural polymers for tissue engineering. *Curr. Med. Chem.* 27 (16), 2658–2680. doi:10.2174/0929867326666190711103956

Tallapaneni, V., Kalaivani, C., Pamu, D., Mude, L., Singh, S. K., and Karri, V. (2021). Acellular scaffolds as innovative biomaterial platforms for the management of diabetic wounds. *Tissue Eng. Regen. Med.* 18 (5), 713–734. doi:10.1007/s13770-021-00344-1

Tang, J., Chen, J., Guo, J., Wei, Q., and Fan, H. (2018). Construction and evaluation of fibrillar composite hydrogel of collagen/konjac glucomannan for potential biomedical applications. *Regen. Biomater.* 5 (4), 239–250. doi:10.1093/rb/rby018

Tang, P., Han, L., Li, P., Jia, Z., Wang, K., Zhang, H., et al. (2019). Mussel-Inspired electroactive and antioxidative scaffolds with incorporation of polydopamine-reduced graphene oxide for enhancing skin wound healing. *ACS Appl. Mat. Interfaces* 11 (8), 7703–7714. doi:10.1021/acsami.8b18931

Tavakoli, S., Mokhtari, H., Kharaziha, M., Kermanpur, A., Talebi, A., and Moshtaghian, J. (2020). A multifunctional nanocomposite spray dressing of Kappa-carrageenan-polydopamine modified ZnO/L-glutamic acid for diabetic wounds. *Mater. Sci. Eng. C* 111, 110837. doi:10.1016/j.msec.2020.110837

Teng, Y. J., Li, Y. P., Wang, J. W., Yang, K. H., Zhang, Y. C., Wang, Y. J., et al. (2010). Bioengineered skin in diabetic foot ulcers. *Diabetes Obes. Metab.* 12 (4), 307–315. doi:10.1111/j.1463-1326.2009.01164.x

Thangavel, P., Ramachandran, B., Chakraborty, S., Kannan, R., Lonchin, S., and Muthuvijayan, V. (2017). Accelerated healing of diabetic wounds treated with L-glutamic acid loaded hydrogels through enhanced collagen deposition and angiogenesis: An *in vivo* study. *Sci. Rep.* 7 (1), 10701. doi:10.1038/s41598-017-10882-1

Thom, S. R. (2011). Hyperbaric oxygen: Its mechanisms and efficacy. *Plastic Reconstr. Surg.* 127 (1), 131s–141s. doi:10.1097/prs.0b013e3181fbe2bf

Tripathi, D., Rastogi, K., Tyagi, P., Rawat, H., Mittal, G., Jamini, A., et al. (2021). Comparative analysis of collagen and chitosan-based dressing for haemostatic and wound healing application. *AAPS PharmSciTech* 22 (3), 76. doi:10.1208/s12249-021-01944-9

Tuhin, R. H., Begum, M. M., Rahman, M. S., Karim, R., Begum, T., Ahmed, S. U., et al. (2017). Wound healing effect of Euphorbia hirta linn. (Euphorbiaceae) in alloxan induced diabetic rats. *BMC Complement. Altern. Med.* 17 (1), 423. doi:10.1186/s12906-017-1930-x

Vermeulen, H., Ubbink, D. T., Goossens, A., de Vos, R., and Legemate, D. A. (2005). Systematic review of dressings and topical agents for surgical wounds healing by secondary intention. *Br. J. Surg.* 92 (6), 665–672. doi:10.1002/bjs.5055

Vogt, L., Ruther, F., Salehi, S., and Boccaccini, A. R. (2021). Poly(Glycerol sebacate) in biomedical applications-A review of the recent literature. *Adv. Healthc. Mat.* 10 (9), e2002026. doi:10.1002/adhm.202002026

Vuerstaek, J. D., Vainas, T., Wuite, J., Nelemans, P., Neumann, M. H., and Veraart, J. C. (2006). State-of-the-art treatment of chronic leg ulcers: A randomized controlled trial comparing vacuum-assisted closure (V.A.C.) with modern wound dressings. *J. Vasc. Surg.* 44 (5), 1029–1037. discussion 1038. doi:10.1016/j.jvs.2006.07.030

Wang, J., Lin, J., Chen, L., Deng, L., and Cui, W. (2022). Endogenous electric-field-coupled electrospun short fiber via collecting wound exudation. *Adv. Mat.* 34 (9), e2108325. doi:10.1002/adma.202108325

Wang, L., Xia, K., Han, L., Zhang, M., Fan, J., Song, L., et al. (2022). Electrospinning of botanicals for skin wound healing. *Front. Bioeng. Biotechnol.* 10, 1006129. doi:10.3389/fbioe.2022.1006129

Wang, W., Lu, K. J., Yu, C. H., Huang, Q. L., and Du, Y. Z. (2019). Nano-drug delivery systems in wound treatment and skin regeneration. *J. Nanobiotechnology* 17 (1), 82. doi:10.1186/s12951-019-0514-y

Wei, S., Xu, P., Yao, Z., Cui, X., Lei, X., Li, L., et al. (2021). A composite hydrogel with co-delivery of antimicrobial peptides and platelet-rich plasma to enhance healing of infected wounds in diabetes. *Acta Biomater.* 124, 205–218. doi:10.1016/j.actbio.2021.01.046

Wolcott, R. D., Rumbaugh, K. P., James, G., Schultz, G., Phillips, P., Yang, Q., et al. (2010). Biofilm maturity studies indicate sharp debridement opens a time-dependent therapeutic window. *J. Wound Care* 19 (8), 320–328. doi:10.12968/jowc.2010.19.8.77709

Wu, K., Fu, M., Zhao, Y., Gerhard, E., Li, Y., Yang, J., et al. (2023). Anti-oxidant anti-inflammatory and antibacterial tannin-crosslinked citrate-based mussel-inspired bioadhesives facilitate scarless wound healing. *Bioact. Mat.* 20, 93–110. doi:10.1016/j.bioactmat.2022.05.017

Wu, S., Yang, Y., Wang, S., Dong, C., Zhang, X., Zhang, R., et al. (2022). Dextran and peptide-based pH-sensitive hydrogel boosts healing process in multidrug-resistant bacteria-infected wounds. *Carbohydr. Polym.* 278, 118994. doi:10.1016/j.carbpol.2021.118994

Wu, Y. Y., Jiao, Y. P., Xiao, L. L., Li, M. M., Liu, H. W., Li, S. H., et al. (2018). Experimental study on effects of adipose-derived stem cell-seeded silk fibroin chitosan film on wound healing of a diabetic rat model. *Ann. Plast. Surg.* 80 (5), 572–580. doi:10.1097/sap.0000000000001355

Xia, G., Zhai, D., Sun, Y., Hou, L., Guo, X., Wang, L., et al. (2020). Preparation of a novel asymmetric wettable chitosan-based sponge and its role in promoting chronic wound healing. *Carbohydr. Polym.* 227, 115296. doi:10.1016/j.carbpol.2019.115296

Xia, Y., Chen, J., Ding, J., Zhang, J., and Chen, H. (2020). IGF1- and BM-MSC-incorporating collagen-chitosan scaffolds promote wound healing and hair follicle regeneration. *Am. J. Transl. Res.* 12 (10), 6264–6276.

Xiao, J., Chen, S., Yi, J., Zhang, H., and Ameer, G. A. (2017). A cooperative copper metal-organic framework-hydrogel system improves wound healing in diabetes. *Adv. Funct. Mat.* 27 (1), 1604872. doi:10.1002/adfm.201604872

Xiao, J., Ma, Y., Wang, W., Zhang, K., Tian, X., Zhao, K., et al. (2021). Incorporation of gelatin improves toughness of collagen films with a homo-hierarchical structure. *Food Chem. x.* 345, 128802. doi:10.1016/j.foodchem.2020.128802

Xie, H., Chen, X., Shen, X., He, Y., Chen, W., Luo, Q., et al. (2018). Preparation of chitosan-collagen-alginate composite dressing and its promoting effects on wound healing. *Int. J. Biol. Macromol.* 107, 93–104. doi:10.1016/j.ijbiomac.2017.08.142

Xin, Y., Xu, P., Wang, X., Chen, Y., Zhang, Z., and Zhang, Y. (2021). Human foreskin-derived dermal stem/progenitor cell-conditioned medium combined with hyaluronic acid promotes extracellular matrix regeneration in diabetic wounds. *Stem Cell Res. Ther.* 12 (1), 49. doi:10.1186/s13287-020-02116-5

Xu, T., Yang, R., Ma, X., Chen, W., Liu, S., Liu, X., et al. (2019). Bionic poly(γ-glutamic acid) electrospun fibrous scaffolds for preventing hypertrophic scars. *Adv. Healthc. Mat.* 8 (13), e1900123. doi:10.1002/adhm.201900123

Yang, Y., Wang, C., Wang, N., Li, J., Zhu, Y., Zai, J., et al. (2022). Photogenerated reactive oxygen species and hyperthermia by Cu(3)SnS(4) nanoflakes for advanced photocatalytic and photothermal antibacterial therapy. *J. Nanobiotechnology* 20 (1), 195. doi:10.1186/s12951-022-01403-y

Yanina, I. Y., Navolokin, N. A., Svenskaya, Y. I., Bucharskaya, A. B., Maslyakova, G. N., Gorin, D. A., et al. (2017). Morphology alterations of skin and subcutaneous fat at NIR laser irradiation combined with delivery of encapsulated indocyanine green. *J. Biomed. Opt.* 22 (5), 055008. doi:10.1117/1.jbo.22.5.055008

Yao, S., Wang, Y., Chi, J., Yu, Y., Zhao, Y., Luo, Y., et al. (2022a). Porous MOF microneedle array patch with photothermal responsive nitric oxide delivery for wound healing. *Adv. Sci. (Weinh).* 9 (3), e2103449. doi:10.1002/advs.202103449

Yao, S., Zhao, Y., Xu, Y., Jin, B., Wang, M., Yu, C., et al. (2022b). Injectable dual-dynamic-bond cross-linked hydrogel for highly efficient infected diabetic wound healing. *Adv. Healthc. Mat.* 11 (14), e2200516. doi:10.1002/adhm.202200516

Ye, J. P., Gong, J. S., Su, C., Liu, Y. G., Jiang, M., Pan, H., et al. (2020). Fabrication and characterization of high molecular keratin based nanofibrous membranes for

wound healing. *Colloids Surfaces B Biointerfaces* 194, 111158. doi:10.1016/j.colsurfb.2020.111158

Yin, M., Wang, X., Yu, Z., Wang, Y., Wang, X., Deng, M., et al. (2020). γ-PGA hydrogel loaded with cell-free fat extract promotes the healing of diabetic wounds. *J. Mat. Chem. B* 8 (36), 8395–8404. doi:10.1039/d0tb01190h

Yin, X., Huang, S., Xu, S., Chang, L., Zhao, X., Chen, Z., et al. (2022). Preparation of pro-angiogenic, antibacterial and EGCG-modified ZnO quantum dots for treating bacterial infected wound of diabetic rats. *Biomater. Adv.* 133, 112638. doi:10.1016/j.msec.2021.112638

Yu, M., Huang, J., Zhu, T., Lu, J., Liu, J., Li, X., et al. (2020). Liraglutide-loaded PLGA/gelatin electrospun nanofibrous mats promote angiogenesis to accelerate diabetic wound healing via the modulation of miR-29b-3p. *Biomater. Sci.* 8 (15), 4225–4238. doi:10.1039/d0bm00442a

Yu, X., Fu, X., Yang, J., Chen, L., Leng, F., Yang, Z., et al. (2022). Glucose/ROS cascade-responsive ceria nanozymes for diabetic wound healing. *Mat. Today Bio* 15, 100308. doi:10.1016/j.mtbio.2022.100308

Zahid, A. A., Augustine, R., Dalvi, Y. B., Reshma, K., Ahmed, R., Raza Ur Rehman, S., et al. (2021). Development of nitric oxide releasing visible light crosslinked gelatin methacrylate hydrogel for rapid closure of diabetic wounds. *Biomed. Pharmacother.* 140, 111747. doi:10.1016/j.biopha.2021.111747

Zehra, M., Zubairi, W., Hasan, A., Butt, H., Ramzan, A., Azam, M., et al. (2020). Oxygen generating polymeric nano fibers that stimulate angiogenesis and show efficient wound healing in a diabetic wound model. *Int. J. Nanomedicine* 15, 3511–3522. doi:10.2147/ijn.s248911

Zeng, Y., Zhu, L., Han, Q., Liu, W., Mao, X., Li, Y., et al. (2015). Preformed gelatin microcryogels as injectable cell carriers for enhanced skin wound healing. *Acta Biomater.* 25, 291–303. doi:10.1016/j.actbio.2015.07.042

Zha, S., Utomo, Y. K. S., Yang, L., Liang, G., and Liu, W. (2022). Mechanic-driven biodegradable polyglycolic acid/silk fibroin nanofibrous scaffolds containing deferoxamine accelerate diabetic wound healing. *Pharmaceutics* 14 (3), 601. doi:10.3390/pharmaceutics14030601

Zhang, H., Cheng, J., and Ao, Q. (2021). Preparation of alginate-based biomaterials and their applications in biomedicine. *Mar. Drugs* 19 (5), 264. doi:10.3390/md19050264

Zhang, H., Wu, X., Quan, L., and Ao, Q. (2022). Characteristics of marine biomaterials and their applications in biomedicine. *Mar. Drugs* 20 (6), 372. doi:10.3390/md20060372

Zhang, L., Ma, Y., Pan, X., Chen, S., Zhuang, H., and Wang, S. (2018). A composite hydrogel of chitosan/heparin/poly (γ-glutamic acid) loaded with superoxide dismutase for wound healing. *Carbohydr. Polym.* 180, 168–174. doi:10.1016/j.carbpol.2017.10.036

Zhang, P., Lu, J., Jing, Y., Tang, S., Zhu, D., and Bi, Y. (2017). Global epidemiology of diabetic foot ulceration: A systematic review and meta-analysis (†). *Ann. Med.* 49 (2), 106–116. doi:10.1080/07853890.2016.1231932

Zhang, X., Liu, Y., Zhang, S., Shen, T., Wang, J., and Liu, C. (2018). Potentiation effect on accelerating diabetic wound healing using 2-N, 6-O-sulfated chitosan-doped PLGA scaffold. *RSC Adv.* 8 (34), 19085–19097. doi:10.1039/c8ra02153h

Zhang, Y., Liang, R. J., Xu, J. J., Shen, L. F., Gao, J. Q., Wang, X. P., et al. (2017). Efficient induction of antimicrobial activity with vancomycin nanoparticle-loaded poly(trimethylene carbonate) localized drug delivery system. *Int. J. Nanomedicine* 12, 1201–1214. doi:10.2147/ijn.s127715

Zhao, C., Chen, R., Chen, Z., Lu, Q., Zhu, H., Bu, Q., et al. (2021). Bioinspired multifunctional cellulose nanofibril-based *in situ* Liquid wound dressing for multiple synergistic therapy of the postoperative infected wound. *ACS Appl. Mat. Interfaces* 13 (43), 51578–51591. doi:10.1021/acsami.1c18221

Zhao, L., Niu, L., Liang, H., Tan, H., Liu, C., and Zhu, F. (2017). pH and glucose dual-responsive injectable hydrogels with insulin and fibroblasts as bioactive dressings for diabetic wound healing. *ACS Appl. Mat. Interfaces* 9 (43), 37563–37574. doi:10.1021/acsami.7b09395

Zhao, X., Lang, Q., Yildirimer, L., Lin, Z. Y., Cui, W., Annabi, N., et al. (2016). Photocrosslinkable gelatin hydrogel for epidermal tissue engineering. *Adv. Healthc. Mat.* 5 (1), 108–118. doi:10.1002/adhm.201500005

Zheng, S., Huang, K., and Tong, T. (2021). Efficacy and mechanisms of oleuropein in mitigating diabetes and diabetes complications. *J. Agric. Food Chem.* 69 (22), 6145–6155. doi:10.1021/acs.jafc.1c01404

Zheng, Z., Liu, Y., Huang, W., Mo, Y., Lan, Y., Guo, R., et al. (2018). Neurotensin-loaded PLGA/CNC composite nanofiber membranes accelerate diabetic wound healing. *Artif. Cells Nanomed. Biotechnol.* 46 (2), 493–501. doi:10.1080/21691401.2018.1460372

Zhou, J., Wang, W., Zhang, Q., Zhang, Z., Guo, J., and Yan, F. (2022). Oxygen-supplied mesoporous carbon nanoparticles for enhanced photothermal/photodynamic synergetic therapy against antibiotic-resistant bacterial infections. *Chem. Sci.* 13 (23), 6967–6981. doi:10.1039/d2sc01740g

Zhu, Y., Hoshi, R., Chen, S., Yi, J., Duan, C., Galiano, R. D., et al. (2016). Sustained release of stromal cell derived factor-1 from an antioxidant thermoresponsive hydrogel enhances dermal wound healing in diabetes. *J. Control. Release* 238, 114–122. doi:10.1016/j.jconrel.2016.07.043

frontiers | Frontiers in Bioengineering and Biotechnology

TYPE Correction
PUBLISHED 06 January 2023
DOI 10.3389/fbioe.2022.1126860

OPEN ACCESS

APPROVED BY
Frontiers Editorial Office,
Frontiers Media SA, Switzerland

*CORRESPONDENCE
Liqun Yang,
yanglq@lnszjk.com.cn
Chenchao Wang,
wangchenchao@139.com

SPECIALTY SECTION
This article was submitted to Biomaterials, a section of the journal Frontiers in Bioengineering and Biotechnology

RECEIVED 18 December 2022
ACCEPTED 20 December 2022
PUBLISHED 06 January 2023

CITATION
Ren S, Guo S, Yang L and Wang C (2023), Corrigendum: Effect of composite biodegradable biomaterials on wound healing in diabetes.
Front. Bioeng. Biotechnol. 10:1126860.
doi: 10.3389/fbioe.2022.1126860

Corrigendum: Effect of composite biodegradable biomaterials on wound healing in diabetes

Sihang Ren[1,2,4], Shuaichen Guo[3], Liqun Yang[1]* and Chenchao Wang[2]*

[1]NHC Key Laboratory of Reproductive Health and Medical Genetics, Liaoning Research Institute of Family Planning, The Affiliated Reproductive Hospital of China Medical University, Shenyang, China, [2]Department of Plastic Surgery, The First Hospital of China Medical University, Shenyang, China, [3]The First Clinical College, China Medical University, Shenyang, China, [4]Department of Plastic Surgery, The Second Hospital of Dalian Medical University, Dalian, China

KEYWORDS

biodegradable biomaterials, diabetic wound, drug delivery systems (DDS), mesenchymal stem cells (MSCs), exosomes

A Corrigendum on
Effect of composite biodegradable biomaterials on wound healing in diabetes

by Ren S, Guo S, Yang L and Wang C (2022). Front. Bioeng. Biotechnol. 10:1060026. doi: 10.3389/fbioe.2022.1060026

In the published article, there was an error regarding the affiliation for "Sihang Ren." As well as having affiliations 1, 2 and 3, they should also have affiliation 4, which is as follows: "Department of Plastic Surgery, The Second Hospital of Dalian Medical University, Dalian, China".

Furthermore, in the published article, there was an error in the **Funding** statement. The Funding statement is not complete. The correct Funding statement appears below.

"This work was sponsored by the Natural Science Foundation of Liaoning Province (2022-YGJC-69) and the support program for excellent young scholars of China Medical University, the National Natural Science Foundation of China (grant/award no. 51872332) and Basic Research Project of the Education Department of Liaoning Province (grant/award no. LJKZ0740)."

The authors apologize for these errors and state that they do not change the scientific conclusions of the article in any way. The original article has been updated.

Publisher's note

All claims expressed in this article are solely those of the authors and do not necessarily represent those of their affiliated organizations, or those of the publisher, the editors and the reviewers. Any product that may be evaluated in this article, or claim that may be made by its manufacturer, is not guaranteed or endorsed by the publisher.

frontiers | Frontiers in Bioengineering and Biotechnology

TYPE Mini Review
PUBLISHED 16 February 2023
DOI 10.3389/fbioe.2023.1096525

OPEN ACCESS

EDITED BY
Shuai Jiang,
Max Planck Institute for Polymer Research, Germany

REVIEWED BY
Dongjin Wu,
The Second Hospital of Shandong University, China
Hailong Yu,
Northern Theater General Hospital, China
Fangqin Fu,
Ocean University of China, China

*CORRESPONDENCE
Qiang Ao,
aoqiang@scu.edu.cn

SPECIALTY SECTION
This article was submitted to Biomaterials, a section of the journal Frontiers in Bioengineering and Biotechnology

RECEIVED 12 November 2022
ACCEPTED 20 January 2023
PUBLISHED 16 February 2023

CITATION
Yu H, Liu H, Shen Y and Ao Q (2023), Synthetic biodegradable polymer materials in the repair of tumor-associated bone defects.
Front. Bioeng. Biotechnol. 11:1096525.
doi: 10.3389/fbioe.2023.1096525

Synthetic biodegradable polymer materials in the repair of tumor-associated bone defects

Honghao Yu[1,2], Haifeng Liu[3], Yuan Shen[1] and Qiang Ao[2,4]*

[1]Departments of Spine Surgery, Shengjing Hospital of China Medical University, Shenyang, China, [2]Department of Tissue Engineering, China Medical University, Shenyang, China, [3]Departments of Neurosurgery, Shengjing Hospital of China Medical University, Shenyang, China, [4]NMPA Key Laboratory for Quality Research and Control of Tissue Regenerative Biomaterial and Institute of Regulatory Science for Medical Device and National Engineering Research Center for Biomaterials, Sichuan University, Chengdu, China

The repair and reconstruction of bone defects and the inhibition of local tumor recurrence are two common problems in bone surgery. The rapid development of biomedicine, clinical medicine, and material science has promoted the research and development of synthetic degradable polymer anti-tumor bone repair materials. Compared with natural polymer materials, synthetic polymer materials have machinable mechanical properties, highly controllable degradation properties, and uniform structure, which has attracted more attention from researchers. In addition, adopting new technologies is an effective strategy for developing new bone repair materials. The application of nanotechnology, 3D printing technology, and genetic engineering technology is beneficial to modify the performance of materials. Photothermal therapy, magnetothermal therapy, and anti-tumor drug delivery may provide new directions for the research and development of anti-tumor bone repair materials. This review focuses on recent advances in synthetic biodegradable polymer bone repair materials and their antitumor properties.

KEYWORDS

synthetic, degradable, polymer materials, bone defect, repair

1 Introduction

Bone tumors and cancer metastasis to bone pose a serious threat to human health, especially osteosarcoma being the most common. For example, the age-standardized incidence rates for 0–79 ranged from 2 cases per million in Southern Asia to 4.2 in Sub-Saharan Africa, and the 5-year survival rate of osteosarcoma treated by amputation surgery has been 5%–20% for decades. The standard clinical treatment strategy for bone cancer involves surgical resection and reconstruction of the involved bone followed by adjuvant radiotherapy or chemotherapy. Surgical resection of bone malignancies can cause bone defects or delayed bone healing, severely affecting the patient's quality of life (Isakoff et al., 2015; Rojas et al., 2021; Chen and Yao, 2022). Finding the ideal repair materials has always been a challenge for orthopedic surgeons. According to the different components of the materials, synthetic bone repair materials can be mainly divided into metal materials, bioceramics, calcium phosphate bone cement, polymer materials, composite materials, tissue engineering materials, *etc.* Among them, polymer materials have been used as bone-filling materials since the mid-1960s, with the advantages

Abbreviations: PLA, polylactic acid; PGA, polyglycolic acid; PLGA, Poly (lactic-co-glycolic acid); PVA, Polyvinyl alcohol; PCL, polycaprolactone.

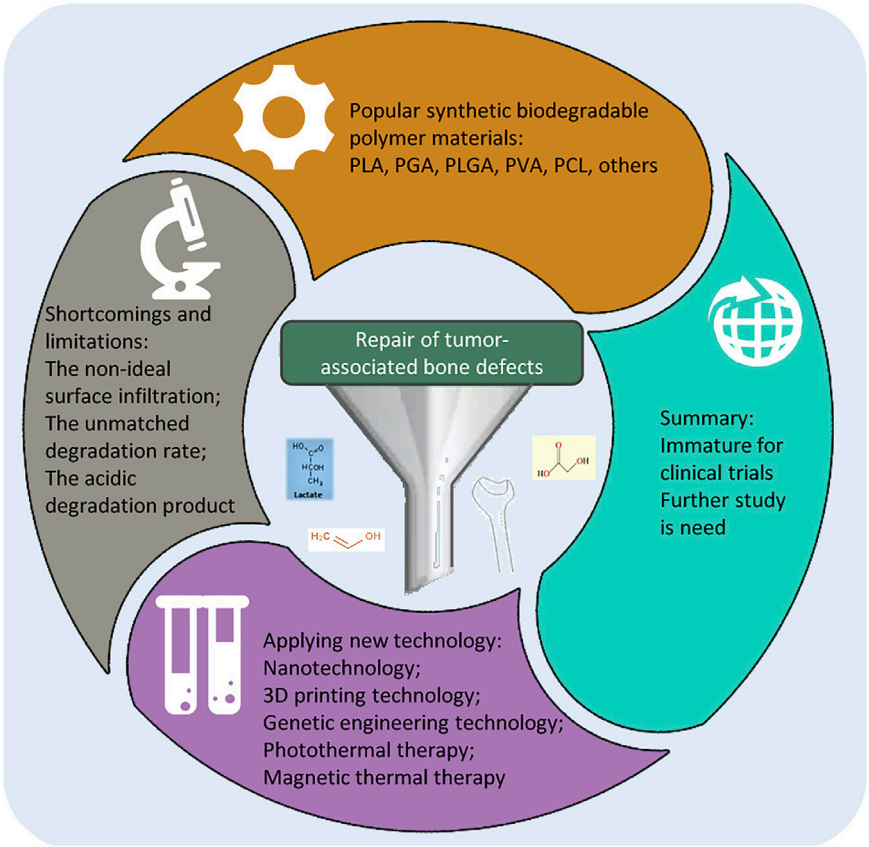

GRAPHICAL ABSTRACT

of immunocompatibility and good biocompatibility (Cao et al., 2021). Polymer materials commonly used in bone tissue engineering research can be divided into natural polymer materials and synthetic polymer materials. Among them, natural polymers include collagen, fibrin, chitin, hyaluronic acid, sodium alginate, chitosan, etc (Zhang et al., 2021; Zhang et al., 2022). Synthetic polymers include polylactic acid (PLA), polyglycolic acid (PGA), poly (lactic-co-glycolic acid) (PLGA), Polyvinyl alcohol (PVA), polycaprolactone (PCL), polyamide and other synthetic polymers (He et al., 2018). Natural polymer materials have good biocompatibility and thus contribute to improving cellular properties. However, they are difficult to design, with limited processing capacity, high contamination risk, and instability and variability of the property. Compared to natural polymer materials, synthetic polymer materials have stable chemical properties, and can be modified to obtain specific properties. Other advantages of synthetic polymer materials include cost-effectiveness, mass-production capacity, and longer storage time (Dwivedi et al., 2020). Synthetic polymer materials mainly exist in the form of scaffolds in bone repair, and composite materials with tissue cells, growth factors, and other materials can improve the biological activity and biocompatibility of the material itself (Yassin et al., 2017). The development of biomaterials provides broad prospects for the future treatment of bone tumors, and worldwide scholars constantly explore biomaterials that can both repair bone defects and inhibit tumor recurrence. This review focuses on new advances in synthetic biodegradable polymer bone repair materials and their antitumor properties.

2 Polymer materials containing polylactic acid, polyglycolic acid or poly (lactic-co-glycolic acid)

PLA, PGA, and PLGA are currently the most widely used extracellular matrix materials for bone tissue engineering. PLA is hydrolyzed *in vivo* to produce lactic acid, and PGA is degraded to hydroxyacetic acid *in vivo*, which can easily participate in the metabolism *in vivo* (Liu and Yu, 2021). PLA and PGA have good biocompatibility, good mechanical properties, and plasticity, which have been approved by the US Food and Drug Administration (FDA) for extensive clinical application. However, these materials have defects such as poor hydrophilic nature and fast degradation rate, and the intermediate products will accumulate in a local range, resulting in low pH values. The effect of the two materials directly used to repair bone defects is not ideal, and other materials need to be added for performance optimization (He et al., 2018). PLGA is also one of the most commonly used synthetic materials for bone defect repair and regeneration. It is a biopolymer material composed of random polymerization of two monomers, lactic acid and hydroxyacetic acid in different proportions. The presence of PGA makes the degradation rate of PLGA faster than PLA, and the degradation time of PLGA is prolonged as the proportion of propylene cross-esters in the copolymer composition increases. This synthetic polymer was first used for biomedical use in the early 1970s and has received extensive attention and research in bone tissue engineering for its good mechanical properties,

controlled degradability, good biocompatibility, and excellent plasticity (Martins et al., 2018; Su et al., 2021). The unique physicochemical properties of the material give it broad biomedical applications, ranging from PLGA polymers for tissue regeneration scaffolds to drug delivery systems, and other applications for parenteral administration, diagnostic, basic, and clinical research, including cancer, cardiovascular disease, tissue engineering, and vaccines (Altındal and Gümüşderelioğlu, 2016; Ray et al., 2017). The synthesis method of PLGA can be divided into two categories: (1) direct polymerization of lactic acid and glycolic acid, which usually yields PLGA with low molecular mass and wide relative molecular mass; (2) ester open ring polymerization of propylene ester, which can obtain higher relative molecular mass and more uniform products (Zhao et al., 2021). There are many modification methods for PLGA scaffold, mainly for blending modification and surface modification. Mixed modification is made by mixing other substances, such as hydroxyapatite, tricalcium phosphate, magnesium hydroxide, and other inorganic substances, which can improve the mechanical properties and hydrophilicity of the scaffold, change cell behavior, and promote bone production. Surface modification is coated on the scaffold surface with a layer of active material that regulates interactions between the cell-scaffold material (Danhier et al., 2012; Rocha et al., 2022). The researchers found that physically mixing the right amount of hydroxyapatite and PLGA into a composite scaffold could improve the scaffold's mechanical strength and that the hydroxyapatite would automerize on the scaffold surface to form a nanostructure, which facilitates cell adhesion and migration and promotes new bone generation. There are also studies to add magnetic nanoparticles to PLGA/hydroxyapatite scaffold, which can effectively inhibit and kill bone tumor cells by magnetic hyperthermia under the external magnetic field, and the addition of magnetic nanoparticles can enhance cell adhesion, proliferation, and differentiation (Li M. et al., 2019). Rong et al. made adriamycin-encapsulated PLGA nanoparticles in a porous nano-hydroxyapatite/collagen scaffold, ADM-PLGA-NHAC, and evaluated the performance of the vehicle scaffold using various techniques such as scanning electron microscopy and *in vitro* sustained release. The results of the *in vitro* tumor-suppressor experiments showed that the ADM-PLGA-NHAC scaffold extract had a strong anti-tumor effect on the MG-63 osteosarcoma cells (Rong et al., 2016). Wang et al. successfully built the bioglass molybdenum disulfide complex (BGM) by fixing the molybdenum disulfide polylactic acid glycolic acid (MoS_2-PLGA) membrane on the surface of the 3D printing bioactive glass bracket. Moreover, they demonstrated the inhibitory effect of this complex on tumor cells *in vitro* and *in vivo* trials (Wang et al., 2020). Bone infection is a serious complication after bone defect repair, and it is often difficult to achieve effective concentrations at the infection site, and the PLGA stent loaded with antibiotics can release high concentrations of antibiotics locally in bone repair to achieve therapeutic purposes. Researchers by studying the antibiotic release curve found that antibiotics in the first few hours of explosive release, then sustained low dose slow release, which is crucial to repair infectious bone defects, early local microenvironment of high concentration of antibiotics to completely kill bacteria, sustained low doses of antibiotics help to inhibit the growth of bacteria (Gao et al., 2016; Aragón et al., 2019). PLGA has shown great potential in drug delivery and tissue engineering, and its application in bone defect repair after tumor resection may become a new choice for orthopedic doctors.

3 Polymer materials containing polyvinyl alcohol

PVA is a linear synthetic polymer with biocompatibility, biodegradability, and chemical stability. PVA is often used in bone repair materials as a component of composite materials to improve the mechanical strength, hydrophilicity, and cell compatibility of scaffold materials (Pourjavadi et al., 2020). Chen et al. prepared the PVA/β-tricalcium phosphate composite scaffolds by melting deposition formation, and with the addition of β-tricalcium phosphate, the maximum stress of the scaffold reached 10.7 kPa, which significantly improved the carrying capacity of the composite scaffold. Chen et al. also verified the cell compatibility of the composite scaffold, and the results showed that the composite scaffold did not inhibit cell growth (Chen et al., 2019). Kaur et al. prepared PVA scaffolds loaded with different concentrations of graphene nanosheets by freeze-drying method. The addition of graphene nanosheets significantly improved the tensile strength of the polyvinyl alcohol scaffold. When the mass fraction of nanographene sheets was 1%, osteoblasts proliferated and differentiated best in the composite scaffold (Kaur et al., 2017). Xia et al. prepared PVA/silica hybrid fiber by electrospinning method. After 3 days of immersion in the simulated body fluid, layered apatite precipitation appeared on the surface of the hybrid fiber, so it is supposed that the fiber has certain bone inducibility conducive to bone repair (Xia et al., 2018). Lan et al. fabricated a well-developed porous carbon nanotube (CNT) reinforced polyvinyl alcohol/biphasic calcium phosphate (PVA/BCP) scaffold by a freeze-thawing and freeze-drying method. The degradation analysis indicated that the degradation ratio of scaffolds can be varied by changing the concentrations of BCP powders and CNTs (Lan et al., 2019). The study of Li Yao et al. determined the ratio of chitosan/polylactic lactate/hydroxyapatite/PVA composite, optimized the mechanical properties of bone scaffold, and the optimal ratio of the composite stent has high porosity and good mechanical properties (YM et al., 2022). The results of Istikharoh et al. demonstrated that polylactic ate glycolic acid/PVA coated hydroxyapatite nanoparticle composites have an optimal aperture, morphology, and degradability, showing their great potential as an effective bone scaffold for the repair of alveolar defects after tooth extraction (Istikharoh et al., 2020).

4 Polymer materials containing PCL

PCL has good degradability, superior biocompatibility, and strong mechanical properties, and it was approved by the FDA in the 1990s. PCL is a polyester organic polymer made by artificial synthesis. At physiological temperatures, the semi-crystalline PCL attains a rubbery state resulting in its high strength, high toughness, and excellent mechanical properties, along with good biocompatibility, slow degradation rate, and strong crystallinity. In addition to being biocompatible and biodegradable, PCL polyester is widely used as a scaffold for absorbable sutures, regenerative therapies, and drug delivery applications for its easy availability and cost-effectiveness, especially for building long-term implant delivery devices. Its longer degradation time makes it widely used to replace hard tissues, and load-bearing tissues by increasing their stiffness, and to replace soft tissues by reducing their molecular weight and degradation time (Dwivedi et al., 2020). In order to make the scaffold has antibacterial properties, Felice et al. prepared mixed with zinc oxide scaffold, the results show that high zinc oxide concentration can induce early mineralization, and adjusting the

TABLE 1 Synthetic biodegradable polymer materials for bone defects (Henslee et al., 2011; Reichert et al., 2012; Jensen et al., 2014; Subramanian et al., 2015; Pang et al., 2019; Ding et al., 2022).

Graft composition	Bone defect	Regeneration outcomes	Limitations	References
3D printed polycaprolactone/β-tricalcium phosphate composite	3 cm, sheep, tibial	Radiographic union; mechanical restoration	Slow graft; resorption	Reichert et al. (2012)
Solid poly (propylene fumarate) rod/porous sleeve with PLGA microparticle	5 mm, rat, femoral	Improved defect fixation by solid rod; improved bone formation	Regeneration impeded by solid rod; no union	Henslee et al. (2011)
Salicylic acid-based poly (anhydride-ester)/polycaprolactone membrane	5 mm, rat, femoral	Ectopic bone formation suppressed; long bone regeneration improved (no mechanical testing)	Poor graft mechanical property; long-term remodelling unclear	Subramanian et al. (2015)
3D printing polylactic acid polymer-bioactive glass loaded with bone cement	5–6 mm in diameter and 5–6 mm in depth, rabbit femoral	Radiographic union; mechanical restoration; osteogenic differentiation ability	Improved scaffold degradation rate	Ding et al. (2022)
Surface-modified functionalized polycaprolactone	10 mm in diameter and 10 mm in depth, porcine, skull	Radiographic union; mechanical restoration	Acceleration of scaffold degradation	Jensen et al. (2014)
polyvinyl alcohol-borosilicate gel hybrid scaffolds	3 mm in diameter and 5 mm in depth, rat, femoral	Radiographic union; mechanical restoration	Unclear degradation rate	Pang et al. (2019)

concentration of zinc oxide and the distribution in the material can realize the regulation of scaffold degradation rate, and the stent has antibacterial effect for S.*aureus* (Felice et al., 2018). Nanoparticles were cultured on a polydopamine-coated polyhexylactone scaffold and were significantly enhanced by the presence of a polydopamine coating by Lee et al. As nanoparticles, this scaffold was found to have good osteogenic activity *in vivo* experiments, which is expected to provide new material options for bony defect repair and regeneration (Lee et al., 2018). Wu et al. made the 3D-printed calcium silicate, PCL, and acellular extracellular matrix scaffolds, and observed that they exhibited excellent biocompatibility, cell adhesion, proliferation, and differentiation by increasing the expression of osteogenesis-related genes (Wu Y. A. et al., 2019). The microporous PCL scaffold matrix found by Palama et al. supports attachment, proliferation, and osteogenic differentiation of osteoblasts, whereas the polyelectrolyte multilayer fixation on the endopore surface maintains local dexamethasone release. These microporous scaffolds demonstrate the ability to treat dexamethasone as a local tumor therapy, and to promote the proliferation and differentiation of osteoblast-like cells *in vitro* (Palamà et al., 2017).

5 Other polymer materials

In addition to the above, there are some new materials, that researchers have brought them to many scholars through in-depth experiments, and may become candidate substitutes for bone defects after tumor resection after more long-term exploration. The applications of emerging technologies such as 3D printing, photothermal effects, and magnetic materials have gradually attracted the attention of researchers (Choi et al., 2017; Lu et al., 2018; Yang et al., 2018). Ma et al. studied an acrylic ester-based composite of polyfumarate as a potential clinical bone repair material with low heat release and suitable mechanical properties, which shows good biocompatibility. Furthermore, the surface morphology and hydrophilic properties can be adjusted by regulating the content of β-calcium phosphate, and maybe a promising bone repair material (Ma et al., 2019). Dang et al. combined 3D printing technology with a solvent thermal method to successfully synthesize $CuFeSe_2$ nanocrystalline bioactive glass scaffold, which was verified to remove bone tumor cells *in vitro* by photothermal effects, and confirmed that the scaffold can kill Saos-2 tumor cells *in vivo* trials (Dang et al., 2018).

Using a strategy of combining 3D printing technology with photothermal properties for *in situ* ablation, Ma et al. made a 3D-printed calcium phosphate composite scaffold and modified it with graphene oxide to transfer the infrared laser energy to the photothermal effect (Ma et al., 2016). Zhang et al. prepared a hydrogenation black titanium dioxide coating with a micro/nano graded morphology by using the induction suspension plasma spraying technology. Good and controlled tumor growth inhibition by 808 nm near-infrared laser irradiation *in vitro* and *in vivo* (Zhang et al., 2019). Mondal et al. synthesized iron oxide, hydroxyapatite, and hydroxyapatite-coated iron oxide nanoparticles, and *in vitro* magnetic hyperthermia studies showed excellent thermal efficacy against MG-63 osteosarcoma cells, killing almost all experimental MG-63 osteosarcoma cells within 30 min of exposure (Mondal et al., 2017). KamitakaharaM et al. have prepared micron-scale magnetic nanoparticles with porous HA particles acting as a scaffold for bone regeneration, and the magnetic nanoparticles generate enough heat to kill tumor cells in an alternating magnetic field (Kamitakahara et al., 2016). Asa et al. have synthesized multifunctional magnetic ZnFe2O4-hydroxyapatite nanoparticles for local anticancer drug delivery and bacterial infection inhibition, and their study has found that drug-borne nanoparticles have the ability to inhibit the proliferation and growth of cancer cells. With the increasing concentration of the nanoparticles, the G292 cancer cell proliferation was inhibited, while the HEK normal cell proliferation was stimulated (Asa et al., 2019). Here listed in Table 1 are the synthetic biodegradable polymer materials for bone defects.

6 Strategies for the development of anti-tumor polymer materials

Modern bone repair materials mainly include polymer materials, tissue-engineered bone, and related derived composites. With the continuous progress of technology in medicine and related fields, the research and technical level of modern materials are more microscopic. New technology is an effective strategy to develop new bone repair materials, and nanotechnology, 3D printing

technology, genetic engineering technology, photothermal therapy, and magnetic thermal therapy have opened up new prospects for the research of anti-tumor bone defect repair materials (Venkatesan and Kim, 2014; Atak et al., 2017; Xu et al., 2022). The application of 3D printing technology makes bone repair stent preparation more refined, and different morphology, porosity, and performance can be made by changing the printing parameters. With the development of 3D printing and computer technology, complex bracket materials are more accurately used for production. Researchers are further studying the three-dimensional structures of prints mixed with living cells, growth factors, or other biomaterials, and 3D printed drug carrier materials are also gaining much attention (Raja and Yun, 2016; Han et al., 2017). Li et al. synthesized a composite scaffold of nano-hydroxyapatite (nHA) and reduced graphene oxide (rGO) sheets fabricated by self-assembly and found that nHA-rGO scaffolds killed all but 8% of osteosarcoma cells (MG-63) under 808 nm near-infrared laser irradiation for 20 min *in vitro* (Li et al., 2018). In order to optimize and make up for the lack of simple stent material performance, the researchers added all kinds of polymer, trace elements, drugs, seeds, cells, and related cytokines, usually different materials, to improve the mechanical properties, degradation properties, biocompatibility, and osteogenic properties, optimize the drug or cytokine load capacity (Li H. et al., 2019).

The composite of multiple materials is an effective way to produce new material properties. The bone stent composed of a single raw material cannot fully meet the needs of bone defect repair. Through the composite of various raw materials, the researchers hope to create an artificial stent that can perfectly fit the needs of bone defect repair. Direct local delivery of anti-tumor agents loaded into stents of bone repair materials is also an effective strategy (Zhou et al., 2017; Qu et al., 2021). Recently, it has been found that HA can inhibit the proliferation and induce apoptosis of various cancer cells, including osteosarcoma, breast cancer, gastric cancer, and colon, and liver cancer cells, but this biomaterial does not inhibit the proliferation of normal cells (Han et al., 2014; Zhao et al., 2018; Wu H. et al., 2019). Qing et al. Using transmission electron microscopy to observe the ultrastructural changes of the 2 cells showed that HA-NPs have a selective effect on different cell types of cells: supporting the proliferation of normal osteocyte cells while causing the apoptosis of osteosarcoma cells (Qing et al., 2012). It has been shown that chitosan plays a tumor-suppressor role by inhibiting glycolysis and reducing glucose uptake and ATP levels in cells, but chitosan has no such effect on normal cells. Moreover, the tumor cell surface has more negative charge than the normal cell surface, and the chitosan is positively charged, thus inhibiting tumor growth and metastasis (Ghezini et al., 2008). Wang et al. used selenium-doped hydroxyapatite nanoparticles (Se-HANs), which could potentially fill the bone defect generated from bone tumor removal while killing residual tumor cells, as an example to study the mechanism by which selenium released from the lattice of Se-HANs induces apoptosis of bone cancer cells *in vitro* and inhibits the growth of bone tumors *in vivo*, finding that Se-HANs induced apoptosis of tumor cells by an inherent caspase-dependent apoptosis pathway synergistically orchestrated with the generation of reactive oxygen species (Wang et al., 2016). Lu et al. reported a polydopamine (PDA)-coated composite scaffold consisting of doxorubicin (DOX)-loaded lamellar hydroxyapatite (LHAp) and poly (lactic-co-glycolic acid) (PLGA) in an attempt to reach dual functions of tumor inhibition and bone repair (Lu et al., 2021). Hess et al. combined a calcium phosphate microsphere with a matrix scaffold and prepared three calcium phosphate/calcium alginate beads as drug carriers by ion gel droplet extrusion method, and combined it into the scaffold matrix by cryogen method, which successfully released cisplatin and doxorubicin in experiments and showed a significant killing effect on osteosarcoma MG-63 cells (Hess et al., 2017).

7 Shortcomings and limitations of synthetic biodegradable polymer materials

Although the artificial synthesis of biodegradable polymer materials has great potential in bone defect repair, some deficiencies and limitations still need to be discussed. Some synthetic polymers are hydrophobic materials, and their surface infiltration is not ideal, affecting the adhesion, proliferation, and differentiation of cells, and then affecting the performance of the material and the repair of bone tissue. While the degradation rate of some materials does not match the speed of bone growth; the degradation product of some polyester materials is acidic and not conducive to new bone regeneration. For example, the degradation of PLA does not depend on enzymes, but through the hydrolysis of the ester bonds. For polylactic acid, the lack of hydrophilic groups in its structure makes the surface of the material hydrophobic. Low hydrophilicity is not conducive to cell adhesion, proliferation, and differentiation. In addition, PLA could produce acidic degradation products like lactic acid. The accumulation of lactic acid cannot be metabolized within a short time and resulting in a pH as low as 3.0 within 4 weeks, this may also dissolve some bone components as well (Liu et al., 2013; Han et al., 2020; Li et al., 2022). The earlier used PCL scaffolds did not provide optimal mechanical properties and biocompatibility, thus attempting to mix PCL with natural or synthetic polymers or ceramics. For example, combining calcium phosphate-based ceramics, bioactive glasses, and polymers into the PCL can improve the biomaterials with better mechanical properties, controllable degradation rates, and enhanced biological activity (Yan et al., 2019). In a word, some synthetic degradable polymer materials may have unsatisfied mechanical properties and biocompatibility and even affect osteogenesis. These problems need to be paid attention to and properly solved.

8 Summary

In recent years, biological materials carrying drugs or biological materials itself has the characteristics of anti-tumor effect have become a new direction, many scholars of malignant bone tumor resection of biological materials after thorough study, but there is not fully meet the requirements of bone repair materials, with bone defect repair and anti-tumor multifunctional materials still have a long distance from clinical trials. With the deepening of the research on the mechanism of osteogenesis, the continuous development of biomaterials, and the progress of material science and technology, it is expected to develop the ideal materials that meet the requirements of human bone repair (He et al., 2018). As a bone repair material, the core design idea is that, by inserting a stent in the damaged bone tissue, this stent can maintain good mechanical properties for a long period of time to support the repair of the defective bone tissue, and can be naturally degraded and replaced by the new bone tissue. The ultimate goal of the bone tissue engineering scaffold is to make an effective repair of the bone tissue, so cytocompatibility and bone inducibility are problems that cannot be

ignored. A synthetic polymer as a scaffold matrix material, on the one hand, we should give full play to its own biocompatibility and biodegradability, and other excellent properties; on the other hand, it should also make up for the shortcomings of unsatisfactory cell compatibility due to their own hydrophobicity. How to better use synthetic polymer materials to simulate the extracellular matrix structure to promote the repair of bone tissue, and the minimum of its negative impact on the human body after implantation are still the problems that scholars need to further study and solve in the future. Different materials have certain advantages and disadvantages, so it is necessary to make optimal choices combined with material characteristics in clinical application. As more and more new biomaterials-related basic and clinical research are developed, the problem of postoperative bone defects and tumor recurrence in bone tumor patients will be solved gradually.

Author contributions

HY drafted the manuscript. HL and YS investigated related publications. QA revised and edited this manuscript. All authors contributed to the article and approved the submitted version.

Funding

This work was funded by the Sichuan Science and Technology Program (2020YFH0008) and the National Key R&D Program of China (2017YFA0105802).

Conflict of interest

The authors declare that the research was conducted in the absence of any commercial or financial relationships that could be construed as a potential conflict of interest.

Publisher's note

References

Altındal, D., and Gümüşderelioğlu, M. (2016). Melatonin releasing PLGA micro/nanoparticles and their effect on osteosarcoma cells. *J. Microencapsul.* 33 (1), 53–63. doi:10.3109/02652048.2015.1115901

Aragón, J., Feoli, S., Irusta, S., and Mendoza, G. (2019). Composite scaffold obtained by electro-hydrodynamic technique for infection prevention and treatment in bone repair. *Int. J. Pharm.* 557, 162–169. doi:10.1016/j.ijpharm.2018.12.002

Asa, B., Sase, A., So, A., and Smn, C. (2019). Multifunctional magnetic ZnFe2O4-hydroxyapatite nanocomposite particles for local anti-cancer drug delivery and bacterial infection inhibition: An *in vitro* study. *J. Taiwan Inst. Chem. Eng.* 96, 503–508. doi:10.1016/j.jtice.2018.10.018

Atak, B. H., Buyuk, B., Huysal, M., Isik, S., Senel, M., Metzger, W., et al. (2017). Preparation and characterization of amine functional nano-hydroxyapatite/chitosan bionanocomposite for bone tissue engineering applications. *Carbohydr. Polym.* 164, 200–213. doi:10.1016/j.carbpol.2017.01.100

Cao, G. D., Pei, Y. Q., Liu, J., Li, P., Liu, P., and Li, X. S. (2021). Research progress on bone defect repair materials. *Zhongguo Gu Shang* 34 (4), 382–388. doi:10.12200/j.issn.1003-0034.2021.04.018

Chen, G., Chen, N., and Wang, Q. (2019). Fabrication and properties of poly(vinyl alcohol)/β-tricalcium phosphate composite scaffolds via fused deposition modeling for bone tissue engineering. *Compos. Sci. Technol.* 172 (MAR.1), 17–28. doi:10.1016/j.compscitech.2019.01.004

Chen, H., and Yao, Y. (2022). Progress of biomaterials for bone tumor therapy. *J. Biomater. Appl.* 36 (6), 945–955. doi:10.1177/08853282211035236

Choi, A. H., Macha, I. J., Akyol, S., Cazalbou, S., and Ben-Nissan, B. (2017). Nanostructured calcium phosphates for drug, gene, DNA and protein delivery and as anticancer chemotherapeutic devices. *Clinical applications of biomaterials*. Springer International Publishing Ag.

Dang, W., Li, T., Li, B., Ma, H., Zhai, D., Wang, X., et al. (2018). A bifunctional scaffold with CuFeSe(2) nanocrystals for tumor therapy and bone reconstruction. *Biomaterials* 160, 92–106. doi:10.1016/j.biomaterials.2017.11.020

Danhier, F., Ansorena, E., Silva, J. M., Coco, R., Le Breton, A., and Préat, V. (2012). PLGA-Based nanoparticles: An overview of biomedical applications. *J. Control Release* 161 (2), 505–522. doi:10.1016/j.jconrel.2012.01.043

Ding, Y., Liu, X., Zhang, J., Lv, Z., Meng, X., Yuan, Z., et al. (2022). 3D printing polylactic acid polymer-bioactive glass loaded with bone cement for bone defect in weight-bearing area. *Front. Bioeng. Biotechnol.* 10, 947521. doi:10.3389/fbioe.2022.947521

Dwivedi, R., Kumar, S., Pandey, R., Mahajan, A., Nandana, D., Katti, D. S., et al. (2020). Polycaprolactone as biomaterial for bone scaffolds: Review of literature. *J. Oral Biol. Craniofac Res.* 10 (1), 381–388. doi:10.1016/j.jobcr.2019.10.003

Felice, B., Sánchez, M. A., Socci, M. C., Sappia, L. D., Gómez, M. I., Cruz, M. K., et al. (2018). Controlled degradability of PCL-ZnO nanofibrous scaffolds for bone tissue engineering and their antibacterial activity. *Mater Sci. Eng. C Mater Biol. Appl.* 93, 724–738. doi:10.1016/j.msec.2018.08.009

Gao, J., Huang, G., Liu, G., Liu, Y., Chen, Q., Ren, L., et al. (2016). *A biodegradable antibiotic-eluting PLGA nanofiber-loaded deproteinized bone for treatment of infected rabbit bone defects.*

Ghezini, R., Sassi, M., Bengueddach, A. J. M., and Materials, M. (2008). Adsorption of carbon dioxide at high pressure over H-ZSM-5 type zeolite. Micropore volume determinations by using the Dubinin–Raduskevich equation and the " t-plot" method. *Microporous Mesoporous Mat.* 113 (1-3), 370–377. doi:10.1016/j.micromeso.2007.11.034

Han, C., Yao, Y., Cheng, X., Luo, J., Luo, P., Wang, Q., et al. (2017). Electrophoretic deposition of gentamicin-loaded silk fibroin coatings on 3D-printed porous cobalt-chromium-molybdenum bone substitutes to prevent orthopedic implant infections. *Biomacromolecules* 18 (11), 3776–3787. doi:10.1021/acs.biomac.7b01091

Han, G., Liu, S., Pan, Z., Lin, Y., Ding, S., Li, L., et al. (2020). Sulfonated chitosan and phosphorylated chitosan coated polylactide membrane by polydopamine-assisting for the growth and osteogenic differentiation of MC3T3-E1s. *Carbohydr. Polym.* 229, 115517. doi:10.1016/j.carbpol.2019.115517

Han, Y., Li, S., Cao, X., Yuan, L., Wang, Y., Yin, Y., et al. (2014). Different inhibitory effect and mechanism of hydroxyapatite nanoparticles on normal cells and cancer cells *in vitro* and *in vivo*. *Sci. Rep.* 4, 7134. doi:10.1038/srep07134

He, W., Fan, Y., and Li, X. (2018). Recent research progress of bioactivity mechanism and application of bone repair materials. *Zhongguo Xiu Fu Chong Jian Wai Ke Za Zhi* 32 (9), 1107–1115. doi:10.7507/1002-1892.201807039

Henslee, A. M., Spicer, P. P., Yoon, D. M., Nair, M. B., Meretoja, V. V., Witherel, K. E., et al. (2011). Biodegradable composite scaffolds incorporating an intramedullary rod and delivering bone morphogenetic protein-2 for stabilization and bone regeneration in segmental long bone defects. *Acta Biomater.* 7 (10), 3627–3637. doi:10.1016/j.actbio.2011.06.043

Hess, U., Shahabi, S., Treccani, L., Streckbein, P., Heiss, C., and Rezwan, K. (2017). Co-delivery of cisplatin and doxorubicin from calcium phosphate beads/matrix scaffolds for osteosarcoma therapy. *Mater Sci. Eng. C Mater Biol. Appl.* 77, 427–435. doi:10.1016/j.msec.2017.03.164

Isakoff, M. S., Bielack, S. S., Meltzer, P., and Gorlick, R. (2015). Osteosarcoma: Current treatment and a collaborative pathway to success. *J. Clin. Oncol.* 33 (27), 3029–3035. doi:10.1200/jco.2014.59.4895

Istikharoh, F., Sujuti, H., Mustamsir, E., and Swastirani, A. (2020). Preparation and biodegradable properties of hydroxyapatite nanoparticle composite coated with poly lactic-co-glycolic acid/polyvinyl alcohol for bone regeneration. *Dent. Med. Probl.* 57 (4), 363–367. doi:10.17219/dmp/125775

Jensen, J., Rölfing, J. H., Le, D. Q., Kristiansen, A. A., Nygaard, J. V., Hokland, L. B., et al. (2014). Surface-modified functionalized polycaprolactone scaffolds for bone repair: *In vitro* and *in vivo* experiments. *J. Biomed. Mater Res. A* 102 (9), 2993–3003. doi:10.1002/jbm.a.34970

Kamitakahara, M., Ohtoshi, N., Kawashita, M., and Ioku, K. (2016). Spherical porous hydroxyapatite granules containing composites of magnetic and hydroxyapatite

nanoparticles for the hyperthermia treatment of bone tumor. *J. Mater Sci. Mater Med.* 27 (5), 93. doi:10.1007/s10856-016-5704-7

Kaur, T., Thirugnanam, A., and Pramanik, K. J. M. T. C. (2017). Effect of carboxylated graphene nanoplatelets on mechanical and *in-vitro* biological properties of polyvinyl alcohol nanocomposite scaffolds for bone tissue engineering. *Mat. Today Commun.* 12, 34–42. doi:10.1016/j.mtcomm.2017.06.004

Lan, W., Zhang, X., Xu, M., Zhao, L., Huang, D., Wei, X., et al. (2019). Carbon nanotube reinforced polyvinyl alcohol/biphasic calcium phosphate scaffold for bone tissue engineering. *RSC Adv.* 9 (67), 38998–39010. doi:10.1039/c9ra08569f

Lee, S. J., Lee, H. J., Kim, S. Y., Seok, J. M., Lee, J. H., Kim, W. D., et al. (2018). *In situ* gold nanoparticle growth on polydopamine-coated 3D-printed scaffolds improves osteogenic differentiation for bone tissue engineering applications: *In vitro* and *in vivo* studies. *Nanoscale* 10 (33), 15447–15453. doi:10.1039/c8nr04037k

Li, C., Lv, H., Du, Y., Zhu, W., Yang, W., Wang, X., et al. (2022). Biologically modified implantation as therapeutic bioabsorbable materials for bone defect repair. *Regen. Ther.* 19, 9–23. doi:10.1016/j.reth.2021.12.004

Li, D., Nie, W., Chen, L., McCoul, D., Liu, D., Zhang, X., et al. (2018). Self-assembled hydroxyapatite-graphene scaffold for photothermal cancer therapy and bone regeneration. *J. Biomed. Nanotechnol.* 14 (12), 2003–2017. doi:10.1166/jbn.2018.2646

Li, H., Chen, X., Xu, T., Sun, T., Huang, H., Lu, M., et al. (2019a). Selenium-substituted hydroxyapatite particles with regulated microstructures for osteogenic differentiation and anti-tumor effects. *Ceram. Int.* 45, 13787–13798. doi:10.1016/j.ceramint.2019.04.075

Li, M., Liu, J., Cui, X., Sun, G., Hu, J., Xu, S., et al. (2019b). Osteogenesis effects of magnetic nanoparticles modified-porous scaffolds for the reconstruction of bone defect after bone tumor resection. *Regen. Biomater.* 6 (6), 373–381. doi:10.1093/rb/rbz019

Liu, X., Liu, H. Y., Lian, X., Shi, X. L., Wang, W., Cui, F. Z., et al. (2013). Osteogenesis of mineralized collagen bone graft modified by PLA and calcium sulfate hemihydrate: *In vivo* study. *J. Biomater. Appl.* 28 (1), 12–19. doi:10.1177/0885328211433618

Liu, Z., and Yu, B. (2021). Development prospect and research value of biodegradable poly(lactic acid) for bone repair. *Zhongguo Zuzhi Gongcheng Yanjiu* 25 (34), 5552–5560.

Lu, J. W., Yang, F., Ke, Q. F., Xie, X. T., and Guo, Y. P. (2018). Magnetic nanoparticles modified-porous scaffolds for bone regeneration and photothermal therapy against tumors. *Nanomedicine* 14 (3), 811–822. doi:10.1016/j.nano.2017.12.025

Lu, Y., Wan, Y., Gan, D., Zhang, Q., Luo, H., Deng, X., et al. (2021). Enwrapping polydopamine on doxorubicin-loaded lamellar hydroxyapatite/poly(lactic-co-glycolic acid) composite fibers for inhibiting bone tumor recurrence and enhancing bone regeneration. *ACS Appl. Bio Mater* 4 (8), 6036–6045. doi:10.1021/acsabm.1c00297

Ma, C., Ma, Z., Yang, F., Wang, J., and Liu, C. (2019). Poly (propylene fumarate)/β-calcium phosphate composites for enhanced bone repair. *Biomed. Mater* 14 (4), 045002. doi:10.1088/1748-605X/ab12ae

Ma, H., Jiang, C., Zhai, D., Luo, Y., Chen, Y., Lv, F., et al. (2016). A bifunctional biomaterial with photothermal effect for Tumor therapy and bone regeneration. *Bone Regen.* 26 (8), 1197–1208. doi:10.1002/adfm.201504142

Martins, C., Sousa, F., Araújo, F., and Sarmento, B. (2018). Functionalizing PLGA and PLGA derivatives for drug delivery and tissue regeneration applications. *Adv. Healthc. Mater* 7 (1), 1701035. doi:10.1002/adhm.201701035

Mondal, S., Manivasagan, P., Bharathiraja, S., Santha Moorthy, M., Nguyen, V. T., Kim, H. H., et al. (2017). Hydroxyapatite coated iron oxide nanoparticles: A promising nanomaterial for magnetic hyperthermia cancer treatment. *Nanomater. (Basel)* 7 (12), 426. doi:10.3390/nano7120426

Palamà, I. E., Arcadio, V., D'Amone, S., Biasiucci, M., Gigli, G., and Cortese, B. (2017). Therapeutic PCL scaffold for reparation of resected osteosarcoma defect. *Sci. Rep.* 7 (1), 12672. doi:10.1038/s41598-017-12824-3

Pang, L., Shen, Y., Hu, H., Zeng, X., Huang, W., Gao, H., et al. (2019). Chemically and physically cross-linked polyvinyl alcohol-borosilicate gel hybrid scaffolds for bone regeneration. *Mater Sci. Eng. C Mater Biol. Appl.* 105, 110076. doi:10.1016/j.msec.2019.110076

Pourjavadi, A., Tehrani, Z. M., Salami, H., Seidi, F., Motamedi, A., Amanzadi, A., et al. (2020). Both tough and soft double network hydrogel nanocomposite based on O-carboxymethyl chitosan/poly(vinyl alcohol) and graphene oxide: A promising alternative for tissue engineering. *A Promis. Altern. Tissue Eng.* 60 (1), 889–899. doi:10.1002/pen.25297

Qing, F., Wang, Z., Hong, Y., Liu, M., Guo, B., Luo, H., et al. (2012). Selective effects of hydroxyapatite nanoparticles on osteosarcoma cells and osteoblasts. *J. Mater Sci. Mater Med.* 23 (9), 2245–2251. doi:10.1007/s10856-012-4703-6

Qu, Y., Zhuang, H., Zhang, M., Wang, Y., Zhai, D., Ma, B., et al. (2021). Bone cements for therapy and regeneration for minimally invasive treatment of neoplastic bone defects. *J. Mater Chem. B* 9 (21), 4355–4364. doi:10.1039/d1tb00703c

Raja, N., and Yun, H. S. (2016). A simultaneous 3D printing process for the fabrication of bioceramic and cell-laden hydrogel core/shell scaffolds with potential application in bone tissue regeneration. *J. Mater Chem. B* 4 (27), 4707–4716. doi:10.1039/c6tb00849f

Ray, S., Saha, S., Sa, B., and Chakraborty, J. (2017). *In vivo* pharmacological evaluation and efficacy study of methotrexate-encapsulated polymer-coated layered double hydroxide nanoparticles for possible application in the treatment of osteosarcoma. *Drug Deliv. Transl. Res.* 7 (2), 259–275. doi:10.1007/s13346-016-0351-6

Reichert, J. C., Cipitria, A., Epari, D. R., Saifzadeh, S., Krishnakanth, P., Berner, A., et al. (2012). A tissue engineering solution for segmental defect regeneration in load-bearing long bones. *Sci. Transl. Med.* 4 (141), 141ra93. doi:10.1126/scitranslmed.3003720

Rocha, C. V., Gonçalves, V., da Silva, M. C., Bañobre-López, M., and Gallo, J. (2022). PLGA-based composites for various biomedical applications. *Int. J. Mol. Sci.* 23 (4), 2034. doi:10.3390/ijms23042034

Rojas, G. A., Hubbard, A. K., Diessner, B. J., Ribeiro, K. B., and Spector, L. G. (2021). International trends in incidence of osteosarcoma (1988-2012). *Int. J. Cancer* 149 (5), 1044–1053. doi:10.1002/ijc.33673

Rong, Z. J., Yang, L. J., Cai, B. T., Zhu, L. X., Cao, Y. L., Wu, G. F., et al. (2016). Porous nano-hydroxyapatite/collagen scaffold containing drug-loaded ADM-PLGA microspheres for bone cancer treatment. *J. Mater Sci. Mater Med.* 27 (5), 89. doi:10.1007/s10856-016-5699-0

Su, Y., Zhang, B., Sun, R., Liu, W., Zhu, Q., Zhang, X., et al. (2021). PLGA-Based biodegradable microspheres in drug delivery: Recent advances in research and application. *Drug Deliv.* 28 (1), 1397–1418. doi:10.1080/10717544.2021.1938756

Subramanian, S., Mitchell, A., Yu, W., Snyder, S., Uhrich, K., and O'Connor, J. P. (2015). Salicylic acid-based polymers for guided bone regeneration using bone morphogenetic protein-2. *Tissue Eng. Part A* 21 (13-14), 2013–2024. doi:10.1089/ten.TEA.2014.0455

Venkatesan, J., and Kim, S. K. (2014). Nano-hydroxyapatite composite biomaterials for bone tissue engineering--a review. *J. Biomed. Nanotechnol.* 10 (10), 3124–3140. doi:10.1166/jbn.2014.1893

Wang, H., Zeng, X., Pang, L., Wang, H., Li, J., Deng, Z., et al. (2020). Integrative treatment of anti-tumor/bone repair by combination of MoS2 nanosheets with 3D printed bioactive borosilicate glass scaffolds. *Chem. Eng. J.* 396, 125081. doi:10.1016/j.cej.2020.125081

Wang, Y., Wang, J., Hao, H., Cai, M., Wang, S., Ma, J., et al. (2016). *In vitro* and *in vivo* mechanism of bone tumor inhibition by selenium-doped bone mineral nanoparticles. *ACS Nano* 10 (11), 9927–9937. doi:10.1021/acsnano.6b03835

Wu, H., Li, Z., Tang, J., Yang, X., Zhou, Y., Guo, B., et al. (2019a). <p>The *in vitro* and *in vivo* anti-melanoma effects of hydroxyapatite nanoparticles: Influences of material factors</p>. *Int. J. Nanomedicine* 14, 1177–1191. doi:10.2147/ijn.S184792

Wu, Y. A., Chiu, Y. C., Lin, Y. H., Ho, C. C., Shie, M. Y., and Chen, Y. W. (2019b). 3D-Printed bioactive calcium silicate/poly-ε-caprolactone bioscaffolds modified with biomimetic extracellular matrices for bone regeneration. *Int. J. Mol. Sci.* 20 (4), 942. doi:10.3390/ijms20040942

Xia, S. H., Teng, S. H., and Wang, P. J. M. L. (2018). Synthesis of bioactive polyvinyl alcohol/silica hybrid fibers for bone regeneration. *Mat. Lett.* 213 (FEB.15), 181–184. doi:10.1016/j.matlet.2017.11.084

Xu, Y., Zhang, F., Zhai, W., Cheng, S., Li, J., and Wang, Y. (2022). Unraveling of advances in 3D-printed polymer-based bone scaffolds. *Polym. (Basel)* 14 (3), 566. doi:10.3390/polym14030566

Yan, F., Shui, X., and Tingfang, W. (2019). Preparation and characterization of sericin/hydroxyapatite/polycaprolactone composite scaffold materials. *Mater. Rep.* 33 (S2), 533–537.

Yang, F., Lu, J., Ke, Q., Peng, X., Guo, Y., and Xie, X. (2018). Magnetic mesoporous calcium sillicate/chitosan porous scaffolds for enhanced bone regeneration and photothermal-chemotherapy of osteosarcoma. *Sci. Rep.* 8 (1), 7345. doi:10.1038/s41598-018-25595-2

Yassin, M. A., Mustafa, K., Xing, Z., Sun, Y., Fasmer, K. E., Waag, T., et al. (2017). A copolymer scaffold functionalized with nanodiamond particles enhances osteogenic metabolic activity and bone regeneration. *Macromol. Biosci.* 17 (6), 1600427. doi:10.1002/mabi.201600427

Ym, L., H, J., and Yf, S. (2022). Preparation and characterization of chitosan/polylactic acid/hydroxyapatite/polyvinyl alcohol composite bone scaffold. *Zhongguo Zuzhi Gongcheng Yanjiu* 26 (18), 2888–2893.

Zhang, H., Cheng, J., and Ao, Q. (2021). Preparation of alginate-based biomaterials and their applications in biomedicine. *Mar. Drugs* 19 (5), 264. doi:10.3390/md19050264

Zhang, H., Wu, X., Quan, L., and Ao, Q. (2022). Characteristics of marine biomaterials and their applications in biomedicine. *Mar. Drugs* 20 (6), 372. doi:10.3390/md20060372

Zhang, W., Gu, J., Li, K., Zhao, J., Ma, H., Wu, C., et al. (2019). A hydrogenated black TiO(2) coating with excellent effects for photothermal therapy of bone tumor and bone regeneration. *Mater Sci. Eng. C Mater Biol. Appl.* 102, 458–470. doi:10.1016/j.msec.2019.04.025

Zhao, D., Zhu, T., Li, J., Cui, L., Zhang, Z., Zhuang, X., et al. (2021). Poly(lactic-co-glycolic acid)-based composite bone-substitute materials. *Bioact. Mater* 6 (2), 346–360. doi:10.1016/j.bioactmat.2020.08.016

Zhao, H., Wu, C., Gao, D., Chen, S., Zhu, Y., Sun, J., et al. (2018). Antitumor effect by hydroxyapatite nanospheres: Activation of mitochondria-dependent apoptosis and negative regulation of phosphatidylinositol-3-kinase/protein kinase B pathway. *ACS Nano* 12 (8), 7838–7854. doi:10.1021/acsnano.8b01996

Zhou, Z. F., Sun, T. W., Chen, F., Zuo, D. Q., Wang, H. S., Hua, Y. Q., et al. (2017). Calcium phosphate-phosphorylated adenosine hybrid microspheres for anti-osteosarcoma drug delivery and osteogenic differentiation. *Biomaterials* 121, 1–14. doi:10.1016/j.biomaterials.2016.12.031

frontiers | Frontiers in Bioengineering and Biotechnology

TYPE Original Research
PUBLISHED 24 February 2023
DOI 10.3389/fbioe.2023.1135248

OPEN ACCESS

EDITED BY
Huihua Yuan,
Nantong University, China

REVIEWED BY
Luzhong Zhang,
Nantong University, China
Liangliang Yang,
Wenzhou Medical University, China

*CORRESPONDENCE
Liqun Yang,
yanglq@lnszjk.com.cn
Guangqi Yan,
yanguangqi_1982@163.com

†These authors have contributed equally to this work

SPECIALTY SECTION
This article was submitted to Biomaterials, a section of the journal Frontiers in Bioengineering and Biotechnology

RECEIVED 31 December 2022
ACCEPTED 16 February 2023
PUBLISHED 24 February 2023

CITATION
Zhang J, Zhang X, Li W, Guo J, Yang L and Yan G (2023), Poly (trimethylene carbonate)/doxycycline hydrochloride films in the treatment of Achilles tendon defect in rats.
Front. Bioeng. Biotechnol. 11:1135248.
doi: 10.3389/fbioe.2023.1135248

Poly (trimethylene carbonate)/doxycycline hydrochloride films in the treatment of Achilles tendon defect in rats

Jinchi Zhang[1,2,3†], Xiaowei Zhang[2†], Wei Li[3], Jing Guo[2], Liqun Yang[1,2*] and Guangqi Yan[4*]

[1]Department of Biomaterials, Shengjing Hospital of China Medical University, Shenyang, China, [2]NHC Key Laboratory of Reproductive Health and Medical Genetics (China Medical University), Liaoning Research Institute of Family Planning (The Affiliated Reproductive Hospital of China Medical University), Shenyang, China, [3]College of Kinesiology, Shenyang Sport University, Shenyang, China, [4]Department of Oral and Maxillofacial Surgery, School of Stomatology, China Medical University, Shenyang, China

Introduction: In this study, Poly (trimethylene carbonate)/Doxycycline hydrochloride (PTMC/DH) films were introduced to repair the Achilles tendon defects for the first time.

Methods: (PTMC/DH) films with different DH content of 10, 20, and 30% (w/w) were prepared by solvent casting. The *in vitro* and *in vivo* drug release of the prepared PTMC/DH films was investigated.

Results: The results of drug release experiments showed that the PTMC/DH films released effective concentrations of doxycycline for more than 7 and 28 days *in vitro* and *in vivo*, respectively. The results of antibacterial activity experiments showed diameters of 25.00 ± 1.00 mm, 29.33 ± 1.15 mm, and 34.67 ± 1.53 mm, respectively, for the inhibition zones produced by the release solutions of PTMC/DH films with 10, 20 and 30% (w/w) DH at 2 h, indicating that the drug-loaded films could inhibit Staphylococcus aureus well. After treatment, the Achilles tendon defects have recovered well, as indicated by the more robust biomechanical properties and the lower fibroblast density of the repaired Achilles tendons. Pathology revealed that the pro-inflammatory cytokine, IL-1β, and the anti-inflammatory factor, TGF-β1, peaked in the first three days and gradually decreased as the drug was released more slowly.

Discussion: These results demonstrated that the PTMC/DH films have great potential for regenerating Achilles tendon defects.

KEYWORDS

poly (trimethylene carbonate), doxycycline hydrochloride, Achilles tendon defect, regeneration, treatment

1 Introduction

The Achilles tendon, one of the thickest and most powerful tendons in the body, is anatomically located approximately 15 cm above the heel tuberosity and consists mainly of a fusion of the tendons of the deep flounder and superficial gastrocnemius muscles. The incidence of traumatic injury and rupture of the Achilles tendon is increasing, whether or not it is associated with a surrounding soft tissue defect. This problem is challenging for tissue engineering technology and regenerative medicine (Bottagisio and Lovati, 2017). Achilles tendon defects

are common in sports and other rigorous movements and can lead to functional impairment and months or years of disability (Dams et al., 2019). In addition to direct injuries, it is estimated that approximately 70% or more of Achilles tendon defects are more commonly involved during sports, especially explosive sports such as ball and track and field (Ganestam et al., 2016). Achilles tendon defects are the most common of all sports injuries, with post-operative Achilles tendon re-rupture rates ranging from approximately 1.7%–5.6% (Cerrato and Switaj, 2017). The injury rate (IR) for Achilles tendon defects in 255 NCAA competitive athletes was calculated to be 2.17% (Chan et al., 2020). It has been calculated that 850 (0.119%) of the 713,456 individuals in the Korean Health Insurance Service-National Sample Cohort database underwent repair of Achilles tendon defects, with the total number of procedures per year increasing with age, peaking and subsequently decreasing at 30–39 years of age (Park et al., 2022). The flexible use of tissue engineering in rehabilitation medicine provides the most favorable support and assurance for repairing Achilles tendon defects. Although there are many surgical approaches to repairing Achilles tendon defects in modern regenerative medicine, there is still no consensus on the simplest, most effective, and safest technique (Chugaev et al., 2018; Monnerie et al., 2019). At this stage, ultrasound imaging is used clinically to examine the early healing of Achilles tendon defects. A unique Achilles tendon defect repair score has also been developed, which assesses the presence or absence of echogenicity in the tendon defect area and the distribution of peritendinous tissue (Hiramatsu et al., 2018). One data showed that in 808 patients with Achilles tendon defects, ultrasound had a sensitivity of 94.8% and a specificity of 98.7% for detecting complete Achilles tendon defects, and the study illustrated the accuracy of ultrasound as a means of providing a diagnostic tool for treating patients with Achilles tendon defects (Aminlari et al., 2021).

Doxycycline hydrochloride (DH) is a commonly used antibiotic in clinical practice. It belongs to the tetracycline group of antibiotics. It is a relatively broad-spectrum antibiotic with a strong antibacterial effect, showing some antibacterial activity against both gram-positive and negative bacteria. Matrix metalloproteinases (MMP) are enzymes involved in the degradation and remodeling of the extracellular matrix (ECM) and play an essential role in the repair of Achilles tendon defects (Molloy et al., 2006; Garofalo et al., 2011; Thomopoulos et al., 2015; Gong et al., 2018; Fernandes de Jesus et al., 2019). Drugs containing MMP have been the first choice in treating Achilles tendinopathy (Smith and Leyden, 2005; Kessler et al., 2014; Nguyen et al., 2017; Baldwin et al., 2019). It is well established in the literature that DH, a drug that inhibits MMP expression *in vivo*, thereby inhibiting the continued expression of inflammatory factors, can have an anti-inflammatory and analgesic effect and reduce swelling. Bedi et al. (2010) (Smith and Leyden, 2005) reported that the immediate administration of doxycycline after surgery could inhibit collagenase activity and play an essential role in improving the structural healing rate. Pasternak et al. (2006) (Bramono et al., 2004) evaluated the effect of doxycycline on Achilles tendon healing in a rat Achilles tendon transection model. This study showed the pharmacological effects of MMP inhibitors on tendon repair for the first time. Sobhani-Eraghi et al. (2020) randomized 20 healthy rats of the same sex into sham-operated and doxycycline groups. The rats underwent surgical intervention with a 2-mm incision on the lateral aspect of the right Achilles tendon. The group was treated with doxycycline 50 mg/kg/d by gavage for 30 days. The study showed significant changes in the repaired tissue in the treated group compared to the sham-operated group, as indicated by a more regular arrangement of collagen fibers, increased cell density, and fibroblast activity. The results indicated that doxycycline improves the extent of the Achilles tendon defect, especially the integrity of the collagen fiber arrangement.

Biodegradable aliphatic polycarbonates have good biodegradability, excellent biocompatibility, and physical properties as an essential class of biodegradable medical polymeric materials (Zhu et al., 1991; Pego et al., 2003; Sachlos and Czernuszka, 2003). Compared with polyesters, such as PLA and PLGA (Albertsson and Eklund, 1995; Athanasiou et al., 1996; Karp et al., 2003), the most significant advantage of biodegradable aliphatic polycarbonates is that no acidic degradation products are generated during the degradation process (Chen et al., 2022), which does not cause side effects such as sterile inflammation in the organism. The most common and widely studied biodegradable aliphatic polycarbonate as a biomedical material is poly (trimethylene carbonate) (PTMC). PTMC has good biocompatibility and biodegradability and is flexible at body temperature. It can be widely used in biodegradable ligature devices, controlled drug release materials, and *in vivo* implant materials. Shieh et al. (1990) found that random copolymers of 90% dimethyltrimethylene carbonate (DMTMC) and 10% trimethylene carbonate (TMC) could be prepared as polymeric material fibers. They retain excellent biomechanical properties and are suitably biodegradable. The basis was laid for the proliferation and migration of peripheral cells in rabbit Achilles tendon defects, further enhancing the activity of stromal cells. Li et al. (2020) prepared a nanofibrous polycaprolactone/poly (trimethyl carbonate) methacrylate (PCL/PTMC-MA) biomaterial polymer scaffold and observed the fibrous morphology of the composite scaffold by scanning electron microscopy. The results showed that this polymer composite scaffold had substantially increased mechanical properties, prevented tissue adhesions, and promoted cell proliferation and differentiation around the Achilles tendon defect. Hence, the application of PTMC as a carrier material for the repair of Achilles tendon defects could be an up-and-coming area of research in the future.

In this study, degradable Doxycycline hydrochloride (DH) loaded poly (trimethylene carbonate) (PTMC) films were developed to achieve slow drug release for a prolonged period. The effect of the DH-loaded PTMC films on the healing process of Achilles tendon rupture after surgical repairment was assessed, confirming that biodegradable PTMC/DH films would enhance the healing process and improve the biomechanical properties of surgically repaired Achilles tendons.

2 Materials and methods

2.1 Materials

Trimethylene carbonate (TMC) was purchased from Daigang Biomaterials Co., Ltd. (Jinan, Shandong, China), recrystallized twice with ethyl acetate and dried under vacuumed at 37°C for 24 h before copolymerization. The catalyst, stannous iso octanoate $Sn(Oct)_2$ (95%) was purchased from Sigma-Aldrich and used as received. Doxycycline hydrochloride (DH) drug was purchased from Aladdin (molecular formula $C_{22}H_{24}N_2O_8{\cdot}HCl{\cdot}0.5H_2O{\cdot}0.5C_2H_6O$, molecular

weight 512.94, purity ≥ 98%) and arrived cold chain and used. All other solvents and reagents were of analytical grade and purified using standard methods.

2.2 Preparation of PTMC polymer

The PTMC polymer (molecular weight Mw ≈ 32,000 Da) was synthesized by ring-opening polymerization (Yang et al., 2015). Briefly, TMC (20.4 g, 0.2 mol) and $Sn(Oct)_2$ (0.2 M; 1/20,000 eq, 25 μL) were added to a glass ampoule. The ampoule was then heat sealed under a high vacuum (5 mmHg) and immersed in an oil bath at 130°C ± 2°C for 24 h. The oil bath was removed, and the ampoule was cooled to room temperature. The polymer was obtained by crushing the ampoule. Subsequently, the crude polymer product was dissolved in chloroform, further purified in ice-methanol, and dried under vacuum to a constant weight. Mn and PDI were calculated using polystyrene as a standard.

2.3 Preparation and characterization of PTMC/DH films

Certain PTMC and 10%, 20%, 30% (w/w) DH were weighted and dissolved in Dichloromethane (DCM). A clear liquid is obtained by magnetic stirring and then left to remove the air bubbles. The solution was poured into a flat-bottomed PTFE Petri dish, allowing the solution to level off naturally, and then placed in a drying oven for 6 h. The drug-carrying film was prepared with an area of 10 mm × 50 mm and a thickness of approximately 0.2 mm. The film was dried under vacuum at room temperature to remove residual organic solvent and water to a constant weight, sealed, and packed at −20°C for storage.

A scanning electron microscope (TESCAN MIRA LMS, Czech Republic) was used to examine the macroscopic morphology of the PTMC and PTMC/DH drug-carrying films. FTIR spectroscopy was performed using a model US Thermo Scientific Nicolet iS50. The resolution in the ATR mode was 4 cm^{-1}, and a total of 27 scans were performed. The drug-carrying film samples were compressed into potassium bromide disks and analysed in the range of 400–4,000 cm^{-1}.

2.4 *In vitro* release behavior of PTMC/DH films

PTMC/DH films of 11 mm in length and 5 mm in width were put in tubes with 5 mL of deionized water. The tubes were then maintained under a temperature shaker at 37°C for 24 h. Then, 5 mL of the eluate was collected and transferred to a centrifuge tube for storage at room temperature, and a further 5 mL of fresh deionized water solution was added to each tube at 2 h, 4 h, 8 h, 12 h, 16 h, 20 h, 1–14 days, respectively. The release amount of doxycycline hydrochloride was measured using a high-performance liquid chromatography (HPLC) (Waters, Milford, MA, United States) with a Waters Model 1515 isocratic HPLC pump to quantify the doxycycline levels in the eluate.

2.5 *In vitro* antibacterial activity assay of PTMC/DH films

The activated *Staphylococcus aureus* was transferred to a nutrient solution and incubated at 37°C for 24 h. The bacteria were then appropriately diluted with this nutrient solution. Subsequently, the *Staphylococcus aureus* bacterial solution was removed with a sterile cotton swab and spread evenly over the nutrient agar plates. Three parallel samples were taken at each time point. The solution was then incubated at a constant temperature for 24 h. The diameter of the inhibition ring was measured using a vernier caliper with an accuracy of 0.1 mm, and the area without visible bacterial growth was visually observed as the edge of the inhibition ring. *Staphylococcus aureus* was also incubated with the control pure PTMC films.

2.6 Establishment of rat model of Achilles tendon defect

Twenty-eight SPF male SD rats, 8–10 weeks and 200 ± 50 g in weight, were selected and randomly divided into 7 groups of 4 rats each for *in vivo* Achilles tendon defect repair experiments. The experimental group 1–3 were treated with 10%, 20% and 30% PTMC/DH films, respectively, and experimental group 4 was treated with doxycycline hydrochloride powder covered with pure PTMC films; the control group 5 was treated with pure PTMC films, the blank group 6 was given no treatment, and the healthy group 7 was normal healthy Achilles tendon without any operation. The rats were anesthetized using Pentobarbital sodium, and after sterilization, longitudinal incisions were made on the skin surface of the bilateral (right and left) Achilles tendons of the rats, with a defect of approximately 1/2 of the Achilles tendon, 5 mm longitudinally, as shown below (Figure 1). All operations were performed according to the Regulations of Experimental Animal Administration issued by The people's Government of Liaoning province.

After surgery, the rat was allowed to move freely in the cage to simulate early functional treatment. two rats of each group were randomly executed at 2 weeks and 4 weeks, respectively. One Achilles tendon specimen was sent for histological analysis and three Achilles tendon specimens were sent for biomechanical analysis in each period.

2.7 Analysis of doxycycline levels *in vivo*

Collect 1 mL of blood on each 1, 3, 5, 7, 14, 21, and 28 days, using two centrifuge tubes separated by 0.5 mL each. One copy of the collected blood sample supernatant was sent for pathological analysis and the other for testing by liquid mass spectrometry Liquid Chromatography-Mass Spectrometry (LC-MS). The collected blood samples were centrifuged using a centrifuge and subsequently stored at ultra-low temperature. Centrifugation conditions: centrifuge speed 10,000 rpm for a total of 10 min at −4°C. The amount of doxycycline hydrochloride in the plasma will be determined by LC-MS(Waters H-Class/Xevo TQD, Germany). The mobile phase acetonitrile water (50:50, v/v) was diluted to obtain calibration standard solutions at concentrations of

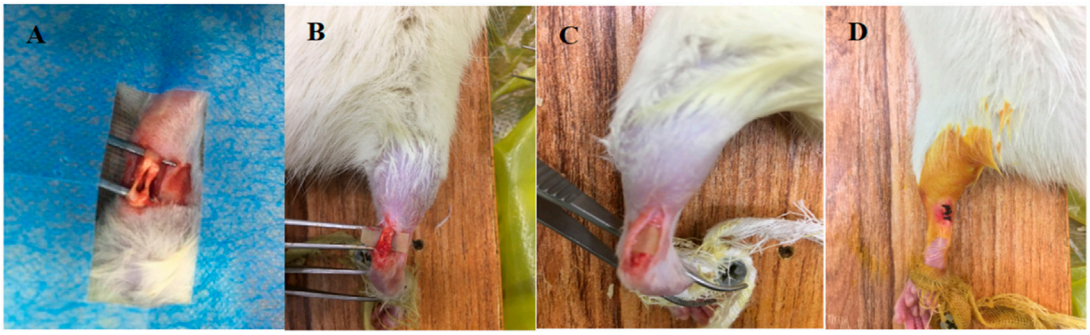

FIGURE 1
(A) Creation of Achilles tendon defect; **(B)** Transfer of PTMC/DH carrier film to Achilles tendon defect; **(C)** Complete encapsulation of Achilles tendon defect with PTMC/DH film; **(D)** Wound Closure.

25, 50, 100, 500 and 1,000 ng/mL^{-1}. These standard solutions (10 μL) were diluted with mixed blank plasma (90 μL) to prepare calibration standards containing 5–1,000 ng/mL^{-1} (2.5, 5, 10, 50, 100 ng/mL^{-1}). For plasma samples, analytes were extracted from rat plasma using a one-step protein precipitation method in methanol. In a 100 μL rat plasma sample, anhydrous methanol (800 μL) was added to a 1.5 mL centrifuge tube and vortexed for 10 min. The sample was then centrifuged at 14,000 rpm for 10 min at 4°C. The supernatant was then separated from the Eppendorf tube and transferred to a glass culture tube. The sample extract was then dried under a stream of nitrogen at 55°C for 45 min using an MD 200 Sample Concentrator (Liaoning Research Institute of Family Planning, Laboratory Equipment). The residue obtained from this process was then reconstituted in 100 μL of mobile phase and collected in an Eppendorf tube. The solution was then vortex mixed for 50 s, sonicated for 10 min and centrifuged at 14,000 rpm at room temperature for 10 min. The supernatant was transferred to an Agilent LC-MS sample vial and 2 μL was sampled in the LC-MS instrument.

2.8 Biomechanical tests

42 rat Achilles tendons collected from 2 to 4 W were moistened with saline, and covered with gauze for testing. The Achilles tendon was fixed on an Instron 5966 universal material testing machine for tensile testing. The Achilles tendon anastomosis was located roughly in the middle of the two tendon clamps. Fixed the Achilles tendon so that the direction of tension was on the same axis as the Achilles tendon, zeroed under complete relaxation of the Achilles tendon, loaded with 0.5 N preload, maintained proper tension on the Achilles tendon and zeroed again. Perform 10 cycles of stretching with a load range of 0–8 N and a loading rate of 3 mm/min. The Achilles tendon was continuously drip-bathed with a soft NS-filled needle during the test. Loaded pull-off test, stretching at a rate of 3 mm/min, with the Achilles tendon not breaking at the jig in the middle position as the criterion for a successful experiment. The computer automatically outputs the maximum load, stiffness and strain at maximum load. After the completion of the mechanical test all specimens are added to a certain amount of Phosphate Buffer Solution (PBS), PH 7.4. They are rapidly frozen with liquid nitrogen and stored for backup.

2.9 Pathological histological analysis

A total of 14 root tendons collected from 2 to 4 weeks were subjected to histological examination, fixed in 10% formalin and embedded in paraffin. The embedded tendons were cut into 4 μm cross-sectional sections and stained with hematoxylin and eosin (HE). An independent examiner completed the histological interpretation at magnifications of ×10 and ×20 and calculated the number and density of Fibroblast (Fb) displacements. In addition, a total of 49 serum samples from 7 blood sampling sites were subjected to Enzyme-linked Immunosorbent Assay (ELISA) to test for the pro-inflammatory factor-rat interleukin IL-1β and the anti-inflammatory factor-growth transforming factor TGF-β1 by double antibody sandwich ELISA, both kits were purchased from Rexin Bio (Size 96T, sensitivity: <0.1 pg/mL, IL-1β test range: 1.25–40 pg/mL, TGF-β1 test range: 2.5–80 ng/mL). Operating procedure All reagents and components are first brought back to room temperature, standards, controls and samples, and it is recommended to do duplicate wells. The operating procedure is as follows:

1) Prepare the working solutions for the various components of the kit as described in the previous instructions. 2) Remove the required slides from the aluminium foil bag and put the remaining slides back into the refrigerator in a sealed self-sealing bag. 3) Set up the standard wells, 0-value wells, blank wells and sample wells. Add 50 μL of standard at different concentrations to each of the standard wells, 50 μL of sample diluent to the 0-value wells, and 50 μL of the sample to be tested to the blank wells. 4) Add 100 μL of Horseradish Peroxidase (HRP)-labelled detection antibody to the standard wells, 0-value wells and sample wells, except for the blank wells. 5) Cover the reaction plate with sealing film. Incubate the plate for 60 min at 37°C in a water bath or thermostat protected from light. 6) Remove the sealing film, discard the liquid, pat dry on blotting paper, fill each well with washing solution, leave for 20 s, shake off the washing solution, pat dry on blotting paper and repeat 5 times. If using an automatic plate washer, follow the operating procedures of the

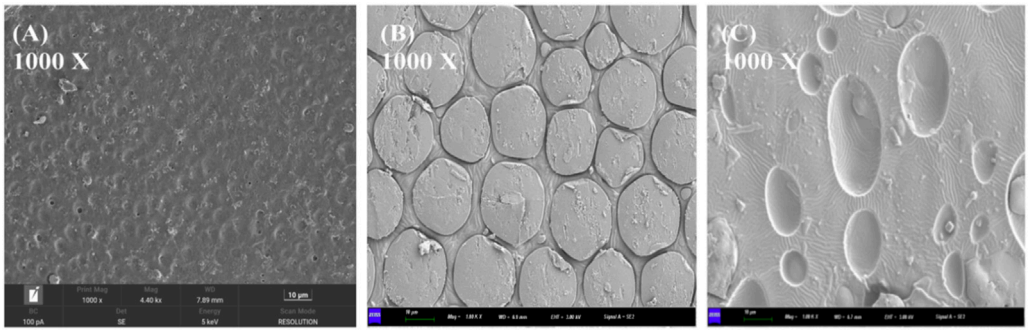

FIGURE 2
Scanning electron microscope images and magnification distribution of **(A)** 10% drug-loaded film; **(B)** 20% drug-loaded film; **(C)** 30% drug-loaded film.

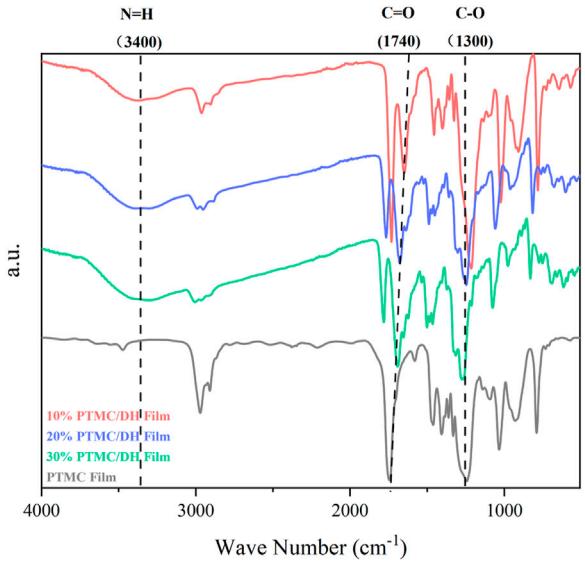

FIGURE 3
FTIR spectra of PMTC/DH films and PTMC films.

washer and add a 30 s soak procedure to improve the accuracy of the assay. At the end of the wash, before adding the substrate, pat the reaction plate dry on clean, non-flaking paper. 7) Mix substrate A and B in a 1:1 volume and add 100 µL of substrate mixture to all wells. Cover the plate with sealing film and incubate for 15 min at 37°C in a water bath or thermostat protected from light. 8) Add 50 µL of termination solution to all wells and read the Optical Density (OD) of each well on an enzyme marker.

3 Results

3.1 Characterization of PTMC/DH films

PTMC/DH films were prepared by the solvent-casting technique. Figures 2A–C shows the SEM images of the drug-loaded films with different concentrations of doxycycline hydrochloride embedded in PTMC. The surface of the PTMC films containing doxycycline hydrochloride is rough. With the amount of doxycycline hydrochloride increased, the grooves and drug particles on the surface of the loaded film become more pronounced.

TABLE 1 Weight loss and PH value of PTMC films after enzymatic digestion.

Time (d)	Weight loss (dry weight)/%	PH
1	15.8 ± 1.68	7.14 ± 0.13
3	35.56 ± 3.69	7.45 ± 0.11
5	49.80 ± 1.88	7.31 ± 0.03
7	64.70 ± 2.21	7.37 ± 0.03
9	89.90 ± 1.48	7.30 ± 0.05

Figure 3 shows the Fourier Transform infrared (FTIR) spectra of the pure PTMC film and the PTMC/DH films. Compared to the spectrum of the PTMC, a new vibrational peak appears at 3,400 cm^{-1} in that of the PTMC/DH films, which can be attributed to the N-H bond of doxycycline hydrochloride, and the peak at around 1,300 cm^{-1} may be the result of increased C-O bonding in doxorubicin (Pasternak et al., 2006; Sun et al., 2017). Furthermore, the vibration at 1,740 cm^{-1} (C=O bond) increases as the DH amount increases in PTMC films. The results of FTIR confimed the successful incorporation of the doxorubicin into the PTMC films. The chemical structure of PTMC has been photographed by using FTIR spectroscopy. Stretching vibrations of the -CH_2- bond (2,971 and 2,909 cm^{-1}) and the C=O bond (1,700 cm^{-1}) were observed in PTMC (Han et al., 2010).

To ensure the PTMC/DH films can be degraded *in vivo*, the degradation behavior of PTMC was performed in lipase solutions. There was a significant change in the weight loss (Dry weight) of the pure PTMC films after enzymatic degradation. The results showed that the weight loss was 15.8% ± 1.68%, 35.56% ± 3.69%, 89.90% ± 1.48% at day 1, 3, 9, respectively, indicating an efficient degradation behavior of the pure PTMC under enzymatic digestion, however, the PH values did not change much (Table 1).

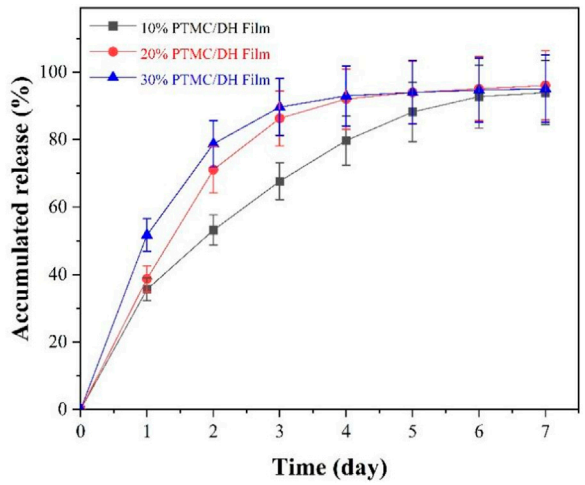

FIGURE 4
In vitro cumulative release of doxycycline hydrochloride.

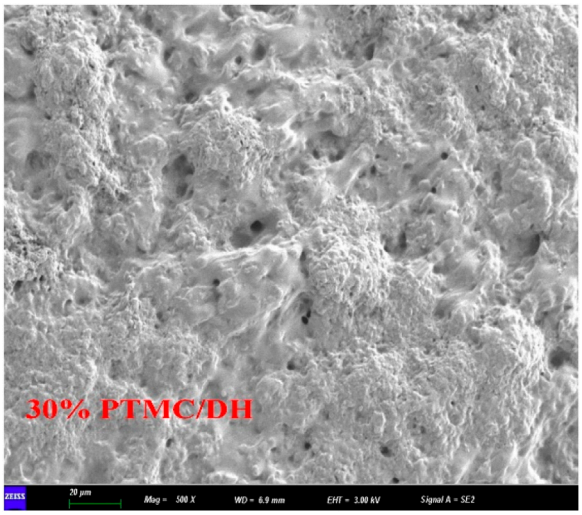

FIGURE 5
SEM images after hydrolysis of drug-loaded films at different ratios.

3.2 *In vitro* release behavior of PTMC/DH films

Figure 4 shows the accumulated release profiles of doxycycline from the PTMC films *in vitro*. The cumulative release profiles suggested that 35.60%, 38.70% and 51.73% of the doxycycline was releasedon day 1, and 67.67%, 86.28%, 89.64% was eluted on day 3 for 10%, 20% and 30% PTMC/DH films, respectively. At 7 days, the accumulated released of doxycycline from all the group reached over 95%. Overall, the PTMC/DH films could provide sustained drug release for more than 7 days *in vitro*, which can be helpful for drug therapy in the acute phase of repairing Achilles tendon defects.

After release, SEM images of the remaining drug-loaded films showed that the surface drugs were all diluted, and there were many grooves and pores on the film surface (Figure 5), allowing nutrients to pass through.

3.3 The *in vitro* antibacterial effect

The *in vitro* antibacterial effect was evaluated semi-quantitatively by measuring the diameter of the antibacterial ring (Figure 6). The results showed that at 2 h post-release, the diameter of the antibacterial ring produced by the release solution of 10% PTMC-DH film against *Staphylococcus aureus* was 25.00 ± 1.00 mm; the diameter of the antibacterial ring produced by the release solution of 20% PTMC-DH film against *Staphylococcus aureus* was 29.33 ± 1.15 mm; and that of the antibacterial ring produced by the release solution of 30% PTMC-DH film against *staphylococcus aureus* was 34.67 ± 1.53 mm, showing that as the drug content increased, the diameter of the inhibition ring was also larger, the inhibition effect of its drug-loaded film was more obvious. On the first day of release, the diameters of the inhibition rings of the three ratios were 12.33 ± 2.08 mm, 17.33 ± 1.53 mm and 18.34 ± 1.15 mm, and on the third day of release, the diameters of the inhibition rings of the three ratios were 11.67 ± 0.58 mm, 15.33 ± 1.15 mm and 16.67 ± 1.15 mm. On the fifth day of release, the inhibition rings of the three ratios were 10.67 ± 0.58 mm, 13.67 ± 1.53 mm and 15.33 ± 0.57 mm. In contrast, no inhibition rings were observed in the control group of pure PTMC.

3.4 *In vivo* release behavior of PTMC/DH films

Figure 7 shows the *in vivo* release patterns of doxycycline *in vivo*. A burst release was observed at day 1. After that, the doxycycline level decreased gradually with time, and the drug can sustained release at the tendon for 28 days.

3.5 Biomechanical studies

Rats were euthanized 2 and 4 weeks after surgery. The repaired Achilles tendons on both sides of the rats were severed from the proximal calf tendon junction, samples were removed and placed in 10% formalin tissue solution for fixation and biomechanical testing was performed. The maximum load on the repaired Achilles tendon at 2 weeks was gradually increased as the drug content increased from 10% to 30% (Figure 8A); At 4 weeks, the experimental group treated with 30% PTMC/DH films showed much stonger maximum load capacity on the Achilles tendon, which was comparable to the strength level of the healthy group. The control and blank groups without treatment of doxycycline hydrochloride showed much lower maximum strength.

At 2 weeks, the rupture elongation of the repaired Achilles tendon in the experimental was also gradually increased as the DH content increased in PTMC films (Figure 8B); At 4 weeks, the experimental group exhibited a rupture elongation almost close to the level of strength of the Achilles tendon in the

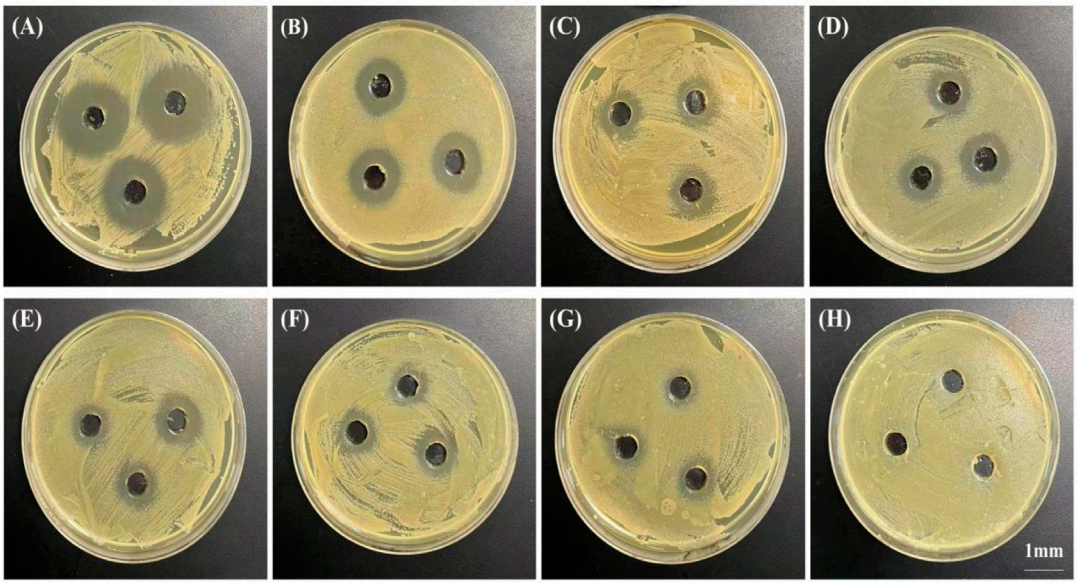

FIGURE 6
Bacteriostatic rings produced by PTMC-loaded doxycycline hydrochloride loaded drug-loaded films releasing solutions at 2 h **(A)**, 4 h **(B)**, 8 h **(C)**, 12 h **(D)**, 20 h **(E)**; Drug-loaded films at 1 day **(F)** and 3 days **(G)** and by blank PTMC leachate at 1 day **(H)**. The scale bar is 1 mm.

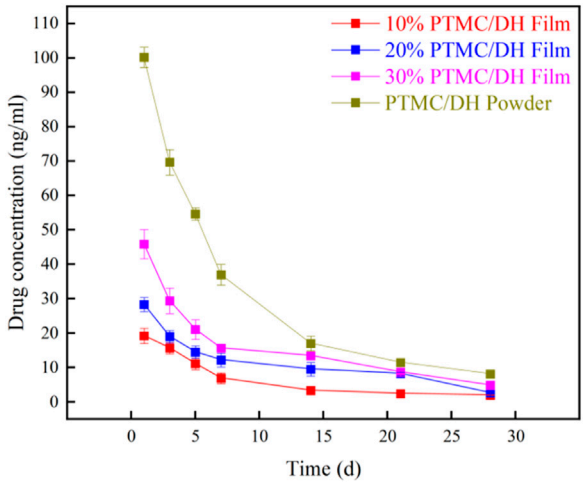

FIGURE 7
In vivo release profile of doxycycline hydrochloride in plasma.

healthy group, which also proved that the rats' Achilles tendon had a greater rupture elongation after the treatment of drug retardation, indicating that the Achilles tendon defect has been well repaired.

In addition, the stress-strain curves of the rat Achilles tendon samples after stretching were also tested and the results showed that the peak of the force-deformation curve tested was significantly greater in the 30% PTMC/DH Film group at 2 weeks than in the 10% and 20% loaded films groups, and the same was true at 4 weeks, but the peak of the overall stress-strain curve at 4 weeks was much improved compared to 2 weeks and the difference was statistically significant (Figure 9). As the area of the stress-strain curve increased at 4 weeks, it demonstrated the greater plasticity, impact resistance and toughness of the repaired Achilles tendon, which was able to withstand greater stress and deformation.

3.6 Histopathological study

After observing the images obtained after H&E staining for evaluation, it was found that the experimental group did not cause a more severe inflammatory response compared to the control group. However, in the experimental group, at 2 weeks, it was evident that a lot of inflammatory factors and new capillaries could be observed. In contrast, a severe inflammatory response was observed in the control group and in the control group as well as a large collagen fibril component; In the experimental group there was only a slight inflammatory factor at 4 weeks, a few mononuclear inflammatory cells and no neovascularisation, indicating that the Achilles tendon defect had been well repaired (Figure 10). In contrast inflammatory cells were still present in the control and control groups, but were reduced relative to 2 weeks.

The leading cause of Achilles tendon adhesion after surgery is that the inflammatory reactions at the Achilles tendon injury cause marked hyperplasia of the fibroblast cells, leading to the proliferation of fibrous connective tissue, granulation tissue and scar formation. The target area of tissue was selected for 400× imaging using CaseViewer 2.2 scanning and viewing software, the number of fibroblasts was measured in each section in fields of view using Image-Pro Plus 6.0 analysis software (Figure 11), and fibroblast density was displayed in Figure 12. As seen in Figure 12, the fibroblasts density in the experimental group treated with 10% PTMC/DH films was 1,605.06 ± 199.26 n/mm^2

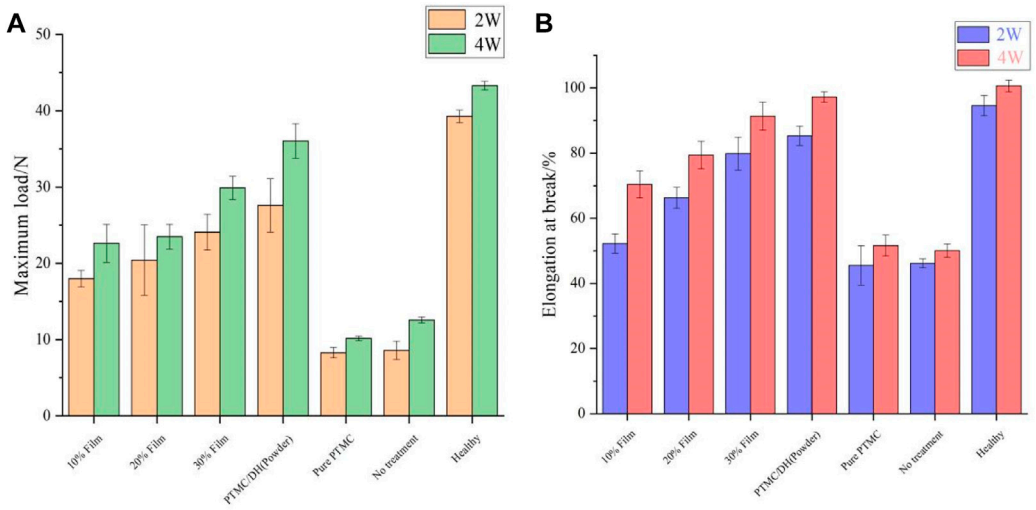

FIGURE 8
Maximum load **(A)** and elongation at rupture **(B)** of Achilles tendon at 2 and 4 weeks after surgery.

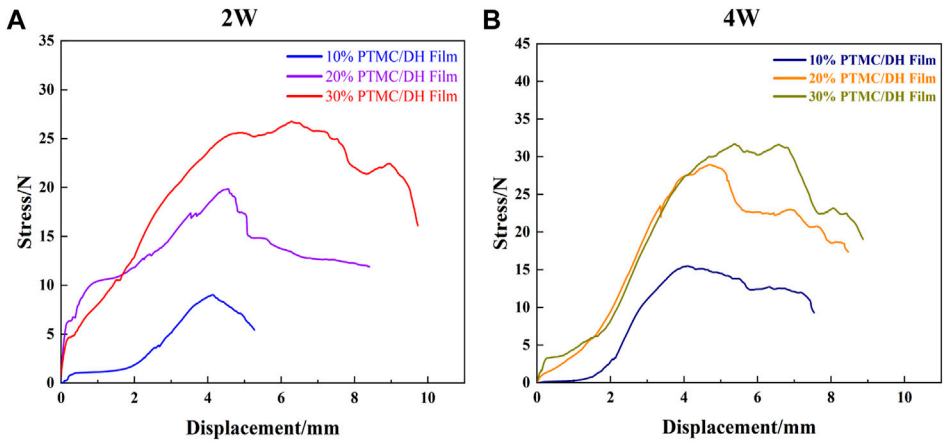

FIGURE 9
Stress-strain curves of the Achilles tendon after stretching at **(A)** 2 W and **(B)** 4 W for 10%, 20% and 30% drug-loaded films.

at 2 weeks and 1,367.27 ± 125.93 n/mm^2 at 4 weeks ($p < 0.01$); The density of Fibroblasts in the experimental group treated with 20% PTMC/DH films was 1,396.89 ± 215.95 n/mm^2, while the density of Fibroblasts in the experimental group treated with 30% PTMC/DH films was 1,329.44 ± 70.67 n/mm^2 at 2 weeks and 821.44 ± 150.64 n/mm^2 at 4 weeks ($p < 0.01$); The density of Fibroblasts in the fourth group was 1,095.16 ± 43.11 n/mm^2 at 2 weeks and 821.44 ± 150.64 n/mm^2 at 4 weeks ($p < 0.01$); In the control group, the fibroblast density was 1,399.70 ± 89.29 n/mm^2 at 2 weeks and 1,007.53 ± 47.49 n/mm^2 at 4 weeks; in the blank group, the Fibroblast density was 1,167.32 ± 156.35 n/mm^2 at 2 weeks and 926.81 ± 142.77 n/mm^2 at 4 weeks; The Fibroblast density in the healthy group was 511.67 ± 33.80 n/mm^2 at 2 weeks and 591.70 ± 28.58 n/mm^2 at 4 weeks, with no statistically significant difference ($p > 0.05$). The decrease in the density of the fibroblast of the Achilles tendon defect verified the reduction of the inflammatory response of the lesion site after treatment, reducing the phenomenon of Achilles tendon adhesion and helping to achieve sound therapeutic effects.

After ELISA enzyme-linked immunosorbent assay, the pro-inflammatory factor rat interleukin IL-1β was measured to show a trend of increasing and then decreasing inflammatory response within 28 days (Figures 13A, B). The experimental group showed the highest inflammatory response on 5 days, with a concentration of 2.7558 pg/mL in the 10% drug-loaded film group; 2.4511 pg/mL in the 20% drug-loaded film group; 2.8695 pg/mL in the 30% drug-loaded film group; and 2.3195 pg/mL in the PTMC/DH (Powder) group.

Similarly, the anti-inflammatory factor TGF-β1 was also measured to show an upward and then downward trend, which in turn maintained a dynamic balance with the pro-inflammatory factors in the organism (Figures 14A, B). The highest levels of

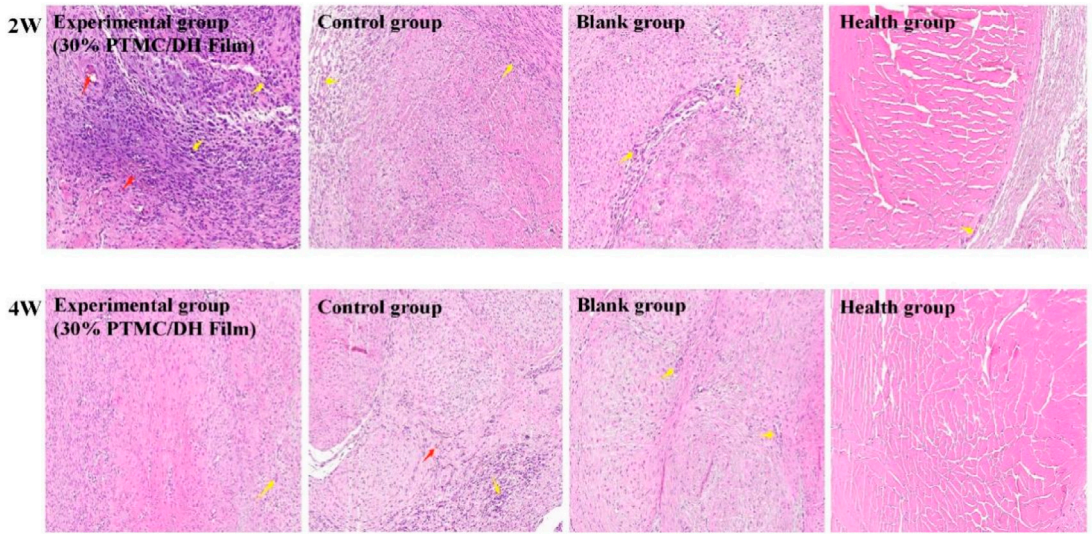

FIGURE 10
Histology of the rat Achilles tendon at 2 weeks and 4 weeks postoperatively (Red arrows show neovascularization, Yellow arrows show inflammatory cells).

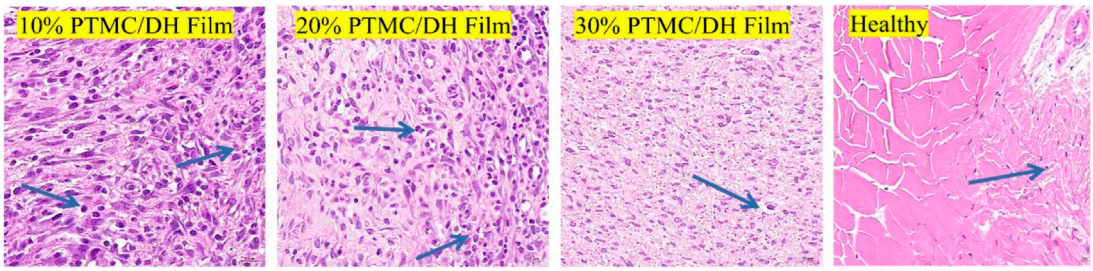

FIGURE 11
Intercepted field of view images of fibroblast density after 4 weeks of treatment (Blue arrows show fibroblast cells).

inflammation were observed in the experimental group at 3 days, with 14.1669 ng/mL in the 10% drug-loaded film group, 15.1968 ng/mL in the 20% drug-loaded film group, 17.4135 ng/mL in the 30% drug-loaded film group and 13.2215 ng/mL in the PTMC/DH (powder) group. Levels were not as pronounced as in the experimental group, which may be related to the addition of the drug, which was able to inhibit the expression of inflammatory factors due to the release of the drug, thus reducing the level of inflammation in the peritendinous area.

4 Discussion

As a new era, human standard of living has been further improved. But with this comes problems that have gradually come to the surface. Nowadays sports injuries happen to everyone and Achilles tendon defects in particular have become a popular sports trauma condition. In adolescence, a large amount of physical inactivity leads to a weakening of the muscles around the Achilles tendon, a decrease in soft tissue flexibility and a decrease in the strength of the ligaments to resist external forces. If high intensity sports training is performed, this can lead to damage to the Achilles tendon, which can be severe enough to cause an Achilles tendon defect. Complications following an Achilles tendon defect are not uncommon, with tendon re-rupture being the most common. Postoperative Achilles tendon re-rupture rate of about 7% (Ingvar et al., 2005). Achilles tendon defects are a common injury in sports and other strenuous activities and can lead to functional impairment and disability. The most common clinical approach to human tendon defects is autograft, however this approach leads to donor area morbidity and further debilitation (Jayasree et al., 2019). From a clinical perspective, there is a desire to develop allogeneic materials to complete the repair of Achilles tendon injuries. Biomedical polymers can be used to treat and repair soft tissues, ligaments, muscles and organs that have been damaged by living organisms.

Biodegradable aliphatic polycarbonate has good biodegradability, excellent biocompatibility and physical and mechanical properties (Zhu et al., 1991; Pego et al., 2003; Zhang et al., 2006), and is an important class of biodegradable medical

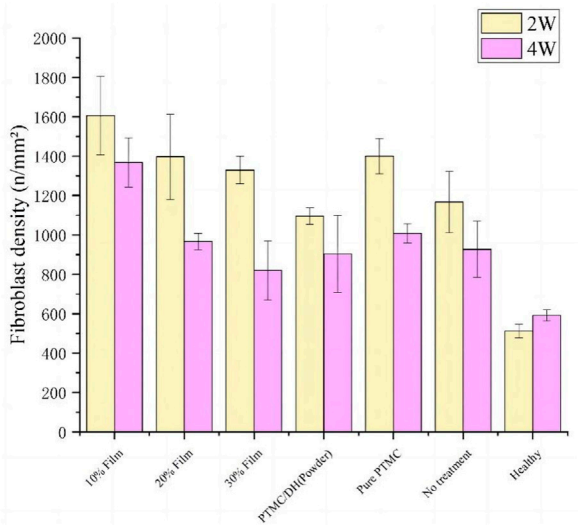

FIGURE 12
Comparison of fibroblast density value counts between groups at 2 weeks and 4 weeks.

polymer materials. Compared with polyhydroxy carboxylic acid esters and their copolymers (Athanasiou et al., 1996; Karp et al., 2003; Sachlos and Czernuszka, 2003), the greatest advantage of biodegradable aliphatic polycarbonates is that no acidic degradation products are generated during the degradation process (Albertsson and Eklund, 1995), which does not cause side effects such as sterile inflammation in the organism. New photothermally responsive elastomeric composites of aliphatic polycarbonates have been reported, which have efficient self-healing properties and controlled mechanical properties (Chen et al., 2022). The most common and widely studied biodegradable aliphatic polycarbonate as a biomedical material is polytrimethylene carbonate because of its better biocompatibility and degradability (Yang et al., 2014; Yang et al., 2016). MMP is an important bioactive substance *in vivo* and a close relationship between MMP and the degree of recovery of the Achilles tendon has been studied (Garofalo et al., 2011; Mitsui et al., 2012). In the course of past studies, it has been demonstrated that doxycycline hydrochloride is effective in the repair of Achilles tendon defects. Doxycycline hydrochloride is considered to be the most effective inhibitor of MMP among the tetracyclines, and many authors have used doxycycline, a tetracycline, in the repair of Achilles tendon injuries with satisfactory results, and this drug has several clinical applications at this stage (Griffin et al., 2011; Dong et al., 2012). Bedi et al. (2010) had a key role in improving the structural healing rate and success of massive tendon sleeve tears by hypothesizing that doxycycline given immediately postoperatively could accelerate healing by inhibiting collagenase activity. In the rat model, MMP-13 activity has returned to lower basal levels, and therefore doxycycline is less sensitive to its inhibition at 4 weeks postoperatively. Nguyen et al. (2017) used oral doxycycline in a rat model of Achilles tendon defect. The results showed that oral doxycycline accelerated matrix remodelling and promoted the rate of recovery of Achilles tendon defect healing. Pasternak et al. (2006) evaluated the effect of doxycycline on Achilles to Achilles tendon healing in a rat Achilles tendon transection model. Compared to our results, force and energy uptake at the time of disruption was significantly lower in mechanical tests at 5, 8 and 14 days compared to control samples. This study shows for the first time the pharmacological effects of MMP inhibitors on tendon repair. This effect is not necessarily detrimental and, at least in theory, MMP has some potentially beneficial applications in tendon tissue, for example, against tendon damage associated with rheumatoid arthritis (Bramono et al., 2004). Weng et al. (2020) used electrostatic spinning to prepare drug-laden nanofibres and investigated their *in vitro* and *in vivo* drug release. The results showed that Polylactide-glycolic acid (PLGA) copolymer nanofibres released effective concentrations of doxycycline for more than 40 days postoperatively, with lower systemic plasma drug concentrations. Rats implanted with

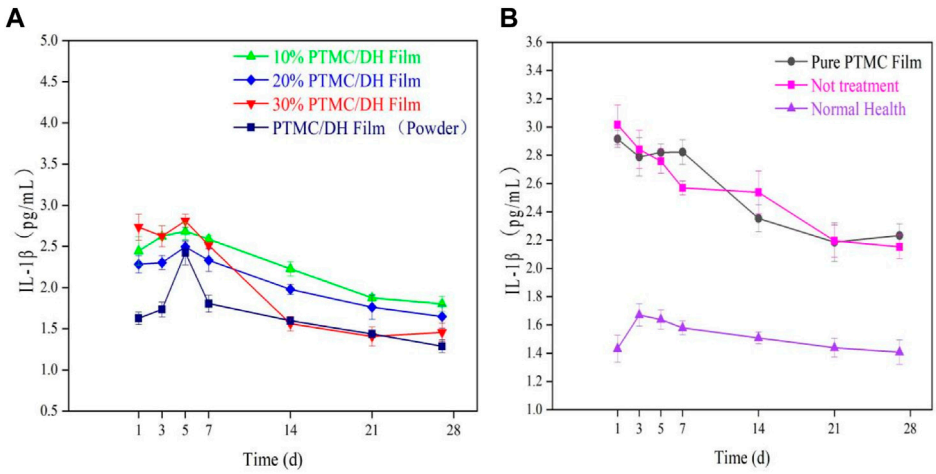

FIGURE 13
(A) IL-1β trend in the experimental group over 28 days; **(B)** IL-1β trend in the control group, blank group and normal healthy group.

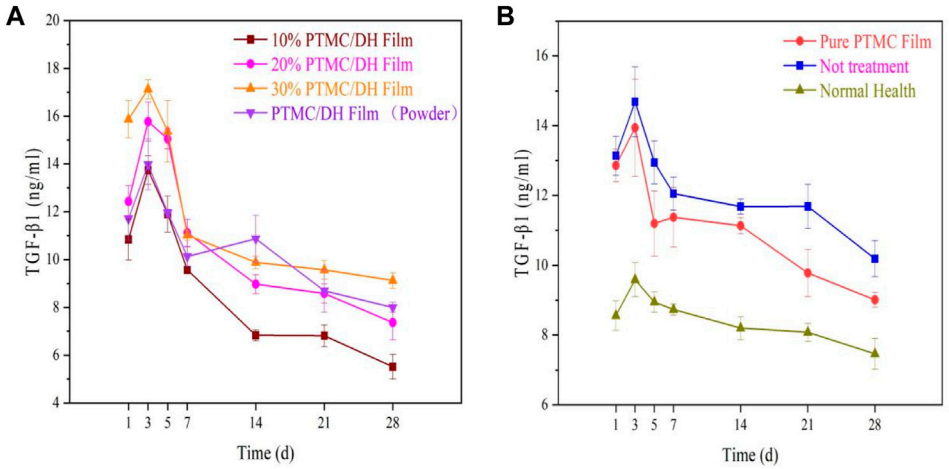

FIGURE 14
(A) TGF-β1 trend in the experimental group over 28 days; **(B)** TGF-β1 trend in the control group, blank group and normal healthy group.

doxycycline nanofibres also exhibited greater postoperative activity and stronger tendons. The findings illustrate the great potential of doxycycline loaded nanofibres in the repair of Achilles tendon ruptures.

In this study, PTMC films were used to embed doxycycline hydrochloride in the drug-carrying film to provide local and sustainable drug release to the lesion site for repair of Achilles tendon defects. However, some of the drug located on the surface of the delivery film then initially shows a burst release, which decreases over time and is excessive in a diffusion-driven manner. *In vivo* drug release peaked on the first day, with the PTMC/DH group releasing the most on the first day, which may be related to the better water solubility of the end of the drug, followed by a gradual decrease in each group until stabilisation around the seventh day. All biomechanical tests showed that the mechanical strength and mechanical properties of the experimental group were better than those of the control and blank groups. Histological analysis showed a gradual decrease in fibroblast density in the experimental group and a tendency for the inflammatory response to first increase and then decrease, both of which were in line with the expected experimental results. In conclusion, this study also demonstrated that locally targeted treatment of Achilles tendon defects in rats also achieved good therapeutic results.

5 Conclusion

In this study, we prepared biodegradable polymer-bound doxycycline hydrochloride drug delivery films and evaluated the safety and efficacy of different concentration ratios of drug delivery films in the repair of Achilles tendon defects in rats using PTMC as the carrier material. The experimental group of rats with Achilles tendon defects repaired with doxycycline hydrochloride showed superior mechanical properties and high Achilles tendon activity. Fibroblast density in the experimental group was gradually reduced and inflammatory factor levels were gradually reduced to normal levels. In conclusion, doxycycline hydrochloride containing drug-loaded films showed effectiveness and feasibility in the repair of Achilles tendon defects in rats.

Data availability statement

The raw data supporting the conclusion of this article will be made available by the authors, without undue reservation.

Ethics statement

The animal study was reviewed and approved by the Ethics Committee of Liaoning Research Institute of Family Planning.

Author contributions

JZ and XZ performed the experiment. JZ wrote the first draft of the manuscript. WL involved in animal experiments. JG organized the database and performed the statistical analysis. LY and GY contributed to the conception and design of the study, and the manuscript revision.

Funding

This work was supported by the Natural Science Foundation of Liaoning Province (2022-YGJC-69), the support program for excellent young scholars of China Medical University and Project supported by the National Science Foundation for Young Scientists of China (Grant No.82204312).

Conflict of interest

The authors declare that the research was conducted in the absence of any commercial or financial relationships that could be construed as a potential conflict of interest.

Publisher's note

References

Albertsson, A. C., and Eklund, M. (1995). Influence of molecular structure on the degradation mechanism of degradable polymers: *In vitro* degradation of poly (trimethylene carbonate), poly (trimethylene carbonate-co-caprolactone), and poly (adipic anhydride). *J. Appl. Polym. Sci.* 57 (1), 87–103. doi:10.1002/app.1995.070570109

Aminlari, A., Stone, J., McKee, R., Subramony, R., Nadolski, A., Tolia, V., et al. (2021). Diagnosing achilles tendon rupture with ultrasound in patients treated surgically: A systematic review and meta-analysis. *J. Emerg. Med.* 61 (5), 558–567. doi:10.1016/j.jemermed.2021.09.008

Athanasiou, K. A., Niederauer, G. G., and Agrawal, C. M. (1996). Sterilization, toxicity, biocompatibility and clinical applications of polylactic acid/polyglycolic acid copolymers. *Biomaterials* 17 (2), 93–102. doi:10.1016/0142-9612(96)85754-1

Baldwin, S. J., Kreplak, L., and Lee, J. M. (2019). MMP-9 selectively cleaves non-D-banded material on collagen fibrils with discrete plasticity damage in mechanically-overloaded tendon. *J. Mech. Behav. Biomed. Mater.* 95, 67–75. doi:10.1016/j.jmbbm.2019.03.020

Bedi, A., Fox, A. J. S., Kovacevic, D., Deng, X. h., Warren, R. F., and Rodeo, S. A. (2010). Doxycycline-mediated inhibition of matrix metalloproteinases improves healing after rotator cuff repair. *Am. J. sports Med.* 38 (2), 308–317. doi:10.1177/0363546509347366

Bottagisio, M., and Lovati, A. B. (2017). A review on animal models and treatments for the reconstruction of Achilles and flexor tendons. *J. Mater. Sci. Mater. Med.* 28 (3), 45–16. doi:10.1007/s10856-017-5858-y

Bramono, D. S., Richmond, J. C., Weitzel, P. P., Kaplan, D. L., and Altman, G. H. (2004). Matrix metalloproteinases and their clinical applications in orthopaedics. *Clin. Orthop. Relat. Research®* 428, 272–285. doi:10.1097/01.blo.0000144166.66737.3a

Cerrato, R., and Switaj, P. (2017). Using arthroscopic techniques for Achilles pathology. *Foot Ankle Clin.* 22 (4), 781–799. doi:10.1016/j.fcl.2017.07.007

Chan, J. J., Chen, K. K., Sarker, S., and Vulcano, E. (2020). Epidemiology of Achilles tendon injuries in collegiate level athletes in the United States. *Int. Orthop.* 44 (3), 2473011419S0013–594. doi:10.1177/2473011419s00134

Chen, C., Hou, Z., Chen, S., Guo, J., Hu, J., et al. (2022). Photothermally responsive smart elastomer composites based on aliphatic polycarbonate backbone for biomedical applications. *Compos. Part B Eng.* 240, 109985. doi:10.1016/j.compositesb.2022.109985

Chugaev, D. V., Konovalchuk, N. S., Sorokin, E. P., Kogan, P. G., Gudz, A. I., Lasunsky, S. A., et al. (2018). Our approach to treatment of neglected achilles tendon ruptures. Is there a simple solution? *Traumatology Orthop. Russ.* 24 (1), 44–52. doi:10.21823/2311-2905-2018-24-1-44-52

Dams, O. C., van den Akker-Scheek, I., Diercks, R. L., Wendt, K. W., Zwerver, J., and Reininga, I. H. F. (2019). Surveying the management of achilles tendon ruptures in The Netherlands: Lack of consensus and need for treatment guidelines. *Knee Surg. Sports Traumatol. Arthrosc.* 27 (9), 2754–2764. doi:10.1007/s00167-018-5049-5

Dong, M., Zhong, L., Chen, W. Q., Ji, X. P., Zhang, M., Zhao, Y. X., et al. (2012). Doxycycline stabilizes vulnerable plaque via inhibiting matrix metalloproteinases and attenuating inflammation in rabbits. *PloS one* 7 (6), e39695. doi:10.1371/journal.pone.0039695

Fernandes de Jesus, J., Spadacci-Morena, D. D., Rabelo, N. D. A., Pinfildi, C. E., Fukuda, T. Y., and Plapler, H. (2019). Photobiomodulation of matrix metalloproteinases in rat calcaneal tendons. *Photobiomodulation, Photomed. laser Surg.* 37 (7), 421–427. doi:10.1089/photob.2019.4633

Ganestam, A., Kallemose, T., Troelsen, A., and Barfod, K. W. (2016). Increasing incidence of acute Achilles tendon rupture and a noticeable decline in surgical treatment from 1994 to 2013. A nationwide registry study of 33,160 patients. *Knee Surg. sports Traumatol. Arthrosc.* 24 (12), 3730–3737. doi:10.1007/s00167-015-3544-5

Garofalo, R., Cesari, E., Vinci, E., and Castagna, A. (2011). Role of metalloproteinases in rotator cuff tear. *Sports Med. Arthrosc. Rev.* 19 (3), 207–212. doi:10.1097/jsa.0b013e318227b07b

Gong, F., Cui, L., Zhang, X., Zhan, X., Gong, X., and Wen, Y. (2018). Piperine ameliorates collagenase-induced Achilles tendon injury in the rat. *Connect. tissue Res.* 59 (1), 21–29. doi:10.1080/03008207.2017.1289188

Griffin, M. O., Ceballos, G., and Villarreal, F. J. (2011). Tetracycline compounds with non-antimicrobial organ protective properties: Possible mechanisms of action. *Pharmacol. Res.* 63 (2), 102–107. doi:10.1016/j.phrs.2010.10.004

Han, J., Branford-White, C. J., and Zhu, L. M. (2010). Preparation of poly(ε-caprolactone)/poly(trimethylene carbonate) blend nanofibers by electrospinning. *Carbohydr. Polym.* 79 (1), 214–218. doi:10.1016/j.carbpol.2009.07.052

Hiramatsu, K., Tsujii, A., Nakamura, N., and Mitsuoka, T. (2018). Ultrasonographic evaluation of the early healing process after achilles tendon repair. *Orthop. J. Sports Med.* 6 (8), 232596711878988. doi:10.1177/2325967118789883

Ingvar, J., Tägil, M., and Eneroth, M. (2005). Nonoperative treatment of achilles tendon rupture: 196 consecutive patients with a 7% re-rupture rate. *Acta Orthop.* 76 (4), 597–601. doi:10.1080/17453670510041619

Jayasree, A., Kottappally Thankappan, S., Ramachandran, R., Sundaram, M. N., Chen, C. H., Mony, U., et al. (2019). Bioengineered braided micro–Nano (multiscale) fibrous scaffolds for tendon reconstruction. *ACS Biomed. Mater. Sci. Eng.* 5 (3), 1476–1486. doi:10.1021/acsbiomaterials.8b01328

Karp, J. M., Shoichet, M. S., and Davies, J. E. (2003). Bone formation on two-dimensional poly(DL-lactide-co-glycolide) (PLGA) films and three-dimensional PLGA tissue engineering scaffolds*in vitro*. *J. Biomed. Mater. Res. Part A An Official J. Soc. Biomaterials, Jpn. Soc. Biomaterials, Aust. Soc. Biomaterials Korean Soc. Biomaterials* 64 (2), 388–396. doi:10.1002/jbm.a.10420

Kessler, M. W., Barr, J., Greenwald, R., Lane, L. B., Dines, J. S., Dines, D. M., et al. (2014). Enhancement of Achilles tendon repair mediated by matrix metalloproteinase inhibition via systemic administration of doxycycline. *J. Orthop. Res.* 32 (4), 500–506. doi:10.1002/jor.22564

Li, X., Chen, H., Xie, S., Wang, N., Wu, S., Duan, Y., et al. (2020). <p>Fabrication of photo-crosslinkable poly(trimethylene carbonate)/polycaprolactone nanofibrous scaffolds for tendon regeneration</p>. *Int. J. nanomedicine* 15, 6373–6383. doi:10.2147/ijn.s246966

Mitsui, Y., Gotoh, M., Shirachi, I., Shibata, H., Yamada, T., Nakamura, H., et al. (2012). Increased matrix metalloprotease-3 gene expression in ruptured rotator cuff tendons is associated with postoperative tendon retear. *J. Shoulder Elb. Surg.* 21 (12), e26–e27. doi:10.1016/j.jse.2012.10.011

Molloy, T. J., Wang, Y., Horner, A., Skerry, T. M., and Murrell, G. A. C. (2006). Microarray analysis of healing rat achilles tendon: Evidence for glutamate signaling mechanisms and embryonic gene expression in healing tendon tissue. *J. Orthop. Res.* 24 (4), 842–855. doi:10.1002/jor.20093

Monnerie, C., Le Nen, D., Hu, W., et al. (2019). Traitement des nécroses du tendon d'Achille sans reconstruction tendineuse: À propos de quatre cas[C]. *Ann. Chir. Plast. Esthétique* 64 (2), 208–214.

Nguyen, Q. T., Norelli, J. B., Graver, A., Ekstein, C., Schwartz, J., Chowdhury, F., et al. (2017). Therapeutic effects of doxycycline on the quality of repaired and unrepaired Achilles tendons. *Am. J. sports Med.* 45 (12), 2872–2881. doi:10.1177/0363546517716637

Park, K. H., Park, J. H., Yoon, Y. K., Kwon, J. B., Kim, J. H., Lee, E., et al. (2022). Association between outdoor temperature and achilles tendon repair: A 14-years nationwide population-based cohort study. *Plos one* 17 (3), e0265041. doi:10.1371/journal.pone.0265041

Pasternak, B., Fellenius, M., and Aspenberg, P. (2006). Doxycycline impairs tendon repair in rats. *Acta Orthop. Belg.* 72 (6), 756–760.

Pego, A. P., Van Luyn, M. J. A., Brouwer, L. A., van Wachem, P. B., Poot, A. A., Grijpma, D. W., et al. (2003). *In vivo* behavior of poly(1,3-trimethylene carbonate) and copolymers of 1,3-trimethylene carbonate withD,L-lactide or ε-caprolactone: Degradation and tissue response. *J. Biomed. Mater. Res. Part A An Official J. Soc. Biomaterials, Jpn. Soc. Biomaterials, Aust. Soc. Biomaterials Korean Soc. Biomaterials* 67 (3), 1044–1054. doi:10.1002/jbm.a.10121

Sachlos, E., and Czernuszka, J. T. (2003). Making tissue engineering scaffolds work. Review: The application of solid freeform fabrication technology to the production of tissue engineering scaffolds. *Eur. Cell Mater* 5 (29), 29–40. doi:10.22203/ecm.v005a03

Shieh, S. J., Zimmerman, M. C., and Parsons, J. R. (1990). Preliminary characterization of bioresorbable and nonresorbable synthetic fibers for the repair of soft tissue injuries. *J. Biomed. Mater. Res.* 24 (7), 789–808. doi:10.1002/jbm.820240702

Smith, K., and Leyden, J. J. (2005). Safety of doxycycline and minocycline: A systematic review. *Clin. Ther.* 27 (9), 1329–1342. doi:10.1016/j.clinthera.2005.09.005

Sobhani-Eraghi, A., Panahi, M., Shirani, A., and H, P. T. (2020). The effect of doxycycline on achilles tendon repair in a rat model. *Malays. Orthop. J.* 14 (3), 155–160. doi:10.5704/moj.2011.024

Sun, X., Xu, C., Wu, G., Ye, Q., and Wang, C. (2017). Poly (lactic-co-glycolic acid): Applications and future prospects for periodontal tissue regeneration. *Polymers* 9 (6), 189. doi:10.3390/polym9060189

Thomopoulos, S., Parks, W. C., Rifkin, D. B., and Derwin, K. A. (2015). Mechanisms of tendon injury and repair. *J. Orthop. Res.* 33 (6), 832–839. doi:10.1002/jor.22806

Weng, C. J., Lee, D., Ho, J., and Liu, S. J. (2020). <p>Doxycycline-Embedded nanofibrous membranes help promote healing of tendon rupture</p>. *Int. J. nanomedicine* 15, 125–136. doi:10.2147/ijn.s217697

Yang, L., Li, J., Li, M., and Gu, Z. (2016). The *in vitro* and *in vivo* degradation of cross-linked poly (trimethylene carbonate)-based networks. *Polymers* 8 (4), 151. doi:10.3390/polym8040151

Yang, L., Li, J., Meng, S., Jin, Y., Zhang, J., Li, M., et al. (2014). The *in vitro* and *in vivo* degradation behavior of poly (trimethylene carbonate-co-ε-caprolactone) implants. *Polymer* 55 (20), 5111–5124. doi:10.1016/j.polymer.2014.08.027

Yang, L., Li, J., Zhang, W., Jin, Y., Liu, Y., et al. (2015). The degradation of poly (trimethylene carbonate) implants: The role of molecular weight and enzymes. *Polym. Degrad. Stab.* 122, 77–87. doi:10.1016/j.polymdegradstab.2015.10.016

Zhang, Z., Kuijer, R., Bulstra, S. K., Grijpma, D. W., and Feijen, J. (2006). The *in vivo* and *in vitro* degradation behavior of poly (trimethylene carbonate). *Biomaterials* 27 (9), 1741–1748. doi:10.1016/j.biomaterials.2005.09.017

Zhu, K. J., Hendren, R. W., Jensen, K., and Pitt, C. G. (1991). Synthesis, properties, and biodegradation of poly (1, 3-trimethylene carbonate). *Macromolecules* 24 (8), 1736–1740. doi:10.1021/ma00008a008

Frontiers in
Bioengineering and Biotechnology

Accelerates the development of therapies, devices, and technologies to improve our lives

A multidisciplinary journal that accelerates the development of biological therapies, devices, processes and technologies to improve our lives by bridging the gap between discoveries and their application.

Discover the latest Research Topics

See more →

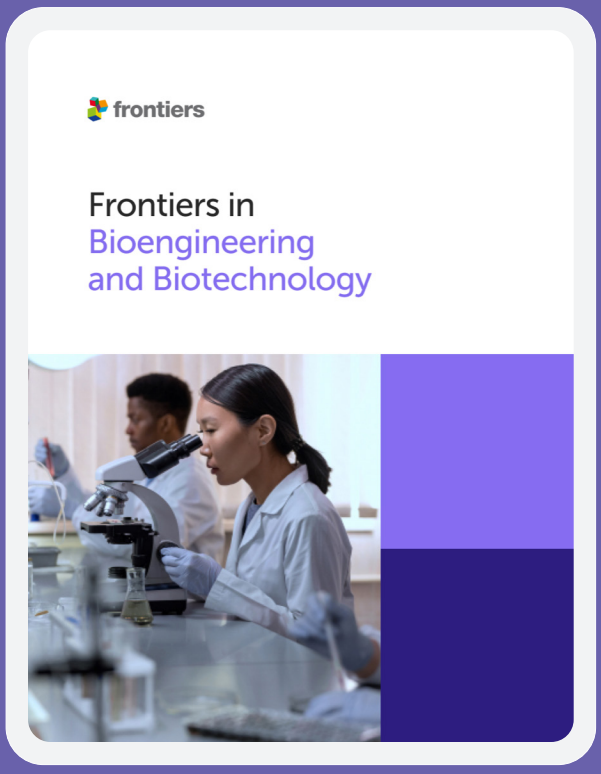

Frontiers

Avenue du Tribunal-Fédéral 34
1005 Lausanne, Switzerland
frontiersin.org

Contact us

+41 (0)21 510 17 00
frontiersin.org/about/contact